

Tuesday

SPDL30

RSNA Diagnosis Live™: Imaging in the Cobra Kai Dojo

Tuesday, Nov. 29 7:15AM - 8:15AM Room: E451B



AMA PRA Category 1 Credit™: 1.00
ARRT Category A+ Credit: 1.00

Participants

Adam E. Flanders, MD, Narberth, PA, (adam.flanders@jefferson.edu) (*Presenter*) Nothing to Disclose
Sandeep P. Deshmukh, MD, Philadelphia, PA, (sandeep.deshmukh@jefferson.edu) (*Presenter*) Nothing to Disclose
Christopher G. Roth, MD, Philadelphia, PA (*Presenter*) Nothing to Disclose

LEARNING OBJECTIVES

1) The participant will be introduced to a series of radiology case studies via an interactive team game approach designed to encourage "active" consumption of educational content. 2) The participant will be able to use their mobile wireless device (tablet, phone, laptop) to electronically respond to various imaging case challenges; participants will be able to monitor their individual and team performance in real time. 3) The attendee will receive a personalized self-assessment report via email that will review the case material presented during the session, along with individual and team performance. This interactive session will use RSNA Diagnosis Live™. Please bring your charged mobile wireless device (phone, tablet or laptop) to participate.

Controversy Session: A New Perspective on Radiation and Sedation Risk in Children: Should ALARA be as 'Low' or as 'Light' as Reasonably Achievable?

Tuesday, Nov. 29 7:15AM - 8:15AM Room: E451A

AMA PRA Category 1 Credit™: 1.00
ARRT Category A+ Credit: 1.00 A small square icon with white text on a dark background containing the letters 'FDA'.
Discussions may include off-label uses.**Participants**Donald P. Frush, MD, Durham, NC, (donald.frush@duke.edu) (*Moderator*) Nothing to DiscloseShreyas S. Vasanaawala, MD, PhD, Stanford, CA (*Presenter*) Research collaboration, General Electric Company; Consultant, Arterys Inc; Research Grant, Bayer AG;Randall Flick, MD, Rochester, MN (*Presenter*) Nothing to Disclose**LEARNING OBJECTIVES**

1) Briefly review current state of low level radiation and risk in children. 2) Emphasize value of non-ionizing radiation MR. 3) Highlight current fast techniques for children. 4) Outline current status of sedation and cognitive impact in children. 5) Provide strategies for team work between anesthesiology and radiology to minimize these risks.

ABSTRACT

The pediatric population is particularly sensitive to the risk of radiation, and radiation risk from CT is estimated as approximately 1/10000 fatal cancers per mSv of radiation. Thus alternative imaging techniques should be utilized when possible, including MRI.

However, MRI often requires sedation or general anesthesia for age groups and indications for which CT does not. Though risks of immediate complications from anesthesia or sedation are generally well appreciated, there is a growing concern of the potential risks related to neurotoxicity of anesthetic agents. This toxicity is thought to carry greatest risk when anesthesia is performed at a particularly young age, for prolonged times, and for repeated procedures. Thus, overall risks to the patient for imaging must be considered in holistic fashion, balancing ionizing radiation against that of anesthesia. Methods to shift this risk profile in a favorable fashion include targeted MR imaging protocols, free-breathing techniques, and volumetric acquisitions.

URL

SPSH30

Hot Topic Session: Multi-Spectral Cardiovascular CT Imaging

Tuesday, Nov. 29 7:15AM - 8:15AM Room: E352



AMA PRA Category 1 Credit™: 1.00
ARRT Category A+ Credit: 1.00

FDA Discussions may include off-label uses.

Participants

Suhny Abbara, MD, Dallas, TX, (Suhny.Abbara@UTSouthwestern.edu) (*Moderator*) Author, Reed Elsevier; Editor, Reed Elsevier; Institutional research agreement, Koninklijke Philips NV; Institutional research agreement, Siemens AG
David A. Bluemke, MD, PhD, Bethesda, MD (*Moderator*) Research support, Siemens AG

LEARNING OBJECTIVES

1) Describe principles of multi-spectral CT for evaluation of the coronary arteries and myocardium. 2) Describe technical principles of various approaches to multi-spectral CT and their differences. 3) Describe applications of multi-spectral CT for optimization of cardiovascular CT.

ABSTRACT

Multi-spectral (multi-energy) CT is increasingly available for cardiovascular applications. Different approaches to multi-spectral CT are implemented on different CT instruments. Current implementations include rapid KV switching, dual scan, split beam, dual-layer detectors, dual source x-ray. While there are strengths and weaknesses of each approach, all share the common goal of providing improved discrimination of abnormal myocardium or arterial wall from normal areas. Multi-spectral CT scanners can generate synthetic monoenergy or combination energy images which in turn can be used to increase conspicuity of atherosclerotic plaque and visualization of calcifications. Multi-spectral CT holds the potential for improved plaque characterization, better detection of myocardial fibrosis and perfusion abnormalities.

URL

Active Handout: David A. Bluemke

http://abstract.rsna.org/uploads/2016/16002345/SPSH30_RSNA_2016_spectral_CV_CTupload.pdf

Sub-Events

SPSH30A Principles of Multi-Spectral CT

Participants

Amir Pourmorteza, PhD, Bethesda, MD, (amir.pourmorteza@nih.gov) (*Presenter*) Researcher, Siemens AG

LEARNING OBJECTIVES

1) Describe the general principles of multi-spectral CT. 2) Describe technical principles of various approaches to multi-spectral CT and their differences.

ABSTRACT

URL

SPSH30B Current Applications of Multi-Spectral Cardiac CT

Participants

David A. Bluemke, MD, PhD, Bethesda, MD (*Presenter*) Research support, Siemens AG

LEARNING OBJECTIVES

1) Describe principles of multi-spectral CT for evaluation of the coronary arteries and myocardium. 2) Describe applications of multi-spectral CT for optimization of cardiovascular CT.

ABSTRACT

Multi-spectral (multi-energy) CT is increasingly available for cardiovascular applications. Different approaches to multi-spectral CT are implemented on different CT instruments. Current implementations include rapid KV switching, dual scan, split beam, dual-layer detectors, dual source x-ray. While there are strengths and weaknesses of each approach, all share the common goal of providing improved discrimination of abnormal myocardium or arterial wall from normal areas. Multi-spectral CT scanners can generate synthetic monoenergy or combination energy images which in turn can be used to increase conspicuity of atherosclerotic plaque and visualization of calcifications. Multi-spectral CT holds the potential for improved plaque characterization, better detection of myocardial fibrosis and perfusion abnormalities.

URL

SPSH30C Opportunities in Spectral Detector Cardiovascular CT

Participants

Suhny Abbara, MD, Dallas, TX (*Presenter*) Author, Reed Elsevier; Editor, Reed Elsevier; Institutional research agreement, Koninklijke Philips NV; Institutional research agreement, Siemens AG

LEARNING OBJECTIVES

View learning objectives under the main course title.

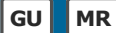
Honored Educators

Presenters or authors on this event have been recognized as RSNA Honored Educators for participating in multiple qualifying educational activities. Honored Educators are invested in furthering the profession of radiology by delivering high-quality educational content in their field of study. Learn how you can become an honored educator by visiting the website at: <https://www.rsna.org/Honored-Educator-Award/>

Suhny Abbara, MD - 2014 Honored Educator

Prostate MRI (Hands-on)

Tuesday, Nov. 29 8:00AM - 10:00AM Room: S401AB

AMA PRA Category 1 Credits™: 1.50
ARRT Category A+ Credit: 0**Participants**

Jelle O. Barentsz, MD, PhD, Nijmegen, Netherlands (*Presenter*) Research Consultant, SPL Medical
Jurgen J. Futterer, MD, PhD, Nijmegen, Netherlands, (jurgen.futterer@radboudumc.nl) (*Presenter*) Research Grant, Medtronic, Inc; Research Grant, Siemens AG
Roel D. Mus, MD, Nijmegen, Netherlands (*Presenter*) Nothing to Disclose
Geert M. Villeirs, MD, PhD, Ghent, Belgium (*Presenter*) Nothing to Disclose
Baris Turkbey, MD, Bethesda, MD (*Presenter*) Nothing to Disclose
Jeffrey C. Weinreb, MD, New Haven, CT (*Presenter*) Nothing to Disclose
Antonio C. Westphalen, MD, Mill Valley, CA, (antonio.westphalen@ucsf.edu) (*Presenter*) Scientific Advisory Board, 3DBiopsy LLC ; Research Grant, Verily Life Sciences LLC
Rianne R. Engels, Cuijk, Netherlands (*Presenter*) Nothing to Disclose
Joyce G. Bomers, Nijmegen, Netherlands (*Presenter*) Nothing to Disclose
Renske L. Van Delft, Nijmegen, Netherlands (*Presenter*) Nothing to Disclose
Laura I. Stoilescu, Nijmegen, Netherlands (*Presenter*) Nothing to Disclose
Daniel J. Margolis, MD, Los Angeles, CA (*Presenter*) Nothing to Disclose
Patrik Zamecnik, MD, Heidelberg, Germany (*Presenter*) Officer, SPL Medical BV
Sadhna Verma, MD, Cincinnati, OH (*Presenter*) Nothing to Disclose

LEARNING OBJECTIVES

1) Understand the PI-RADS v2 Category assessment to detect and localize significant cancer for both peripheral zone and transitional zone lesions. 2) Recognize benign pathology like inflammation and BPH and to differentiate these from significant prostate cancers.

ABSTRACT

In this Hands-On Workshop, the participants will be able to review up to 40 multi-parametric MRI cases with various prostatic pathology using a dedicated workstation. Focus will be on the overall assessment of PI-RADS v2 category, which enables them to score the probability of the presence of a significant cancer in patients with elevated PSA and/or clinical suspicion. All cases are from daily non-academic practice, and have various levels of difficulty. The cases include: easy and difficult significant peripheral-transition- and central zone cancers, inflammation, BPH, and the most common pitfalls. Internationally renowned teachers will guide the participants during their PI-RADS v2 scoring. There will be 50 workstations available. Participants will be able to use their own laptops through a secure WiFi connection.

Active Handout: Renske Lian Van Delft

http://abstract.rsna.org/uploads/2016/16002001/RCA_Coursebook_Prostate_hands_on_course.pdf

MSAS31

The Evolution of the Imaging Technologist (Sponsored by the Associated Sciences Consortium) (An Interactive Session)

Tuesday, Nov. 29 8:30AM - 10:00AM Room: S105AB

OT

AMA PRA Category 1 Credits™: 1.50
ARRT Category A+ Credits: 1.50

Participants

David B. Nicholson, Charlottesville, VA (*Moderator*) Nothing to Disclose
Charlotte Beardmore, MBA, London, United Kingdom (*Moderator*) Nothing to Disclose

LEARNING OBJECTIVES

1) To understand the changing role of the radiographer in the UK in supporting streamlined patient care. 2) To consider the impact of these changes upon education and training requirements; in relation to higher levels of practice. 3) To consider the importance of impact reporting with changing scope of practice.

Sub-Events

MSAS31A The Integration of Simulation into the Education and Training of Imaging Technologists

Participants

David B. Nicholson, Charlottesville, VA (*Presenter*) Nothing to Disclose

LEARNING OBJECTIVES

View learning objectives under main course title.

MSAS31B Changing Scope of Practice in the UK

Participants

Charlotte Beardmore, MBA, London, United Kingdom (*Presenter*) Nothing to Disclose

LEARNING OBJECTIVES

View learning objectives under main course title.

MSCC31

Case-based Review of Nuclear Medicine: PET/CT Workshop-Head and Neck Cancers (In Conjunction with SNMMI) (An Interactive Session)

Tuesday, Nov. 29 8:30AM - 10:00AM Room: S406A



AMA PRA Category 1 Credits™: 1.50
ARRT Category A+ Credits: 1.50

Participants

Janis P. O'Malley, MD, Birmingham, AL, (jomalley@uabmc.edu) (*Moderator*) Nothing to Disclose
Jonathan E. McConathy, MD, PhD, Birmingham, AL (*Presenter*) Research Consultant, Eli Lilly and Company; Research Consultant, Blue Earth Diagnostics Ltd; Research Consultant, Siemens AG; Research Consultant, General Electric Company;

LEARNING OBJECTIVES

1) Participants will use FDG-PET/CT and FDG-PET/MRI more effectively in their clinical practice through better understanding of the anatomy, clinical scenarios, and differential diagnoses relevant to the diagnostic imaging of head and neck cancers.

ABSTRACT

MSES31

Essentials of Genitourinary Imaging

Tuesday, Nov. 29 8:30AM - 10:00AM Room: S100AB

GU

AMA PRA Category 1 Credits™: 1.50
ARRT Category A+ Credits: 1.50

Participants

Sub-Events

MSES31A Acute Pelvic Pain

Participants

Marcia C. Javitt, MD, Haifa, Israel (*Presenter*) Consultant, Bayer AG;

LEARNING OBJECTIVES

1) How to classify the many causes of acute pelvic pain. 2) When and how to triage patients to appropriate imaging. 3) How to identify surgical emergencies. 4) Whether to recommend specific therapy quickly. 5) How to prevent unnecessary interventions. 6) Ways to minimize health care expenses.

ABSTRACT

Acute pelvic pain is pain of less than about 3 months duration. Patients with acute pelvic pain can be categorized into patients with a positive versus those with a negative pregnancy test (beta-human chorionic gonadotropin). The objectives of this talk are to: 1) provide a scheme to understand the causes of acute pelvic pain; 2) triage the diagnostic imaging workup using the clinical presentation and laboratory data; and 3) achieve a tailored differential diagnosis useful to guide appropriate treatment in female patients presenting with acute pelvic pain. The course will cover obstetrical, postpartum, gynecologic, infectious, inflammatory, and neoplastic causes of acute pelvic pain. Patients with acute pelvic pain may have characteristic findings on US, CT, and MRI that permit specific diagnosis of their conditions. Becoming familiar with these patterns on cross-sectional imaging empowers the radiologist to identify the cause of the pain and aid the referring clinicians to institute prompt and appropriate treatment for these important and sometimes life-threatening conditions.

MSES31B Sonography in Patients with Renal Colic

Participants

Ruth B. Goldstein, MD, San Francisco, CA (*Presenter*) Nothing to Disclose

LEARNING OBJECTIVES

1) To state the advantage and safety of using sonography in the initial evaluation of patients with renal colic. 2) To state the risk/benefits of starting the imaging evaluation with sonography vs CT. 3) To be able to optimize the renal/bladder sonogram in patients with renal colic. 4) To state the most common locations of ureteral stones in patients presenting to the ED with renal colic.

MSES31C Imaging of Hematuria

Participants

Alessandro Furlan, MD, Pittsburgh, PA, (furlana@upmc.edu) (*Presenter*) Book contract, Reed Elsevier; Research Grant, General Electric Company

LEARNING OBJECTIVES

1) Identify the role of imaging studies in the assessment of patients with hematuria according to current national and international guidelines. 2) Describe basic technical aspects of cross-sectional imaging tests used in patients with hematuria. 3) List the most common causes of hematuria and the key diagnostic imaging features.

ABSTRACT

Hematuria, defined as the presence of red blood cell in the urine, is a common presentation of multiple genitourinary diseases including benign (e.g. stones) and malignant disorders. Imaging plays a key role for the evaluation of patients with hematuria as delineated in multiple guidelines. This presentation will discuss 1) the current guidelines for the management of patients with hematuria, 2) the basic technical imaging aspects of CT urography and MR urography and 3) the key imaging findings for the diagnosis of the most common causes of hematuria.

MSES31D Interventional Management of Uterine Bleeding-Not Just Fibroids

Participants

Philip D. Orons, DO, Pittsburgh, PA, (oronspd@upmc.edu) (*Presenter*) Nothing to Disclose

LEARNING OBJECTIVES

1) Define causes of acute and chronic uterine bleeding. 2) Identify appropriate patients for transcatheter, medical, or surgical therapy based on patient presentation, imaging findings, and clinical circumstances. 3) Describe the clinical presentation and imaging findings of uterine arteriovenous malformations. 4) Compare outcomes of surgical and percutaneous therapy for the treatment and prevention of postpartum hemorrhage.

ABSTRACT

Uterine bleeding is a common and serious condition that may be associated with a high degree of morbidity and even mortality, particularly when occurring postpartum. The clinical presentation and potential long-term effects of uterine bleeding vary by etiology. Appropriate treatment is dictated by patient presentation and clinical and imaging findings. This presentation will discuss etiology, clinical presentation, and treatment options for multiple causes of acute and chronic uterine bleeding.

MSQI31

Quality Improvement Symposium: What is Value?

Tuesday, Nov. 29 8:30AM - 10:00AM Room: S406B

SQ

AMA PRA Category 1 Credits™: 1.50
ARRT Category A+ Credits: 1.50

Participants

Ella A. Kazerooni, MD, Ann Arbor, MI, (ellakaz@umich.edu) (*Moderator*) Nothing to Disclose

LEARNING OBJECTIVES

ABSTRACT

Sub-Events

MSQI31A Value Through the Patient's Eyes: Patient and Family Centered Care

Participants

Kelly Parent, Ann Arbor, MI, (parentk@med.umich.edu) (*Presenter*) Nothing to Disclose

LEARNING OBJECTIVES

1) Demonstrate the value of patient and family engagement to promote high quality and safe care.

ABSTRACT

Handout: Kelly Parent

http://abstract.rsna.org/uploads/2016/16000814/RSNA_final.pdf

MSQI31B Delivering Value to Patients: The Radiologist's Perspective

Participants

James V. Rawson, MD, Augusta, GA (*Presenter*) Nothing to Disclose

LEARNING OBJECTIVES

1) Identify opportunities to increase value to patients. 2) Develop infrastructure to sustain bringing new value to patients.

ABSTRACT

Opportunities exist both inside and outside of the traditional Radiologist's workflow to bring additional value to the patient. By including patients and families in the practice/hospital committees, equipment renovations or other operational projects, patients and families can help identify changes that would be important to them.

MSQI31C Patient/Family Engagement as Part of the QI

Participants

Paul G. Nagy, PhD, Baltimore, MD, (pnagy@jhu.edu) (*Presenter*) Institutional license agreement, Analytical Informatics, Inc

LEARNING OBJECTIVES

1) Describe QI as an effective management method to drive organizational change. 2) Discuss the need for patient advocacy for alignment of teams. 3) Illustrate projects with Patient experience as the focus. 4) Identify how we communicate and interact with patients.

ABSTRACT

Improving patient experience is a valid and important focus for quality improvement projects. This discussion will illustrate lessons learned with projects having a patient experience focus as opposed to traditional patient safety, provider coordination, and operations project topics.

Honored Educators

Presenters or authors on this event have been recognized as RSNA Honored Educators for participating in multiple qualifying educational activities. Honored Educators are invested in furthering the profession of radiology by delivering high-quality educational content in their field of study. Learn how you can become an honored educator by visiting the website at: <https://www.rsna.org/Honored-Educator-Award/>

Paul G. Nagy, PhD - 2014 Honored Educator

MSRO31

BOOST: Breast-Oncology Anatomy (An Interactive Session)

Tuesday, Nov. 29 8:30AM - 10:00AM Room: S103AB



AMA PRA Category 1 Credits™: 1.50
ARRT Category A+ Credits: 1.50

Participants

Jean L. Wright, MD, New York, NY (*Presenter*) Nothing to Disclose

Susan C. Harvey, MD, Lutherville, MD, (sharvey7@jhmi.edu) (*Presenter*) Nothing to Disclose

LEARNING OBJECTIVES

1) Understand breast and regional lymph node anatomy. 2) Be familiar with how the basic anatomic structures appear on a variety of imaging modalities. 3) Be familiar with breast and regional lymph node contouring techniques used in radiation treatment planning for breast cancer. 4) Apply contouring knowledge to inform radiation treatment planning for breast cancer.

ABSTRACT

Review breast and axillary anatomy.

BOOST: Lung-Oncology Anatomy (An Interactive Session)

Tuesday, Nov. 29 8:30AM - 10:00AM Room: S103CD

CH **RO**AMA PRA Category 1 Credits™: 1.50
ARRT Category A+ Credits: 1.50**Participants**Meng X. Welliver, MD, Columbus, OH, (meng.welliver@osumc.edu) (*Moderator*) Nothing to DiscloseMichelle S. Ginsberg, MD, New York, NY (*Presenter*) Nothing to DiscloseGregory Videtic, MD, FRCPC, Cleveland, OH, (videtig@ccf.org) (*Presenter*) Nothing to DiscloseFeng-Ming Kong, MD, PhD, Augusta, IN (*Presenter*) Research Grant, Varian Medical Systems, Inc; Speaker, Varian Medical System, Inc; Travel support, Varian Medical System, Inc**LEARNING OBJECTIVES**

1) Review the Radiologist's approach to thoracic anatomy that impacts treatment decision making in the treatment of lung cancer regarding tumors and proximity to great vessels/heart; involvement of airway/esophagus/chest wall; involvement of diaphragm/pericardium/phrenic nerve; involvement of vertebral column; and mediastinal and hilar nodes. 2) Understand the terminology used by Radiation Oncologists when defining targets for treatment and normal structures for avoidance including a) review the contouring of gross tumor volume (GTV), clinical target volume (CTV), and planning target volume (PTV) for stereotactic body radiotherapy for medically inoperable early stage non-small cell lung cancer; b) review the contouring of gross tumor volume (GTV), clinical target volume (CTV), and planning target volume (PTV) for conventional external beam radiotherapy for non-metastatic non-small cell lung cancer and small cell lung cancer. c) review the contouring of, and standardized definitions for, critical organs at risk (OARs) in the thorax: e.g. esophagus, brachial plexus, heart, airways, lungs, as they relate to definitive radiotherapy

ABSTRACT

Lung Cancer is a challenging disease to treat. It typically presents in advanced stage and even in the curative setting, the normal structures in the thorax make it challenging to treat with radiotherapy because of their inherent sensitivity. In this course, the Radiologist's perspective will inform a review the normal anatomy of the chest and how its structures relate to, and can predict, the acute and late manifestations of radiotherapy on these organs and tissues. Then, the parameters by which Radiation Oncologists design their treatment targets in order to maximize treatment of cancer and minimize injury to organs-at-risk will be reviewed.

RC301

Non-Vascular Thoracic MR: Ready for Prime Time!

Tuesday, Nov. 29 8:30AM - 10:00AM Room: E451A

CH **MR**

AMA PRA Category 1 Credits™: 1.50
ARRT Category A+ Credits: 1.50

FDA

Discussions may include off-label uses.

Participants

Jeanne B. Ackman, MD, Boston, MA (*Moderator*) Nothing to Disclose

LEARNING OBJECTIVES

1) Discuss what it takes to build a non-vascular thoracic MR practice. 2) Create simple mediastinal, pleural, and lung protocols which answer clinical questions. 3) Become more comfortable interpreting these various types of non-vascular thoracic MR examinations.

ABSTRACT

Despite MRI's long-demonstrated advantages regarding tissue contrast and diagnostic specificity and its absence of radiation, MRI remains an underutilized imaging modality for thoracic evaluation. The aim of this course is to cover the basics needed to build a non-vascular thoracic MR practice and to perform and interpret thoracic MRI, whether of the mediastinum, the pleura, or the lung. Fast and robust examination protocols, applicable and ready to use on currently available MR equipment, will be shared. Clinical indications for thoracic MRI and commonly encountered lesions will be discussed, with the goal of further improving patient care.

Sub-Events

RC301A Building a Clinical Program

Participants

Jeanne B. Ackman, MD, Boston, MA (*Presenter*) Nothing to Disclose

LEARNING OBJECTIVES

1) Discuss the challenges to building a clinical non-vascular thoracic MR practice. 2) Understand how to surmount these challenges. 3) Outline a multifaceted approach to building a practice. 4) Understand the benefit of building a clinical non-vascular thoracic MR practice.

ABSTRACT

There are many challenges to building a clinical non-vascular thoracic MR practice, many of which can be surmounted by: 1) identifying a knowledgeable and capable radiologist within your practice to take this initiative and build a team of interested colleagues to move forward 2) educating technologists, referring physicians, trainees, and colleagues as to its performance, interpretation, and benefits, 3) building a few simple MR protocols which can answer most clinical questions, 4) regularly sharing MR cases to enhance the knowledge of your group, 5) patience and recognition of the fact that those in your group insufficiently trained in thoracic MRI may not at first be comfortable with protocoling, interpreting, and recommending these examinations; these colleagues will need to be convinced of MR's benefits and, if interested, will be open to learning what they need to learn to maximize the benefits that can be achieved for patient care as a result of MR's higher tissue contrast, diagnostic specificity, and lack of ionizing radiation.

RC301B MRI of the Pleura: Value Added

Participants

Jeanne B. Ackman, MD, Boston, MA (*Presenter*) Nothing to Disclose

LEARNING OBJECTIVES

1) Discuss MR's added value beyond computed tomography for pleural lesion assessment in terms of tissue characterization, diagnostic specificity, gauging extent of disease, and guidance to the surgeon. 2) Outline the essential components of a basic pleural MR protocol. 3) Discuss typical features of various cystic and solid pleural lesions.

ABSTRACT

MRI adds value beyond computed tomography (CT) with regard to tissue characterization, diagnostic specificity, assessment of extent of pleural disease, and guidance to the thoracic surgeon. This brief lecture will cover the basics of pleural MR imaging and interpretation and show how pleural MR imaging can improve patient care. Typical features of various cystic and solid pleural lesions, including mesothelioma, solitary fibrous tumors, endometriomas, intrapleural bronchogenic cysts, and extralobar sequestration, will be discussed.

RC301C MRI of the Lung: The Ace Up the Sleeve

Participants

Jurgen Biederer, MD, Heidelberg, Germany, (biederer@radiologie-darmstadt.de) (*Presenter*) Nothing to Disclose

LEARNING OBJECTIVES

1) Estimate the diagnostic scope of lung MRI for evaluation of the lung parenchyma and airways. 2) Appreciate the diagnostic yield

of MRI for the evaluation and characterization of lung nodules and the detection of malignancy. 3) Consider MRI as potential first choice modality for imaging and follow up of pulmonary disease in young and/or pregnant patients--e.g. cystic fibrosis. 4) Discuss the potential role of lung MRI as an alternative or adjunct to other modalities--e.g. in COPD or interstitial lung disease.

ABSTRACT

Besides X-ray and CT, MRI of the lung can play an interesting role as "the ace up the sleeve" in your clinical practice. The sensitivity of MRI for infiltrates is at least similar to X-ray and CT, lung nodule detection is superior to X-ray and slightly inferior to CT and unique options for tissue characterization (exclusion of malignancy) and functional imaging capacities (perfusion, ventilation, respiratory motion) are available with standardized protocols. Given this, MRI may serve as a radiation-free alternative in patients who should not be exposed to ionizing radiation (children and young subjects, pregnant patients), e.g. as your first choice modality in patients with cystic fibrosis. It may well serve as an adjunct to other modalities for comprehensive lung imaging in COPD and some cases of interstitial lung diseases, e.g. sarcoidosis (dark lymph node sign). In young patients, it may well be used for the long term follow-up of malignancy (e.g. seminoma) or inflammatory disease (e.g. GPA/Wegener's disease). As an adjunct or alternative to other modalities, MRI can be helpful in lung cancer staging and follow-up (differentiation of atelectasis and lung cancer) or the characterization of lung nodules ("actionable nodules" with contrast uptake, high NPV of nodules with no or low contrast uptake, fatty content in hamartoma). Finally, MRI might even play a role in early detection of lung cancer, either as the screening tool or for the further diagnostic work-up of detected lesions.

RC301D Practical Mediastinal MRI

Participants

Constantine A. Raptis, MD, Saint Louis, MO (*Presenter*) Nothing to Disclose

LEARNING OBJECTIVES

1) Identify scenarios in which MRI is helpful in the evaluation of patients with known or suspected mediastinal pathology. 2) Discuss the components of efficient MRI protocols for the evaluation of mediastinal pathologies. 3) Understand key imaging findings which can be encountered on MRI examinations of the mediastinum.

ABSTRACT

While CT has long been the primary imaging modality for cross sectional evaluation of the thorax, MRI has emerged as a complimentary, and in some cases superior, means of evaluating mediastinal pathologies. This presentation will discuss the role MRI plays in the evaluation of mediastinal pathologies, focusing on important indications, protocol components, and imaging findings. This information will remain centered on practical aspects of mediastinal MRI that can be readily applied in any practice setting. Ultimately, the goal of this presentation is to give the audience the framework needed to utilize mediastinal MRI to improve patient care.

RC302

Leadership: How Can We Teach It and Promote It?

Tuesday, Nov. 29 8:30AM - 10:00AM Room: N227B



AMA PRA Category 1 Credits™: 1.50
ARRT Category A+ Credit: 0

Participants

Valerie P. Jackson, MD, Tucson, AZ (*Moderator*) Nothing to Disclose

Sub-Events

RC302A Leadership: The Resident's Point of View

Participants

Zachary E. Ballenger, MD, Indianapolis, IN, (zaballen421@gmail.com) (*Presenter*) Nothing to Disclose

LEARNING OBJECTIVES

1) Appreciate the role of leadership education for residency/fellowship curriculum. 2) Develop leadership educational programs at their institutions. 3) Prepare their radiology trainees for the leadership roles they will need to fill upon entering the radiology workforce in order to better serve their patients and practices in the changing healthcare environment.

ABSTRACT

RC302B Leadership: The Program Director's Point of View

Participants

Angelisa M. Paladin, MD, Seattle, WA (*Presenter*) Nothing to Disclose

LEARNING OBJECTIVES

1. Develop an appreciation for the value of a leadership curriculum for trainees 2. Identify successful strategies for program directors to develop a leadership curriculum

RC302C Promoting Leadership for Junior Faculty

Participants

Valerie P. Jackson, MD, Tucson, AZ (*Presenter*) Nothing to Disclose

LEARNING OBJECTIVES

1) Describe the value of leadership skills for young faculty. 2) Discuss resources available. 3) Describe the professional development needs of junior faculty. 4) Promote career development and leadership education for junior faculty.

ABSTRACT

Honored Educators

Presenters or authors on this event have been recognized as RSNA Honored Educators for participating in multiple qualifying educational activities. Honored Educators are invested in furthering the profession of radiology by delivering high-quality educational content in their field of study. Learn how you can become an honored educator by visiting the website at: <https://www.rsna.org/Honored-Educator-Award/>

Valerie P. Jackson, MD - 2014 Honored Educator

Cardiac Series: Emerging Cardiac MR and CT Imaging Techniques

Tuesday, Nov. 29 8:30AM - 12:00PM Room: S504AB



AMA PRA Category 1 Credits™: 3.25
ARRT Category A+ Credits: 4.00

FDA Discussions may include off-label uses.

Participants

Konstantin Nikolaou, MD, Tuebingen, Germany, (konstantin.nikolaou@med.uni-tuebingen.de) (*Moderator*) Speakers Bureau, Siemens AG; Speakers Bureau, Bracco Group; Speakers Bureau, Bayer AG
Robert M. Steiner, MD, Philadelphia, PA (*Moderator*) Consultant, Educational Symposia; Consultant, Johnson & Johnson
Suhny Abbara, MD, Dallas, TX (*Moderator*) Author, Reed Elsevier; Editor, Reed Elsevier; Institutional research agreement, Koninklijke Philips NV; Institutional research agreement, Siemens AG

Sub-Events**RC303-01 Spectral Detector CT**

Tuesday, Nov. 29 8:30AM - 8:55AM Room: S504AB

Participants

Suhny Abbara, MD, Dallas, TX, (Suhny.Abbara@UTSouthwestern.edu) (*Presenter*) Author, Reed Elsevier; Editor, Reed Elsevier; Institutional research agreement, Koninklijke Philips NV; Institutional research agreement, Siemens AG

LEARNING OBJECTIVES

1) Describe the technical characteristics of dual and single energy approaches resulting in spectral CT images. 2) Describe the potential applications of dual layer spectral detector cardiovascular CT.

ABSTRACT

Spectral energy CT images can be acquired via several routes, including dual scan, rapid kV switching, Dual source, split beam, and dual layer, as well as photon counting. This presentation will review the general differences between the various approaches and will then focus on dual layer spectral detector CT and its potential applications in cardiovascular imaging

Honored Educators

Presenters or authors on this event have been recognized as RSNA Honored Educators for participating in multiple qualifying educational activities. Honored Educators are invested in furthering the profession of radiology by delivering high-quality educational content in their field of study. Learn how you can become an honored educator by visiting the website at: <https://www.rsna.org/Honored-Educator-Award/>

Suhny Abbara, MD - 2014 Honored Educator

RC303-02 Triple-Rule-Out CT Angiography with Prospective ECG-trigger Dual-Energy Spectral Imaging and Low Concentration Contrastmedium

Tuesday, Nov. 29 8:55AM - 9:05AM Room: S504AB

Participants

Qi Yang, Xianyang, China (*Presenter*) Nothing to Disclose
Taiping He, Xianyang, China (*Abstract Co-Author*) Nothing to Disclose
Yong Yu, Xianyang City, China (*Abstract Co-Author*) Nothing to Disclose
Haifeng Duan, Xianyang City, China (*Abstract Co-Author*) Nothing to Disclose
Tian Xin, MMed, Xianyang City, China (*Abstract Co-Author*) Nothing to Disclose

PURPOSE

To investigate the use of low dose Spectral imaging mode with low concentration contrast medium in triple-rule-out CT angiography (CTA).

METHOD AND MATERIALS

Forty consecutive patients (HR<65BPM) with acute chest pain were randomly assigned into two groups to undergo triple-rule-out CTA on a Discovery CT750HD scanner. 20 patients in the study group (group A) were examined using prospective ECG-triggering dual-energy Spectral CT mode with a biphasic contrast injection of Iohexol (300mgI/ml). Images were reconstructed at 65keV with 60%ASIR. The control group (group B) of 20 patients underwent a conventional 120kVp retrospective ECG-gated spiral CT with auto mA and contrast concentration of 350mgI/ml. 120 kVp images were reconstructed with 40%ASIR. Region-of-interest was placed on coronary artery, pulmonary artery, thoracic aorta and muscle to measure CT number and standard deviation, and to calculate the contrast-to-noise ratio (CNR) and signal-to-noise ratio (SNR) for arteries. Two experienced radiologists also evaluated image quality double-blindly using a 4-point scoring system on MIP and VR images. Kappa test was used to test the interobserver consistency. The effective dose was obtained. Measurements between the two groups were statistically compared.

RESULTS

The CT number, SNR, CNR, subjective score of the two groups were statistically the same ($p>0.05$), and the agreement between the two observers were excellent ($k>0.80$). There was a significant difference in CTI

CONCLUSION

Spectral CT with prospective ECG-triggering and low concentration contrast medium reduces both radiation dose and contrast dose while maintaining image quality in triple-rule-out CT angiography compared with the conventional scanning protocol

CLINICAL RELEVANCE/APPLICATION

Prospective ECG-triggering Spectral CT may be used in triple-rule-out CT angiography

RC303-03 Multicenter Study of Utility of Left and Right Ventricular Strain Analysis for Diagnosis of Arrhythmogenic Right Ventricular Dysplasia (ARVD/C)

Tuesday, Nov. 29 9:05AM - 9:15AM Room: S504AB

Awards**Student Travel Stipend Award****Participants**

Mounes Aliyari Ghasabeh, MD, Baltimore, MD (*Presenter*) Nothing to Disclose
Anneline S. te Riele, MD, Utrecht, Netherlands (*Abstract Co-Author*) Nothing to Disclose
Manijeh Zarghampour, MD, Baltimore, MD (*Abstract Co-Author*) Nothing to Disclose
Cynthia James, PhD, Baltimore, MD (*Abstract Co-Author*) Nothing to Disclose
Crystal Tichnell, MSc, Baltimore, MD (*Abstract Co-Author*) Nothing to Disclose
Britney Murray, MS, Baltimore, MD (*Abstract Co-Author*) Nothing to Disclose
Bharath Ambale Venkatesh, PhD, Baltimore, MD (*Abstract Co-Author*) Nothing to Disclose
Elzbieta Chamera, Baltimore, MD (*Abstract Co-Author*) Nothing to Disclose
Joao A. Lima, MD, Baltimore, MD (*Abstract Co-Author*) Research Grant, Toshiba Corporation
Birgitta K. Velthuis, MD, Utrecht, Netherlands (*Abstract Co-Author*) Nothing to Disclose
David A. Bluemke, MD, PhD, Bethesda, MD (*Abstract Co-Author*) Research support, Siemens AG
Harikrishna Tandri, Baltimore, MD (*Abstract Co-Author*) Nothing to Disclose
Hugh Calkins, Baltimore, MD (*Abstract Co-Author*) Nothing to Disclose
Ihab R. Kamel, MD, PhD, Baltimore, MD (*Abstract Co-Author*) Research Grant, Siemens AG
Stefan L. Zimmerman, MD, Baltimore, MD (*Abstract Co-Author*) Nothing to Disclose

PURPOSE

Purpose: ARVD/C is a challenging diagnosis. The aim of this study was to assess regional and global wall motion using cardiac MRI strain analysis in suspected ARVD/C patients.

METHOD AND MATERIALS

Method: Retrospective, multi-center, international, IRB-approved and HIPPA compliant study. We enrolled 397 consecutive ARVD-suspected patients with MRI examinations who had been referred to two different tertiary centers in the United States and Holland for ARVD evaluation. After complete Task Force Criteria work-up, patients were divided into five groups: 1: definite ARVD, 2: at-risk (mutation positive without symptomatic disease), 3: structural heart disease (not ARVD), 4: electrical heart disease and 5: normal subjects. Regional and global strain analysis was performed on cine SSFP CMR images (Myocardial Tissue Tracking, Toshiba, Tokyo, Japan). RV and LV longitudinal strains were measured on long axis views. Short-axis views were used for circumferential strain measurements.

RESULTS

Results: There were 67, 74, 55, 78, and 123 patients in groups 1-5, respectively. RV global longitudinal strain was significantly worse in ARVD patients compared to all other groups. Mean strain values for RV and LV are summarized in table 1. The at-risk group showed strain values between ARVD and normal patients. LV strain was worst in the structural heart disease group, and similar between other groups. Longitudinal strains showed stronger differences between groups than circumferential strains, both for the RV and LV. By ROC analysis, RV basal longitudinal strain was the best parameter for ARVD diagnosis. A cutpoint of -27 was 82% sensitive and 83% specific for differentiating ARVD from groups 3,4, and 5 combined (at-risk group excluded).

CONCLUSION

Conclusion: In a large, multicenter study of patients referred to tertiary care centers for possible ARVD, RV longitudinal strain analysis was able to reliably differentiate between ARVD and non-ARVD patients. At-risk patients showed RV functional decline, with strain values midway between normals and phenotypically positive ARVD.

CLINICAL RELEVANCE/APPLICATION

Clinical relevance/Application: RV longitudinal strain analysis by MRI shows promise as an objective, quantifiable measure for diagnosis of ARVD and may have utility as an adjunct to current Task Force Criteria.

Honored Educators

Presenters or authors on this event have been recognized as RSNA Honored Educators for participating in multiple qualifying educational activities. Honored Educators are invested in furthering the profession of radiology by delivering high-quality educational content in their field of study. Learn how you can become an honored educator by visiting the website at: <https://www.rsna.org/Honored-Educator-Award/>

Ihab R. Kamel, MD, PhD - 2015 Honored Educator
Stefan L. Zimmerman, MD - 2012 Honored Educator

Stefan L. Zimmerman, MD - 2015 Honored Educator

RC303-04 Non-binary Myocardial Infarct Quantification Technique Accounting for Partial Volume Averaging Predicts Segmental Left Ventricular Myocardial Contraction

Tuesday, Nov. 29 9:15AM - 9:25AM Room: S504AB

Participants

Balazs Ruzsics, MD, PhD, Charleston, SC (*Presenter*) Nothing to Disclose
Pal Suranyi, MD, PhD, Charleston, SC (*Abstract Co-Author*) Nothing to Disclose
Rob J. van der Geest, PhD, Leiden, Netherlands (*Abstract Co-Author*) Nothing to Disclose
Carlo N. De Cecco, MD, PhD, Charleston, SC (*Abstract Co-Author*) Nothing to Disclose
Moritz H. Albrecht, MD, Charleston, SC (*Abstract Co-Author*) Nothing to Disclose
U. Joseph Schoepf, MD, Charleston, SC (*Abstract Co-Author*) Research Grant, Astellas Group; Research Grant, Bayer AG; Research Grant, General Electric Company; Research Grant, Siemens AG; Research support, Bayer AG; Consultant, Guerbet SA; ; ;
Taylor M. Duguay, Charleston, SC (*Abstract Co-Author*) Nothing to Disclose
Gabriel A. Elgavish, PhD, Birmingham, AL (*Abstract Co-Author*) Owner, Elgavish Paramagnetics, Inc; Consultant, Elgavish Paramagnetics, Inc; President, Elgavish Paramagnetics, Inc
Akos Varga-Szemes, MD, PhD, Charleston, SC (*Abstract Co-Author*) Consultant, Guerbet SA

PURPOSE

Binary myocardial infarct (MI) quantification techniques do not take partial volume averaging into consideration, resulting in an overestimation in MI size. Non-binary approaches, such as Percent Infarct Mapping (PIM), are able to address these shortcomings. The aim of this study was to investigate the influence of true MI content determined by PIM on segmental myocardial contraction.

METHOD AND MATERIALS

Twenty patients (57±11 years, 16 males) with prior MI underwent 1.5T MRI (Avanto, Siemens). Short-axis balanced steady-state free-precession (bSSFP) cine imaging, post-contrast (0.1mmol/kg gadobenate dimeglumine) T1-mapping (modified Look-Locker inversion recovery (IR), scheme 4(1)3(1)2), and late gadolinium enhancement (LGE) imaging (bSSFP with IR pulse) were performed. Myocardial contraction was quantified as radial wall thickening (RWT) using the centerline method according to the 17-segment model. Segmental MI content was calculated based on both T1 and LGE images applying the previously described PIM algorithm (PIMT1 and PIMLGE, respectively) using an in-house developed application. MI was also quantified based on LGE images using a binary approach (full-width at half-maximum, FWHM). Relationship between MI percentage (MI%) and RWT was tested using a linear regression.

RESULTS

Sixteen segments were excluded due to image artifacts. MI was observed in 69 of the remaining 324 segments. The FWHM method measured significantly higher global MI% compared to PIMT1 and PIMLGE (13.3±3.1%, 8.3±2.9%, and 8.7±3.5%, respectively, P=0.0024), as well as higher segmental MI% (66.1±26.1%, 47.4±18.0%, and 44.9±16.7%, respectively, P=0.0009). Average RWT in the normal and MI segments was 149.6±47.3% and 43.1±46.4%, respectively (P<0.0001). Strong correlation between MI% and RWT was observed using PIMT1 (r=-0.605, P=0.0012) and PIMLGE (r=-0.757, P<0.0001) methods, while the correlation was weaker using the binary FWHM threshold (r=-0.399, P=0.0319).

CONCLUSION

Both PIMT1 and PIMLGE showed good correlation with segmental myocardial contraction. The PIM-based methods measured lower MI% due to their ability to account for partial volume averaging. Non-binary approaches may become preferred techniques for quantitative LGE evaluation.

CLINICAL RELEVANCE/APPLICATION

Non-binary MI quantification is able to account for partial volume averaging thus provides more reliable MI measurement and better prediction of segmental myocardial contraction.

RC303-05 Quantifying Regional Myocardial Function-Strain, Torsion and Twist

Tuesday, Nov. 29 9:25AM - 9:50AM Room: S504AB

Participants

Bernd J. Wintersperger, MD, Toronto, ON, (bernd.wintersperger@uhn.ca) (*Presenter*) Speakers Bureau, Siemens AG; Research support, Siemens AG

LEARNING OBJECTIVES

1) Describe the principles of regional myocardial function assessment. 2) Compare different imaging approaches for quantification of regional myocardial function. 3) Identify possible applications of regional function analysis in clinical cardiac imaging.

ABSTRACT

Active Handout: Bernd J. Wintersperger

http://abstract.rsna.org/uploads/2016/16001381/RC303_05_RC_Strain,TorsionandTwist.pdf

LEARNING OBJECTIVES

1) Describe the principles of regional myocardial function assessment. 2) Compare different imaging approaches for quantification of regional myocardial function. 3) Identify possible applications of regional function analysis in clinical cardiac imaging.

ABSTRACT

A complex joint effort of the entire heart muscle is required in order to provide normal ventricular output. While the evaluation of global cardiac function and volumes aims at assessment of the gross ventricular status, measures of regional myocardial function aim at a more detailed analysis of the myocardial function. Parameters of regional myocardial function generally describe the relationship between force and resulting deformation of finite elements. Furthermore, such regional parameters are used to describe these relationships along various directions of the cardiac axis and coordinate system. Different modalities (Echo, MRI, CT) have been proposed for the assessment of such parameters. While in MRI regional parameters have predominately been used for research purposes, the development of speckle-tracking echocardiography (STE) and its evaluation has pushed towards clinical applications of regional myocardial functional parameters. The clinical use of such techniques may allow for earlier identification of subclinical pathology and as such may trigger therapy decisions at earlier time points.

RC303-06 Integrated Electroanatomic Mapping With Three-Dimensional Computed Tomographic Images for Real-Time Guide to Ablations: Comparison with Standard Procedure

Tuesday, Nov. 29 9:50AM - 10:00AM Room: S504AB

Participants

Anna Palmisano, MD, Milan, Italy (*Presenter*) Nothing to Disclose
Antonio Esposito, MD, Milan, Italy (*Abstract Co-Author*) Nothing to Disclose
Caterina Colantoni, MD, Milan, Italy (*Abstract Co-Author*) Nothing to Disclose
Sofia Antunes, Milan, Italy (*Abstract Co-Author*) Nothing to Disclose
Francesco A. De Cobelli, MD, Milan, Italy (*Abstract Co-Author*) Nothing to Disclose
Alessandro Del Maschio, MD, Milan, Italy (*Abstract Co-Author*) Nothing to Disclose

PURPOSE

Aim of the study was to validate a CT acquisition protocol and image post-processing for the creation of 3D model of the heart containing information about cardiac anatomy and myocardial scar substrate of ventricular tachycardia (VT), than to compare the performance of VT ablation guided by electroanatomic map (EAM) merged with CT-3D model versus ablation guided by EAM only, that is the clinical standard procedure.

METHOD AND MATERIALS

Eighty-seven patients with recurrent VT were enrolled. 32 patients underwent standard ablation; 55 patients underwent DE-CT before VT-ablation, including an angiographic-scan and a delayed-scan (80KV). A 3D-model of the heart, representing the cardiac cavities, aortic root, left ventricular wall and myocardial scar, was obtained by the fusion of angiographic and delayed scan, separately segmented. The 3D-model were uploaded on CARTO@system and co-registered with EAMs using CARTO-merge. Agreement between low voltages at EAM and scar at CT was evaluated, and time of procedure (TOP), complication and success rate between standard and CT-3D model guided ablation

RESULTS

CT identified segments characterized by low voltages with good sensitivity (76%), good specificity (86%), and very high negative predictive value (95%). Point-by-point quantitative comparison revealed good correlation between the average area of scar detected at CT and at bipolar mapping (CT: 4.901mm², bipolar voltages -EAM: 4.070mm²; R: 0.78; p<0.0001). 70% and 84% of low-amplitude bipolar points were mapped at a maximum distance of 5 mm and 10 mm from CT-segmented scar, respectively. TOP was 258±84 minutes for standard procedures and 204±60 minutes for CT-EAM guided ablations (p=0.012). A significant difference was found in the TOP for most complex procedure performed with both endo-epicardial approach (p=0.04). No significant differences were observed in term of procedural complication and success rate.

CONCLUSION

CT merged with EAM may be an effective tool for reduction of TOP and real-time guidance of VT ablation.

CLINICAL RELEVANCE/APPLICATION

Delayed enhancement CT resulted effective for identification of myocardial scars substrate of VT. Moreover, CT-3D model may be effective for real time guiding of EAM and radio frequency ablation

RC303-07 Predicting the Size of Left Atrial Appendage Occluder using a Printed MDCT 3D Model- A Proof of Concept

Tuesday, Nov. 29 10:00AM - 10:10AM Room: S504AB

Participants

Orly Goitein, MD, Ramat Gan, Israel (*Presenter*) Research Grant, Koninklijke Philips NV
Noam Fink, Ramat Gan, Israel (*Abstract Co-Author*) Nothing to Disclose
Victor Guetta, Tel Hashomer, Israel (*Abstract Co-Author*) Nothing to Disclose
Eli Konen, MD, Ramat Gan, Israel (*Abstract Co-Author*) Research Consultant, RadLogics Inc
Roy Beinart, MD, Baltimore, MD (*Abstract Co-Author*) Nothing to Disclose
David Goitein, Ramat Gan, Israel (*Abstract Co-Author*) Nothing to Disclose
Elio Di Segni, MD, Tel Hashomer, Israel (*Abstract Co-Author*) Nothing to Disclose
Michael Glikson, MD, Tel Hashomer, Israel (*Abstract Co-Author*) Nothing to Disclose

PURPOSE

Background: LAA occlusion is an effective alternative to oral anticoagulation in non valvular atrial fibrillation patients. The LAA varies significantly in size, morphology and spatial orientation making percutaneous occlusion challenging. MDCT provides three dimensional (3D) datasets allowing accurate imaging. Our objective was to evaluate the ability of printed 3D LAA models based on MDCT datasets in predicting LAA

occluder size.

METHOD AND MATERIALS

Patients planned for LAA occluder implantation were included. All patients underwent MDCT before implantation; this data was used for creating and printing 3D LAA models. Three cardiologists (informed which type of occluder was inserted) were asked to use the 3D models in vitro to predict the size of the device by fitting the device into the model. The chosen device size was compared with the actual device implanted during the procedure.

RESULTS

This retrospective study cohort included 29 patients (78±7 years, 64% males). Watchman™ and ACP™ devices were deployed in 17 and 12 patients, respectively. Two procedures were aborted (Watchman™) all three physicians predicted it. There was poor agreement between the 3D models and the inserted device for Watchman™ devices; Lin's concordance correlation coefficient 0.3 (95% CI -0.13, 0.76) as compared with a very good correlation between the 3D models and the inserted device for ACP™ devices; Lin's concordance correlation coefficient 0.8 (95% CI 0.5, 1.0). Average intra-class correlation for Watchman™ and ACP™ devices were 0.816 (95% CI 0.559, 0.933) and 0.915 (95% CI 0.559, 0.933), respectively.

CONCLUSION

LAA printed 3D models were accurate in predicting both device size for ACP™ device and procedure failures. However, no such correlation was demonstrated for predicting Watchman™ device size. Further studies are required in order to evaluate the potential role of printed 3D LAA models in assisting LAA occluder procedures.

CLINICAL RELEVANCE/APPLICATION

LAA occluder is challenging due to the diverse anatomy of the appendage. Printed models based on MDCT data might help device selection and procedure planning.

RC303-08 T1 and T2 Mapping Cardiovascular Magnetic Resonance to Differentiate Acute from Chronic Myocardial Infarction

Tuesday, Nov. 29 10:10AM - 10:20AM Room: S504AB

Awards

Student Travel Stipend Award

Participants

Enver G. Tahir, MD, Hamburg, Germany (*Presenter*) Nothing to Disclose
Martin Sinn, Hamburg, Germany (*Abstract Co-Author*) Nothing to Disclose
Maxim Avanesov, MD, Hamburg, Germany (*Abstract Co-Author*) Nothing to Disclose
Sebastian Bohnen, Hamburg, Germany (*Abstract Co-Author*) Nothing to Disclose
Kai Muellerleile, Hamburg, Germany (*Abstract Co-Author*) Nothing to Disclose
Christian Stehning, Hamburg, Germany (*Abstract Co-Author*) Employee, Koninklijke Philips NV
Ulf K. Radunski, Hamburg, Germany (*Abstract Co-Author*) Nothing to Disclose
Bernhard Schnackenburg, PhD, Hamburg, Germany (*Abstract Co-Author*) Nothing to Disclose
Gerhard B. Adam, MD, Hamburg, Germany (*Abstract Co-Author*) Nothing to Disclose
Gunnar K. Lund, MD, Hamburg, Germany (*Abstract Co-Author*) Nothing to Disclose

PURPOSE

Quantitative tissue characterization by novel T1 and T2 Mapping CMR techniques could provide incremental information to differentiate acute from chronic myocardial infarction (MI). We investigated the clinical utility of an approach using novel Mapping techniques in comparison to standard T2-weighted CMR to discriminate acute from chronic MI.

METHOD AND MATERIALS

Sixty-seven patients with first reperfused AMI were enrolled. T2w, T2, T1 mapping and late gadolinium enhancement (LGE) CMR were obtained at 2 time points after AMI at 8 ±5 days after infarction (baseline) and 6 ±1.4 months. CMR acquisitions were performed on end-diastolic LV short-axes. Myocardial T2 relaxation times were quantified using a free-breathing, navigator-gated multiecho sequence. Myocardial T1 relaxation times were measured using the modified Look-Locker inversion recovery sequence before and after administration of 0.075 mmol/kg gadobenate dimeglumine. T2, T1, and ECV maps were generated using a plug-in for OsiriX software (Pixmeo, Bernex, Switzerland). Two experienced observers independently placed regions of interest in the infarcted areas using LGE as a reference standard. A T2w-ratio was generated using the formula: T2w-ratio = Mean S1infarct / Mean S1remote.

RESULTS

Native T1 had an almost perfect discriminative performance to differentiate between acute (baseline CMR) and the chronic stage (6 months follow-up) with an AUC of 0.984. The AUC of native T1 was significantly superior to the T2w-ratio with an AUC of 0.906 (P<0.05) and to T2 with an AUC of 0.903 (P<0.05). ECV of infarcted myocardium had a poor discriminative performance with an AUC of 0.655, which was significantly inferior compared to native T1, T2w-ratio and T2, respectively (P<0.001). The optimal cutoff of ≥1138 ms for native T1 provided a sensitivity and specificity of 96% and 100%, respectively. The optimal cutoffs for the other CMR parameters were: ≥3.3 for T2w-ratio, ≥69ms for T2 and ≥39% for ECV.

CONCLUSION

Native T1 of infarcted myocardium is the best discriminator between acute and chronic myocardial infarction and should preferably be used as an objective and truly quantitative parameter to differentiate between the acute and chronic stage of myocardial infarction.

CLINICAL RELEVANCE/APPLICATION

Major clinical application would be identification of the culprit lesion in patients presenting with recent myocardial infarction and multi-vessel disease.

RC303-09 Multiparametric Myocardial MR Mapping (T1, T2 and T2*)

Tuesday, Nov. 29 10:30AM - 10:55AM Room: S504AB

Participants

Kate Hanneman, MD, FRCPC, Toronto, ON, (kate.hanneman@uhn.ca) (*Presenter*) Nothing to Disclose

LEARNING OBJECTIVES

1) Describe the basic methods of myocardial T1, T2 and T2* mapping and the advantages and limitations of each technique. 2) Explain the role of myocardial MR mapping as a diagnostic and prognostic tool to quantify disease and detect diffuse myocardial abnormalities. 3) Identify findings of common diseases on T1, T2 and T2* maps.

RC303-10 Doppler Ultrasound Triggering for Cardiac Magnetic Resonance Imaging at 7 Tesla: Initial Results

Tuesday, Nov. 29 10:55AM - 11:05AM Room: S504AB

Participants

Fabian Kording, Hamburg, Germany (*Presenter*) Nothing to Disclose
Christian Ruprecht, Hamburg, Germany (*Abstract Co-Author*) Nothing to Disclose
Bjoern Schoennagel, MD, Hamburg, Germany (*Abstract Co-Author*) Nothing to Disclose
Mathias Kladeck, Hamburg, Germany (*Abstract Co-Author*) Nothing to Disclose
Jin Yamamura, MD, Hamburg, Germany (*Abstract Co-Author*) Nothing to Disclose
Gerhard B. Adam, MD, Hamburg, Germany (*Abstract Co-Author*) Nothing to Disclose
Juliane Schelhorn, MD, Essen, Germany (*Abstract Co-Author*) Nothing to Disclose
Kai Nassenstein, Essen, Germany (*Abstract Co-Author*) Nothing to Disclose
Stefan Madenwald, PhD, MSc, Essen, Germany (*Abstract Co-Author*) Nothing to Disclose
Harald H. Quick, PhD, Essen, Germany (*Abstract Co-Author*) Nothing to Disclose
Oliver Kraff, MSc, Essen, Germany (*Abstract Co-Author*) Nothing to Disclose

PURPOSE

A prerequisite for cardiac magnetic resonance imaging (CMR) is adequate synchronization of image acquisition with the cardiac cycle. However, ECG is an inherently electrical measurement and distortions increase with higher magnetic field strengths. The purpose of this work was to evaluate the feasibility of Doppler Ultrasound (DUS) for CMR image synchronization at 7T.

METHOD AND MATERIALS

A custom build cardiocardiogram was used to derive DUS signals. In order to reduce common-mode currents effects, six cable traps tuned to 297 MHz were placed within the transmission line. A sufficient MR compatibility was evaluated using field probes and by flip angle maps. Cardiac MRI was performed at a 7T (Magnetom 7T, Siemens Healthcare GmbH, Germany) in 3 healthy subjects. The ultrasound transducer was placed in an apical location under the RF coil. The E-wave in early diastole was selected as a trigger time point. For validation of the trigger signal, ECG, pulse, and DUS signals were recorded simultaneously outside of the MR room and compared in terms of RR interval length and time delay. Breath hold 2D cine FLASH sequences were acquired in short axis and four chamber view. To assess the image quality, endocardial blurring (EB) was measured in the left ventricle as a mean over all cardiac phases.

RESULTS

The maximal measured change in the E- and H-field distribution with and without transducer was 5%. As a consequence, no interferences were observed between DUS and MRI in the B1 maps and during CMR imaging. The validation of the DUS trigger signal resulted in a high correlation to the ECG signal of $r = 0.99$. The DUS signal showed a mean time delay compared to the R-wave of 516 ± 20 ms and a similar variation of 51 ms. Analysis of endocardial blurring between ventricular blood and myocardium resulted in 3.4 ± 0.8 pixel.

CONCLUSION

Doppler Ultrasound was applied as a new trigger method in cardiac MRI at 7T. The DUS transmission line and transducer were approved for RF safety and successfully tested for CMR image synchronization at 7T. In future, this method needs to be evaluated in more detail in a larger patient population.

CLINICAL RELEVANCE/APPLICATION

With the merit of not being influenced by the electromagnetic field of the MRI, DUS may provide a reliable trigger method for cardiac imaging at high field strength.

RC303-11 Estimates of Fractional Flow Reserve from Coronary CT Angiography Using Contrast Opacification Gradients to Determine Coronary Branch Flow Distribution

Tuesday, Nov. 29 11:05AM - 11:15AM Room: S504AB

Participants

Satoru Kishi, MD, Tokyo, Japan (*Abstract Co-Author*) Nothing to Disclose
Andreas Giannopoulos, MD, Boston, MA (*Abstract Co-Author*) Nothing to Disclose
Nahoko Kato, Tokyo, Japan (*Abstract Co-Author*) Nothing to Disclose
Joao A. Lima, MD, Baltimore, MD (*Abstract Co-Author*) Research Grant, Toshiba Corporation
Frank J. Rybicki III, MD, PhD, Ottawa, ON (*Abstract Co-Author*) Nothing to Disclose

Dimitris Mitsouras, PhD, Boston, MA (*Presenter*) Research Grant, Toshiba Corporation;
Anji Tang, Boston, MA (*Abstract Co-Author*) Nothing to Disclose
Andrea L. Vavere, Baltimore, MD (*Abstract Co-Author*) Nothing to Disclose

PURPOSE

To validate a CT-FFR algorithm that can be reproduced by the readership with or without a proprietary basis, and to determine changes in CT-FFR accuracy for different methods to estimate the distribution of coronary blood flow in the coronary tree.

METHOD AND MATERIALS

The following four-step CT-FFR algorithm was retrospectively applied to 61 patients with 320-detector row CTA and invasive FFR: coronary lumen segmentation, myocardial segmentation with estimation of blood flow based on myocardial mass, estimation of the relative distribution of coronary blood flow to each coronary branch, and computational fluid dynamic simulation. Diagnostic performance of CT-FFR was tested for three different strategies to estimate the relative distribution of blood flow. The first two, Murray's Law and Huo-Kassab's rule, used coronary diameter, and the third used contrast opacification gradients to estimate resting-state flow. The algorithms were compared using the area under the receiver operating characteristic curve (AUC) to detect $FFR \leq 0.8$. Correlation coefficients and Bland-Altman limits of agreement with invasive FFR were also calculated.

RESULTS

Two patients were excluded from analysis due to motion artifact. FFR was measured on average 36.5 days after CTA. 25 lesions (41%) had $FFR \leq 0.8$. AUC to detect $FFR \leq 0.8$ was significantly higher using the contrast gradient (AUC=0.95), than using the Huo-Kassab (AUC=0.88, $p=0.033$) or Murray law models (AUC=0.87, $p=0.041$, Figure). Correlation coefficients were highest for the gradients (Spearman $\rho=0.81$), followed by the Huo-Kassab ($\rho=0.67$) and Murray law models ($\rho=0.65$). Bland-Altman limits of agreement were narrowest for the gradients (-0.181-0.150), followed by the Huo-Kassab (-0.246-0.152) and Murray law models (-0.286-0.260).

CONCLUSION

A simple, transparent four-step CT-FFR algorithm accurately detects a significant $FFR \leq 0.8$, the invasive gold-standard to determine the need for percutaneous coronary intervention. Estimating the relative blood flow distribution in a coronary tree using coronary contrast gradients can improve CT-FFR accuracy.

CLINICAL RELEVANCE/APPLICATION

Cardiovascular imagers can perform CT-FFR using a simple four-step approach with or without a proprietary basis to accurately detect a significant FFR0.8.

Honored Educators

Presenters or authors on this event have been recognized as RSNA Honored Educators for participating in multiple qualifying educational activities. Honored Educators are invested in furthering the profession of radiology by delivering high-quality educational content in their field of study. Learn how you can become an honored educator by visiting the website at: <https://www.rsna.org/Honored-Educator-Award/>

Frank J. Rybicki III, MD, PhD - 2016 Honored Educator

RC303-12 The Extracellular Volume Fraction using Contrast-enhanced T1 Mapping Cardiac Magnetic Resonance Imaging is Constant with Hematocrit Change: Evaluation with an Anemic Rat Model

Tuesday, Nov. 29 11:15AM - 11:25AM Room: S504AB

Participants

Yoo Jin Hong, MD, Seoul, Korea, Republic Of (*Presenter*) Nothing to Disclose
Pan Ki Kim, Seoul, Korea, Republic Of (*Abstract Co-Author*) Nothing to Disclose
Joshua Jinhun Kim, Seoul, Korea, Republic Of (*Abstract Co-Author*) Nothing to Disclose
Donghyun Hong, MS, Essen, Germany (*Abstract Co-Author*) Nothing to Disclose
Chul Hwan Park, MD, Seoul, Korea, Republic Of (*Abstract Co-Author*) Nothing to Disclose
Jin Young Kim, MD, Seoul, Korea, Republic Of (*Abstract Co-Author*) Nothing to Disclose
Byoung Wook Choi, MD, Seoul, Korea, Republic Of (*Abstract Co-Author*) Nothing to Disclose

PURPOSE

The aim of this study was to evaluate the stability of extracellular volume fraction (ECV) based on cardiac magnetic resonance imaging (CMR) according to hematocrit (Hct) change using a rat model of anemia.

METHOD AND MATERIALS

Sixteen adult male Sprague-Dawley rats (weight, 300-500 g) underwent pre-model CMR without intervention. Six days after the MR scan, anemia was modeled and post-model CMR scanning was performed. For modeling anemia, an experienced veterinarian withdrew 15% of the total circulating blood by volume from the tail vein and replaced it by Hartmann's solution. A Hct drop of more than 15% was regarded as successful modeling of anemia. All CMR, including cine, pre T1, and post T1 mapping, were performed using a 9.4T MR scanner (Bruker Biospin Co., Billerica, MA). Pre- and post-T1 values were measured from 6 segments of the mid-LV and the LV cavity. The partition coefficient and ECV were calculated. After post-model MR scanning, all rats were sacrificed and histology was performed on their hearts.

RESULTS

After anemia modeling, the Hct level was $46.4\% \pm 4.09\%$ (range: 39-54%), which was significantly lower than pre-modeling levels ($59.0\% \pm 3.37\%$, range: 56-65%, $p < 0.001$). The mean Hct drop was 22%. The LVFV of the pre-modeling group was not significantly different from the post-modeling group ($72.5\% \pm 2.6\%$ vs. $72.7\% \pm 4.5\%$, respectively; $p = 0.83$). Post-contrast T1 values in the LV cavity in the anemia group were significantly lower than the pre-model group (629.6 ± 175.3 vs. 721.7 ± 104.1 , respectively; $p = 0.02$). The partition coefficient of the anemia group was significantly lower than the pre-model group (30.2 ± 3.5 vs. 37.4 ± 5.4 , respectively; $p < 0.001$). The ECV of the anemia group was not significantly different from the pre-model group (15.9 ± 2.1 vs. 15.6 ± 2.1 , respectively; $p = 0.70$).

CONCLUSION

CMR ECV is stable according to Hct change in a rat model of anemia; this supports the constant linear equilibrium between myocardial extracellular interstitial space and intravascular plasma.

CLINICAL RELEVANCE/APPLICATION

Anemia is a very common clinical condition in patients with heart failure. It is clinically important to evaluate the stability of ECV in anemic patients. Contrast enhanced T1 mapping MRI is simple, non-invasive, and safe. ECV based on contrast enhanced T1 mapping could be a robust tool for monitoring myocardial characteristics in patients with anemia.

RC303-13 Assessment of Left Ventricular Regional Wall Motion on the Basis of MR Sequences Featuring Sparse Data Sampling and Iterative Reconstruction (SSIR) with and without Breath-hold Commands - Segment-based Analysis

Tuesday, Nov. 29 11:25AM - 11:35AM Room: S504AB

Awards

Student Travel Stipend Award

Participants

Sonja Sudarski, MD, Mannheim, Germany (*Presenter*) Nothing to Disclose
Thomas Henzler, MD, Mannheim, Germany (*Abstract Co-Author*) Research support, Siemens AG; Speaker, Siemens AG
Holger Haubenreisser, Mannheim, Germany (*Abstract Co-Author*) Speaker, Siemens AG Speaker, Bayer AG
Johannes Budjan, MD, Mannheim, Germany (*Abstract Co-Author*) Nothing to Disclose
Stefan O. Schoenberg, MD, PhD, Mannheim, Germany (*Abstract Co-Author*) Institutional research agreement, Siemens AG
Theano Papavassiliu, Mannheim, Germany (*Abstract Co-Author*) Nothing to Disclose

PURPOSE

To evaluate the accuracy of regional wall motion (RWM) assessment using a 2D-real-time-CINE-TrueFISP MR-sequence featuring sparse data sampling and iterative reconstruction (SSIR) acquired with and without breath-hold commands at 3 Tesla in patients scheduled for LV analysis.

METHOD AND MATERIALS

60 patients prospectively underwent a segmented multi-breath-hold cine sequence as reference standard (RS) and a prototype undersampled SSIR-sequence acquired once during a single breath-hold (SSIR-sBH) and once during free shallow breathing (SSIR-non-BH). RWM was visually assessed in 16 segments (basal segments 1-6; mid-cavity segments 7-12; apical segments 13-16) as normal wall motion, hypokinetic, akinetic or dyskinetic segments.

On SSIR datasets for each segment compared to the RS the percentage of correctly evaluated, false worse and false better evaluated segments was assessed. To compare concordance of RWM evaluation, weighted Cohen's kappa testing for each of the 16 myocardial wall segments evaluated was performed.

RESULTS

In the final analysis of 52 patients, of the 832 analyzed segments, 603 segments were rated as normal, 186 segments were rated as hypokinetic and 43 segments akinetic in RS readout. None of the analyzed segments was dyskinetic. Agreement of RWM-assessment with the RS was similar for SSIR-sBH and SSIR-non-BH (86% agreement vs. 85%). Segment-based analysis showed equally high rates of RWM rated as false better, false worse and equal to the RS (around 5%, 10% and 85%) and a tendency in SSIR datasets to underestimate wall motion of septal segments, yet not reaching statistical significance.

CONCLUSION

Segment-based analysis of regional wall motion assessment with SSIR-data at 3 Tesla leads to similar results as RWM assessment on the basis of the RS sequences. Yet, a tendency to underestimate RWM in septal segments was observed with SSIR-data irrespective of breath-hold commands.

CLINICAL RELEVANCE/APPLICATION

Left ventricular regional wall motion assessment with SSIR-data at 3 Tesla leads to similar results compared to the reference standard sequences.

RC303-14 Valvular Flow Quantification with Phase Contrast Imaging (2D, 4D)

Tuesday, Nov. 29 11:35AM - 12:00PM Room: S504AB

Participants

Christopher J. Francois, MD, Madison, WI, (cfrancois@uwhealth.org) (*Presenter*) Research support, General Electric Company

Active Handout: Christopher Jean-Pierre Francois

http://abstract.rsna.org/uploads/2016/16001383/RC30314_RSNA2016_ValveFlowQuantification_handouts.pdf

LEARNING OBJECTIVES

1) Describe the physics of imaging blood flow with MRI from 2D to 4D phase contrast MRI. 2) Classify the categories of valve disease that can be characterized using MRI. 3) Illustrate how phase contrast MRI is used to assess normal and abnormal valve function.

ABSTRACT

MRI flow imaging is based on flow-sensitive, phase contrast sequences. This presentation will introduce the basic MRI physics responsible for imaging flow, extending 1-directional flow imaging to 3-directional flow imaging used in 4D flow MRI. Normal cardiac valve anatomy and function will be reviewed and serve as a basis to classify valvular heart disease - including congenital abnormalities, valvular stenosis and valvular regurgitation. The presentation will initially focus on the use of standard 2D phase contrast MRI for quantifying the severity of disease. The future potential for 4D phase contrast MRI to be used to quantify velocities and flow in patients with valvular disease will be described. In addition, more advanced hemodynamic parameters that can be quantified with 4D phase contrast MRI will be identified.

RC304

Musculoskeletal Series: Ultrasound

Tuesday, Nov. 29 8:30AM - 12:00PM Room: E450A



AMA PRA Category 1 Credits™: 3.25
ARRT Category A+ Credits: 4.00

Participants

Marnix T. van Holsbeeck, MD, Detroit, MI, (marnix@rad.hfh.edu) (*Moderator*) Consultant, General Electric Company; Stockholder, Koninklijke Philips NV; Stockholder, General Electric Company; Stockholder MedEd3D; Grant, Siemens AG; Grant, General Electric Company;

Connie Y. Chang, MD, Boston, MA, (cychang@mgh.harvard.edu) (*Moderator*) Nothing to Disclose

Jon A. Jacobson, MD, Ann Arbor, MI, (jjacobsn@umich.edu) (*Moderator*) Consultant, BioClinica, Inc; Royalties, Reed Elsevier; ; ;
Ogonna K. Nwawka, MD, New York, NY (*Moderator*) Research Grant, General Electric Company

LEARNING OBJECTIVES

1) The "Ultrasound" Series Course will review musculoskeletal sonography through live instruction by expert refresher course instructors, interspersed with scientific presentations.

Sub-Events

RC304-01 Shoulder Ultrasound (Demonstration)

Tuesday, Nov. 29 8:30AM - 9:00AM Room: E450A

Participants

Jon A. Jacobson, MD, Ann Arbor, MI, (jjacobsn@umich.edu) (*Presenter*) Consultant, BioClinica, Inc; Royalties, Reed Elsevier; ; ;

LEARNING OBJECTIVES

1. List the fundamental steps in performing an ultrasound examination of the shoulder
2. Understand common pitfalls in shoulder ultrasound
3. Utilize dynamic imaging in the evaluation of shoulder pathology

ABSTRACT

LEARNING OBJECTIVES

View learning objectives under main course title.

Honored Educators

Presenters or authors on this event have been recognized as RSNA Honored Educators for participating in multiple qualifying educational activities. Honored Educators are invested in furthering the profession of radiology by delivering high-quality educational content in their field of study. Learn how you can become an honored educator by visiting the website at: <https://www.rsna.org/Honored-Educator-Award/>

Jon A. Jacobson, MD - 2012 Honored Educator

RC304-02 Impact of Musculoskeletal Shoulder Ultrasound on Clinical Decision Making

Tuesday, Nov. 29 9:00AM - 9:10AM Room: E450A

Participants

Michael V. Friedman, MD, Saint Louis, MO (*Presenter*) Nothing to Disclose

Travis J. Hillen, MD, Saint Louis, MO (*Abstract Co-Author*) Consultant, Biomedical Systems; Instructor, DFine, Inc

David V. Holland, MD, Saint Louis, MO (*Abstract Co-Author*) Nothing to Disclose

James M. Essenberg, MD, Saint Louis, MO (*Abstract Co-Author*) Nothing to Disclose

Jennifer L. Demertzis, MD, Saint Louis, MO (*Abstract Co-Author*) Nothing to Disclose

PURPOSE

To evaluate the impact of musculoskeletal (MSK) shoulder ultrasound (US) on clinical decision making.

METHOD AND MATERIALS

IRB approval was obtained. 912 patients with 1037 consecutive MSK shoulder US, ordered and performed at our institution over a 12 month period, were retrospectively reviewed. 125 patients had bilateral exams which were managed and scored independently. 102 patient exams were excluded from the study. (89 exams had no follow up or initial clinic note; 11 exams were duplicate; and two exams were performed for contralateral comparison.) 935 total patient exams had both pre- and post-US clinical evaluations, meeting inclusion criteria. The medical records and clinic notes of each patient were analyzed, recording immediate pre- and post-US diagnoses and treatment plans. Management plans were categorized as: 1-No plan/No further treatment; 2-Conservative/physical therapy; 3-Therapeutic injection; 4-Surgical Intervention; 5-Change in diagnosis; 6-Need additional imaging. Data was analyzed for changes in clinical management based upon US results using nonparametric statistical methods.

RESULTS

Of 935 patient exams, 679 (72.6%) had a post-US treatment plan that differed from pre-US management, demonstrating a statistically significant impact of shoulder US on patient management ($p < 0.001$). The diagnosis was changed to non-shoulder pathology in 23 patients (2.5%), and 12 patients (1.3%) were referred for additional imaging. In 450 patient exams (48%), the treating physician refrained from making a treatment plan until the shoulder US was obtained. Of the 485 patient exams with a defined pre-US management plan, the invasiveness of the plan was increased in 108 (22.3%) subjects based on the shoulder US

results. Clinical management was altered in nine patients (1.9%) from surgical to nonsurgical treatment, and in 78 patients (16.1%) from nonsurgical to surgical management. US also played a role in surgical planning, with 25 studies (2.7%) specifically performed to evaluate rotator cuff integrity and muscle atrophy when deciding between conventional and reverse shoulder arthroplasty.

CONCLUSION

MSK shoulder US is a useful diagnostic imaging modality with significant impact on clinical decision making.

CLINICAL RELEVANCE/APPLICATION

Musculoskeletal shoulder US is a validated diagnostic imaging modality for the evaluation of rotator cuff pathology, and has a significant impact on clinical decision making and patient management.

RC304-03 T2/T2* Maps and Ultrasound Shear Wave Elastography: A Potential Relationship that Could Improve the Quantitative Assessment of the Supraspinatus Tendon on MRI

Tuesday, Nov. 29 9:10AM - 9:20AM Room: E450A

Participants

Konstantin Kreplin, MD, New York, NY (*Abstract Co-Author*) Nothing to Disclose
Alexander N. Merkle, MD, New York, NY (*Presenter*) Nothing to Disclose
Mary Bruno, RT, New York, NY (*Abstract Co-Author*) Nothing to Disclose
Jose Maria Raya Garcia Del Olmo, PhD, New York, NY (*Abstract Co-Author*) Nothing to Disclose
Ronald S. Adler, MD, PhD, New York, NY (*Abstract Co-Author*) Nothing to Disclose
Soterios Gyftopoulos, MD, New York, NY (*Abstract Co-Author*) Nothing to Disclose

PURPOSE

To determine whether there is an association between T2/T2* mapping and supraspinatus tendon mechanical properties as assessed by shear-wave ultrasound elastography (SWE).

METHOD AND MATERIALS

This HIPAA compliant prospective study received approval from our hospital's institutional review board. Eight patients (3 males/5 females; age range 44-72 years) and 9 shoulders underwent conventional shoulder MRI and T2/T2* mapping on a 3T scanner, and ultrasound evaluation with SWE. All ultrasound examinations were performed by a single musculoskeletal radiologist with more than 20 years of musculoskeletal ultrasound experience. Shear wave velocities (SWV) were obtained in multiple 1.5 mm square regions of interest (ROIs) drawn within the insertional 1-2 cm of the supraspinatus tendon at the mid-portion of the superior greater tuberosity facet. The ROIs were organized, and averaged when necessary, into one of 3 locations within the insertional portion of the tendon: lateral, medial and middle. Two musculoskeletal radiologists reviewed the MRI exams in consensus for evidence of supraspinatus tendon pathology, with tear size and retraction measured for full-thickness tears. T2 and T2* values were calculated from coronal T2/T2* maps using equidistant ROIs corresponding to the same medial, middle, and lateral locations as on ultrasound. Pearson correlation coefficients between T2/T2* values and SWV, as well as between T2, T2*, SWV and tear size and retraction were calculated.

RESULTS

There was a significant negative correlation between T2* and SWV in the lateral location ROI ($r = -0.86$, $p = 0.013$) and overall mean ROI ($r = -0.90$, $p = 0.006$). There was significant positive correlation between T2 and measures of tear size in the lateral and mean ROIs (r range 0.71 – 0.77, p range 0.016 – 0.034). There was significant negative correlation between SWV and tear size in the middle and mean ROIs (r range -0.79 – -0.68, p range 0.011 – 0.046).

CONCLUSION

This pilot study shows the feasibility of doing T2/T2* mapping in the supraspinatus tendon and reveals a potential relationship between the tendon's T2* values and its mechanical properties.

CLINICAL RELEVANCE/APPLICATION

T2/T2* mapping has the potential to improve our description of rotator cuff disease on MRI by providing a more objective measure of tendon quality; information that can be useful to the patient and surgeon considering rotator cuff repair surgery.

RC304-04 Early Detection of Brachial Plexus Neuritis by Means of High-Resolution Ultrasonography of the Suprascapular Nerve

Tuesday, Nov. 29 9:20AM - 9:30AM Room: E450A

Participants

Alexander Loizides, MD, Innsbruck, Austria (*Presenter*) Nothing to Disclose
Leonhard Gruber, Innsbruck, Austria (*Abstract Co-Author*) Nothing to Disclose
Wolfgang Loescher, Innsbruck, Austria (*Abstract Co-Author*) Nothing to Disclose
Hannes Gruber, MD, PhD, Innsbruck, Austria (*Abstract Co-Author*) Nothing to Disclose

PURPOSE

Brachial plexus neuritis (BPN) is a rare condition with initial shoulder pain up to two weeks after symptom onset and consecutive shoulder girdle paresis. We assessed the diagnostic value of ultrasound examinations of the suprascapular nerve (SSN) in the early diagnosis of BPN.

METHOD AND MATERIALS

The cross-section areas (CSA) of the SSN at the root and at the omohyoid muscle were assessed in seven patients with clinically definitive BPN and 30 healthy volunteers. To compare group means, an ordinary one-sided ANOVA with Holm-Sidak's multiple testing correction was performed. To determine ideal cut-offs, receiver-operator-characteristics (ROC) curves were generated and according contingency tables were constructed to calculate sensitivity, specificity, positive (PPV) and negative predictive values (NPV), likelihood ratios (LR) and odds ratios (OR). To account for confounding factors, a bootstrapped binary regression analysis

(10.000 iterations, 95% bias-corrected and accelerated confidence intervals [CI]) was carried out.

RESULTS

Patients with BNP had significantly higher CSAs of the SSN at the omohyoid muscle (5.99 ± 2.08 vs. 2.79 ± 0.82 mm², $p < 0.0001$) and significantly higher ratios of SSN CSAs of the affected to contralateral side at the omohyoid muscle ($223.0 \pm 94.4\%$ vs. $127.7 \pm 51.1\%$, $p = 0.0016$) as well as ratios of SSN CSA at the omohyoid muscle to the root ($180.7 \pm 91.3\%$ vs. $99.9 \pm 28.3\%$, $p = 0.0006$). SSN root CSAs did not differ significantly (3.63 ± 1.23 vs. 2.90 ± 0.90 mm², $p = 0.14$). With a SSN CSA at the omohyoid muscle greater than 4.2 mm², the ROC area under the curve was 0.933. Sensitivity was 85.7% (42.1–99.6%), specificity 96.7% (82.8–99.9%), PPV 85.7% (42.1–99.6%), NPV 96.7% (82.8–99.9%), OR 174.0 (9.5–3190.0) and LR 25.7 (95% CI in parentheses). Multivariate analysis identified SSN swelling at the omohyoid muscle as a strong predictor ($B = -344.3 \pm 55.1$; $p = 0.001$). Age ($B = -14.1 \pm 2.3$; $p = 0.001$) and BMI ($B = 17.8 \pm 5.3$; $p = 0.005$) had a minor influence, gender none ($B = -20.0 \pm 26.2$; $p = 0.22$).

CONCLUSION

Increased SSN CSA at the omohyoid muscle can reliably identify BNP in case of clinical suspicion of neuralgic shoulder amyotrophy.

CLINICAL RELEVANCE/APPLICATION

An increase in CSA beyond 4.2 mm² of the suprascapular nerve at the level of the omohyoid muscle is highly indicative of brachial plexus neuritis. Further studies should focus on treatment strategies.

RC304-05 Stress Ultrasound to Diagnose UCL Tears at the Elbow: Which Joint Gapping Threshold to Use?

Tuesday, Nov. 29 9:30AM - 9:40AM Room: E450A

Participants

Johannes B. Roedl, MD, PhD, Philadelphia, PA (*Presenter*) Nothing to Disclose

Adam C. Zoga, MD, Philadelphia, PA (*Abstract Co-Author*) Nothing to Disclose

William B. Morrison, MD, Philadelphia, PA (*Abstract Co-Author*) Consultant, General Electric Company Consultant, AprioMed AB Patent agreement, AprioMed AB Consultant, Zimmer Holdings, Inc

Mika T. Nevalainen, MD, PhD, Philadelphia, PA (*Abstract Co-Author*) Nothing to Disclose

Levon N. Nazarian, MD, Philadelphia, PA (*Abstract Co-Author*) Nothing to Disclose

PURPOSE

To assess different joint gapping thresholds for stress ultrasound in the diagnosis of ulnar collateral ligament (UCL) tears in baseball players.

METHOD AND MATERIALS

Throwing athletes with surgically or arthroscopically proven UCL tears underwent stressUS. The interval gapping of the medial elbow joint was measured between rest and valgus stress both at the injured (ipsilateral) and at the uninjured (contralateral) elbow. The relative gapping between both elbows (ipsilateral gapping minus contralateral gapping) was calculated. Throwing athletes without UCL tears were available as a control group. Receiver operator curve (ROC) analysis determined retrospectively the most accurate thresholds to predict UCL tears. Institutional review board approval was obtained and the requirement for informed consent was waived. The study is compliant with HIPAA.

RESULTS

In this retrospective analysis, 71 athletes with UCL tears were compared to 122 athletes without UCL tears. The ROC analysis determined the following thresholds in order of decreasing specificity: A relative joint gapping threshold of 2.6 mm had a specificity of 100% and a sensitivity of 53% in predicting UCL tears. A threshold of 1.5 mm resulted in a specificity of 91% and a sensitivity of 81%. A threshold of 1.0 mm yielded a specificity of 81% and a sensitivity of 96%.

CONCLUSION

The above listed thresholds can be used and it depends on the clinical practice whether higher specificity or sensitivity is desired.

CLINICAL RELEVANCE/APPLICATION

Elbow stress ultrasound is an emerging technique and the thresholds provided will help the Radiologist in the diagnosis of UCL tears.

RC304-06 Elbow Ultrasound (Demonstration)

Tuesday, Nov. 29 9:40AM - 10:10AM Room: E450A

Participants

Marnix T. van Holsbeeck, MD, Detroit, MI (*Presenter*) Consultant, General Electric Company; Stockholder, Koninklijke Philips NV;

Stockholder, General Electric Company; Stockholder MedEd3D; Grant, Siemens AG; Grant, General Electric Company;

Kathy Quenneville, BS, RT, Commerce Township, MI (*Presenter*) Nothing to Disclose

LEARNING OBJECTIVES

View learning objectives under main course title.

RC304-07 Knee Ultrasound (Demonstration)

Tuesday, Nov. 29 10:20AM - 10:50AM Room: E450A

Participants

Ronald S. Adler, MD, PhD, New York, NY (*Presenter*) Nothing to Disclose

LEARNING OBJECTIVES

View learning objectives under main course title.

RC304-08 Medial Meniscal Extrusion on Weight? Bearing Ultrasound of the Knee

Tuesday, Nov. 29 10:50AM - 11:00AM Room: E450A

Participants

Sandra Rutigliano, MD, Philadelphia, PA (*Abstract Co-Author*) Nothing to Disclose
William B. Morrison, MD, Philadelphia, PA (*Presenter*) Consultant, General Electric Company Consultant, AprioMed AB Patent agreement, AprioMed AB Consultant, Zimmer Holdings, Inc
Suzanne S. Long, MD, Philadelphia, PA (*Abstract Co-Author*) Nothing to Disclose
Adam C. Zoga, MD, Philadelphia, PA (*Abstract Co-Author*) Nothing to Disclose
Johannes B. Roedel, MD, PhD, Philadelphia, PA (*Abstract Co-Author*) Nothing to Disclose

PURPOSE

To evaluate the potential role of screening ultrasound in identifying unstable meniscal tears. Specifically, the presence of medial meniscal extrusion on dynamic ultrasound, with and without weightbearing, will be utilized to identify unstable meniscal tears.

METHOD AND MATERIALS

12 patients with unilateral knee pain underwent dynamic ultrasound of the medial meniscus of both knees. Ultrasound images were obtained of the medial meniscus in the coronal plane with the knee extended, with and without weight bearing. Abbreviated MR examination of both the symptomatic and asymptomatic knees was performed on a 1.5 T MR unit. Coronal T2 fat-suppressed and sagittal proton density weighted images were obtained. The degree of meniscal extrusion on weight bearing and non weight bearing ultrasound, as well as a change in meniscal extrusion, were correlated with demographic and clinical factors such as age, sex, weight, and duration of symptoms, as well as findings on MRI.

RESULTS

Medial meniscal extrusion was readily observed on ultrasound. All but one meniscus demonstrated increased extrusion with weight bearing. Of the 24 menisci, there were 5 tears (1 radial /2 oblique /2 complex). Extrusion averaged 2.4mm at rest and 3.5mm with weight bearing (avg difference 1.1mm) in menisci without tear on MRI; extrusion was 2.3mm at rest and 4.3mm with weight bearing (avg difference 2.0mm) in menisci with tear on MRI. In the symptomatic knee, difference in extrusion averaged 1.6mm vs 0.8mm in the asymptomatic knee. Only one individual had medial compartment chondrosis. Regarding pain chronicity, difference in extrusion averaged 1.3mm with pain <1 year versus 1.8mm with pain >1 year. Knees in individuals with weight <200lb showed average difference in extrusion of 1.1mm and 1.1mm in individuals >200lb. Difference in extrusion for age > 50 years averaged 0.9mm versus 1.2mm for age <50.

CONCLUSION

Dynamic ultrasound with and without weight bearing may be useful to distinguish unstable from stable (or chronic) tears.

CLINICAL RELEVANCE/APPLICATION

Weight-bearing ultrasound of the medial meniscus may serve as a quick, economical means to triage patients with medial knee pain and suspected unstable medial meniscal tears.

RC304-09 Role of Real-Time (RTE) and Shear-Wave (SWE) Sonoelastography in the Follow-up of Muscle Thigh Injury in Athletes: A Three-Years Longitudinal Study

Tuesday, Nov. 29 11:00AM - 11:10AM Room: E450A

Participants

Davide Orlandi, MD, PhD, Genova, Italy (*Presenter*) Nothing to Disclose
Angelo Corazza, MD, Genova, Italy (*Abstract Co-Author*) Nothing to Disclose
Luca Maria Sconfienza, MD, PhD, Milano, Italy (*Abstract Co-Author*) Travel support, Bracco Group
Enzo Silvestri, MD, Genoa, Italy (*Abstract Co-Author*) Nothing to Disclose

PURPOSE

The aim of the current study is to assess the reliability and effectiveness of the RTE and SWE in the evaluation and follow-up of traumatic lower limb muscle tears in a cohort of professional athletes using MRI as a reference standard.

METHOD AND MATERIALS

143 male athletes (aged 23 ± 5) with MRI confirmed indirect thigh muscle injury was included in our study and evaluated with ultrasound (US) over a period of 36 months and for a total of 112 muscles. Muscle tears were evaluated with B-mode US, RTE and SWE using two different US apparatuses (LOGIQ E9, GE Healthcare; RS80 Prestige, Samsung Medical) at baseline, 2, 4 and 6 weeks in order to evaluate the healing process of the injury also comparing the obtained results with the healthy contralateral side. Statistical analysis of the obtained data was performed, also assessing intra- and inter-observer reproducibility with the Bland-Altman test.

RESULTS

The results derived from the current study highlight a direct relationship between the clinical recovery of the injured muscle and its appearance and the elastic features of the regenerative scar tissue. In particular SWE quantitative elasticity assessment was able to provide meaningful data about the quality of the regenerated tissue, furnishing thresholds (11.3 ± 7.6 kPa: newly formed healing tissue; 28.3 ± 4.6 kPa: complete recovery) and contralateral normal muscle (15.4 ± 5.8 kPa) with high measurement reliability index (RMI): 0.7 ± 0.2 .

CONCLUSION

The dynamic features of US, combined with RTE and SWE techniques are able to provide qualitative and quantitative elasticity assessment of the healing process of an injured muscle. This can be crucial in the management and early recovery of athletes.

CLINICAL RELEVANCE/APPLICATION

SWE is able to perform a quantitative assessment of muscle healing process and could be extremely useful in athletes follow-up.

RC304-10 Carpal Tunnel Ultrasonography in Diabetics: Missing the Mark?

Tuesday, Nov. 29 11:10AM - 11:20AM Room: E450A

Participants

Alexander Loizides, MD, Innsbruck, Austria (*Presenter*) Nothing to Disclose
Leonhard Gruber, Innsbruck, Austria (*Abstract Co-Author*) Nothing to Disclose
Gabriele Morsdorf, Innsbruck, Austria (*Abstract Co-Author*) Nothing to Disclose
Ingrid Gruber, Innsbruck, Austria (*Abstract Co-Author*) Nothing to Disclose
Hannes Gruber, MD, PhD, Innsbruck, Austria (*Abstract Co-Author*) Nothing to Disclose

PURPOSE

To assess whether commonly used ultrasound (US) measurements for carpal tunnel syndrome (CTS) are reliable in diabetics.

METHOD AND MATERIALS

We retrospectively assessed the cross-section area (CSA) of the median nerve at the level of the carpal tunnel (CT) and the pronator quadratus muscle in 236 wrists of 157 symptomatic patients with clinical suspicion of CTS and calculated the wrist-to-forearm-ratio (WFR). Furthermore 14 wrists in seven asymptomatic diabetics were examined. HbA1c values at the time of US-examination were collected. Values for CSAs and WFR of patients grouped by presence or absence of diabetes and by HbA1c values were compared via an ordinary one-way ANOVA with Holm-Sidak correction for multiple testing after logarithmic transformation to achieve normal distribution. Correlations between HbA1c and WFR as well as CSAs were furthermore quantified through a linear regression analysis. Finally receiver-operator characteristics (ROC) curves were generated to assess the diagnostic utility of WFR measurements.

RESULTS

The average WFR was 1.90 ± 0.55 in asymptomatic diabetics, 2.10 ± 0.77 in symptomatic diabetics and 2.37 ± 0.75 in symptomatic non-diabetics. Diabetic patients had a significantly lower WFR than otherwise healthy patients with CTS ($p=0.037$). There were no other significant differences between CSA values between groups, but a trend towards higher CSA values at the CT ($p = 0.278$). No difference was found for CSA values at the CT ($p=0.52$). There was no correlation between HbA1c values and WFR ($R^2 = 0.0072$), CSA at the CT ($R^2 = 0.0004$) or CSA at the pronator quadratus ($R^2 = 0.0009$). ROC curve analysis demonstrated a lack of discriminatory power of US between diabetics with and without CTS (area under the curve 0.551).

CONCLUSION

Ultrasound should not be used in the evaluation of CTS in diabetic patients, as its discriminatory power is very low in this patient group, probably due to prevalent neuropathic changes.

CLINICAL RELEVANCE/APPLICATION

Ultrasound is not suited for confirmation of primary CTS in diabetics, but still can be used to rule out other secondary causes of neural compression.

RC304-11 Median Nerve Evaluation by Shear Wave Elastosonography: Impact of "Bone-proximity" Hardening Artifacts and Inter-observer Agreement

Tuesday, Nov. 29 11:20AM - 11:30AM Room: E450A

Participants

Elena Turpini, MD, Pavia, Italy (*Presenter*) Nothing to Disclose
Paolo F. Felisaz, MD, Pavia, Italy (*Abstract Co-Author*) Nothing to Disclose
Chandra Bortolotto, MD, Pavia, Italy (*Abstract Co-Author*) Nothing to Disclose
Fabrizio Calliada, MD, Pavia, Italy (*Abstract Co-Author*) Research Grant, Toshiba Corporation; Speakers Bureau Member, Hitachi, Ltd; Speakers Bureau Member, Shenzhen Mindray Bio-Medical Electronics Co, Ltd

PURPOSE

Elastosonography widely expanded his area of applicability in the last years, including peripheral nerves evaluation. Frequently peripheral nerves travels close to bone surfaces and are therefore prone to elastosonographic "bone-proximity" hardening artifacts. The impact of these artifacts on median nerve stiffness quantitative measurements performed by shear wave elastosonography has not yet been explored. Our aim is to assess normal median nerves stiffness values at various locations and, as a secondary endpoint, to evaluate inter-observer agreement.

METHOD AND MATERIALS

36 healthy volunteers (24 women and 12 men) aged between 25 and 40 years were evaluated. Two operators performed the evaluation: expert (6 years of ultrasound experience) and inexperienced (6 months' experience). The nerve was sampled in cross section in three different location: at mid-forearm, immediately before the carpal tunnel and within the tunnel. We used a Toshiba Aplio 500 scanner (Toshiba MS, Otawara-shi, Japan) equipped with 14 MHz linear probe. Measurement were performed using a ROI corresponding to the diameter of the nerve.

RESULTS

Median nerve mean stiffness values were: 4.92 kPa at the forearm (95% confidence interval = 4.31-5.53); 21.33 kPa before the tunnel (95% CI = 19.11-23.55); 31.28 kPa within the tunnel (95% CI = 22.30-40.25). Inter-observer agreement (Bland Altman analysis) was excellent at the forearm (mean difference 1.3 CI 8.2 to -10.8) and good at the other two levels (6.2 CI 40.3 to -52.7; 4.1 CI 38.2 to -46.2).

CONCLUSION

The stiffness of the median nerve progressively increases in its distal portions, where the nerve approaches the bone surfaces. Therefore, when evaluating nerve pathologies, stiffness must be compared to the same portion of the contralateral nerve rather than its proximal or distal portions in order to avoid possible "bone-proximity" hardening artifacts. Measurements inter-observer agreement is generally good.

CLINICAL RELEVANCE/APPLICATION

Median nerve stiffness increases from forearm to its distal portion. Therefore, when evaluating nerve pathologies, stiffness must be compared to the same portion of the contralateral nerve rather than its proximal or distal portions.

RC304-12 Hand and Wrist Ultrasound (Demonstration)

Tuesday, Nov. 29 11:30AM - 12:00PM Room: E450A

Participants

Viviane Khoury, MD, Philadelphia, PA, (Viviane.khoury@uphs.upenn.edu) (*Presenter*) Nothing to Disclose

LEARNING OBJECTIVES

View learning objectives under main course title.

RC305

Neuroradiology Series: Brain Tumors

Tuesday, Nov. 29 8:30AM - 12:00PM Room: S102AB

NR

AMA PRA Category 1 Credits™: 3.25
ARRT Category A+ Credits: 4.00

FDA

Discussions may include off-label uses.

Participants

Yvonne W. Lui, MD, New York, NY, (yvonne.lui@nyumc.org) (*Moderator*) Nothing to Disclose
Whitney B. Pope, MD, PhD, Los Angeles, CA (*Moderator*) Research Consultant, F. Hoffmann-La Roche Ltd; Research Consultant, Amgen Inc; Research Consultant, Tocagen Inc; ;

LEARNING OBJECTIVES

This session will highlight cutting-edge advances in brain tumor imaging including classification, radiogenomics, and quantitative pitfalls from leaders in the field.

ABSTRACT

Sub-Events

RC305-01 WHO Decided to Reclassify Brain Tumors?

Tuesday, Nov. 29 8:30AM - 9:00AM Room: S102AB

Participants

Soonmee Cha, MD, San Francisco, CA (*Presenter*) Nothing to Disclose

LEARNING OBJECTIVES

1) Present salient features of the new 2016 WHO Classification of Tumors of the Central Nervous System. 2) Discuss rationale and implication of the new classification in clinical practice of neuro-oncology and neuroradiology. 3) Apply tissue-based data outlined in the new classification to understand complex and heterogeneous brain tumor biology and to improve diagnostic imaging interpretation of brain tumors before, during, and after treatment.

ABSTRACT

RC305-02 Implications of 2-Hydroxyglutarate in Gliomas with IDH1/2 Mutations

Tuesday, Nov. 29 9:00AM - 9:10AM Room: S102AB

Participants

Liya Wang, MD, Atlanta, GA (*Abstract Co-Author*) Nothing to Disclose
Jeffrey Olson, PHD, Atlanta, GA (*Abstract Co-Author*) Nothing to Disclose
James Ross, Atlanta, GA (*Abstract Co-Author*) Nothing to Disclose
Erwin G. Van Meir, Atlanta, GA (*Abstract Co-Author*) Nothing to Disclose
Zhou Liu, MD, Shenzhen, China (*Abstract Co-Author*) Nothing to Disclose
Hui Mao, PhD, Atlanta, GA (*Presenter*) Nothing to Disclose

PURPOSE

Mutations in isocitrate dehydrogenase 1 or 2 (IDH1/2) occur in 80% of low grade gliomas. Onco-metabolite, R(-)-2-hydroxyglutarate (2HG) is a biomarker for IDH mutation (mIDH) for molecular classification of tumors and can be detected with magnetic resonance spectroscopy (MRS) for predicting prognosis[1,2]. To determine whether MRS measurement of 2HG can provide more prognostic and therapeutic information, we investigated the correlations of 2HG level with chromosome 1p/19q co-deletion status, tumor progressions, and other metabolites.

METHOD AND MATERIALS

2HG concentrations were measured from tissue specimens of 47 gliomas with mIDH by 2D Correlation Spectroscopy using solid state NMR. All tumors were categorized into three WHO grades. 1p/19q co-deletion was determined using fluorescence in situ hybridization. Progression free survival (PFS) of patients with mIDH and wild type (WT) IDH was determined. 2HG levels were compared with WHO grades, PFS, 1p/19q status and selected metabolites, such as lactate (Lac), glutamate (Glu) and glutamine (Gln). Nonparametric Mann-Whitney test for comparison/Spearman for correlation were used for statistical analysis.

RESULTS

2HG level is elevated in tumors of higher grades. Patients with mIDH have increased PFS compared to those with WT IDH. However, PFS is negatively correlated with the 2HG concentration. 1p/19q co-deletion was found in 27 out of 34 mIDH tumors. mIDH gliomas with 1p/19q co-deleted produced more 2HG. The metabolite measurements showed that the increased 2HG level is related to increases of Glu and Gln, indicating that 2HG may trigger a metabolic shift since Glu/Gln can be converted to α -ketoglutarate, the substrate of mIDH. Furthermore, the levels of Lac and 2HG are found to be positively correlated, possibly due to increase of glucose consumption related to high mutant enzyme activity.

CONCLUSION

2HG level correlates with several prognostic indices, such as PFS and 1p/19q co-deletion status. MRS analysis allows for examining the metabolic flux involving 2HG. Imaging methods capable of monitoring 2HG level may enable non-invasive and longitudinal assessment of prognosis and treatment responses.

CLINICAL RELEVANCE/APPLICATION

MRS detecting 2HG enables genetic classifying gliomas with IDH mutation. The role of 2HG in prognosis and treatment and the need of measuring 2HG level are important to apply this biomarker in precision medicine.

RC305-03 Evaluation of Recurrent High-Grade Gliomas Treated with Bevacizumab: A Three-Dimensional Pseudo-continuous Arterial Spin Labeling (3D-pcASL) Study

Tuesday, Nov. 29 9:10AM - 9:20AM Room: S102AB

Participants

Yuelei Lyu, Beijing, China (*Presenter*) Nothing to Disclose
Shuai Liu, Beijing, China (*Abstract Co-Author*) Nothing to Disclose
Hui You, Beijing, China (*Abstract Co-Author*) Nothing to Disclose
Bo Hou, BA, Beijing, China (*Abstract Co-Author*) Nothing to Disclose
Yu Wang, Beijing, China (*Abstract Co-Author*) Nothing to Disclose
Wenbin Ma, Beijing, China (*Abstract Co-Author*) Nothing to Disclose
Feng Feng SR, MD, Beijing, China (*Abstract Co-Author*) Nothing to Disclose

PURPOSE

The aim of this study is to investigate the role of cerebral blood flow (CBF) from a 3D fast spin echo (FSE) pcASL sequence in predicting the response of recurrent high-grade gliomas (rHGGs) treated with bevacizumab (BEV).

METHOD AND MATERIALS

Sixteen patients with rHGGs underwent 3D FSE pcASL imaging 1-2 days before (baseline) and within one month after BEV initiation (post-BEV) were included in this study. Average (aCBF) and maximum (mCBF) cerebral blood flow of the enhanced tumor, their normalized values to contralateral normal appearing white matter (rCBF_wm and mCBF_wm) and cerebellum (rCBF_cb and mCBF_cb), and their changes between baseline and post-BEV were evaluated. ROC curve analysis was utilized to define the optimal cutoff perfusion values for PFS and OS prediction. Kaplan-Meier analysis with log-rank test was applied to assess and compare progression-free survival (PFS) and overall survival (OS) rates.

RESULTS

Cutoffs of aCBF pre-BEV for OS, rCBF_cb pre-BEV for PFS and OS, and Δ aCBF for PFS were of statistical significance in survival prediction ($P=0.026$, 0.044 , 0.046 and 0.048 respectively). Specifically, if aCBF was >43.72 (ml/100g/min) at baseline, the median OS was 140 days compared with 404 days when aCBF ≤ 43.72 (ml/100g/min) ($P=0.026$). The percent changes of aCBF predicted a longer PFS than otherwise, if aCBF decreased more than 37% post-BEV (267 days vs 116 days, $P=0.048$). With a threshold value of 1.09, rCBF_cb predicted a longer PFS and OS in 9/16 patients when it was less than 1.09 (251 days vs 112 days for PFS; 404 days vs 194 days for OS) ($P=0.044$, $P=0.046$).

CONCLUSION

Three-dimensional FSE pcASL technique has the potential to predict the OS and PFS in patients with rHGGs treated with bevacizumab. Average CBF at baseline is a promising imaging biomarker to evaluate the prognosis of recurrent high-grade gliomas.

CLINICAL RELEVANCE/APPLICATION

Three-dimensional pcASL can predict the OS and PFS in patients with recurrent high-grade gliomas treated with bevacizumab and is recommended to evaluate the prognosis of recurrent high-grade gliomas.

RC305-04 Non-Invasively Detecting Isocitrate Dehydrogenase 1 (IDH1) Mutation Using Non-Gaussian Diffusion MR Imaging in Low-grade Gliomas

Tuesday, Nov. 29 9:20AM - 9:30AM Room: S102AB

Participants

Yan Ren, MD, Shanghai, China (*Presenter*) Nothing to Disclose
Haopeng Pang, Shanghai, China (*Abstract Co-Author*) Nothing to Disclose
Hong Chen, Shanghai, China (*Abstract Co-Author*) Nothing to Disclose
Zhenwei Yao, Shanghai, China (*Abstract Co-Author*) Nothing to Disclose
Jinsong Wu, PhD, Shanghai, China (*Abstract Co-Author*) Nothing to Disclose
Xiaoyuan Feng, MD, Shanghai, China (*Abstract Co-Author*) Nothing to Disclose

PURPOSE

To explore the feasibility of non-invasively detecting the status of IDH1 mutation (isocitrate dehydrogenase 1) using non-Gaussian-derived diffusion MR imaging in brain gliomas.

METHOD AND MATERIALS

Fifty-three cases with pathologically confirmed low-grade glioma (WHO grade II) were enrolled in this prospective study, who performed MR scans with the imaging protocol of T1WI, T2WI, T2-Flair, DWI (0,1000 s/mm²), eDWI (22 b-value DWI of 0-5000 s/mm²) and enhanced-T1WI. In tumor regions of T2-Flair hypertense, excluding remarkable cystic parts, four diffusion parameters of monoexponential-derived apparent diffusion parameter (ADC), biexponential-derived slow diffusion coefficient (Dslow), stretched exponential-derived distributed diffusion coefficient (DDC) and α were measured to correlate with the status of IDH1 mutation, which was determined by immunohistologic chemistry staining and molecular sequencing. Based on the status of IDH1 mutation, 53 gliomas were divided into two groups of IDH1mut (n=37) and IDH1wild (n=16). Four parameters of ADC, Dslow, DDC and α were employed to make comparisons between two groups of IDH1 mut and IDH1 wild. And ROC curve analyses were used to compare the capability of differentiating gliomas of IDH1 mut from IDH1 wild.

RESULTS

There were significantly increased values of Dslow (mm²/s) and α for groups of IDH1mut than IDH1wild (Dslow: 0.69 ± 0.114 vs. 0.61 ± 0.124 ; α : 0.87 ± 0.053 vs. 0.82 ± 0.058) with P values of 0.019 and 0.003, respectively. Meanwhile, the increasing signal was

shown in diffuse astrocytoma with IDH1 mut than that with IDH1wild for α and Dslow. Otherwise, no significant difference for ADC and DDC were demonstrated between groups of IDH1mut and IDH1wild. ROC curve analyses showed slightly higher AUC of 0.743 ($P=0.011$) for α than that of 0.722 ($P=0.005$) for Dslow, respectively.

CONCLUSION

Non-Gaussian-derived parameters of α and Dslow may identify the status of IDH1 mutation in low-grade gliomas. In low-grade gliomas, the water molecules behave more freely and heterogeneously in groups of IDH1mut than IDH1wild.

CLINICAL RELEVANCE/APPLICATION

Non-gaussian diffusion MR imaging may non-invasively identify the status of IDH mutation (isocitrate dehydrogenase) in low-grade gliomas and this exam is recommended when the patients with gliomas hope to take conservative management and pathological samples are not available.

RC305-05 The Impact of Prebolus T1 Measurement Over a Fixed T1 Value in the Differentiation of True Progression from Pseudoprogession in Patients with Glioblastoma after Concurrent Radiation Therapy and Chemotherapy with Temozolomide

Tuesday, Nov. 29 9:30AM - 9:40AM Room: S102AB

Participants

Ju G. Nam, MD, Seoul, Korea, Republic Of (*Presenter*) Nothing to Disclose
Koung Mi Kang, Seoul, Korea, Republic Of (*Abstract Co-Author*) Nothing to Disclose
Seung Hong Choi, MD, PhD, Seoul, Korea, Republic Of (*Abstract Co-Author*) Nothing to Disclose
Tae Jin Yoon, MD, Seoul, Korea, Republic Of (*Abstract Co-Author*) Nothing to Disclose
Roh-Eul Yoo, MD, Seoul, Korea, Republic Of (*Abstract Co-Author*) Nothing to Disclose
Ji-Hoon Kim, MD, Seoul, Korea, Republic Of (*Abstract Co-Author*) Nothing to Disclose
Chul-Ho Sohn, MD, Seoul, Korea, Republic Of (*Abstract Co-Author*) Nothing to Disclose

PURPOSE

To evaluate the diagnostic performance of the DCE pharmacokinetic parameters and the impact of tissue T1 measurement versus fixed T1 value in differentiating true progression from pseudoprogession of glioblastoma after concurrent radiation therapy and chemotherapy (CCRT) with Temozolomide

METHOD AND MATERIALS

This retrospective study included thirty four histopathologically proven glioblastoma patients who had developed any new enhancing lesion after CCRT, which was defined to be either true ($n=14$) or pseudoprogession ($n=20$) following RANO criteria. DCE pharmacokinetic parameters, including the volume transfer constant (Ktrans), the rate transfer constant (Kep), the extravascular extracellular space per unit volume of tissue (Ve), and the blood plasma volume per unit volume of tissue (Vp), for each lesion were calculated twice, using both a fixed T1 of 1000ms and tissue T1 measurement using variable flip angle method. Intraobserver reproducibility was assessed using intraclass correlation coefficient (ICC). The mean of each parameter was compared between two groups using unpaired t test and multivariate analysis. The diagnostic performance was evaluated by receiver operating characteristic (ROC) analysis with Bonferroni correction.

RESULTS

ICC of all eight parameters was excellent (0.760 to 0.999). The mean Ktrans from both fixed T1 and T1 measurement and mean Kep from fixed T1 were significantly higher in the true progression group (true vs. pseudoprogession: $0.14 /\text{min} \pm 0.15$ vs. $0.07 /\text{min} \pm 0.04$, $0.12 /\text{min} \pm 0.14$ vs. $0.06 /\text{min} \pm 0.04$, and $0.30 /\text{min} \pm 0.26$ vs. $0.18 /\text{min} \pm 0.09$; $P = .037$, $.039$, and $.026$, respectively). Multivariable analysis revealed that Kep from fixed T1 was the only independent differentiating variable ($P = .019$). In ROC analysis, Kep and Ktrans from fixed T1 showed significant diagnostic power distinguishing true from pseudoprogession (AUC 0.718 and 0.714; $P = .015$ and $.016$, respectively). None from T1 measurement showed proper diagnostic performance (all $P_s > .05$).

CONCLUSION

Semiquantitative DCE-derived parameters, Kep and Ktrans, calculated from a fixed T1 act as preferable tools to differentiate true progression from pseudoprogession compared with the parameters from tissue T1 measurement.

CLINICAL RELEVANCE/APPLICATION

Early differentiation of true progression against Temozolomide might help nonreactive patients stop suffering from side effects and give them opportunity for another treatment.

RC305-06 Practical Radiogenomics: Lessons Learned from the Cancer Genome Atlas

Tuesday, Nov. 29 9:40AM - 10:10AM Room: S102AB

Participants

Rajan Jain, MD, Hartsdale, NY (*Presenter*) Consultant, Cancer Panels; Royalties, Thieme Medical Publishers, Inc

LEARNING OBJECTIVES

1) Describe The Cancer Imaging Archive, Glioma phenotype research group organization and VASARI feature set. 2) Role of imaging in the new age of tumor genomics: How it can improve understanding of tumor biology. 3) Describe imaging characteristics of gliomas based on genomic differences: Phenotype-genotype correlation (Imaging Genomics/Radio-genomics).

ABSTRACT

Recent advances in glioma genomics have significantly changed our understanding of tumor biology and hence, affected how these patients are treated. Similarly, integrating imaging data with genomic markers has also helped create better prognostic and predictive biomarkers which offer promising future for personalized medicine. This session will highlight a multi-disciplinary approach with the focus on advanced imaging and genomics markers before and after therapy in gliomas.

RC305-07 Participants

Processing Pitfalls in Quantitative Brain Tumor Imaging

Tuesday, Nov. 29 10:20AM - 10:50AM Room: S102AB

Bradley J. Erickson, MD, PhD, Rochester, MN, (bje@mayo.edu) (*Presenter*) Stockholder, OneMedNet Corporation; Stockholder, VoiceIt Technologies, LLC; Stockholder, FlowSigma

LEARNING OBJECTIVES

1) Become familiar with common image processing techniques applied to MRI images obtained in brain tumor patients, and the ways in which they can lead to incorrect conclusions. This will primarily focus on diffusion and perfusion imaging.

ABSTRACT

Diffusion and perfusion imaging is commonly used for brain tumor patients. These methods provide unique insights into what is happening in tumors, particularly during and after therapeutic intervention. Understanding how these methods work can substantially impact interpretation of MRI examinations in these patients. However, the processing of diffusion and perfusion images is complex, and can often lead to incorrect conclusions if artifacts and other differences are not understood. While the computation of ADC images from DWI acquisitions is straightforward, one must be careful when making conclusions based on minimum values seen in an ROI due to filtering that may or may not be applied to the images. Registration and subtraction can also be useful, but can also have errors in them. Perfusion images, particularly DSC images, involve very complex processing based on assumptions about what is happening in tissues. Those assumptions substantially impact calculations that are used to produce rCBV and other types of perfusion images. Even seemingly simple things like selection of the normal-appearing white matter can substantially change measured values. Understanding basic principles used in processing can help to avoid or minimize errors in interpretation.

RC305-08 Assessment of the Prognostic Value of Contrast Enhancement and FLAIR for Overall Survival in Newly Diagnosed Glioblastoma Treated With and Without Bevacizumab: Results from the ACRIN 6686/RTOG 0825 Central Reader Study

Tuesday, Nov. 29 10:50AM - 11:00AM Room: S102AB

Participants

Jerrold L. Boxerman, MD, PhD, Providence, RI (*Presenter*) Medical Advisor, Imaging Biometrics, LLC

Zheng Zhang, PhD, Providence, RI (*Abstract Co-Author*) Nothing to Disclose

Yair Safriel, MBBCh, Clearwater, FL (*Abstract Co-Author*) Principal, PharmaScan Clinical Trials

Jeffrey M. Rogg, MD, Providence, RI (*Abstract Co-Author*) Nothing to Disclose

Ronald L. Wolf, MD, PhD, Philadelphia, PA (*Abstract Co-Author*) Nothing to Disclose

Helga Marques, MS, Providence, RI (*Abstract Co-Author*) Nothing to Disclose

James Gimpel, Philadelphia, PA (*Abstract Co-Author*) Nothing to Disclose

A. Gregory Sorensen, MD, Malvern, PA (*Abstract Co-Author*) CEO, Siemens USA Consultant, sanofi-aventis Group Research support,

sanofi-aventis Group Consultant, Bayer AG Research support, Exelixis, Inc Research support, Schering-Plough Corporation

Consultant, Mitsubishi Corporation Consultant, Biogen Idec Inc Research support, Takeda Pharmaceutical Company Limited

Mark Gilbert, Houston, TX (*Abstract Co-Author*) Nothing to Disclose

Daniel P. Barboriak, MD, Durham, NC (*Abstract Co-Author*) Advisory Board, General Electric Company

PURPOSE

ACRIN 6686/RTOG 0825 is a phase III double-blinded placebo-controlled trial of conventional chemoradiation and adjuvant temozolomide with or without bevacizumab (BEV) in newly diagnosed glioblastoma. We aim to assess the association between changes in tumor size measured by contrast enhancement (post-Gd T1) or FLAIR after 3 treatment cycles and overall survival (OS).

METHOD AND MATERIALS

284 patients (171 men; ages 19-79 years, median 57; 159 on BEV arm) had post-op (baseline) and 22-week (pre-cycle 4) MRI. Central readers measured unidimensional (1D), bidimensional (2D) and volumetric (3D) lesion post-Gd T1 and FLAIR hyperintensity at both time points, and determined change from baseline at week 22 for all six imaging markers. Hazard ratio (HR) from Cox proportional hazards model either with or without treatment and marker interaction term and Kaplan-Meier survival estimates with log-rank test were used for inference.

RESULTS

T1: Increasing 2D-T1 was significantly associated with worse survival (n=261, HR=2.19, 95% CI 1.49-2.93, p<0.0001 adjusting for treatment). Median OS (days) was significantly shorter for patients with increasing versus decreasing 2D-T1 in both BEV (443 vs. 535, p=0.004) and non-BEV (526 vs. 887, p=0.001) arms. **T2:** Increasing 2D-FLAIR was significantly associated with worse survival (n=272, HR=1.72, 95% CI 1.24-2.39, p=0.001 adjusting for treatment). Median OS was significantly shorter for patients with increasing versus decreasing 2D-FLAIR in the non-BEV arm (595 vs. 872, p=0.001), but not in the BEV arm (499 vs. 535, p=0.12). Results for 1D and 3D measures were similar. **T1+T2:** Increasing 2D-FLAIR for patients without increasing 1D-T1 tumor enhancement was associated with worse survival overall (HR=1.63, 95% CI 1.15-2.32, p=0.006 adjusting for treatment), with similar association for non-BEV and BEV arms (HR=2.07 vs. 1.65, respectively, p=0.64).

CONCLUSION

Post-Gd T1 has predictive value for OS in BEV and non-BEV subgroups. FLAIR has independent prognostic value for OS overall, and may further dichotomize patients by OS in both subgroups when there is no increased enhancement on post-Gd T1.

CLINICAL RELEVANCE/APPLICATION

Post-therapy increased T1 enhancement is a useful MRI marker for failed BEV and non-BEV therapy, with added prognostic value of FLAIR particularly in non-BEV therapies. Funded by NCI U01-CA080098 and U01-CA079778.

Honored Educators

Presenters or authors on this event have been recognized as RSNA Honored Educators for participating in multiple qualifying educational activities. Honored Educators are invested in furthering the profession of radiology by delivering high-quality educational content in their field of study. Learn how you can become an honored educator by visiting the website at:

Daniel P. Barboriak, MD - 2013 Honored Educator

RC305-09 Biopsy Tissue Validation of Amide Proton Transfer-Weighted MRI Signal as a Biomarker to Differentiate Recurrent Gliomas from Treatment Effect

Tuesday, Nov. 29 11:00AM - 11:10AM Room: S102AB

Participants

Shanshan Jiang, MD, Baltimore, MD (*Presenter*) Nothing to Disclose
Jinyuan Zhou, PhD, Baltimore, MD (*Abstract Co-Author*) License agreement, Koninklijke Philips NV
Charles Eberhart, MD, PhD, Baltimore, MD (*Abstract Co-Author*) Nothing to Disclose
Michael Lim, Baltimore, MD (*Abstract Co-Author*) Nothing to Disclose
Alfredo Quinones-Hinojosa, Baltimore, MD (*Abstract Co-Author*) Nothing to Disclose
Huamin Qin, Baltimore, MD (*Abstract Co-Author*) Nothing to Disclose
Hye-Young Heo, Baltimore, MD (*Abstract Co-Author*) Nothing to Disclose
Yi Zhang, Baltimore, MD (*Abstract Co-Author*) Nothing to Disclose
Lindsay Blair, Baltimore, MD (*Abstract Co-Author*) Nothing to Disclose
Zhibo Wen, Guangzhou, China (*Abstract Co-Author*) Nothing to Disclose
Peter B. Barker, DPhil, Baltimore, MD (*Abstract Co-Author*) Nothing to Disclose
Martin G. Pomper, MD, PhD, Baltimore, MD (*Abstract Co-Author*) Shareholder, CTS, Inc; Board Member, CTS, Inc; Research Grant, CTS, Inc; Advisor, CTS, Inc; Institutional license agreement, Progenics Pharmaceuticals, Inc; Institutional license agreement, Advanced Accelerator Applications SA; Institutional license agreement, LI-COR, Inc; Institutional license agreement, BIND Therapeutics, Inc
John Laterra, Baltimore, MD (*Abstract Co-Author*) Nothing to Disclose
Peter C. Van Zijl, PhD, Baltimore, MD (*Abstract Co-Author*) Speakers Bureau, Koninklijke Philips NV; License agreement, Koninklijke Philips NV
Jaishri Blakeley, Baltimore, MD (*Abstract Co-Author*) Nothing to Disclose

PURPOSE

The surveillance of post-treatment gliomas remains a formidable radiologic dilemma. Protein-based amide proton transfer-weighted (APTw) MRI has showed promising diagnostic values for gliomas. Here, we performed a radiopathologic correlation analysis via APTw image-directed stereotactic biopsy to determine the accuracy of the APTw signal as an imaging biomarker of active tumor.

METHOD AND MATERIALS

21 patients with suspected malignant glioma recurrence underwent a volumetric APTw imaging sequence at 3T. 64 APTw imaging-guided biopsy specimens were obtained and analyzed for tumor cellularity, necrosis, and proliferation. Specimens were classified as active, quiescent, or mixed by neuropathology. Active and mixed were grouped as recurrence, while quiescent and no tumor were grouped as treatment effect.

RESULTS

20/64 specimens were active tumor, 13 quiescent tumor, and 27 mixed. No tumor was found in four specimens. 9/21 patients had multiple categories within the same lesion. The mean APTw signal intensities were $3.14 \pm 0.68\%$ in active specimens, $1.97 \pm 1.04\%$ in mixed specimens, and $1.22 \pm 0.60\%$ specimens, independent of Gd enhancement. There were moderate to strong positive correlations between APTw and tumor status ($R = 0.728$), cellularity ($R = 0.523$), and proliferation ($R = 0.407$), a mild negative correlation between APTw and necrosis ($R = -0.328$). Multiple linear regression showed that tumor status was the most powerful predictor of APTw intensities ($R^2 = 0.575$). The APTw intensities showed significant difference between the treatment effect group ($1.61 \pm 0.93\%$) and recurrence group ($3.14 \pm 0.68\%$), having a cut-off value of 1.64% and an AUC of 0.962 to differentiate these two groups.

CONCLUSION

APTw hyperintensity within heterogeneous tumors is associated with active recurrent tumor. The APTw imaging signal as a biomarker of active glioma has the potential to non-invasively identify the status of malignant gliomas post-treatment.

CLINICAL RELEVANCE/APPLICATION

APTw imaging signal has the potential to non-invasively differentiate tumor recurrence from treatment effect that may eventually avoid surgery where tissues sampling is only for diagnosis.

RC305-10 Presurgical fMRI and DTI as a Predictive Imaging Marker for Postoperative Focal Neural Deficits in Glioblastoma

Tuesday, Nov. 29 11:10AM - 11:20AM Room: S102AB

Participants

Mohamed Zaid, MBCh, Houston, TX (*Abstract Co-Author*) Nothing to Disclose
Islam S. Hassan, MD, Houston, TX (*Abstract Co-Author*) Nothing to Disclose
Wei Wei, Houston, TX (*Abstract Co-Author*) Nothing to Disclose
Ashok J. Kumar, MD, Houston, TX (*Abstract Co-Author*) Nothing to Disclose
Sujit Prabhu, MD, Houston, TX (*Abstract Co-Author*) Nothing to Disclose
Jeffrey S. Weinberg, MD, Houston, TX (*Abstract Co-Author*) Nothing to Disclose
Raymond Sawaya, MD, Houston, TX (*Abstract Co-Author*) Nothing to Disclose
Pascal O. Zinn, MD, Boston, MA (*Abstract Co-Author*) Nothing to Disclose
Rivka R. Colen, MD, Houston, TX (*Abstract Co-Author*) Nothing to Disclose
Nabil A. Elshafeey, MD, Houston, TX (*Presenter*) Nothing to Disclose

PURPOSE

To evaluate the ability of combined fMRI and tractography to predict postoperative focal deficits in GBM patients undergoing surgery.

METHOD AND MATERIALS

We enrolled 220 patients who underwent presurgical fMRI in this IRB approved study. Our inclusion criteria were pathologically proven diagnosis of GBM, full pre and postoperative neurological examination, preoperative task based motor fMRI as well as diffusion tensor imaging (DTI). We obtained multiple fMRI and DTI parameters including Lesion to activation distance (LAD) in T1+C (T1LAD) and T2 FLAIR (FLAIRLAD). both from center of activity to center of lesion and from margin of activity to margin of lesion. DTI was done to measure distance between neoplasms margin, edema margin and corticospinal tract (CST) in T1+C and T2 FLAIR respectively. KruskalWallis test was used to compare distance between patient groups, all tests were 2 sided and p-values of 0.05 or less we reconsidered statistically significant.

RESULTS

Our cohort was 53% females, 47% males; majority showed Rt. handedness (90%). GBMs were located in Lt. hemisphere in 63% of patients, 38% in the right, 48% in frontal lobe, 30% and 22.5% in parietal and temporal lobes respectively. Gross total resection was achieved in 70 %; 30% underwent subtotal. The most important imaging marker for determining the postoperative status of motor focal neurological deficit (MFND) was Distance between lesion edge and Edema edge with the worst prognosis in development of MFND in patients with FLAIRLAD of less than 1 mm (P=0.0004). The second best marker was T1LAD measured from edge of tumor to edge of activation; distance below 6.6 mm was associated with deterioration in motor functions (P= 0.002). Similarly, a statistically significant deterioration occurred in T1LAD less than 2.9 mm measured from center of tumor to center of activity (p-value= 0.007). The distance of contrast enhancement and FLAIR signal abnormality to corticospinal tract showed no statistical significance.

CONCLUSION

LAD is an important functional imaging marker for predicting Motor FND in GBM patients. GBM has a significant edema portion that contributes to the potential outcome of patients

CLINICAL RELEVANCE/APPLICATION

Combination of both DTI and fMRI in presurgical mapping for patients with Glioblastoma in close vicinity to motor area is of supreme importance to avoid postoperative deficits while maximizing resection.

RC305-11 Differentiating and Predicting True Progression versus Pseudoprogression: Comparing ASL, DSC, DCE and MRS

Tuesday, Nov. 29 11:20AM - 11:30AM Room: S102AB

Participants

Ahmed T. Shaaban, MD, Houston, TX (*Abstract Co-Author*) Nothing to Disclose
Nabil A. Elshafeey, MD, Houston, TX (*Presenter*) Nothing to Disclose
Ahmed A. Hassan, MBCh, Houston, TX (*Abstract Co-Author*) Nothing to Disclose
Ho-Ling Liu, PhD, Houston, TX (*Abstract Co-Author*) Nothing to Disclose
Ping Hou, PhD, Houston, TX (*Abstract Co-Author*) Nothing to Disclose
Vinodh A. Kumar, MD, Houston, TX (*Abstract Co-Author*) Nothing to Disclose
Ashok J. Kumar, MD, Houston, TX (*Abstract Co-Author*) Nothing to Disclose
Norman E. Leeds, MD, Houston, TX (*Abstract Co-Author*) Nothing to Disclose
Rivka R. Colen, MD, Houston, TX (*Abstract Co-Author*) Nothing to Disclose

PURPOSE

To evaluate the predictive value of Magnetic Resonance Spectroscopy (MRS) as well as different magnetic resonance perfusion (MRP) parameters including dynamic susceptibility contrast (DSC), Dynamic contrast enhanced (DCE), arterial spin labeling (ASL) in discriminating Pseudoprogression (PsP) from true progression (PD) in Glioblastoma (GBM) patients.

METHOD AND MATERIALS

Our Institutional review board has approved this HIPAA-compliant retrospective study. We identified a total of 69 patients (45 Males: 24 females) (average age =50, median age = 51) with pathologically proven GBM. All patients underwent advanced MRI studies (DSC, DCE, ASL and MRS). All patients had pathological proof of either PD or PsP after the advanced MRI studies. For each patient, three board-certified neuroradiologists, blinded to the pathology report, evaluated all the advanced imaging features using a designed qualitative questionnaire to determine PD and PsP. The questionnaire included the following parameters: DCE (PEI 3, 60, Curves), DSC (rCBV, NEI, Curves), ASL (CBF), MRS (Nacetylaspartate, choline/creatine, lipid). Statistical analysis was performed to evaluate the ability of each imaging feature in discriminating PD from PsD.

RESULTS

According to the pathology reports, 7 patients had PsP while remaining 62 patients had PD. While MRS was the most superior imaging features in accurately discriminating PD from PsP followed by DSC, ASL and DCE respectively, yet, combination of the aforementioned features yielded the best discriminatory results. The ability to predict Psp versus true progression as compared to the gold standard (pathological confirmation) was 97%

CONCLUSION

DCE, DSC, ASL, MRS can be valid reliable imaging markers with statistically significant predictive values to differentiate PD versus PsP. The combination of those different advanced MRI technique can eventually yield an accurate platform for diagnosis of PD vs PsP

CLINICAL RELEVANCE/APPLICATION

Advanced Imaging analysis can be used as a distinguishable method between the true and pseudoprogression in GBM Patients

RC305-12 Brain Tumor Imaging with MR/PET

Tuesday, Nov. 29 11:30AM - 12:00PM Room: S102AB

Participants

Fernando E Boada, New York, NY, (Fernando.Boada@nyumc.org) (*Presenter*) Nothing to Disclose

RC306

RSNA Diagnosis Live™: Do You Know Your Head and Neck Anatomy? (An Interactive Session)

Tuesday, Nov. 29 8:30AM - 10:00AM Room: E451B



AMA PRA Category 1 Credits™: 1.50
ARRT Category A+ Credits: 1.50

Participants

LEARNING OBJECTIVES

This interactive session will use RSNA Diagnosis Live™. Please bring your charged mobile wireless device (phone, tablet or laptop) to participate.

Sub-Events

RC306A Temporal Bone Anatomy

Participants

Richard H. Wiggins III, MD, Salt Lake City, UT (*Presenter*) Nothing to Disclose

LEARNING OBJECTIVES

1) Review important temporal bone anatomy. 2) Understand complex imaging anatomy of the temporal bone. 3) Describe imaging techniques of the temporal bone.

ABSTRACT

The temporal bone has some of the most intricate anatomy of the human body. This refresher course will review the complex anatomy of the temporal bone, including the external auditory canal, middle ear, inner ear, and petrous apex, as well as the imaging techniques to best evaluate this region. The anatomy and normal imaging appearances will be described and reviewed.

Honored Educators

Presenters or authors on this event have been recognized as RSNA Honored Educators for participating in multiple qualifying educational activities. Honored Educators are invested in furthering the profession of radiology by delivering high-quality educational content in their field of study. Learn how you can become an honored educator by visiting the website at: <https://www.rsna.org/Honored-Educator-Award/>

Richard H. Wiggins III, MD - 2012 Honored Educator

RC306B Skull Base Anatomy

Participants

C. Douglas Phillips, MD, New York, NY, (dphillips@med.cornell.edu) (*Presenter*) Stockholder, MedSolutions, Inc Consultant, Guerbet SA

LEARNING OBJECTIVES

1) Understand the embryologic development of the skull base. 2) Identify a number of developmental anomalies of the skull base and describe their imaging findings. 3) Compare developmental lesions from inflammatory/infectious or neoplastic lesions.

RC306C Larynx and Hypopharynx

Participants

Hugh D. Curtin, MD, Boston, MA, (Hugh_Curtin@meei.harvard.edu) (*Presenter*) Nothing to Disclose

LEARNING OBJECTIVES

1) Review the major anatomic structures of the larynx. 2) Specifically identify the laryngeal ventricle and its bordering tissues. 3) Describe the contents of the paraglottic space and describe its importance in tumor growth.

ABSTRACT

The larynx is a complex system of cartilage, muscle and ligaments that work together to produce speech and to facilitate breathing. Imaging can identify many of the different structures of the larynx. Particularly important are the laryngeal ventricle and the paraglottic space. These structures will be emphasized along with other anatomy that is of key importance in imaging evaluation.

Predicting Outcomes for Genitourinary Malignancies: Role of Radiomics in Clinical Practice

Tuesday, Nov. 29 8:30AM - 10:00AM Room: S405AB

GU

AMA PRA Category 1 Credits™: 1.50
ARRT Category A+ Credits: 1.50

FDA

Discussions may include off-label uses.

Participants

Ivan Pedrosa, MD, Dallas, TX (*Coordinator*) Nothing to Disclose

Ivan Pedrosa, MD, Dallas, TX (*Presenter*) Nothing to Disclose

Maryellen R. Sun, MD, Boston, MA, (msun@bidmc.harvard.edu) (*Presenter*) Nothing to Disclose

Masoom A. Haider, MD, Toronto, ON (*Presenter*) Consultant, Bayer AG; ;

LEARNING OBJECTIVES

1) Recognize the differences in the biologic behavior and prognosis between cystic and solid renal cancers and learn how the imaging phenotype can be helpful in guiding management decisions when incorporated into the radiology report. 2) Assess tumor aggressiveness of urothelial carcinomas of the upper tract and bladder with imaging and understand the added value of this information in disease management. 3) Use imaging characteristics of aggressive prostate cancer and the 'index lesion' to distinguish clinically significant prostate cancers from indolent ones.

ABSTRACT

The development of imaging phenotypes in genitourinary (GU) malignancies, supported by the application of Radiomics, has improved our understanding of the relationship between imaging phenotypes and clinical outcomes. Radiomics are based on the extraction of more information than what may be obvious to the eye with the use of quantitative and advanced feature analysis techniques. Radiomics provide a platform for whole-tumor analysis in vivo, and offer the opportunity for investigating pathophysiologic phenomena (e.g. blood flow, vascular permeability, tumor proliferation) that are difficult to examine in ex vivo tissue - these image-based features may serve as surrogate biomarkers of tumor aggressiveness. Furthermore, radiomics correlate with genetic profiles that predict tumor aggressiveness and provides a pathway toward the understanding of tumor heterogeneity, classification, and risk stratification. This refresher course will review the correlation between imaging phenotypes and the clinical behavior of renal, prostate, and urothelial malignancies. We will show how radiomics can be incorporated into radiology reports in patients with GU malignancies and emphasize how radiomics features can be used to affect patient care.

Emergency Radiology Series: Imaging of Thoracic and Related Emergencies

Tuesday, Nov. 29 8:30AM - 12:00PM Room: N230B



AMA PRA Category 1 Credits™: 3.50
ARRT Category A+ Credits: 4.00

Participants

Martin L. Gunn, MBChB, Seattle, WA, (marting@uw.edu) (*Moderator*) Research Grant, Koninklijke Philips NV; Royalties, Cambridge University Press; Spouse, Consultant, Reed Elsevier; Spouse, Consultant, athenahealth, Inc; ; Stephen Ledbetter, MD, Boston, MA (*Moderator*) Nothing to Disclose

Active Handout: Martin Lee David Gunn

http://abstract.rsna.org/uploads/2016/16000652/RC308_Gunn_Aortic_Injury.pdf

Sub-Events**RC308-01 Esophageal Emergencies**

Tuesday, Nov. 29 8:30AM - 9:00AM Room: N230B

Participants

Francis J. Scholz, MD, Burlington, MA, (francis.j.scholz@lahey.org) (*Presenter*) Owner, FSpoon Company

LEARNING OBJECTIVES

After this presentation the radiologist will: Understand how to optimally examine for pharyngeal and esophageal trauma using fluoroscopy Recognize and stage trauma as either A. Mucosal Tear B Intramural Dissection C Transmural Tear

ABSTRACT

Esophageal trauma is common in practice and includes a broad spectrum of clinical and radiologic entities including perforation, hematoma, and foreign body ingestion that must be recognized promptly in order to reduce morbidity and mortality. Imaging findings are often subtle or may not be demonstrable by conventional radiography or CT. Recognizing subtle fluoroscopic findings of disease may avoid additional work up including more invasive endoscopy. Radiologists frequently perform esophageal fluoroscopy for not only possible spontaneous trauma but also complex post-surgical and endoscopic trauma. In addition, spontaneous or post traumatic pneumomediastinum or air in soft tissues of the neck lead to an urgent request to evaluate for esophageal perforation. This presentation will provide concise details of our fluoroscopic technique and the findings that permit staging of traumatic insults for clinical treatment choices, correlated with CT findings. Mucosal tears, intramural dissections, and transmural perforations are shown. Classic eponymic esophageal traumas - Boerhaave and Mallory Weiss - are discussed and illustrated.

ABSTRACT

Esophageal trauma is common in practice and includes a broad spectrum of clinical and radiologic entities including perforation, hematoma, and foreign body ingestion that must be recognized promptly in order to reduce morbidity and mortality. Imaging findings are often subtle or may not be demonstrable by conventional radiography or CT. Recognizing subtle fluoroscopic findings of disease may avoid additional work up including more invasive endoscopy. Radiologists frequently perform esophageal fluoroscopy for not only possible spontaneous trauma but also complex post-surgical and endoscopic trauma. In addition, spontaneous or post traumatic pneumomediastinum or air in soft tissues of the neck lead to an urgent request to evaluate for esophageal perforation. This presentation will provide concise details of our fluoroscopic technique and the findings that permit staging of traumatic insults for clinical treatment choices, correlated with CT findings. Mucosal tears, intramural dissections, and transmural perforations are shown. Classic eponymic esophageal traumas - Boerhaave and Mallory Weiss - are discussed and illustrated.

Active Handout: Francis Joseph Scholz

http://abstract.rsna.org/uploads/2016/16000653/rc30801_Esophageal_Emergencies_DONE_6p.pdf

LEARNING OBJECTIVES

1) Understand presentations of esophageal trauma that warrant prompt fluoroscopic imaging. 2) Know esophageal anatomy and structure required for fluoroscopic imaging. 3) Use techniques that optimally define esophageal pathology. 4) Diagnose esophageal trauma, and stage perforations.

ABSTRACT

Esophageal emergencies are common and the radiologist is a key member of the team involved in the diagnosis, staging, and treatment of many esophageal emergencies. CT and Fluoroscopy remain the principle diagnostic tools in patients with emergent esophageal symptoms. Introduction to esophageal perforation, fluoroscopy and CT technique, diagnostic findings, and staging concepts will be discussed and illustrated, including classic diagnoses: Taco Tear, Mallory Weiss, Boerhaave Syndrome Signs and symptoms of esophageal trauma: odynophagia, pain after endoscopy, neck crepitus, abnormal breath sounds.

PERFORATION ETIOLOGIES: Instrumentation and Surgery

Ingestion/vomiting: Mallory Weiss, Boerhaave, Taco Tear, often alcohol associated

Fragile mucosa: Bullous Dermatoses, Eosinophilic Esophagitis

Radiation Stricture

Caustic agents TECHNIQUE: If critically ill: CT and/or straight to surgery. If not critically ill and high suspicion, fluoroscopy is the FIRST BEST TEST for esophageal trauma. It is best suited for finding subtle intramural perforations and for severity staging. FLUOROSCOPY: Review prior swallow, find prior stricture site

Water-soluble, 90 cc, 4/s AP pharynx; 1/sec AP Esophagus.

If negative: barium Esophagus: 1/s, upright AP, LAO and prone LPO. Pharynx: 4/s AP, Lateral ESOPHAGEAL TRAUMA STAGING Mucosal Intramural

Transmural
Distant tracking, pleural and mediastinal inflammation

RC308-02 Chest Pain CT in the Emergency Department: Watch Out the Myocardium

Tuesday, Nov. 29 9:00AM - 9:10AM Room: N230B

Participants

Kai Higashigaito, Zurich, Switzerland (*Abstract Co-Author*) Nothing to Disclose
Ricarda M. Hinzpeter, MD, Zurich, Switzerland (*Presenter*) Nothing to Disclose
Stephan Baumuller, Zurich, Switzerland (*Abstract Co-Author*) Nothing to Disclose
Hatem Alkadhi, MD, Zurich, Switzerland (*Abstract Co-Author*) Nothing to Disclose
Fabian Morsbach, Zurich, Switzerland (*Abstract Co-Author*) Nothing to Disclose

PURPOSE

To evaluate the frequency and significance of hypodense myocardium (HM) and coronary culprit lesions in chest-pain CT in the emergency department.

METHOD AND MATERIALS

In this IRB- and ethics committee approved study, ECG-triggered chest-pain CT examinations of 300 consecutive patients (mean age 59±17 years, 71% male) with acute chest pain referred to our emergency department for DRO (rule-out pulmonary embolism (PE) and aortic dissection (AD), n=179) and TRO (n=121) between 06/2012 and 11/2015 were retrospectively analyzed. Chest-pain CT for TRO was performed with s.l. nitroglycerine and without nitroglycerine for DRO. Each myocardial segment was assessed for the presence of hypodense myocardium (HM). Attenuation of HM was measured and compared to normal myocardium. Coronary arteries were searched for the presence of culprit lesions and coronary plaques were classified into non-calcified, mixed and calcified. Presence of positive remodeling was noted. Patient histories were reviewed for the indications of CT, cardiovascular risk factors, known previous myocardial infarction (MI), and final diagnosis causing acute chest pain.

RESULTS

HM was identified in 27/300 patients (9%): 12/179 in DRO-CT (7%) and 15/121 in TRO-CT (12%). Mean attenuation of HM (59±40HU) was significantly lower than that of healthy myocardium (112±20HU, p<0.05), with a mean difference of 83±32HU. In 16/27 patients (59%) with HM, the final diagnosis was acute MI, and in the remaining 11/27 patients (41%) previous MI was found in the patients' history. DRO-CT identified HM and the corresponding culprit lesion in 6/16 patients (37%) with a final diagnosis of acute MI. In 13/16 patients (81%), a culprit lesion causing MI was correctly identified and subsequently confirmed with catheter angiography. Of the identified 13 plaques in culprit lesions, 4 (31%) were non-calcified, 4 (31%) mixed, and 5 (38%) calcified. 9/13 (69%) plaques showed positive remodeling.

CONCLUSION

Hypodense myocardium and the culprit coronary lesion causing acute MI is encountered often in chest-pain CT examinations, even if only a DRO-CT was performed. This indicates that the myocardium should be analyzed for hypodense regions also if no dedicated CT of the coronaries and heart was asked for.

CLINICAL RELEVANCE/APPLICATION

Acute MI can be detected in both DRO- and TRO- chest-pain CT examinations and may facilitate the diagnostic workup of acute chest pain patients.

RC308-03 MDCT of Aortic Dissection

Tuesday, Nov. 29 9:10AM - 9:40AM Room: N230B

Participants

Stephen Ledbetter, MD, Boston, MA, (sledbetter@partners.org) (*Presenter*) Nothing to Disclose

LEARNING OBJECTIVES

To optimize imaging approach for the ED patient
To review the typical CT imaging findings
To understand the spectrum of disease

RC308-04 Novel CT Predictors of Type A Aortic Dissection

Tuesday, Nov. 29 9:40AM - 9:50AM Room: N230B

Awards

Student Travel Stipend Award

Participants

Nigel R. Munce, MD, PhD, Hamilton, ON (*Presenter*) Founder, Conavi Medical Inc; Shareholder, Conavi Medical Inc
Michael N. Patlas, MD, FRCPC, Hamilton, ON (*Abstract Co-Author*) Nothing to Disclose
Ali Alsagheir, MD, Hamilton, ON (*Abstract Co-Author*) Nothing to Disclose
Forough Farrokhyar, DPhil, PhD, Hamilton, ON (*Abstract Co-Author*) Nothing to Disclose
Dominic Parry, MD, Hamilton, ON (*Abstract Co-Author*) Nothing to Disclose

PURPOSE

To retrospectively evaluate the clinical relevance of novel MDCT parameters in patients with type A aortic dissection when compared to a control group having MDCT for the evaluation of thoracic aorta.

METHOD AND MATERIALS

An IRB- approved retrospective review of patients presenting with Type A aortic dissection at our institution (n=51 with available

MDCT) was conducted from January 2008 - January 2016. MDCT parameters measured were: length of the ascending aorta (AA), maximal AA diameter, aortic root diameter, the left ventricular outflow tract (LVOT) angle (the angle between an imaginary line drawn at right angles to the plane of the aortic annulus and a second line representing the transverse plane) and the cardiac apex (CA) angle (the angle between an imaginary line drawn from left ventricular apex to the mid point of the aortic valve and a second line representing the transverse plane). Similar measurements were performed in an age and gender matched control group (n=76). Statistical comparison were made with Student's t-tests.

RESULTS

51 cases of acute Type A dissection with available MDCT were identified (mean age= 61; M:F= 35:16). Review of 123 urgent CTs of the complete aorta yielded 76 cases without significant acute aortic pathology or prior thoracic aortic intervention which served as age and gender matched controls. The mean length of the ascending aorta in the Type A dissection population versus control group was 12.00 vs 9.27 cm ($p < .0001$). The maximal aortic diameter was 4.97 vs 3.15 cm ($p < .0001$) and aortic root diameter was 4.35 vs 2.89 cm ($p < .001$). The LVOT and CA angles were both significantly less in the type A dissection group measuring 31.70 vs 44.13 degrees ($p < .0001$) and 20.44 vs 30.34 degrees ($p < .0001$), respectively.

CONCLUSION

Our study shows, for the first time to our knowledge, that there is a statistically significant increase in the length of the ascending aorta in patients with Type A dissection as compared to control group. We also demonstrate that there is a decrease in the angle of the LVOT and CA angle.

CLINICAL RELEVANCE/APPLICATION

AA length, LVOT angle and CA angle are significantly different in patients with Type A dissection as compared to a control group and thus may serve as novel predictors for type A aortic dissection.

RC308-05 Morphological Changes between Acute and Chronic Type B Communicating Aortic Dissection on MDCT: A Retrospective Study

Tuesday, Nov. 29 9:50AM - 10:00AM Room: N230B

Participants

Yumi Imamura, Tokyo, Japan (*Presenter*) Nothing to Disclose

Satoru Morita, MD, PhD, Shinjuku-ku, Japan (*Abstract Co-Author*) Nothing to Disclose

Shuji Sakai, MD, Shinjuku-Ku, Japan (*Abstract Co-Author*) Nothing to Disclose

PURPOSE

No reports have systematically clarified the differences between acute and chronic type B communicating aortic dissection on computed tomography (CT), though such clarification is sometimes required clinically. Thorough understanding of these differences from disease onset is important for determining optimal therapeutic methods and accurately estimating the prognosis. The purpose of this study was to compare the morphological changes between acute and chronic type B communicating aortic dissection on multidetector row CT (MDCT).

METHOD AND MATERIALS

We analyzed 21 patients with type B communicating aortic dissection who underwent acute-phase contrast-enhanced MDCT. The flap curvature, flap thickness, long and short diameter of the aorta, and false lumen length were measured at a representative portion of the descending aorta. The numbers of slices with 5-mm thickness with a fluttering flap, calcification on the flap, and thrombosis in the false lumen were counted. These findings in the acute and chronic phases before any intervention (median 0 and 181 days after onset) were compared using the Mann-Whitney U test.

RESULTS

The mean flap curvature in the acute phase was significantly larger than in the chronic phase (66.0 ± 18.0 vs. 35.5 ± 30.9 1/m, $p = 0.009$). The median number of slices with a fluttering flap in the acute phase was larger than in the chronic phase (10 vs. 1, $p = 0.008$). The mean ratio of the long to short diameter in the acute phase was relatively lower than in the chronic phase (1.07 ± 0.06 vs. 1.14 ± 0.12 , $p = 0.073$). The mean ratio of the false lumen length to long diameter in the acute phase was significantly lower than in the chronic phase (0.41 ± 0.10 vs. 0.59 ± 0.16 , $p < 0.001$). No significant differences in the mean flap thickness, median number of slices with calcification on the flap, and median number of slices with thrombosis in the false lumen were observed (2.4 ± 0.5 vs. 2.7 ± 0.6 , $p = 0.176$; 8 vs. 10, $p = 0.651$; and 2 vs. 12, $p = 0.086$).

CONCLUSION

Acute and chronic type B communicating aortic dissection can be differentiated on MDCT. Findings suggestive of acute phase are a curved flap, flap fluttering, and complete round shape of the descending aorta.

CLINICAL RELEVANCE/APPLICATION

MDCT findings of a curved flap, flap fluttering, and complete round shape of the descending aorta suggest the acute rather than chronic phase of type B communicating aortic dissection.

RC308-06 Aortic MRA Can Guide ED Management of Suspected Acute Aortic Dissection

Tuesday, Nov. 29 10:00AM - 10:10AM Room: N230B

Participants

Gary X. Wang, MD, PhD, Boston, MA (*Presenter*) Nothing to Disclose

Sandeep S. Hedgire, MD, Boston, MA (*Abstract Co-Author*) Nothing to Disclose

Thang Le, MD, Cambridge, MA (*Abstract Co-Author*) Nothing to Disclose

Jonathan Sonis, MD, Boston, MA (*Abstract Co-Author*) Nothing to Disclose

Brian Yun, MD, MBA, Boston, MA (*Abstract Co-Author*) Nothing to Disclose

Michael H. Lev, MD, Boston, MA (*Abstract Co-Author*) Consultant, General Electric Company; Institutional Research Support, General Electric Company; Stockholder, General Electric Company; Consultant, MedyMatch Technology, Ltd; Consultant, Takeda Pharmaceutical Company Limited; Consultant, D-Pharm Ltd

Ali Raja, MD, MBA, Boston, MA (*Abstract Co-Author*) Nothing to Disclose
Anand M. Prabhakar, MD, Somerville, MA (*Abstract Co-Author*) Nothing to Disclose

PURPOSE

Though ACR Appropriateness Criteria recommends MRA for suspected acute aortic dissection when CTA is not possible, the feasibility and utility of this strategy in the ED is unclear. This study examines the indications and outcomes of MRA in suspected acute aortic dissection evaluation in the ED.

METHOD AND MATERIALS

This study was completed in an urban, academic Level 1 trauma center. An IRB approved retrospective electronic medical record review identified patients who underwent MRA in the ED for suspected acute thoracic aortic dissection from 2010-2015. Age, gender, clinical assessment, CTA contraindications, MRA results, clinical outcomes, and times of ED arrival and dismissal, and of MRA completion were analyzed.

RESULTS

47 patients (mean age 58 years old) underwent MRA: 19 (40%) due to iodinated contrast allergy, 21 (45%) due to renal insufficiency (eGFR < 30 ml/min/1.73 m² or clinical concern for declining renal function), 2 (4%) due to both, 2 (4%) to spare ionizing radiation, 2 (4%) for further work-up after CTA, and 1 (2%) due to prior contrast-enhanced CT within 24 hours. Mean ED arrival to MRA completion time was 381±279 min. 40 studies were fully diagnostic; 7 were limited. Two (4%) patients had acute dissection on MRA and 45 (96%) had negative exams. 18 (38%) received gadolinium: 14 (78%) had iodinated contrast allergy and none had renal insufficiency. 29 (62%) patients did not receive gadolinium: 21 (72%) had renal insufficiency and 2 (6%) were on hemodialysis; 7 (24%) had iodinated contrast allergy. No significant difference exists in ability to achieve a fully diagnostic MRA with or without gadolinium ($p = 0.225$, Fisher's exact test). 16 (34%) of patients were discharged home from the ED; 2 (4%) were admitted for acute dissection seen on MRA and 29 (62%) for further evaluation after dissection was excluded or to manage an alternative diagnosis.

CONCLUSION

MRA has a clear role in the evaluation for acute thoracic aortic dissection in the ED, where it can guide management and facilitate safe discharge to home. Nearly all MRA exams in this study cohort were performed when CTA was not possible, which follows ACR Appropriateness Criteria and demonstrates its feasibility in the ED.

CLINICAL RELEVANCE/APPLICATION

With increased MRI availability in the ED, MRA can be useful in evaluating suspected acute aortic dissection in ED patients unable to undergo CTA and can allow for safe discharge to home.

RC308-07 Advanced Imaging of Traumatic Thoracic Aortic Emergencies

Tuesday, Nov. 29 10:10AM - 10:40AM Room: N230B

Participants

Martin L. Gunn, MBChB, Seattle, WA, (marting@uw.edu) (*Presenter*) Research Grant, Koninklijke Philips NV; Royalties, Cambridge University Press; Spouse, Consultant, Reed Elsevier; Spouse, Consultant, athenahealth, Inc ;

Active Handout: Martin Lee David Gunn

http://abstract.rsna.org/uploads/2016/16000655/ACTIVE_RC308_07.pdf

LEARNING OBJECTIVES

1) Review multi-modality imaging findings of traumatic thoracic aortic injuries. 2) Describe the most appropriate use of CT in the patient at risk of traumatic aortic injury. 3) Explain recent advances in the understanding of blunt aortic injuries, and current evidence-based management. 4) Identify imaging pitfalls and explain how to differentiate "pseudo-disease" from a true injury.

ABSTRACT

RC308-08 The Incidence and Effect on Mortality of Costochondral Fractures in Blunt Polytrauma Patients- A Review of 1461 Consecutive Whole Body CT Studies for Trauma

Tuesday, Nov. 29 10:40AM - 10:50AM Room: N230B

Awards

Student Travel Stipend Award

Participants

Mari Nummela, MD, Helsinki, Finland (*Presenter*) Nothing to Disclose
Frank Bensch, MD, PhD, Helsinki, Finland (*Abstract Co-Author*) Nothing to Disclose
Seppo K. Koskinen, MD, PhD, Stockholm, Sweden (*Abstract Co-Author*) Nothing to Disclose

PURPOSE

To evaluate the incidence of costal cartilage fractures (CCfx's) in blunt polytrauma patients, related injuries, trauma mechanism and mortality.

METHOD AND MATERIALS

All patients with a history of blunt trauma in a level I trauma center over a period of 36 months were included. All whole body CT (WBCT) studies were initially double read and retrospectively reviewed by a board certified radiologist blinded to initial reports.

RESULTS

A total of 1461 WBCT studies were found, of which 574 (39%) had thoracic injuries (M 425; 74.0%, mean age 46.6 (range 18-91), F 149; 26.0%, mean age 48.9 (range 18-97)). Of these, 118 patients (M 101; 85.6%, mean age 48.8 (range 18-84), F 17; 14.4%

mean age 47.4 (range 20-82)) had a total of 225 CCfx's. The incidence of CCfx's was 8.1% (118/1461) in all WBCT studies and 20.6% (118/574) in thoracic trauma patients. CCfx's were categorized as costochondral (101; 44.9%), midchondral (112; 49.8%) or costosternal (12; 5.3%). Costal cartilages of ribs 6 (37/225; 16.4%) and 7 (38/225; 16.9%) were most commonly injured. Multiple CCfx's were found in 50% (59/118) and 16/118 patients (13.6%) had bilateral CCfx's. No correlation between CC calcifications and fractures was found. However, posttraumatic calcifications were seen adjacent or in the fracture line on follow up CT-studies of 16 patients starting from 21 days after initial trauma. No internal mammary or subclavian artery injuries were detected. Acute traumatic aortic injury was rare (4/118; 3.4%). Multiple bony rib fx's occurred in 96 cases of 118 (81.4%) of which 42 cases had bilateral fx's. Associated intrathoracic injuries were pneumothorax (76; 64.4%), hemothorax (61; 51.7%), and pulmonary contusions (62; 52.5%). Intra-abdominal injuries were seen in 29 patients (24.6%). The main trauma mechanisms were MVA (40; 33.9%) and fall (34; 28.8%). The 30-day mortality of patients with CCfx's was 7.63% (9/118) in comparison to 4.61% (21/456) of patients with no CCfx's (OR 1.71, 95% CI (0.762-3.839)).

CONCLUSION

Costochondral fractures are common in blunt thoracic trauma. CC fx's are related to high-energy trauma; patients with CCfx's had a slightly higher mortality rate than thoracic trauma patients with no CCfx's.

CLINICAL RELEVANCE/APPLICATION

Costochondral fractures increase rib cage instability and often contribute to the formation of a flail chest. They are usually painful and may impair respiratory function of chest trauma patients.

RC308-09 Prognostic Value of CT-derived Left Atrial and Left Ventricular Measures in Patients with Acute Chest Pain

Tuesday, Nov. 29 10:50AM - 11:00AM Room: N230B

Participants

Paul Apfaltrer, MD, Vienna, Austria (*Presenter*) Nothing to Disclose

Rozemarijn Vliegenthart, MD, PhD, Groningen, Netherlands (*Abstract Co-Author*) Nothing to Disclose

U. Joseph Schoepf, MD, Charleston, SC (*Abstract Co-Author*) Research Grant, Astellas Group; Research Grant, Bayer AG; Research Grant, General Electric Company; Research Grant, Siemens AG; Research support, Bayer AG; Consultant, Guerbet SA; ; ;

John W. Nance JR, MD, Baltimore, MD (*Abstract Co-Author*) Nothing to Disclose

Richard A. Takx, MD, Boston, MA (*Abstract Co-Author*) Nothing to Disclose

PURPOSE

The aim of this study was to determine the prognostic value of computed tomography (CT)-derived measures of left ventricular (LV) and left atrial (LA) geometry and function for future major adverse cardiac events (MACE).

METHOD AND MATERIALS

We retrospectively analyzed data of 225 subjects who had undergone coronary CT angiography (CCTA) using a dual-source CT system for acute chest pain evaluation between September 2006 and March 2009. LV mass, LV ejection fraction (EF), LV end-systolic volume (ESV) and LV end-diastolic volume (EDV), LA ESV and LA diameter, septal wall thickness and cardiac chamber diameters were measured. MACE was defined as cardiac death, non-fatal myocardial infarction, unstable angina, or late revascularization. The association between cardiac CT measures and the occurrence of MACE was quantified using Cox proportional hazard analysis, adjusting for traditional risk factors (age, sex, body mass index, hypertension and Framingham risk score), coronary calcium score, and obstructive coronary artery disease on CCTA.

RESULTS

225 subjects (mean age±SD, 56.2±11.2; 140 males) were analyzed, of whom 42 (18.7%) experienced a MACE during a median follow-up of 13 months (range 9-17 months). LA diameter (HR: 1.07, 95% confidence interval [CI] 1.01-1.13 per mm) and LV mass (HR: 1.05, 95% CI 1.00-1.10 per gram) remained significant prognostic factor of MACE after controlling for Framingham risk score. LA diameter and LV mass were also found to have prognostic value independent of each other. The other morphologic and functional cardiac measures were no significant prognostic factors for MACE.

CONCLUSION

CT-derived LA diameter and LV mass are associated with future MACE in patients undergoing evaluation for chest pain, and portend independent prognostic value beyond traditional risk factors, coronary calcium score, and obstructive coronary artery disease on CCTA.

CLINICAL RELEVANCE/APPLICATION

The results of the study indicate that CT-derived left atrial diameter and left ventricular mass are prognostic markers of cardiovascular events in patients with acute chest pain independent of traditional risk factors, coronary calcium score, and obstructive coronary artery disease on coronary CT angiography.

RC308-10 Multi-modality Imaging of Deep Venous Thrombosis

Tuesday, Nov. 29 11:00AM - 11:30AM Room: N230B

Participants

Douglas S. Katz, MD, Mineola, NY, (dkatz@winthrop.org) (*Presenter*) Nothing to Disclose

LEARNING OBJECTIVES

1) To review the multi-modality current imaging of deep venous thrombosis (DVT) of the upper and lower extremities. 2) To review the advantages and disadvantages of the individual modalities for imaging known or suspected DVT in the upper and lower extremities - ultrasound, CT, MR, and conventional venography. 3) To demonstrate typical and less typical examples of acute as well as chronic DVT. 4) To review the potential pitfalls in the imaging of DVT.

ABSTRACT

Honored Educators

Presenters or authors on this event have been recognized as RSNA Honored Educators for participating in multiple qualifying educational activities. Honored Educators are invested in furthering the profession of radiology by delivering high-quality educational content in their field of study. Learn how you can become an honored educator by visiting the website at: <https://www.rsna.org/Honored-Educator-Award/>

Douglas S. Katz, MD - 2013 Honored Educator
Douglas S. Katz, MD - 2015 Honored Educator

RC308-11 A Review of Modified Well's Criteria Score as a Predictor of Lower Limb Venous Thromboembolism

Tuesday, Nov. 29 11:30AM - 11:40AM Room: N230B

Participants

Ronan Waldron, MBCh, Galway, Ireland (*Abstract Co-Author*) Nothing to Disclose
Brian M. Moloney, MBCh, Galway, Ireland (*Presenter*) Nothing to Disclose
Mary Clare Casey, Co Mayo, Ireland (*Abstract Co-Author*) Nothing to Disclose

PURPOSE

We aim to assess the use of the Modified Wells Criteria (MWC) score as a determinant for eligibility for Doppler Ultrasound (DUS) and to determine the diagnostic accuracy of D-Dimers in positively predicting the presence of deep venous thrombosis (DVT)

METHOD AND MATERIALS

All patients who underwent lower limb DUS following suspicion of DVT between November 2012 and September 2014 were reviewed. Pre-imaging MWC score was recorded and D-Dimer result noted if performed.

RESULTS

A total of 764 patients underwent lower limb DUS. 415(54.3%) of patients involved were female. 10.34% (n=80) of those who underwent Lower Limb DUS had a positive finding of DVT. 364 patients had a MWC Score of 2, with a positive result in 23(6.32%). 257 patients had a MWC Score of 3, with a positive result in 24 (9.33%). 114 patients had a MWC score of 4, with a positive result for DVT identified in 21 (18.42%). 29 patients had a MWC score of 5, 9(31.01%) of whom had a DVT. 7 patients had a MWC score of 6, with a positive result for DVT in 3 (42.85%). The most common presenting symptoms were lower limb oedema (n= 731, 95.7%) and pain (n=715, 93.6%). D-Dimer was elevated in all cases it was performed (n=564 (73.8%)). A mean elevation of 6.3 times normal level was recorded with a DVT diagnosed at DUS.

CONCLUSION

Requests for DUS has increased significantly over the past decade in order to provide diagnostic certainty with consequent significant burden on radiology services. The low positive outcome (10.3%) following DUS, as compared to antiquated international comparisons of 12-25% supports suggestions of a deluge in reliance on this investigation for a negative diagnosis. Average pre-test MWC scores suggested the majority of patients were within 'likely range' for existence of a lower limb DVT, which may suggest a need to reassess interpretation of the MWC

CLINICAL RELEVANCE/APPLICATION

Venous thromboembolism is a common cause of morbidity and a potentially fatal complication of hospitalization. DVT is the most common form of venous thrombosis with an estimated incidence of 67 per 100,000 in the general population and a cumulative lifetime incidence of 2 to 5%. The diagnosis of DVT is initially based on clinical suspicion, clinical examination and the use of the MWC. DUS is only indicated to confirm the diagnosis of a DVT in a patient with a MWC score of two or greater. A D-Dimer test may be utilized as an adjunct to an elevated MWC score to support a diagnosis.

RC308-12 Clinical Utility of CT Pulmonary Angiography in the Emergency Department when Providers Override Evidence-Based Clinical Decision Support

Tuesday, Nov. 29 11:40AM - 11:50AM Room: N230B

Awards

Student Travel Stipend Award

Participants

Zihao Yan, BS, Boston, MA (*Presenter*) Nothing to Disclose
Ali Raja, MD, MBA, Boston, MA (*Abstract Co-Author*) Nothing to Disclose
Ivan Ip, MD, MPH, Brookline, MA (*Abstract Co-Author*) Nothing to Disclose
Joshua Kosowsky, MD, Boston, MA (*Abstract Co-Author*) Nothing to Disclose
Jeremiah Schuur, MD, Boston, MA (*Abstract Co-Author*) Nothing to Disclose
Ramin Khorasani, MD, Boston, MA (*Abstract Co-Author*) Consultant, Medicalis Corp

PURPOSE

Assess frequency of clinically useful diagnoses other than pulmonary embolism (PE) found on CT pulmonary angiography (CTPA) in emergency department (ED) patients with suspected PE when providers' imaging request is inconsistent with evidence-based clinical decision support (CDS).

METHOD AND MATERIALS

This Institutional Review Board-approved study was performed at a tertiary-care, academic medical center ED with approximately 60,000 annual visits. We included all adult patients with suspected PE undergoing CTPA between 1/1/2011-8/31/2013. Each order was exposed to CDS based on the Wells Criteria. We compared the frequency of clinically useful alternative diagnoses (alternative diagnoses/ number of CTPAs) when providers overrode CDS alerts (e.g., CTPAs in patients with Well Score (WS) ≤ 4 with normal or no-D-dimer) to orders adherent to CDS (CTPAs in patients with WS > 4 or WS ≤ 4 with elevated D-dimer). We defined clinically useful alternative diagnosis as imaging findings other than PE that could potentially explain the patient's signs and symptoms (e.g. shortness of breath) and result in changes in clinical management within 3 months (e.g. thoracentesis 2 days post-CTPA for pleural

effusion not seen on prior X-ray). Incidental findings resulting in changes in clinical management within 3 months (e.g. newly discovered enlarged mediastinal or hilar lymph nodes resulting in oncology admission) were also included. We hypothesized 20% rate of alternative diagnoses in the CDS adherent group, and 35% in the non-adherent group, requiring a sample size of 138 CTPAs in each group to provide 80% power ($\alpha = 0.05$; two-tailed test). After removing positive PE studies in both groups, 150 CTPAs were randomly selected from each group. We performed patient chart review to investigate existence of alternative diagnosis. Chi-squared test was used for statistical analysis.

RESULTS

Among 2993 CTPA studies, 589 studies were performed against CDS recommendations. The frequency of alternative diagnoses in the override group was 32% (48/150), compared to 15% (22/150) in the adherent group ($p < 0.001$).

CONCLUSION

CTPAs performed against the recommendation of evidence-based CDS were more than twice as likely to result in alternative diagnoses.

CLINICAL RELEVANCE/APPLICATION

CTPA use inconsistent with evidence-based CDS may provide clinical utility in nearly 1/3 of patients, prompting further research to determine if alternative tests would be more optimal in such patients.

RC308-13 Cardiac and Hemodynamic Effects of Arterial Obstruction in Cancer-related Acute Pulmonary Embolism

Tuesday, Nov. 29 11:50AM - 12:00PM Room: N230B

Participants

Juana M. Plasencia-Martinez, MD, Murcia, Spain (*Presenter*) Nothing to Disclose
Alberto Carmona-Bayonas, MD, Murcia, Spain (*Abstract Co-Author*) Nothing to Disclose
David Calvo-Temprano, MD, Oviedo, Spain (*Abstract Co-Author*) Nothing to Disclose
Paula Jimenez-Fonseca, MD, Oviedo, Spain (*Abstract Co-Author*) Nothing to Disclose

PURPOSE

To analyze the impact of acute pulmonary embolism (PE) on right ventricle (RV), and their hemodynamic effects in patients with cancer.

METHOD AND MATERIALS

303 consecutive patients with symptomatic cancer-related PE were ambispectively enrolled in the multicenter (14 hospitals) observational EPIPHANY study. All PEs were diagnosed by computed tomography pulmonary angiography. Arterial obstruction severity was quantified with the Qanadli index (QI). Patients were stratified by PE location as central (trunk, main and/or lobar) or peripheral (segmentary and/or subsegmentary branches). RV-dysfunction signs were defined as dilated RV (≥ 39 mm), increased right-to-left ventricle (RV/LV) diameter ratio (≥ 1) and abnormal (flattened or inverted) interventricular septum (IVS).

RESULTS

Mean QI scores were higher in subjects with dilated RVs (30.4 ± 21.7 vs. 23.6 ± 18.5 , $P = 0.007$) and abnormal IVSs (39.5 ± 20.7 vs. 22.1 ± 18.2 , $P < 0.001$). QI measurements correlated with the RL/LV ratio and RV diameter ($r = 0.39$ and 0.28 , respectively, $P < 0.001$). Correlation between QIs and systemic blood pressure (SBP) was weak overall. However, progressively decreased heart adaptive capacity, as expressed by dilated RVs or abnormal IVSs, QI showed an inverse correlation with SBP that increased gradually ($r = -0.56$, $P = 0.09$; $r = -0.998$, $P < 0.001$, respectively). Correlations between QI measurements, RV/LV ratios and RV diameters were stronger in hypotensive subjects ($r = 0.55$ and $r = 0.64$, respectively, $P < 0.001$). In subjects with RV-dysfunction, the QI increased from normotensive to hypotensive patients (28.7 ± 21.8 vs. 42.1 ± 17.6 , $P = 0.004$). All those effects were unrelated with PE location (central or strictly peripheral).

CONCLUSION

In acute pulmonary embolism, the arterial obstruction index, assessed by Qanadli index, affects the hemodynamic status, but only when the right-sided heart adaptive capacity fails.

CLINICAL RELEVANCE/APPLICATION

The evaluation of right ventricular dilation by CT pulmonary angiography is more useful than the degree of occlusion of the pulmonary vasculature in predicting the outcome of cancer-related pulmonary embolism, likely because it evaluates better the hemodynamic impact of the increased afterload produced by PE on ventricular function, especially in patients with reduced cardiac contractility.

RC309

Gastrointestinal Series: Liver Imaging

Tuesday, Nov. 29 8:30AM - 12:00PM Room: E350

GI

AMA PRA Category 1 Credits™: 3.25
ARRT Category A+ Credits: 3.50

Participants

Mustafa R. Bashir, MD, Cary, NC (*Moderator*) Research support, Siemens AG; Research support, Guerbet SA; Research support, General Electric Company; Imaging Core Lab, NGM Biopharmaceuticals; Imaging Core Lab, TaiwanJ Pharma
Jay P. Heiken, MD, Saint Louis, MO (*Moderator*) Patent agreement, Guerbet SA; Patent agreement, Bayer AG
Frank H. Miller, MD, Chicago, IL (*Moderator*) Research Grant, Siemens AG

Sub-Events

RC309-01 Hypervascular Liver Lesions in Non-cirrhotic Patients

Tuesday, Nov. 29 8:30AM - 8:50AM Room: E350

Participants

Dushyant V. Sahani, MD, Boston, MA (*Presenter*) Research support, General Electric Company; Medical Advisory Board, Allena Pharmaceuticals, Inc

Honored Educators

Presenters or authors on this event have been recognized as RSNA Honored Educators for participating in multiple qualifying educational activities. Honored Educators are invested in furthering the profession of radiology by delivering high-quality educational content in their field of study. Learn how you can become an honored educator by visiting the website at: <https://www.rsna.org/Honored-Educator-Award/>

Dushyant V. Sahani, MD - 2012 Honored Educator
Dushyant V. Sahani, MD - 2015 Honored Educator
Dushyant V. Sahani, MD - 2016 Honored Educator

RC309-02 Distinguishing Benign from Malignant Hyperenhancing Hepatic Nodules in Post-Fontan Patients

Tuesday, Nov. 29 8:50AM - 9:00AM Room: E350

Participants

Michael L. Wells, MD, Rochester, MN (*Presenter*) Nothing to Disclose
David M. Hough, MD, Rochester, MN (*Abstract Co-Author*) Nothing to Disclose
Jeff L. Fidler, MD, Rochester, MN (*Abstract Co-Author*) Nothing to Disclose
Joseph Poterucha, Rochester, MN (*Abstract Co-Author*) Nothing to Disclose
Patrick S. Kamath, MD, Rochester, MN (*Abstract Co-Author*) Nothing to Disclose
Sudhakar K. Venkatesh, MD, FRCR, Rochester, MN (*Abstract Co-Author*) Nothing to Disclose

PURPOSE

Describe the imaging characteristics and pathological etiology of hyperenhancing hepatic nodules arising in post-Fontan patients (pts).

METHOD AND MATERIALS

Post-Fontan pts with hyperenhancing hepatic nodules found at dedicated abdominal multiphasic CT and/or MRI were identified by retrospective review of medical records. Imaging findings were reviewed by consensus agreement of four staff radiologists using LIRADs criteria. Nodules with characteristic imaging findings of focal nodular hyperplasia (FNH) were defined as typical, and nodules with findings associated with hepatocellular carcinoma (HCC) (LIRADS 4 or 5) were defined as atypical. Alpha fetoprotein levels (AFP) and central venous pressures (CVP) were recorded. Eight atypical nodules had histological confirmation.

RESULTS

32 pts, 17 with cirrhosis, had average age of 26.5 years (range 10-41 years) at diagnosis of a liver nodule. CVP was elevated (>8mmHg) in 22/23 (96%) pts. AFP was elevated (>20ng/mL) in 4/27 (15%) pts. 291 hyperenhancing nodules (257 typical, 34 atypical) were detected. 13/32 (41%) pts had one or more atypical nodule. Pts with atypical nodules had significantly higher CVP (19.2 vs 14.2mmHg, P=0.016) and number of nodules (13 vs 4, P=0.01). Atypical nodules showed washout in 33 (portal phase in 7, delayed phase in 33), pseudocapsule in 2, threshold growth in 3, tumor in vein in 1, and ancillary features favoring malignancy in 6 (mosaic architecture in 5). 20 atypical nodules showed washout without additional concerning features. Pathology confirmed HCC in 5 atypical nodules in 4 pts and FNH in 3 atypical nodules in 2 pts and 4 typical nodules in 2 pts. 2 atypical nodules were present in a pt with clinical diagnosis of HCC. Atypical nodules were significantly more likely to be HCC than FNH (either biopsy-proven or stable >24 months without biopsy) when showing portal venous phase washout (P<.001), threshold growth (P=0.006), mosaic architecture (P<.001) or when AFP was elevated (P<.001).

CONCLUSION

Benign masses in Fontan pts may demonstrate washout and be mistaken as HCC by imaging criteria. Portal phase washout, threshold growth, mosaic architecture and elevated AFP were associated with HCC in this population.

CLINICAL RELEVANCE/APPLICATION

Post-Fontan patients with chronic passive hepatic congestion commonly develop benign arterial hyperenhancing masses within the liver which may show washout and be mistaken for HCC.

RC309-03 Dealing with Liver Incidentalomas

Tuesday, Nov. 29 9:00AM - 9:20AM Room: E350

Participants

Jay P. Heiken, MD, Saint Louis, MO, (heikenj@wustl.edu) (*Presenter*) Patent agreement, Guerbet SA; Patent agreement, Bayer AG

LEARNING OBJECTIVES

1) Identify the imaging characteristics of common incidentally discovered liver lesions. 2) Recommend the most appropriate test to characterize an indeterminate incidentally discovered liver lesion. 3) Recognize the differences in risk of an incidentally discovered liver lesion being malignant based on history of extrahepatic malignancy or cirrhosis.

RC309-04 Colorectal Cancer Liver Metastases: Enhancement Pattern on Hepatobiliary Phase of Gadoteric Acid-enhanced MRI and Its Prognostic Value

Tuesday, Nov. 29 9:20AM - 9:30AM Room: E350

Participants

Seunghyun Park, Seoul, Korea, Republic Of (*Presenter*) Nothing to Disclose
Jin-Young Choi, Seoul, Korea, Republic Of (*Abstract Co-Author*) Nothing to Disclose
Honsoul Kim, MD, PhD, Seoul, Korea, Republic Of (*Abstract Co-Author*) Nothing to Disclose
Myeong-Jin Kim, MD, PhD, Seoul, Korea, Republic Of (*Abstract Co-Author*) Research Grant, Bayer AG
Eun Kyung Kim, Seoul, Korea, Republic Of (*Abstract Co-Author*) Nothing to Disclose

PURPOSE

To investigate factors associated with hepatobiliary phase (HBP) enhancement of gadoteric acid-enhanced MRI and whether quantitative and qualitative analysis of HBP images could be used to predict prognosis in patients with liver metastases (LM) from colorectal cancer.

METHOD AND MATERIALS

Ninety-eight patients who underwent surgical resection for LM were retrospectively analyzed. We evaluated HBP enhancement pattern of LM, qualitatively and classified into mixed and clearly hypointense groups. For quantitative measurement, 4 parameters were calculated by the following equations. (1) Relative intensity ratio on HBP image (RIRpost) = SI of the nodule/SI of the liver parenchyma on HBP image. (2) Relative intensity ratio on precontrast image (RIRpre). (3) Relative enhancement ratio (RER) = RIRpost/RIRpre. (4) Contrast to noise ratio (CNR). To investigate factors associated with HBP enhancement, the amount of tumor components (fibrosis, necrosis, tumor cellularity) was scored on a semi-quantitative 4 point scale. Immunohistochemistry was performed to evaluate the presence of organic anionic transporting polypeptide 1B3 (OATP1B3). Univariate and multivariate analyses were done to determine significant factors for visual enhancement in both subgroups based on preoperative chemotherapy. Overall survival and disease-free survival after tumor removal were analyzed using Kaplan-Meier method and differences in survival curve were analyzed using the log-rank test.

RESULTS

Of the total 98 nodules, mixed and clearly hypointense group was 67 (68%), and 31 nodules (32%), respectively. In surgically resected 55 nodules without preoperative chemotherapy, a multivariate analysis revealed that OATP1B3 expression was the only significant factor regarding the HBP enhancement (P= 0.049). In this subgroup, nodules with OATP1B3 expression showed significantly higher RIRpost and RER than nodules without OATP1B3 expression (P= 0.0285, 0.0014, respectively). Mixed hypointense group showed worse survival rate and disease free survival rate with statistical significance (P= 0.0169, 0.0466, respectively).

CONCLUSION

The enhancement pattern of CRLM could be associated with OATP1B3 expression in non-chemotherapy group. The quantitative and qualitative analyses of enhancement patterns on HBP may predict prognosis in patients with CRLM.

CLINICAL RELEVANCE/APPLICATION

HBP may predict prognosis in patients with CRLM and is recommended before making treatment plan.

RC309-05 The Difficult Hepatocellular Carcinoma

Tuesday, Nov. 29 9:30AM - 9:50AM Room: E350

Participants

Cher Heng Tan, MBBS, FRCR, Singapore, Singapore, (Cher_Heng_Tan@ttsh.com.sg) (*Presenter*) Nothing to Disclose

LEARNING OBJECTIVES

1) Relate the classic imaging features of hepatocellular carcinoma (HCC) to its histological characteristics. 2) Explain the limitations of the criteria set forth by current clinical guidelines for the imaging diagnosis of HCC. 3) Assess the potential of diffusion weighted MRI and hepatocyte specific contrast MRI agents for improving detection of HCC.

ABSTRACT

Hepatocellular carcinoma (HCC) is widely known for its association with chronic hepatitis and liver cirrhosis. The classic imaging features of HCC can be explained by its unique histological characteristics. This enables patients to proceed to definitive treatment without lesion biopsy, provided that specific criteria for imaging diagnosis are met. However, due to the heterogeneous nature of HCC, non-classical imaging findings are frequently encountered. Diffusion weighted MRI and hepatocyte specific contrast MRI agents may play a bigger role in imaging diagnosis in such instances.

Active Handout: Cher Heng Tan

http://abstract.rsna.org/uploads/2016/16000479/The_Difficult_HCC_Cher_Heng_Tan_handouts.pdf

RC309-06 Added Value of Peripheral Dark Rim in the Hepatobiliary Phase of Gadoteric Acid-enhanced MRI in Detecting Capsule and Diagnosing Hepatocellular Carcinoma

Tuesday, Nov. 29 9:50AM - 10:00AM Room: E350

Participants

Chae Jung Park, MD, Seoul, Korea, Republic Of (*Presenter*) Nothing to Disclose
Chansik An, MD, Seoul, Korea, Republic Of (*Abstract Co-Author*) Nothing to Disclose
Sungwon Kim, MD, Seoul, Korea, Republic Of (*Abstract Co-Author*) Nothing to Disclose
Sumi Park, MD, Seoul, Korea, Republic Of (*Abstract Co-Author*) Nothing to Disclose
Song-Ee Baek, MD, Seoul, Korea, Republic Of (*Abstract Co-Author*) Nothing to Disclose
Yeun Yoon Kim, MD, Seoul, Korea, Republic Of (*Abstract Co-Author*) Nothing to Disclose
Myeong-Jin Kim, MD, PhD, Seoul, Korea, Republic Of (*Abstract Co-Author*) Research Grant, Bayer AG

PURPOSE

To examine the added value of peripheral smooth dark rim in the hepatobiliary phase (HBP) of gadoteric acid-enhanced magnetic resonance imaging (MRI) in detecting tumor capsule and in diagnosing hepatocellular carcinoma (HCC).

METHOD AND MATERIALS

Between Jan 2008 and Dec 2011, 349 consecutive patients at risk for HCC underwent hepatic resection after gadoteric acid-enhanced MRI at a single tertiary hospital. A total of 379 pathologically confirmed hepatic lesions from these patients were our final study subjects: 330 HCCs, 35 non-HCC malignancies, and 13 benign lesions. For each hepatic lesion, two abdominal radiologists determined in consensus the presence or absence of arterial enhancement, washout, conventional capsule appearance (defined as peripheral rim of smooth hyper-enhancement in the portal or delayed phase), and HBP capsule appearance (defined as peripheral smooth dark rim in the HBP), as well as Liver Imaging Reporting and Database system (LI-RADS) category (LR-5 and LR-5V were considered positive for HCC). Diagnostic accuracy was compared using generalized estimating equation method.

RESULTS

Using the results of pathologic examination as the reference standard, 249 (75.5%) of 330 HCCs and 8 (16.7%) of 48 non-HCC lesions had fibrous capsules. Diagnostic accuracy for the presence of fibrous capsule was significantly higher when the presence of either conventional or HBP capsule appearance was considered positive than when only conventional capsule appearance was considered (54% vs. 70.9%, $P < 0.001$). Diagnostic accuracy of LI-RADS for HCC was also significantly higher when HBP capsule appearance was included for the definition of capsule appearance in addition to conventional capsule appearance (61.4% vs. 79.4%, $P < 0.001$).

CONCLUSION

Peripheral smooth dark rim seen in the HBP should be included for the definition of capsule appearance on gadoteric acid-enhanced MRI.

CLINICAL RELEVANCE/APPLICATION

Capsule appearance can be masked when hepatobiliary contrast agents are used. This may be overcome by using the smooth dark rim in hepatobiliary phase as a complement to conventional capsule appearance.

RC309-07 Long-term Observation of Hypovascular Hypointense Nodules (HHNs) on Gadoteric Acid-enhanced MRI

Tuesday, Nov. 29 10:00AM - 10:10AM Room: E350

Participants

Tatsuya Shimizu, MD, Yamanashi, Japan (*Presenter*) Nothing to Disclose
Utaroh Motosugi, MD, Yamanashi, Japan (*Abstract Co-Author*) Nothing to Disclose
Katsuhiko Sano, MD, PhD, Chuo, Japan (*Abstract Co-Author*) Nothing to Disclose
Shintaro Ichikawa, MD, Chuo-Shi, Japan (*Abstract Co-Author*) Nothing to Disclose
Hiroshi Onishi, MD, Yamanashi, Japan (*Abstract Co-Author*) Nothing to Disclose

PURPOSE

Hepatocellular carcinomas (HCCs) commonly develop via multistep carcinogenesis, which first appear as hypovascular HCCs also known as early HCCs. Early HCCs show hypointensity on gadoteric acid-enhanced hepatobiliary phase images. In this study, we call these nodules "hypovascular hypointense nodule (HHN)". We investigated outcomes of HHNs with long-term observation, and conducted a retrospective study to perform risk analysis of development of hypervascular HCC from HHNs (hypervascularization).

METHOD AND MATERIALS

We reviewed the radiological records about the patients who underwent gadoteric acid-enhanced MRI for the purpose of screening for HCC at our hospital from February 2008 to February 2011. We included all patients who had HHN and follow-up MRI (222 HHNs in 92 patients). Endpoint of this study was the development of hypervascular HCC in the liver. Risk factors of hypervascular HCC were analyzed by univariate and multivariate Cox proportional hazard model with the following factors: age, sex, tumor size, signal intensity on T2-weighted images and fat-saturated T1-weighted images, fat-containing appearance on opposed-phase T1-weighted images, growth rate in size. The incidence rate of hypervascular HCC was assessed using Kaplan-Meier curves.

RESULTS

Median of observation period was 775 days (184-2858). During the follow-up, 123 HHNs became hypervascular HCCs. Incidence rate of hypervascularization at 3 years and 5 years were 41.21% and 68.61%, respectively. Multivariate analysis revealed that, fat-saturated T1-weighted images (1.85 [1.09 - 3.08]), larger tumor size (>10mm, 1.56 [1.01 - 2.41]) were the independent risk factors of hypervascularization.

CONCLUSION

Cumulative rate of hypervascularization from HHNs were ever-increasing over 5 years. Size of >10 mm were one of the independent

risk of becoming hypervascular HCCs.

CLINICAL RELEVANCE/APPLICATION

Cirrhotic patients with large hypovascular hypointense nodules on gadoxetic acid-enhanced MRI should be intensely followed up, especially when the size is large ($\geq 10\text{mm}$).

RC309-08 Assessing the Risk of Developing Hepatocellular Carcinoma by Gadoxetic Acid-enhanced MRI and MR Elastography: A Prospective Study

Tuesday, Nov. 29 10:10AM - 10:20AM Room: E350

Participants

Tatsuya Shimizu, MD, Yamanashi, Japan (*Presenter*) Nothing to Disclose
Utaroh Motosugi, MD, Yamanashi, Japan (*Abstract Co-Author*) Nothing to Disclose
Shintaro Ichikawa, MD, Chuo-Shi, Japan (*Abstract Co-Author*) Nothing to Disclose
Hiroshi Onishi, MD, Yamanashi, Japan (*Abstract Co-Author*) Nothing to Disclose

PURPOSE

Hypovascular hypointense nodules (HHNs) in the liver, as depicted in gadoxetic acid-enhanced hepatobiliary phase (HBP) images, and higher liver stiffness in MR elastography are risk factors for hepatocellular carcinoma (HCC) development in patients with chronic liver disease. In this study, we conducted a prospective study to investigate whether those MR features are risk factors for HCC.

METHOD AND MATERIALS

From March 2012 to May 2014, 110 chronic liver disease patients without a history of HCC were prospectively enrolled. All patients underwent MRI for screening HCC. The patients were classified on the basis of presence of HHN in the liver on gadoxetic acid-enhanced HBP images (present [non-clean liver], $n=34$; absent [clean liver], $n=76$), and stiffness value by MR elastography (soft liver, $<4.0\text{kPa}$, $n=53$; and stiff liver, $\geq 4.0\text{kPa}$, $n=45$). Risk factors for incidence of hypervascular HCC were analyzed by univariate and multivariate Cox regression analyses of the following factors: age, gender, liver cirrhosis, fatty liver, alcohol abuse, diabetes mellitus, non-clean liver, stiff liver. Then, we calculated the incidence rates of hypervascular HCC using Kaplan–Meier curves. The log-rank tests were used to analyze significant differences.

RESULTS

During the follow-up period (median, 25.0 months), 16 patients developed HCC. Patients with non-clean liver showed higher incidence of HCC compared to those with clean liver (3 year HCC incidence rates, 52.0% and 6.4%; $p<0.05$). However, no significant difference in incidence of HCC was observed between patients with soft and stiff livers. Cox-proportional model analysis revealed that non-clean liver was an independent risk of HCC development, with a relative risk of 18.75 (95%CI, 4.83–128.63, $p<0.0001$).

CONCLUSION

Patients showing HHNs on gadoxetic acid-enhanced HBP images are at high risk for developing HCC.

CLINICAL RELEVANCE/APPLICATION

Hypovascular hypointense nodule (HHN) on gadoxetic acid-enhanced MRI is a strong indicator of subsequent development of hypervascular HCCs in patients with chronic liver disease.

RC309-09 Diffuse Liver Disease: Fat and Iron

Tuesday, Nov. 29 10:40AM - 11:00AM Room: E350

Participants

Aliya Qayyum, MBBS, Houston, TX (*Presenter*) Spouse, Founder, In Context Reporting

RC309-10 Hepatic Proton Density Fat Fraction Measurements: Same-Day Agreement between Readers and Across Scanner Manufacturers

Tuesday, Nov. 29 11:00AM - 11:10AM Room: E350

Participants

Suraj Serai, PhD, Cincinnati, OH (*Abstract Co-Author*) Nothing to Disclose
Jonathan R. Dillman, MD, Cincinnati, IA (*Abstract Co-Author*) Research Grant, Siemens AG; Research Grant, Guerbet SA; Travel support, Koninklijke Philips NV; Research Grant, Toshiba
Andrew T. Trout, MD, Cincinnati, OH (*Presenter*) Advisory Board, Koninklijke Philips NV; Travel support, Koninklijke Philips NV; Author, Reed Elsevier; Research Grant, Siemens AG

PURPOSE

Given the accuracy of MRI based proton density fat-fraction (PDFF) sequences in determination of hepatic steatosis. These sequences may ultimately replace biopsy for the diagnosis & monitoring of patients with steatosis and may serve to monitor response to treatment. This is particularly important for long-term follow-up as patients may be imaged on different scanners and possibly at different field strengths. The purpose of this study was to examine the agreement of hepatic MRI based PDFF measurements between readers, scanner manufacturers and field strengths.

METHOD AND MATERIALS

Following informed consent, 24 adult volunteers were scanned on one 1.5T (Philips) & two different 3T (GE 750W & Philips) MR scanners on the same day in order to estimate hepatic PDFF. A single breath-hold Dixon-based acquisition was performed (mDIXON Quant [Philips], IDEAL IQ [GE]). One large region of interest (ROI), inclusive of as much liver parenchyma as possible in the right lobe while avoiding large vessels, was placed by 5 readers on scanner generated parametric maps to measure PDFF. Two-way ICCs were used to assess inter-reader agreement and agreement across 3 scanner platforms.

RESULTS

There was excellent inter-reader agreement for hepatic PDFF measurements obtained using mDIXON Quant on the Philips 1.5T scanner (ICC = 0.995, 95% CI: 0.991–0.998), mDIXON Quant on the Philips 3T scanner (ICC = 0.992, 95% CI: 0.986–0.996), and IDEAL IQ on the GE 3T scanner (ICC = 0.966, 95% CI: 0.939–0.984). Individual reader (n=5) ICCs for hepatic PDFF measurements across all three scanner manufacturer/field strength combinations also showed excellent inter-scanner agreement, ranging from 0.917 to 0.942.

CONCLUSION

Our study shows that hepatic PDFF estimation using mDIXON Quant and IDEAL IQ is highly reproducible across MRI scanner platforms (including different manufacturers & field strengths), with only minimal average bias. Additionally, PDFF measurement made by multiple readers show excellent inter-reader agreement.

CLINICAL RELEVANCE/APPLICATION

PDFF is a robust and reliable noninvasive biomarker of hepatic steatosis that will likely be increasingly important in the initial assessment and follow-up of fatty liver disease. Furthermore, it is also likely that this technique will play an important role in the evaluation of pharmacologic therapies that are currently under development for the treatment of fatty liver disease, serving as a noninvasive, radiologic surrogate end-point.

Honored Educators

Presenters or authors on this event have been recognized as RSNA Honored Educators for participating in multiple qualifying educational activities. Honored Educators are invested in furthering the profession of radiology by delivering high-quality educational content in their field of study. Learn how you can become an honored educator by visiting the website at: <https://www.rsna.org/Honored-Educator-Award/>

Jonathan R. Dillman, MD - 2016 Honored Educator

RC309-11 Metabolic Effects Resulting from Changes of Liver Volume, Intrahepatic Fat and Body Weight in the Course of a Lifestyle Interventional Study

Tuesday, Nov. 29 11:10AM - 11:20AM Room: E350

Participants

Malte N. Bongers, MD, Tuebingen, Germany (*Presenter*) Nothing to Disclose
Norbert Stefan, Tubingen, Germany (*Abstract Co-Author*) Nothing to Disclose
Hans-Ulrich Haering, Tuebingen, Germany (*Abstract Co-Author*) Nothing to Disclose
Andreas Fritsche, Tuebingen, Germany (*Abstract Co-Author*) Nothing to Disclose
Konstantin Nikolaou, MD, Tuebingen, Germany (*Abstract Co-Author*) Speakers Bureau, Siemens AG; Speakers Bureau, Bracco Group; Speakers Bureau, Bayer AG
Fritz Schick, MD, PhD, Tuebingen, Germany (*Abstract Co-Author*) Nothing to Disclose
Juergen Machann, MD, Tuebingen, Germany (*Abstract Co-Author*) Nothing to Disclose

PURPOSE

To investigate associations between changes of liver volume, intrahepatic lipids (IHL) and body weight during lifestyle intervention and to delineate effects on metabolic markers of liver function and systemic low grade-inflammation.

METHOD AND MATERIALS

Participants were retrospectively selected from prospective cohort studies, characterizing the risk of developing a type 2 diabetes mellitus. All participants followed a caloric restriction diet for 6-9 months. 66 females and 45 males, mean age 48 years (22–71years) with an average body mass index (BMI) of 31kg/m² (20–47kg/m²) were enrolled. The liver volume was determined using three-dimensional MRI (figure 1, A) and IHL were quantified by volume-selective 1H-MRS (figure 1, B). Liver enzymes and high sensitive C-reactive protein (hsCRP) as surrogate marker for systemic low grade inflammation were determined. Gender stratified correlation analyses were performed.

RESULTS

Δ LV was significantly correlated with Δ IHL in females and males (females: $r=0.64$, $p<.0001$; males: $r=0.51$, $p<.005$). Δ LV was significantly associated with Δ GGT in both genders (females: $r=0.36$, $p=0.005$; male: $r=0.5$, $p=0.001$), but not associated with Δ BW. In females, a significant correlation between Δ IHL and Δ GGT ($r=0.45$, $p<.005$) respectively Δ ALT ($r=0.28$, $p=0.02$) was present. Males showed a significant correlation between Δ IHL and Δ ALT ($r=0.49$, $p<.005$) and Δ AST ($r=0.40$, $p=0.008$). In females, but not in males a significant association between Δ IHL and Δ CRP could be identified (females: $r=0.45$, $p<.005$).

CONCLUSION

The change of liver volume during lifestyle intervention is independent of change in body weight and is primarily determined by the change of IHL. Changes of liver volume seems to be directly connected to changes of GGT in both genders. Reduction of IHL seems to have gender-specific effects on liver enzymes, mainly reducing GGT in females and ALT in males as well as having a positive effect in reducing the systemic low grade inflammation only in females. These results of a lifestyle intervention show the reversibility of augmented liver volume in steatosis and the resulting gender-specific benefits on metabolism.

CLINICAL RELEVANCE/APPLICATION

Knowing the details about hepatic steatosis and the effects on liver volume, liver function and systemic low-grade inflammation is of highest importance to determine effective lifestyle interventions.

RC309-12 MR Elastography and Liver Fibrosis

Tuesday, Nov. 29 11:20AM - 11:40AM Room: E350

Participants

Frank H. Miller, MD, Chicago, IL, (fmiller@northwestern.edu) (*Presenter*) Research Grant, Siemens AG

LEARNING OBJECTIVES

1) Understand the role of MR elastography in the diagnosis of hepatic fibrosis and cirrhosis. 2) Understand the advantages and limitations of MR elastography. 3) Recognize uncommon causes of elevated stiffness.

ABSTRACT

MR imaging plays an important role in the diagnosis of cirrhosis and hepatic. Invasive biopsy is currently the standard approach to diagnosis and stage liver fibrosis and inflammation. Biopsies however are invasive, prone to sampling error and poor patient acceptance. Magnetic resonance elastography can measure fibrosis-associated changes in liver stiffness. MR elastography is rapid and allows differentiation between the different stages of fibrosis and can be easily added to conventional liver MR examinations. Studies in the literature using MR elastography to assess hepatic fibrosis will be discussed. Comparisons with conventional imaging features of cirrhosis will be described. The role of MR elastography will also be discussed in diagnosing conditions such as nonalcoholic steatohepatitis in patients with nonalcoholic fatty liver disease. Uncommon causes of elevated hepatic stiffness values on MR elastography will be discussed. In addition, challenges faced with MR elastography including iron overload will be discussed.

Honored Educators

Presenters or authors on this event have been recognized as RSNA Honored Educators for participating in multiple qualifying educational activities. Honored Educators are invested in furthering the profession of radiology by delivering high-quality educational content in their field of study. Learn how you can become an honored educator by visiting the website at: <https://www.rsna.org/Honored-Educator-Award/>

Frank H. Miller, MD - 2012 Honored Educator

Frank H. Miller, MD - 2014 Honored Educator

RC309-13 Test-Retest Repeatability of Magnetic Resonance Elastography of Liver-A Meta-Analysis

Tuesday, Nov. 29 11:40AM - 11:50AM Room: E350

Participants

Suraj Serai, PhD, Cincinnati, OH (*Presenter*) Nothing to Disclose

Nancy A. Obuchowski, PhD, Cleveland, OH (*Abstract Co-Author*) Research Consultant, Siemens AG; Research Consultant, QT Ultrasound Labs; Research Consultant, Elucid Bioimaging Inc

Sudhakar K. Venkatesh, MD, FRCR, Rochester, MN (*Abstract Co-Author*) Nothing to Disclose

Claude B. Sirlin, MD, San Diego, CA (*Abstract Co-Author*) Research Grant, General Electric Company; Research Grant, Siemens AG; Research Grant, Guerbet SA; ;

Patricia E. Cole, MD, PhD, East Hanover, NJ (*Abstract Co-Author*) Nothing to Disclose

Edward Ashton, Pittsford, NY (*Abstract Co-Author*) Officer, VirtualScopics, Inc

Mark Palmeri, MD, PhD, Durham, NC (*Abstract Co-Author*) Nothing to Disclose

Frank H. Miller, MD, Chicago, IL (*Abstract Co-Author*) Research Grant, Siemens AG

Richard L. Ehman, MD, Rochester, MN (*Abstract Co-Author*) CEO, Resoundant, Inc; Stockholder, Resoundant, Inc;

PURPOSE

Magnetic resonance elastography (MRE) is a non-invasive tool for staging liver fibrosis and is suitable for repeated use, to assess disease progression & treatment response. Multiple studies of the test-retest repeatability of MRE have been published. The purpose of this work was to conduct a critical meta-analysis to generate a summary estimate of the repeatability coefficient from these multiple studies. This work was conducted to develop a longitudinal MRE "claim" by the RSNA QIBA MRE workgroup.

METHOD AND MATERIALS

A systematic search of PubMed, EMBASE, SCORPUS, Cochrane, Web of Science, CINAHL and Google scholar databases was performed for publications on MRE during the ten year period 2006-2015 at two major institution libraries. Studies performed on humans & published in English or translations available were included. The following data were extracted: (1) Author, journal and year of publication; (2) within-subject Coefficient of variation (wCV); (3) number of subjects; (4) number of readers; and (5) notes on method used to calculate the wCV. Two reviewers independently determined the percent repeatability coefficient (%RC) and effective sample size from each article. The wCV were recalculated & validated as reported. A forest plot was constructed of the %RC estimates from the various studies. A 95% percentile bootstrap confidence interval (CI) was constructed for the summary %RC.

RESULTS

Library 1 search found 309 articles and library 2 search found 350 articles. Duplicate articles were removed and a list of 450 articles was collected in a single end note library. The identified studies were screened independently and then verified reciprocally by two observers. Twelve studies comprising of 299 patients met the inclusion criteria and were included for analysis. The studies %RC ranged from 10 to 37% (Figure 1). The estimated summary RC was 22.2%, with 95% CI of [16.4 – 27.8].

CONCLUSION

An accurate assessment of the degree of hepatic fibrosis has therapeutic & prognostic implications. The meta-analysis results provide the basis for the following draft longitudinal QIBA MRE claim: a measured change in hepatic stiffness of 22% or greater indicates that a true change in stiffness has occurred with 95% confidence.

CLINICAL RELEVANCE/APPLICATION

Our estimated Meta-analysis summary RC for MRE was 22.2% with 95% CI of [16.4–27.8]. Assuming no change in MRE hardware & software, a measured change exceeding the RC can be considered a true change over time.

Honored Educators

Presenters or authors on this event have been recognized as RSNA Honored Educators for participating in multiple qualifying educational activities. Honored Educators are invested in furthering the profession of radiology by delivering high-quality educational content in their field of study. Learn how you can become an honored educator by visiting the website at: <https://www.rsna.org/Honored-Educator-Award/>

Frank H. Miller, MD - 2012 Honored Educator
Frank H. Miller, MD - 2014 Honored Educator
Richard L. Ehman, MD - 2016 Honored Educator

RC309-14 Comparing the Accuracy of Magnetic Resonance Elastography with that of Liver Biopsy Samples for Diagnosing Liver Fibrosis

Tuesday, Nov. 29 11:50AM - 12:00PM Room: E350

Participants

Hiroyuki Morisaka, MD, Kofu, Japan (*Presenter*) Nothing to Disclose
Utaroh Motosugi, MD, Yamanashi, Japan (*Abstract Co-Author*) Nothing to Disclose
Shintaro Ichikawa, MD, Chuo-Shi, Japan (*Abstract Co-Author*) Nothing to Disclose
Tadao Nakazawa, MD, PhD, Chuo, Japan (*Abstract Co-Author*) Nothing to Disclose
Tetsuo Kondo, MD, PhD, Chuo, Japan (*Abstract Co-Author*) Nothing to Disclose
Masanori Matsuda, MD, Yamanashi, Japan (*Abstract Co-Author*) Nothing to Disclose
Katsuhiko Sano, MD, PhD, Chuo, Japan (*Abstract Co-Author*) Nothing to Disclose
Tomoaki Ichikawa, Hidaka-shi, Japan (*Abstract Co-Author*) Nothing to Disclose

PURPOSE

Liver biopsy for the staging of liver fibrosis has some clinical concerns: sampling errors, inter-observer variability, and rare but serious complications. Sampling error can happen in the assessment of biopsy specimen, because liver fibrosis is heterogeneous. Therefore, large volume of non-tumorous liver tissue as obtained by surgical resection is necessary for correct staging of liver fibrosis. In this study, we aimed to compare the diagnostic accuracy of magnetic resonance elastography (MRE) and liver biopsy for liver fibrosis staging by using surgically resected liver specimens as a standard of reference.

METHOD AND MATERIALS

This retrospective study included 170 patients with normal liver and chronic liver disease who underwent preoperative MRE on a 1.5 or 3-Tesla clinical MR scanner and subsequent surgical liver resection. Fifty patients, 10 patients each for 5 fibrosis stages (F0-F4) corresponding to the METAVIR scoring system, were used to calculate optimal threshold liver stiffness values (kPa) and mean and standard deviation of liver stiffness in each 5 liver fibrosis stage. Liver biopsy samples were directly obtained from surgically resected liver tissues in the other 120 patients by using an 18-gauge biopsy needle. Liver fibrosis was graded by a pathologist by using Masson trichrome stain. Liver stiffness of the 120 patients was then measured using MRE, and these results were used to make MRE-based fibrosis staging by using the threshold and Bayesian prediction methods. Diagnostic accuracy was determined as the proportion of correct staging of liver fibrosis with use of whole tissue specimens as reference standards. The equivalence in accuracy between liver biopsy samples and the threshold and Bayesian prediction MRE methods within a given range of $\pm 20\%$ was tested using a modified McNemar's test.

RESULTS

Diagnostic accuracy of liver fibrosis stages were 51.6% [62/120] for liver biopsy samples, 50.8% [61/120] for MRE with threshold method, and 56.6% [68/120] for MRE with the Bayesian prediction method. The diagnostic accuracies of both MRE-based methods were not inferior to that of liver biopsy ($p < 0.009$), indicating that diagnostic accuracies of liver biopsy samples and MRE-based methods were statistically similar.

CONCLUSION

MRE provides equal diagnostic accuracy as liver biopsy for staging liver fibrosis.

CLINICAL RELEVANCE/APPLICATION

Liver MRE can be used as an alternative to liver biopsy in clinical practice.

RC310

First Trimester Ultrasound

Tuesday, Nov. 29 8:30AM - 10:00AM Room: S402AB



AMA PRA Category 1 Credits™: 1.50
ARRT Category A+ Credits: 1.50

Participants

Active Handout: Carol Beer Benson

http://abstract.rsna.org/uploads/2016/16000395/ACTIVE_RC310.pdf

Sub-Events

RC310A Ectopic Pregnancy

Participants

Peter M. Doubilet, MD, PhD, Boston, MA (*Presenter*) Nothing to Disclose

LEARNING OBJECTIVES

1) More accurately diagnose tubal ectopic pregnancies. 2) Diagnose unusual ectopic pregnancies, including cervical and interstitial pregnancies. 3) Distinguish early intrauterine pregnancy from ectopic pregnancy.

ABSTRACT

Active Handout: Peter Michael Doubilet

http://abstract.rsna.org/uploads/2016/16000396/rc310a_Doubilet-Ectopic_Pregnancy_handout.pdf

RC310B Diagnosis of Failed Pregnancy

Participants

Mindy M. Horrow, MD, Philadelphia, PA, (horrowm@einstein.edu) (*Presenter*) Spouse, Employee, Merck & Co, Inc

LEARNING OBJECTIVES

1) Review normal embryonic development in the first trimester. 2) Describe issues related to safe interpretation of first trimester pregnancy including definitely normal, definitely abnormal and indeterminate findings that require follow up. 3) List criteria that are diagnostic for pregnancy failure and distinguish from those that are suspicious for pregnancy failure.

ABSTRACT

Honored Educators

Presenters or authors on this event have been recognized as RSNA Honored Educators for participating in multiple qualifying educational activities. Honored Educators are invested in furthering the profession of radiology by delivering high-quality educational content in their field of study. Learn how you can become an honored educator by visiting the website at: <https://www.rsna.org/Honored-Educator-Award/>

Mindy M. Horrow, MD - 2013 Honored Educator
Mindy M. Horrow, MD - 2016 Honored Educator

RC310C Mid-late First Trimester

Participants

Carol B. Benson, MD, Boston, MA (*Presenter*) Nothing to Disclose

LEARNING OBJECTIVES

1) Recognize the importance of evaluating the developing fetal head during the late first trimester for early detection of large neural tube defects. 2) Incorporate measurement of the nuchal translucency into their assessment of the fetuses of gestational age 11-14 weeks. 3) Recognize sonographic abnormalities of the ventral wall to distinguish normal physiologic bowel herniation from defects including omphalocele and gastroschisis.

ABSTRACT

This lecture will discuss the sonographic appearance of fetal anatomy in the latter part of the third trimester in order to help participants recognize abnormalities of the fetus at this early gestational age. While many anomalies cannot be detected until later in pregnancy, the discussion will focus on those anomalies that can be detected in the first trimester. Specific topics covered will be central nervous system anomalies, including anencephaly, encephalocele and holoprosencephaly, ventral wall defects including omphalocele and gastroschisis, bladder outlet obstruction, and skeletal anomalies including skeletal dysplasias. Detection of anomalies early in gestation, before the second trimester, permits time to assess the fetus for other anomalies, syndromes, and aneuploidy.

RC311

Nuclear Medicine Series: Assessment of Cancer Treatment Response: Updates

Tuesday, Nov. 29 8:30AM - 12:00PM Room: S505AB



AMA PRA Category 1 Credits™: 3.50
ARRT Category A+ Credits: 4.00

FDA Discussions may include off-label uses.

Participants

Haesun Choi, MD, Houston, TX, (hchoi@mdanderson.org) (Moderator) Nothing to Disclose

LEARNING OBJECTIVES

1) The currently available response evaluation criteria of solid tumors and its limitations. 2) New concept of response evaluation of solid tumors. 3) Future of response evaluation of solid tumors.

ABSTRACT

Sub-Events

RC311-01 Response Assessment Recommendations in Solid Tumors: RECIST vs PERCIST

Tuesday, Nov. 29 8:30AM - 9:00AM Room: S505AB

Participants

Heather Jacene, MD, Boston, MA (Presenter) Nothing to Disclose

LEARNING OBJECTIVES

1) To compare anatomic and metabolic imaging for response assessment. 2) To discuss limitations of current widely used criteria for assessing response. 3) To discuss the benefits and limitations of metabolic imaging for response assessment.

ABSTRACT

RC311-02 Fasting Glucose Level Observations in Oncologic FDG PET - A 10 Year Multi-Institutional Review Based on NCTN Clinical Trials

Tuesday, Nov. 29 9:00AM - 9:10AM Room: S505AB

Participants

Katherine Binzel, PhD, Columbus, OH (Presenter) Nothing to Disclose
David Poon, BS, Columbus, OH (Abstract Co-Author) Nothing to Disclose
Preethi Subramanian, MS, BEng, Columbus, OH (Abstract Co-Author) Nothing to Disclose
Tim Sbory, BS, Columbus, OH (Abstract Co-Author) Nothing to Disclose
Marcel M. Knopp, Atlanta, GA (Abstract Co-Author) Nothing to Disclose
Michael V. Knopp, MD, PhD, Columbus, OH (Abstract Co-Author) Nothing to Disclose
Chadwick L. Wright, MD, PhD, Lewis Center, OH (Abstract Co-Author) Nothing to Disclose
Jun Zhang, PhD, Columbus, OH (Abstract Co-Author) Nothing to Disclose

PURPOSE

While it is standard practice to determine the blood glucose level at the time of FDG PET imaging, no current assessment reports on trends and observations and changes exist. We utilized access to the clinical trial data of the National Clinical Trial Network to develop a 10 year perspective.

METHOD AND MATERIALS

Patient blood glucose levels (BGL) are routinely determined as point of care testing to insure eligibility as most FDG PET protocols require a confirmation that the level is not above 200 mg/dl. Within the quality assurance assessment we perform for clinical trials within the NCI cooperative groups (NCTN), we record and assess the BGL. We developed query tools and pivot tables to assess the distribution and changes over time for BGL. We analyzed a portfolio of 5 clinical trials that include FDG PET within the last 10 years and evaluated more than 2000 examinations.

RESULTS

The distribution of fasting BGLs for each study included in our analysis were fairly similar. In general, BGLs were found to be within the limit of 200 mg/dL required for compliance within each clinical trial protocol. We found trends that point to population differences in regard to disease state and therapeutic status. Consistently, more than 90% of subjects had a BGL less than 150 at the time of injection, A representative trial including 411 FDG PET examinations found an average BGL at 107 ± 24 mg/dL, range was between 59 and 212 mg/dL. The majority of subjects had a BGL below 110 at the time of injection, less than one third of subjects had a BGL above 110, and only 8% had a BGL above 150. Overall, only 0.5% of studies had BGL above the threshold level. There were no significant trends found relating BGL to recorded fasting time.

CONCLUSION

On average, blood glucose levels of patients enrolled in these clinical trials were below 110 mg/dL at the time of injection. Overall protocol compliance is exceptional, however stricter BGL limits could be achieved with a reduced threshold at 150 mg/dl without greatly impacting recruitment if reduced glycolytic status variability would be desired especially for quantitative assessments.

CLINICAL RELEVANCE/APPLICATION

Compliance to blood glucose thresholds in clinical trials and implications to high quality data collection and analysis.

Compliance to blood glucose thresholds in clinical trials and practice is high. Opportunity exists to refine guidelines if more normoglycolytic populations are desirable for quantitative imaging.

RC311-03 Feasibility of Ultra-Early Treatment Response Assessment in Non-Hodgkin Lymphoma by Means of [18F]-FDG-PET/MR: Do Changes in Glucose Metabolism and Cell Density Occur Simultaneously?

Tuesday, Nov. 29 9:10AM - 9:20AM Room: S505AB

Participants

Marius E. Mayerhoefer, MD, PhD, Vienna, Austria (*Presenter*) Nothing to Disclose
Daniela Senn, Vienna, Austria (*Abstract Co-Author*) Nothing to Disclose
Alexander Haug, MD, Munich, Germany (*Abstract Co-Author*) Nothing to Disclose
Chiara Giraud, MD, Vienna, Austria (*Abstract Co-Author*) Nothing to Disclose
Markus Raderer, MD, Vienna, Austria (*Abstract Co-Author*) Nothing to Disclose

PURPOSE

To determine, in patients with Non-Hodgkin lymphoma (NHL), whether (1) quantitative assessment of treatment response by [18F]-FDG-PET/MR is possible with the first 72 h, or the first week, after initiation of the first cycle of rituximab-based immunochemotherapy; and (2) whether treatment-induced changes in glucose metabolism and cell density occur simultaneously.

METHOD AND MATERIALS

Patients with histologically proven diffuse large B-cell lymphoma (DLBCL) or follicular lymphoma (FL) were included in this prospective IRB-approved study. Patients underwent [18F]-FDG-PET/MR before, and then 48-72 h (follow-up 1, FU-1), as well as one week (FU-2) after initiation of the first cycle of R-CHOP (for DLBCL), or R-BENDA (for FL). For the up to 3 lesions per patient, matched ROIs were used to assess standardized [18F]-FDG uptake values (SUV_{max}, SUV_{mean}), and apparent diffusion coefficients (ADC_{min}, ADC_{mean}) derived from free-breathing EPI-DWI (b50, b800), at each time point (baseline, FU-1, FU-2). ANOVA and pairwise post-hoc tests were used to test for significant changes in SUVs and ADCs between baseline and FU-1, and baseline and FU-2. Rates of change were also compared between FU-1 and FU-2, and Pearson correlation coefficients were calculated.

RESULTS

Eighteen patients (DLBCL, 8; FL, 10) with 36 lesions were analyzed. Lesion-based mean rates of change between baseline and FU-1 were -41.8%, -37.4%, +37.2%, and +26.1%, for SUV_{max}, SUV_{mean}, ADC_{min}, and ADC_{mean}, respectively; whereas mean rates of change between baseline and FU-2 were -54.7%, -51.2%, +73.0%, and +55.2%, for SUV_{max}, SUV_{mean}, ADC_{min}, and ADC_{mean}, respectively. These changes between baseline and FU-1, and baseline and FU-2, were statistically significant for all quantitative parameters (P<0.001). A substantial, significant negative correlation was observed between baseline-to-FU-1 SUV_{mean} and ADC_{mean} changes (r=-0.63); whereas a significant, moderate, negative correlation was also observed between baseline-to-FU2 SUV_{mean} and ADC_{mean} changes (r=-0.48).

CONCLUSION

In Non-Hodgkin lymphoma, significant changes of glucose metabolism and cell density occur as early as 48-72 hours after initiation of the first cycle of rituximab-based immunochemotherapy, and can be captured by [18F]-FDG-PET/MR.

CLINICAL RELEVANCE/APPLICATION

In Non-Hodgkin lymphoma, [18F]-FDG-PET/MR may enable assessment of treatment response within the first 72 hours after treatment initiation.

RC311-04 Role of TRIPLET FDG-PET in Lymphoma (HL and DLBCL): If Interim PET is Negative is END of Therapy PET Mandated?

Tuesday, Nov. 29 9:20AM - 9:30AM Room: S505AB

Participants

Shanker Raja, MD, Bellaire, TX (*Presenter*) Nothing to Disclose
Sharad P. George, MD, Dhahran, Saudi Arabia (*Abstract Co-Author*) Nothing to Disclose
Shaima H. Shousha, MD, MBCh, Muharraq, Bahrain (*Abstract Co-Author*) Nothing to Disclose
Imran K. Tailor, MD, MBBS, Riyadh, Saudi Arabia (*Abstract Co-Author*) Nothing to Disclose
Belal M. Albtoosh, BSN, Riyadh, Saudi Arabia (*Abstract Co-Author*) Nothing to Disclose
Mohammed O. Al Harbi, Riyadh, Saudi Arabia (*Abstract Co-Author*) Nothing to Disclose
M Salman, Riyadh, Saudi Arabia (*Abstract Co-Author*) Nothing to Disclose
Abdullah S. Aldosary, MBBS, Riyadh, Saudi Arabia (*Abstract Co-Author*) Nothing to Disclose

PURPOSE

Introduction: FDG-PET in staging lymphomas has been validated, while the role of triplet [triPET @ (baseline (basP), interim (intP) and end of Rx (endRxP))] in pt. management strategies is evolving. Compelling data favors the inclusion of intP in PET-directed adaptive therapies in HL; however, for DLBCL the role of intP is questionable. We evaluated the role of triPET in pts. with lymphoma.

METHOD AND MATERIALS

Methods Retrospective review of PET archives revealed a total of 37 pts (HL=22, DLBCL=15). Majority of the HL and DLBCL were Rxd with ABVD and RCHOP respectively. TriPET were acquired per accepted protocol, the images were reviewed by an expert (SR) and a novice (SH). SUV_{max} and Deauville scores (DSc) were obtained from five target lesions, the avg -composite SUV_{max} & DSc were computed for each pt. Statistical analyses were performed with the composite maxSUV (cSUV) and Deauville scores (cDSc) (EXCEL). Following statistics were performed (separately and combined in HL and DLBCL); mean+SD, PPV and NPV for CR Vs. progressive disease (PD) on intP using the variables cSUV and cDSc and delta change (DELTA). Median PFS was the clinical endpoint for response.

RESULTS

Results: In HL median PFS 17 months, 86% overall survival. In DLBCL median PFS 15 months, 93% overall survival. At baseline

SUVmax in all pts was 15.0+/-5.2, (HL12.9+/-4.6 vs DLBCL 18.0+/-4.7; t-test p 0.003). Using cut off thresholds for intP to predict CR at cSUV <=2.0, cDSC <=2.0 and DELT >=80%,. In HL: for cSUV- PPV 67%, NPV 95%; for DELT of cSUV PPV 100%, NPV 95%; for cDSC-PPV 30%, NPV 100%. In DLBCL: for cSUV- PPV 25%, NPV 100%; for DELT of cSUV PPV 33%, NPV 100%; for cDSC- PPV 50%, NPV 100%.

CONCLUSION

Conclusion: The results from our series suggest that intP has a promising role in managing HL as well as DLBCL. As opposed to recent work from other groups, in our modest cohort a negative intP in DLBCL had a NPV of 100% across cSUV, cDSc and DELT, with regards to CR Vs progressive disease; it appears that if intP is -ve then endofRxP is not mandated. In the results for HL subset, the role of intP parallels the emerging results from other groups. Our results need to be validated in a larger series, and alternate different management strategies.

CLINICAL RELEVANCE/APPLICATION

Clinical relevance: If our results in DLBCL are corroborated in larger series by other groups, a neg. intP would suffice and potentially preclude/defer end of therapy PET.

Handout:Shanker Raja

http://abstract.rsna.org/uploads/2016/16015014/RSNA2016_Lymphoma_TRIPET.pdf

RC311-05 Question and Answer

Tuesday, Nov. 29 9:30AM - 9:40AM Room: S505AB

Participants

RC311-06 Imaging Response - Earning Biomarker Status

Tuesday, Nov. 29 9:40AM - 10:10AM Room: S505AB

Participants

Terence Z. Wong, MD, PhD, Chapel Hill, NC (*Presenter*) Nothing to Disclose

LEARNING OBJECTIVES

1) Compare and contrast prognostic, predictive, and pharmacodynamic biomarkers. 2) Understand the difference between integrated and integral biomarkers in clinical trials. 3) Discuss advantages and limitations of imaging biomarkers.

ABSTRACT

Serum, pathological, and imaging biomarkers are becoming increasingly important to define potential biological targets, select which patients may benefit from a particular targeted agent, and to follow patients during and following therapy. Traditionally, imaging has not been formally recognized as a biomarker, and standardization of quantitative imaging techniques remains a major challenge. However, functional and quantitative imaging techniques are now being used routinely to evaluate early response to therapy. Unlike conventional cytotoxic chemotherapy, targeted therapy can be cytostatic and selects only susceptible populations of cells. Imaging response criteria is therefore often different from standard anatomic (RECIST, WHO) criteria, and the response may be heterogeneous. In the future, both serum and imaging biomarkers will have an increasingly important role in managing patients undergoing conventional and targeted therapy.

RC311-07 Treatment Response Evaluation with 18F-FDG PET/CT and 18F-NaF PET/CT in Multiple Myeloma Patients Undergoing High-dose Chemotherapy and Autologous Stem Cell Transplantation

Tuesday, Nov. 29 10:10AM - 10:20AM Room: S505AB

Participants

Christos Sachpekidis, Heidelberg, Germany (*Abstract Co-Author*) Nothing to Disclose

Jens Hillengass, MD, Heidelberg, Germany (*Abstract Co-Author*) Nothing to Disclose

Hartmut Goldschmidt, MD, Heidelberg, Germany (*Abstract Co-Author*) Nothing to Disclose

Uwe Haberkorn, MD, Heidelberg, Germany (*Abstract Co-Author*) Nothing to Disclose

Antonia Dimitrakopoulou-Strauss, Heidelberg, Germany (*Abstract Co-Author*) Nothing to Disclose

Heinz-Peter W. Schlemmer, MD, Heidelberg, Germany (*Abstract Co-Author*) Nothing to Disclose

Frederik L. Giesel, MD, MBA, Heidelberg, Germany (*Presenter*) Patent application for F18-PSMA-1007

PURPOSE

NaF PET/CT is suggested as a potential valuable tool in the assessment of MM. The aim of this study was to assess the combined use of the radiotracers FDG and NaF in treatment response evaluation of a group of multiple myeloma (MM) patients undergoing high-dose chemotherapy (HDT) followed by autologous stem cell transplantation (ASCT) by means of static (whole-body) and dynamic PET/CT (dPET/CT).

METHOD AND MATERIALS

35 patients with primary, previously untreated MM were enrolled in the study. All patients underwent PET/CT scanning with FDG and NaF before and after therapy. Treatment response by means of FDG PET/CT was assessed according to the EORTC 1999 criteria. NaF PET/CT therapy response assessment was based on visual evaluation of the patients' scans. Clinical criteria served as gold standard.

RESULTS

5 MM patients had a negative baseline FDG PET/CT scan and were excluded from the statistical analysis. Of the remaining 30 patients, 4 demonstrated complete response (CR) and 26 demonstrated non-CR (13 patients near complete response-nCR, 4 patients very good partial response-VGPR, 9 patients partial response-PR). After treatment, FDG PET/CT was negative in 15/30 patients and positive in 15/30 patients, showing a sensitivity of 57.7% and a specificity of 100%, in comparison to clinical criteria. Regarding NaF PET/CT, 5/30 pts (16.7%) had a negative baseline scan, thus failed to depict MM. NaF PET/CT depicted 56/129 18F-

FDG positive lesions (43%). Follow-up NaF PET/CT showed persistence of 81.5% of the baseline 18F-NaF positive MM lesions after treatment, despite the fact that 64.7% of them had turned to 18F-FDG negative. Dynamic FDG and NaF PET/CT studies showed that SUV_{average}, SUV_{max}, as well as the kinetic parameters K₁, influx and FD from reference bone marrow and skeleton responded to therapy with a significant decrease (p<0.001).

CONCLUSION

FDG PET/CT demonstrated satisfactory results in treatment response evaluation of MM. On the other hand, NaF PET/CT does not seem to aid significantly in treatment response evaluation of MM patients undergoing HDT and ASCT, at least in an early phase.

CLINICAL RELEVANCE/APPLICATION

Our study confirms the role of FDG PET/CT and at the same time stresses the limitations of NaF PET/CT in treatment response evaluation of MM patients.

RC311-08 Investigation of Quantitative [I-123] MIBG SPECT/CT in a Pediatric Population with Neuroblastoma

Tuesday, Nov. 29 10:20AM - 10:30AM Room: S505AB

Participants

Samuel L. Brady, MS, PhD, Memphis, TN (*Presenter*) Nothing to Disclose

Barry L. Shulkin, MD, MBA, Memphis, TN (*Abstract Co-Author*) Nothing to Disclose

PURPOSE

SPECT has traditionally been regarded as a non-quantitative imaging modality. With recent advances in reconstruction and attenuation correction algorithms, quantitation in SPECT/CT is available. In this study a manufacturer-independent quantitative SPECT/CT reconstruction algorithm was investigated.

METHOD AND MATERIALS

Our institutional IRB deemed this study to be exempt from informed consent. All data were managed in compliance with HIPPA. 106 [I-123] MIBG SPECT/CT examinations were retrospectively reconstructed using SUV SPECT® (HERMES Medical Solutions Inc., Montreal Quebec), where 43 examinations were imaged using a GE Infinia Hawkeye 4, and 63 were imaged using a Siemens Symbia Intevo. Inter-scanner SUV analysis of nine regions of normal [I-123] MIBG tissue uptake (left/right parotids, left/right sub mandibular gland, left ventricle of the heart, liver, left/right adrenal glands, and the bladder) was conducted. Intra-patient SUV_{mean} variability was calculated by measuring normal liver uptake within patients scanned on both scanners. Additionally, neoplastic tissue present in the examination data was quantified using SUV_{max} and trended with time.

RESULTS

A total of 44 patients (22 male) with median age of 3.9 years (range 0.8-17.4 years) were analyzed. Inter-scanner SUV variability measured no statistical difference (average p-value of 0.38) among the nine normal tissues analyzed. Intra-patient liver SUV_{mean} varied by no more than 14% as calculated for 25 patients (87 examinations) scanned on both scanners. In one clinical example a posterior thoracic tumor was evaluated over eight time points (2/2015-2/2016) and demonstrated a 74% (3.1/12.0) reduction in SUV_{max} with treatment.

CONCLUSION

The results demonstrate low intra-patient measurement variability for scanner-independent quantitative SPECT/CT SUV analysis in a pediatric population with neuroblastoma. Furthermore, quantitative SPECT/CT may offer the opportunity for objective analysis of tumor response using the conventional single photon emitting agent [I-123] MIBG, by normalizing the uptake to injected dose, patient weight, and injection to imaging interval as is done for PET.

CLINICAL RELEVANCE/APPLICATION

Quantitative SPECT/CT may assist inter-institutional trials that require tumor response measurement using single photon emitting radiotracers and facilitate evaluation using radionomic techniques.

RC311-09 Imaging of Osteosarcoma using Bone Scintigraphy, Sodium Fluoride-18-PET/CT and Fluoro-18-Deoxyglucose PET/CT - Evaluation of Treatment Response in a Phase I Trial with Radium-223 Therapy

Tuesday, Nov. 29 10:30AM - 10:40AM Room: S505AB

Participants

Kalevi J. Kairemo, MD, PhD, Houston, TX (*Presenter*) Nothing to Disclose

Eric M. Rohren, MD, PhD, Houston, TX (*Abstract Co-Author*) Nothing to Disclose

Gregory C. Ravizzini, MD, Houston, TX (*Abstract Co-Author*) Nothing to Disclose

Arvind Rao, Houston, TX (*Abstract Co-Author*) Nothing to Disclose

Homer A. Macapinlac, MD, Houston, TX (*Abstract Co-Author*) Nothing to Disclose

Vivek Subbiah, MD, Houston, TX (*Abstract Co-Author*) Nothing to Disclose

PURPOSE

The aim was to investigate the role of different imaging modalities in a phase I clinical trial of radium-223 (223RaCl₂) in the treatment of patients (N=18) with high-risk relapsed bone-forming osteosarcoma (NCT01833520).

METHOD AND MATERIALS

Patients received 1-6 cycles of 223RaCl₂, doses varied from 6.84 MBq to 57.81 MBq. Bone scintigraphy, FDG-PET or sodium fluoride-18 (NaF) PET was used to characterize the disease. All 18 patients had multiple lesions. Bone scintigraphy and FDG-PET or NaF-PET studies could be compared in 10 patients at two time points. Lesion number, locations, and volumes were analyzed using FDG-PET and NaF-PET. We also developed a measure in analogue to PERCIST analyze response in NaF-PET, called NAFCIST.

RESULTS

Of the 18 patients, 17 had bone lesions. In four of the seven patients with multiple skeletal lesions (>5), FDG-PET and NaF-PET studies could be compared. The skeletal tumor locations varied in our patient population: two patients lesions in the skull, seven in the extremities, 10 patients in pelvis, 12 in the spine, and nine patients in the ribs. The FDG-PET and NaF-PET studies could be compared in all four patients who had multiple lung lesions (>5): the lung volume, calcified lung nodules, and pathologic NaF and FDG volumes varied substantially. Most of the patients (14/18) had soft-tissue metastases, and at least some of the metastases were calcified in all 14 patients. Soft-tissue lesions were found in lungs, brain, liver and lymph nodes. In many patients, the soft-tissue lesions were extensions of bone tumors. Overall response was seen in only one patient, but 4 patients experienced mixed responses, in which most often the bone lesion decreased in intensity, and the surrounding soft tissues increased in intensity. The NaF-PET response criteria (NAFCIST change) demonstrated a correlation with changes in alkaline phosphatases, and with cumulative administered activity.

CONCLUSION

NAFCIST may be a new tool for high-risk osteosarcoma response evaluation, because NaF demonstrates also soft tissue metastases in osteosarcoma (lung, liver, brain, lymph node), and 5 lesions in multiple organs can be found. Our results indicate that NaF-PET is an essential part of osteosarcoma staging and NaF PET and FDG PET are complementary in osteosarcoma.

CLINICAL RELEVANCE/APPLICATION

We have developed new criteria for osteosarcoma response evaluation based on fluoride-PET.

Honored Educators

Presenters or authors on this event have been recognized as RSNA Honored Educators for participating in multiple qualifying educational activities. Honored Educators are invested in furthering the profession of radiology by delivering high-quality educational content in their field of study. Learn how you can become an honored educator by visiting the website at: <https://www.rsna.org/Honored-Educator-Award/>

Eric M. Rohren, MD, PhD - 2015 Honored Educator

RC311-10 Question and Answer

Tuesday, Nov. 29 10:40AM - 10:50AM Room: S505AB

Participants

RC311-11 Challenges of Solid Tumor Measurements and Techniques to Address This

Tuesday, Nov. 29 10:50AM - 11:20AM Room: S505AB

Participants

Haesun Choi, MD, Houston, TX, (hchoi@mdanderson.org) (*Presenter*) Nothing to Disclose

LEARNING OBJECTIVES

1) The currently available response evaluation criteria of solid tumors and its limitations. 2) New concept of response evaluation of solid tumors. 3) Future of response evaluation of solid tumors.

ABSTRACT

LEARNING OBJECTIVES

1) The currently available response evaluation criteria of solid tumors and its limitations. 2) New concept of response evaluation of solid tumors. 3) Future of response evaluation of solid tumors.

ABSTRACT

RC311-12 Comparison of Novel Multi-level Otsu and Conventional PET Segmentation Methods for Measuring FDG Metabolic Tumor Volume in Patients with Soft Tissue Sarcoma

Tuesday, Nov. 29 11:20AM - 11:30AM Room: S505AB

Participants

Inki Lee, MD, Madison, WI (*Presenter*) Nothing to Disclose

Hyung-Jun Im, MD, Madison, WI (*Abstract Co-Author*) Nothing to Disclose

Meiyappan Solaiyappan, Baltimore, MD (*Abstract Co-Author*) Nothing to Disclose

Steve Cho, MD, Madison, WI (*Abstract Co-Author*) Nothing to Disclose

PURPOSE

There are various strategies that may be used for PET tumor segmentation. We have developed a novel and highly consistent segmentation algorithm using a multi-level Otsu PET method (MO-PET) (JNM 2015 May 1;56(supplement 3):452). We evaluated the reliability of MO-PET compared to conventional PET segmentation methods for measuring FDG PET metabolic tumor volume (MTV) in patients with soft tissue sarcoma (STS).

METHOD AND MATERIALS

Clinical and imaging data were obtained from the NCI Cancer Imaging Archive (<http://dx.doi.org/10.7937/K9/TCIA.2015.7GO2GSKS>). Forty-eight STS patients with FDG PET/CT and MR prior to therapy were analyzed. MTV of the tumor using MO-PET was compared to other conventional methods (absolute SUV threshold values of 2.0, 2.5 or 3.0, and percentage of SUVmax values of 30%, 40%, 50% or 60%). The reference volume was defined as an MR based gross tumor volume (GTV), which was contoured on T2-weighted fat-suppression images. Intra-class analysis and Bland-Altman analysis were performed to evaluate the correlation and agreement of MTV to GTV.

RESULTS

MTVs obtained using each parameter including SUV 30%, 2.0, 2.5, 3.0, and MO-PET were highly correlated with the GTV in intra-

class correlation analysis (all $p < 0.01$ except for SUV 30% $p < 0.05$). MO-PET had the highest correlation of MTV to GTV with a correlation coefficient of 0.93. The highest correlation coefficient using absolute and percent SUV threshold was 2.0 and 30% (correlation coefficients; 0.79 and 0.42, respectively). The Bland-Altman bias results showed highest agreement for MTV using MO-PET with GTV ($26.0 \pm 489.6 \text{ cm}^3$) compared to other methods (SUV 2.0 with $-69.3 \pm 765.8 \text{ cm}^3$ and SUV 30% with $-255.0 \pm 876.6 \text{ cm}^3$).

CONCLUSION

PET MTV segmented with MO-PET method showed higher correlation and agreement with MRI-based GTV in comparison to conventional percent and absolute SUV-based PET segmentation methods. MO-PET is a reliable and consistent method for measuring tumor MTV.

CLINICAL RELEVANCE/APPLICATION

Quantitation of tumor metabolic burden using the MO-PET segmentation method shows promise for future clinical applications.

RC311-13 Pilot Comparison of 4DST and FDG PET/CT for Early Therapy Monitoring of Advanced Non Small Cell Lung Cancer

Tuesday, Nov. 29 11:30AM - 11:40AM Room: S505AB

Participants

Ryogo Minamimoto, MD, PhD, Tokyo, Japan (*Abstract Co-Author*) Nothing to Disclose
Masatoshi Hotta, Shinjyuku-ku, Japan (*Presenter*) Nothing to Disclose
Miyako Morooka, MD, Tokyo, Japan (*Abstract Co-Author*) Nothing to Disclose
Masashi Kameyama, Tokyo, Japan (*Abstract Co-Author*) Nothing to Disclose
Kazuo Kubota, MD, Tokyo, Japan (*Abstract Co-Author*) Nothing to Disclose
Jun Toyohara, Tokyo, Japan (*Abstract Co-Author*) Nothing to Disclose

PURPOSE

$4'$ -[Methyl- ^{11}C] Thiothymidine (4DST) PET-CT provides DNA synthesis imaging, which represented higher correlation with proliferation of advanced non small cell lung cancer (NSCLC) compared to FDG. The aim of this prospective study is to evaluate the potential of 4DST for early therapy monitoring of advanced NSCLC, and comparing the result to the assessments with CT and FDG PET-CT.

METHOD AND MATERIALS

The patients pathologically diagnosed with advanced NSCLC scheduled to receive platinum-doublet chemotherapy (PDC) were eligible. 4DST and FDG PET-CT scan, and CT were performed at baseline and after 2 cycles of PDC. Patients were evaluated after 2 cycles of PDC by RECIST 1.1 (response evaluation criteria in solid tumors) based on CT measurements, EORTC (European Organization for Research and Treatment of Cancer criteria) and PERCIST 1.0 (PET Response Criteria in Solid Tumors) based on PET-CT measurements. 4DST PET-CT was evaluated according to modified EORTC criteria (difference of SUV_{max} as $-35\% >$ was regarded as inadequate therapeutic response). The reference standard for the assessment of patient's prognosis was based on the medical records and the follow-up radiographic assessments.

RESULTS

A total of 20 patients were included in this study. Three patient showed PD before early interim PET, finally 17 patients (male: 13, female 4, mean age: 72 ± 7 , range: 56-84) were used for the analysis. The results of prognosis for patients after following up of average four months were 12 patients of recurrence and five patients without disease progression. 4DST had a significantly higher PPV (75%, $p < 0.001$) to predict disease progression than RECIST (50%), EORTC (25%) and PERCIST (33%). No difference in NPV was found between 4DST (80%) and RECIST (100%), EORTC (100%), and PERCIST (100%)

CONCLUSION

4DST PET/CT had a potential for early therapy monitoring of advanced NSCLC.

CLINICAL RELEVANCE/APPLICATION

4DST PET/CT had a potential for early therapy monitoring of advanced NSCLC.

RC311-15 Question and Answer

Tuesday, Nov. 29 11:50AM - 12:00PM Room: S505AB

Participants

RC312

Peripheral Artery Disease (PAD)

Tuesday, Nov. 29 8:30AM - 10:00AM Room: S403A



AMA PRA Category 1 Credits™: 1.50
ARRT Category A+ Credits: 1.50

FDA Discussions may include off-label uses.

Participants

Stephen T. Kee, MD, Stanford, CA (*Moderator*) Nothing to Disclose

LEARNING OBJECTIVES

1) Discuss the basic pathology of peripheral artery disease. 2) Describe the risk factors associated with the development of peripheral artery disease. 3) Outline the benefits of providing a comprehensive clinical service in the management of PVD. 4) Discuss how to build a PVD practice. 5) Describe the basic techniques employed in the treatment of PVD.

ABSTRACT

Sub-Events

RC312A Clinical Overview of PAD

Participants

Stephen T. Kee, MD, Stanford, CA (*Presenter*) Nothing to Disclose

LEARNING OBJECTIVES

View learning objectives under main course title.

RC312B Lower Extremity CTA

Participants

Richard L. Hallett II, MD, Stanford, CA, (xraydoc97@yahoo.com) (*Presenter*) Nothing to Disclose

LEARNING OBJECTIVES

1) Describe techniques for patient selection, acquisition, reconstruction, and interpretation of lower extremity CTA. 2) Describe evidence-based results for lower extremity CTA, and expected impact on patient care. 3) Describe a coherent plan that integrates lower extremity CTA into cost-effective clinical care.

ABSTRACT

Peripheral arterial disease (PAD) is a common cause of morbidity and mortality in developed countries. Traditionally, imaging for risk stratification and therapeutic planning involved catheter angiography. In recent years, cross-sectional imaging by CTA and MRA has proven a robust technique for non-invasive PAD assessment. Given ubiquity of CT scanning technology, CTA is widely available. High resolution datasets can be acquired rapidly, which facilitates assessment of clinically labile or trauma patients. To be optimally effective, CTA techniques require particular attention to contrast medium and scan protocol. With appropriate protocol design, data acquisition requires limited operator dependence. The acquired 3D dataset is rich with information, but requires careful scrutiny by the interpreting physician. Volumetric review of these datasets produces the most accurate results. Extensive small vessel calcification remains a potential barrier to full assessment of pedal vessels by CTA. Recent published data validates the clinical effectiveness of CTA for diagnosis of PAD and for the direction of treatment planning. Ongoing research aims to exploit the newest generation of CT scanners to acquire additional information, including dual energy data, time-resolved information, and radiation dose savings.

Active Handout: Richard Lee Hallett

http://abstract.rsna.org/uploads/2016/13012018/ACTIVE_RC312B_Hallett_LE_CTA.pdf

RC312C Lower Extremity MRA

Participants

Harald Kramer, MD, Munich, Germany, (harald.kramer@med.lmu.de) (*Presenter*) Nothing to Disclose

LEARNING OBJECTIVES

1) Identify the appropriate technique for peripheral MRA depending on the available hardware and the clinical question and condition of the patient. 2) Differentiate between different contrast agents and their specific characteristics. 3) Choose between different contrast agent application schemes depending on the technique used and the clinical question. 4) Compare the pros and cons of contrast-enhanced and non contrast-enhanced techniques for peripheral MRA.

ABSTRACT

The prevalence of symptomatic peripheral artery disease (PAD) ranges around 3% in patients aged 40 and 6% at an age of 60 years. Additionally, the prevalence of asymptomatic PAD lies between 3% and 10% in the general population increasing to 15% to 20% in persons older than 70 years of age. However, these data still might underestimate the total prevalence of PAD since screening studies showed that between 10% and 50% of all patients with intermittent claudication (IC) never consult a doctor

about their symptoms. These data prove the need for an accurate and reliable method for assessment of the peripheral vasculature. Digital subtraction angiography (DSA) still serves as the reference standard for all vascular imaging techniques. However, because of the absence of ionizing radiation, the use of non-nephrotoxic contrast agents or even non contrast-enhanced sequences and the large toolbox of available techniques for high-resolution static and dynamic imaging Magnetic Resonance Angiography (MRA) constitute an excellent non-invasive alternative. Different acquisition schemes and contrast agent application protocols as well as different types of data sampling for static, dynamic, contrast- and non contrast-enhanced imaging enable to tailor each exam to a specific question and patient respectively.

RC312D Endovascular Treatment of PAD

Participants

Stephen T. Kee, MD, Stanford, CA (*Presenter*) Nothing to Disclose

LEARNING OBJECTIVES

View learning objectives under main course title.

RC313

Pediatric Series: CV/Chest

Tuesday, Nov. 29 8:30AM - 12:00PM Room: N228



AMA PRA Category 1 Credits™: 3.25
ARRT Category A+ Credits: 3.50

FDA Discussions may include off-label uses.

Participants

R. Paul Guilleman, MD, Houston, TX (*Moderator*) Nothing to Disclose
Elizabeth F. Sheybani, MD, Saint Louis, MO (*Moderator*) Nothing to Disclose

Sub-Events

RC313-01 Imaging of Childhood Interstitial Lung Disease

Tuesday, Nov. 29 8:30AM - 8:50AM Room: N228

Participants

Catherine M. Owens, MD, London, United Kingdom (*Presenter*) Nothing to Disclose

LEARNING OBJECTIVES

1) To understand and define the Childhood Interstitial Lung disease ChILD classification. 2) To illustrate examples within this classification. 3) To update on more recent additions with clinicopathological examples.

ABSTRACT

RC313-02 Radiologic Evaluation of Drug-Induced Pneumonitis following Carmustine (BCNU)-Based Preparative Regimens in Children

Tuesday, Nov. 29 8:50AM - 9:00AM Room: N228

Participants

Yu Jin Kim, MD, Seoul, Korea, Republic Of (*Presenter*) Nothing to Disclose
Woo Sun Kim, MD, Seoul, Korea, Republic Of (*Abstract Co-Author*) Nothing to Disclose
Young Hun Choi, MD, Seoul, Korea, Republic Of (*Abstract Co-Author*) Nothing to Disclose
Jung-Eun Cheon, MD, Seoul, Korea, Republic Of (*Abstract Co-Author*) Nothing to Disclose
In-One Kim, MD, Seoul, Korea, Republic Of (*Abstract Co-Author*) Nothing to Disclose
Ji-Eun Park, Seoul, Korea, Republic Of (*Abstract Co-Author*) Nothing to Disclose
Young Jin Ryu, MD, Seoul, Korea, Republic Of (*Abstract Co-Author*) Nothing to Disclose

PURPOSE

To describe radiologic findings of drug-induced pneumonitis following carmustine (BCNU)-based preparative regimens for autologous peripheral blood stem cell transplantation (aPBSCT) in children.

METHOD AND MATERIALS

From 2010 through 2014 in our institution, among 35 patients who received carmustine-based preparative regimens for aPBSCT, 9 patients (6 boys and 3 girls; 3-17 years, mean 10 years; 7 lymphoma and 2 leukemia patients) presented respiratory symptoms and radiologic abnormalities. They had no evidence of infection, cardiogenic edema, and other explainable causes. The chief complaints were fever (n=8, 89%), dyspnea (n=4, 44%), and cough (n=2, 22%). The symptoms developed at 40th day on average (range 34-51 days) after receiving carmustine-based preparative regimens. Chest radiographs and CT scans performed under the impression of infection at the first of respiratory symptoms were reviewed by 2 pediatric radiologists who reached consensus in analyzing the presence and distribution of ground-glass opacity (GGO), consolidation, septal thickening and other various patterns of interstitial pneumonitis, and pleural effusion.

RESULTS

Radiographic findings were bilateral patchy GGO (n=9, 100%) combined with consolidation (n=3, 33%) and septal thickening (n=6, 67%). Pleural effusion were noted in 5 patients (56%). CT findings were patchy GGO (n=9, 100%), localized consolidations (n=4, 44%) and septal thickening (n=7, 78%). The distribution of lesions were bilateral (n=9, 100%) and lower lobar predominant (n=6, 67%). There was no central/peripheral, or anterior/posterior predilection. Pleural effusion was seen in 6 patients (67%) at CT scans and was bilateral in all.

CONCLUSION

Bilateral patchy GGO combined with or without consolidation, septal thickening and bilateral pleural effusion were common radiologic findings in drug-induced pneumonitis following carmustine-based preparative regimens. It should be differentiated from pulmonary infection which is critical and frequently encountered in oncologic patients.

CLINICAL RELEVANCE/APPLICATION

Carmustine can cause pneumonitis. Common radiologic findings of this pneumonitis were bilateral patchy GGO combined with or without consolidation, septal thickening and bilateral pleural effusion.

RC313-03 High-temporal Resolution Chest CT Examinations in Infants and Young Children without Sedation or General Anesthesia: Frequency and Severity of Motion Artifacts

Participants

Suonita Khung, MD, Lille, France (*Abstract Co-Author*) Nothing to Disclose
Nicolas Lasalle, Lille, France (*Abstract Co-Author*) Nothing to Disclose
Younes Arous, MD, Lille, France (*Abstract Co-Author*) Nothing to Disclose
Antoine Deschildre, Lille, France (*Abstract Co-Author*) Nothing to Disclose
Jacques Remy, MD, Mouvaux, France (*Abstract Co-Author*) Research Consultant, Siemens AG
Martine J. Remy-Jardin, MD, PhD, Lille, France (*Abstract Co-Author*) Research Grant, Siemens AG
Antoine Hutt, MD, Lille, France (*Presenter*) Nothing to Disclose

PURPOSE

To evaluate the frequency and severity of motion artifacts on chest CT examinations acquired without sedation nor general anesthesia in infants and children younger than 5 years.

METHOD AND MATERIALS

The study population included all consecutively registered infants and young children (age <5 years) who had been referred for a standard chest CT examination on a third-generation, dual-source CT system. The examinations were obtained with a high-pitch and high-temporal resolution protocol (pitch: 3.0; rotation time: 250 ms). Children were scanned while freely breathing, without sedation or general anaesthesia. In order to scan quiet children, each examination was supervised by a paediatric nurse practitioner. For each examination, we recorded (a) the number of acquisitions necessary to reach a diagnostic image quality, (b) the frequency and severity of motion artifacts in the upper, mid and lower lung zones using a 4-point scale (0 : no artifact ; 1 : mild; 2 : moderate ; 3 : severe) and (c) the diagnostic value of each acquisition.

RESULTS

The study population comprised 343 patients (mean age: 14.92 months) who underwent a contrast (n=240) or noncontrast (n=103) chest CT examinations; the mean duration of data acquisition was 0.23 ± 0.05 s (range: 0.11 – 0.52). For 330 patients (96.2%), the investigation comprised a single acquisition which was rated as follows: (a) no motion artifact over the entire thorax (n=193); (b) presence of motion artifacts that did not affect the overall diagnostic value of the examination (n=137) with a mean score of artifact of 0.72 (median: 0.67; range: 0.33 – 2.33). In 13 patients (3.8%): (a) the acquisition was rated as nondiagnostic due to the presence of severe artifacts (mean score: 1.62; range: : 1.67-2.67); (b) a second acquisition was then performed, rated as diagnostic in 13 cases (mean score of artifact: 0.47; median: 0.17; range: 0-2) and nondiagnostic in 1 patient.

CONCLUSION

Diagnostic image quality is obtained with a single examination in 96.2% of children scanned while freely breathing.

CLINICAL RELEVANCE/APPLICATION

High-quality chest CTA can be routinely obtained in freely-breathing infants and young children when evaluated with high-temporal resolution, making sedation and anesthesia unnecessary.

RC313-04 Correlation of High Resolution Computed Tomography Findings and Clinical Severity of Bronchopulmonary Dysplasia

Tuesday, Nov. 29 9:10AM - 9:20AM Room: N228

Participants

Min Yeong Kim, MD, Seoul, Korea, Republic Of (*Presenter*) Nothing to Disclose

PURPOSE

To analyze high resolution computed tomography (HRCT) findings in neonate with bronchopulmonary dysplasia (BPD). To evaluate correlation between HRCT findings and clinical severity.

METHOD AND MATERIALS

From 2008 to 2015, fifty very low birth weight infants with BPD underwent HRCT exams at the mean postmenstrual age of 38.7 weeks. HRCT findings were classified as two categories and 7 findings: 1) hyperaeration; area of decreased lung attenuation, mosaic attenuation, bulla/bleb and 2) parenchymal lesions; linear lesions, consolidation, bronchial wall thickening, bronchiectasis. These HRCT findings were recorded in each lobe of lungs. Clinical severity was graded as mild, moderate and severe. Each HRCT finding, sum of hyperaeration scores, sum of parenchymal lesion scores and total scores of HRCT findings were analyzed for correlation with clinical severity of BPD.

RESULTS

The total scores of HRCT findings were significantly correlated with clinical severity of BPD ($r>0.6$, $p=0.03$). Parenchymal lesion scores were well correlated with clinical severity of BPD while hyperaeration scores were not significantly correlated with clinical severity of BPD. The best correlated HRCT finding is consolidation ($p=0.006$). Area of decreased lung attenuation was frequent findings regardless of clinical severity of BPD.

CONCLUSION

Total scores of HRCT findings are correlated with clinical severity of BPD and parenchymal lesion scores have a key part, especially consolidation. Unlike previous reports about HRCT of BPD, hyperaeration scores are not correlated with clinical severity of BPD.

CLINICAL RELEVANCE/APPLICATION

On HRCT of infants with BPD, hyperaeration is not specific for clinical severity of BPD but consolidation is predictive findings of that of BPD.

RC313-05 Assessment of the Severity of Disease in Patients with Cystic Fibrosis using MRI of the Lung: Signal Intensity and Lung Volumes Compared to the Lung-Clearance-Index and Forced Expiratory-Volume-in-1-Second

Participants

Sabrina Fleischer, MD, Tuebingen, Germany (*Abstract Co-Author*) Nothing to Disclose
Ilias Tsiflikas, MD, Tuebingen, Germany (*Abstract Co-Author*) Nothing to Disclose
Verena Langlouis, Tuebingen, Germany (*Abstract Co-Author*) Nothing to Disclose
Matthias Teufel, Tuebingen, Germany (*Abstract Co-Author*) Nothing to Disclose
Ute Graepler-Mainka, Tuebingen, Germany (*Abstract Co-Author*) Nothing to Disclose
Joachim Riethmuller, MD, Tuebingen, Germany (*Abstract Co-Author*) Nothing to Disclose
Andreas Hector, Tuebingen, Germany (*Abstract Co-Author*) Nothing to Disclose
Konstantin Nikolaou, MD, Tuebingen, Germany (*Abstract Co-Author*) Speakers Bureau, Siemens AG; Speakers Bureau, Bracco Group; Speakers Bureau, Bayer AG
Juergen F. Schaefer, MD, Tuebingen, Germany (*Presenter*) Nothing to Disclose

PURPOSE

Morphological assessment of lung damage is already part of diagnostic work-up in cystic fibrosis (CF). Imaging biomarkers as lung volume (Vol) or signal intensity (SI) can be calculated at baseline and in follow-up. Aim of this study was to correlate MR values of regional pulmonary function with lung clearance index (LCI) and forced expiratory volume in 1 second (FEV1) as the most important parameter for the monitoring the disease.

METHOD AND MATERIALS

IRB waived informed consent and approved this retrospective, HIPAA-compliant study. 49 consecutive CF-patients (23 f, 26 m) mean age 17 +/- 7 y (7-40y) received MRI at 1.5 T of the lung as standard of care in our institution. In this protocol, a 2D GRE sequence with very-short echo time was applied in submaximal inspiration as well as expiration. Semiautomatic segmentation of ventilated areas was performed. Absolute Vol and SI values at in- and expiration, relative differences (Vol_Delta and SI_Delta) and cumulative histograms for relative SI values across entire lung volume were computed.

RESULTS

Strong correlation between Vol_Delta and SI_Delta was found ($R=0.86$; $P<0.0001$). Individual Vol-SI-curves created by cumulative histograms allowed visually the differentiation between clinically minimal and strongly affected patients ($LCI > 10$). The expiratory volume at a relative SI of 100% correlated significantly with LCI and FEV1 ($R=0.63$ and $R=0.81$; $P<0.0001$).

CONCLUSION

A close relation of pulmonary volume and SI during respiration was observed. Individual Vol-SI-curves were suitable to estimate the severity of disease clinically assessed by LCI. The cross correlation with LCI and FEV1 might be promising for the quantification of areas with low SI values due to air trapping.

CLINICAL RELEVANCE/APPLICATION

Cumulative histograms for relative SI values across lung volume by unenhanced MRI offer information of regional ventilation and can estimate the severity of disease in CF.

RC313-06 Characterization of All-Terrain Vehicle-Related Chest Injury Patterns in Children

Participants

Kelly N. Hagedorn, MD, Houston, TX (*Presenter*) Nothing to Disclose
Jennifer H. Johnston, MD, Cerritos, CA (*Abstract Co-Author*) Nothing to Disclose
Sean K. Johnston, MD, Houston, TX (*Abstract Co-Author*) Nothing to Disclose
Nagaramesh Chinapuvvula, MBBS, Houston, TX (*Abstract Co-Author*) Nothing to Disclose
Chunyan Cai, Houston, TX (*Abstract Co-Author*) Nothing to Disclose

PURPOSE

To evaluate chest injury patterns in pediatric patients involved in all-terrain vehicle (ATV) accidents.

METHOD AND MATERIALS

A retrospective review of the trauma registry at a level I trauma institution from 1992-2013 was performed for patients between 0-18 years admitted after ATV-related incidents. Only patients with chest imaging were included. Type of chest injuries, mechanism of injury, driver/passenger status and demographic data were recorded. Clinical data such as length of hospital stay and intensive care unit (ICU) admission were documented. Comparison of demographic data and clinical data between patients with and without chest injury was conducted using the Chi-square test for categorical variables and two-sample t test for continuous variables.

RESULTS

A total of 455 pediatric patients were admitted after an ATV injury during the study period. Of these, 102 patients (22%) had a chest injury. Most injuries occurred due to a rollover (44/102, 43%), collision with landscape (20/102, 20%) or falls (16/102, 16%). The patient was the driver in 41 (40%) and passenger in 33 (32%) cases (others unknown). Patients with chest injuries were older (13 vs 11 years, $P 0.0027$), taller (157 cm vs 148 cm, $P 0.0012$), and heavier (57 kg vs 48 kg, $P 0.0006$) than those without chest injury. The most common injury was pulmonary contusion (62/102, 61%), followed by pneumothorax (46/102, 45%) and non-flail rib fracture(s) (35/102, 34%). There were no cardiac, esophageal, or airway injuries, and no vascular injury other than a case of subclavian artery transection. Patients with chest injury more often required ICU care (41/102, 40%, compared to 77/353, 22%, $P 0.0002$) and had longer median hospital stay (3 days vs 2 days, $P 0.0054$) compared to patients without chest injury. Eight patients with chest injury died (8%).

CONCLUSION

Chest injuries are a relatively common occurrence in children following ATV accidents, which remain a significant public health issue in terms of morbidity and mortality. Patients with chest injuries were more likely to require ICU care and to have a longer hospital

stay.

CLINICAL RELEVANCE/APPLICATION

Chest injuries following ATV accidents in the pediatric population are common and increased public awareness of these potentially devastating injuries is needed.

RC313-07 Does a Normal Chest X-ray Obviate the Need for Thoracic CT Scanning in Pediatric Trauma?

Tuesday, Nov. 29 9:40AM - 9:50AM Room: N228

Participants

Mohammed F. Mohammed, MBBS, Vancouver, BC (*Presenter*) Nothing to Disclose
Reem S. Zakzouk, MD, Riyadh, Saudi Arabia (*Abstract Co-Author*) Nothing to Disclose
Nizar Bhulani, MD, Houston, TX (*Abstract Co-Author*) Nothing to Disclose
Savvas Nicolaou, MD, Vancouver, BC (*Abstract Co-Author*) Institutional research agreement, Siemens AG
Hesham M. Alshaalan, MD, Toronto, ON (*Abstract Co-Author*) Nothing to Disclose
Amna A. Kashgari, MD, Halifax, NS (*Abstract Co-Author*) Nothing to Disclose

PURPOSE

Motor vehicle collisions and road traffic related injuries constitute one of the leading causes of premature death worldwide. In children with multiple injuries, the presence of chest trauma increases the mortality rate by 20 times. Whole-body CT has become the mainstay in assessment of patients involved in traumas of various causes. The drawback has been an increase in exposure to medical imaging. Pediatric patients are more sensitive to the negative effects of ionizing radiation, and minimizing exposure is a priority. We assess the role of a negative chest x-ray in obviating the need for further chest CT in stable pediatric patients that have sustained trauma in an attempt to reduce unnecessary imaging.

METHOD AND MATERIALS

A retrospective study was carried out on all patients under 14 years of age that presented to our institution, a level 1 trauma center, from 2010 to 2013. A total of 304 patients received whole-body trauma CT and had received chest x-rays within 30 minutes of the CT. The chest x-rays and thoracic CT scans were independently reviewed by two radiologists who were blinded to the clinical outcome. The presence of pulmonary contusions/consolidations, pneumothorax, pneumomediastinum, subcutaneous emphysema, pleural effusion and fractures was recorded.

RESULTS

165 (54.3%) of the chest x-rays were normal. Of these, 41 (24.8%) demonstrated minimal airspace opacity on CT. These were confined to one lobe and were small. They did not warrant further management in all 41 patient. 2 out of the 41 patients had tiny pneumothoraces on CT which did not require further follow up or intervention. The remaining 139 chest x-rays had at least 1 positive finding and demonstrated good correlation to significant CT findings that required further intervention and management ($p < 0.01$). The likelihood of significant CT findings was greater when pleural effusion was present on the x-ray or when 2 or more findings were positive on the chest x-ray.

CONCLUSION

A normal chest x-ray virtually excludes the presence of significant findings on the thoracic CT scan; however, if the chest x-ray demonstrates any pathology, particularly pleural effusion, a chest CT is required to exclude significant findings which may require immediate intervention.

CLINICAL RELEVANCE/APPLICATION

In a stable, assessable pediatric patient with a low suspicion mechanism of injury, a normal chest x-ray likely obviates the need for further assessment or intervention.

RC313-08 Imaging of Vascular Rings

Tuesday, Nov. 29 9:50AM - 10:10AM Room: N228

Participants

Elizabeth F. Sheybani, MD, Saint Louis, MO, (elizabeth.sheybani@wustl.edu) (*Presenter*) Nothing to Disclose

LEARNING OBJECTIVES

1) Describe the presentation and clinical significance and developmental anatomy of vascular rings. 2) Identify major findings indicative of vascular rings on multiple modalities including radiography, fluoroscopy, CT and MRI. 3) Classify vascular rings and identify key features on cross-sectional imaging for surgical planning. 4) Compare available modalities and optimize evaluation of vascular rings.

ABSTRACT

RC313-09 Imaging of Tetralogy of Fallot

Tuesday, Nov. 29 10:30AM - 10:50AM Room: N228

Participants

Taylor Chung, MD, Oakland, CA, (tchung@mail.cho.org) (*Presenter*) Travel support, Koninklijke Philips NV;

Active Handout: Taylor Chung

http://abstract.rsna.org/uploads/2016/16000461/rc31309_RSNA2016_TOF_talk.pdf

LEARNING OBJECTIVES

1) Understand the clinical indications therefore imaging goals for post-operative imaging of patients with tetralogy of Fallot. 2) Review practical clinical MR protocol for post-operative imaging of patients with tetralogy of Fallot.

RC313-10 Assessment of the Reliability of Ventricular Function and Flow Evaluation for Repaired Tetralogy of Fallot with 4D Flow MRI

Tuesday, Nov. 29 10:50AM - 11:00AM Room: N228

Participants

Qiong Yao, MD, Shanghai, China (*Presenter*) Nothing to Disclose

Michael A. Kadoch, MD, Stanford, CA (*Abstract Co-Author*) Nothing to Disclose

Floris-Jan S. Ridderbos, BSc, Stanford, CA (*Abstract Co-Author*) Nothing to Disclose

Shreyas S. Vasanawala, MD, PhD, Stanford, CA (*Abstract Co-Author*) Research collaboration, General Electric Company; Consultant, Arterys Inc; Research Grant, Bayer AG;

Francis P. Chan, MD, PhD, San Francisco, CA (*Abstract Co-Author*) Nothing to Disclose

PURPOSE

Patients with repaired tetralogy of Fallot (rTOF) require regular monitoring by MRI to assess for right ventricular enlargement and pulmonary regurgitation. 4D flow, a time-resolved, volumetric, accelerated phase contrast technique, may efficiently acquire this information in 10 minutes. We evaluate (1) the consistency between ventricular volumes and flows within 4D flow data and (2) the agreement of these parameters with conventional 2D SSFP-cine and 2D phase contrast acquisitions in patients with rTOF.

METHOD AND MATERIALS

Following IRB approval, patients diagnosed with uncomplicated rTOF who underwent combined 2D and 4D flow MRI studies were identified. Patients with residual shunts, pulmonary conduits, pulmonary stenosis, and/or significant non-pulmonary valvular regurgitation were excluded. Using post-processing software (Arterys for 4D data, Medis for 2D data), pulmonary and systemic flows (Qp, Qs), pulmonary regurgitant volume (PRV), and left/right diastolic/systolic ventricular volumes (LVEDV, RVEDV, LVESV and RVESV) were quantified. From these measurements, stroke volumes (LVSV, RVSV), ejection fractions (LVEF, RVEF), pulmonary regurgitant fraction (PRF), and left/right ventricular outputs (LVO, RVO) were calculated. Internal consistency between Qp and Qs as well as between PRV and RVO-LVO difference was measured using intra-class correlation (ICC). Agreement with 2D data was measured using Pearson correlation and Bland-Altman plot.

RESULTS

24 patients (10 males, 6.4 ± 4.8 years) were identified. For 4D MRI, Qp and Qs had good agreement (ICC 0.446-0.866) as did PRV with RVO-LVO difference (ICC 0.315-0.820). 4D and 2D results were well correlated ($r = 0.885$ for LVEDV, 0.974 for RVEDV, 0.898 for LVESV, 0.980 for RVESV, 0.863 for EFI, 0.925 for EF_r, 0.447 for Qp/Qs and 0.764 for PRF). Bland-Altman analysis showed wider limits of agreement for flow relative to ventricular function.

CONCLUSION

Ventricular function and flow measurements can be accomplished with 4D flow MRI and are consistent with 2D results.

CLINICAL RELEVANCE/APPLICATION

Monitoring of patients with uncomplicated rTOF can be achieved in under 10 minutes with an MRI protocol consisting of a single 4D flow sequence, improving patient experience and reducing costs.

RC313-11 A Prospective Evaluation of Contrast and Radiation Dose and Image Quality in Cardiac CT in Children with Complex Congenital Heart Disease using Low-Concentration Iodinated Contrast Agent and Low Tube Voltage and Current

Tuesday, Nov. 29 11:00AM - 11:10AM Room: N228

Participants

Qiaoru Hou, MD, Shanghai, China (*Abstract Co-Author*) Nothing to Disclose

Li Wei Hu, DIPLENG, MENG, Pudong, China (*Abstract Co-Author*) Nothing to Disclose

Haisheng Qiu, Shanghai, China (*Abstract Co-Author*) Nothing to Disclose

Yumin Zhong, MD, Shanghai, China (*Presenter*) Nothing to Disclose

PURPOSE

To assess image quality and contrast and radiation dose in cardiac CT in children with congenital heart disease using low-concentration iodinated contrast agent and low tube voltage and tube current.

METHOD AND MATERIALS

110 consecutive patients (54 male, 56 female, 5kg)

RESULTS

There was no difference in age, weight between the two groups (all $p > 0.05$). The iodine load in Group A was 30% lower than in Group B (3.98 ± 0.75 gI vs. 5.76 ± 1.02 gI, $p < 0.001$). And CT DIvol, DLP and ED in Group A (1.35 mGy, 15.29 ± 1.91 mGy/cm and 0.60 ± 0.07 mSv) were lower than in Group B (1.81 mGy, 20.11 ± 2.12 mGy/cm and 0.77 ± 0.10 mSv) (all $p < 0.001$). However, the mean CT value, noise, CNR and SNR for Group A and Group B were similar (all $p > 0.05$), and the mean image quality score for Group A and Group B was also similar with good agreement between the two observers. Comparing to the surgery results ($n = 26$ in Group A and $n = 38$ in Group B), Group A was 96% accurate in the diagnosis for extracardiac defects and 92% accurate for intracardiac defects, while Group B was 95% accurate in the diagnosis for extracardiac defects and 93% accurate for intracardiac defects.

CONCLUSION

The scanning protocol using low tube voltage (80kVp), low tube current (120mA) and low-concentration iodinated contrast agent (270mgI/mL) enables reduction in iodine load and radiation dose while maintaining compatible image quality.

CLINICAL RELEVANCE/APPLICATION

Low tube voltage (80kVp), low tube current (120mA) and low-concentration iodinated contrast agent (270mgI/mL) may be used

effectively to examine complex congenital heart disease in infants.

RC313-12 Comparison of 3 Different Carotid Artery Intima Media Thickness (IMT) Measurements According to Math's System Software, Non Invasive Vascular Elastography (NIVE) Platform and Radiofrequency (RF) Generated Ultrasound Sequences in a Pediatric COH

Tuesday, Nov. 29 11:10AM - 11:20AM Room: N228

Participants

Ramy El Jalbout, MD, Montreal, QC (*Presenter*) Nothing to Disclose

Guy Cloutier, PhD, Montreal, QC (*Abstract Co-Author*) Nothing to Disclose

Melanie Henderson, Montreal, QC (*Abstract Co-Author*) Nothing to Disclose

Chantale Lapierre, MD, Montreal, QC (*Abstract Co-Author*) Nothing to Disclose

Gilles P. Soulez, MD, Montreal, QC (*Abstract Co-Author*) Speaker, Bracco Group Speaker, Siemens AG Research Grant, Siemens AG Research Grant, Bracco Group Research Grant, Cook Group Incorporated Research Grant, Object Research Systems Inc

Josee Dubois, MD, Montreal, QC (*Abstract Co-Author*) Nothing to Disclose

PURPOSE

To compare IMT measurements in children according to three different techniques: Math's system software, radiofrequency generated ultrasound sequences and NIVE software. To compare IMT measurements between two groups of normal and overweight/obese children using 3 different techniques

METHOD AND MATERIALS

Children aged between 8 and 10 years (n=120) were randomly chosen such that 60 children were of normal weight (group A) and 60 children were overweight (group B). We compared 3 methods of IMT measurement of the far away common carotid artery wall relative to the transcutaneously placed linear ultrasound probe. The first used a dedicated software Math's system allowing an automated measurement of IMT on B-mode ultrasound images. The second measured IMT automatically using an echotracking system based on the amplitude of radiofrequency (RF) signal. The third used a semi automated segmentation analysis generated by the NIVE platform of video sequences obtained with radiofrequency ultrasound.

RESULTS

There is no significant correlation between any of the three different techniques neither in group A nor in group B. In group A, the interclass correlation coefficients were as follows: IMT B-mode-IMT RF ICC=0.010 (p=0.28), IMT B-mode-IMT NIVE ICC=0.003 (p=0.45), IMT RF-IMT NIVE ICC=0.0006 (p=0.52). In group B, IMT B-mode-IMT RF ICC=0.003 (p=0.42), IMT B-mode-IMT NIVE ICC=0.005 (p=0.43) and IMT RF-IMT NIVE ICC=0.002 (p=0.42). Each technique has its limitations in the pediatric population. However, when comparing IMT values across weight, IMT was significantly lower for normal weight youth using all 3 techniques: using B-mode (0.553 mm versus 0.573 mm for groups A and B respectively; p=0.026); using RF (0.457 mm for group A vs 0.489 mm for group B; p=0.031 and using NIVE algorithm (0.325 mm vs 0.355 mm for groups A and B; p=0.010).

CONCLUSION

Significant IMT measurement variation was observed between the different techniques. However, overweight children tend to have higher IMT values regardless of the method used. There is no gold standard technique and future studies are needed to validate our results.

CLINICAL RELEVANCE/APPLICATION

Risk factors for atherosclerosis begin in childhood. IMT using the same technique can be used to target children at risk and follow them in time until one technique proves to be the gold standard.

RC313-13 Utility of 1.5-T Three-dimensional Steady-State Free Precession Whole-heart MRI in the Assessment of Coronary Artery Anatomy with and without Contrast Enhancement in Children

Tuesday, Nov. 29 11:20AM - 11:30AM Room: N228

Participants

Quanli Shen, Shanghai, China (*Presenter*) Nothing to Disclose

Xihong Hu, PhD, Shanghai, China (*Abstract Co-Author*) Nothing to Disclose

Qiong Yao, MD, Shanghai, China (*Abstract Co-Author*) Nothing to Disclose

PURPOSE

To compare the performance of a contrast-enhanced with a noncontrast 1.5-T three-dimensional (3D) steady-state free precession (SSFP) sequence for magnetic resonance coronary angiography (MRCA) in children.

METHOD AND MATERIALS

The study was approved by the institutional review board. Seventy-nine children in the age range of 1 month to 18 years were enrolled in this study. They were classified into three groups according to the age: group 1 = patients 2 years or younger (n = 19), group 2 = patients older than 2 years to 5 years (n = 17), group 3 = patients older than 5 years (n = 43). A free-breathing, navigator-gated, 3D SSFP whole-heart protocol at 1.5-T was used before and after injection of Gadolinium-DTPA. The image quality, vessel length, signal-to-noise ratio (SNR) and contrast-to-noise ratio (CNR) of the left main trunk (LMT), left anterior descending coronary artery (LAD), left circumflex coronary artery (LCX), and right coronary artery (RCA) were assessed by using Wilcoxon signed-rank test.

RESULTS

The application of Gadolinium-DTPA improved the image quality of all the coronary arteries in group 1 (P 0.05). Contrast-enhanced 3D SSFP sequence revealed longer length for LAD and LCX in group 1, and LCX in group 2 (P 0.05). SNR and CNR of all the coronary arteries in group 1 and 2, and the LCX and RCA in group 3 increased after application of Gadolinium-DTPA (P 0.05).

CONCLUSION

Contrast-enhanced 3D SSFP whole-heart MRCA at 1.5-T significantly improves the image performance in young children but the

Contrast enhanced 3D SSFP whole heart MRCA at 1.5 T significantly improves the image performance in young children, but the overall performance is not significantly improved in older children.

CLINICAL RELEVANCE/APPLICATION

3D SSFP whole-heart MRCA can be used young children with congenital heart disease or Kawasaki Disease.

RC313-14 Feasibility of Low Iodine Containing Iodixanol 270 Contrast Media for Cardiac Computed Tomography Angiography Using a Peak Tube Voltage of 80kV in Neonates and Infants

Tuesday, Nov. 29 11:30AM - 11:40AM Room: N228

Participants

Ki Seok Choo, MD, Yangsan, Korea, Republic Of (*Abstract Co-Author*) Nothing to Disclose

Jae-Yeon Hwang, MD, Yangsan-si, Korea, Republic Of (*Abstract Co-Author*) Research Grant, Bayer AG; Research Grant, Guerbet SA

Jin Hyeok Kim, MD, Yangsan-si, Korea, Republic Of (*Abstract Co-Author*) Nothing to Disclose

Yoon Young Choi, MD, Yangsan, Korea, Republic Of (*Abstract Co-Author*) Nothing to Disclose

Hwaseong Ryu, Yangsan-si, Korea, Republic Of (*Abstract Co-Author*) Nothing to Disclose

Junhee Han, Yangsan-si, Korea, Republic Of (*Abstract Co-Author*) Nothing to Disclose

Jun Woo Lee, MD, Pusan, Korea, Republic Of (*Abstract Co-Author*) Nothing to Disclose

Jeongmin Lee, MD, Yangsancity, Korea, Republic Of (*Presenter*) Nothing to Disclose

PURPOSE

Contrast media (CM) of different concentrations are widely used for pediatric cardiac computed tomography angiography (CCTA). However, lower concentration < 300 mgI/ml CM is not routinely used in CTA due to concerns of suboptimal enhancement of cardiac structures and smaller vessels. The aim of the present study was to evaluate the feasibility of using iso-osmolar CM containing a low iodine dose for CCTA in neonates and infants.

METHOD AND MATERIALS

The iodixanol 270 group consisted of 79 CT scans and the iopromide 370 group of 62 CT scans in patients less than one old year. Radiation dose, volume of contrast media, and total iodine dose were retrospectively reviewed. Regarding objective measurements, enhancement and image noise of the ascending aorta (AA), main pulmonary artery (MPA), descending aorta (DA), and left ventricle (LV) were analyzed and contrast-to-noise ratios (CNRs) of the AA and LV were calculated. Regarding subjective measurement, a visual analytic scoring system was devised to evaluate degrees of contrast enhancement, image noise, motion artifact, and overall image quality of each image set. Reader performance for correctly differentiating iodixanol 270 and iopromide 370 by visual assessment was evaluated.

RESULTS

No significant intergroup differences were found between radiation doses or volumes of contrast media. However, iodine doses differed in the two groups (2.1 ± 0.94 g in the iodixanol 270 group and 2.94 ± 1.3 g in iopromide 370 group, $P < .001$). Group objective and subjective measurements were non-significantly different. Overall sensitivity, specificity, positive predictive value, and negative predictive value for correctly differentiating iodixanol 270 and iopromide 370 by visual assessment were 44.3 %, 57.3 %, 57.8 %, and 43.8 %. Overall area under the curve was 0.51.

CONCLUSION

In conclusion, the application of iodixanol 270 was found to be feasible for performing pediatric CCTA at 80 kVp in neonates and infants. Objective measurements of contrast enhancement and subjective image quality assessments were not statistically different in the iodixanol 270 and iopromide 370 groups.

CLINICAL RELEVANCE/APPLICATION

Low-iodine containing contrast media was not inferior to the high-iodine containing contrast media for cardiac CT angiography using 80 kVp in neonates and infants.

RC313-15 Coronary Artery Imaging in Children

Tuesday, Nov. 29 11:40AM - 12:00PM Room: N228

Participants

Lorna Browne, MD, FRCR, Aurora, CO (*Presenter*) Nothing to Disclose

RC314

Interventional Series: Dialysis Interventions

Tuesday, Nov. 29 8:30AM - 12:00PM Room: E353A

IR

AMA PRA Category 1 Credits™: 3.25
ARRT Category A+ Credits: 3.75

FDA

Discussions may include off-label uses.

Participants

Charles E. Ray JR, MD, PhD, Chicago, IL (*Moderator*) Data Safety Monitoring Board, Novate Medical Ltd; Editor, Thieme Medical Publishers, Inc; Consultant, W. L. Gore & Associates, Inc; Consultant, Medtronic plc; ; ; ; ;
Ziv J. Haskal, MD, Baltimore, MD (*Moderator*) Advisory Board, W. L. Gore & Associates Research Consultant, W. L. Gore & Associates Advisory Board, IC Sciences Corporation Royalties, Cook Group Incorporated Research Support, C. R. Bard, Inc Research Consultant, C. R. Bard, Inc Advisory Board, NovaShunt AG Advisory Board, Endoshape, Inc

Sub-Events

RC314-01 Advanced Stent Grafting

Tuesday, Nov. 29 8:30AM - 8:45AM Room: E353A

Participants

Ziv J. Haskal, MD, Baltimore, MD (*Presenter*) Advisory Board, W. L. Gore & Associates Research Consultant, W. L. Gore & Associates Advisory Board, IC Sciences Corporation Royalties, Cook Group Incorporated Research Support, C. R. Bard, Inc Research Consultant, C. R. Bard, Inc Advisory Board, NovaShunt AG Advisory Board, Endoshape, Inc

RC314-02 Debate - Early Stenting?

Tuesday, Nov. 29 8:45AM - 9:00AM Room: E353A

Participants

Charles E. Ray JR, MD, PhD, Chicago, IL (*Presenter*) Data Safety Monitoring Board, Novate Medical Ltd; Editor, Thieme Medical Publishers, Inc; Consultant, W. L. Gore & Associates, Inc; Consultant, Medtronic plc; ; ; ; ;
James T. Bui, MD, Chicago, IL (*Presenter*) Nothing to Disclose

LEARNING OBJECTIVES

1) Discuss outcomes of angioplasty for treatment of failing HD access circuits. 2) Critique role of stenting in failing HD access circuits. 3) Debate merits of angioplasty versus stenting in HD access circuits. 4) Apply personalized management of HD access circuits.

ABSTRACT

RC314-03 Currently Available Stent Grafts

Tuesday, Nov. 29 9:00AM - 9:15AM Room: E353A

Participants

Charles E. Ray JR, MD, PhD, Chicago, IL (*Presenter*) Data Safety Monitoring Board, Novate Medical Ltd; Editor, Thieme Medical Publishers, Inc; Consultant, W. L. Gore & Associates, Inc; Consultant, Medtronic plc; ; ; ; ;

RC314-04 Hemodialysis Reliable Outflow (HeRO) Opportunities and Challenges

Tuesday, Nov. 29 9:15AM - 9:30AM Room: E353A

Participants

James T. Bui, MD, Chicago, IL (*Presenter*) Nothing to Disclose

LEARNING OBJECTIVES

1) Describe applications for use of Hemodialysis Reliable Outflow (HeRO). 2) List potential challenges or complications for HeRO placement and maintenance. 3) Examine options to overcome challenges during use. 4) Identify device and the varying locations on radiographs.

ABSTRACT

RC314-05 Near Infrared Fluorescence Imaging of Matrix Metalloprotease Activity as a Biomarker of Vascular Remodeling in Hemodialysis Access

Tuesday, Nov. 29 9:30AM - 9:40AM Room: E353A

Awards

Student Travel Stipend Award

Participants

Charles N. Weber, MD, Boston, MA (*Presenter*) Nothing to Disclose
Stephen J. Hunt, MD, PhD, Philadelphia, PA (*Abstract Co-Author*) Nothing to Disclose
Terence P. Gade, MD, PhD, New York, NY (*Abstract Co-Author*) Research Grant, Guerbet SA
Gregory J. Nadolski II, MD, Philadelphia, PA (*Abstract Co-Author*) Nothing to Disclose

PURPOSE

Fistulography images the late morphologic changes of vascular remodeling. To better prevent and treat stenosis, imaging of the biological process preceding these late structural changes must be developed. The purpose of this study is to establish the capability of near-infrared fluorescence (NIRF) imaging of MMP activity to be a biomarker of vascular remodeling within an in vivo animal model of hemodialysis access stenosis.

METHOD AND MATERIALS

Arteriovenous fistulae (AVF) were made in 12wk old Sprague Dawley rats (n=10) using an end-to-side anastomosis between the right common femoral artery and vein with interrupted 10-0 suture. Sham operations were performed on the contralateral femoral vessels in all animals. Four weeks after creation, fistulography was performed via a left common carotid artery approach using a 1.5F catheter that was positioned at the aortic bifurcation. At the time of fistulography, 2 nmol of MMP activated NIRF probe (MMPsense 750) was injected from catheter immediately above the aortic bifurcation. NIRF imaging was performed on explanted AVFs and control vessels after 24hrs using Spectrum IVUS (excitation 750nm, detection 780nm). NIRF signal normalized to background was calculated in AVF and control vessels and compared using paired student's t-test. The AVF and control explants were stained with alpha SMA, MMP2, DAPI, and CD31 for immunohistochemical analysis.

RESULTS

AVFs were successfully created in all animals. Fistulography confirmed AVF with >50% peri-anastomotic stenosis in 8 animals 4-weeks post-AVF creation. In the remaining two animals, AVFs were thrombosed. The mean normalized MMP activated NIRF signal was 45.5 in AVFs compared to 16.2 in the contralateral control vessels. The mean increase in total radiant efficiency of AVFs over the control vessels was 2.6-fold (SD = 0.98, p=0.012). Increased NIRF signal correlated with neointimal hyperplasia containing increased alpha-SMA and MMP2 expression.

CONCLUSION

NIRF optical imaging can detect increased MMP activity in stenotic AVFs compared to contralateral normal vessels, which correlated with MMP expression and neointimal hyperplasia on immunohistochemistry. These findings suggest NIRF imaging of MMP may be used as a biomarker for the vascular remodeling underlying stenosis.

CLINICAL RELEVANCE/APPLICATION

Advancement of this technology may provide a mechanism for earlier detection and treatment of vascular remodeling that leads to stenosis in AVF.

RC314-06 Visualization and Quantification of 4D-flow MRI in the Native Radiocephalic Fistula for Hemodialysis

Tuesday, Nov. 29 9:40AM - 9:50AM Room: E353A

Awards

Student Travel Stipend Award

Participants

Yigang Pei, MD, Changsha, China (*Presenter*) Nothing to Disclose

Wenzheng Li, MD, PhD, Changsha, China (*Abstract Co-Author*) Nothing to Disclose

PURPOSE

To evaluate the feasibility of 4D-flow MRI for visualizing and quantifying the hemodynamics of the native radiocephalic fistula (RCF) in hemodialysis patients.

METHOD AND MATERIALS

This prospective study was approved by the institutional review board. Written informed consent was obtained from all participants prior to examination. ECG gated flow-sensitive 4D MRIs with velocity 200cm/s, 400cm/s and 600cm/s were performed respectively on a 3 Tesla scanner (Ingenia, Philips Medical Systems) in 24 consecutive dialysis patients by native RCF for at least 6months. A 4D-flow MRI with mostly distinctly presented native RCF from them for each subject was chosen to achieve the visualization of blood flow's streamline bundles and to evaluate the hemodynamics for the native RCF. The regional peak and mean velocities were quantitatively analyzed at the 3 points of the RCF (the vascular anastomosis, artery and vein proximate segments at 1cm from the anastomosis), which were compared to the referenced standard Doppler ultrasound (DUS).

RESULTS

22 out of 24 subjects were undergone successfully 4D-flow MRI, including 8 native RCF with stenosis and 5 with turbulent blood flow. 3D blood flow's streamline bundles of native RCF were obtained on 4D-flow MRI from dialysis patients' wrist, which was more excellent and extended than DUS. At the anastomosis point, there was no significant difference and had good agreement for peak velocities (p>0.05, r = 0.69) and for mean velocities (p>0.05, r = 0.64) between 4D-flow MR and DUS. At arterial proximate segment, there was no significant difference and had excellent agreement for peak velocities (p>0.05, r = 0.82) and good agreement for mean velocities (p>0.05, r = 0.78). At vein position, there was no significant difference and good agreement for peak velocities (p>0.05, r = 0.65) and for mean velocities (p>0.05, r = 0.58).

CONCLUSION

4D-flow MRI is a promising, non-invasive and safe method for a good visualization of native RCF, and for providing a detailed blood flow's hemodynamics in those hemodialysis patients, which can help to guide the interventional therapy of native RCF relative complications.

CLINICAL RELEVANCE/APPLICATION

4D-flow MRI is a promising, non-invasive and safe method for visualizing and quantifying the hemodynamics of the native RCF in those hemodialysis patients, which can help to guide the interventional treatment of RCF relative complications.

RC314-07 MSCT Vascular Mapping of AV Fistula Related Vascular Complications in Hemodialysis Patients;

Adjuvant Role in Correlation with CDUS

Tuesday, Nov. 29 9:50AM - 10:00AM Room: E353A

Participants

Hazem Soliman, MD, Cairo, Egypt (*Presenter*) Nothing to Disclose
rami sulaiman, Bridgeport, CT (*Abstract Co-Author*) Nothing to Disclose

PURPOSE

To evaluate the role and usefulness of Multislice CT angiography (CTA) and color Doppler US (CDUS) in assessment of vascular tree of AVFs and comprehensive evaluation of possible shunt complications in ESRD patients on hemodialysis.

METHOD AND MATERIALS

Prospective analysis of vascular access related data was obtained from 30 patients (10 Male, 20 Female and age range 18–80 years) referred from hemodialysis unit via CTA and CDUS examination of the upper limbs. All patients were examined to identify the different types of fistula shunt related complications utilizing Doppler indices (PSV, EDV and RI) and different CTA 2D image reconstruction and 3D volume rendering techniques followed by surgical procedures as a gold standard within 2–7 days.

RESULTS

The study showed 15 patients with shunt related complications; aneurysm 33.3% (10 patients) followed by venous thrombosis 23.3% (7 patients), and arterial steal syndrome 13.3% (4 patients), and finally venous hypertension 6.6% (2 patients). Considering surgery as a gold standard the sensitivity and specificity of CDUS and CTA, in detecting aneurysms and stenosis was 100% and 100% respectively. The detection of subclavian occlusion sensitivity and specificity by CDUS was 70% and 85% respectively on the other hand CTA sensitivity and specificity was 100% and 100% respectively.

CONCLUSION

The adjuvant diagnostic value of CTA with CDUS maximizes the evaluation of AV fistula related vascular complications approaching that of surgery.

CLINICAL RELEVANCE/APPLICATION

The MDCT angiography has facilitated non invasive imaging of the vascular system. CT angiography (CTA) demonstrates vessel abnormalities such as stenosis, thrombosis, aneurysms, pseudoaneurysms, calcifications, intimal thickening, stent ingrowth and perivascular complications

RC314-08 Endovascular Hemodialysis AVF Creation

Tuesday, Nov. 29 10:00AM - 10:15AM Room: E353A

Participants

Dheeraj K. Rajan, MD, Toronto, ON (*Presenter*) Consultant, TVA Medical, Inc; Shareholder, TVA Medical, Inc;

LEARNING OBJECTIVES

- 1) Discuss current surgical outcomes for AVF creation.
- 2) Describe the potential advantages of endovascular creation of an AVF.
- 3) Describe current published outcomes with this new procedure.

ABSTRACT

RC314-09 Competitive Outflow Vein Embolization

Tuesday, Nov. 29 10:30AM - 10:45AM Room: E353A

Participants

John E. Aruny, MD, New Haven, CT (*Presenter*) Speakers Bureau, W. L. Gore & Associates, Inc

RC314-10 Clinical and Imaging Assessment of the Failing Dialysis Access

Tuesday, Nov. 29 10:45AM - 11:00AM Room: E353A

Participants

Paul J. Rochon, MD, Denver, CO (*Presenter*) Nothing to Disclose

LEARNING OBJECTIVES

- 1) Clinically evaluate a patient with a failing arteriovenous fistula.

RC314-11 In Vivo Endothelial Cell Gene Expression Analysis of Venous Outflow Stenoses in Hemodialysis Arteriovenous Fistulas Utilizing a Novel Endovascular Sampling Technique

Tuesday, Nov. 29 11:00AM - 11:10AM Room: E353A

Awards

Trainee Research Prize - Fellow

Participants

Hugh C. McGregor, MD, San Francisco, CA (*Presenter*) Research Grant, HealthTronics, Inc
Zhengda Sun, San Francisco, CA (*Abstract Co-Author*) Nothing to Disclose
Miles B. Conrad, MD, Tucson, AZ (*Abstract Co-Author*) Nothing to Disclose
Mark W. Wilson, MD, San Francisco, CA (*Abstract Co-Author*) Nothing to Disclose
Daniel L. Cooke, MD, Seattle, WA (*Abstract Co-Author*) Nothing to Disclose

PURPOSE

To elucidate the mechanisms underlying venous outflow stenosis by evaluating endothelial cell (EC) dysfunction on a molecular level using a novel endovascular sampling technique.

METHOD AND MATERIALS

Informed consent was obtained for this IRB approved proof of concept study. A venous outflow stenosis of a radiocephalic arteriovenous fistula was identified angiographically and with intravascular ultrasound. A Rosen guidewire was advanced into the stenosis and retracted at 1 cm intervals 20 times. Identical sampling technique was used in a morphologically normal outflow vein (control). ECs were identified by immunofluorescence staining with endothelial specific CD31 and sorted by single cell fluorescence activated cell sorting. Gene expression analysis was performed by single-cell quantitative polymerase chain reaction (PCR) using the Fluidigm BioMark HD system. Fluidigm Real-Time PCR Analysis software and SINGuLAR Analysis Toolset 2.1 were used for single-cell quantitative PCR data processing and statistical analysis. Violin plots were used to identify the distribution of expression for each gene between stenosis and control sites.

RESULTS

Immunofluorescence staining for endothelial specific CD31 demonstrated viable ECs. Seventy-five ECs were sorted from the stenosis and 40 from the control vein. Twenty-four ECs from each group were then selected for microfluidic single cell quantitative PCR analysis. Statistically significant differential expression of TIMP metalloproteinase inhibitor 1 (TIMP1) and angiotensin 1 converting enzyme (ACE) between control ECs and ECs sampled from the outflow stenosis were identified. Elevated transcriptional levels of TIMP1 were present in control ECs and elevated transcriptional levels of ACE were present in ECs from the region of stenosis.

CONCLUSION

Endovascular sampling and single cell gene expression analysis of ECs is feasible and may help elucidate the molecular mechanisms underlying venous outflow stenoses in dialysis arteriovenous fistulas. Preliminary data suggests genes involved in inhibition of tissue metalloproteinases may be underexpressed and genes involved in vasoconstriction overexpressed in ECs from stenotic regions when compared to morphologically normal controls.

CLINICAL RELEVANCE/APPLICATION

Understanding the molecular mechanisms underlying vascular stenoses in dialysis arteriovenous fistulas will enable identification of specific drug targets to prolong fistula patency.

RC314-12 Vector Flow Imaging in Arteriovenous Fistulas: New Tool to Evaluate Complex Flow

Tuesday, Nov. 29 11:10AM - 11:20AM Room: E353A

Participants

Ilaria Fiorina, Pavia, Italy (*Presenter*) Travel support, Shenzhen Mindray Bio-Medical Electronics Co, Ltd; Consultant, Esaote SpA; Consultant, Shenzhen Mindray Bio-Medical Electronics Co, Ltd; Consultant, SuperSonic Imagine; Consultant, Hitachi, Ltd; Consultant, Toshiba Corporation
Maria Vittoria Raciti, MD, Pavia, Italy (*Abstract Co-Author*) Nothing to Disclose
Alfredo Goddi, MD, Varese, Italy (*Abstract Co-Author*) Nothing to Disclose
Fabrizio Calliada, MD, Pavia, Italy (*Abstract Co-Author*) Research Grant, Toshiba Corporation; Speakers Bureau Member, Hitachi, Ltd; Speakers Bureau Member, Shenzhen Mindray Bio-Medical Electronics Co, Ltd

PURPOSE

Color Doppler (CD) and Spectral Doppler are the first-line of non invasive imaging techniques to evaluate the flow in hemodialytic fistulas. We assessed a new ultrasound technique: Vector Flow Imaging (VFI).

METHOD AND MATERIALS

We prospectively examined 14 patients (2 females and 12 males), age ranging from 32 to 86 years (mean age 59 years), with functioning upper arm arteriovenous fistulas. We realized the examinations with Resona 7 (Mindray, Shenzhen, China), through high frequency linear array transducer (L11-U3). The scans were performed just before the hemodialytic session, through CD, Spectral Doppler and Vector Flow Imaging.

RESULTS

Vector Flow Imaging (VFI) shows the blood flow direction and velocity, through multiple coloured arrows real-time within a color box. This technique doesn't necessitate of adequate insonation angle and, for that reason, is less prone to operator-related mistakes. In 2 patients the flow in the arteriovenous fistula showed the same features through CD and VFI. Eleven patients demonstrated complex flow, not adequately valuable with conventional color, characterized by orthogonal components (8/11), inverted flow (5/11) and vortices (4/11). Instead in one case, in correspondence of a stenotic tract evidenced through CD, where the velocities were faster, we didn't obtain any signal with VFI.

CONCLUSION

VFI is an intuitive method to study the complex flow in the vascular accesses, that provides additional information despite of conventional CD examination. Furthermore, VFI allows to identify the components of a complex flow, such as vortices and inverted flow.

CLINICAL RELEVANCE/APPLICATION

Vector Flow Imaging can demonstrate singular components of the flow in the arteriovenous fistulas in hemodialysis patients and should be useful for the surveillance of the vascular access.

RC314-13 Comparison of Standard and Extended Lyse- and- Wait Technique for Acute Thrombosed Hemodialysis Fistulas

Tuesday, Nov. 29 11:20AM - 11:30AM Room: E353A

Participants

Susanne Regus, Erlangen, Germany (*Presenter*) Nothing to Disclose
Werner Lang, MD, Erlangen, Germany (*Abstract Co-Author*) Nothing to Disclose
Marco Heinz, Erlangen, Germany (*Abstract Co-Author*) Nothing to Disclose
Axel Schmid, MD, Erlangen, Germany (*Abstract Co-Author*) Nothing to Disclose

PURPOSE

Local thrombolysis with an exposure time of recombinant- tissue plasminogen activator (rtPA) for about 15 to 150 minutes is commonly used to de clot acutely thrombosed hemodialysis fistulas. There is still an ongoing discussion about short or long time thrombolysis for restoration of arteriovenous blood flow. Catheters in case of sudden failure of fistulas or grafts should be avoided, if possible 1 The aim of this study was to compare long (3 hours and more) (LTT) to short (less than 3 hours) (STT) thrombolysis treatment at our institution.

METHOD AND MATERIALS

We retrospectively analyzed 86 interventional declotting procedures (28 STT and 58 LTT) for thrombosed hemodialysis fistulas. Special interest was focused on the intervention time (IT) from first fistulography to the end of angioplasty maneuvers and the risk for temporary catheter placement (TCP).

RESULTS

The IT was reduced after LTT (63.3 ± 9.3 minutes) in contrast to STT (106.7 ± 24.7) ($p < 0.001$), whereas there was no difference in success rate (85.7 % STT, 89.7% LTT; $p = 0.722$). Despite the extended procedure, the need for TCP was not increased after LTT (10.7%) compared to STT (12.1%) ($p = 0.982$), while the major complication rate was reduced (3.4% after LTT and 28.6% after STT; $p = 0.004$).

CONCLUSION

LTT results in shorter and less complicated percutaneous stenosis treatment. Despite the long time interval up to 25 hours until access was punctable for dialysis, there was no increased risk for TCP or major adverse events as bleeding and access rupture after LTT.

CLINICAL RELEVANCE/APPLICATION

we demonstrate our results comparing lyse-and -wait thrombolysis for acute thrombosed hemodialysis access using rtPA with prolonged local reaction time

RC314-14 What the Surgeon Needs to Know

Tuesday, Nov. 29 11:30AM - 11:45AM Room: E353A

Participants

Thomas M. Vesely, MD, Saint Louis, MO (*Presenter*) Research Consultant, W.L. Gore & Associates; Research Consultant, Phase One Medical; Medical Advisory Board, Elcam Medical; Research Consultant, Lutonix

LEARNING OBJECTIVES

Following this course the participant will:1. Learn the advantages of surgical intervention for hemodialysis access.2.Understand the limitations of endovascular interventions.3. Improve patient referral patterns.

RC314-15 Debate: Cephalic Arch: Advanced Interventions vs. Repeat PTA

Tuesday, Nov. 29 11:45AM - 12:00PM Room: E353A

Participants

Ziv J. Haskal, MD, Baltimore, MD (*Presenter*) Advisory Board, W. L. Gore & Associates Research Consultant, W. L. Gore & Associates Advisory Board, IC Sciences Corporation Royalties, Cook Group Incorporated Research Support, C. R. Bard, Inc Research Consultant, C. R. Bard, Inc Advisory Board, NovaShunt AG Advisory Board, Endoshape, Inc
Thomas M. Vesely, MD, Saint Louis, MO (*Presenter*) Research Consultant, W.L. Gore & Associates; Research Consultant, Phase One Medical; Medical Advisory Board, Elcam Medical; Research Consultant, Lutonix

LEARNING OBJECTIVES

After completing this course the participant will:1. Understand the etiology(s) of cephalic arch stenosis.2. Recognize typical and atypical patterns of cephalic arch stenosis.3. Know appropriate indications for treatment of cephalic arch stenosis.

ABSTRACT

RC315

Breast Series: MRI Emerging Technology in Breast Imaging

Tuesday, Nov. 29 8:30AM - 12:00PM Room: Arie Crown Theater



AMA PRA Category 1 Credits™: 3.25
ARRT Category A+ Credits: 4.00

FDA Discussions may include off-label uses.

Participants

Fiona J. Gilbert, MD, Cambridge, United Kingdom (*Moderator*) Research Grant, GlaxoSmithKline plc; Research Grant, General Electric Company; Research Grant, Hologic, Inc
Habib Rahbar, MD, Seattle, WA, (hrahbar@uw.edu) (*Moderator*) Research Grant, General Electric Company

LEARNING OBJECTIVES

Sub-Events

RC315-01 Screening MRI

Tuesday, Nov. 29 8:30AM - 8:50AM Room: Arie Crown Theater

Participants

Constance D. Lehman, MD, PhD, Boston, MA (*Presenter*) Research Grant, General Electric Company; Medical Advisory Board, General Electric Company

RC315-02 Unenhanced Magnetic Resonance Screening using Fused Diffusion-weighted Imaging and Maximum Intensity Projection in Patients with Personal History of Breast Cancer

Tuesday, Nov. 29 8:50AM - 9:00AM Room: Arie Crown Theater

Participants

Ji-Won Kang, MD, Seoul, Korea, Republic Of (*Presenter*) Nothing to Disclose
Hee Jung Shin, MD, Seoul, Korea, Republic Of (*Abstract Co-Author*) Nothing to Disclose
Eun Young Chae, Seoul, Korea, Republic Of (*Abstract Co-Author*) Nothing to Disclose
Woo Jung Choi, MD, Seoul, Korea, Republic Of (*Abstract Co-Author*) Nothing to Disclose
Hak Hee Kim, MD, Seoul, Korea, Republic Of (*Abstract Co-Author*) Nothing to Disclose
Joo Hee Cha, MD, Seoul, Korea, Republic Of (*Abstract Co-Author*) Nothing to Disclose
Ki Chang Shin, Seoul, Korea, Republic Of (*Abstract Co-Author*) Nothing to Disclose

PURPOSE

To assess the diagnostic performance of unenhanced abbreviated protocols (AP) consisting of fused DWI using T1-weighted imaging (T1WI) with DWI maximum intensity projections (DWI MIPs), compared with conventional protocol (CP) consisting of dynamic contrast-enhanced T1WI with MIPs in the screening setting of patients with personal history of breast cancer.

METHOD AND MATERIALS

We conducted a retrospective observational reader study in 351 patients with personal history of breast cancer. Three breast radiologists reviewed the two sets of AP and CP images as follows: First, three readers reviewed the DWI MIP initially to search for the significant lesion and then reviewed the remaining images of AP to characterize the detected lesion on DWI MIPs and establish BIRADS final assessment. Second, MIPs of CP was evaluated, and then the remaining images of CP were assessed. Time to make each decision was measured and recorded.

RESULTS

MRI acquisition time was 5 minutes for the AP and 15 minutes for the CP. For AP, average times to read the DWI MIP and complete AP images were 5.51 and 22.14 seconds, respectively. For CP, average times to read MIP and complete CP images were 7.80 and 39.62 seconds, respectively. Ten in-breast recurrences (7 invasive ductal carcinomas and 3 ductal carcinoma in situ) were diagnosed. Among them, one DCIS was missed by all three readers, which were calcifications alone on mammography and not visible on MRI. On DWI MIP, three readers detected 9, 8, and 9 of 10 cancers, respectively and negative predictive values (NPVs) were 99.6%, 99.3%, and 99.6%, respectively. Complete AP showed sensitivities of 80%, 90%, and 80% and specificities of 94.9%, 93.2%, and 95.2%, respectively. On CP MIP, three readers detected 9, 8, and 9 of 10, respectively, and NPVs were 99.6%, 99.3%, and 98.6%, respectively. Complete CP showed sensitivities of 90.9 %, 90.0 %, and 80.0 % and specificities of 93.8%, 93.8%, and 96.3%, respectively.

CONCLUSION

An unenhanced AP showed short acquisition time of 5 minutes, and DWI MIP showed high NPVs more than 99% across three readers. Diagnostic performance of complete AP was equivalent to that of CP in the screening of patients with personal history of breast cancer.

CLINICAL RELEVANCE/APPLICATION

Diagnostic performance of an unenhanced AP was equivalent to that of CP with short acquisition time and no usage of contrast material in the screening of patients with personal history of breast cancer.

RC315-03 Head-to-head Comparison of Diffusion-weighted Imaging to Dynamic Contrast-Enhanced Magnetic Resonance Imaging of the Breast: Stand-Alone or Complimentary Parameter for Breast Cancer Detection?

Participants

Katja Pinker-Domenig, MD, Vienna, Austria (*Presenter*) Nothing to Disclose
Elizabeth J. Sutton, MD, New York, NY (*Abstract Co-Author*) Nothing to Disclose
Michael Weber, Vienna, Austria (*Abstract Co-Author*) Nothing to Disclose
Nina Purvis, MSc, PhD, New York City, NY (*Abstract Co-Author*) Nothing to Disclose
Sunitha Thakur, PhD, MS, New York, NY (*Abstract Co-Author*) Nothing to Disclose
Thomas H. Helbich, MD, Vienna, Austria (*Abstract Co-Author*) Research Grant, Medicor, Inc Research Grant, Siemens AG Research Grant, C. R. Bard, Inc
Maxine S. Jochelson, MD, New York, NY (*Abstract Co-Author*) Nothing to Disclose
Elizabeth A. Morris, MD, New York, NY (*Abstract Co-Author*) Nothing to Disclose

PURPOSE

Diffusion weighted imaging (DWI) is increasingly used in clinical practice and together with dynamic contrast-enhanced MRI (DCE-MRI) as multiparametric (MP) MRI achieves excellent sensitivities and increases specificity. The aim of this study was to assess whether DWI can be used as a stand-alone parameter for breast cancer detection and to compare it to DCE-MRI and MP MRI.

METHOD AND MATERIALS

In this two-center study prospectively populated data-bases were searched for patients with a BI-RADS 0,4/5 finding, who underwent MP MRI of the breast with DCE-MRI and DWI and subsequent histopathologic verification. 100 patients were randomly selected and MP MRI data was retrospectively evaluated by two experienced readers in consensus. All DCE images and DWI with ADC maps were randomly assessed in an independent review, i.e. readers assessed DWI without being provided DCE-MRI and vice-versa. Examinations were classified as either normal or abnormal (suspicious finding, further assessment necessary). A BI-RADS rating (1-5) was assigned. Lesion size and ADC values were recorded. MP MRI with DWI and DCE-MRI was assessed using a reading method that adapted ADC-thresholds to the BI-RADS classification. Histopathology was used as the reference standard. Appropriate statistical tests were used to assess sensitivity, specificity, and diagnostic accuracy.

RESULTS

There were 42 malignant and 58 benign tumors. DCE-MRI was the most sensitive test for breast cancer detection with a sensitivity of 100%. DWI as a stand-alone parameter was significantly less sensitive with 80% ($p=0.001$) but more specific with 78.6% compared to DCE-MRI with 66.7%. Diagnostic accuracy was 80% for DWI and 86% for DCE-MRI respectively. Except for a mucinous carcinoma and a ILC, missed cancers with DWI (11/42) were consistently lesions <12mm. When both parameters were used complementary as MP MRI, sensitivity with 96.7% was not significantly different from DCE-MRI ($p=0.45$) and specificity almost as good as DWI with 76.2% ($p=1$) resulting in the best diagnostic accuracy of 88%.

CONCLUSION

DWI cannot be used as a stand-alone parameter for breast cancer detection with sensitivities decreasing in smaller lesions. MP MRI with DWI and DCE-MRI achieves the best diagnostic accuracy for breast cancer detection.

CLINICAL RELEVANCE/APPLICATION

Radiologist should be aware that DWI should not be used as a stand-alone parameter for breast cancer detection but used complementary to DCE-MRI.

RC315-04 High Risk Breast Cancer Screening with an Ultrafast High Spatiotemporal Resolution MRI Sequence; Less Costly and as Reliable as a Full Diagnostic MRI Protocol

Tuesday, Nov. 29 9:10AM - 9:20AM Room: Arie Crown Theater

Participants

Jan Van Zelst, MD, Nijmegen, Netherlands (*Abstract Co-Author*) Nothing to Disclose
Albert Gubern-Merida, PhD, Nijmegen, Netherlands (*Abstract Co-Author*) Nothing to Disclose
Suzan Vreemann, MSc, Nijmegen, Netherlands (*Abstract Co-Author*) Nothing to Disclose
Jeroen Veltman, MD, Hengelo, Netherlands (*Presenter*) Nothing to Disclose
Monique D. Dorrius, MD, PhD, Groningen, Netherlands (*Abstract Co-Author*) Nothing to Disclose
Claudette E. Loo, MD, Amsterdam, Netherlands (*Abstract Co-Author*) Nothing to Disclose
Katya M. Duvivier van Hoof, Utrecht, Netherlands (*Abstract Co-Author*) Nothing to Disclose
Nico Karssemeijer, PhD, Nijmegen, Netherlands (*Abstract Co-Author*) Shareholder, Matakina Technology Limited Consultant, QView Medical, Inc Shareholder, QView Medical, Inc Director, ScreenPoint Medical BV Shareholder, ScreenPoint Medical BV
Ritse M. Mann, MD, PhD, Nijmegen, Netherlands (*Abstract Co-Author*) Research agreement; Siemens AG; Research agreement, Seno Medical Instruments, Inc

PURPOSE

High costs of breast cancer screening with MRI are mainly due to the costs of MRI itself. TWIST is an ultrafast dynamic contrast enhanced MRI (UDCE) sequence with a temporal resolution of 4.3s and a diagnostic spatial resolution, thus allowing morphologic and kinetic evaluation of breast lesions. A dynamic TWIST series can be obtained in 102s and may decrease the costs of breast MRI substantially compared to a standard full diagnostic protocol (FDP) that typically takes about 15-20 minutes. The purpose of our study is to investigate whether breast cancer screening with an UDCE only is as accurate as screening with a FDP.

METHOD AND MATERIALS

The need for informed consent was waived by the IRB. Women at >20% risk who underwent a hybrid breast MRI screening protocol including a standard FDP (T1w dynamic contrast-enhanced (VIBE) series, T2w imaging and diffusion weighted imaging) and a UDCE on a 3-Tesla scanner (SIEMENS, Erlangen, Germany) with a dedicated 16-channel breast coil were eligible for this study. We included all screening exams with a screen-detected malignant ($n=31$) or benign ($n=54$) lesion between 2011 and 2015. Furthermore, 115 randomly selected normal exams with >2 years of negative follow-up were included. Four dedicated breast radiologists were asked to read all 200 exams twice in two separate reading sessions; once reading the FDP (without UDCE) and once only the UDCE series. Reading sessions were at least 4 weeks apart and the reading modes and order of the cases were

randomized for each reader. Suspicious findings were scored using the BI-RADS scoring system and a likelihood scale from 0-100. Multi-case-multi-reader ROC analysis was used to evaluate reader performance. McNemar tests were used to compare the mean sensitivity and specificity.

RESULTS

The mean AUC for the FDP was 0.87 and 0.89 for UDCE only reading ($p=0.21$). Readers worked on a slightly different operating point of the ROC curve; the mean sensitivity of UDCE vs FDP was slightly lower (80 vs 85%; $p=0.1$), while the specificity was significantly higher (81 vs 77%; $p=0.001$), respectively.

CONCLUSION

UDCE only is as accurate as a standard FDP for screening women at increased risk of developing breast cancer.

CLINICAL RELEVANCE/APPLICATION

Ultrafast high spatiotemporal resolution MRI such as a UDCE can be performed within 102 seconds, substantially decreasing the time needed to perform accurate breast MRI and thus the costs.

RC315-05 Breast MRI: Is Background Parenchymal Enhancement (BPE) Predicted By Serum Sex Hormone Levels?

Tuesday, Nov. 29 9:20AM - 9:30AM Room: Arie Crown Theater

Participants

Glen Lo, MBBS, Perth, Australia (*Presenter*) Nothing to Disclose
Rachel P. Fleming, MD, Etobicoke, ON (*Abstract Co-Author*) Nothing to Disclose
Anabel M. Scaranelo, MD, PhD, Toronto, ON (*Abstract Co-Author*) Nothing to Disclose
Karina Bukhanov, MD, Toronto, ON (*Abstract Co-Author*) Nothing to Disclose
Divjot Minhas, , ON (*Abstract Co-Author*) Nothing to Disclose
Hadas Moshonov, PhD, Toronto, ON (*Abstract Co-Author*) Nothing to Disclose
Pavel Crystal, MD, Toronto, ON (*Abstract Co-Author*) Nothing to Disclose

PURPOSE

Background parenchymal enhancement (BPE) at breast magnetic resonance imaging (MRI) has been shown to be associated with breast cancer risk. The factors responsible for BPE were not sufficiently studied. Our study aimed to evaluate a correlation between BPE and plasma sex hormone levels and ability to predict BPE based on a combination of sex hormone levels.

METHOD AND MATERIALS

Eligible MRI studies included high-risk screening and diagnostic studies. Exclusion criteria were prior breast carcinoma or radiation therapy and current anti-oestrogen medication (e.g. tamoxifen). MRI studies were performed on Siemens units at 1.5 T or 3 T with standard protocol (T1 and T2-weighted imaging without and with fat saturation, diffusion-weighted imaging and ADC maps) with Gadavist enhancement (0.1 mmol/kg at 2.0 mL/s with 20 mL saline flush, scanning at 35 s, 1, 2 and 6 min). MRI studies were post-processed on an automated viewing platform to calculate BPE (MultiView software, HOLOGIC). Serum drawn at time of MRI measured estradiol, progesterone, follicular stimulating hormone (FSH), luteinizing hormone (LH) and prolactin. Patient demographic data collected included MRI indication, menopausal status, menarche, HRT use, date of LMP (day of cycle), prior oophorectomy, height and mass (BMI).

RESULTS

86 women were enrolled, with sex hormone levels measured and automated BPE measurement obtainable. Median age was 49 years (29-70). We observed a negative correlation between each sex hormone and BPE, however, none of these correlations were statistically significant: estradiol ($r=0.05$, $p=0.63$); progesterone ($r=0.003$, $p=0.98$); FSH ($r=-0.05$, $p=0.63$); LH ($r=-0.1$, $p=0.36$); prolactin ($r=0.02$, $p=0.85$). Based on multiple regression (with stepwise selection), there was no combination of sex hormones that could significantly predict BPE.

CONCLUSION

We observed no association between individual or combination serum sex hormone levels and BPE.

CLINICAL RELEVANCE/APPLICATION

Our results suggest that factors other than blood sex hormones may play a significant role in predicting background parenchymal enhancement (BPE). Our study does not provide direct support for current practice of scheduling breast MRI during the second week of the menstrual cycle.

RC315-06 Diagnostic MRI

Tuesday, Nov. 29 9:30AM - 9:50AM Room: Arie Crown Theater

Participants

Elizabeth A. Morris, MD, New York, NY (*Presenter*) Nothing to Disclose

RC315-07 Estimation of T2* Relaxation Time of Breast Cancer: Correlation with Clinical, Imaging and Pathological Features

Tuesday, Nov. 29 9:50AM - 10:00AM Room: Arie Crown Theater

Participants

Mirinae Seo, MD, Seoul, Korea, Republic Of (*Presenter*) Nothing to Disclose
Jung Kyu Ryu, MD, PhD, Seoul, Korea, Republic Of (*Abstract Co-Author*) Nothing to Disclose
Geon-Ho Jahng, PhD, Seoul, Korea, Republic Of (*Abstract Co-Author*) Nothing to Disclose
Hye Shin Ahn, MD, Seoul, Korea, Republic Of (*Abstract Co-Author*) Nothing to Disclose
Sun Jung Rhee, MD, Seoul, Korea, Republic Of (*Abstract Co-Author*) Nothing to Disclose

PURPOSE

The purpose of this study was to estimate the T2* relaxation time in breast cancer and to evaluate the relationship of the T2* value of breast cancer with clinical-imaging-pathological features.

METHOD AND MATERIALS

Between January 2011 and July 2013, 107 consecutive women with 107 breast cancers underwent multi-echo T2* weighted imaging on a 3.0 T clinical magnetic resonance image system. The Student's t-test and one-way analysis of variance (ANOVA) were used to compare the T2* values of cancer for different groups based on clinical-imaging-pathological features (age at diagnosis, menopausal status, symptoms at diagnosis, family history, mammographic density, calcification at mammography, lesion location, size, and signal intensity on T2-weighted image (T2WI) at MRI, pathologic subtype, LN metastasis, histologic grade, ER, PR, HER2, p53, Ki-67, CK 5/6, and molecular subtype). In addition, multiple linear regression analysis was performed to find independent predictive factors associated with T2* values.

RESULTS

The mean T2* value of 92 invasive cancers was significantly longer than that of 15 ductal carcinomas in situ (DCIS) ($p=0.029$). Signal intensity on T2-weighted MR images (T2WI) and histologic grade of invasive breast cancers showed significant correlation with T2* relaxation time in univariate and multivariate analysis. Breast cancer group with higher signal intensity compared with breast parenchyma on T2WI showed longer T2* relaxation time ($p=0.006$). Cancer group with higher histologic grade showed longer T2* relaxation time ($p=0.014$).

CONCLUSION

T2* value was significantly longer in invasive cancer than DCIS. In invasive cancers, T2* relaxation time was significantly longer in cancer with high histologic grade and high signal intensity on T2WI. Based on these preliminary data, quantitative T2* mapping is a potentially useful technique for the characterization of breast cancer.

CLINICAL RELEVANCE/APPLICATION

Quantitative T2* mapping is a potentially useful technique for the characterization of breast cancer in yielding information of the tumor microstructure.

RC315-08 Feasibility Analysis of Early Temporal Kinetic features in an Abbreviated MRI Protocol as a Surrogate Marker for Tumor Type, Grade, and Prognosis

Tuesday, Nov. 29 10:00AM - 10:10AM Room: Arie Crown Theater

Awards

Trainee Research Prize - Fellow

Participants

Laura Heacock, MD, MS, New York, NY (*Presenter*) Nothing to Disclose
Yiming Gao, MD, New York, NY (*Abstract Co-Author*) Nothing to Disclose
Alana A. Lewin, MD, New York, NY (*Abstract Co-Author*) Nothing to Disclose
Neeti Bagadiya, MD, New York, NY (*Abstract Co-Author*) Nothing to Disclose
Amy N. Melsaether, MD, New York, NY (*Abstract Co-Author*) Nothing to Disclose
James S. Babb, PhD, New York, NY (*Abstract Co-Author*) Nothing to Disclose
Samantha L. Heller, MD, PhD, New York, NY (*Abstract Co-Author*) Nothing to Disclose
Linda Moy, MD, New York, NY (*Abstract Co-Author*) Nothing to Disclose

PURPOSE

To evaluate the role of early temporal kinetics in differentiating invasive ductal carcinoma (IDC) and ductal carcinoma in situ (DCIS) by tumor grade, tumor type and prognostic markers.

METHOD AND MATERIALS

In this institutional review board-approved study, 152 women with 178 pathology-proven lesions underwent breast DCE-MRI on a 3.0T magnet with a 7 channel breast coil. The protocol consisted of pre-contrast, first post-contrast and subtraction images. Lesion size, shape, morphology, initial enhancement ratio (IER; % signal increase over baseline at the first post-contrast acquisition), pathology, axillary metastases, Oncotype DX score, background parenchymal enhancement (BPE) and peritumoral BPE were evaluated. Statistical analysis included Fisher's exact tests, Mann-Whitney U tests and Spearman rank correlation.

RESULTS

Cancers were 76% (135/178) IDC and 24% (43/178) DCIS. For IDC, 57% (77/135) were estrogen receptor/progesterone receptor-positive (ER/PR+), 21% (28/135) were triple negative breast cancer (TNBC) and 22% (31/135) were human epidermal growth factor receptor 2-positive (HER2+). IER was higher for IDC than DCIS ($p<0.001$) and for high-grade DCIS and IDC compared to low-grade DCIS ($p<0.001$). IER increased as tumor grade increased ($r=0.38$, $p<0.001$), as ki-67 increased ($r=0.28$, $p=0.002$), as BPE increased ($r=0.31$, $p<0.001$), and as size increased ($r=0.37$, $p<0.001$). Mean IER was higher for IDC with positive nodes (211% [82-452%]) than for no nodes (156% [44-359%], $p=0.00$) and for HER2+ (mean=213% [100-359%]) and TNBC (mean=227% [110-452%]) than for ER/PR+ tumors (mean=164% [54-298%], $p=0.026$). There was no correlation between Oncotype DX score and IER. There was no correlation between BPE/peritumoral BPE and size, tumor grade, ki-67, or positive axillary nodes.

CONCLUSION

High IER at the first post-contrast imaging can differentiate high-grade malignancy, HER2+/TNBC cancers, axillary invasion, and high ki-67 tumors, all predictors of tumor recurrence after therapy. There is a growing clinical interest in an abbreviated breast MRI protocol for breast cancer screening; IER is an important temporal kinetic marker that can be easily assessed with such a protocol.

CLINICAL RELEVANCE/APPLICATION

Initial enhancement ratio (IER) correlates with likelihood of a biologically significant breast cancer and is easily incorporated into screening abbreviated breast MRI (AB-MRI).

RC315-09 Electronic Property Tomography (EPT): A New Breast MRI Application for Differentiating between Malignant and Benign Breast Lesions

Tuesday, Nov. 29 10:10AM - 10:20AM Room: Arie Crown Theater

Participants

Keiko Tsuchiya, Otsu, Japan (*Abstract Co-Author*) Nothing to Disclose
Naoko Mori, MD, PhD, Sendai, Japan (*Abstract Co-Author*) Nothing to Disclose
Deepa Sheth, MD, Chicago, IL (*Presenter*) Nothing to Disclose
David V. Schacht, MD, Chicago, IL (*Abstract Co-Author*) Nothing to Disclose
Ulrich Katscher, Hamburg, Germany (*Abstract Co-Author*) Employee, Koninklijke Philips NV
Hiroyuki Abe, MD, Chicago, IL (*Abstract Co-Author*) Nothing to Disclose

PURPOSE

To evaluate the diagnostic value of Electronic Property Tomography (EPT) in differentiating malignant from benign breast lesions

METHOD AND MATERIALS

EPT is a method that maps the conductivity and permittivity using phase-based conductivity images reconstructed from clinical MR sequences. The causes of elevated conductivity in tumors are the presence of necrosis and cell membrane breakdown, increased cell membrane charge, increased sodium concentration, and changes in water content. We obtained phase images reconstructed from the 3D TSE sequence (TR/TE=2000/210 ms, voxel size=0.7x0.7x0.8mm³) using a 3T system (Philips Achieva TX) with a 16 channel breast coil. A tissue conductivity map was then made from phase images using the EPT technique. 69 patients with 32 benign and 51 malignant breast lesions were enrolled in this study. All malignant lesions and 24 benign lesions were confirmed pathologically, and 8 benign lesions were confirmed by clinical follow-up for more than 2 years. The lesions were segmented semi-automatically on pre/post-contrast subtraction images, and the segmented volume of the lesions was registered to the phase images. Subsequently, reconstruction of the conductivity map was performed. The conductivity reconstruction was made only inside the lesions. The mean conductivity of benign and malignant breast lesions was compared. Statistical analysis was performed using paired Wilcoxon and Mann-Whitney U tests.

RESULTS

The mean conductivity of malignant lesions was -0.0964 ± 1.80403 S/m, and that of benign lesions was 1.3017 ± 1.21225 S/m. There was a statistically significant difference between two groups ($p = 0.0001$). The corresponding ROC yielded an AUC of 75% (Sensitivity, specificity, PPV and NPV were 71, 79, 84 and 63% using the cut-off point of 0.88512 S/m).

CONCLUSION

Our study revealed that there was a statistically significant difference in mean conductivity between benign and malignant breast lesions. The result suggests that EPT could be useful in differentiating benign and malignant breast lesions.

CLINICAL RELEVANCE/APPLICATION

The novel technique of EPT has the potential to differentiate benign and malignant breast lesions.

RC315-10 Dual-Parametric MR Imaging with Read-Out Segmented Diffusion-Weighted and High Temporal Resolution Dynamic Contrast-Enhanced Imaging Improves the Differentiation of Breast Lesions

Tuesday, Nov. 29 10:20AM - 10:30AM Room: Arie Crown Theater

Awards

Student Travel Stipend Award

Participants

Yanqiong Chen, MD, Shanghai, China (*Presenter*) Nothing to Disclose
Bin Wu, MD, Shanghai, China (*Abstract Co-Author*) Nothing to Disclose
Hui Liu, Shanghai, China (*Abstract Co-Author*) Employee, Siemens AG
Yan Xu, Shanghai, China (*Abstract Co-Author*) Nothing to Disclose
Caixia Fu, Shenzhen, China (*Abstract Co-Author*) Employee, Siemens AG
Dan Wang, Shanghai, China (*Abstract Co-Author*) Nothing to Disclose
Jian Mao, Shanghai, China (*Abstract Co-Author*) Nothing to Disclose
Ya Jia Gu, MD, Shanghai, China (*Abstract Co-Author*) Nothing to Disclose

PURPOSE

To investigate the clinical value of a dual-parameter classification method in differentiating benign and malignant breast lesions using RS-DWI and quantitative DCE.

METHOD AND MATERIALS

One hundred and seven patients with 125 breast lesions were scanned with DCE-MRI (a prototype TWIST-Dixon VIBE sequence was used to achieve a temporal resolution of 5.3 s) and RS-DWI (RESOLVE, $b = 50, 800$ s/mm²) in a 3T MR scanner. ADC was calculated inline and Ktrans was calculated using a commercially available software package. Volume of interest was semi-automatically delineated on the last phase of DCE. ADC map was rigidly registered into DCE images. For each ADC and Ktrans 1D histogram, the following parameters were calculated for the entire tumor volume: the mean, median, low quantile, upper quantile, kurtosis and skewness. A 2D histogram (Ktrans-ADC) was also generated using a dual-parameter mapping package, and then the 2D parameters were calculated from the normalized Ktrans-ADC map. Each parameter was correlated with a pathologic result, and its Receiver Operating Characteristic was calculated.

RESULTS

All the patients underwent breast lumpectomy or radical resection after MR imaging. Breast lesions included 98 malignant and 27 benign lesions. For ADC analysis, AUC of median, low quantile and skewness had statistically diagnostic value in ROC test (mean: 0.738, low quantile: 0.713, upper quantile: 0.572, kurtosis: 0.509, skewness: 0.703); for Ktrans histogram, AUC value of mean, upper quantile and kurtosis had diagnostic value (mean: 0.841, low quantile: 0.585, upper quantile: 0.807, kurtosis: 0.642,

skewness: 0.601); for dual-parametric Ktrans-ADC 2D histogram approach, all the parameters had diagnostic value (Xm: 0.852, Ym: 0.743, kurtosis: 0.809, skewness: 0.803).

CONCLUSION

The major limitation of DCE MR imaging in breast disease is that benign lesions like fibroadenoma can also cause a local perfusion increase. The implementation of dual-parametric MR imaging in combination with DCE MR imaging and DWI optimizes the diagnostic accuracy in our study of breast tumors at 3T. Further investigation on the clinical usage of dual-parameter analysis in a larger population base is a necessity, and it also might be useful in classifying pathological subtypes of breast cancer and monitoring the changes of neoadjuvant chemotherapy.

CLINICAL RELEVANCE/APPLICATION

To improve the diagnostic value of MRI in breast lesions.

RC315-11 Difference in Enhancement Pattern between Malignant and Benign Non-Mass Enhancement Lesions at Very Early Post-Contrast Phase on Ultra-Fast Breast MRI

Tuesday, Nov. 29 10:30AM - 10:40AM Room: Arie Crown Theater

Participants

Hiroyuki Abe, MD, Chicago, IL (*Presenter*) Nothing to Disclose
Andrea L. Magee, MD, Chicago, IL (*Abstract Co-Author*) Nothing to Disclose
Naoko Mori, MD, PhD, Sendai, Japan (*Abstract Co-Author*) Nothing to Disclose
Keiko Tsuchiya, Otsu, Japan (*Abstract Co-Author*) Nothing to Disclose
Deepa Sheth, MD, Chicago, IL (*Abstract Co-Author*) Nothing to Disclose
David V. Schacht, MD, Chicago, IL (*Abstract Co-Author*) Nothing to Disclose
Gregory S. Karczmar, PhD, Chicago, IL (*Abstract Co-Author*) Nothing to Disclose
Federico Pineda, PhD, Chicago, IL (*Abstract Co-Author*) Nothing to Disclose
Kirti M. Kulkarni, MD, Chicago, IL (*Abstract Co-Author*) Nothing to Disclose

PURPOSE

To evaluate the kinetic data of benign and malignant breast non-mass enhancement lesions in the ultra-early phase after contrast injection, using a whole breast ultrafast (UF) MR scanning technique.

METHOD AND MATERIALS

29 non-mass enhancing breast lesions (biopsy-proven 12 benign and 17 malignant lesions) were obtained with an acquisition protocol of UF-MRI, consisting of pre and 8 post-contrast bilateral, fat-suppressed T1 weighted images of the whole breasts, with temporal resolution of 7 second on a Philips Achieva 3T-TX. Regular scans (temporal resolution of 75 second) were followed immediately after UF-MRI. The size of malignant lesions ranged from 15 to 112 mm (mean 46 mm) and that of benign lesions ranged from 9 to 34 mm (mean 22 mm). All benign lesions were proven by MR-guided biopsy, and all malignant lesions were surgically excised and confirmed with surgical pathology. The kinetic curve of the highest enhancing voxel in each lesion during the UF phase (0 – 56 sec) was assessed with a commercially available CAD system (DynaCAD). To compensate for differences in time-of-arrival of contrast media, time points in the ultrafast scans were relative to the initial contrast enhancement in the descending aorta: we referred to the time point when the aorta began to enhance as 'C1', and referred to subsequent time points as 'C2,' 'C3,' etc. Enhancement rate (ER: % increase in signal after contrast injection) and area under the kinetic curve (kinetic-AUC) of UF-MRI and Signal enhancement rate (SER) of the regular scans were compared between malignant and benign lesions. Wilcoxon test and ROC test were performed for statistical analysis.

RESULTS

ER and kinetic-AUC both showed significant differences between malignant and benign non-mass lesions ($p < 0.0001$ at C2 – C5), but SER of the regular scans did not show a significant difference. With ROC analysis, area under curve for ER was over 0.94 at C2 – C5, and that for kinetic-AUC was over 0.94 at C3 – C6.

CONCLUSION

The kinetic curve obtained during the very early post-contrast phase was quite useful in differentiating malignant and benign non-mass enhancement breast lesions. Kinetic data from a voxel of the highest enhancement in a lesion is critical to performing this task.

CLINICAL RELEVANCE/APPLICATION

The kinetic curve of a voxel of the highest enhancement in a lesion obtained from Ultrafast MRI is useful in differentiating malignant and benign non-mass enhancement breast lesions.

RC315-12 Quantitative Breast MRI

Tuesday, Nov. 29 10:50AM - 11:10AM Room: Arie Crown Theater

Participants

Despina Kontos, PhD, Philadelphia, PA, (Despina.Kontos@uphs.upenn.edu) (*Presenter*) Nothing to Disclose

LEARNING OBJECTIVES

1) Review fundamental principles of quantitative breast MRI. 2) Identify key factors that affect quality and standardization of quantitative breast MRI measures. 3) Describe emerging clinical applications of quantitative breast MRI in diagnostic interpretation, prognostication, and evaluation of response to treatment.

ABSTRACT

RC315-13 Breast Cancer Heterogeneity Assessed by Texture Analysis in Magnetic Resonance Imaging: Its Relationship with Survival Outcomes

Participants

Eun Sook Ko, MD, Seoul, Korea, Republic Of (*Presenter*) Nothing to Disclose
Boo-Kyung Han, MD, PhD, Seoul, Korea, Republic Of (*Abstract Co-Author*) Nothing to Disclose
Eun Young Ko, MD, PhD, Seoul, Korea, Republic Of (*Abstract Co-Author*) Nothing to Disclose
Jungmin Bae, Seoul, Korea, Republic Of (*Abstract Co-Author*) Nothing to Disclose
Ji Soo Choi, MD, PhD, Seoul, Korea, Republic Of (*Abstract Co-Author*) Nothing to Disclose

PURPOSE

To determine the relationship between tumor heterogeneity assessed by magnetic resonance imaging (MRI) texture analysis and survival outcomes in patients with primary breast cancer.

METHOD AND MATERIALS

This study was approved by the institutional review board, and the need for informed consent was waived. Between January 2010 and August 2010, texture analysis of the entire primary tumor was performed using T2-weighted and contrast-enhanced T1-weighted subtraction MR images obtained from 203 patients for preoperative staging. Histogram-based uniformity and entropy were calculated. To dichotomize texture parameters for survival analysis, the 10-fold cross-validation method was used to determine cutoff points in the receiver operating characteristic curve analysis. The Cox proportional hazards model and Kaplan-Meier analysis were used to determine the association of MRI texture parameters and morphologic or volumetric information obtained from MRI or clinicopathological variables with recurrence-free survival (RFS).

RESULTS

There were 26 events, including 22 recurrences (10 locoregional and 12 distant) and 4 deaths, after a mean follow-up time of 56.2 months. In multivariate analysis, higher N stage (RFS hazard ratio, 11.15 [N3 stage]; $P = 0.003$), triple-negative subtype (RFS hazard ratio = 16.91; $P < 0.001$), high risk of T1 entropy (less than the cutoff value, RFS hazard ratio = 4.55; $P = 0.018$), and T2 entropy (equal to or higher than the cutoff value, RFS hazard ratio = 9.84; $P = 0.001$) were associated with worse outcomes.

CONCLUSION

Patients with more heterogeneous breast cancers on T2-weighted images (higher entropy) and less heterogeneous tumors on contrast-enhanced T1-weighted subtraction images (lower entropy) exhibited poorer RFS.

CLINICAL RELEVANCE/APPLICATION

No study determined whether tumor texture is related to survival outcomes based on preoperative breast MRI. Our study suggests that magnetic resonance imaging texture analysis for measurements of tumor heterogeneity can be used as an additional risk stratification method for patients with primary breast cancer.

RC315-14 Predicting Level of Tumor Infiltrating Lymphocyte in Patients with Triple Negative Breast Cancer: Usefulness of Breast MRI Computer-aided Detection & Diagnosis

Tuesday, Nov. 29 11:20AM - 11:30AM Room: Arie Crown Theater

Participants

Seon Jeong Oh, MD, Seoul, Korea, Republic Of (*Presenter*) Nothing to Disclose
Hak Hee Kim, MD, Seoul, Korea, Republic Of (*Abstract Co-Author*) Nothing to Disclose
You Jin Ku, Incheon, Korea, Republic Of (*Abstract Co-Author*) Nothing to Disclose
Joo Hee Cha, MD, Seoul, Korea, Republic Of (*Abstract Co-Author*) Nothing to Disclose
Hee Jung Shin, MD, Seoul, Korea, Republic Of (*Abstract Co-Author*) Nothing to Disclose
Hee Jin Lee, Seoul, Korea, Republic Of (*Abstract Co-Author*) Nothing to Disclose
Gyungyub Gong, Seoul, Korea, Republic Of (*Abstract Co-Author*) Nothing to Disclose

PURPOSE

Triple negative breast cancer (TNBC) is a heterogeneous malignancy with varying prognosis. Recently, the importance of tumor-infiltrating lymphocytes (TILs) has been determined. That is, increased TILs positively correlated with the pathological complete response and patient survival. The purpose of this study is to evaluate the usefulness of MRI computer-aided detection & diagnosis (CAD) in TNBC patients for prediction of tumor infiltrating lymphocyte.

METHOD AND MATERIALS

We retrospectively enrolled 60 lesions in 59 patients with TNBC (mean age, 48.7 years; range, 25-81 years) who underwent dynamic contrast-enhanced MRI. The CAD for all lesions were obtained, and the analyzed quantitative kinetic features included degree of initial peak enhancement; enhancement profiles including lesion percentages of washout, plateau and persistent enhancement; worst kinetic curve and predominant kinetic curve. According to level of TIL, we divided the tumors into two groups (<50% TILs as the low TIL group and $\geq 50\%$ TILs as the high TIL group). Kinetic parameters in low TIL group versus high TIL group were compared using student t-test and chi-square test. We developed empirical model to predict high TIL group and low TIL group using logistic regression analysis and receiver operating characteristics (ROC) analysis

RESULTS

There were 48 low TIL and 12 high TIL lesions. Among enhancement profiles of MRI CAD, persistent portion of tumors were negatively correlated with the TIL level of tumor (mean proportion of persistent on high TIL group was 43%, $p = 0.003$). The persistent-washout value of low TIL group was significantly higher than that of high TIL group ($p = 0.008$). The odds ratios were 0.944 (95% confidence interval (CI), 0.896-0.982; $p=0.012$) for persistent and 0.971 (95% CI, 0.948-0.991; $p=0.008$) for persistent - washout value. The area under the receiver operating characteristic curve (AUC) was >0.7 with the optimal cutoff values of 26 for persistent and -19 for persistent-washout.

CONCLUSION

The prediction model using quantitative kinetic parameters, particularly plateau proportion and plateau-washout value, could be helpful for identifying TIL level of patient with triple negative breast cancer and may be used as an imaging biomarker to guide the

treatment plan.

CLINICAL RELEVANCE/APPLICATION

Kinetic parameters acquired by MRI CAD can be a useful tool for assessing TIL level of patient with triple negative breast cancer.

RC315-15 Quantitative Radiogenomics: Association between Breast MRI Functional Tumor Volume and Oncotype DX Recurrence Score

Tuesday, Nov. 29 11:30AM - 11:40AM Room: Arie Crown Theater

Participants

Lina Nayak, MD, San Francisco, CA (*Abstract Co-Author*) Nothing to Disclose
Kimberly M. Ray, MD, San Francisco, CA (*Presenter*) Nothing to Disclose
Genevieve A. Woodard, MD, PhD, Pittsburgh, PA (*Abstract Co-Author*) Nothing to Disclose
Bonnie N. Joe, MD, PhD, San Francisco, CA (*Abstract Co-Author*) Nothing to Disclose
Nola M. Hylton, PhD, San Francisco, CA (*Abstract Co-Author*) Nothing to Disclose
Elissa R. Price, MD, San Francisco, CA (*Abstract Co-Author*) Nothing to Disclose
Jessica Gibbs, San Francisco, CA (*Abstract Co-Author*) Nothing to Disclose
Iryna Lobach, San Francisco, CA (*Abstract Co-Author*) Nothing to Disclose
David Newitt, PhD, San Francisco, CA (*Abstract Co-Author*) Nothing to Disclose
Rick Baehner, MD, San Francisco, CA (*Abstract Co-Author*) Stockholder, Agendia BV

PURPOSE

To investigate the association between MRI functional tumor volume (FTV), a non-invasive quantitative measure of contrast kinetics, and breast cancer recurrence risk as determined by a validated gene expression assay.

METHOD AND MATERIALS

This is an IRB-approved, HIPAA-compliant retrospective review of 82 patients with ER+ HER2- invasive breast cancer treated at our institution between 2005 and 2013 who underwent breast MRI and an Oncotype DX (ODx) assay (Genomic Health, Inc.) at the time of diagnosis. MRI signal enhancement ratio (SER), a relative measure of contrast uptake and washout, was calculated on a per-voxel basis. Functional tumor volume (FTV) was defined as the volume of enhancing voxels above an initial enhancement level of 70%. Fraction of Washout and Plateau (FWP) was defined as the volume of enhancing voxels with "washout" or "plateau" kinetics (SER > 0.9) divided by FTV. Fraction of Washout (FW) was defined as the volume of voxels with "washout" kinetics only (SER > 1.3) divided by FTV. Concordance between ODx score and MRI parameters was examined using Spearman correlation correlation ρ , χ^2 tests, and linear regression models.

RESULTS

FTV measurements [mean(cm³) +/-SD] for patients with high, intermediate and low risk ODx scores were 3.7 ± 3.84 , 2.7 ± 3.9 and 1.95 ± 2.39 , respectively. ODx scores were significantly associated with FTV ($\beta=1.4$, $p=0.006$, $R^2=0.31$) in a model adjusted for age, tumor size (measured on MRI), tumor grade, and lymph node status. In a subset of tumors measuring 14-25mm (25-75th percentile of observed tumor size), FWP and ODx scores were concordant ($p=0.34$, $p=0.025$). FW alone was not significantly correlated with ODx score.

CONCLUSION

Higher FTV is significantly associated with higher ODx score, independent of patient age, tumor size, tumor grade or lymph node status. Larger FWP is significantly correlated with higher ODx score for tumors 14-25 mm in size, which represent the majority of tumors in our dataset.

CLINICAL RELEVANCE/APPLICATION

Quantitative MRI FTV measurements may serve as imaging biomarkers of breast cancer recurrence risk.

RC315-16 Evaluating Breast Cancer by Using Mono-exponential, Bi-exponential, Stretched-exponential Diffusion-weighted MR Imaging and Diffusion Kurtosis MR Imaging

Tuesday, Nov. 29 11:40AM - 11:50AM Room: Arie Crown Theater

Participants

Kun Sun, Shanghai, China (*Presenter*) Nothing to Disclose
Xu Yan, Shanghai, China (*Abstract Co-Author*) Employee, Siemens AG
Caixia Fu, Shenzhen, China (*Abstract Co-Author*) Employee, Siemens AG
Fuhua Yan, MS, Shanghai, China (*Abstract Co-Author*) Nothing to Disclose

PURPOSE

To quantitatively compare the potential of various diffusion parameters obtained from mono-exponential, bi-exponential, and stretched-exponential diffusion weighted imaging and diffusion kurtosis imaging in evaluating breast cancer.

METHOD AND MATERIALS

Institutional review board approval and written informed consent were obtained. Both diffusion-weighted-imaging and diffusion-kurtosis-imaging were performed in 94 patients with pathologically proven breast lesions by using a 1.5 T MRI unit. Apparent diffusion coefficient(ADC) was by using a mono-exponential model. Diffusion coefficient(D), pseudo-diffusion coefficient(D*) and perfusion fraction(f) were calculated by using a bi-exponential model. A water molecular diffusion heterogeneity index(α) and distributed diffusion coefficient(DDC) were calculated by using a stretched-exponential model. Mean diffusivity(MD) and mean kurtosis(MK) was calculated from diffusion kurtosis images. All values were compared between benign and malignant breast lesions and different proliferative breast cancer. Student t test, Wilcoxon signed-rank test, ROC curves, and Spearman correlation were used for statistical analysis.

RESULTS

ADC.D.DDC.and MD were significantly lower in malignant lesions than in benign lesions(respectively: $P < .0001$). α . D* and MK were

MD and MK were significantly better in malignant lesions than in benign lesions (respectively; $P = .0001$ and $P = .0001$) were significantly higher in malignant lesions than in benign lesions (respectively; $P < .0001$). Both MD and MK had significantly greater AUC (0.967 and 0.960) than D^* , α , and f (0.677 vs 0.692 vs 0.522) in the differentiation of benign and malignant lesions ($P < .0001$). In patients with invasive breast cancer, kurtosis and water molecular diffusion heterogeneity index was positively correlated with expression of the Ki-67 protein ($r=0.55$ and 0.43).

CONCLUSION

DKI model may provide additional information and improve the characterizing of breast lesions compared with conventional diffusion parameters. The kurtosis and water molecular diffusion heterogeneity index derived from DKI and stretched Exponential DWI may be helpful for the preoperative differentiation of proliferative activity of breast cancer.

CLINICAL RELEVANCE/APPLICATION

Non-Gaussian water diffusion with use of DKI and SE, as compared with conventional mono- and bi-exponential DWI, could lead to a substantial improvement in the diagnosis of breast disease. The K and α value derived from the DKI and SE model may be helpful for the preoperative differentiation of proliferative activity of breast cancer.

RC315-17 Magnetic Resonance Spectroscopy of Breast Cancer for Assessing Early Treatment Response: Results from the ACRIN 6657 MRS Trial

Tuesday, Nov. 29 11:50AM - 12:00PM Room: Arie Crown Theater

Participants

Patrick J. Bolan, PhD, Minneapolis, MN (*Presenter*) Research Consultant, Breast-Med, Inc
Eunhee Kim, Chapel Hill, NC (*Abstract Co-Author*) Nothing to Disclose
Benjamin A. Herman, MS, Providence, RI (*Abstract Co-Author*) Nothing to Disclose
Gillian M. Newstead, MD, Chicago, IL (*Abstract Co-Author*) Medical Advisory Board, Bayer AG Consultant, Three Palm Software LLC Consultant, VuCOMP, Inc Medical Advisor, Quantitative Insights, Inc
Mark A. Rosen, MD, PhD, Philadelphia, PA (*Abstract Co-Author*) Nothing to Disclose
Mitchell D. Schnall, MD, PhD, Philadelphia, PA (*Abstract Co-Author*) Nothing to Disclose
Etta D. Pisano, MD, Charleston, SC (*Abstract Co-Author*) Researcher, Koninklijke Philips NV; Researcher, FUJIFILM Holdings Corporation; Researcher, Alan Penn & Associates, Inc; Stockholder, NextRay, Inc; Board Member, NextRay, Inc
Paul T. Weatherall, MD, Dallas, TX (*Abstract Co-Author*) Nothing to Disclose
Elizabeth A. Morris, MD, New York, NY (*Abstract Co-Author*) Nothing to Disclose
Constance D. Lehman, MD, PhD, Boston, MA (*Abstract Co-Author*) Research Grant, General Electric Company; Medical Advisory Board, General Electric Company
Michael G. Garwood, PhD, Minneapolis, MN (*Abstract Co-Author*) Stockholder, Steady State Imaging, LLC
Michael Nelson, MD, Minneapolis, MN (*Abstract Co-Author*) I hold license and patents on a breast marker named VizMark
Douglas Yee, MD, Minneapolis, MN (*Abstract Co-Author*) Nothing to Disclose
Sandra Polin, Washington, DC (*Abstract Co-Author*) Nothing to Disclose
Laura J. Esserman, MD, , (*Abstract Co-Author*) Nothing to Disclose
Constantine Gatsonis, PhD, Providence, RI (*Abstract Co-Author*) Consultant, WILEX AG Consultant, Endocyte, Inc
Gregory J. Metzger, PhD, Minneapolis, MN (*Abstract Co-Author*) Nothing to Disclose
David Newitt, PhD, San Francisco, CA (*Abstract Co-Author*) Nothing to Disclose
Savannah C. Partridge, PhD, Seattle, WA (*Abstract Co-Author*) Nothing to Disclose
Nola M. Hylton, PhD, San Francisco, CA (*Abstract Co-Author*) Nothing to Disclose

PURPOSE

To estimate the accuracy of predicting response to neoadjuvant chemotherapy (NACT) in patients with locally advanced breast cancer using magnetic resonance spectroscopy (MRS) measurements made very early in treatment.

METHOD AND MATERIALS

The HIPAA-compliant protocol and the informed consent process were approved by the American College of Radiology and local-site institutional review boards. 119 women with invasive breast cancer of 3 cm or greater undergoing NACT with a paclitaxel-based regimen in followed by an anthracycline-cyclophosphamide regimen were enrolled between September 2007 and April 2010. Each site received MRS-specific training and was required to submit MRS measurements with acceptable accuracy and spectral quality from a trial-specific spectroscopy phantom prior to enrolling patients. MRS measurements of the concentration of choline-containing compounds ([tCho]) were performed prior to the first chemotherapy regimen (time point 1, TP1) and 20-96 hours after the first cycle of treatment (TP2). The change in [tCho] was assessed for its ability to predict pathologic complete response (pCR) and radiologic response using the area under the receiver operating characteristic curve (AUC) and logistic regression models.

RESULTS

Of the 119 subjects enrolled, only 29 cases (24%) with 8 pCRs provided usable data for the primary analysis. Technical challenges in acquiring quantitative MRS data in a multi-site trial setting limited the capture of usable data. In this limited data set, the decrease in tCho from TP1 to TP2 had poor ability to predict either pCR (AUC = 0.53, 95% CI: [0.27, 0.79]) or radiologic response (AUC = 0.51, 95% CI: [0.27, 0.75]). An exploratory analysis found that water T2 (measured by MRS) was more easily measured (data yield 59%, 60/102) and was associated with pathologic complete response ($p < 0.01$).

CONCLUSION

The technical difficulty of acquiring quantitative MRS data in a multi-site clinical trial setting led to a low yield of analyzable data, which was insufficient to accurately measure the ability of early MRS measurements to predict response to NACT. These findings suggest that further technical developments are needed to produce more robust methods for breast MRS.

CLINICAL RELEVANCE/APPLICATION

The low data yield of this study suggests that current methods used for acquiring quantitative magnetic resonance spectroscopy data in the breast are not sufficiently robust for use in clinical practice.

Honored Educators

Presenters or authors on this event have been recognized as RSNA Honored Educators for participating in multiple qualifying

educational activities. Honored Educators are invested in furthering the profession of radiology by delivering high-quality educational content in their field of study. Learn how you can become an honored educator by visiting the website at: <https://www.rsna.org/Honored-Educator-Award/>

Mitchell D. Schnall, MD, PhD - 2013 Honored Educator

RC316

International Medical Student Imaging Education (Sponsored by the Committee on International Radiology Education)

Tuesday, Nov. 29 8:30AM - 10:00AM Room: S102D

ED

AMA PRA Category 1 Credits™: 1.50
ARRT Category A+ Credits: 1.50

Participants

Kristen K. DeStigter, MD, Burlington, VT (*Moderator*) Medical Advisory Board, Koninklijke Philips NV; Luminary, McKesson Corporation; Research collaboration, Koninklijke Philips NV;

Sub-Events

RC316A Introduction

Participants

Kristen K. DeStigter, MD, Burlington, VT (*Presenter*) Medical Advisory Board, Koninklijke Philips NV; Luminary, McKesson Corporation; Research collaboration, Koninklijke Philips NV;

LEARNING OBJECTIVES

1) Define the role of the RSNA Committee on International Radiology Education (CIRE) in advancing radiology education through its various programs. 2) Assess opportunities for radiology education in other countries especially those with the most need. 3) Assess the different educational programs administered by the CIRE, the specific areas of emphasis of each program and the qualifications of candidates for these programs.

ABSTRACT

The RSNA Committee on International Radiology Education (CIRE) administers four educational programs each targeting a different population of radiologists. The International Visiting Professor program sends a team of radiologists with different areas of expertise, based on the needs expressed by the host country. The team lectures at national radiology society annual meetings, local hospitals and teaching institutions during a two week period. The Derek Harwood Nash fellowship selects junior faculty within 10 years after completion of training from all over the world who desire to have focused training on a specific radiologic specialty in an institution chosen by the applicant. They train for 6-12 weeks in the U. S. institution prior to returning to their countries. The Introduction to Research for Young Academics selects international residents or fellows interested in academics. They join selected residents from U.S. programs for one week of research workshops during RSNA week. The Education Materials and Journal award program selects institutions of learning from developing or newly-developed nations to receive gratis online or print subscriptions to *Radiology* and *RadioGraphics* in addition to other materials from the RSNA Education Center. Background information and updated data will be provided for each program.

RC316B Best Practices for Introducing Radiology into the Medical Student Curriculum (Why, When, Where, Who, How for Radiology Departments and Radiologists)

Participants

Petra J. Lewis, MD, Lebanon, NH, (petra.lewis@hitchcock.org) (*Presenter*) Book contract, Oxford University Press; Consultant, Siemens AG

LEARNING OBJECTIVES

1) List 3 reasons why medical students should learn medical imaging. 2) Identify the most appropriate places in the curriculum for this to occur. 3) Compare the advantages and disadvantages of different instructor types. 4) Describe 3 different methods of integrating medical imaging into the curriculum.

RC316C How Training Radiology during Medical School is Performed in Europe

Participants

Valerie Vilgrain, MD, Clichy, France (*Presenter*) Nothing to Disclose

LEARNING OBJECTIVES

1) Describe the different approaches to training radiology during medical school in Europe. 2) Compare the advantages and disadvantages of the different approaches. 3) Describe how training should be performed.

ABSTRACT

RC316D Medical Imaging: The Basics and the Safety

Participants

Francesco Sardanelli, MD, San Donato Milanese, Italy, (f.sardanelli@grupposandonato.it) (*Presenter*) Speakers Bureau, Bracco Group Research Grant, Bracco Group Speakers Bureau, Bayer AG Research Grant, Bayer AG Research Grant, IMS International Medical Scientific

LEARNING OBJECTIVES

1) To learn a simple way to link technology and safety through the distinction between *ionizing radiation-free imaging modalities* and *non-ionizing radiation-free modalities*. 2) To understand the assumption of *linear relationship between dose and effect of low*

dose ionizing radiation and its consequences in terms of *appropriateness and justification*, *ALARA principle*, and *renewal cycle of radiological equipment*, with special attention to CT. 3) To understand the *huge technological innovation for CT dose reduction* during the last ten years. 4) To become familiar with *MR contraindications and classification of medical devices as MR-safe, MR-conditional, and MR-unsafe*. 5) To understand *contrast materials safety issues*.

ABSTRACT

Imaging modalities should be subdivided into: I) *ionizing radiation-free techniques* such as US, MRI, and optical imaging; II) *non-ionizing radiation-free techniques* such as radiography, tomosynthesis, fluoroscopy, DSA, CT, DEXA, scintigraphy, SPECT, and PET. Metrics of radiation dose should be presented for *absorbed, equivalent* (considering the radiation type), and *effective dose* (considering the exposed tissue, too). The assumption of a *linear relationship between dose and effect of low dose radiation* has to be presented together with the lack of evidence for any increase of cancer incidence for pilots and crews of commercial flight companies or for populations living in regions at high altitudes. Examples for explaining radioprotection should be provided, such as *translating radiological procedures into number of chest x-ray radiograms*. Reducing radiation dose should be presented as a "must" with three key points: 1. Evidence-based *appropriateness and justification*; 2. *Optimization* (ALARA principle); 3. *Renewal of equipment*, with special attention to CT. Simple criteria should be provided such as considering alternatives to CT especially for young patients under 35. On the other hand, the huge technological innovation cycle for CT dose reduction during the last ten years has to be highlighted, showing the advantages of more sensitive detectors combined with iterative algorithms for image noise reduction. *MR contraindications* and classification of *medical devices as MR-safe, MR-conditional, and MR-unsafe* have to be presented. Finally, *contrast materials safety issues* should be illustrated, including the prohibition of barium when a gastrointestinal perforation is suspected and the attention to renal function and history of allergy for both iodinated and Gd-based contrast materials for intravascular injection. In the light of the Hippocrates' principle *Primum, non nocere*, the recent report of Gd accumulation in brain nuclei should be taken into consideration, especially when multiple injections are probable.

RC316E Diagnostic Imaging-related Mini-research as a Part of Medical Student Education: Current Status and Perspective

Participants

Kunihiko Fukuda, MD, Tokyo, Japan, (fukuda@jikei.ac.jp) (Presenter) Nothing to Disclose

LEARNING OBJECTIVES

1) Describe the possible topics for undergraduate imaging-related mini-research. 2) List the advantages and disadvantages of research for students and educators. 3) Describe the suitable timing for image related mini-research. 4) Describe how image related mini-research should be performed.

ABSTRACT

RC317

Emerging Technology: PET/MRI - Opportunities and Challenges

Tuesday, Nov. 29 8:30AM - 10:00AM Room: S504CD



AMA PRA Category 1 Credits™: 1.50
ARRT Category A+ Credits: 1.50

Discussions may include off-label uses.

Participants

Rathan M. Subramaniam, MD, PhD, Dallas, TX (*Moderator*) Nothing to Disclose

Sub-Events

RC317A PET/MRI: The Evolving Imaging Field of Structure and Function

Participants

Rathan M. Subramaniam, MD, PhD, Dallas, TX (*Presenter*) Nothing to Disclose

RC317B PET/MRI Physics: The Opportunities and Challenges

Participants

Georges El Fakhri, PhD, Boston, MA (*Presenter*) Nothing to Disclose

RC317C PET/MRI Clinical Applications: Brain and Head and Neck

Participants

Alexander Drzezga, MD, Cologne, Germany (*Presenter*) Consultant, Siemens AG; Consultant, Bayer AG; Consultant, General Electric Company; Consultant, Eli Lilly and Company; Consultant, The Piramal Group; Speakers Bureau, Siemens AG; Speakers Bureau, Bayer AG; Speakers Bureau, General Electric Company; Speakers Bureau, Eli Lilly and Company; Speakers Bureau, The Piramal Group

LEARNING OBJECTIVES

1) Review relevant clinical applications for PET/MR in the diagnostic work-up of disorders of the brain. 2) Review strengths of PET/MR for disorders of the head and neck. 3) Understand the value of different currently available tracers for neuroimaging and oncological applications. 4) Review challenges and limitations of PET/MR in brain/head&neck and expected future developments.

RC317D PET/MRI Clinical Applications: Body

Participants

Thomas A. Hope, MD, San Francisco, CA, (thomas.hope@ucsf.edu) (*Presenter*) Research Grant, Consultant, GE Healthcare

LEARNING OBJECTIVES

1) Review common current applications for abdominopelvic oncologic PET/MRI, including hepatic malignancies, rectal cancer, and cervical cancer. 2) Understand the role of novel tracers in prostate cancer (PSMA PET) and neuroendocrine tumors (somatostatin receptor PET). 3) Present the current limitations and future advances in PET/MRI that will help increase the clinical acceptance and applicability of body PET/MRI.

ABSTRACT

RC317E PET/MRI Clinical Applications: Cardiac

Participants

Pamela K. Woodard, MD, Saint Louis, MO, (woodardp@mir.wustl.edu) (*Presenter*) Research Grant, Astellas Group; Research Grant, Bayer AG; Research agreement, Siemens AG; ; ; ;

LEARNING OBJECTIVES

1) Discuss clinical cardiac PET/MR imaging applications, including myocardial perfusion and viability, nonischemic cardiomyopathy, and tumor assessment.

ABSTRACT

RC318

Interactive Game: When Do Imaging Findings Make a Difference?

Tuesday, Nov. 29 8:30AM - 10:00AM Room: E450B



AMA PRA Category 1 Credits™: 1.50
ARRT Category A+ Credits: 1.50

Participants

Sub-Events

RC318A Neuro

Participants

Birgit B. Ertl-Wagner, MD, Munich, Germany, (Birgit.Ertl-Wagner@med.lmu.de) (*Presenter*) Board Member, Koninklijke Philips NV; Board Member, Bracco Group; Board Member, Springer Science+Business Media; Consultant, MMI Munich Medical International GmbH; Consultant, Koninklijke Philips NV; Consultant, Springer Science+Business Media; Consultant, Thieme Medical Publishers, Inc; Consultant, Bracco Group; Institutional Research Grant, Eli Lilly and Company; Institutional Research Grant, F. Hoffmann-La Roche Ltd; Institutional Research Grant, Guerbet SA; Institutional Research Grant, Merck KGaA; Institutional Research Grant, Bayer AG; Institutional Research Grant, Novartis AG; Speaker, Siemens AG; Author, Springer Science+Business Media; Author, Thieme Medical Publishers, Inc; Author, Bracco Group; Royalties, Springer Science+Business Media; Royalties, Thieme Medical Publishers, Inc; Stockholder, Siemens AG; Travel support, Siemens AG;

LEARNING OBJECTIVES

1) To comprehend the importance of signs in neuroimaging for diagnostic decision making. 2) To understand in which instances imaging findings have a direct consequence for therapeutic decision making. 3) To appreciate the therapeutic consequences of selected neuroimaging findings.

RC318B Musculoskeletal

Participants

David M. Panicek, MD, New York, NY, (panicekd@mskcc.org) (*Presenter*) Nothing to Disclose

LEARNING OBJECTIVES

1) Assess imaging features that facilitate specific diagnoses of musculoskeletal lesions. 2) Describe scenarios in which various imaging features of musculoskeletal lesions lead to more accurate tumor staging and treatment response assessment. 3) Detect musculoskeletal complications of tumors and their treatment.

RC318C Pelvis

Participants

Caroline Reinhold, MD, MSc, Montreal, QC (*Presenter*) Consultant, GlaxoSmithKline plc

LEARNING OBJECTIVES

1) Understand the role of imaging in the management of gynaecological malignancies. 2) Assess imaging features that allow accurate staging of gynaecological malignancies. 3) Be familiar with pitfalls that can result in staging errors using imaging. 4) Understand the changes in imaging appearance post treatment.

ABSTRACT

Honored Educators

Presenters or authors on this event have been recognized as RSNA Honored Educators for participating in multiple qualifying educational activities. Honored Educators are invested in furthering the profession of radiology by delivering high-quality educational content in their field of study. Learn how you can become an honored educator by visiting the website at: <https://www.rsna.org/Honored-Educator-Award/>

Caroline Reinhold, MD, MSc - 2013 Honored Educator
Caroline Reinhold, MD, MSc - 2014 Honored Educator

RC320

Challenges in Hodgkin's Lymphoma Management Across the Age Spectrum

Tuesday, Nov. 29 8:30AM - 10:00AM Room: S102C

RO

AMA PRA Category 1 Credits™: 1.50
ARRT Category A+ Credits: 1.50

Participants

Stephanie A. Terezakis, MD, Baltimore, MD (*Moderator*) Nothing to Disclose
Satish P. Shanbhag, MBBS, MPH, Baltimore, MD (*Presenter*) Nothing to Disclose
Bradford Hoppe, MD, Jacksonville, FL (*Presenter*) Nothing to Disclose
Chelsea C. Pinnix, MD, PhD, Houston, TX (*Presenter*) Nothing to Disclose
Stacy L. Cooper, MD, Baltimore, MD, (scoope30@jhmi.edu) (*Presenter*) Nothing to Disclose

LEARNING OBJECTIVES

1) Compare pediatric and adult adaptive therapy trials in Hodgkin Lymphoma. 2) Examine the pattern of relapse amongst pediatric and adult patients with Hodgkin Lymphoma. 3) Critique radiation doses used in pediatric and adult patients with Hodgkin Lymphoma.

ABSTRACT

RC321

Advances in CT: Technologies, Applications, Operations-Quantitative CT (QIBA)

Tuesday, Nov. 29 8:30AM - 10:00AM Room: E352



AMA PRA Category 1 Credits™: 1.50
ARRT Category A+ Credits: 1.50

Participants

Ehsan Samei, PhD, Durham, NC (*Coordinator*) Research Grant, General Electric Company; Research Grant, Siemens AG
Norbert J. Pelc, ScD, Stanford, CA (*Coordinator*) Research support, General Electric Company; Research support, Koninklijke Philips NV; Consultant, Varian Medical Systems, Inc; Consultant, NanoX; Scientific Advisory Board, RefleXion Medical Inc; Scientific Advisory Board, Prismatic Sensors AB; Medical Advisory Board, OurCrowd, LP ;

Sub-Events

RC321A Volumetry

Participants

Michael F. McNitt-Gray, PhD, Los Angeles, CA (*Presenter*) Institutional research agreement, Siemens AG Research support, Siemens AG

Active Handout: Michael F. McNitt-Gray

http://abstract.rsna.org/uploads/2016/16001076/RC321_Volumetry.pdf

RC321B Material Identification

Participants

Daniele Marin, MD, Durham, NC, (daniele.marin@duke.edu) (*Presenter*) Research support, Siemens AG

LEARNING OBJECTIVES

1) Review different dual-energy CT imaging techniques for material identification. 2) Provide an overview of clinically available applications of material identification using dual-energy CT. 3) Identify factors that can affect the reproducibility of quantitative measurements of material composition using dual-energy CT.

ABSTRACT

RC321C Texture Characterization

Participants

Samuel G. Armato III, PhD, Chicago, IL, (s-armato@uchicago.edu) (*Presenter*) Consultant, Aduro Biotech, Inc
Maryellen L. Giger, PhD, Chicago, IL (*Presenter*) Stockholder, Hologic, Inc; Stockholder, Quantitative Insights, Inc; Co-founder, Quantitative Insights, Inc; Royalties, Hologic, Inc; Royalties, General Electric Company; Royalties, MEDIAN Technologies; Royalties, Riverain Technologies, LLC; Royalties, Mitsubishi Corporation; Royalties, Toshiba Corporation;

LEARNING OBJECTIVES

1) Understand the concept of texture-based image characterization. 2) Identify radiologic tasks in CT that could benefit from image texture analysis. 3) Describe the limitations of these techniques.

RC322

Imaging for Personalized Medicine: Thorax

Tuesday, Nov. 29 8:30AM - 10:00AM Room: S502AB

CH RO PH

AMA PRA Category 1 Credits™: 1.50
ARRT Category A+ Credits: 1.50

Participants

Carri Glide-Hurst, Detroit, MI (*Moderator*) Research Consultant, Koninklijke Philips NV; Research agreement, Koninklijke Philips NV; Research agreement, Modus Medical Devices Inc

Sub-Events

RC322A Managing Anatomical Change and Respiration during Radiotherapy

Participants

Geoffrey Hugo, PhD, Richmond, VA (*Presenter*) Research Grant, Koninklijke Philips NV; Research Grant, Varian Medical Systems, Inc

LEARNING OBJECTIVES

- 1) Understand how respiration impacts radiotherapy imaging and delivery and how to implement strategies to mitigate these issues.
- 2) Understand types and magnitude of geometric changes in thoracic anatomy during radiotherapy, and determine approaches to correct for discrepancies between the planned and delivered dose to the patient.

ABSTRACT

Radiotherapy is in widespread use for both early and advanced stage lung cancer, as a sole modality and also in combination with other modalities such as chemotherapy. Due to the potential for both acute and late toxicities in organs adjacent to treated regions, modern techniques seek to limit the extent of the high dose volume. The purpose of this session is to develop an understanding for how geometric and anatomic changes during radiotherapy can be managed. The focus will be on solutions readily available in the clinic today, particularly with respect to imaging modalities and planning solutions.

RC322B Functional Targeting and Adaptation

Participants

Carri Glide-Hurst, Detroit, MI (*Presenter*) Research Consultant, Koninklijke Philips NV; Research agreement, Koninklijke Philips NV; Research agreement, Modus Medical Devices Inc

LEARNING OBJECTIVES

- 1) Understand the opportunities for targeting and avoidance based on functional imaging in lung.
- 2) Discuss the technical details of functional targeting for tumor and functional avoidance in normal tissue for lung cancer in the pre-treatment and adaptive settings.

ABSTRACT

Radiation therapy continues to play an important role in the treatment of lung cancer although many opportunities remain to improve local control and survival as well as reduce toxicity, especially in advanced stage lung cancer. The use of functional imaging and biomarkers to predict tumor burden and response as well as measure and predict normal tissue toxicity has begun to increase in the community. This session aims to summarize the different modalities and types of information available to perform functional targeting or avoidance of tumor and normal tissue in lung cancer, including imaging (such as PET and SPECT) and other data (such as blood-based biomarkers). The session will also highlight the technical details associated with the use of functional data for treatment planning, treatment response, and adaptation.

RC323

Molecular Imaging Mini-Course: Basics of Molecular Imaging

Tuesday, Nov. 29 8:30AM - 10:00AM Room: S403B



AMA PRA Category 1 Credits™: 1.50
ARRT Category A+ Credits: 1.50

Participants

Sub-Events

RC323A Developing Molecular Imaging Agents

Participants

Julie L. Sutcliffe, PhD, Sacramento, CA (*Presenter*) Nothing to Disclose

LEARNING OBJECTIVES

1) Describe the ideal properties of a molecular imaging agent and molecular target. 2) Describe the in vitro and in vivo validation of the molecular imaging agent. 3) Describe specific examples of successful molecular imaging agents.

ABSTRACT

RC323B Instrumentation (PET and CT) and Image Reconstruction

Participants

John Sunderland, PhD, Iowa City, IA, (john-sunderland@uiowa.edu) (*Presenter*) Research Grant, Siemens AG

LEARNING OBJECTIVES

1) Identify the primary design components of a modern PET/CT system. 2) Design and implement a PET/CT quality control program to assure high quality and quantitatively accurate clinical imaging. 3) Describe commonly used PET reconstruction algorithms and the practical impact of reconstruction parameters upon image quality and quantitation.

ABSTRACT

RC323C Basic Clinical Applications

Participants

Hubert J. Vesselle, MD, PhD, Seattle, WA (*Presenter*) Consultant, MIM Software Inc

ABSTRACT

RC324

Why Do Radiologists Burn out, and What Can We Do About It?

Tuesday, Nov. 29 8:30AM - 10:00AM Room: E353C

OT **PR**

AMA PRA Category 1 Credits™: 1.50
ARRT Category A+ Credit: 0

Participants

Richard B. Gunderman, MD, PhD, Indianapolis, IN, (rbguneer@iu.edu) (*Moderator*) Nothing to Disclose

LEARNING OBJECTIVES

1) Identify common causes of burnout. 2) Describe techniques for avoiding burnout. 3) Develop strategies to enhance resilience and thriving.

ABSTRACT

Burnout is becoming an increasingly important problem in medicine, with adverse consequences for patients, health care organizations, and physicians themselves. In this course, we explore the causes of burnout in contemporary radiology practice, strategies for preventing and remedying it when it develops, and steps radiologists can take to enhance their professional resiliency and fulfillment.

Sub-Events

RC324A Causes of Burnout

Participants

Richard B. Gunderman, MD, PhD, Indianapolis, IN (*Presenter*) Nothing to Disclose

RC324B Strategies for Avoiding Burnout

Participants

Norman J. Beauchamp JR, MD, Seattle, WA (*Presenter*) Research Grant, Koninklijke Philips NV

ABSTRACT

Burnout is becoming an increasingly important problem in medicine, with adverse consequences for patients, health care organizations, and physicians themselves. In this course, we explore the causes of burnout in contemporary radiology practice, strategies for preventing and remedying it when it develops, and steps radiologists can take to enhance their professional resiliency and fulfillment.

RC324C Resiliency and Thriving

Participants

David P. Fessell, MD, Ann Arbor, MI, (fessell@umich.edu) (*Presenter*) Nothing to Disclose

LEARNING OBJECTIVES

ABSTRACT

RC325

Medical Physics 3.0: Re-envisioning Medical Physics in the Era of Value-based and Precision Healthcare

Tuesday, Nov. 29 8:30AM - 10:00AM Room: N229

PH

AMA PRA Category 1 Credits™: 1.50
ARRT Category A+ Credits: 1.50

Participants

Todd Pawlicki, PhD, La Jolla, CA (*Presenter*) Nothing to Disclose

Ehsan Samei, PhD, Durham, NC, (samei@duke.edu) (*Presenter*) Research Grant, General Electric Company; Research Grant, Siemens AG

LEARNING OBJECTIVES

1) Understand the broad trajectory of advances in the contribution of medical physics to human health. 2) Understand the attributes of excellent in clinical physics. 3) Outline processes to position physicists to have the competence and the confidence to fulfill their unique calling as scientific agents of precision and innovation in healthcare.

RC327

Prospering in the Era of Payment Reform

Tuesday, Nov. 29 8:30AM - 10:00AM Room: N226

HP

AMA PRA Category 1 Credits™: 1.50
ARRT Category A+ Credit: 0

Participants

James A. Brink, MD, Boston, MA (*Moderator*) Nothing to Disclose

James A. Brink, MD, Boston, MA (*Coordinator*) Nothing to Disclose

LEARNING OBJECTIVES

1) To understand the Merit-Based Incentive Payment System (MIPS) and Alternative Payment Models (APMs) required as part of the Medicare Access and CHIP Reauthorization Act of 2015. 2) To explore mechanisms to respond to the shift from volume to value-based reimbursement models. 3) To consider ways to provide both personalized and population-based imaging care.

Sub-Events

RC327A MACRA Mandates and How to Deal with Them

Participants

Ezequiel Silva III, MD, San Antonio, TX (*Presenter*) Nothing to Disclose

LEARNING OBJECTIVES

View learning objectives on main course title.

RC327B Involving Patients In Their Radiological Care: Radiologist Visibility, Personalized Care and Improving Outcomes

Participants

Geraldine B. McGinty, MD, MBA, New York, NY, (gbm9002@med.cornell.edu) (*Presenter*) Nothing to Disclose

LEARNING OBJECTIVES

View learning objectives on main course title.

RC327C The Radiologist's Role in Population Health Management: Leveraging Technology for Better Outcomes

Participants

James A. Brink, MD, Boston, MA (*Presenter*) Nothing to Disclose

LEARNING OBJECTIVES

View learning objectives on main course title.

Should I Scan That Patient: Updates and an Interactive Session on MR Safety and Regulations (A Very Interactive Session)

Tuesday, Nov. 29 8:30AM - 10:00AM Room: E351



AMA PRA Category 1 Credits™: 1.50
ARRT Category A+ Credits: 1.50

Participants

Jerry W. Froelich, MD, Minneapolis, MN, (froel005@umn.edu) (*Presenter*) Researcher, Siemens AG
Thomas L. Chenevert, PhD, Ann Arbor, MI (*Presenter*) Consultant, Koninklijke Philips NV
Jay K. Pahade, MD, New Haven, CT (*Presenter*) Consultant, Precision Imaging Metrics, LLC

LEARNING OBJECTIVES

1) Gain a better understanding of how to manage life threatening emergencies that may occur within the MRI scanner and when or if to quench the magnet. 2) Learn the proposed guidelines for performing needed MRI's in patients with Implanted Cardiac Electronic Devices (IECD's). 3) Answer questions regarding real-life MR safety questions and how to analyze potential issues and make an educated decision as to weather to perform an MRI on a particular patient. and 4) Ask and discuss MR safety issues from their own practice experiences. Based on these learning objectives the participants should be able to provide a safer MRI environment for their patients, technologists and visitors.

ABSTRACT

With 100's of millions of MRI scans having been performed worldwide there is a sense that the number of MR safety related injuries and medical-legal cases resulting from injuries is increasing and thus there is a need for greater MRI safety education and regulation. As practitioners of MRI examinations, the safety of patients undergoing MRI studies is critically important and there are frequent questions regarding a number of safety issues; i.e., implanted metal devices, implanted electronic devices, tattoos, drug patches, post surgical devices, medical conditions, retained metals and wires, etc. The landscape of new questions regarding the pre-scan risk / safety of patients, technologists and visitors continues to expand almost daily and thus a need for rapid updating of MRI safety related education and the opportunity to ask questions. This refresher course will provide four distinctive opportunities for MRI safety education: The initial presentation will be on "When to Push the Red Button" to quench the MRI system, the second presentation will be a status report on the developing standards to perform clinically needed MRI scans on patients with implanted cardiac electronic devices (ICED's), the third will be an highly interactive session on real-life examples of MR safety questions and a final session of audience directed questions and discussion. The presenters will utilized the "audience response system" and web initiated questions to enhance the overall participation and discussion.

Tumor Ablation beyond the Liver: Practical Techniques for Success

Tuesday, Nov. 29 8:30AM - 10:00AM Room: S104A



AMA PRA Category 1 Credits™: 1.50
ARRT Category A+ Credits: 1.50

Participants

Debra A. Gervais, MD, Boston, MA (*Presenter*) Nothing to Disclose

Terrance T. Healey, MD, Providence, RI (*Presenter*) Nothing to Disclose

Anil N. Kurup, MD, Rochester, MN, (kurup.anil@mayo.edu) (*Presenter*) Research Grant, Galil Medical Ltd; Royalties, UpToDate, Inc

Muneeb Ahmed, MD, Wellesley, MA, (mahmed@bidmc.harvard.edu) (*Presenter*) Nothing to Disclose

LEARNING OBJECTIVES

1) Describe indications for tumor ablation in extrahepatic sites. 2) Describe approaches and techniques to help prevent and manage organ specific complications. 3) Review results of tumor ablation in the lung, kidney, and bone.

ABSTRACT

Pulmonary malignancies, and specifically lung cancer, are a leading cause of death worldwide. Utilization of best current therapies results in an overall five-year relative survival rate for all stages combined to be only 15%, necessitating the use of alternative therapies. Image-guided ablation of lung malignancies is a revolutionary concept whose clinical applications are just beginning to be developed. It has some advantages over traditional radiotherapy and chemotherapy. Its safety profile is similar to percutaneous image guided lung biopsy. Almost all image-guided ablative procedures can be performed in an outpatient setting, mostly with conscious sedation. Multiple applications can be performed without any additional risks. Contraindications are few and include uncontrollable bleeding diathesis and recent use of anticoagulants. Image-guided ablation of lung malignancies is performed with two basic rationales. In the first group it is used with an intention of achieving definitive therapy. These are patients who are not candidates for surgery because of co-morbid medical contraindications to surgery, like poor cardiopulmonary reserve or patients refusing to undergo operation. This cohort could potentially derive significant benefit from a minimally invasive alternative therapy. In the second group it is used as a palliative measure as follows: (a) to achieve tumor reduction before chemotherapy (b) to palliate local symptoms related to aggressive tumor growth, such as chest pain, chest wall pain or dyspnea (c) hematogenous painful bony metastatic disease (d) tumor recurrence in patients who are not suitable for repeat radiation therapy or surgery. Image-guided ablation is expanding treatment options for the local control of non-small cell lung cancer and metastatic disease.

Honored Educators

Presenters or authors on this event have been recognized as RSNA Honored Educators for participating in multiple qualifying educational activities. Honored Educators are invested in furthering the profession of radiology by delivering high-quality educational content in their field of study. Learn how you can become an honored educator by visiting the website at: <https://www.rsna.org/Honored-Educator-Award/>

Debra A. Gervais, MD - 2012 Honored Educator

RC332

Research Management

Tuesday, Nov. 29 8:30AM - 10:00AM Room: E260

LM

AMA PRA Category 1 Credits™: 1.50
ARRT Category A+ Credits: 1.50

Participants

LEARNING OBJECTIVES

1) Understand how one can create an organizational culture that encourages innovation in Radiology. 2) Learn about the historical high impact of imaging research and the importance of inventions in Radiology. 3) Understand how contemporary rules and regulations affect the opportunities and challenges for academic-industrial partnerships in imaging innovation.

Sub-Events

RC332A Promoting Innovation Within Your Team: Practical Pearls for Pragmatic People

Participants

Thomas M. Grist, MD, Madison, WI (*Presenter*) Institutional research support, General Electric Company; Institutional research support, Bracco Group; Stockholder, Collectar Biosciences, Inc;

LEARNING OBJECTIVES

View learning objectives under main course title.

RC332B Inventions in Radiology: From k-Space to Pasteur's Quadrant

Participants

Richard L. Ehman, MD, Rochester, MN (*Presenter*) CEO, Resoundant, Inc; Stockholder, Resoundant, Inc;

LEARNING OBJECTIVES

View learning objectives under main course title.

Honored Educators

Presenters or authors on this event have been recognized as RSNA Honored Educators for participating in multiple qualifying educational activities. Honored Educators are invested in furthering the profession of radiology by delivering high-quality educational content in their field of study. Learn how you can become an honored educator by visiting the website at: <https://www.rsna.org/Honored-Educator-Award/>

Richard L. Ehman, MD - 2016 Honored Educator

RC332C Academic Radiology - Industry Partnerships in the 21st Century

Participants

Steven E. Seltzer, MD, Boston, MA, (sseltzer@partners.org) (*Presenter*) Institutional research agreement, General Electric Company; Institutional research agreement, Siemens AG; Advisory Board, General Electric Company; Travel support, General Electric Company

LEARNING OBJECTIVES

1) Understand how one can create an organizational culture that encourages innovation in Radiology. 2) Learn about the historical high impact of imaging research and the importance of inventions in Radiology. 3) Understand how contemporary rules and regulations affect the opportunities and challenges for academic-industrial partnerships in imaging innovation.

ABSTRACT

By attending this refresher course, participants will: -understand how one can create an organizational culture that encourages innovation in Radiology-learn about the historical high impact of imaging research and the importance of inventions in Radiology-understand how contemporary rules and regulations affect the opportunities and challenges for academic-industrial partnerships in imaging innovation

RC332D Questions and Discussion

Participants

LEARNING OBJECTIVES

View learning objectives under main course title.

RC350

CTA from Head to Toe

Tuesday, Nov. 29 8:30AM - 10:00AM Room: E353B



AMA PRA Category 1 Credits™: 1.50
ARRT Category A+ Credits: 1.50

Participants

Christopher Lee, MD, Los Angeles, CA, (christopher.lee.1@med.usc.edu) (*Moderator*) Nothing to Disclose

ABSTRACT

CT angiography (CTA) is essential for diagnosis and evaluation of arterial vascular pathology of the head and neck. Protocol adjustments for optimal imaging will be discussed. Advanced data post-processing including multiplanar reformations, maximum intensity projection (MIP) reconstructions, and volume rendering will also be discussed. By the end of the presentation, participants should be able to set up CTA protocols for the head and neck and understand how advanced imaging post-processing techniques can be used in everyday practice.

Acute aortic syndrome (AAS) represents the triad of aortic dissection, intramural hematoma, and penetrating atherosclerotic ulcer. Imaging with CTA is essential for the accurate diagnosis of AAS. CTA protocols should optimally image the aorta while minimizing radiation exposure and intravenous contrast administration. Newer CT technology can reduce radiation dose and contrast delivery while preserving image quality. Minimally invasive treatment of acute aortic syndrome with thoracic endovascular aortic repair (TEVAR) has become increasingly popular. The radiologist should be aware of TEVAR's potential complications and their imaging appearances.

Cardiac CTA involves slightly more preparation than standard CTA acquisition. Heart rate control is one of the most important factors that needs to be addressed prior to performing cardiac CTA. Periprocedural issues mostly involve how to optimize technique while having the lowest radiation dose, especially in the new age of dose reduction. Almost as important as heart rate management is how to treat postprocedural complications. This presentation will discuss these aspects and include treatment options as well as their alternatives.

Sub-Events

RC350A Head and Neck CTA

Participants

Alexander Lerner, MD, Los Angeles, CA (*Presenter*) Research Grant, Koninklijke Philips NV; Research Grant, Bracco Group

LEARNING OBJECTIVES

1) Describe techniques for CTA of the neck, upper and lower extremities. 2) Distinguish common artifacts on CTA of these anatomic regions. 3) Evaluate protocol/scanner modifications for optimal CTA imaging.

Active Handout:Alexander Lerner

[http://abstract.rsna.org/uploads/2016/9001497/RC350A Head and Neck CTA Final Handout.pdf](http://abstract.rsna.org/uploads/2016/9001497/RC350A%20Head%20and%20Neck%20CTA%20Final%20Handout.pdf)

RC350B Aortic CTA

Participants

Christopher Lee, MD, Los Angeles, CA, (christopher.lee.1@med.usc.edu) (*Presenter*) Nothing to Disclose

LEARNING OBJECTIVES

1) Formulate a CTA protocol to optimally image acute aortic syndrome. 2) Distinguish the imaging appearances and pitfalls of acute aortic syndrome. 3) Summarize the important measurements and vessel variants that help guide therapy. 4) Describe the common complications following TEVAR and their appearances on CTA.

Active Handout:Christopher Lee

[http://abstract.rsna.org/uploads/2016/9001496/ACTIVE RC350B.pdf](http://abstract.rsna.org/uploads/2016/9001496/ACTIVE%20RC350B.pdf)

RC350C Cardiac CTA

Participants

Cameron Hassani, MD, Los Angeles, CA (*Presenter*) Nothing to Disclose

LEARNING OBJECTIVES

1) Describe pre-procedural patient preparation including appropriate patient selection, contraindications, and beta-blockade. 2) Evaluate peri-procedural issues including vasodilation, continued heart rate control, and breathholding. 3) Evaluate Image acquisition including radiation dose reduction techniques and technique choice. 4) Describe postprocedural complications including contrast reactions and their management.

Liver Elastography (Hands-on)

Tuesday, Nov. 29 8:30AM - 10:00AM Room: E264

GI

AMA PRA Category 1 Credits™: 1.50

ARRT Category A+ Credits: 1.50

FDA

Discussions may include off-label uses.

Participants

Richard G. Barr, MD, PhD, Youngstown, OH (*Presenter*) Consultant, Siemens AG; Consultant, Koninklijke Philips NV; Research Grant, Siemens AG; Research Grant, SuperSonic Imagine; Speakers Bureau, Koninklijke Philips NV; Research Grant, Bracco Group; Speakers Bureau, Siemens AG; Consultant, Toshiba Corporation; Research Grant, Esaote SpA; Research Grant, B and K Ultrasound; Research Grant, Hitachi Aloka Ultrasound

Giovanna Ferraioli, MD, Pavia, Italy, (giovanna.ferraioli@unipv.it) (*Presenter*) Speaker, Koninklijke Philips NV; Speaker, Hitachi Ltd; Speaker, Toshiba Corporation

Carlo Filice, MD, Pavia, Italy (*Presenter*) Speaker, Koninklijke Philips NV; Speaker, Hitachi, Ltd ; Research Grant, Bracco Group; Research Grant, Hitachi, Ltd; Research Grant, Toshiba Corporation; Research Grant, Esaote SpA

Vito Cantisani, MD, Rome, Italy, (vito.cantisani@uniroma1.it) (*Presenter*) Speaker, Toshiba Corporation; Speaker, Bracco Group; Speaker, Samsung Electronics Co, Ltd;

Fabrizio Calliada, MD, Pavia, Italy (*Presenter*) Research Grant, Toshiba Corporation; Speakers Bureau Member, Hitachi, Ltd; Speakers Bureau Member, Shenzhen Mindray Bio-Medical Electronics Co, Ltd

Ann E. Podrasky, MD, Coral Gables, FL (*Presenter*) Nothing to Disclose

Michelle L. Robbin, MD, Birmingham, AL (*Presenter*) Consultant, Koninklijke Philips NV;

Nitin G. Chaubal, MD, MBBS, Mumbai, India, (thaneultrasound@gmail.com) (*Presenter*) Nothing to Disclose

Hisham A. Tchelepi, MD, Los Angeles, CA (*Presenter*) Research Grant, General Electric Company; Research Grant, Roper Industries, Inc

Norihisa Yada, Osaka-Sayama, Japan, (yada@med.kindai.ac.jp) (*Presenter*) Nothing to Disclose

Paul S. Sidhu, MRCP, FRCR, London, United Kingdom, (paulsidhu@nhs.net) (*Presenter*) Speaker, Koninklijke Philips NV; Speaker, Bracco Group; Speaker, Hitachi, Ltd; Speaker, Siemens AG

Juergen K. Willmann, MD, Stanford, CA, (willmann@stanford.edu) (*Presenter*) Research Consultant, Bracco Group; Research Grant, Siemens AG; Research Grant, Bracco Group; Research Grant, Koninklijke Philips NV; Research Grant, General Electric Company; Advisory Board, Lantheus Medical Imaging, Inc; Advisory Board, Bracco Group

Laura Maiocchi, MD, Pavia, Italy (*Presenter*) Nothing to Disclose

LEARNING OBJECTIVES

1) Improve basic knowledge and skills relevant to clinical practice in Liver elastography of the participants. 2) Teach how to practice liver elastography. 3) Show live how to do a proper examination, providing tips and tricks and updating current knowledge on different techniques. 4) Practical hands-on and slide presentation with key messages will be used.

ABSTRACT

RC353

Practical Informatics for the Practicing Radiologist: Part One (In conjunction with the Society for Imaging Informatics in Medicine)

Tuesday, Nov. 29 8:30AM - 10:00AM Room: S404CD

IN

AMA PRA Category 1 Credits™: 1.50
ARRT Category A+ Credits: 1.50

Participants

Marc D. Kohli, MD, San Francisco, CA (*Moderator*) Nothing to Disclose

LEARNING OBJECTIVES

1) Define and describe the fundamental components of imaging informatics in a very practical and easy-to-understand way. 2) Understand methods to minimize distraction and reporting time when using speech recognition and structured reporting. 3) Understand the history and basic principles of business analytics.

ABSTRACT

Sub-Events

RC353A A Patient's Journey through Imaging Informatics

Participants

Marc D. Kohli, MD, San Francisco, CA (*Presenter*) Nothing to Disclose

LEARNING OBJECTIVES

1) Describe the three major systems used in radiology departments and their function. 2) Provide details regarding the HL7 and DICOM standards including how they are important in radiology workflow. 3) Describe the function of an interface engine in a modern healthcare system.

ABSTRACT

Understanding how the basic systems in a radiology department interact to provide complete workflow is an important building-block for radiologists interested in informatics. This presentation will outline the RIS, PACS, and Voice recognition systems and illustrate how they interact as we follow a patient through the radiology department.

RC353B Challenges in Enterprise Imaging

Participants

Alex Towbin, MD, Cincinnati, OH, (alexander.towbin@cchmc.org) (*Presenter*) Author, Reed Elsevier; Grant, Guerbet SA; Grant, Siemens AG;

LEARNING OBJECTIVES

1) Describe the concept of an enterprise imaging archive. 2) Describe the differences between DICOM-based imaging and non-DICOM-based imaging. 3) Identify the unique challenges associated with incorporating non-DICOM images into an enterprise imaging archive.

ABSTRACT

Over the past 20 years, the field of radiology has built an impressive digital infrastructure, automating many portions of the imaging process from the time of order entry through image distribution. With the advent of small, low-cost, high quality digital cameras, other medical specialties have turned to imaging to visualize and document disorders yet, they have not implemented the same type of digital infrastructure as radiology. Today, thousands of medical images are obtained in hospitals each day. With the increasing reliance on imaging, there is a greater need to build systems and processes to obtain, store, and distribute these images across the enterprise so that health care providers can better care for their patients. Even though many of these problems have been solved in radiology, the solutions are not easily transferred to other specialties due to the differences in imaging hardware and the image acquisition workflow. The purpose of this talk is to describe the problems facing hospitals as they begin to build enterprise imaging archives and to discuss potential solutions to these problems.

Honored Educators

Presenters or authors on this event have been recognized as RSNA Honored Educators for participating in multiple qualifying educational activities. Honored Educators are invested in furthering the profession of radiology by delivering high-quality educational content in their field of study. Learn how you can become an honored educator by visiting the website at: <https://www.rsna.org/Honored-Educator-Award/>

Alex Towbin, MD - 2014 Honored Educator

RC353C Breaching the Moat: Current Concepts in IT Security

Participants

James Whitfill, MD, Scottsdale, AZ (*Presenter*) President, Lumetis, LLC;

LEARNING OBJECTIVES

1) Understand how the changing nature of security threats requires a new approach to security within the healthcare enterprise. 2)

Understand how changes from HIPAA and HITECH affect managing breaches and leaks of PHI.

ABSTRACT

The role of security continues to be elevated as more organizations find themselves victims of hacking and breaches. Banks, retail organizations, insurers and even Children's Hospitals have all been victims of security breaches. While efficient workflow for healthcare providers remains a key focus of imaging informatics, the growing threats from international hacking require greater and greater focus by IT and Healthcare organizations. In response to these developments, an increasing regulatory burden exists to report and mitigate against such breaches. Managing both of these challenges will take increasing amounts of resources in the near future.

Preparing your Radiology Practice and IT Department for Big Data

Tuesday, Nov. 29 8:30AM - 10:00AM Room: S404AB



AMA PRA Category 1 Credits™: 1.50
ARRT Category A+ Credits: 1.50

Participants

Paul J. Chang, MD, Chicago, IL, (pchang@radiology.bsd.uchicago.edu) (*Moderator*) Co-founder, Stentor/Koninklijke Philips NV; Researcher, Koninklijke Philips NV; Medical Advisory Board, lifeIMAGE Inc; Advisory Board, Bayer AG

LEARNING OBJECTIVES

1) The potential of applying "Big Data" approaches to radiology will be discussed. 2) The participant will be introduced to the importance of developing a comprehensive IT architecture and capability beyond the EMR in order to effectively use "Big Data" tools. 3) Strategies for preparing IT for "Big Data" will be discussed.

ABSTRACT

Current and near future requirements and constraints will require radiology practices to continuously improve and demonstrate the value they add to the enterprise. Merely "managing the practice" will not be sufficient; groups will be required to compete in an environment where the goal will be measurable improvements in efficiency, productivity, quality, and safety. This will require optimally leveraging IT enabled business intelligence, analytics, and data driven workflow. In many ways, this challenge can be described as a "Big Data" problem, requiring the application of newer "Big Data" approaches and tools. Unfortunately, many have discovered that an "EMR centric" IT perspective may severely limit the ability for the enterprise to maximally leverage these newer tools to create differentiable value. This session will provide an introduction to the importance of developing a comprehensive architectural strategy to augment the existing EMR to more effectively consume "Big Data" tools.

Sub-Events

RC354A Getting Your IT Infrastructure Ready for Big Data

Participants

Paul J. Chang, MD, Chicago, IL, (pchang@radiology.bsd.uchicago.edu) (*Presenter*) Co-founder, Stentor/Koninklijke Philips NV; Researcher, Koninklijke Philips NV; Medical Advisory Board, lifeIMAGE Inc; Advisory Board, Bayer AG

LEARNING OBJECTIVES

1) The potential of applying "Big Data" and noSQL approaches to radiology will be discussed. 2) The participant will be introduced to the importance of developing a comprehensive IT architecture and capability beyond the EMR in order to effectively use "Big Data" tools. 3) Strategies for preparing IT for business intelligence and analytics will be discussed.

ABSTRACT

Current and near future requirements and constraints will require radiology practices to continuously improve and demonstrate the value they add to the enterprise. Merely "managing the practice" will not be sufficient; groups will be required to compete in an environment where the goal will be measurable improvements in efficiency, productivity, quality, and safety. This will require optimally leveraging IT enabled business intelligence, analytics, and data driven workflow. In many ways, this challenge can be described as a "Big Data" problem, requiring the application of newer "Big Data" approaches and tools. Unfortunately, many have discovered that an "EMR centric" IT perspective may severely limit the ability for the enterprise to maximally leverage these newer tools to create differentiable value. This session will provide an introduction to the importance of developing a comprehensive architectural strategy to augment the existing EMR to more effectively consume "Big Data" approaches and fully leverage business intelligence and analytics.

RC354B NoSQL Approaches: Beyond the Traditional Relational Database

Participants

Paul J. Chang, MD, Chicago, IL, (pchang@radiology.bsd.uchicago.edu) (*Presenter*) Co-founder, Stentor/Koninklijke Philips NV; Researcher, Koninklijke Philips NV; Medical Advisory Board, lifeIMAGE Inc; Advisory Board, Bayer AG

LEARNING OBJECTIVES

1) The distinction between the traditional relational (SQL) database and "NoSQL" approaches will be discussed. 2) The attendees will be given a basic introduction to how "NoSQL" tools, such as Hadoop, MapReduce, MongoDB can be complementary to existing approaches. 3) NoSQL applications and their relevance to radiology will be discussed.

ABSTRACT

Current and near future requirements and constraints will require radiology practices to continuously improve and demonstrate the value they add to the enterprise. Merely "managing the practice" will not be sufficient; groups will be required to compete in an environment where the goal will be measurable improvements in efficiency, productivity, quality, and safety. This will require optimally leveraging IT enabled business intelligence, analytics, and data driven workflow. These approaches will require the ability to consume and utilize all available enterprise data, including unstructured reports, multimedia objects, etc. Other industries have realized that traditional IT approaches, such as the relational (SQL) database, cannot optimally address these "difficult" data objects. Many outside of the medical domain have successfully augmented traditional approaches by newer "Big Data" and "NoSQL" methodologies, such as Hadoop, MapReduce, MongoDB, etc. In this session, an introduction to these newer tools will be presented.

RC354C Deep Learning: An Example of Big Data Applications

Participants

William W. Boonn, MD, Penn Valley, PA, (wboonn@gmail.com) (*Presenter*) Officer, Nuance Communications, Inc; Shareholder, Nuance Communications, Inc

LEARNING OBJECTIVES

1) A technical overview of machine learning and deep learning will be presented. 2) Applications of machine learning and deep learning in radiology will be illustrated. 3) Challenges in deploying machine learning and deep learning in radiologist workflow and productivity demands will be discussed.

ABSTRACT

Computers in radiology have often promised to deliver faster clinical decisions, more accurate diagnoses, and transformative visualizations. Computer aided diagnostics (CAD) has been deployed to guide radiologists in their detection of abnormalities and identification of disease. Historically, CAD has been based on domain-driven heuristics, and more recently used simple machine learning on structured data. Both of these require extensive manual engineering making them very slow to build, limited in their flexibility, and less accurate than we would like. Deep learning is a new paradigm that offers a transformative solution. Instead of demanding countless human hours of painstaking feature generation and selection, deep learning automatically discovers clinically-relevant features by first architecting a hierarchy of patterns (loosely modelled on the brain's own neural neural networks) and then updating those patterns upon observing examples. As radiology requires complex associative pattern recognition, deep learning is the ideal companion tool. Enlitic is developing a deep neural network of the entire human body that will offer a new way forward in which the radiologist has immediate access to the most relevant clinical information. In this talk, we will present a technical overview of machine learning and deep learning, illustrate its applications in radiology, and detail some of the challenges improving radiological workflow using deep learning poses.

Honored Educators

Presenters or authors on this event have been recognized as RSNA Honored Educators for participating in multiple qualifying educational activities. Honored Educators are invested in furthering the profession of radiology by delivering high-quality educational content in their field of study. Learn how you can become an honored educator by visiting the website at: <https://www.rsna.org/Honored-Educator-Award/>

William W. Boonn, MD - 2012 Honored Educator

RCB31

Hands-on Introduction to Social Media (Hands-on)

Tuesday, Nov. 29 8:30AM - 10:00AM Room: S401CD

IN

AMA PRA Category 1 Credits™: 1.50
ARRT Category A+ Credit: 0

Participants

Amy L. Kotsenas, MD, Rochester, MN, (kotsenas.amy@mayo.edu) (*Presenter*) Nothing to Disclose
Neil U Lall, MD, Cincinnati, OH, (nulall@gmail.com) (*Presenter*) Nothing to Disclose
Tirath Y. Patel, MD, Houston, TX (*Presenter*) Nothing to Disclose
Tessa S. Cook, MD, PhD, Philadelphia, PA, (tessa.cook@uphs.upenn.edu) (*Presenter*) Nothing to Disclose
Saad Ranginwala, MD, Cincinnati, OH, (sranginwala@gmail.com) (*Presenter*) Nothing to Disclose

LEARNING OBJECTIVES

1) Appreciate the professional relevance of social media for radiologists. 2) Understand the differences between social media in personal and professional roles. 3) Understand the differences between and advantages/disadvantages of multiple social media networks. 4) Set up and use a Twitter account. 5) Understand the purpose of hashtags, lists, and DMs. 6) Get acquainted with other radiologists and radiology organizations on Twitter. 7) Use a variety of social media venues to share images for educational purposes. 8) Understand the difference between and utility of professionally oriented social networking sites such as Doximity and LinkedIn. 9) Understand how to safely /securely communicate via social media while maintaining HIPAA requirements.

ABSTRACT

URL

<http://bit.ly/RSNASocialMediaIntro>

Active Handout: Amy Louise Kotsenas

http://abstract.rsna.org/uploads/2016/11035016/RCB31_RSNA16_Hands_On_Social_Media_-_Twitter_Kotsenas.pdf

Active Handout: Tessa S. Cook

http://abstract.rsna.org/uploads/2016/11035016/RCB31_socialmedia-handout-cook.pdf

RCC31

Imaging Informatics: Year in Review (RSNA/AMIA/SIIM Joint Sponsorship)

Tuesday, Nov. 29 8:30AM - 10:00AM Room: S501ABC

IN

AMA PRA Category 1 Credits™: 1.50
ARRT Category A+ Credits: 1.50

FDA

Discussions may include off-label uses.

Participants

Charles E. Kahn JR, MD, MS, Philadelphia, PA, (charles.kahn@uphs.upenn.edu) (*Moderator*) Nothing to Disclose
William Hsu, PhD, Los Angeles, CA (*Presenter*) Nothing to Disclose

LEARNING OBJECTIVES

1) Review the year's most significant advances in imaging informatics. 2) Understand current directions in biomedical informatics research of importance to radiology, including ontologies, data mining, natural language processing, reporting systems, and decision support. 3) Describe recent advances in image processing and analysis, and their applications in radiology, including image reconstruction, filtering and post-processing, pattern recognition, computer-aided detection and diagnosis, and visualization.

ABSTRACT

The field of imaging informatics is rapidly advancing in its ability to address challenges related to clinical big data and harnessing this information for precision medicine. In the past year, the field has experienced growth in a variety of areas including radiomics (the generation of high dimensional features from images), development of new ontologies and standards for capturing information from images and reports, and unsupervised learning from images to predict the course of a disease and treatment response. In addition, we have seen a remarkable growth in novel approaches that go beyond pixel data by integrating imaging with other biomedical data, standardizing imaging workflows, and improving the quality and utility of image-derived information in clinical practice. This session, developed in partnership with the American Medical Informatics Association (AMIA) and the Society of Imaging Informatics in Medicine (SIIM), highlights the year's most important advances in imaging informatics. This course provides a comprehensive "Year in Review" of informatics in medical imaging.

URL

<http://www.rsna.org/Informatics/2016/>

MSAS32

Radiation Dose: Optimisation and Safety (Sponsored by the Associated Sciences Consortium) (An Interactive Session)

Tuesday, Nov. 29 10:30AM - 12:00PM Room: S105AB

SQ

AMA PRA Category 1 Credits™: 1.50
ARRT Category A+ Credits: 1.50

Participants

Charlotte Beardmore, MBA, London, United Kingdom (*Moderator*) Nothing to Disclose
Nancy McDonald, MS, Chicago, IL (*Moderator*) Nothing to Disclose

Sub-Events

MSAS32A Optimisation of Clinical Radiographic Examinations in a Digital Era

Participants

Andrew England, PhD, Salford, United Kingdom, (a.England@salford.ac.uk) (*Presenter*) Nothing to Disclose

LEARNING OBJECTIVES

1) Explain the rationale for optimising radiographic examinations. 2) Describe the common methods for assessing radiographic image quality and estimating radiation dose in a digital era. 3) Appraise the various methods for optimising digital radiographic examinations.

ABSTRACT

Within the United Kingdom (UK) and many other countries it is a legal requirement for radiographic studies, involving humans, to use the lowest possible radiation dose whilst producing an image of acceptable quality. This practise of producing an adequate image together with the lowest possible dose is termed **dose optimisation** and forms part of the UK Ionising Radiation Medical Exposure Regulations. Other countries have adopted similar practises with Image Gently and Image Wisely being examples. Making a decision regarding the adequacy of a radiographic image is largely based on visual perception. This is a highly subjective process and decisions surrounding the acceptability of radiographic images can be prone to significant observer variability. Radiographic technique is largely based around historical practises. There is a general lack of evidence regarding the most appropriate acquisition factors in order to generate an optimised radiographic examination. This problem in part extends from the issue of defining an acceptable or adequate image and an overall lack of any validated methods for measuring perceptual image quality. The problem has been further exacerbated by the widespread role out of digital radiographic systems and move away from images acquired using film-screen systems. In this new arena the relationship between image quality and radiation dose has changed and the effects of changes to acquisition parameters are often poorly understood. The proposed presentation will seek to highlight current knowledge, including our own research findings, around the current methods of dose optimisation for digital radiographic examinations. This will include a short discussion on the assessment of image quality (perceptual), appropriate measures for estimating radiation dose and the various options for optimising the examination. Such options can include the adjustment of the X ray tube to detector distance, modifying the orientation of the patient, changes to the beam energy and the inclusion of additional tube filtration. In many instances acquisition factor changes can be complimentary, however, in some instances multiple changes can be counter productive and effective processes for dose optimisation are needed.

MSAS32B Dose Optimisation in CT

Participants

Yifang Zhou, PhD, Los Angeles, CA (*Presenter*) Nothing to Disclose

LEARNING OBJECTIVES

1) Understand the CT dose concept and the need to minimize unnecessary radiation. 2) Understand the technical factors affecting CT dose and image quality. 3) Understand the special need to minimize the pediatric dose. 4) Learn the methods to optimize CT dose following the principle of ALARA.

ABSTRACT

This lecture will discuss technical factors affecting CT dose and image quality and demonstrate the practical methods for CT dose optimization using phantoms. The cases include chest, abdomen, elbow and brain CT. Pediatric dose reduction is discussed in the context of consistent image quality. Possible pitfalls and misunderstanding on dose reduction are addressed.

MSAS32C Dose Optimisation in Interventional Radiology

Participants

David B. Nicholson, Charlottesville, VA (*Presenter*) Nothing to Disclose

Case-based Review of Nuclear Medicine: PET/CT Workshop-Chest Cancers (In Conjunction with SNMMI) (An Interactive Session)

Tuesday, Nov. 29 10:30AM - 12:00PM Room: S406A



AMA PRA Category 1 Credits™: 1.50
ARRT Category A+ Credits: 1.50

Participants

Janis P. O'Malley, MD, Birmingham, AL, (jomalley@uabmc.edu) (*Moderator*) Nothing to Disclose
Ciaran J. Johnston, MD, Dublin, Ireland, (cjohnston@stjames.ie) (*Presenter*) Nothing to Disclose

LEARNING OBJECTIVES

1. Discuss the strengths and limitations of PET-CT of the chest with reference to staging the common cancers (lung, breast, esophageal).
2. Discuss confounding factors in chest PET-CT including non-neoplastic hyper metabolic lesions and conversely tumours that demonstrate little or no FDG avidity.
3. Demonstrate the importance of CT correlation, particularly in suspected lung cancer.
- 4) Describe the role of PET CT in assessing patient response to radiation therapy and chemotherapy, including early assessment and PET influenced treatment strategies.

MSES32

Essentials of Musculoskeletal Imaging

Tuesday, Nov. 29 10:30AM - 12:00PM Room: S100AB



AMA PRA Category 1 Credits™: 1.50
ARRT Category A+ Credits: 1.50

Participants

Sub-Events

MSES32A Target Area Approach to Arthritis

Participants

Donald L. Resnick, MD, San Diego, CA (*Presenter*) Nothing to Disclose

LEARNING OBJECTIVES

1) Review the classic target sites of common articular disorders emphasizing the hand, wrist, and foot. 2) Summarize the important differences in distribution of these disorders, allowing accurate diagnosis.

ABSTRACT

The accurate diagnosis of articular disorders is based on two observations: the morphologic or structural abnormalities; and the distribution of these abnormalities. In this presentation, classic patterns of distribution of common and a few uncommon articular disorders will be reviewed with emphasis on the hand, wrist, heel, and foot. Points of differential diagnosis will be summarized.

MSES32B State of Art Imaging of Osteoporosis

Participants

Leon Lenchik, MD, Winston-Salem, NC, (llechik@wakehealth.edu) (*Presenter*) Nothing to Disclose

LEARNING OBJECTIVES

1) Discuss diagnosis and monitoring of osteoporosis. 2) Discuss fracture risk assessment. 3) Describe pitfalls in DXA scan interpretation.

ABSTRACT

MSES32C The Essentials of Hip MRI

Participants

Scott D. Wuertzer, MD, MS, Winston-Salem, NC, (swuertze@wakehealth.edu) (*Presenter*) Nothing to Disclose

LEARNING OBJECTIVES

1) Discuss some key concepts on the techniques of hip MRI. 2) Recognize common extra-articular hip pathology on MRI. 3) Differentiate labral variants from tears. 4) Identify MRI features of femoroacetabular impingement (FAI).

ABSTRACT

MSES32D Altered Marrow Signal in the Knee: Diagnostic Considerations

Participants

Christine B. Chung, MD, San Diego, CA (*Presenter*) Nothing to Disclose

LEARNING OBJECTIVES

1) Describe histopathologic marrow changes producing findings of bone marrow edema on MRI. 2) Review traumatic pathomechanisms producing commonly encountered marrow edema patterns and associated soft tissue and osseous injuries. 3) Discuss bone marrow edema findings encountered in setting of altered mechanical loading, chronic repetitive trauma, and articular degeneration.

MSQI32

Quality Improvement Symposium: Measuring Value

Tuesday, Nov. 29 10:30AM - 12:00PM Room: S406B

SQ

AMA PRA Category 1 Credits™: 1.50
ARRT Category A+ Credits: 1.50

Participants

Paul G. Nagy, PhD, Baltimore, MD, (pnagy@jhu.edu) (*Moderator*) Institutional license agreement, Analytical Informatics, Inc

ABSTRACT

Quality improvement (QI) is a data driven method for leading change, reducing waste, and being patient centric. Without data and goals we cannot assess where we are, where we want to go, or even if we are heading in the right direction. The metrics chosen to set goals direct institutional resources. They are a reflection of the values of an organization and what it intends to achieve. This session will explore metrics used in radiology to assess value to our patients.

Sub-Events

MSQI32A Patient Perspective

Participants

Olga R. Brook, MD, Boston, MA, (obrook@bidmc.harvard.edu) (*Presenter*) Research Grant, Toshiba Medical Systems Corporation

LEARNING OBJECTIVES

1) Learn how to measure patient's satisfaction in Radiology and what are important components of patient's satisfaction.

ABSTRACT

Patient satisfaction has been identified as important metric in quality of care in medicine. Radiology departments are somewhat unique as patients primarily interact with technologists, receptionist and rarely with doctors and nurses. Furthermore, patients can rarely assess quality of imaging studies or reports. So, what patient satisfaction really means in Radiology? In this presentation, we will describe how we perform patient satisfaction surveys in a large Radiology department and what we have learnt from patient responses and ratings.

MSQI32B How a Radiology Department Measures and Tracks Values

Participants

Jonathan B. Kruskal, MD, PhD, Boston, MA, (jkruskal@bidmc.harvard.edu) (*Presenter*) Author, UpToDate, Inc

LEARNING OBJECTIVES

1) provide an overview of the following material as relates to value metrics: a) What are metrics and how are these used to drive improved performance? b) What metrics reflect the value that we add with our clinical services c) What value metrics should we currently be using?

ABSTRACT

Honored Educators

Presenters or authors on this event have been recognized as RSNA Honored Educators for participating in multiple qualifying educational activities. Honored Educators are invested in furthering the profession of radiology by delivering high-quality educational content in their field of study. Learn how you can become an honored educator by visiting the website at: <https://www.rsna.org/Honored-Educator-Award/>

Jonathan B. Kruskal, MD, PhD - 2012 Honored Educator

Jonathan B. Kruskal, MD, PhD - 2016 Honored Educator

MSQI32C How Payers Measure Value

Participants

Daniel Durand, MD, Baltimore, MD (*Presenter*) Consultant, National Decision Support Company;

MSRO32

BOOST: Breast-Science Session with Keynote

Tuesday, Nov. 29 10:30AM - 12:00PM Room: S103AB



AMA PRA Category 1 Credits™: 1.50
ARRT Category A+ Credits: 1.50

FDA Discussions may include off-label uses.

Participants

Anna Shapiro, MD, Syracuse, NY (*Moderator*) Nothing to Disclose
Tracy M. Sherertz, MD, San Francisco, CA (*Moderator*) Nothing to Disclose

Sub-Events

MSRO32-01 Invited Speaker: Proton Therapy for Breast Cancer

Tuesday, Nov. 29 10:30AM - 10:50AM Room: S103AB

Participants

L. Christine Fang, MD, Seattle, WA (*Presenter*) Nothing to Disclose

MSRO32-03 An Abbreviated Interval Between Radiotherapy and Follow-up Mammography in Breast Conservation Surgery May Lead to Unnecessary Downstream Work-up

Tuesday, Nov. 29 10:50AM - 11:00AM Room: S103AB

Participants

Stephen Abel, BS, Pittsburgh, PA (*Abstract Co-Author*) Nothing to Disclose
Shaakir Hasan, MD, Pittsburgh, PA (*Presenter*) Nothing to Disclose
LaShondria Camp, MD, Pittsburgh, PA (*Abstract Co-Author*) Nothing to Disclose
Meredith Witten, Pittsburgh, PA (*Abstract Co-Author*) Nothing to Disclose
Leslie Teng, DO, Pittsburgh, PA (*Abstract Co-Author*) Nothing to Disclose
Luis Aguilera, DO, Pittsburgh, PA (*Abstract Co-Author*) Nothing to Disclose
Frances Philp, Pittsburgh, PA (*Abstract Co-Author*) Nothing to Disclose
Thomas B. Julian, MD, Pittsburgh, PA (*Abstract Co-Author*) Nothing to Disclose
Stephen M. Karlovits, MD, Allison Park, PA (*Abstract Co-Author*) Nothing to Disclose
Michael Cowher, Cleveland, OH (*Abstract Co-Author*) Nothing to Disclose

PURPOSE

Surveillance mammography for breast conservation therapy (BCT) is frequently conducted within 6 months upon completion of adjuvant radiotherapy (XRT). We retrospectively analyzed the effect of post-XRT mammographic timing and radiation technique in relation to additional downstream workup for 569 BCT patients treated with adjuvant XRT following their initial surveillance mammogram (MMG).

METHOD AND MATERIALS

From January 2011 to December 2014, 1959 consecutive breast cancer patients were reviewed, 569 of whom had breast conservation surgery and adjuvant XRT with a follow-up MMG. Patients between the ages 31 and 91 (median 63) with stages 0(Tis) to IIIA of ductal, lobular, mixed, and metaplastic histologies were included. Patients were stratified by the time interval until their first post-XRT MMG, and by XRT technique – whole breast (472), accelerated partial breast (96), conventional fractionation (373), hypofractionation (94), surgical cavity boosts (407) or no boost (66). The primary endpoint was further imaging after the initial MMG. P values were generated from Chi square testing via MedCalc. IRB approval was received for this retrospective study.

RESULTS

Additional workup for those receiving a MMG within 3 months of completing XRT was 51% (73/143), compared to 40% (84/210) with MMG between 3 to 6 months, and 34.5% (75/217) with MMG after 6 months (P = 0.04). Two of ten biopsies were positive for recurrence among those with surveillance MMG within 6 months, compared to 1 of 2 patients with MMG after 6 months. Accelerated partial breast irradiation, hypofractionation, and surgical cavity boosts did not correlate with further downstream imaging.

CONCLUSION

BCT patients who underwent screening MMG prior to 6 months after completion of XRT were more likely to undergo downstream workup, including additional biopsies. Comparatively aggressive radiation techniques were not associated with the need for supplementary workup. Further study is needed to assess appropriate selection of high risk patients and possible negative implications of earlier post-radiotherapy screening MMG such as healthcare costs and quality of life.

CLINICAL RELEVANCE/APPLICATION

Premature surveillance mammography relative to adjuvant radiation in breast conservation therapy is common and likely results in excessive downstream workup, costs, and patient discomfort.

MSRO32-04 Analysis of Radiation Lung Fibrosis after Hypo-fractionated Breast Radiotherapy: 3 Dimensional Volume Measurement

Tuesday, Nov. 29 11:00AM - 11:10AM Room: S103AB

Participants

ABSTRACT

Purpose/Objective(s): Hypo-fractionated breast radiotherapy is widely accepted as an alternative treatment option for early stage breast cancer. However, long term clinical outcome of late toxicity is relatively scarce compared to conventional radiotherapy regime. To evaluate whether hypo-fractionated breast radiotherapy can cause more late lung toxicity, instead of using subjective grading system, we have directly measured volume of fibrotic lung tissues in the region of tangential radiation fields. **Materials/Methods:** Fifty-three early stage breast cancer patients who were treated with hypo-fractionated radiotherapy and the same number of early stage breast cancer patients with conventional radiotherapy were retrospectively analyzed. All patients had multiple follow up chest CT images for more than three years. With deformable registration with radiation treatment planning data, lung fibrosis tissues within radiotherapy fields were segmented and 3 dimensional volumes of lung fibrosis were directly measured. Radiation therapy techniques and protocols were the exactly same, but only dose scheme was different. **Results:** The volume of lung fibrosis appeared to be slightly larger in the group of hypo-fractionated breast radiotherapy. Mean volume of lung fibrosis in patients with hypo-fractionated radiotherapy arm was 14.1 cc, and the volume in patients with conventional radiotherapy arm was 12.3 cc. We compared histogram of volume distribution of each patient group. Conventional radiotherapy group appeared to show slightly smaller volume of lung fibrosis compared to hypo-fractionated radiotherapy group, however, which was not statistically significant (p). **Conclusion:** Even though the lung fibrosis in this study was subclinical, hypofractionated radiotherapy may cause slightly more lung fibrosis, caution is needed when patient irradiation lung volume is significantly exceeded as usual.

MSRO32-07 Evaluating Candidacy for Endocrine Therapy, Accelerated Partial Breast Irradiation, and Hypofractionated Radiation Therapy following Breast Conserving Surgery: A Surveillance Epidemiology and End Results (SEER) Analysis

Tuesday, Nov. 29 11:30AM - 11:40AM Room: S103AB

Participants

Bindu Manyam, Oak Brook, IL (*Presenter*) Nothing to Disclose

ABSTRACT

Purpose/Objective(s): Standard breast conserving therapy consists of lumpectomy followed by whole breast irradiation. Alternative strategies in appropriately selected patients (pts) include endocrine therapy (ET) alone, accelerated partial breast irradiation (APBI), and hypofractionated radiation therapy (HFRT), which can limit treatment duration, and potentially reduce morbidity and cost. However, limited data are available on the percentage of pts eligible for these alternative treatments; therefore, a Surveillance Epidemiology and End Results (SEER) analysis was performed to assess candidacy for these alternative options in women with early stage breast cancer according to current consensus guidelines and trial eligibility criteria. **Materials/Methods:** Women treated for breast cancer between the years of 2010-2012 were identified in the SEER database. Pts with metastatic disease, T3/T4 disease, and node positive disease were excluded. Pts were defined as eligible for ET alone according to the CALGB 9343 inclusion criteria (Age \geq 70 years; T1; Estrogen receptor positive [ER+]) and PRIME II inclusion criteria (Age \geq 65 years; T1/T2; ER+ and/or Progesterone receptor positive [PR+]). Pts were defined as eligible for HFRT according to ASTRO consensus guidelines (Age \geq 50 years; T1/T2). Pts eligible for APBI were evaluated based on ASTRO consensus guidelines (Age \geq 60 years; T1; ER+), American Brachytherapy Society (ABS) and the GEC-ESTRO consensus guidelines (Age \geq 50 years; T1/T2), and the GEC-ESTRO APBI trial criteria (Age \geq 40 years; T1-T2). Additional pathologic features, dosimetric data, and chemotherapy receipt were not available. **Results:** 110,858 women with early stage breast cancer who met aforementioned inclusion criteria were identified. Of these pts, 23,286 (21.0 %) were eligible for ET alone according to CALGB 9343 criteria and 43,278 (39.0%) according to PRIME II criteria. Based on ASTRO consensus guidelines, there were 91,492 (82.5%) pts eligible for HFRT. There were 44,528 (40.2%) pts who were eligible for APBI according to ASTRO consensus guidelines, 88,945 (80.2%) pts eligible according to ABS consensus guidelines, and 88,945 (80.2%) pts eligible according to the GEC-ESTRO consensus guidelines. There were 107,235 (96.7%) pts who were eligible for APBI according to the GEC-ESTRO APBI trial criteria. **Conclusion:** This SEER analysis demonstrates there is a substantial proportion of women with early stage breast cancer who may be eligible for ET alone, HFRT, and/or APBI following breast conserving surgery according to consensus guidelines and prospective trial criteria. Moving forward, with incorporation of additional pathologic, dosimetric, and chemotherapy data, quality assurance pathways may use such data to help ensure pts are receiving appropriate risk stratified treatment recommendations.

BOOST: Lung-Science Session with Keynote

Tuesday, Nov. 29 10:30AM - 12:00PM Room: S103CD



AMA PRA Category 1 Credits™: 1.50
ARRT Category A+ Credits: 1.50

Participants

John C. Grecula, MD, Columbus, OH (*Moderator*) Research Grant, Teva Pharmaceutical Industries Ltd Research Grant, Soligenix, Inc
Matthew M. Harkenrider, MD, Maywood, IL (*Moderator*) Nothing to Disclose

Sub-Events**MSRO35-01 Invited Speaker:**

Tuesday, Nov. 29 10:30AM - 10:50AM Room: S103CD

Participants

Meng X. Welliver, MD, Columbus, OH (*Presenter*) Nothing to Disclose

MSRO35-04 Dynamic Contrast-Enhanced Perfusion MRI vs Dynamic Contrast-Enhanced Area-Detector CT vs FDG-PET/CT: Capability for Therapeutic Outcome Prediction in NSCLC Patients with Chemoradiotherapy

Tuesday, Nov. 29 11:00AM - 11:10AM Room: S103CD

Participants

Yoshiharu Ohno, MD, PhD, Kobe, Japan (*Abstract Co-Author*) Research Grant, Toshiba Corporation; Research Grant, Koninklijke Philips NV; Research Grant, Bayer AG; Research Grant, DAIICHI SANKYO Group; Research Grant, Eisai Co, Ltd; Research Grant, Fuji Pharma Co, Ltd; Research Grant, FUJIFILM RI Pharma Co, Ltd; Research Grant, Guerbet SA;
Yuji Kishida, MD, Kobe, Japan (*Abstract Co-Author*) Nothing to Disclose
Shinichiro Seki, Kobe, Japan (*Abstract Co-Author*) Nothing to Disclose
Hisanobu Koyama, MD, PhD, Kobe, Japan (*Abstract Co-Author*) Nothing to Disclose
Takeshi Yoshikawa, MD, Kobe, Japan (*Abstract Co-Author*) Research Grant, Toshiba Corporation
Yasuko Fujisawa, MS, Otawara, Japan (*Abstract Co-Author*) Employee, Toshiba Corporation
Masao Yui, Otawara, Japan (*Abstract Co-Author*) Employee, Toshiba Corporation
Shigeharu Ohyu, MEng, Otawara, Japan (*Abstract Co-Author*) Employee, Toshiba Corporation
Naoki Sugihara, MEng, Otawara, Japan (*Abstract Co-Author*) Employee, Toshiba Corporation
Wakiko Tani, RT, Kobe, Japan (*Presenter*) Nothing to Disclose
Kiyosumi Kagawa, Kobe, Japan (*Abstract Co-Author*) Nothing to Disclose
Noriyuki Negi, RT, Kobe, Japan (*Abstract Co-Author*) Nothing to Disclose
Yuichiro Somiya, Kobe, Japan (*Abstract Co-Author*) Nothing to Disclose
Katsusuke Kyotani, RT, Kobe, Japan (*Abstract Co-Author*) Nothing to Disclose
Kazuro Sugimura, MD, PhD, Kobe, Japan (*Abstract Co-Author*) Research Grant, Toshiba Corporation Research Grant, Koninklijke Philips NV Research Grant, Bayer AG Research Grant, Eisai Co, Ltd Research Grant, DAIICHI SANKYO Group

PURPOSE

To directly compare the capability for therapeutic outcome prediction between dynamic first-pass CE-perfusion area-detector CT (ADCT) and MRI assessed by same mathematical method and FDG-PET/CT in non-small cell lung cancer (NSCLC) patients treated with chemoradiotherapy.

METHOD AND MATERIALS

43 consecutive Stage IIIB NSCLC patients (25 male, 18 female; mean age 67 year old) underwent PET/CT, dynamic CE-perfusion ADCT and MRI, chemoradiotherapy, and follow-up examination. In each patient, therapeutic outcomes were assessed as therapeutic effect based on RECIST guideline, disease free interval and overall survival. Then, all patients were divided into two groups as follows: 1) CR+PR (n=23) and 2) SD+PD (n=20) groups. In each patient, total tumor perfusion (TP) and tumor perfusions from pulmonary (TPP) and systemic (TPS) circulations calculated by dual-input maximum slope method from dynamic ADCT and MRI data and SUVmax on PET/CT were assessed at each targeted lesion, and averaged to determine final values. To compare the capability for distinguishing two groups, ROC analyses were performed. Then, disease free and overall survivals between responders and non-responders assessed by each index were compared by Kaplan-Meier method followed by log-rank test.

RESULTS

Area under the curves (Azs) of TP (MRI: Az=0.90, ADCT: Az=0.87) and TPS (MRI: Az=0.84, ADCT: Az=0.84) were significantly larger than that of TPP (MRI: Az=0.72, p<0.05; ADCT: Az=0.72, p<0.05). Disease free survivals of responder were significantly longer than that of non-responder by TP (MRI: p=0.01, ADCT: p=0.03) and TPS (MRI: p=0.01, ADCT: p=0.001). Overall survivals of responder were also significantly longer than that of non-responder by TP (MRI: p=0.007, ADCT: p=0.004), TPS (MRI: p=0.001; ADCT: p=0.0001) and SUVmax (p=0.04).

CONCLUSION

Dynamic first-pass CE-perfusion ADCT and MRI has equal to or better potential to predict therapeutic outcome than PET/CT in NSCLC patients treated with chemoradiotherapy. Perfusion parameters from dynamic first-pass CE-perfusion ADCT and MRI may be applicable as new biomarkers in this setting.

CLINICAL RELEVANCE/APPLICATION

Dynamic first-pass CE-perfusion ADCT and MRI has equal to or better potential to predict therapeutic outcome than PET/CT in NSCLC patients treated with chemoradiotherapy. Perfusion parameters may be applicable as new biomarkers in this setting.

MSRO35-07 Biological Effective Dose (BED) Influence on Clinical Outcomes of Stage I Non-Small Cell Lung Cancer (NSCLC) Treated with Fiducial-based Robotic Stereotactic Body Radiation Therapy (SBRT) with Respiratory Motion Tracking

Tuesday, Nov. 29 11:30AM - 11:40AM Room: S103CD

Awards

Student Travel Stipend Award

Participants

Jonathan W. Lischalk, MD, Washington, DC (*Presenter*) Nothing to Disclose

ABSTRACT

Purpose/Objective(s): SBRT for early stage NSCLC is an established treatment option for medically inoperable patients. Previous research has supported a biological effective dose (BED) threshold to achieve superior control rates. Fiducial-based robotic SBRT allows for intrafractional respiratory motion management, which avoids the requirement to create an internal target volume (ITV). We report the long-term outcomes of patients treated using this novel unique technique, in particular whether this respiratory motion management strategy is also subject to a reported BED threshold. **Materials/Methods:** In this single institutional retrospective series we reviewed clinical outcomes of stage I inoperable NSCLC. Inclusion criteria was as follows: (1) AJCC 7th edition stage I tumors, (2) pathologic confirmation of malignancy, (3) pre-treatment PET/CT for mediastinal staging, and (4) medical inoperability determined by multidisciplinary evaluation. All patients were treated using a robotic fiducial-based SBRT system with respiratory motion tracking in 3 or 5 fraction of 10 to 20 Gy to a minimum BED of 100 Gy using a NSCLC tumor α/β of 10. Locoregional failure was defined as recurrence within the locally treated field, involved lobe, or ipsilateral nodal region (N1-2). Local control, locoregional control, and overall survival were calculated using the Kaplan-Meier method and comparisons between BED above and below 105 Gy were calculated using the generalized Wilcoxon test. **Results:** Sixty-one patients with a median age of 75 years were included. The majority of patients determined to be surgically inoperable due to pulmonary dysfunction. The majority of patients (75%) were diagnosed with AJCC prognostic stage IA NSCLC. Patients were treated using robotic SBRT to a median total dose of 50 Gy with a median BED of 112.5 Gy (range, 100 to 180 Gy). Thirty-one patients were treated with a BED greater than 105 Gy and the remaining 30 with a BED below 105 Gy. Five year local control, locoregional control, and overall survival for those patients treated above and below a BED of 105 Gy were 90.5% vs. 82.6% ($p = 0.26$), 78.6% vs. 64.8% ($p = 0.03$), and 38.7% vs. 42.9% ($p = 0.97$). **Conclusion:** Statistically significant improvements in locoregional control were observed in patients treated with a BED greater than 105 Gy, although this did not translate into an improvement in overall survival. Treatment of stage I NSCLC with fiducial-based robotic SBRT using advanced respiratory motion management does not preclude the necessity of delivering an adequate BED to the tumor target.

MSRO35-08 Effect of Tumor Contouring on the Prediction Performance of Using Radiomic Approach to Predict Gene Mutational Status in Non-Small Lung Cancer Patients With Gefitinib Treatment

Tuesday, Nov. 29 11:40AM - 11:50AM Room: S103CD

Participants

Lin Lu, New York, NY (*Abstract Co-Author*) Nothing to Disclose

Qiao Huang, New York, NY (*Abstract Co-Author*) Nothing to Disclose

Yajun Li, Fort Lee, NJ (*Abstract Co-Author*) Nothing to Disclose

Qian Yin, MD, Xian, China (*Abstract Co-Author*) Nothing to Disclose

Min Zong Jr, MD, PhD, Nanjing, China (*Abstract Co-Author*) Nothing to Disclose

Binsheng Zhao, DSc, New York, NY (*Presenter*) License agreement, Varian Medical Systems, Inc; License agreement, Keosys SAS ; License agreement, Hinacom Software and Technology, Ltd; License agreement, ImBio, LLC ; Research funded, ImBio, LLC; License agreement, AG Mednet, Inc

Lawrence H. Schwartz, MD, New York, NY (*Abstract Co-Author*) Committee member, Celgene Corporation Committee member, Novartis AG Committee member, ICON plc Committee member, BioClinica, Inc

PURPOSE

Radiomic delta-features describe the change of tumor imaging phenotype between baseline and follow-up scan images. Prior to computation of radiomic delta-features, tumor regions-of-interest (ROI) on baseline and follow-up images need to be delineated by radiologist. This study was to explore the effect of different tumor ROIs drawn by different radiologists on the performance of using radiomic delta-features to predict the epidermal growth factor receptor (EGFR) gene mutational status in non-small cell lung cancers (NSCLC) patient with gefitinib treatment.

METHOD AND MATERIALS

This was a retrospective analysis on a clinical trial data of 46 early stage NSCLC patients with a total of 46 tumors (one tumor per patient) whose EGFR mutation status were known (EGFR+:EGFR- = 20:26). All of the patients had non-contrast enhanced, 1.25mm and lung reconstruction images at both CT scan time points. Three radiologists, with reading experiences of 23, 15 and 8 years respectively, used an identical in-house algorithm to independently delineate baseline and three-week follow-up tumor ROIs, upon which 89 radiomic features to describe the change of tumor size, intensity histogram, shape, edge and texture were extracted. Delta-features were the differences between baseline and follow-up features. The area under the curve (AUC) of the receiver operator characteristic (ROC) was calculated to assess the power of radiomic delta-features on predicting the EGFR mutational status of patients.

RESULTS

Tumor ROIs delineated by different radiologists resulted in different performance on the prediction of the EGFR mutational status. The highest AUCs (number of significant features: AUC > 0.8) of the three radiologists' were 0.91 (3), 0.85 (5), and 0.79 (0), respectively. A same feature can have different prediction power if calculated from different tumor ROIs. For example, the AUCs of feature Run_PLU (Run-Length Primitive Length Uniformity) were 0.88, 0.75 and 0.73 for three different ROIs.

CONCLUSION

Radiomic delta-features are able to be used as potential imaging biomarkers to predict the gene mutational status of patient. However, tumor delineation induced differences in predicting EGFR mutations warrants further investigation.

CLINICAL RELEVANCE/APPLICATION

With the rapid growth of the field of radiogenomics, our findings are valuable because they increase awareness of variations in the performance of predicting EGFR mutations using radiomic features.

MSRO35-09 Multiparametric Imaging of the Tumor Response in Non-small Cell Lung Cancer to Stereotactic Ablative Radiation Therapy

Tuesday, Nov. 29 11:50AM - 12:00PM Room: S103CD

Participants

Dae-Myoung Yang, MSc, London, ON (*Presenter*) Nothing to Disclose

David Palma, MD, FRCPC, London, ON (*Abstract Co-Author*) Nothing to Disclose

Ting-Yim Lee, MSc, PhD, London, ON (*Abstract Co-Author*) License agreement, General Electric Company

PURPOSE

To determine whether metabolism as measured with dynamic fluorine-18 fluorodeoxyglucose (FDG) positron emission tomography (PET) and perfusion as measured with dynamic contrast-material enhanced (DCE) computed tomography (CT) scanning can help predicting and assessing the integration and true pathological rate of stereotactic ablative radiation therapy (SABR) in non-small cell lung cancer (NSCLC).

METHOD AND MATERIALS

After Research Ethics Board approval was obtained, 13 patients who have histologically confirmed early stage T1 or T2a NSCLC that has a tumour diameter ≤ 5 cm and no nodal metastases (T1T2N0) underwent dynamic FDG-PET and DCE-CT pre- and post-SABR since September 2014. The post scans were acquired 8 weeks after SABR. Dynamic FDG-PET measures maximum standardized uptake values (SUVmax) in the tumour. DCE-CT imaging allows quantitative mapping of blood flow (BF) and blood volume (BV) in the tumours. Since free-breathing was allowed during DCE-CT scanning, breathing motion was minimized by non-rigid image registration before the BF and BV functional maps were generated. Lobectomy surgery was performed 10 weeks after SABR, to allow sufficient time for reactive response to SABR to subside.

RESULTS

Analysis of dynamic FDG-PET and DCE-CT scans of the first 10 patients showed difference from pre- to post-SABR. Following SABR, there were a reduction in BF (41.3%, $P = 0.001$), BV (27.8%, $P = 0.062$) and SUVmax (46.0%, $P = 0.005$). The included 3D scatter plot shows the distinct characteristic response of NSCLC to SABR.

CONCLUSION

Dynamic FDG-PET and DCE-CT can assess and measure the response of NSCLC to SABR. In future analysis, sensitivity and specificity of this imaging technique and quantitative measurements of glucose kinetics can be calculated.

CLINICAL RELEVANCE/APPLICATION

Novel combination of neoadjuvant SABR plus surgery is being evaluated as a cure for T1T2N0 NSCLC. Dynamic FDG-PET and DCE-CT are a useful adjunct to standard follow-up in assessing true response rate.

MSRP31

RSNA Resident and Fellow Symposium: Career 101: Contract Negotiation (An Interactive Session)

Tuesday, Nov. 29 10:30AM - 12:00PM Room: E451B

ED

AMA PRA Category 1 Credits™: 1.50
ARRT Category A+ Credit: 0

Participants

Sub-Events

MSRP31A Academics

Participants

Bhumin Patel, MD, Memphis, TN, (bhuminpatel@gmail.com) (*Presenter*) Nothing to Disclose

David M. Yousem, MD, Baltimore, MD, (dyousem1@jhu.edu) (*Presenter*) Royalties, Reed Elsevier; Royalties, Oakstone Publishing, LLC

LEARNING OBJECTIVES

1) Understand the typical issues that are addressed in a contract for an academic radiologist's position. 2) Recount strategies for getting the "extras" that you need/want to be successful. 3) Identify pitfalls in radiology contracts.

ABSTRACT

Most physicians are so excited to finally be employed after training that they often fail to exercise caution in agreeing to a contract that may lead to troubles in later life. While one may typically focus on salary, benefits, and vacation time, the factors leading to one's success in academia more often focus on 1) research time, 2) mentorship, 3) start-up resources, and 4) promotion criteria. If one focuses on mission and vision and values with the Chairperson, one can often frame a request for more resources in a win-win arrangement that leads to successful negotiation. By the same token, making sure that non-compete clauses and restrictions on practice are reasonable can prevent misunderstandings and limitations on practice in the future.

MSRP31B Private Practice

Participants

Thomas G. Tullius JR, MD, Chicago, IL, (thomas.tulliusjr@uchospitals.edu) (*Presenter*) Nothing to Disclose

J. Raymond Geis, MD, Fort Collins, CO (*Presenter*) Shareholder, Montage Healthcare Solutions, Inc; Advisor, Nuance Communications, Inc;

LEARNING OBJECTIVES

1) Understand the typical employment process in private practices. 2) Learn what to look for when assessing a private practice job offer. 3) Learn how to prioritize pros and cons of a private practice situation.

ABSTRACT

To find a satisfying private radiology practice job involves understanding one's priorities. Any job will offer pros and cons; finding the right job involves being comfortable with the compromises between the two. This presentation will discuss what to look for, and look out for, when job searching, and then negotiating the employment contract.

Handout: J. Raymond Geis

[http://abstract.rsna.org/uploads/2016/16019609/RSNA 2016 Resident Job Talk handout MSRP31B GEIS .pdf](http://abstract.rsna.org/uploads/2016/16019609/RSNA_2016_Resident_Job_Talk_handout_MS RP31B_GEIS_.pdf)

MSRP31C Leadership Skills for Trainees

Participants

Ajwad S. Bajwa, MD, Royal Oak, MI (*Presenter*) Nothing to Disclose

Jonathan A. Flug, MD, MBA, Denver, CO, (Jonathan.Flug@Ucdenver.edu) (*Presenter*) Nothing to Disclose

LEARNING OBJECTIVES

1) Understand what networking is and why it is important for their future success. 2) Learn how to build and maintain an effective network. 3) Recognize how to reap the largest benefit out of a network by focusing on helping and advancing the career of others in your network.

ABSTRACT

Networking involves the exchange of information or services among individuals, groups, or institutions. Numerous studies both within healthcare and outside of healthcare have highlighted the multitude of benefits associated with establishing and maintaining a network. This lecture will define what a true network is, review the science and data behind effective networks, and provide practical advice for attendees which can be implemented early in one's career to reap the lifelong benefits of a highly functioning network.

3D Printing (Mimics) Hands-on

Tuesday, Nov. 29 10:30AM - 12:00PM Room: S401AB

IN

AMA PRA Category 1 Credits™: 1.50
ARRT Category A+ Credits: 1.50

Participants

Adnan M. Sheikh, MD, Ottawa, ON, (asheikh@toh.on.ca) (*Moderator*) Nothing to Disclose
 Adnan M. Sheikh, MD, Ottawa, ON, (asheikh@toh.on.ca) (*Presenter*) Nothing to Disclose
 Frank J. Rybicki III, MD, PhD, Ottawa, ON, (frybicki@toh.ca) (*Presenter*) Nothing to Disclose
 Dimitris Mitsouras, PhD, Boston, MA, (dmitsouras@alum.mit.edu) (*Presenter*) Research Grant, Toshiba Corporation;
 Leonid Chepelev, MD, PhD, Ottawa, ON (*Presenter*) Nothing to Disclose
 Taryn Hodgdon, MD, Ottawa, ON (*Presenter*) Nothing to Disclose
 Carlos H. Torres, MD, FRCPC, Ottawa, ON, (catorres@toh.ca) (*Presenter*) Nothing to Disclose
 Ai-Li Wang, Ottawa, ON (*Presenter*) Nothing to Disclose
 Ekin P. Akyuz, BSc, Ottawa, ON (*Presenter*) Nothing to Disclose
 Nicole Wake, MS, New York, NY (*Presenter*) Nothing to Disclose
 Peter C. Liacouras, PhD, Bethesda, MD (*Presenter*) Nothing to Disclose
 Gerald T. Grant, MD, MS, Louisville, KY (*Presenter*) Nothing to Disclose
 Satheesh Krishna, MD, Ottawa, ON, (dr.satheeshkrishna@gmail.com) (*Presenter*) Nothing to Disclose
 John P. Lichtenberger III, MD, Bethesda, MD, (john.lichtenberger@usuhs.edu) (*Presenter*) Author, Reed Elsevier
 Ashish Gupta, MD, Ottawa, ON (*Presenter*) Grant, Medtronic plc
 Elizabeth George, MD, Boston, MA (*Presenter*) Nothing to Disclose
 Jane S. Matsumoto, MD, Rochester, MN (*Presenter*) Nothing to Disclose
 Amy E. Alexander, BEng, Rochester, MN (*Presenter*) Nothing to Disclose
 Jonathan M. Morris, MD, Rochester, MN (*Presenter*) Nothing to Disclose

LEARNING OBJECTIVES

1) To become familiar with the computational processing of cross-sectional images required to enable 3D printing using practical examples. 2) To learn to use software to identify and extract anatomical parts from cross-sectional images using manual and semi-automated segmentation tools, including thresholding, region growing, and manual sculpting. 3) To gain exposure to techniques involving model manipulation, refinement, and addition of new elements to facilitate creation of customized models. 4) To learn the application of tools and techniques, including "wrapping" and "smoothing" to enable the accurate printing of the desired anatomy, pathology, and model customizations using Computer Aided Design (CAD) software. 5) To become exposed to Standard Tessellation Language (STL) file format and interfacing with a 3D printer.

ABSTRACT

"3D printing" refers to fabrication of a tangible object from a digital file by a 3D printer. Materials are deposited layer-by-layer and then fused to form the final object. There are several 3D printing technologies that share similarities but differ in speed, cost, and resolution of the product. Digital Imaging and Communications in Medicine (DICOM) image files cannot be used directly for 3D printing; further steps are necessary to make them readable by 3D printers. The purpose of this hands-on course is to convert a set of DICOM files into a 3D printed model through a series of simple steps. Some of the initial post-processing steps may be familiar to the radiologist, as they share common features with 3D visualization tools that are used for image post-processing tasks such as 3D volume rendering. However, some are relatively or completely new to radiologists, including the manipulation of files in Standard Tessellation Language (STL). It is the STL format that is read by the 3D printer and used to reproduce a part of the patient's anatomy. This 90 minute session will begin with a DICOM file and review the commonest tools and techniques required to create a customized printable STL model. An extensive training manual will be provided before the meeting. It is highly recommended that participants review the training manual to optimize the experience at the workstation.

Honored Educators

Presenters or authors on this event have been recognized as RSNA Honored Educators for participating in multiple qualifying educational activities. Honored Educators are invested in furthering the profession of radiology by delivering high-quality educational content in their field of study. Learn how you can become an honored educator by visiting the website at: <https://www.rsna.org/Honored-Educator-Award/>

Frank J. Rybicki III, MD, PhD - 2016 Honored Educator

Getting Stuff Done: A Hands-on Technology Workshop to Enhance Personal Productivity (Hands-on)

Tuesday, Nov. 29 10:30AM - 12:00PM Room: S401CD



AMA PRA Category 1 Credits™: 1.50
ARRT Category A+ Credits: 1.50

Participants

Matthew B. Morgan, MD, Sandy, UT (*Presenter*) Consultant, Reed Elsevier
Puneet Bhargava, MD, Shoreline, WA, (bhargp@uw.edu) (*Presenter*) Editor, Reed Elsevier
Dushyant V. Sahani, MD, Boston, MA (*Presenter*) Research support, General Electric Company; Medical Advisory Board, Allena Pharmaceuticals, Inc
Amanda Lackey, MD, Columbus, OH (*Presenter*) Editor, Reed Elsevier

LEARNING OBJECTIVES

- 1) Introduce the concept of "Getting Things Done".
- 2) Learn the concepts of Inbox Zero and other email management techniques.
- 3) Using tools such as note-taking applications, citation and password managers.

ABSTRACT**Honored Educators**

Presenters or authors on this event have been recognized as RSNA Honored Educators for participating in multiple qualifying educational activities. Honored Educators are invested in furthering the profession of radiology by delivering high-quality educational content in their field of study. Learn how you can become an honored educator by visiting the website at: <https://www.rsna.org/Honored-Educator-Award/>

Puneet Bhargava, MD - 2015 Honored Educator
Dushyant V. Sahani, MD - 2012 Honored Educator
Dushyant V. Sahani, MD - 2015 Honored Educator
Dushyant V. Sahani, MD - 2016 Honored Educator

RCC32

Initiatives to Support Quality Measurement and Effectiveness Research in Radiology

Tuesday, Nov. 29 10:30AM - 12:00PM Room: S501ABC



AMA PRA Category 1 Credits™: 1.50
ARRT Category A+ Credits: 1.50

Participants

Charles E. Kahn JR, MD, MS, Philadelphia, PA, (charles.kahn@uphs.upenn.edu) (*Moderator*) Nothing to Disclose

LEARNING OBJECTIVES

1) Describe current Federal incentive payment systems and their impact on radiology. 2) Learn how radiology data registries are being used to support research and performance-based payments to radiologists. 3) Discover new radiology informatics tools to facilitate participation in data registries. 4) Gain an overview of progress in using registries to measure quality.

Sub-Events

RCC32A Overview and Current Status of Federal Health IT Programs and Payment Incentives

Participants

Jeffrey Smith, MPP, Bethesda, MD, (jsmith@amia.org) (*Presenter*) Nothing to Disclose

LEARNING OBJECTIVES

1) Describe how major regulations will impact their practice in the near-term. 2) Understand the role Congress plays in setting policy after legislation passes, and how they impact regulation without legislation. 3) Learn how health informatics policy is evolving to meet a constant set of challenges in healthcare.

ABSTRACT

While headlines depict contentious election year politics and constant gridlock in the nation's Capital, it's far from the whole story. Significant activities inside the Beltway by both the Obama Administration and Congress have shifted how healthcare is delivered and paid for across the country. Join AMIA Vice President of Public Policy, Jeffrey Smith, M.P.P., for a review of what policies are driving Washington, DC and what's in store for the clinical community over the next several months.

RCC32B Current Use of Registries in Radiology

Participants

Richard L. Morin, PhD, Jacksonville, FL (*Presenter*) Nothing to Disclose

LEARNING OBJECTIVES

View learning objectives under the main course title.

RCC32C New Radiology Informatics Tools Designed to Facilitate Registry Participation

Participants

Charles E. Kahn JR, MD, MS, Philadelphia, PA, (charles.kahn@uphs.upenn.edu) (*Presenter*) Nothing to Disclose

LEARNING OBJECTIVES

View learning objectives under the main course title.

Honored Educators

Presenters or authors on this event have been recognized as RSNA Honored Educators for participating in multiple qualifying educational activities. Honored Educators are invested in furthering the profession of radiology by delivering high-quality educational content in their field of study. Learn how you can become an honored educator by visiting the website at: <https://www.rsna.org/Honored-Educator-Award/>

Charles E. Kahn JR, MD, MS - 2012 Honored Educator

RCC32D Progress Toward the Use of Registries to Measure Quality

Participants

Douglas Fridsma, MD, PhD, Bethesda, MD (*Presenter*) Nothing to Disclose

LEARNING OBJECTIVES

View learning objectives under the main course title.

SPCP31

Turkey Presents: The Meaning of Evolution for Radiology and Advances in Neuroradiology

Tuesday, Nov. 29 10:30AM - 12:00PM Room: E353C

NR

AMA PRA Category 1 Credits™: 1.50
ARRT Category A+ Credits: 1.50

Participants

Ayşe Sezin Gunes, Eskisehir, Turkey (*Presenter*) Nothing to Disclose

Sub-Events

SPCP31A Opening Remarks

Participants

Richard L. Baron, MD, Chicago, IL (*Presenter*) Nothing to Disclose

SPCP31B Presentation about the Activities of Turkish Society of Radiology

Participants

Aysenur Oktay Alfati, MD, Izmir, Turkey (*Presenter*) Nothing to Disclose

SPCP31C Hemodynamic Basics Governing Endovascular Treatment of Intracranial Aneurysms

Participants

Civan Islak, Istanbul, Turkey (*Presenter*) Nothing to Disclose

LEARNING OBJECTIVES

1) Understand underlying hemodynamic factors leading to aneurysm formation (plastic deformation of vessel wall) and biomechanical definition of endovascular aneurysm treatment. 2) Learn probable Flow effects of so called flow modifier devices and their role in final aneurysm sac thrombosis and its long term result. 3) Understand the differences between morphologic and hemodynamic treatment.

SPCP31D Meaning of Evolution for Radiology and Medicine

Participants

Tamer Kaya, PhD , ESKISEHIR, Turkey (*Presenter*) Nothing to Disclose

LEARNING OBJECTIVES

After Darwin's implementation of the theory over 150 years ago, evolution has been a reality. Thanks to the increasing curiosity and putting in a new vision to the medicine, evolutionary medicine is growing. As a radiology specialist, nearly all of our practice is about three dimensional imaging of the body. Evolution shows us another dimension different than these three dimensional approaching of anatomical detail and pathology. Various pathological conditions have close relations with evolution. At the time of intrauterine and pediatric development period, there is very most evolutionary effect. Differentiation of cells and the process of the formation of new tissues are mainly related to ancestral family tree. Blocking this process in some cell differentiation may cause many congenital diseases and variational anatomic changes. Classification systems are insufficient for classifying some pathologies. But it will be very effective to classify and understand pathologies on the basis of evolution. In this presentation, some anatomical variations and some pathologies will be displayed and discussed on the point of evolution.

SPCP31E Imaging the Human Brain beyond Anatomy: The Human Connectome Project

Participants

Kamil Ugurbil, PhD, Minneapolis, MN (*Presenter*) Stockholder, MR Instruments, Inc; Consultant, MR Instruments, Inc; Consultant, Varian, Inc

SPCP31F Closing Remarks

Participants

James P. Borgstede, MD, Colorado Springs, CO (*Presenter*) Nothing to Disclose

SSG01

Breast (Tomosynthesis Diagnostic)

Tuesday, Nov. 29 10:30AM - 12:00PM Room: E451A

BR **DM** **MR**

AMA PRA Category 1 Credits™: 1.50
ARRT Category A+ Credits: 1.50

FDA Discussions may include off-label uses.

Participants

Emily F. Conant, MD, Philadelphia, PA (*Moderator*) Consultant, Hologic, Inc; Consultant, Siemens AG
Debra S. Copit, MD, Philadelphia, PA (*Moderator*) Grant, Hologic, Inc

Sub-Events

SSG01-01 **BI-RADS 3 Re-defined with Tomosynthesis: Mammographic Features and Imaging Frequency**

Tuesday, Nov. 29 10:30AM - 10:40AM Room: E451A

Participants

Madhavi Raghu, MD, New Haven, CT (*Presenter*) Nothing to Disclose
Thomas McCann, MD, New Haven, CT (*Abstract Co-Author*) Nothing to Disclose
Taraneh Hashemi-Zonouz, MD, New Haven, CT (*Abstract Co-Author*) Nothing to Disclose
Sarah H. O'Connell, MD, New Haven, CT (*Abstract Co-Author*) Nothing to Disclose
Laura S. Sheiman, MD, New Haven, CT (*Abstract Co-Author*) Nothing to Disclose
Reni S. Butler, MD, Madison, CT (*Abstract Co-Author*) Nothing to Disclose
Regina J. Hooley, MD, New Haven, CT (*Abstract Co-Author*) Consultant, FUJIFILM Holdings Corporation; Consultant, Siemens AG
Liane E. Philpotts, MD, New Haven, CT (*Abstract Co-Author*) Nothing to Disclose

PURPOSE

Tomosynthesis can improve diagnostic confidence with potential fewer BI-RADS 3 (BR 3) mammographic follow-up recommendations. As this rate declines, the criteria and frequency of imaging lesions previously classified as probably benign may need to be re-defined. The purpose of this study is to determine the frequency, timing, and duration of follow-up imaging for probably benign lesions with tomosynthesis.

METHOD AND MATERIALS

A retrospective, IRB approved review of the breast imaging database was conducted to identify all diagnostic mammograms categorized as BR3 and performed with tomosynthesis over 3 years (1/12-1/15). 1-3 year follow-up data was collected. Biopsy outcomes of all studies re-classified as BR4 or 5 at follow-up were collected to determine malignancy rate, timing of cancers diagnosis (6,12,24 or 36 months) and mammographic features (focal asymmetries, masses, calcifications or architectural distortions).

RESULTS

12611 diagnostic studies were performed with tomosynthesis and 2535 (20%) were categorized as BR3. 12-36 month follow up data was available in 2212 patients (87%). 145 patients were re-classified as BR4 or 5 at follow-up resulting in 25 malignancies (1.0%): 16 invasive cancers & 9 DCIS. 24/25 malignancies were node negative and presented as masses (12), calcifications (11) or distortions (2). No asymmetries resulted in malignancy. A majority of cancers 22 (88%) were diagnosed at the first follow up imaging: 15 at 6 month interval, 3 at 12 months and 4 at 24 months. Three were diagnosed during the second follow up imaging: 1 invasive, 2 DCIS. The only node positive case was in a 52 year old woman with new onset nipple retraction and a new mass diagnosed as invasive lobular carcinoma at the 6 month interval.

CONCLUSION

The BR3 malignancy rate remained low at 1.0% with most cancers manifesting as masses or calcifications, suggesting that focal asymmetries may be categorized as benign. Most malignancies were diagnosed at the first follow up study, indicating that continued surveillance for 2-3 years may be unnecessary when the diagnostic work-up is performed with tomosynthesis.

CLINICAL RELEVANCE/APPLICATION

Mammography with tomosynthesis may alter diagnostic workflow patterns and may ultimately also re-define the imaging features and follow up intervals for probably benign lesions.

SSG01-02 **Detection of Non-Calcified T1-stage Invasive Breast Cancer using Digital Breast Tomosynthesis and Full-field Digital Mammography: Factors Affecting Tumor Visibility and the Effect on Diagnostic Performances**

Tuesday, Nov. 29 10:40AM - 10:50AM Room: E451A

Participants

Jung Min Chang, MD, Seoul, Korea, Republic Of (*Presenter*) Nothing to Disclose
Ann Yi, MD, PhD, Seoul, Korea, Republic Of (*Abstract Co-Author*) Nothing to Disclose
Su Hyun Lee, MD, PhD, Seoul, Korea, Republic Of (*Abstract Co-Author*) Nothing to Disclose
Sung Ui Shin, MD, Seoul, Korea, Republic Of (*Abstract Co-Author*) Nothing to Disclose
Nariya Cho, MD, PhD, Seoul, Korea, Republic Of (*Abstract Co-Author*) Nothing to Disclose
Woo Kyung Moon, Seoul, Korea, Republic Of (*Abstract Co-Author*) Nothing to Disclose

PURPOSE

To identify the significant variables associated with visibility of non-calcified T1-stage invasive breast cancers on digital breast tomosynthesis (DBT) interpretation combined with 2D full-field digital mammography (FFDM), and to evaluate the effect of variables on diagnostic performance.

METHOD AND MATERIALS

This retrospective study was approved by our institutional review board, and the requirement to obtain informed consent was waived. Between January 2012 and December 2014, a total of 265 patients (106 non-calcified T1-stage invasive breast cancers and 159 negative controls) who underwent FFDM and DBT were included. The visibility scores (1-3; poorly, fairly, definitely visible) of 106 cancers were assessed on DBT+FFDM and FFDM images in a separate session. Independent variables associated with poorly visible tumors were identified using the logistic regression model. In a total of 265 patients stratified by the independent variable, diagnostic performances of DBT+FFDM and FFDM were compared using the McNemar's test.

RESULTS

For 106 cancers, the mean visibility score was higher in DBT+FFDM compare to FFDM (2.5 vs.1.8; P=.001). Extremely dense breast was the only independent factor associated with poorly visible tumors (odds ratio, 0.02; P<.001). In 55 patients with extremely dense breasts, sensitivity (63.6% vs.59.1%; P=.642) and specificity (84.8%vs.75.8%; P=.078) were not improved by addition of DBT compared to FFDM, whereas were significantly improved (94.0%vs.69.0%; P<.001), (98.4%vs.81.7%; P=.002) in 210 patients with the other mammographic densities.

CONCLUSION

Extremely dense breast was associated with poor visibility in interpreting DBT combined with FFDM for non-calcified T1-stage invasive breast cancers, and no additional diagnostic yield was observed compared to FFDM in women with extremely dense breasts.

CLINICAL RELEVANCE/APPLICATION

Our study supports the benefit of adding DBT to FFDM for detection of non-calcified T1 breast cancers in non-extremely dense breast, whereas the role is minimal in extremely dense breasts.

SSG01-03 Tomosynthesis Increases Detection of Invasive Lobular Carcinoma and Less Aggressive Breast Cancer

Tuesday, Nov. 29 10:50AM - 11:00AM Room: E451A

Participants

Serine E. Baydoun, MD, Iowa City, IA (*Presenter*) Nothing to Disclose

Limin Yang, MD, PhD, Iowa City, IA (*Abstract Co-Author*) Nothing to Disclose

Jinhu Xiong, Iowa City, IA (*Abstract Co-Author*) Nothing to Disclose

Laurie L. Fajardo, MD, MBA, Park City, UT (*Abstract Co-Author*) Consultant, Hologic, Inc; Scientific Advisory Board, Hologic, Inc; Consultant, Koninklijke Philips NV; Advisory Board, Koninklijke Philips NV; Consultant, Siemens AG; Consultant, FUJIFILM Holdings Corporation; Advisory Board, Galena Biopharma, Inc

PURPOSE

To evaluate the added benefit of using Tomosynthesis (3D) in invasive breast cancer detection on screening and diagnostic mammograms with correlation to pathology, receptor status and breast density.

METHOD AND MATERIALS

An IRB approved retrospective review of all mammogram reports from October 2012-May 2015 was performed to identify biopsy-proven invasive breast cancer cases. Cancer detection rate on screening and diagnostic mammograms by digital 2D only versus 2D+3D was compared. Correlation with breast density, pathology and receptor status was performed.

RESULTS

Of 22238 screening mammograms & 7848 diagnostic mammograms, 2D+3D was used in 12543 screening & 4093 diagnostic cases. 177 cases were biopsy proven invasive breast cancer; 59 detected on exams performed with 2D only (24 screening, 35 diagnostic) & 118 detected on exams performed with the adjunct use of 3D (53 screening, 65 diagnostic). 3D significantly improved cancer detection rate in both screening & diagnostic mammograms (4.2 vs 2.5 per 1000; 15.9 vs 9.3 per 1000, p<0.01). Of the 118 cancers diagnosed on 2D+3D exams, the malignancy was either only or better detected by 3D in 62 patients. Characteristics of cancers depicted on 3D included: higher frequency of invasive lobular carcinoma (ILC) (12/118 vs 3/118, p<0.01); higher frequency of less aggressive invasive carcinoma (Grade 1, grade 2, ER/PR positive, Her2 negative cancers, p<0.01); similar frequency of aggressive carcinoma (Grade 3, positive Her2, triple negative). Tomosynthesis also detected more invasive carcinoma in patients with dense breasts (p<0.01).

CONCLUSION

Tomosynthesis increases breast cancer detection in both the screening and diagnostic population. Depiction of ILC & less aggressive invasive cancer (low and intermediate grade, ER/PR positive, Her2 negative) was higher by tomosynthesis. Compared with 2D mammography, tomosynthesis demonstrates enhanced detection of architectural distortion and subtle asymmetries, a feature commonly seen in less aggressive, slower growing tumors as well as invasive lobular carcinoma.

CLINICAL RELEVANCE/APPLICATION

Tomosynthesis improves the detection of subtle asymmetries and architectural distortions associated with ILC and less aggressive cancers, as well as in patients with dense breasts.

SSG01-04 Usefulness of Synthetic MMG (SMMG) and Thick Slab Images with DBT (Digital Breast Tomosynthesis) for Optimization of Clinical Workflow

Tuesday, Nov. 29 11:00AM - 11:10AM Room: E451A

Participants

Nachiko Uchiyama, MD, Tokyo, Japan (*Presenter*) Nothing to Disclose

Mari Kikuchi, MD, Chuou-ku, Japan (*Abstract Co-Author*) Nothing to Disclose
Minoru Machida, MD, PhD, Tokyo, Japan (*Abstract Co-Author*) Nothing to Disclose
Ryusuke Murakami, Tokyo, Japan (*Abstract Co-Author*) Nothing to Disclose
Yasuaki Arai, Tokyo, Japan (*Abstract Co-Author*) Nothing to Disclose

PURPOSE

Concurrent usage of 2D MMG (MMG) and DBT is inevitable in diagnostic usage currently. The number of images with MMG and DBT increases by dozens of times compared with MMG only. The reprocessing of DBT data to generate a 2D MMG-like image and thick slab images of DBT will provide decrease of radiation dose and number of images. In this study, we evaluated the diagnostic accuracy of SMMG with or without DBT and compared with MMG and compared the diagnostic accuracy between two different DBT slab thickness settings.

METHOD AND MATERIALS

The pixel pitch of the MMG and the DBT images was 0.085×0.085 mm. The SMMG images were reconstructed from the 25 raw and processed projection images utilizing 3D volume ray casting method. With one-view MMG and DBT, the radiation doses, utilizing the ACR phantom 156, were 1.20 and 1.80 mGy. All patients received a full two-view MMG and DBT. MMG, SMMG, and SMMG plus DBT images from 108 cases (38 cases of breast cancer and 70 cases of normal or benign) were analyzed and the mean age was 57.0 y.o. The images were evaluated independently by four readers utilizing ROC analysis with the BI-RADS and POM (Probability of Malignancy) scale. In addition, the diagnostic performance between images of 2mm slice thickness with 1mm overlap as current setting and that of 6mm thick synthetic slabs with 3mm overlap reconstructed with a special edge preserving algorithm were compared respectively utilizing ROC analysis.

RESULTS

With DBT, the AGDs were 1.65 mGy in CC view and 1.59 mGy in MLO view. With BIRADS, the average AUC for MMG, SMMG, and SMMG plus DBT were 0.817, 0.813 and 0.892. With POM scale, those were 0.822, 0.813, and 0.898. SMMG plus DBT demonstrated superior diagnostic accuracy compared with MMG and SMMG alone ($p < 0.01$). On the other hand, between SMMG and MMG alone, there were no statistical differences in each ($p > 0.05$). The average AUC for 2mm and 6mm slab images with BIRADS were 0.893 and 0.893. With POM scale, those were 0.896 and 0.895. There were no statistical differences between 2mm and 6mm slab images ($p > 0.05$).

CONCLUSION

SMMG plus DBT will offer the benefit of increased diagnostic accuracy compared with MMG and a 40% decrease of radiation dose compared with MMG plus DBT. Thick slab DBT images will contribute to decrease reading overload compared with current setting without impairing diagnostic accuracy.

CLINICAL RELEVANCE/APPLICATION

SMMG and thick slab images with DBT will be useful to optimize clinical workflow.

SSG01-05 Preoperative Staging in Women with Known Breast Cancers: Comparison between Digital Breast Tomosynthesis (DBT) and Magnetic Resonance Imaging (MRI)

Tuesday, Nov. 29 11:10AM - 11:20AM Room: E451A

Participants

Federica Pediconi, MD, Rome, Italy (*Presenter*) Nothing to Disclose
Francesca Galati, MD, Rome, Italy (*Abstract Co-Author*) Nothing to Disclose
Elena Miglio, Rome, Italy (*Abstract Co-Author*) Nothing to Disclose
Maria L. Luciani, MD, Rome, Italy (*Abstract Co-Author*) Nothing to Disclose
Giovanna Panzironi, MD, Roma, Italy (*Abstract Co-Author*) Nothing to Disclose
Carlo Catalano, MD, Rome, Italy (*Abstract Co-Author*) Nothing to Disclose

PURPOSE

To evaluate the accuracy in tumor extent and size assessment of Digital Breast Tomosynthesis (DBT) and Magnetic Resonance Imaging (MRI) in women with known breast cancers.

METHOD AND MATERIALS

From May 2014 to January 2016, 44 patients (mean age 54.9) with known breast cancer were enrolled. All patients underwent MR exam using a GE DISCOVERY 750 3T, with bilateral breast coil and dedicated protocol, and a DBT projection with Siemens Mammomat Inspiration system. A radiologist with 15 years of experience in breast imaging, evaluated blindly each imaging set. Sensitivity, PPV and accuracy of MRI and DBT were calculated, using histology as the gold standard. The correspondence of the number of lesions identified on MRI vs Histological Examination and on DBT vs Histological Examination was calculated. The maximum tumor size of the lesions on MRI vs DBT was also evaluated and the measurements were considered concordant if they were within ± 3 mm.

RESULTS

On histological examination 58 lesions were detected. MRI had a sensitivity of 98%, PPV 89%, and accuracy 88%; TDM sensitivity was 85%, PPV 95%, and accuracy 84%. The correspondence of the number of identified lesions was good (MRI vs Histological Examination 94%, DBT vs Histological Examination 78%) and the correspondence of the dimensional values of the lesions was moderate (MRI vs DBT 64%).

CONCLUSION

MRI provided higher diagnostic performance than DBT in the pre-operative evaluation of disease, especially in dense breasts. MRI was the most accurate technique, however DBT showed good accuracy, and proved to be a valid tool in patients with known breast cancer.

CLINICAL RELEVANCE/APPLICATION

In cases when MRI couldn't be done, DBT could be a valid tool for preoperative staging.

SSG01-06 Synthetic Digital Mammography with Additional Digital Tomosynthesis Compared to Conventional Full-field Digital Mammography with Additional Digital Tomosynthesis

Tuesday, Nov. 29 11:20AM - 11:30AM Room: E451A

Participants

Nicole Berger, MD, Zurich, Switzerland (*Abstract Co-Author*) Nothing to Disclose
Andrea Luparia, Trento, Italy (*Abstract Co-Author*) Nothing to Disclose
Luca A. Carbonaro, MD, San Donato Milanese, Italy (*Presenter*) Nothing to Disclose
Giovanni Di Leo, San Donato Milanese, Italy (*Abstract Co-Author*) Travel support, Bracco Group
Marco Ali, Milan, Italy (*Abstract Co-Author*) Nothing to Disclose
Francesco Sardanelli, MD, San Donato Milanese, Italy (*Abstract Co-Author*) Speakers Bureau, Bracco Group Research Grant, Bracco Group Speakers Bureau, Bayer AG Research Grant, Bayer AG Research Grant, IMS International Medical Scientific

PURPOSE

To compare the diagnostic accuracy of synthetic digital mammography (SM) with additional digital tomosynthesis (DBT) to full-field digital mammography (FFDM) with DBT.

METHOD AND MATERIALS

IRB approved retrospective study including consecutive patients with FFDM, which were recalled after a suspicious mammogram for screening at our institution between March and November 2015; they all performed a DBT exam (Giotto Tomo system, IMS, Italy) and an ultrasound as work up. Three breast imagers rated FFDM with DBT and SM with DBT independently for Breast Imaging Reporting and Data System (BI-RADS) and density (ACR). Inter-reader agreement was used to compare the two techniques for negative (BI-RADS 1-2) and positive (BI-RADS 3-5) findings. Bland-Altman Plots of each reader were assessed to compare the BI-RADS and ACR rating of both techniques. $P < 0.05$ was regarded as significant. Radiation doses for FFDM vs. DBT were noted and compared.

RESULTS

146 patients were evaluated. Inter-reader agreement was substantial for both FFDM 0.69 (95% coefficient interval, 95%CI 0.62 – 0.76) and SM 0.73 (95%CI 0.66 – 0.79) regarding positive and negative rating. Comparing FFDM to SM reading all readers, the differences were not statistically significant ($P = 0.054$). Out of 11 cancers diagnosed at work up, one cancer was undetected by all both at FFDM and SM. Only one reader showed a significant higher rating ($P = 0.009$) of BI-RADS for using FFDM compared to SM. All three readers showed no difference ($P > 0.058$) between both methods by rating the density rated by using the ACR and $> 85\%$ of all measurements lay between the 95%CI showing a good comparison between the two techniques. Radiation dose for FFDM vs. DBT was for the cranio-caudal projection 1.49 ± 0.56 mGy vs. 1.97 ± 0.87 mGy ($P < 0.001$) and for the medio-lateral oblique projection 1.73 ± 0.67 mGy vs. 2.09 ± 0.87 mGy ($P < 0.001$).

CONCLUSION

Overall, no statistically significant differences were found between SM with DBT and FFDM with DBT readings regarding BI-RADS- and ACR, with just a 21-32% increase in radiation dose.

CLINICAL RELEVANCE/APPLICATION

Synthetic digital mammography (SM) plus tomosynthesis (DBT) is comparable to digital mammography (FFDM) plus DBT regarding BI-RADS- and ACR-ratings and could be applied in screening programs.

SSG01-07 Imaging Features of Breast Cancers on Digital Breast Tomosynthesis According to the Subtypes

Tuesday, Nov. 29 11:30AM - 11:40AM Room: E451A

Participants

Su Hyun Lee, MD, PhD, Seoul, Korea, Republic Of (*Presenter*) Nothing to Disclose
Jung Min Chang, MD, Seoul, Korea, Republic Of (*Abstract Co-Author*) Nothing to Disclose
Sung Ui Shin, MD, Seoul, Korea, Republic Of (*Abstract Co-Author*) Nothing to Disclose
Ann Yi, MD, PhD, Seoul, Korea, Republic Of (*Abstract Co-Author*) Nothing to Disclose
Nariya Cho, MD, PhD, Seoul, Korea, Republic Of (*Abstract Co-Author*) Nothing to Disclose
Woo Kyung Moon, Seoul, Korea, Republic Of (*Abstract Co-Author*) Nothing to Disclose

PURPOSE

To evaluate imaging features of breast cancers on digital breast tomosynthesis (DBT) according to the subtypes and to determine whether it affects the visibility of breast cancers on DBT.

METHOD AND MATERIALS

This study was approved by our institutional review board and the requirement for written informed consent was waived. Between December 2011 and February 2014, a retrospective database review identified 277 invasive breast cancers in 273 women who underwent DBT for preoperative evaluation. Three blinded radiologists independently reviewed DBT images to determine the visibility of cancers and morphologies in terms of mass and microcalcification. Visibility score of each breast cancer was determined by the number of readers correctly detected the cancer (0-3) and divided into low (0-1) and high (2-3) visibility groups. Morphologies of breast cancers were reviewed by two unblinded readers in consensus. Clinicopathologic factors associated with the visibility groups were evaluated using chi-square tests or independent samples t-test. Morphologic imaging features of breast cancer subtypes were analyzed using chi-square tests.

RESULTS

The median age was 49 years (range, 22-78). Breast density was almost entirely fatty in 4% (11/273), scattered fibroglandular in 16% (44/273), heterogeneously dense in 58% (159/273), and extremely dense in 22% (59/273). Of 277 invasive cancers (mean size 2.2 cm; range, 0.2-9.5 cm), 186 (67%) were HR(+)HER2(-), 47 (17%) were HR(+/-)HER2(+), and 44 (16%) were HR(-)HER2(-). The most common findings on DBT was spiculated mass for HR(+)HER2(-) cancers; fine linear branching microcalcifications with non-spiculated mass for HR(+/-)HER2(+) cancers; and non-spiculated mass without microcalcification for HR(-)HER2(-) cancers ($P < .001$). Low visibility of breast cancers on DBT was more frequent in extremely dense breasts ($P = .020$), small pathologic tumor

size ($P < .001$). Breast cancer subtype was not a significant factor associated with the visibility on DBT.

CONCLUSION

Breast cancers showed different imaging findings on DBT according to the subtypes, however, it did not affect the visibility of breast cancers.

CLINICAL RELEVANCE/APPLICATION

Typical findings of breast cancers on DBT according to the subtypes may help to interpret DBT.

SSG01-08 Use of Digital Breast Tomosynthesis (DBT) as a Guide in a Consecutive Series of 178 Vacuum Assisted Biopsies (VAB): Feasibility and Clinical Usefulness

Tuesday, Nov. 29 11:40AM - 11:50AM Room: E451A

Participants

Vincenzo Sabatino, MD, Trento, Italy (*Presenter*) Nothing to Disclose
Anna Ventriglia, MD, Verona, Italy (*Abstract Co-Author*) Nothing to Disclose
Marco Pellegrini, MD, Trento, Italy (*Abstract Co-Author*) Nothing to Disclose
Paolina Tuttobene, MD, Trento, Italy (*Abstract Co-Author*) Nothing to Disclose
Carmine Fanto, MD, Trento, Italy (*Abstract Co-Author*) Nothing to Disclose
Marvi Valentini, MD, Trento, Italy (*Abstract Co-Author*) Nothing to Disclose
Andrea Luparia, Trento, Italy (*Abstract Co-Author*) Nothing to Disclose
Daniela Bernardi, MD, Trento, Italy (*Abstract Co-Author*) Nothing to Disclose

PURPOSE

To analyze the diagnostic accuracy and clinical usefulness of DBT-guided VAB in the assessment of suspicious mammographic nonpalpable lesions

METHOD AND MATERIALS

The study included 178 consecutive breast lesions that, after IRB approval, between January and December 2013, underwent mammographic-guided VAB biopsy. Inclusion criteria: non palpable mammographic findings, suspicious grades R3-R5 according to European Guidelines, biopsied using DBT-guide. Exclusion criteria: lesions biopsied using standard stereotactic-guide, 7/178. The study considered 166 subjects (average age, 55 years; range, 31-83) with 171 lesions. Samplings were performed using 9G needles and an added on system. Patient were in sitting position (144/171) or lateral decubitus (27/171). Specimen radiographs were performed in 133/171 cases. Age of women (59 years), degree of suspicious (R3,R4,R5), lesion morphology (microcalcifications, opacity, distortion) and size (2 cm) were analysed, checking their possible correlation with VAB histological outcomes (B1-B5) by chi-square test. Procedure time for all DBT-guide biopsies was measured. Reference standards were surgical histology and/or a follow-up at least of 12 months

RESULTS

67,8% of the women were 50 years and older. Lesions had at imaging a level of suspicion classified R3 in 91, R4 in 60 and R5 in 20 cases. Lesions were microcalcifications (141, 82.5%), small opacities (6, 3.5%), distortions (24, 14%) with sizes 2cm in 67/171 cases. VAB histology report was negative (B1=4; B2=49) in 53 (31%) cases; borderline (B3) in 47 (27,5%) cases, 33 of them with atypia; suspicious (B4) in 4 (2,3%) cases; positive (B5) in 66 (38,6%) cases. 1/171 (0,6%) was a lymphoma. Age and suspicious grades significantly correlated with VAB histology ($p < 0.005$). 102 patients underwent surgery without any downgrading of VAB histology. In the remaining cases during follow up there was no development of carcinoma. On average DBT biopsy time was 9 minutes, lower than that reported in literature

CONCLUSION

DBT-guided VAB showed an high diagnostic accuracy and an excellent clinical performance proving to be a fast and feasible system for sampling suspicious mammographic nonpalpable lesions

CLINICAL RELEVANCE/APPLICATION

In the future DBT-guide may replace standard stereotactic-system for the assessment of suspicious non palpable lesions

SSG01-09 Added Cancer Yield of Screening Breast MRI in the Modern Era of Digital Breast Tomosynthesis

Tuesday, Nov. 29 11:50AM - 12:00PM Room: E451A

Awards

Student Travel Stipend Award

Participants

Ashley A. Roark, MD, Boston, MA (*Presenter*) Nothing to Disclose
Pragya A. Dang, MD, Boston, MA (*Abstract Co-Author*) Nothing to Disclose
Bethany L. Niell, MD, Tampa, FL (*Abstract Co-Author*) Nothing to Disclose
Elkan F. Halpern, PhD, Boston, MA (*Abstract Co-Author*) Research Consultant, Hologic, Inc; Research Consultant, Real Imaging Ltd; Research Consultant, Gamma Medica, Inc; Research Consultant, K2M Group Holdings, Inc
Geoffrey M. Rutledge, MD, Boston, MA (*Abstract Co-Author*) Nothing to Disclose
Constance D. Lehman, MD, PhD, Boston, MA (*Abstract Co-Author*) Research Grant, General Electric Company; Medical Advisory Board, General Electric Company

PURPOSE

To compare the added cancer yield and performance of screening breast MRI in high-risk women screened with digital breast tomosynthesis (DBT) versus digital mammography (DM).

METHOD AND MATERIALS

Following IRB approval, medical record review identified 4,418 screening breast MRI exams: 2,127 performed 1/2013-1/2015 with a

negative DBT exam in the prior year (DBT group) and 2,291 performed 1/2010-1/2012 with a negative DM exam in the prior year (DM group). Specific MRI exam indications (genetic mutation, family history, prior chest irradiation, personal history of breast cancer or of high-risk lesion) were recorded. Added cancer yield, abnormal interpretation rate (AIR) and positive predictive values (PPV1,2,3) were calculated using ACR BI-RADS 5th edition definitions. Logistic regression analysis was used to compare the groups, adjusting for differences in patient demographics (age, exam indication, mammographic breast density, presence of prior MRI exam).

RESULTS

Mean patient age was 52 years (range 25-86 years). 34 cancers were identified by MRI in the DBT group with an added cancer yield of 16 cancers/1000 screens (30/1000 prevalence screens and 14/1000 incidence screens) compared to 11 cancers/1000 MRI screens in the DM group (7/1000 prevalence screens and 12/1000 incidence screens). No significant differences were found in cancer detection before or after adjusting for differences in patient demographics (age, exam indication, mammographic breast density, presence of prior MRI exam) ($p=0.20$ vs. $p=0.23$). The AIR (BI-RADS 0, 3, 4, 5) was 7.3% (155/2127) in the DBT group and 7.4% (170/2291) in the DM group. PPV1, PPV2, and PPV3 were 22% (34/155), 33% (32/98) and 35% (32/92) in the DBT group and 15% (26/170), 23% (18/77), and 28% (18/64) in the DM group. Of the cancers detected in the DBT group, 79% (27/34) were invasive; of these, 74% (20/27) were <1 cm in size and 85% (23/27) node negative.

CONCLUSION

In high-risk women screened with DBT, the added cancer yield with supplemental MRI screening is similar to the added cancer yield of MRI after DM, with most cancers being invasive, sub-centimeter and node negative.

CLINICAL RELEVANCE/APPLICATION

In the modern era of screening mammography with DBT, MRI continues to be an important supplemental screening modality for high-risk women and detects otherwise occult early-stage invasive cancers.

Science Session with Keynote: Cardiac (Coronary Artery Disease)

Tuesday, Nov. 29 10:30AM - 12:00PM Room: S502AB



AMA PRA Category 1 Credits™: 1.50
ARRT Category A+ Credits: 1.50

Participants

Sanjeev Bhalla, MD, Saint Louis, MO (*Moderator*) Nothing to Disclose
 Albert De Roos, MD, Leiden, Netherlands (*Moderator*) Nothing to Disclose
 Hajime Sakuma, MD, Tsu, Japan (*Moderator*) Departmental Research Grant, Siemens AG; Departmental Research Grant, Bayer AG; Departmental Research Grant, Guerbet SA; Departmental Research Grant, DAIICHI SANKYO Group; Departmental Research Grant, FUJIFILM Holdings Corporation; Departmental Research Grant, Nihon Medi-Physics Co, Ltd

Sub-Events**SSG02-01 Cardiac Keynote Speaker: Correlation of Coronary Anatomy and Pathology with Functional Evaluation on CT Angiography**

Tuesday, Nov. 29 10:30AM - 10:50AM Room: S502AB

Participants

Ethan J. Halpern, MD, Philadelphia, PA (*Presenter*) Nothing to Disclose

PURPOSE

Evaluations of cardiac chamber size and geometry, cardiac structural anatomy, as well as ventricular function are essential components of a cardiac evaluation. A major criticism of cardiac CT is that it evaluates coronary anatomy, but does not provide functional information. Echocardiography and cardiac MRI are often preferred for evaluation of cardiac morphology and function, though CTA clearly excels in evaluation of coronary anatomy. Many investigators have used newer techniques to expand the domain of coronary CTA for evaluation of perfusion. However, precise anatomic evaluation of cardiac chamber morphology and function are available as part of the basic gated cardiac CTA. This information should be combined with a detailed assessment of coronary anatomy and valves in order to derive the most benefit from the cardiac CT evaluation. This presentation will highlight the application of cardiac CTA for evaluation of cardiac function, intracardiac shunts, obstructive physiology, and valvular pathology, in order to demonstrate the complementary information that may be combined along with visualization of coronary anatomy, to provide a more complete understanding of cardiac pathology.

SSG02-03 Clinically Equivalent Coronary Artery Calcification Scoring at 75% Lower Dose Radiation with Forward Projected Model Based Iterative Reconstruction

Tuesday, Nov. 29 10:50AM - 11:00AM Room: S502AB

Participants

Andrew Choi, MD, Washington, DC (*Presenter*) Nothing to Disclose
 Sujata Shanbhag, Bethesda, MD (*Abstract Co-Author*) Nothing to Disclose
 Jeannie Yu, Bethesda, MD (*Abstract Co-Author*) Nothing to Disclose
 Shirley Rollison, Bethesda, MD (*Abstract Co-Author*) Nothing to Disclose
 John Schuzer, Vernon Hills, IL (*Abstract Co-Author*) Employee, Toshiba Corporation
 Chloe Steveson, MS, Otawara, Japan (*Abstract Co-Author*) Employee, Toshiba Corporation;
 Marcus Y. Chen, MD, Bethesda, MD (*Abstract Co-Author*) Institutional research agreement, Toshiba Corporation

PURPOSE

Coronary artery calcification (CAC) quantification is important for cardiovascular risk assessment, but exposes patients to radiation. Forward projected model based iterative reconstruction (FiRST) reduces image noise and enables lower radiation; however, it has not been prospectively validated against conventional filtered back projection (FBP). The purpose of this study was to test whether FiRST with 75% radiation dose reduction results in similar Agatston coronary calcium as standard radiation dose FBP.

METHOD AND MATERIALS

Under Institutional Review Board approved protocol, 100 consecutive patients (61% male, 58.8±8.5 yrs, 27.7±5.8 BMI) prospectively underwent both a low radiation dose coronary calcium score using FiRST and a standard dose coronary calcium score using conventional FBP on a 320 detector row scanner (Aquilion ONE VISION, Toshiba Medical Systems, Otawara, Japan). CAC was quantified using the Agatston method and compared using linear regression, Bland-Altman and weighted kappa for standard clinical Agatston risk groups (0, 1-10, 11-100, 101-400, >400).

RESULTS

Radiation exposure was 75% lower for low vs. standard dose scans (30.5 mGy.cm [IQR 16.2-35.5] vs 98 mGy.cm [IQR 64.3-140.5], $p < 0.0001$). Low FiRST compared to standard FBP showed no significant difference in Agatston score [mean 156.6 vs 147.3 (range 0-1590), mean difference 9.4 ± 28.4, $p = \text{NS}$] and near perfect correlation ($R = 0.99$). Clinical equivalence of low FiRST vs standard FBP was similar to 2 standard FBP scans with 81% (81/100) subjects classified in the same Agatston group and a 0.884 weighted K (95% CI 0.834 – 0.933).

CONCLUSION

Low dose FiRST, when compared to standard FBP, achieves 75% radiation dose reduction with similar image quality and near-clinically equivalent CAC scoring.

CLINICAL RELEVANCE/APPLICATION

Forward projected model based iterative reconstruction for coronary artery calcium scoring significantly reduces radiation exposure to patients with clinically equivalent scoring.

SSG02-04 Coronary Artery Calcium Scoring at the Radiation Dose of a Chest X-ray: The Impact of 3rd Generation Dual-Source CT with Tin Filtration

Tuesday, Nov. 29 11:00AM - 11:10AM Room: S502AB

Awards

Student Travel Stipend Award

Participants

Christian Tesche, MD, Charleston, SC (*Presenter*) Nothing to Disclose
Carlo N. De Cecco, MD, PhD, Charleston, SC (*Abstract Co-Author*) Nothing to Disclose
Moritz H. Albrecht, MD, Charleston, SC (*Abstract Co-Author*) Nothing to Disclose
Akos Varga-Szemes, MD, PhD, Charleston, SC (*Abstract Co-Author*) Consultant, Guerbet SA
Ullrich Ebersberger, MD, Charleston, SC (*Abstract Co-Author*) Nothing to Disclose
U. Joseph Schoepf, MD, Charleston, SC (*Abstract Co-Author*) Research Grant, Astellas Group; Research Grant, Bayer AG; Research Grant, General Electric Company; Research Grant, Siemens AG; Research support, Bayer AG; Consultant, Guerbet SA; ; ;
Christian Canstein, Charleston, SC (*Abstract Co-Author*) Employee, Siemens AG
Richard Bayer, Charleston, SC (*Abstract Co-Author*) Nothing to Disclose
Ellen Hoffmann, Munich, Germany (*Abstract Co-Author*) Nothing to Disclose

PURPOSE

To prospectively investigate the diagnostic performance and potential radiation dose reduction of 3rd generation dual-source CT (DSCT) with tin filtration for coronary artery calcium scoring (CACS) compared to the standard acquisition protocol.

METHOD AND MATERIALS

We prospectively enrolled 50 subjects (61% male, 62.1±10.8 years) who underwent a clinically indicated coronary artery calcium scoring study using the 120kV convention for image acquisition. These participants were investigated with a second 100kV coronary artery calcium scan as the research test using a tin filter comprised within the DSCT x-ray tube. Tin filtration reduces the portion of weaker photons that would unnecessarily contribute to effective radiation exposure without generating a signal. Agatston scores and MESA percentiles were derived from 120kV and 100kV studies and their correlation determined. Radiation dose estimates were compared between the low-dose acquisition protocol and the established standard acquisition protocol as the reference standard.

RESULTS

The low- vs. standard-dose mAs was 402.2±119.5mAs vs. 110.1±51.2mAs ($p=0.34$), computed tomography dose index volume (CTDIvol) was 1.2±1.4mGy for low-dose and 4.2±1.9mGy for standard dose ($p=0.08$). The effective radiation dose resulted in 0.20±0.05mSv for low-dose scans and 0.86±0.37 for standard acquisition ($p<0.0001$). Mean image noise was 26.5±5.9 for low-dose scans and 17.5±4.0 for standard dose ($p=0.019$). Mean Agatston scores were 239.3±434.7 with low-dose and 263.4±467.9 in standard dose acquisitions with a range of scores from 0 to 2263. A good correlation of Agatston scores between low-dose and standard dose was shown ($r=0.994$, $p<0.0001$). Comparison of Agatston score categories and percentile-based risk categories showed excellent agreement for standard acquisition and low-dose scans ($\kappa=0.923$ and $\kappa=0.972$).

CONCLUSION

Coronary artery calcium scoring using CT tin-filtration showed excellent correlation and agreement for cardiac risk categories with the standard acquisition protocol based on the Agatston method, while reducing radiation dose to the levels of a chest x-ray. Such radiation dose reductions appear desirable for a screening test to be used in a priori healthy subjects.

CLINICAL RELEVANCE/APPLICATION

3rd Generation Dual-Source CT with Tin Filtration significantly decreases radiation dose while maintaining excellent accuracy for coronary calcium detection and quantification.

SSG02-05 Gender and CT Coronary Artery Calcium Score Differences in Patients Offered No-Cost PCP Referred Screening vs Standard Clinical Referrals

Tuesday, Nov. 29 11:10AM - 11:20AM Room: S502AB

Participants

Leslie Ciancibello, RT, Cleveland, OH (*Presenter*) Consultant, Cassling Group; Consultant, Siemens AG
Robert C. Gilkeson, MD, Cleveland, OH (*Abstract Co-Author*) Research Consultant, Riverain Technologies, LLC; Research support, Koninklijke Philips NV; Research support, Siemens AG; Research support, General Electric Company
Ronald D. Novak, PhD, Cleveland, OH (*Abstract Co-Author*) Nothing to Disclose
Hiram Bezerra, Cleveland, OH (*Abstract Co-Author*) Nothing to Disclose
Daniel I. Simon, MD, Cleveland, OH (*Abstract Co-Author*) Nothing to Disclose
Robin Rowell, Cleveland, OH (*Abstract Co-Author*) Nothing to Disclose

PURPOSE

Clinical evidence indicates that females underestimate the prevalence of CV disease and their individual-specific CV risk. The purpose of this study was to determine if a greater proportion of females participated in a PCP referred no-cost CAC screening program and had higher mean CAC scores than female patients traditionally referred for CAC scoring (\$99 out-of-pocket cost) based on medical evaluation.

METHOD AND MATERIALS

We compared the gender participation and CAC score data between 3 groups. Group 1 received mailed invitations for a no-cost PCP referred CAC screening during 06/2015, (N= 876, M=436, F=440). Groups 2 and 3 (self-pay 99 \$) were referred for CAC

evaluation in 06/2014, (N=94, M=60, F=34) and 11/2014-05/2015, (N= 911, M=508, F=403), respectively. The difference in mean CAC scores between groups was evaluated using ANOVA. Group differences were evaluated by the χ^2 test and the Marascuilo procedure. P values < 0.05 were considered to be significant.

RESULTS

Female subjects had significantly higher CAC scores in Group 1 (124.6±353.5) when compared to Group 3 (74.1±202.3), $p=0.028$. Significantly more females were screened in Group 1 (50.2%) compared to females in Groups 2 (42.6%) and 3 (44.2%) and fewer males were in Group 1 than Groups 2 and 3 ($\chi^2=10.79$, $p=0.005$). The number of females in Groups 2 and 3 were not significantly different ($p=0.30$). Finally, Group 1 had a significantly larger proportion of females with CAC scores ≥ 400 (9.6%) when compared to both Groups 2 (0%) and 3 (4.7%), ($p=0.008$). Males in Group 1 also had a significantly higher proportion of CAC scores ≥ 400 when compared to Group 3 ($p=0.013$).

CONCLUSION

Offering CAC as a no cost screening exam increased our one month volume six fold during the screening period with an increase of 32% in overall average volumes following the no cost pilot. No-cost PCP referred CAC screening identified a significantly larger proportion of females with CAC scores in the critical range of ≥ 400 and larger average CAC scores when compared to the other groups. Males had significantly overall higher CAC scores than females but also had more individuals with CAC scores ≥ 400 in Group 1.

CLINICAL RELEVANCE/APPLICATION

These results suggest that males and particularly females, may benefit from no-cost CAC screening to identify those at high risk for future CV disease.

SSG02-06 Association between Alcohol Consumption and Presence of Coronary Artery Disease

Tuesday, Nov. 29 11:20AM - 11:30AM Room: S502AB

Awards

Trainee Research Prize - Fellow

Participants

Julia Karady, MD, Budapest, Hungary (*Presenter*) Nothing to Disclose
Balint Szilveszter, MD, Boston, MA (*Abstract Co-Author*) Nothing to Disclose
Zsafia D. Drobni, Budapest, Hungary (*Abstract Co-Author*) Nothing to Disclose
Marton Kolossvary, Budapest, Hungary (*Abstract Co-Author*) Nothing to Disclose
Andrea Bartykowszki, Budapest, Hungary (*Abstract Co-Author*) Nothing to Disclose
Mihaly Karolyi, Budapest, Hungary (*Abstract Co-Author*) Nothing to Disclose
Adam Jermendy, Budapest, Hungary (*Abstract Co-Author*) Nothing to Disclose
Alexisz Panajotu, Budapest, Hungary (*Abstract Co-Author*) Nothing to Disclose
Zsolt Bagyura, Budapest, Hungary (*Abstract Co-Author*) Nothing to Disclose
Pal Maurovich-Horvat, MD, PhD, Pecs, Hungary (*Abstract Co-Author*) Nothing to Disclose

PURPOSE

It has been suggested that light alcohol consumption is associated with reduced risk for coronary artery disease (CAD). However, data regarding regular alcohol consumption and its association with the presence of CAD still remain controversial. The aim of this study was to assess the association between alcohol consumption and the presence of CAD as detected by coronary CT angiography (CTA).

METHOD AND MATERIALS

Consecutive patients referred for coronary CTA were enrolled in our study. We excluded patients with history of stroke, acute myocardial infarction or coronary revascularization. The weekly alcohol consumption was registered using a questionnaire. Alcohol units were calculated as follows: 1 unit equals 2 dl beer or 1 dl wine or 4 cl spirit. Based on the presence of any plaque on coronary CTA we classified the patients into CAD and no CAD groups.

RESULTS

In total, 1925 patients were enrolled (mean age 57.3±16.1 years, females 43.1%). Atherosclerotic plaque was present in at least one coronary segment in 74.3% of the patients. Alcohol consumption was reported by 37.3% of the patients with a median of 6.7 (IQR:3.3;10.8, range:0.2-66.7) units weekly. Using univariate analysis to compare CAD and no CAD patients we found significant difference regarding cardiovascular risk factors ($p<0.001$) but no difference in alcohol consumption ($p=0.35$). After adjusting for cardiovascular risk factors with logistic regression we found no association between alcohol intake and the presence of CAD (OR:1.00;CI:0.98-1.02; $p=0.76$). We performed a secondary analysis to assess the relationship between alcohol consumption and CAD among no drinkers and light drinkers (maximum 14 units per week; 82.7% of alcohol drinkers) and found no association (OR:1.02;CI:0.98-1.06; $p=0.33$). Furthermore, we analyzed the effect of different alcohol types (wine, beer, spirit) on the presence of CAD, but no relationship was found.

CONCLUSION

Our study suggests that the amount of weekly alcohol consumption does not show association with the presence of CAD. We did not detect any association between alcohol intake and CAD among light drinkers either. In addition, we did not find any association between the different alcohol types and the presence of coronary atherosclerosis.

CLINICAL RELEVANCE/APPLICATION

It seems that there is no association between light to moderate alcohol consumption and coronary artery disease.

SSG02-07 Photon-counting CT for Coronary Artery Calcium Scoring: Potential for Dose Reduction in a Human Population

Tuesday, Nov. 29 11:30AM - 11:40AM Room: S502AB

Participants

Veit Sandfort, MD, Bethesda, MD (*Abstract Co-Author*) Nothing to Disclose
Amir Pourmorteza, PhD, Bethesda, MD (*Abstract Co-Author*) Researcher, Siemens AG
Rolf Symons, MD, Washington, DC (*Abstract Co-Author*) Nothing to Disclose
Marissa Mallek, Bethesda, MD (*Abstract Co-Author*) Nothing to Disclose
Tyler E. Cork, BS, Bethesda, MD (*Abstract Co-Author*) Nothing to Disclose
Mark A. Ahlman, MD, Bethesda, MD (*Abstract Co-Author*) Nothing to Disclose
David A. Bluemke, MD, PhD, Bethesda, MD (*Presenter*) Research support, Siemens AG

PURPOSE

The Agatston coronary calcium score (CAC) is one of the best known quantitative radiologic measurements. Photon counting CT detectors (PCD) have the potential to reduce noise at very low doses and therefore may enable ultra-low dose calcium scoring. The purpose of this study was to compare CAC scoring with PCD versus energy-integrating detector (EID).

METHOD AND MATERIALS

We used a hybrid (dual-source) whole-body prototype CT system (Siemens Healthcare, Germany), which consists of an energy integrating detector and a photon-counting detector. We compared 40 datasets from 10 subjects. Subjects were scanned with radiation dose-matched conventional EID and PCD at 120 kVp using two preset quality reference standards (standard dose: 80 mAs, low dose: 20 mAs), 3 mm slice thickness and kernel B35f. Calcium scoring was performed using Vitrea (Vital Images). Multiple areas were measured (LM/LAD, LCX, RCA, ascending aorta, descending aorta, total). Agreement of measurements was assessed using intra-class correlation (ICC) and Bland-Altman analysis. Noise was measured in the blood pool. An analysis of number of pixels >130 HU was performed, which relates to the practicality of calcium scoring.

RESULTS

Average dose-length-product (DLP) was 78.2 ± 22.5 mGy x cm for standard dose and 21.4 ± 4.9 mGy x cm for low dose CAC, resulting in effective radiation doses of 1.1 ± 0.3 mSv and 0.3 ± 0.1 mSv, respectively. Agreement between EID and PCD in standard dose calcium scores was excellent (ICC=0.98). Using the standard dose EID scan as a reference, the agreement of the low dose PCD CAC was superior to the low dose EID CAC (ICC 0.93 vs 0.98, respectively (figure 1A)). Using EID standard dose CAC as reference, PCD low dose showed less bias for CAC scores compared with EID low dose (-10.8 vs -24.8, respectively) (figure 1B) with smaller limits of agreement ([-52, 30.4] vs [-85.6, 36], respectively). Noise levels were similar between EID and PCD, but the fraction of voxels >130 in the blood pool (which may complicate semiautomatic calcium scoring) was higher for low dose EID (p=0.047).

CONCLUSION

The findings suggest that photon counting technology has the potential to reduce radiation dose further in low dose calcium scoring.

CLINICAL RELEVANCE/APPLICATION

Radiation exposure remains an obstacle to calcium scoring for risk prediction purposes. CT detector innovations like photon counting may enable ultra-low dose calcium scoring protocols.

SSG02-08 Darkfield Imaging in Coronary Atherosclerosis

Tuesday, Nov. 29 11:40AM - 11:50AM Room: S502AB

Participants

Nicole Webber, Munich, Germany (*Presenter*) Nothing to Disclose
Marian Willner, Munchen, Germany (*Abstract Co-Author*) Nothing to Disclose
Julia Herzen, Garching, Germany (*Abstract Co-Author*) Nothing to Disclose
Sigrid Auweter, Munich, Germany (*Abstract Co-Author*) Nothing to Disclose
Fabian Bamberg, MD, MPH, Tuebingen, Germany (*Abstract Co-Author*) Speakers Bureau, Bayer AG; Speakers Bureau, Siemens AG; Research Grant, Bayer AG; Research Grant, Siemens AG;
Holger Hetterich, MD, Munich, Germany (*Abstract Co-Author*) Nothing to Disclose
Tobias Saam, MD, Munich, Germany (*Abstract Co-Author*) Research Grant, Diamed Medizintechnik GmbH Research Grant, Pfizer Inc

PURPOSE

Microcalcifications have been recognized as an important marker for atherosclerotic plaque instability. Darkfield imaging based on small angle X-ray scattering has been shown to be highly sensitive for calcifications, e.g. in breast tissue. We hypothesized that high signal areas in darkfield imaging of atherosclerotic plaque are associated with microcalcifications and that darkfield imaging is more sensitive for microcalcifications than absorption-X-ray techniques.

METHOD AND MATERIALS

Fifteen coronary artery specimens were examined at an experimental set-up consisting of X-ray tube, grating-interferometer and detector. Tomographic darkfield-, absorption- and phase-contrast data were simultaneously acquired. Ten cross-sections with high darkfield signal but no signs of calcification in absorption- and phase-contrast were identified. Ten positive and ten negative controls were selected. Histopathology served as standard of reference. A simulation of darkfield and absorption signal for a clinically realistic system for different pixel sizes and different amounts and particle size distributions of calcifications was performed.

RESULTS

According to histopathology microcalcifications were present in 10/10 (100%) cross-sections with high darkfield signal and without evidence of calcifications in absorption- or phase contrast. In positive controls with high signal areas in all three modalities 10/10 (100%) cross-sections showed macrocalcifications and 9/10 (90%) additional microcalcifications. In negative controls without high

signal areas, no micro- or macrocalcifications were detected in histopathology (0/10). In simulations for bigger pixel sizes the darkfield signal is highly sensitive especially for small particle sizes, while showing similar behaviour with the increasing amount of calcifications like the absorption signal.

CONCLUSION

Darkfield imaging can detect microcalcifications with a higher sensitivity than other x-ray contrast imaging techniques and might provide complementary information in the assessment of plaque instability.

CLINICAL RELEVANCE/APPLICATION

Currently darkfield imaging might serve as a non-destructive method for accurate ex-vivo assessment of microcalcifications in cardiovascular research.

SSG02-09 Effect of a Cardiac Motion Correction Algorithm on Coronary CT Angiography Image Quality of Patients with Heart Rates over 70bpm

Tuesday, Nov. 29 11:50AM - 12:00PM Room: S502AB

Participants

Yong Yu, Xianyang City, China (*Presenter*) Nothing to Disclose
Yongjun Jia, MMed, Xianyang City, China (*Abstract Co-Author*) Nothing to Disclose
Chenglong Ren, Shanxi, China (*Abstract Co-Author*) Nothing to Disclose
Ma Guangming, MMed, Xianyang City, China (*Abstract Co-Author*) Nothing to Disclose
Chuangbo Yang, MMed, Xianyang City, China (*Abstract Co-Author*) Nothing to Disclose
Shan Dang, Xianyang, China (*Abstract Co-Author*) Nothing to Disclose
Dong Han, MA, Xianyang, China (*Abstract Co-Author*) Nothing to Disclose

PURPOSE

To explore the value of a cardiac motion correction algorithm (snapshot freeze (SSF)) to improve the image quality of coronary computed tomography angiography (CCTA) for patients with high heart rates.

METHOD AND MATERIALS

65 patients with heart rates (HR) over 70 beats per minute (71-93bpm) who underwent retrospective ECG-gated CCTA were included in the study. Cardiac images were reconstructed with both SSF and the standard (STD) methods. Image quality was evaluated. Two independent readers assessed the overall image quality of the two reconstruction methods using a five-point scale (0-4), and the results were statistically analyzed.

RESULTS

Image quality was higher by using SSF than STD reconstruction on a per-patient level (3.34 ± 0.76 vs. 2.28 ± 0.96), with statistical significance ($Z = -9.21$, $P < 0.05$). 96.9% of the patients could be diagnosed confidently by the SSF reconstruction while only 80% by the STD reconstruction. The difference in the interpretability on a per-patient level was statistically significant between the two groups ($\chi^2 = 9.12$, $P < 0.05$).

CONCLUSION

The motion correction algorithm (SSF) can effectively decrease artifacts caused by the cardiac motion to significantly improve image quality and interpretability in cardiac patients with high heart rates undergoing CCTA.

CLINICAL RELEVANCE/APPLICATION

The motion correction algorithm (SSF) can effectively decrease artifacts caused by the cardiac motion to significantly improve image quality and interpretability in cardiac patients with high heart rates undergoing CCTA.

SSG03

Chest (Diffuse Lung Disease)

Tuesday, Nov. 29 10:30AM - 12:00PM Room: S404CD



AMA PRA Category 1 Credits™: 1.50
ARRT Category A+ Credits: 1.50

Participants

Jonathan D. Dodd, MD, Dublin 4, Ireland (*Moderator*) Nothing to Disclose

Brett M. Elicker, MD, San Francisco, CA (*Moderator*) Nothing to Disclose

Sub-Events

SSG03-01 Transitional Changes in Interstitial Lung Disease Using HRCT to Assess the Impact of Treatment with Cyclophosphamide or Mycophenolate: Results of Scleroderma Lung Study II

Tuesday, Nov. 29 10:30AM - 10:40AM Room: S404CD

Participants

Hyung J. Kim, PhD, Los Angeles, CA (*Presenter*) Nothing to Disclose

Pechin Lo, Los Angeles, CA (*Abstract Co-Author*) Nothing to Disclose

Donald P. Tashkin, MD, Los Angeles, CA (*Abstract Co-Author*) Nothing to Disclose

Matthew S. Brown, PhD, Los Angeles, CA (*Abstract Co-Author*) Nothing to Disclose

David W. Gjertson, PhD, Los Angeles, CA (*Abstract Co-Author*) Nothing to Disclose

Peiyun Lu, Los Angeles, CA (*Abstract Co-Author*) Nothing to Disclose

Danny Chong, MS, Los Angeles, CA (*Abstract Co-Author*) Nothing to Disclose

Jonathan G. Goldin, MBChB, PhD, Los Angeles, CA (*Abstract Co-Author*) Nothing to Disclose

PURPOSE

Systemic sclerosis (scleroderma, SSc) is a complex life-threatening autoimmune disease that affects multiple organ systems. Lung involvement is the leading cause of morbidity and mortality. The aim is to quantify the changes for monitoring the progression or improvement in interstitial lung disease (ILD) over time using voxel-by-voxel transitional scores.

METHOD AND MATERIALS

We report transitional scores using volumetric HRCT scans obtained from participants in SLSII who received either cyclophosphamide (CYC) (n=47) or mycophenolate mofetil (MMF)(n=50). The steps in this process include (1) lobar segmentation and classification of ILD patterns of quantitative lung fibrosis (QLF), quantitative ground glass (QGG), quantitative honeycomb (QHC), and quantitative normal lung (QNL); (2) registration of lobes between two paired scans; (3) mapping each voxel (<27mm³) using a nearest neighbor algorithm; (4) summarizing the transitional patterns into a ratio, where the ratio expresses the counts of changes from one pattern to the other to the counts of patterns at baseline; (5) integrating the transitional net-improvement into a matrix across all patterns. Mixed effect models were used to compare the differences.

RESULTS

Means of the differences in the transitional proportions in the most severe lobe were as follows: CYC group 16% from fibrotic reticulation to GG, 21% from reticulation to normal pattern, and 31% from GG to normal pattern; MMF group 12%, 17%, and 28%, respectively. Similar means were found in whole lung. Mean transitional net improvement from GG or fibrotic pattern to normal patterns and from fibrotic pattern to GG were significant in the two arms (all p<0.001).

CONCLUSION

Using voxel-by-voxel transitional scores on paired HRCT scans 24 months apart, we found obvious changes in extent of ILD patterns, indicating significant transitions from ground glass opacity or fibrotic reticulation to normal patterns and regionally dependent changes between fibrotic patterns and ground glass opacity in patients with SSc-ILD treated with either CYC or MMF. These findings demonstrate the utility of serial HRCT scans and quantitative technique in monitoring the response to treatment in SSc-ILD, and provide insights into the nature of the therapeutic effects

CLINICAL RELEVANCE/APPLICATION

Registration-based transitional texture-based CT scores are effective in characterizing structural changes to therapy at each neighboring voxel level.

SSG03-02 Rheumatoid Arthritis Related Interstitial Lung Disease: Identification of Patients with an Idiopathic Pulmonary Fibrosis Equivalent Outcome using Automated CT Analysis

Tuesday, Nov. 29 10:40AM - 10:50AM Room: S404CD

Participants

Joseph Jacob, MBBS, MRCP, London, United Kingdom (*Presenter*) Nothing to Disclose

Brian J. Bartholmai, MD, Rochester, MN (*Abstract Co-Author*) License agreement, ImBio, LLC; Scientific Advisor, ImBio, LLC

Anne Laure Brun, MD, Paris, France (*Abstract Co-Author*) Nothing to Disclose

Ryoko Egashira, MD, Saga, Japan (*Abstract Co-Author*) Nothing to Disclose

Srinivasan Rajagopalan, PhD, Rochester, MN (*Abstract Co-Author*) Patent agreement, Imbio, LLC

Ronald Karwoski, BS, Rochester, MN (*Abstract Co-Author*) Patent agreement, Imbio, LLC

Maria Kokosi, MD, London, United Kingdom (*Abstract Co-Author*) Nothing to Disclose

Athol U. Wells, London, United Kingdom (*Abstract Co-Author*) Speaker, F. Hoffmann-La Roche Ltd; Speaker, Boehringer Ingelheim

GmbH; Speaker, Gilead Sciences, Inc; Speaker, Merck & Co, Inc; Speaker, Bayer AG; Speaker, Chiesi Farmaceutici SpA; ;

David M. Hansell, MD, London, England, United Kingdom (*Abstract Co-Author*) Research Consultant, AstraZeneca PLC Research

PURPOSE

Patients with rheumatoid arthritis-interstitial lung disease (RA-ILD) with a usual interstitial pneumonia pattern on histopathology are thought to have a disease outcome similar to IPF. Our study evaluated CTs using visual and computer analysis to identify CT variables that predicted an IPF-like outcome in RA-ILD.

METHOD AND MATERIALS

Consecutive patients with a rheumatological and multi-disciplinary team diagnosis of RA-ILD (n=50) were included. Visual and computer-based (using CALIPER software) parenchymal features evaluated against mortality included: total ILD extent, honeycombing, reticular pattern, ground glass opacities, pulmonary vessel volume (PVV), emphysema, traction bronchiectasis and consolidation. Pulmonary function tests recorded were FEV1, FVC, DLco, Kco and a composite physiologic index (CPI). Variables predictive of survival were evaluated against mean survival in a study group of consecutive patients with IPF (n=186).

RESULTS

Visual and computer-based measures of pulmonary fibrosis, DLco, Kco and CPI were predictive of mortality on univariate analysis. Independent predictors of mortality in RA included: age (HR=1.07;p=0.007), visual honeycombing presence (HR=5.19;p=0.04), Kco (HR=0.97;p=0.02) and CALIPER PVV (HR=1.61;p=0.0003). Following exclusion of patients with end-stage disease (n=5), patients with RA-ILD (n=45) were evaluated alongside IPF patients using Kaplan Meier and Cox mortality analysis. Binary CT thresholds identifying RA-ILD patients with either good or IPF-like outcomes included: VISUAL: honeycombing presence (n=30); traction bronchiectasis >5/18 (n=27); fibrosis extent >20% (n=32). CALIPER: honeycombing >0.25% (n=22); PVV >3.5% (n=26); fibrosis extent >2% (n=35). Stratification into more detailed prognostic groups was possible with visual fibrosis extent: <20%, 20-35%, >35% and PVV thresholds: <2.5%, 2.5-5.5%, >5.5%.

CONCLUSION

Automated computer-analysis of CTs can predict an IPF-like outcome in RA patients with a similar sensitivity to visual analysis and is not constrained by observer variation.

CLINICAL RELEVANCE/APPLICATION

Automated computer CT analysis can be used to stratify patients with RA-interstitial lung disease in proposed upcoming large-scale multicentre studies. The technique is fast, sensitive and identifies a new CT variable with no visual correlate, thereby obviating the need for arduous visual CT analysis with its associated interobserver variation.

SSG03-03 Functional Differences of Cystic Lesions between IPF and Distal Acinar Emphysema on Relative Regional Air Volume Change Map

Tuesday, Nov. 29 10:50AM - 11:00AM Room: S404CD

Participants

Kum Ju Chae, MD, Seoul, Korea, Republic Of (*Presenter*) Nothing to Disclose
Chang Hyun Lee, MD, PhD, Seoul, Korea, Republic Of (*Abstract Co-Author*) Nothing to Disclose
Ji Woong Choi, Iowa city, IA (*Abstract Co-Author*) Nothing to Disclose
Gong Yong Jin, MD, PhD, Jeonju, Korea, Republic Of (*Abstract Co-Author*) Nothing to Disclose
Hye-Ryun Kang, Seoul, Korea, Republic Of (*Abstract Co-Author*) Nothing to Disclose
Ching-Long Lin, PhD, Iowa City, IA (*Abstract Co-Author*) Nothing to Disclose
Eric A. Hoffman, PhD, Iowa City, IA (*Abstract Co-Author*) Founder, VIDA Diagnostics, Inc Shareholder, VIDA Diagnostics, Inc Advisory Board, Siemens AG
Jin Mo Goo, MD, PhD, Seoul, Korea, Republic Of (*Abstract Co-Author*) Nothing to Disclose

PURPOSE

Honeycombing cyst is a hallmark of idiopathic pulmonary fibrosis (IPF), but differentiation of paraseptal cysts on CT scans alone is at times difficult. The purpose of this study was to investigate if identification of functional differences between honeycombing cysts and paraseptal low attenuation areas (LAAs) is possible using a relative regional air volume change (RRAVC) map.

METHOD AND MATERIALS

10 normal, 19 emphysema, and 20 idiopathic interstitial lung disease (11 IPF and 9 NSIP) were included in our study. VIDA Apollo software (Coralville, IA) and mass preserving image registration technique were used to compute low ventilation area (LVA) from inspiration and expiration CT scans. LVA0.8 is defined as percent lung volume reflecting less ventilation than 80% of the whole lung mean value. LVA0.8 in the whole lung and fractional air volume change in upper and lower lobes were compared between the three groups using analysis of variance test (ANOVA). The honeycombing cysts in IPF and LAAs in emphysema were visually inspected on the RRAVC map.

RESULTS

LVA0.8 was higher in emphysema patients than IPF or normal subjects (p=0.001). (emphysema: 29.1+/-5.1%, IPF: 19.3+/-5.8%, normal: 20.6+/-5.7) in both lungs. There were significant differences between ILD and emphysema patients in both upper and lower lobe fractional air volume change, where emphysema patients had significantly higher fractional air volume change than normal patients in the upper lobe and ILD patients had lower fractional air volume change than normal patients in the lower lobe. In the RRAVC map, distal acinar emphysema cysts showed decreased air volume change between inspiration and expiration, which represents regional obstruction, characteristic of COPD. Whereas relatively higher ventilation was noted in honeycombing cysts compared to emphysema, suggesting a relatively preserved airway flow in IPF patients.

CONCLUSION

LAAs in distal acinar emphysema were demonstrated as low ventilation areas while cysts in honeycombing did not demonstrate a decreased ventilation on the RRAVC map. This could provide a method for differentiating between distal acinar emphysema and honeycombing cysts.

CLINICAL RELEVANCE/APPLICATION

Cystic lesions which can be seen in IPF and emphysema could be differentiated by the quantitation of acinar scale functional impairment assessed by image matching method, using pairs of inspiratory/expiratory CT data sets.

SSG03-04 Pleuroparenchymal Fibroelastosis (PPFE) Predicts Survival in Idiopathic Pulmonary Fibrosis (IPF)

Tuesday, Nov. 29 11:00AM - 11:10AM Room: S404CD

Participants

Joseph Jacob, MBBS, MRCP, London, United Kingdom (*Presenter*) Nothing to Disclose
Angelo De Laurentis, London, United Kingdom (*Abstract Co-Author*) Nothing to Disclose
Hersh S. Basra, MBBS, BSC, Hitchin, United Kingdom (*Abstract Co-Author*) Nothing to Disclose
Wasim Hakim, MBBS, London, United Kingdom (*Abstract Co-Author*) Nothing to Disclose
Martina Boniface, London, United Kingdom (*Abstract Co-Author*) Nothing to Disclose
Dina Visca, London, United Kingdom (*Abstract Co-Author*) Nothing to Disclose
Maria Kokosi, MD, London, United Kingdom (*Abstract Co-Author*) Nothing to Disclose
Elisabetta Renzoni, London, United Kingdom (*Abstract Co-Author*) Nothing to Disclose
David M. Hansell, MD, London, England, United Kingdom (*Abstract Co-Author*) Research Consultant, AstraZeneca PLC Research Consultant, Boehringer Ingelheim GmbH Research Consultant, InterMune, Inc Research Consultant, F. Hoffmann-La Roche Ltd
Athol U. Wells, London, United Kingdom (*Abstract Co-Author*) Speaker, F. Hoffmann-La Roche Ltd; Speaker, Boehringer Ingelheim GmbH; Speaker, Gilead Sciences, Inc; Speaker, Merck & Co, Inc; Speaker, Bayer AG; Speaker, Chiesi Farmaceutici SpA; ;

PURPOSE

Pleuroparenchymal fibroelastosis (PPFE) is a rare interstitial lung disease (ILD) entity characterized by pleural and parenchymal fibrosis with a striking upper-lobe predominance. PPFE can occasionally coexist with other ILDs. The aim of this retrospective study was to estimate the prevalence and prognostic significance of PPFE in a large group of IPF patients.

METHOD AND MATERIALS

CT imaging from 285 consecutive IPF patients were reviewed (mean age:66±1.1, males:77%, ever smokers:66%, mean FVC:68.4%±2.5, mean DLco:36.3%±1.6, mean CT ILD extent:38.4%±1.6). The presence of PPFE on CT was assessed by two thoracic radiologists and average CT disease extent was used as a measure of disease severity. Mortality, time to irreversible decline in FVC levels of >10% and DLco levels of >15% from baseline, were quantified using proportional hazards analysis.

RESULTS

Kappa values for interobserver agreement for the identification of PPFE were excellent at 0.78. 94 (33%) IPF patients met CT criteria for PPFE. Compared to patients without PPFE, subjects with PPFE were less likely to be ever smokers (p=0.02), had lower FVC measurements (p=0.0005) and more extensive ILD on CT (p=0.03). Freestanding bronchiectasis was identified in 34% of PPFE cases versus < 2% of patients without PPFE (p<0.0001). PPFE was significantly associated with increased mortality (HR:1.54; CI:1.16-2.05, p=0.003), decreased time to decline in FVC (HR:1.82; CI:1.28-2.6, p=0.001) and DLco (HR:2.29 CI:1.6-3.3, p<0.0001). After adjusting for age, gender, smoking status and ILD severity, the association of PPFE with survival and FVC and DLco decline was confirmed.

CONCLUSION

PPFE is an independent predictor of survival and functional worsening in IPF and demonstrates good interobserver agreement. Studies evaluating prevalence and outcome in other diffuse fibrosing lung diseases are needed.

CLINICAL RELEVANCE/APPLICATION

The presence of PPFE in patients with IPF is important to recognize given its independent links with reduced survival.

SSG03-05 Quantitative Follow-Up of Interstitial Pneumonia Using 3D-Curved High-Resolution CT Imaging Parallel to the Chest Wall

Tuesday, Nov. 29 11:10AM - 11:20AM Room: S404CD

Participants

Hiroyasu Umakoshi, Nagoya, Japan (*Presenter*) Nothing to Disclose
Shingo Iwano, MD, Nagoya, Japan (*Abstract Co-Author*) Nothing to Disclose
Tutomu Inoue, Tokyo, Japan (*Abstract Co-Author*) Employee, FUJIFILM Holdings Corporation
Yuanzhong Li, Tokyo, Japan (*Abstract Co-Author*) Employee, FUJIFILM Holdings Corporation
Shinji Naganawa, MD, Nagoya, Japan (*Abstract Co-Author*) Nothing to Disclose

PURPOSE

The imaging findings of patients with interstitial pneumonia (IP) were quantified and compared using three-dimensional curved high-resolution computed tomography (3D-cHRCT) at a depth of 1 cm from the chest wall and pulmonary function testing (PFT), including the predicted percent vital capacity (%VC), forced expiratory volume in 1 second (FEV1), and the predicted percent diffusing capacity of the lungs for carbon monoxide (%DLco).

METHOD AND MATERIALS

We retrospectively reviewed patients with IP who underwent multi-detector row CT (MDCT) scanning and PFT at least twice. Thirty-one patients with IP (25 males and 6 females; mean age, 65 years) were enrolled. Based on MDCT data, 3D-cHRCT images of the lung at a depth of 1 cm from the chest wall were automatically reconstructed using original software. The total area (TA), high-attenuation area (HAA) >-500 HU, and %HAA = (HAA/TA) × 100 were calculated. Moreover, the %HAA ratio (current %HAA / past %HAA) was calculated.

RESULTS

Clinically, 12 patients had stable IP and 19 patients had progressive IP. The mean %HAA of all patients was increased from 8.34% to 9.83% during follow-up, and the mean %DLco was decreased from 77.9% to 73.3%. The mean %HAA ratio was significantly lower in the stable IP group than the progressive IP group (1.05±0.28% vs. 1.43±0.40%, p<0.01). Patients with progressive IP had

a significantly greater decrease in %DLco during follow-up than stable IP patients. The mean %HAA ratio of patients with a > 10% decrease in %DLco was significantly higher than other patients (1.52 vs. 1.10, $p = 0.030$).

CONCLUSION

The %HAA ratio, as determined by 3D curved HRCT in parallel with chest wall data, was significantly correlated with the clinical IP course, and is a novel quantitative parameter by which a decrease in diffusion capacity can be evaluated.

CLINICAL RELEVANCE/APPLICATION

An increase in the %HAA ratio by computed 3D curved HRCT based on routine follow-up HRCT data indicates progressive IP and a lower diffusion capacity

SSG03-06 Evaluation of the Association of Emphysema with Pulmonary Hypertension and Effects on Mortality in Idiopathic Pulmonary Fibrosis

Tuesday, Nov. 29 11:20AM - 11:30AM Room: S404CD

Participants

Joseph Jacob, MBBS, MRCP, London, United Kingdom (*Presenter*) Nothing to Disclose
Brian J. Bartholmai, MD, Rochester, MN (*Abstract Co-Author*) License agreement, ImBio, LLC; Scientific Advisor, ImBio, LLC
Srinivasan Rajagopalan, PhD, Rochester, MN (*Abstract Co-Author*) Patent agreement, Imbio, LLC
Maria Kokosi, MD, London, United Kingdom (*Abstract Co-Author*) Nothing to Disclose
Arjun Nair, MD, FRCR, London, United Kingdom (*Abstract Co-Author*) Nothing to Disclose
Ronald Karwoski, BS, Rochester, MN (*Abstract Co-Author*) Patent agreement, Imbio, LLC
Simon I. Walsh, MD, PhD, London, United Kingdom (*Abstract Co-Author*) Speaker, Boehringer Ingelheim GmbH
Athol U. Wells, London, United Kingdom (*Abstract Co-Author*) Speaker, F. Hoffmann-La Roche Ltd; Speaker, Boehringer Ingelheim GmbH; Speaker, Gilead Sciences, Inc; Speaker, Merck & Co, Inc; Speaker, Bayer AG; Speaker, Chiesi Farmaceutici SpA; ;
David M. Hansell, MD, London, England, United Kingdom (*Abstract Co-Author*) Research Consultant, AstraZeneca PLC Research Consultant, Boehringer Ingelheim GmbH Research Consultant, InterMune, Inc Research Consultant, F. Hoffmann-La Roche Ltd

PURPOSE

There is conflicting evidence regarding the impact on mortality when emphysema coexists in patients with IPF. We investigated effects on outcome resulting from emphysema in a large IPF cohort, using visual and computer-based (CALIPER) CT analysis.

METHOD AND MATERIALS

Consecutive patients with a multi-disciplinary team diagnosis of IPF (n=272) had CT extents of interstitial lung disease (ILD) and emphysema scored visually on a lobar basis and volumetrically by CALIPER. CT scores were evaluated against functional indices (FVC, DLco, Kco and a composite physiologic index [CPI]), to determine the independent effects of ILD and emphysema extent on functional indices. Logistic regression identified variables predictive of the presence of pulmonary hypertension as measured by echocardiography. Finally, the independent effects of emphysema and ILD extent on mortality were investigated.

RESULTS

IPF patients with emphysema (114/272 [42%]) had significantly less ILD than patients without emphysema ($p=0.004$). After correction for DLco, age and gender, the presence/extent of emphysema scored visually and by CALIPER had no impact on the presence of pulmonary hypertension (Table 1). Findings were maintained at emphysema thresholds of >5% and >10% of the lung. On Cox mortality analysis, when correcting for baseline disease severity with DLco, patients with and without emphysema had the same outcome with results maintained at emphysema thresholds of >5% and >10% of the lung.

CONCLUSION

The presence and/or extent of emphysema does not influence the likelihood of having pulmonary hypertension. When correcting for baseline disease severity, the presence/extent of emphysema is not linked to a worsened outcome in IPF.

CLINICAL RELEVANCE/APPLICATION

Using both visual and computer scoring of emphysema on CTs: IPF patients with emphysema were shown not to constitute a disease subgroup with a worsened outcome and as such do not require targeted interventions

SSG03-07 Evaluation of the Impact of Emphysema when using FVC Change to Predict Mortality in Patients with Idiopathic Pulmonary Fibrosis

Tuesday, Nov. 29 11:30AM - 11:40AM Room: S404CD

Participants

Joseph Jacob, MBBS, MRCP, London, United Kingdom (*Presenter*) Nothing to Disclose
Brian J. Bartholmai, MD, Rochester, MN (*Abstract Co-Author*) License agreement, ImBio, LLC; Scientific Advisor, ImBio, LLC
Srinivasan Rajagopalan, PhD, Rochester, MN (*Abstract Co-Author*) Patent agreement, Imbio, LLC
Maria Kokosi, MD, London, United Kingdom (*Abstract Co-Author*) Nothing to Disclose
Arjun Nair, MD, FRCR, London, United Kingdom (*Abstract Co-Author*) Nothing to Disclose
Ronald Karwoski, BS, Rochester, MN (*Abstract Co-Author*) Patent agreement, Imbio, LLC
Simon I. Walsh, MD, PhD, London, United Kingdom (*Abstract Co-Author*) Speaker, Boehringer Ingelheim GmbH
Athol U. Wells, London, United Kingdom (*Abstract Co-Author*) Speaker, F. Hoffmann-La Roche Ltd; Speaker, Boehringer Ingelheim GmbH; Speaker, Gilead Sciences, Inc; Speaker, Merck & Co, Inc; Speaker, Bayer AG; Speaker, Chiesi Farmaceutici SpA; ;
David M. Hansell, MD, London, England, United Kingdom (*Abstract Co-Author*) Research Consultant, AstraZeneca PLC Research Consultant, Boehringer Ingelheim GmbH Research Consultant, InterMune, Inc Research Consultant, F. Hoffmann-La Roche Ltd

PURPOSE

FVC change represents the cardinal variable used to identify clinical deterioration in patients with IPF. However evidence now suggests that emphysema, by preserving lung volumes, may curtail the magnitude of FVC decline in IPF patients undergoing real function deterioration. Our study aimed to evaluate the ability of FVC change to predict mortality in IPF patients with and without emphysema.

METHOD AND MATERIALS

Consecutive patients with a multi-disciplinary team diagnosis of IPF (n=148) with serial FVC, DLco and composite physiologic index (CPI) measurements at 9-18 month intervals had emphysema scored on baseline CTs by two experienced thoracic radiologists. Baseline demographics between groups were analysed using the T-test. Mortality prediction was evaluated using Cox regression analysis.

RESULTS

Significant differences were identified between patients with and without emphysema in baseline FVC, CPI and relative FVC change, but not DLco values (Table 1). With correction for baseline disease severity with the CPI, FVC change was strongly predictive of mortality in patients without emphysema (n=74), but not patients with emphysema (n=65)[Table 2]. DLco and CPI change were predictive of mortality in both groups (Table 2). Based on average relative FVC change values in the two groups, it was calculated that a 10% relative FVC decline in patients without emphysema equated to a 4% relative FVC decline in patients with emphysema. In our cohort, a 4% relative FVC decline threshold identified 5/67 (7%) more patients with a significant functional decline.

CONCLUSION

The presence of emphysema negatively impacts the ability of FVC change to predict mortality in IPF.

CLINICAL RELEVANCE/APPLICATION

When relying on FVC change to identify a clinical deterioration in IPF, patients with emphysema on CT are likely to have disease progression under-recognised and therefore may be undertreated when compared to patients without emphysema

SSG03-08 Serial CT in Cryptogenic Organizing Pneumonia: Evolutional Findings and Prognostic Factors

Tuesday, Nov. 29 11:40AM - 11:50AM Room: S404CD

Participants

Boda Nam, MD, Seoul, Korea, Republic Of (*Presenter*) Nothing to Disclose
Kyung S. Lee, MD, PhD, Seoul, Korea, Republic Of (*Abstract Co-Author*) Nothing to Disclose
Man Pyo Chung, Seoul, Korea, Republic Of (*Abstract Co-Author*) Nothing to Disclose
Min Jae Cha, Seoul, Korea, Republic Of (*Abstract Co-Author*) Nothing to Disclose
Tae Jung Kim, MD, PhD, Seoul, Korea, Republic Of (*Abstract Co-Author*) Nothing to Disclose
Joungho Han, Seoul, Korea, Republic Of (*Abstract Co-Author*) Nothing to Disclose
Jung Hwa Hwang, MD, Seoul, Korea, Republic Of (*Abstract Co-Author*) Nothing to Disclose
Jai Soung Park, Bucheon, Korea, Republic Of (*Abstract Co-Author*) Nothing to Disclose

PURPOSE

Most patients with COP have some remaining lesions on CT, simulating a fibrotic nonspecific interstitial pneumonia (fNSIP) pattern, although generally favorable prognosis. However, we do not know what clinical or imaging features are determinant for the remaining disease. The purpose of this study was to observe serial CT features of COP and to investigate prognostic determinants for the remaining disease.

METHOD AND MATERIALS

52 patients with pathologically confirmed COP were studied (20 men and 32 women; mean age, 55.3 years; median follow-up period, 22 months; range, 1-155 months). Clinical findings and pulmonary function test (PFT) results at the time of pathologic diagnosis were assessed. The presence, extent, and distribution of CT findings were reviewed. Overall changes in disease extent were classified as cured, improved (i.e., $\geq 10\%$ decrease in extent), not changed, or progressed (i.e., $\geq 10\%$ increase in extent). Uni- and multivariate analyses were performed to seek for prognostic factors among clinical or imaging features.

RESULTS

The most common patterns of lung abnormality on initial CT were GGO (100.0%) and consolidation (70.2%), which were distributed along the bronchovascular bundles (41.4%) or subpleural lungs (27.9%). In 13.5% of patients, the disease disappeared completely; in 63.5%, the disease decreased in extent; in 9.6%, the extent did not change; and in 13.4%, the disease increased in extent. When lesions remained, the most common patterns of follow-up CT were GGO (81.7%) and reticulation (43.3%), which seemed to be like patterns of fNSIP. The prognostic factors related to residual lesions on final CT were the PFT findings (FEV1, FVC and DLco) at the presentation and the patient's age at the diagnosis on univariate analysis ($p < .05$). The extent of consolidation on initial CT differed between the patient with complete resolution and remaining lung lesion, but statistically not significant ($p = .08$).

CONCLUSION

In 86.5% of COP patients, the lung abnormalities are remaining on follow-up CT with corticosteroid treatment. The most common patterns of residual disease are GGO and reticulation, thus simulated fNSIP pattern on the final follow-up CT. The results of initial PFT and patient's age are related to the presence of residual lung lesions.

CLINICAL RELEVANCE/APPLICATION

Higher initial FEV1, FVC and DLco levels and younger age at presentation in patient of COP may allow the prediction of complete resolution of lung parenchymal lesion on follow-up CT.

SSG03-09 Computer Based Quantitative CT Analysis of Hypersensitivity Pneumonitis Patients: Predicting Outcome Using Advanced Stratification Techniques

Tuesday, Nov. 29 11:50AM - 12:00PM Room: S404CD

Participants

Joseph Jacob, MBBS, MRCP, London, United Kingdom (*Presenter*) Nothing to Disclose
Brian J. Bartholmai, MD, Rochester, MN (*Abstract Co-Author*) License agreement, ImBio, LLC; Scientific Advisor, ImBio, LLC
Maria Kokosi, MD, London, United Kingdom (*Abstract Co-Author*) Nothing to Disclose
Srinivasan Rajagopalan, PhD, Rochester, MN (*Abstract Co-Author*) Patent agreement, ImBio, LLC
Ronald Karwoski, BS, Rochester, MN (*Abstract Co-Author*) Patent agreement, ImBio, LLC

Wing Yan Mok, MBBS, BS, London, United Kingdom (*Abstract Co-Author*) Nothing to Disclose
Sze Mun Mak, MBBS, FRCR, London, United Kingdom (*Abstract Co-Author*) Nothing to Disclose
Keishi Sugino, Tokyo, Japan (*Abstract Co-Author*) Nothing to Disclose
Giovanni Della Casa, MD, Spilamberto, Italy (*Abstract Co-Author*) Nothing to Disclose
Simon I. Walsh, MD, PhD, London, United Kingdom (*Abstract Co-Author*) Speaker, Boehringer Ingelheim GmbH
Athol U. Wells, London, United Kingdom (*Abstract Co-Author*) Speaker, F. Hoffmann-La Roche Ltd; Speaker, Boehringer Ingelheim GmbH; Speaker, Gilead Sciences, Inc; Speaker, Merck & Co, Inc; Speaker, Bayer AG; Speaker, Chiesi Farmaceutici SpA; ;
David M. Hansell, MD, London, England, United Kingdom (*Abstract Co-Author*) Research Consultant, AstraZeneca PLC Research Consultant, Boehringer Ingelheim GmbH Research Consultant, InterMune, Inc Research Consultant, F. Hoffmann-La Roche Ltd

PURPOSE

Computer algorithms quantifying interstitial lung disease (ILD) patterns on volumetric CT acquisitions (such as CALIPER) have dramatically increased in sophistication in recent years. However, application of computer tools to the evaluation of interspaced CTs, (still relevant in young adults and select regional centres), has not been evaluated. Our study assessed the ability of CALIPER to predict mortality in chronic hypersensitivity pneumonitis (CHP) patients undergoing interspaced CTs, and independently analysed the cohort using advanced stratification techniques.

METHOD AND MATERIALS

Interspaced CTs in 98 CHP patients had parenchymal pattern extents evaluated by CALIPER and on a lobar basis by two experienced radiologists. Mortality prediction was calculated using Cox analyses. Independent stratification of the cohort was performed using pairwise comparisons of a dissimilarity metric which identified similar clusters using affinity propagation and analysis of similarities.

RESULTS

Indicators of fibrosis: (VISUAL: honeycombing, traction bronchiectasis) and CALIPER (ILD extent, ground glass opacity, reticular pattern, pulmonary vessel volume) and all pulmonary function tests (PFTs) were strongly predictive of mortality on univariate analysis ($p < 0.01$). On multivariate analysis, DLco ($p < 0.0001$) and CALIPER reticular pattern ($p = 0.001$) were independently predictive of mortality. Stratification identified 3 clusters of patients (illustrated in three dimensional space, with differing outcomes on Kaplan Meier survival curves (Log rank test $p < 0.0001$) which correlated well with PFTs.

CONCLUSION

Quantitative tools designed for volumetric CT evaluation have a role in the evaluation of interspaced CTs. Stratification can identify population subgroups with differing outcome. Both findings may have relevance to the use of quantitative CT in drug trials.

CLINICAL RELEVANCE/APPLICATION

Automated stratification when allied to computer based CT analysis allows standardized and objective evaluation of disease burden and mortality prediction. Both techniques could influence patient selection and outcome measures in clinical trials.

SSG04

Gastrointestinal (CT Technique and Contrast)

Tuesday, Nov. 29 10:30AM - 12:00PM Room: E352



AMA PRA Category 1 Credits™: 1.50
ARRT Category A+ Credits: 1.50

Participants

Vahid Yaghmai, MD, Chicago, IL (*Moderator*) Nothing to Disclose
Naveen Kulkarni, MD, Milwaukee, WI (*Moderator*) Nothing to Disclose
Christine O. Menias, MD, Chicago, IL (*Moderator*) Nothing to Disclose

Sub-Events

SSG04-01 Fine Focal Spot CT Improves Image Quality in Abdominal CT Imaging

Tuesday, Nov. 29 10:30AM - 10:40AM Room: E352

Participants

Yin P. Goh, MBBS, Clayton, Australia (*Presenter*) Nothing to Disclose
Sidney M. Levy, MBBS, BMedSc, Melbourne, Australia (*Abstract Co-Author*) Nothing to Disclose
Kenneth K. Lau, MBBS, FRANZCR, Melbourne, Australia (*Abstract Co-Author*) Nothing to Disclose
Keat Y. Low, MBBS, FRANZCR, Melbourne, Australia (*Abstract Co-Author*) Nothing to Disclose

PURPOSE

CT tubes usually have two focal-spot sizes, with the finer focal spot providing higher spatial resolution. The aim of this retrospective study is to compare the image quality of the abdominal viscera between fine focal spot size (FFSS) and standard focal spot size (SFSS).

METHOD AND MATERIALS

All contrast-enhanced CT abdomen and pelvis (CTAP) of all adult patients between June and September 2014 were included. Two blinded radiologists assessed the margin clarity of the abdominal viscera and the detected lesions using a 5-point grading scale. Cohen's kappa test was used to examine the inter-observer reliability amongst the two reviewers for organ margin clarity. Mann-Whitney U test was used to assess the statistical differences of the margin clarity of the abdominal viscera and the detected lesions between the two groups.

CONCLUSION

FFSS improves the image quality in abdominal CT imaging in terms of better organ and lesion margin clarity.

SSG04-02 Effect of Different Reconstruction Algorithms of MDCT Examinations for Quantitative Imaging Features: Comparison with Liver Parenchyma, Focal Liver Lesion and Renal Cyst

Tuesday, Nov. 29 10:40AM - 10:50AM Room: E352

Participants

Su Joa Ahn, Seoul, Korea, Republic Of (*Abstract Co-Author*) Nothing to Disclose
Jung Hoon Kim, MD, Seoul, Korea, Republic Of (*Presenter*) Nothing to Disclose
Sang Joon Park, PhD, Seoul, Korea, Republic Of (*Abstract Co-Author*) Nothing to Disclose
Joon Koo Han, MD, Seoul, Korea, Republic Of (*Abstract Co-Author*) Nothing to Disclose

PURPOSE

To determine whether different reconstruction algorithms affect quantitative features of CT imaging in liver parenchyma, focal liver lesions and renal cysts.

METHOD AND MATERIALS

We included 300 adult patients (192 men, 108 women; mean age, 58 years) who underwent MDCT with one CT scanner. Among 300 patient, normal liver parenchyma without chronic liver disease nor malignant disease (n=200), well circumscribed focal liver lesion (n=100; 81 metastases, 9 hepatocellular carcinoma, 6 hemangioma, 4 hepatic abscess), and renal cysts larger than 1cm (n=34) were included. All CT images were reconstructed with filtered back projection (FBP), adaptive statistical iterative reconstruction (IRT), and iterative model reconstruction (IMR) algorithms. Computerized texture analysis was performed by extracting 16 quantitative imaging features including histogrammic parameter (mean attenuation, standard deviation, skewness, kurtosis, entropy, homogeneity), volumetric parameter (volume, effective diameter, surface area), and morphologic features (sphericity, discrete compactness, GLCM moments, GLCM ASM, GLCM IDM, GLCM Contrast, GCLM entropy) using semi-automatic segmentation of target lesions.

RESULTS

Different reconstruction algorithms had a significant effect on quantitative imaging features. IMR had more significant effect on than IRT. IRT had a significant effect on five, eight, and three of the features for liver parenchyma, focal liver lesion, and renal cysts ($P < .005$), whereas IMR had a significant effect on seven, 11, and five of the features for respectively ($P < .005$). Focal liver lesion had more significant effect on different reconstruction algorithms (eight on IRT, 11 on IMR) than liver parenchyma (five on IRT, seven on IMR) or renal cysts (three on IRT, five on IMR). Although quantitative imaging features were significantly affected by different reconstruction algorithms, the volumetric features did not effect on reconstruction algorithm ($p > .03$).

CONCLUSION

Different reconstruction algorithms affect quantitative features of CT imaging. In focal liver lesion. reconstruction algorithms show

Different reconstruction algorithms affect quantitative features of CT imaging. In renal artery, reconstruction algorithms show more significant effect on the quantitative features than liver parenchyma or renal cysts.

CLINICAL RELEVANCE/APPLICATION

Because of different reconstruction algorithms affect quantitative features of CT imaging, imaging quantification using uniform reconstruction algorithms would be increased their reliability level.

SSG04-03 Sub-Second High-Pitch Abdominopelvic CT Angiography With Ultra-Low Dose Contrast Media (<30 mL) at 80kV: A Feasibility Study

Tuesday, Nov. 29 10:50AM - 11:00AM Room: E352

Awards

Student Travel Stipend Award

Participants

Faezeh Sodagari, MD, Chicago, IL (*Presenter*) Grant, Siemens AG
Alan L. Goodwin, RT, Chicago, IL (*Abstract Co-Author*) Nothing to Disclose
Jeremy D. Collins, MD, Chicago, IL (*Abstract Co-Author*) Nothing to Disclose
Vahid Yaghmai, MD, Chicago, IL (*Abstract Co-Author*) Nothing to Disclose

PURPOSE

To evaluate homogeneity of vascular enhancement and image quality in sub-second high-pitch abdominopelvic CT angiography (CTA) with ultra-low dose contrast media at 80 kV.

METHOD AND MATERIALS

In this HIPAA-compliant IRB-approved prospective study, twelve patients underwent high-pitch sub-second abdominopelvic CTA at 80kV with ultra-low dose (<30 mL) of non-ionic iodinated contrast media (iopamidol 370) in a large academic institution. All scans were performed using third generation dual source CT scanner. The homogeneity of the intravascular contrast attenuation at suprarenal aorta, infrarenal aorta, and right common iliac artery was assessed. Image noise, contrast-to-noise ratio, and signal-to-noise ratio were measured to assess the objective image quality. Subjective image quality was evaluated on a 5-point scale (1 = unacceptable; 5 = excellent). Volume CT dose index (CTDIvol) was extracted from dose reports to assess radiation dose. Repeated-measures analysis of variances was used for data analysis. Significance was set at 0.05.

RESULTS

Six men and 6 women with the mean \pm standard deviation (SD) age of 64.2 ± 13 years and the mean weight of 75.8 ± 16.2 kg were included in this study. The patients received 15 to 28 mL of contrast with a mean of 20 ± 3.4 mL. The mean CTDIvol was 3.8 ± 1.1 mGy. Mean CNR and SNR were 9.2 ± 4.9 and 9.9 ± 4.1 , respectively. Mean image noise was 24.4 ± 5.0 Hounsfield units (HU). All images had diagnostic image quality with the median subjective image quality score of 4 (Good). The contrast attenuation was homogeneous across suprarenal aorta, infrarenal aorta, and right common iliac artery levels with the mean attenuation of 228.6 ± 74.3 , 249.3 ± 59.7 , and 249.2 ± 56.1 HU, respectively ($P = 0.16$).

CONCLUSION

Abdominopelvic CTA with ultra-low dose (<30 mL) contrast at 80kV is technically and clinically feasible with good diagnostic image quality and homogenous attenuation across vascular levels.

CLINICAL RELEVANCE/APPLICATION

This study shows the potential for reducing the contrast dose to as low as 15 mL for high-pitch abdominopelvic CT angiography at 80kV. This may have clinical implications in abdominopelvic CT angiography in patients with renal impairment.

Honored Educators

Presenters or authors on this event have been recognized as RSNA Honored Educators for participating in multiple qualifying educational activities. Honored Educators are invested in furthering the profession of radiology by delivering high-quality educational content in their field of study. Learn how you can become an honored educator by visiting the website at: <https://www.rsna.org/Honored-Educator-Award/>

Vahid Yaghmai, MD - 2012 Honored Educator

Vahid Yaghmai, MD - 2015 Honored Educator

SSG04-04 Low-kV CT Can Reduce the Frequency of Acute Adverse of Intravenous Iodine Contrast Medium

Tuesday, Nov. 29 11:00AM - 11:10AM Room: E352

Participants

Tomoki Maebayashi, Kobe, Japan (*Abstract Co-Author*) Nothing to Disclose
Satoru Takahashi, MD, Suita, Japan (*Presenter*) Nothing to Disclose
Tatsuya Nishii, MD, PhD, Kobe, Japan (*Abstract Co-Author*) Nothing to Disclose
Atsushi K. Kono, MD, PhD, Kobe, Japan (*Abstract Co-Author*) Nothing to Disclose
Noriyuki Negi, RT, Kobe, Japan (*Abstract Co-Author*) Nothing to Disclose
Kiyosumi Kagawa, Kobe, Japan (*Abstract Co-Author*) Nothing to Disclose
Erina Suehiro, RT, Kobe, Japan (*Abstract Co-Author*) Nothing to Disclose
Wakiko Tani, RT, Kobe, Japan (*Abstract Co-Author*) Nothing to Disclose
Toshinori Sekitani, MS, Kobe, Japan (*Abstract Co-Author*) Nothing to Disclose
Hideaki Kawamitsu, MD, Kobe, Japan (*Abstract Co-Author*) Nothing to Disclose
Kazuro Sugimura, MD, PhD, Kobe, Japan (*Abstract Co-Author*) Research Grant, Toshiba Corporation Research Grant, Koninklijke Philips NV Research Grant, Bayer AG Research Grant, Eisai Co, Ltd Research Grant, DAIICHI SANKYO Group

PURPOSE

Acute adverse reactions of CM are either allergy-like reactions or physiologic reactions. Although dose and concentration of CM

unlikely affect allergic-like contrast reactions, physiologic reactions (chemotoxic or osmotoxic reactions) are often dose and concentration dependent. Because recently introduced low-kV CT has enabled the reduction of contrast dosage in daily clinical practices, the incidence of acute adverse events would decrease in low-kV post-contrast body CT (CECT). The purpose of this retrospective study was to compare the incidence of acute adverse events in low-kV CT with reduced CM and conventional CT with full-dose CM.

METHOD AND MATERIALS

Routine CECT in 3rd generation dual-source CT has been acquired at 70 kV with 60% dose of 270 mgI/Kg CM (70 kV protocol), while in remaining scanners it has been acquired at 120 kV with a standard dose of 450 mgI/Kg CM (120 kV protocol) in our institution. Because injection duration and scan delay time are fixed for routine CECT, iodine deliver rate at 70 kV protocol is also 60% of 120 kV protocol. Between January 20, 2015 and February 26, 2016, contrast reaction reports and medical records of patients were reviewed.

RESULTS

1,317 patients underwent with 70 kV protocol, while 4,234 with 120 kV. Mean body weight in 70 kV protocol was smaller than 120 kV protocol ($p < .001$). Mean injection dose and rate of CM for 70 kV protocol (50.6 ± 9.4 mL, 1.1 ± 0.2 mL/sec) were significantly smaller than those for 120 kV protocol (82.1 ± 15.2 mL, 1.8 ± 0.3 mL/sec), respectively ($p < .001$). Among all 5,551 patients, allergic-type reactions occurred in 64 (1.15%) of patients, while physiologic reaction in 28 (0.50%): 86 (93%) reactions were mild and 6 (7%) were moderate. Seven (0.52%) patients showed allergic-type reactions in 70 kV protocol, while 57 (1.35%) in 120 kV protocol ($p < .05$; χ^2). Three (0.22%) patients demonstrated physiologic reaction in 70 kV protocol, while 25 (0.59%) in 120 kV protocol ($p = .16$; χ^2).

CONCLUSION

Low kV CT with reduced CM injection may decrease the incidence of acute adverse events, especially allergic-like reaction.

CLINICAL RELEVANCE/APPLICATION

Although further larger prospective study is essential, reduced CM dosage with low-kV CT may reduce the chance of adverse events.

SSG04-05 Prospective Evaluation of Reduced Dose Computed Tomography for the Detection of Low-contrast Liver Lesions: Direct Comparison with Concurrent Standard Dose Imaging

Tuesday, Nov. 29 11:10AM - 11:20AM Room: E352

Awards

Student Travel Stipend Award

Participants

B. Dustin Pooler, MD, Madison, WI (*Presenter*) Nothing to Disclose
Meghan G. Lubner, MD, Madison, WI (*Abstract Co-Author*) Grant, Koninklijke Philips NV; Grant, Johnson & Johnson;
David H. Kim, MD, Middleton, WI (*Abstract Co-Author*) Consultant, Viatronix, Inc; Co-founder, VirtuoCTC, LLC; Medical Advisory Board, Digital ArtForms, Inc; Stockholder, Celectar Biosciences, Inc
Oliver T. Chen, MD, Frederick, MD (*Abstract Co-Author*) Nothing to Disclose
Ke Li, PhD, Madison, WI (*Abstract Co-Author*) Nothing to Disclose
Guang-Hong Chen, PhD, Madison, WI (*Abstract Co-Author*) Research funded, General Electric Company Research funded, Siemens AG
Perry J. Pickhardt, MD, Madison, WI (*Abstract Co-Author*) Co-founder, VirtuoCTC, LLC; Stockholder, Celectar Biosciences, Inc; Stockholder, SHINE Medical Technologies, Inc; Research Grant, Koninklijke Philips NV

PURPOSE

To prospectively compare diagnostic performance of reduced-dose (RD) contrast-enhanced CT (CECT) with standard-dose (SD) CECT for detection of low-contrast liver lesions.

METHOD AND MATERIALS

70 adults with non-liver primary malignancies underwent abdominal SD-CECT immediately followed by RD-CECT, aggressively targeted at 60-70% dose reduction. SD series were reconstructed using FBP. RD series were reconstructed with FBP, ASIR, and MBIR. Three readers—blinded to clinical history and comparison studies—reviewed all series, identifying liver lesions ≥ 4 mm. Non-blinded review by two experienced abdominal radiologists—assessing SD against available clinical and radiologic information—established the reference standard.

RESULTS

RD-CECT mean effective dose was 2.01 ± 1.36 mSv (median, 1.71), a $64.1 \pm 8.8\%$ reduction. Pooled per-patient performance data were (sensitivity/specificity/PPV/NPV/accuracy) 0.91/0.78/0.60/0.96/0.81 for SD-FBP, compared with RD-FBP 0.79/0.75/0.54/0.91/0.76; RD-ASIR 0.84/0.75/0.56/0.93/0.78; and RD-MBIR 0.84/0.68/0.49/0.92/0.72. ROC AUC values were 0.896/0.834/0.858/0.854 for SD-FBP/RD-FBP/RD-ASIR/RD-MBIR, respectively. RD-FBP ($P = 0.005$) and RD-MBIR ($P = 0.047$) AUC were significantly lower than SD-FBP; RD-ASIR was not ($P = 0.084$). Reader confidence was lower for all RD series ($P < 0.001$) compared with SD-FBP, especially when calling patients entirely negative.

CONCLUSION

Aggressive CT dose reduction resulted in inferior diagnostic performance and reader confidence for detection of low-contrast liver lesions compared to SD. Relative to RD-ASIR, RD-FBP showed decreased sensitivity and RD-MBIR showed decreased specificity.

CLINICAL RELEVANCE/APPLICATION

Aggressive CT dose reduction may result in mischaracterization of low-contrast liver lesions at contrast-enhanced CT, including both false positive and false negative cases.

Honored Educators

Presenters or authors on this event have been recognized as RSNA Honored Educators for participating in multiple qualifying educational activities. Honored Educators are invested in furthering the profession of radiology by delivering high-quality educational content in their field of study. Learn how you can become an honored educator by visiting the website at: <https://www.rsna.org/Honored-Educator-Award/>

Meghan G. Lubner, MD - 2014 Honored Educator
Meghan G. Lubner, MD - 2015 Honored Educator
Perry J. Pickhardt, MD - 2014 Honored Educator

SSG04-06 Contrast Agent Dose Reduction in Combination with Low-Tube Voltage and Adaptive Statistical Iterative Reconstruction Algorithm in CT Enterography: Effect on Image Quality and Radiation Dose

Tuesday, Nov. 29 11:20AM - 11:30AM Room: E352

Participants

Cui Feng, MD, Wuhan, China (*Presenter*) Nothing to Disclose
Zhen Li, MD, PhD, Wuhan, China (*Abstract Co-Author*) Nothing to Disclose

PURPOSE

The aim of the study was to investigate the image quality and radiation exposure of contrast enhanced CT enterography with low-tube-voltage, low-concentration contrast agent combined with adaptive statistical iterative reconstruction (ASIR).

METHOD AND MATERIALS

From October 2015 to February 2016, 137 patients (65 female, 72 male, mean age 54±14 years) underwent contrast enhanced CT enterography using a 64-slice MDCT scanner (Discovery CT750 HD, GE Healthcare, USA). All the cases were randomly assigned into two groups. Group A (n=79) were examined on CT with low-tube-voltage according to BMI (BMI < 23 kg/m², 80- kVp; BMI ≥ 23 kg/m², 100- kVp), and low-concentration contrast agent (270 mgI/mL). The raw data were reconstructed with standard filtered back projection (FBP) and 50% ASIR respectively. Group B (n=58) underwent conventional CT at 120- kVp, 350 mgI/mL contrast agent with FBP. The CT DI_{vol}, DLP were recorded, effective dose (ED) and total contrast medium dosage were calculated and compared. The CT value, SNR, CNR of the bowel wall, gastrointestinal lesions, mesenteric vessel were assessed and compared statistically. The subjective image quality was assessed by two radiologists using five-point Likert scale (1=poor; 2=acceptable; 3=moderate; 4=good; 5=excellent).

RESULTS

There were 63 gastrointestinal cancers, 21 gastrointestinal inflammation proved pathologically by surgery or endoscopy. Compared with group B, CT DI_{vol}, ED, DLP and total iodine contrast medium dosage in group A were decreased by 25.2%, 25.7%, 25.7%, 26.07% respectively. The average qualitative image quality score of FBP image of group A (4.02±0.39), 50% ASIR image of group A (4.02±0.37) were lower than FBP image of group B (4.21±0.55), the difference was not statistically significant (P > 0.05). SD of 50% ASIR image of group A was significantly lower than FBP image of group A (13.18±2.687 vs. 15.69±3.60, p < 0.001). CT value, CNR and SNR were significantly higher in SMA, SMV, gastrointestinal lesions in 50% ASIR image of group A (P < 0.05).

CONCLUSION

Compared with conventional protocol, CT enterography performed at low tube voltage and low-concentration contrast agent combined with 50% ASIR produced diagnostically acceptable image quality with a mean ED of 6.34 mSv and a total iodine dose reduction of 26.07%.

CLINICAL RELEVANCE/APPLICATION

Contrast agent dose reduction, low tube voltage with ASIR is feasible in contrast enhanced CT enterography, reduce the radiation dose and the risk of contrast induced nephropathy (CIN), without impairment of image quality.

SSG04-07 Reduction of Patient Radiation Dose with a New Organ based Dose Modulation Technique for Chest Abdomen Pelvis CT

Tuesday, Nov. 29 11:30AM - 11:40AM Room: E352

Participants

Marie Fillon, MD, Lyon, France (*Presenter*) Nothing to Disclose
Philippe Coulon, PhD, Suresnes, France (*Abstract Co-Author*) Employee, Koninklijke Philips NV
Salim Si-Mohamed, Bron, France (*Abstract Co-Author*) Nothing to Disclose
Aurelie Vuillod, Lyon, France (*Abstract Co-Author*) Nothing to Disclose
Paul Klahr, PhD, Cleveland, OH (*Abstract Co-Author*) Researcher, Koninklijke Philips NV
Loic Bousset, MD, Lyon, France (*Abstract Co-Author*) Nothing to Disclose

PURPOSE

In a single scan for chest, abdomen and pelvis (CAP) CT, using standard Automatic Exposure Control (AEC), the requirement for contrast resolution in the liver is setting the target image quality for the whole scan, and, as a result, the radiation dose. The purpose of this study was to evaluate dose reduction and image quality resulting from a new organ based dose modulation system allowing setting different image quality in the liver than in the chest and the pelvis.

METHOD AND MATERIALS

Our retrospective study included 37 patients who had CAP CT scans for oncology follow up in less than a year time difference, on 2 scanners, one using standard AEC (Standard AEC) and one using new Liver DoseRight Index organ based dose modulation system (Liver DRI). For each acquisition, average Water Equivalent Diameter (WED), CT Dose Index (CTDI) and Size-Specific Dose Estimates (SSDE) were calculated for the total scan and for lung, breast, liver and pelvis area. Signal to Noise Ratio (SNR) was measured in the muscle at each anatomic level and diagnostic confidence was evaluated by 2 radiologists. Quantitative and qualitative variables were compared using respectively paired t-test and Wilcoxon signed rank tests with Bonferroni correction.

RESULTS

While no significant WED difference was observed between the two scans (all p values > 0.05), patient radiation dose was

while no significant web difference was observed between the two scans (all p-values > 0.05), patient radiation dose was significantly reduced with Liver DRI compared to Standard AEC (all p-values <0.01) in the total scan, lung, breast and pelvis area, with a CTDI reduction of respectively 26.9%, 22.6%, 24.0% and 30.6% and a SSDE reduction of 23.2%, 20.5%, 22.6% and 28.7%. There was no significant dose reduction (p>0.08) in the liver area. SNR reduction was only significant (p<0.02) in the pelvis (4.2±1.2 vs 5.2±1.7). There was no significant difference (p>0.05) in diagnostic confidence between the 2 types of scan, in any of the anatomic regions with a good inter-observers correlation (kappa=0.72).

CONCLUSION

Liver DoseRight Index organ based dose modulation technique allows significant dose reduction compared to standard AEC while preserving diagnostic image quality in all CAP body areas.

CLINICAL RELEVANCE/APPLICATION

Liver DoseRight Index organ based dose modulation technique allows an optimization of dose and image quality in the different body areas individually and thus decreases the total radiation exposure in Chest Abdomen Pelvis CT.

SSG04-09 Photon-Counting-Detector CT for the Evaluation of Non-contrast Enhanced Abdominal Imaging in Patients

Tuesday, Nov. 29 11:50AM - 12:00PM Room: E352

Awards

Trainee Research Prize - Fellow

Participants

Roy Marcus, MD, Rochester, MN (*Presenter*) Institutional research agreement, Siemens AG; Research support, Siemens AG
Joel G. Fletcher, MD, Rochester, MN (*Abstract Co-Author*) Grant, Siemens AG ;
Shannon P. Sheedy, MD, Rochester, MN (*Abstract Co-Author*) Nothing to Disclose
Jeff L. Fidler, MD, Rochester, MN (*Abstract Co-Author*) Nothing to Disclose
Zhoubo Li, Rochester, MN (*Abstract Co-Author*) Nothing to Disclose
Zhicong Yu, Rochester, MN (*Abstract Co-Author*) Nothing to Disclose
Felicity Enders, Rochester, MN (*Abstract Co-Author*) Nothing to Disclose
Ahmed Halaweish, PhD, Rochester, MN (*Abstract Co-Author*) Employee, Siemens AG
Cynthia H. McCollough, PhD, Rochester, MN (*Abstract Co-Author*) Research Grant, Siemens AG

PURPOSE

To assess in patients the overall clinical image quality of routine unenhanced abdominal CT on a preclinical photon-counting-detector CT (PCCT) compared to the conventional CT using energy integrating detectors.

METHOD AND MATERIALS

Thirty patients received a routine unenhanced exam of the abdomen on a commercial 2nd generation dual-source CT (SOMATOM Flash, Siemens Healthcare) in dual energy mode (DECT). DECT scans were acquired using 80/140Sn kV or 100/140Sn kV, dependent on patient size. PCCT scans were acquired at 140 kV in macro-mode with energy thresholds set at 25 and 75 keV. CTDIvol values were matched between exams. 5 mm slices at 2.5 mm interval with reconstructed for both scanners using filtered back projection and a D30 kernel. Low threshold PCCT images (25–140 keV) and mixed DECT (mDECT) images were evaluated by 3 abdominal radiologists in a blinded side-by-side comparison. After evaluating solid and hollow abdominal organs, readers independently selected one of the datasets as their preference according to a 2-point scale (1=preferred but no effect on diagnostic confidence; 2=definitely preferred and resulted in improved diagnostic confidence); ties were not allowed. Overall preference was decided by a majority rules criterion. Patient size was recorded as diameter at the level of the right renal vein.

RESULTS

There was no overall preference regarding the subjective image quality for routine unenhanced abdominal CT (16 cases preferred for PCCT vs. 14 cases for mDECT). On a per reader basis, the preference showed a nonsignificant trend towards PCCT (p= 0.28). Subjective image preference was not patient size dependent (p=0.81). Both modalities performed equally in displaying small structures and parenchymal lesions, such as para aortal lymph nodes or parenchymal masses. However PCCT was beneficial in better demarcating small low attenuation structures such as biliary and pancreatic ducts, and reducing the osseous blooming effect.

CONCLUSION

No difference was found in image quality between PCCT images and conventional DECT mixed images for non-enhanced abdominal CT. PCCT appears promising for displaying small low attenuation structures. Patient's size did not influence reader preference.

CLINICAL RELEVANCE/APPLICATION

PCCT has previously been shown to offer improved contrast-to-noise ratio for iodine imaging. This study demonstrated clinical benefit for unenhanced imaging as well.

SSG05

Genitourinary (Multiparametric Prostate MRI)

Tuesday, Nov. 29 10:30AM - 12:00PM Room: N229



AMA PRA Category 1 Credits™: 1.50
ARRT Category A+ Credits: 1.50

Participants

Andrew B. Rosenkrantz, MD, New York, NY (*Moderator*) Nothing to Disclose
Antonio C. Westphalen, MD, Mill Valley, CA (*Moderator*) Scientific Advisory Board, 3DBiopsy LLC ; Research Grant, Verily Life Sciences LLC
Ronaldo H. Baroni, MD, Sao Paulo, Brazil (*Moderator*) Nothing to Disclose

Sub-Events

SSG05-01 Comparison of Initial and Subspecialist Second Opinion Reads of Multiparametric Magnetic Resonance Imaging of the Prostate Prior to Repeat Biopsy

Tuesday, Nov. 29 10:30AM - 10:40AM Room: N229

Participants

Nienke L. Hansen, MD, Aachen, Germany (*Presenter*) Nothing to Disclose
Brendan C. Koo, MBBCh, Cambridge, United Kingdom (*Abstract Co-Author*) Nothing to Disclose
Ferdia A. Gallagher, PhD, FRCR, Cambridge, United Kingdom (*Abstract Co-Author*) Research support, General Electric Company
Anne Warren, Cambridge, United Kingdom (*Abstract Co-Author*) Nothing to Disclose
Christof Kastner, Cambridge, United Kingdom (*Abstract Co-Author*) Nothing to Disclose
Tristan Barrett, MBBS, BSc, Guildford, United Kingdom (*Abstract Co-Author*) Nothing to Disclose

PURPOSE

To investigate the value of second-opinion evaluation of multiparametric magnetic resonance imaging (mpMRIs) of the prostate by subspecialised urologists at a tertiary center for the detection of significant cancer in transperineal MR/US fusion prostate biopsy.

METHOD AND MATERIALS

Evaluation of prospectively acquired initial and second-opinion radiology reports of 158 patients who underwent mpMRI at regional hospitals prior to transperineal MR/US fusion biopsy at a tertiary referral center over a 3-year period. Gleason score (GS) 7-10 cancer and all cancer detection rates, positive (PPV) and negative (NPV) predictive values ($\pm 95\%$ confidence intervals) were calculated for mpMRIs that were reported as negative, equivocal, or suspicious for cancer and compared by Fisher's exact test.

RESULTS

Disagreement between the initial and the second-opinion report was observed in 54% of cases (86/158). mpMRIs were more often called negative in subspecialist reads than in initial reports (41% vs. 20%; $p=0.0001$) with significantly higher NPV for GS 7-10 in subspecialist second-reads (0.89 (± 0.08) vs. 0.72 (± 0.16) for external reports; $p=0.04$). mpMRIs were less often called suspicious in subspecialist reads than in initial reports (39% vs. 51%; $p=0.04$) with significantly higher PPV for subspecialist second-reads (0.56 (± 0.12) vs. 0.34 (± 0.10) for external reports; $p=0.01$). For equivocal cancer suspicion, the PPV was 0.18 (± 0.13) for subspecialist reads and 0.24 (± 0.12) for external reads; $p=1.00$.

CONCLUSION

Second reading of prostate mpMRIs by subspecialised urologists significantly improved the NPV and PPV. If biopsy is to be avoided on the basis of a negative MRI, Urologists need to be aware of the experience of the reporter and potential for variation in negative predictive values. Reporter experience may also reduce overcalling and therefore avoid overtargeting of lesions.

CLINICAL RELEVANCE/APPLICATION

Variation in reporting performance needs to be acknowledged, particularly with mpMRI being increasingly used in order to target or avoid prostate biopsy.

SSG05-02 Negative Predictive Value of Prostate Magnetic Resonance Imaging among Men with Negative Prostate Biopsy and Elevated PSA: A Retrospective Cohort Study

Tuesday, Nov. 29 10:40AM - 10:50AM Room: N229

Awards

Student Travel Stipend Award

Participants

Kirsteen R. Burton, MD, MBA, Toronto, ON (*Presenter*) Nothing to Disclose
Glen Lo, MBBS, Perth, Australia (*Abstract Co-Author*) Nothing to Disclose
Neil Fleshner, Toronto, ON (*Abstract Co-Author*) Nothing to Disclose
Antonio Finelli, Toronto, ON (*Abstract Co-Author*) Nothing to Disclose
Masoom A. Haider, MD, Toronto, ON (*Abstract Co-Author*) Consultant, Bayer AG; ;
Sangeet Ghai, MD, Toronto, ON (*Abstract Co-Author*) Nothing to Disclose

PURPOSE

To estimate the negative predictive value (NPV) of multiparametric-MRI (mp-MRI) for clinically significant cancer at a mean follow up of 6.8 years.

METHOD AND MATERIALS

IRB approved, retrospective cohort study of diagnostic performance of prostate MRI examinations performed between 2004-2009. The oldest MRI per individual patient was eligible for study inclusion. Patients with Gleason score 6 disease at outset and negative initial MRI who remained on active surveillance were included in the study. Presence of any volume Gleason 4 component or higher at follow-up biopsy was considered as clinically significant disease. Follow-up duration and subsequent prostate cancer diagnoses (and scores) were determined by chart review in July 2015, by the most recent prostate biopsy result, outpatient clinic letter and from data linkage to the hospital's Cancer Registry. Diagnostic performance was estimated from contingency tables.

RESULTS

During the study period, 727 prostate MRI studies were performed, with 541 MRI examinations ultimately included in the analysis. Median patient age was 63 years. Within our sample of 541 men, 132 men (24.4%) had a negative initial MRI (73 with previous negative biopsy and median PSA 10; and 59 with low-volume Gleason 6 disease, median PSA 6). At median follow up 81.4 months, 115/132 men (87.1%) remained on watchful waiting or active surveillance without any disease or clinically significant disease. Within this group, 70/73 men (95.9%) remained free of clinical disease at a median follow up of 81 months. A total of 409 men (75.6%) had a positive MRI at the initial read. Of these, clinically significant cancer was present in 237/409 on biopsy (positive predictive value (PPV) = 58%). Within this group, the PPV of MRI in patients with prior negative biopsy was significantly lower (16.7%) in comparison to patients on active surveillance (63.4%).

CONCLUSION

Our long-term study showed that mp-MRI demonstrated a high clinical NPV and is very useful to rule out clinically significant prostate cancer, more so in patients with prior negative biopsy.

CLINICAL RELEVANCE/APPLICATION

In men with prior negative biopsy and a negative MRI, the risk of developing clinically significant disease over a median of 6.7 years is extremely low therefore these patients could be clinically followed less frequently.

SSG05-03 Abbreviated Prostate MRI: Magnetic Resonance Imaging Validation Study to Screen Patients for Initial Biopsy

Tuesday, Nov. 29 10:50AM - 11:00AM Room: N229

Awards

Student Travel Stipend Award

Participants

Ge Gao, MD, Beijing, China (*Presenter*) Nothing to Disclose

Xiaoying Wang, MD, Beijing, China (*Abstract Co-Author*) Nothing to Disclose

PURPOSE

To investigate whether an abbreviated prostate MRI protocol-based on revised Prostate Imaging and Data System (PI-RADS v2) is sufficient to screen clinical significant prostate cancer in a cohort of patients for initial biopsy.

METHOD AND MATERIALS

240 consecutive patients (mean age, 66.4±8.8 years; range, 40-82 years) with normal digital rectal examination (DRE) results but elevated total prostate-specific antigen (t-PSA) levels (4-20/ml) or normal t-PSA but falling f/t PSA (<0.16) were enrolled in this retrospective study. All patients underwent 3-T abbreviated prostate MRI protocol including T2WI and DWI. Transrectal ultrasound guided random systematic biopsy was performed subsequently. All MRI image data were read by 2 experienced radiologists, who were blinded to the PSA data, in consensus according to PI-RADS v2. The effectiveness of abbreviated prostate MRI protocol in screening clinical significant PCa was evaluated by the receiver operating characteristic (ROC) analysis. The thresholds to recommend biopsy were obtained from the Youden J statistics.

RESULTS

There were finally 104/240 men (43.3%) diagnosed with clinical significant PCa, with normal DRE but moderate elevated t-PSA (mean, 10.59 ng/ml; range, 4.09-19.85 ng/ml). Abbreviated prostate MRI based on PI-RADS v2 achieved high areas under ROC curve of 0.905. For the threshold of PI-RADS v2 score of 4 or greater, the sensitivity, specificity, PPV and NPV were 0.885, 0.904, 0.876 and 0.911. The accuracy of abbreviated prostate MRI protocol for PCa detection is 89.5%. While for the score threshold of 3 or greater, the sensitivity, specificity, PPV, NPV and accuracy were 0.933, 0.750, 0.740, 0.936 and 0.829.

CONCLUSION

Abbreviated prostate MRI based on PI-RADS v2 allows screen clinical significant PCa in men with normal DRE and moderate elevated t-PSA for initial biopsy.

CLINICAL RELEVANCE/APPLICATION

Abbreviated prostate MRI based on PI-RADS v2 might be a promising screen method for men with equivocal biopsy indications, which would reduce overdiagnosis and overtreatment for this cohort of patients in some extent.

SSG05-04 B-Value and Mode Dependence of Diffusion Weighted Imaging in Peripheral Zone Prostate Cancer Detection

Tuesday, Nov. 29 11:00AM - 11:10AM Room: N229

Participants

Xiangde Min, MD, Wuhan, China (*Presenter*) Nothing to Disclose

Liang Wang, MD, PhD, Wuhan, China (*Abstract Co-Author*) Nothing to Disclose

Zhaoyan Feng, MD, Wuhan, China (*Abstract Co-Author*) Nothing to Disclose

Debo Zhi, MS, Hefei, China (*Abstract Co-Author*) Nothing to Disclose

Yuping Chen, Hefei, China (*Abstract Co-Author*) Nothing to Disclose

PURPOSE

To evaluate the b value and mode dependence of diffusion weighted imaging in peripheral zone prostate cancer detection.

METHOD AND MATERIALS

78 patients with peripheral PCa underwent DW-MRI using 21 b-values (0-4500s/mm²) at 3.0T. The mean signal intensities of ROIs placed in normal peripheral tissue and peripheral PCa were fitted using the four models (conventional mono-exponential, bi-exponential, stretched-exponential, and kurtosis). To validate the dependence of modes on the b-values, the b-values were divided into four different ranges: 0-1000, 0-2000, 0-3200, and 0-4500 s/mm², titled as groups A, B, C, and D, respectively. ADC, D, D*, f, DDC, α , Dapp, Kapp were estimated for every group. In order to test goodness-of-fit, adjusted coefficient of determinant (R²) for groups were calculated among different models. Receiver operating characteristic curve (ROC) analysis was performed and the area under the curve (AUC) was obtained to evaluate and compare the diagnostic accuracy of parameters in distinguishing cancerous tissues from normal PZ.

RESULTS

The bi-exponential and the stretched-exponential models provide the highest adjusted R² among the four models in every group. The kurtosis model provide the medium goodness-of-fit. The mono-exponential model provide the lowest goodness-of-fit in the four groups. Whether in the benign PZ or in the cancerous tissue, the mean value of ADC, D, D* α , Dapp significantly decrease with the increasing of b value. Yet, the mean value of f and Kapp significantly increase with the decreasing of the b value. Different from the parameters above, the DDC and α calculated from the stretched exponential model have no significant variation with the increasing of b value. ADC, DDC and Kapp of group B, C and D provide the highest AUC. No significant differences between group B, C and D about AUC value of ADC, DDC and Kapp (all p>0.05).

CONCLUSION

Higher b-value and more complicated models provide no additional diagnostic value than conventional mono-exponential at b-value about 2000s/mm² in peripheral zone prostate cancer detection. However, DDC derived from stretched-exponential model is an promising parameter for it's good diagnostic performance and stability though the b-value adopted.

CLINICAL RELEVANCE/APPLICATION

Higher b-value and more complicated models provide no additional diagnostic value than conventional mono-exponential at b-value about 2000s/mm² in peripheral zone prostate cancer detection.

SSG05-05 Computer-Aided Diagnosis for Prostate Cancer mpMRI: A Multi-Reader Study

Tuesday, Nov. 29 11:10AM - 11:20AM Room: N229

Awards

Trainee Research Prize - Medical Student

Participants

Matthew Greer, BS, Cleveland Heights, OH (*Presenter*) Nothing to Disclose
Nathan S. Lay, PhD, Bethesda, MD (*Abstract Co-Author*) Nothing to Disclose
Joanna Shih, Bethesda, MD (*Abstract Co-Author*) Nothing to Disclose
Tristan Barrett, MBBS, BSc, Guildford, United Kingdom (*Abstract Co-Author*) Nothing to Disclose
Leonardo K. Bittencourt, MD, PhD, Rio De Janeiro, Brazil (*Abstract Co-Author*) Nothing to Disclose
Samuel Borofsky, MD, Washington, DC (*Abstract Co-Author*) Nothing to Disclose
Ismail M. Kabakus, MD, PhD, Ankara, Turkey (*Abstract Co-Author*) Nothing to Disclose
Yan Mee Law, MBBS, Singapore, Singapore (*Abstract Co-Author*) Nothing to Disclose
Jamie Marko, MD, Bethesda, MD (*Abstract Co-Author*) Nothing to Disclose
Haytham M. Shebel, MD, Mansoura, Egypt (*Abstract Co-Author*) Nothing to Disclose
Francesca Mertan, BS, Bethesda, MD (*Abstract Co-Author*) Nothing to Disclose
Maria Merino, MD, Bethesda, MD (*Abstract Co-Author*) Nothing to Disclose
Peter Pinto, Bethesda, MD (*Abstract Co-Author*) Nothing to Disclose
Peter L. Choyke, MD, Rockville, MD (*Abstract Co-Author*) Researcher, Koninklijke Philips NV; Researcher, General Electric Company; Researcher, Siemens AG; Researcher, iCAD, Inc; Researcher, Aspyrian Therapeutics, Inc; Researcher, ImaginAb, Inc; Researcher, Aura Biosciences, Inc
Ronald M. Summers, MD, PhD, Bethesda, MD (*Abstract Co-Author*) Royalties, iCAD, Inc; ;
Baris Turkbey, MD, Bethesda, MD (*Abstract Co-Author*) Nothing to Disclose

PURPOSE

Computer-aided diagnosis (CAD) of prostate mpMRI has the potential to assist inexperienced readers and improve agreement among readers. We conducted a multi-reader study to assess the accuracy and agreement of CAD-assisted mpMRI.

METHOD AND MATERIALS

9 radiologists (with n=3 high, n=3 moderate, n=3 low experience with prostate MRI) from 8 institutions participated. In order to detect a 10% difference in sensitivity between MRI and CAD 77 total patients were needed. Test cases were consecutive patients with ERC MRI at 3T (T2W, ADC, b2000, and DCE MRI) and subsequent prostatectomy. Control cases were patients with no lesions on ERC MRI and no positive TRUS biopsy. Readers were blinded to all outcomes, asked to detect up to 3 lesions, and use PIRADS v2 for evaluation of MRI without CAD. After 5 weeks, readers evaluated MRI with CAD by detecting lesions on CAD alone and then accepted or rejected these lesions using PIRADS v2 criteria on MRI. Lesions were correlated to whole mount prostatectomy specimens processed with customized 3D-printed molds. Average sensitivity, specificity, and positive predictive value (PPV) were calculated on a per-patient and per-lesion basis. Index of specific agreement (ISA) was calculated among all readers and experience levels. Paired student t-test was used to compare time to make reads.

RESULTS

There were 163 patients (n=110 cases, n=53 controls) with a median PSAD of 0.19 ng/ml² for cases and 0.09 ng/ml² for controls. On lesion based analysis the average sensitivity for detecting index lesions of any grade was 78% for MRI and 86% for CAD (p=0.02). When all lesions of any grade were included the sensitivity was 52% for MRI and 60% for CAD (p=0.001). Index lesion sensitivity increased 7.6% on average for each reader with CAD (p=0.02). On a per-patient basis the average specificity of CAD

and MRI were 57% and 70% ($p=0.003$), respectively. ISA was 72% for detection of lesions with CAD versus 57% ($p<0.001$) for MRI alone. Agreement between high and low experience readers improved from 60% to 72% with CAD ($p<0.001$). No difference was observed in time to make reads ($p=0.645$).

CONCLUSION

With the assistance of CAD, readers of varying experience were able to detect intermediate and high grade index lesions on mpMRI with high sensitivity and agreement.

CLINICAL RELEVANCE/APPLICATION

The addition of CAD to mpMRI could bridge the gap between readers of varying experience for detecting high grade prostate cancer.

SSG05-06 Multiparametric Magnetic Resonance Imaging Versus Partin Tables and Memorial Sloan Kettering Cancer Center Nomogram in Assessing Risk Category of Prostate Cancer: A Study in Patients Addressed to External Beam Radiation Therapy

Tuesday, Nov. 29 11:20AM - 11:30AM Room: N229

Participants

Rossano Girometti, MD, Udine, Italy (*Presenter*) Nothing to Disclose
Marco A. Signor, MD, Udine, Italy (*Abstract Co-Author*) Nothing to Disclose
Michele Zerial, Udine, Italy (*Abstract Co-Author*) Nothing to Disclose
Martina Urbani, MD, AVIANO, Italy (*Abstract Co-Author*) Nothing to Disclose
Daniele Maruzzi, Pordenone, Italy (*Abstract Co-Author*) Nothing to Disclose
Chiara Zuiani, MD, Udine, Italy (*Abstract Co-Author*) Nothing to Disclose

PURPOSE

To evaluate the impact on risk stratification of prostate cancer (PCa) of Multiparametric Magnetic Resonance Imaging (mpMRI) as compared to Partin Tables (PT) and Memorial Sloan Kettering Cancer Center (MSKCC) nomogram in patients addressed to External Beam Radiation Therapy (EBRT).

METHOD AND MATERIALS

In this bicentric study, we prospectively performed pre-ERBT staging mpMRI in fifty-three patients with biopsy-proven PCa. Examination were acquired on a 3.0T magnet, with a protocol including high-resolution multiplanar T2-weighted imaging, diffusion-weighted imaging (maximum b-value 2000 sec/mm²) and dynamic contrast-enhanced imaging after i.v. injection of 0.1 mmol/Kg of Gd-BOPTA. Patients' risk group was assessed in accordance with the National Comprehensive Cancer Network (NCCN) categories, by combining prostate-specific-antigen level, Gleason score and the T-stage as defined by mpMRI vs PT or MSKCC. On a per-patient basis, we calculated the agreement between mpMRI and nomograms in assessing $\leq T2$ vs $\geq T3$ stage (Cohen's kappa), as well as mpMRI-induced rate of changes in risk group assignment (\leq low risk vs intermediate risk vs \geq high risk). Additional thirty-five patients with post-operative histological diagnosis served as a validation group for mpMRI.

RESULTS

mpMRI showed poor agreement with PT ($k=0.30$) and MSKCC ($k=0.33$) in defining $\leq T2$ vs $\geq T3$ stage. In particular, mpMRI modified the T stage in 18/53 patients (34.0%;95%C.I. 21.9-48.4) compared to both nomograms, mainly in terms of downstaging (18.9% and 28.3% for PT and MSKCC, respectively). This translated into mpMRI-induced change in risk group assignment in 17/53 of both PT and MSKCC cases (32.1%;95%C.I. 20.3-46.4), with a prevalent effect of downgrading \geq high risk to intermediate risk category (17% of patients). In the validation group of surgical patients, mpMRI showed 85.7% accuracy in assessing $\geq T3$ stage.

CONCLUSION

mpMRI changed PT- and MSKCC-related T staging of PCa in about one-third of patients, translating into a modification of risk category in 32.1% of cases, mainly in terms of \geq high-to-intermediate risk downgrading.

CLINICAL RELEVANCE/APPLICATION

mpMRI refines nomograms-based risk stratification, especially in patients initially assessed as \geq high-risk, thus impacting on the EBRT regimen (e.g., duration of concomitant hormonal therapy).

SSG05-07 Utility of Multi-parametric MRI to Predict Pathological Stage and Surgical Margins in Anterior Prostate Cancers

Tuesday, Nov. 29 11:30AM - 11:40AM Room: N229

Awards

Student Travel Stipend Award

Participants

Muhammad Idris, MBBS, Ottawa, ON (*Presenter*) Nothing to Disclose
Nicola Schieda, MD, Ottawa, ON (*Abstract Co-Author*) Nothing to Disclose
Christopher Lim, MD, Ottawa, ON (*Abstract Co-Author*) Nothing to Disclose
Robert Lim, MD, Ottawa, ON (*Abstract Co-Author*) Nothing to Disclose
Wael M. Shabana, MD, Ottawa, ON (*Abstract Co-Author*) Nothing to Disclose
Satheesh Krishna, MD, Ottawa, ON (*Abstract Co-Author*) Nothing to Disclose
Trevor A. Flood, MD, FRCPC, Ottawa, ON (*Abstract Co-Author*) Nothing to Disclose
Rodney H. Breau, MD, Ottawa, ON (*Abstract Co-Author*) Nothing to Disclose
Christopher Morash, MD, Ottawa, ON (*Abstract Co-Author*) Nothing to Disclose

PURPOSE

Clinical staging of anterior prostate cancer (APC) is limited and studies evaluating MRI for staging of APC are lacking. Moreover, there are higher rates of positive surgical margins (PSM) after radical prostatectomy (RP) in APC. This study evaluates subjective

and quantitative MRI, to predict extraprostatic extension (EPE) and PSM in APC.

METHOD AND MATERIALS

With IRB approval, 25 patients underwent RP with APC (>2/3 of tumor anterior to urethra; 21 transition zone, 4 anterior peripheral zone tumors) and MRI between 2012-2015. Two blinded radiologists assessed MRI for: tumor size (mm), invasion of anterior fibromuscular stroma (AFMS), whether tumor crosses midline and EPE. Radiologists measured leading edge of tumor (relative to prostate capsule) on b₂≥1000 mm²/sec EPI fused onto T2W. Comparisons were performed using chi-square, regression and ROC.

RESULTS

Age and PSA were 65.2 ± 5.9 years and 9.91 ± 7.62 ng/mL with no difference by EPE or PSM (p>0.05). Rates of EPE and PSM were 52% (13/25) and 40% (10/25). Gleason scores were: 3+3=6 (N=1), 3+4=7 (N=12), 4+3=7 (N=9), 4+4=8 (N=1) and 4+5=9 (N=2). Tumor size was 19.0 ± 8.3 (7-33) mm overall; larger tumors were associated with EPE and PSM (p=0.009 and 0.011). AUC for size predicting EPE/PSM were 0.79 (SE=0.09, CI 0.62-0.97) and 0.77 (0.11, 0.55-0.99) with size ≥16mm yielding sensitivity/specificity (SENS/SPEC) of 76.9/66.7% and 80/60% respectively. 52% (13/25) of tumors crossed the midline, this was associated with EPE and PSM (p=0.009 and 0.002). 72% (18/25) tumors invaded AFMS, this was not associated with EPE or PSM (p>0.05). Radiologist impression of EPE had SENS/SPEC of 61.5/75.0%. Leading edge of tumor was 1.3 ± 3.7 (-7 - 10) mm overall and was associated with both EPE and PSM (p=0.011 and 0.013). AUC for leading edge predicting EPE/PSM were 0.79 (SE=0.09, CI 0.61-0.98) and 0.77 (0.09, 0.59-0.96) with ≥2mm extension yielding SENS/SPEC of 76.9/75% and 70/73.3% respectively.

CONCLUSION

In anterior prostate cancers, size of tumor, extension across midline and the leading edge of tumor are findings associated with extraprostatic extension and positive surgical margins after RP.

CLINICAL RELEVANCE/APPLICATION

Diagnosis of extraprostatic spread of tumor in anterior prostate cancers is possible with MRI. These findings correlate with positive surgical margin rates after radical prostatectomy and may alter surgical approach or management.

SSG05-08 PI-RADS Version 2: Quantitative Analysis Helps Reliable Interpretation of Diffusion-Weighted Imaging for Peripheral Zone Prostate Cancer

Tuesday, Nov. 29 11:40AM - 11:50AM Room: N229

Participants

Sung Yoon Park, Seoul, Korea, Republic Of (*Presenter*) Nothing to Disclose
Young Taik Oh, MD, Seoul, Korea, Republic Of (*Abstract Co-Author*) Nothing to Disclose
Su-Jin Shin, Seoul, Korea, Republic Of (*Abstract Co-Author*) Nothing to Disclose
Dae Chul Jung, MD, Seoul, Korea, Republic Of (*Abstract Co-Author*) Nothing to Disclose
Nam Hoon Cho, Seoul, Korea, Republic Of (*Abstract Co-Author*) Nothing to Disclose
Young Deuk Choi, Seoul, Korea, Republic Of (*Abstract Co-Author*) Nothing to Disclose
Koon Ho Rha, MD, PhD, Seoul, Korea, Republic Of (*Abstract Co-Author*) Nothing to Disclose
Sung Joon Hong, Seoul, Korea, Republic Of (*Abstract Co-Author*) Nothing to Disclose

PURPOSE

To analyze whether quantitative analysis of apparent diffusion coefficient (ADC) helps reliable interpretation of diffusion-weighted imaging (DWI) for peripheral zone (PZ) prostate cancer.

METHOD AND MATERIALS

Consecutive 76 patients with PZ cancer who underwent 3T DWI and surgery were included. Based on the location of an index tumor from surgical specimens, two independent readers performed DWI scoring of revised Prostate Imaging Reporting and Data System (PI-RADSv2). Then, ADC ratio of benign PZ-to-cancer was also measured in consensus. The ADC ratio was compared between agreement (i.e., score ≥ 4 for both readers) and disagreement groups (i.e., score ≥ 4 only for one reader). The cutoff and area under the curve (AUC) of ADC ratio were analyzed for DWI score ≥ 4.

RESULTS

The rate of inter-reader disagreement regarding DWI score ≥ 4 or not was 11.8% (9/76). The ADC ratio of benign PZ-to-cancer was significantly higher in agreement group than in disagreement group (median, 1.7 versus 1.3; p < 0.001). For DWI score ≥ 4, the cutoff and AUC of ADC ratio were more than 1.2 and 0.921 with reader 1, and more than 1.3 and 0.949 with reader 2, respectively. For patients with ADC ratio > 1.3, the rate of inter-reader disagreement was 6% (3/50). The application of ADC ratio > 1.3 allowed 100% (50/50) positive predictive value for clinically significant cancer that met Epstein criteria.

CONCLUSION

The quantitative analysis of ADC ratio between benign PZ and PZ cancer may be useful for reliable interpretation of DWI score ≥ 4 in PI-RADSv2.

CLINICAL RELEVANCE/APPLICATION

In PI-RADSv2, DWI score is determined by visual analysis, which may be associated with inter-reader disagreement. The quantitative analysis of ADC may help reliable interpretation for the detection of CSC

SSG05-09 Rapid Biparametric MRI and Targeted Biopsy in Patients with Elevated PSA Before Their First Biopsy: Initial Finding of a Multi-Institutional Prospective Registered Clinical Trial

Tuesday, Nov. 29 11:50AM - 12:00PM Room: N229

Participants

Ivan Jambor, MD, Turku, Finland (*Presenter*) Nothing to Disclose
Aida K. Kiviniemi, MD, Turku, Finland (*Abstract Co-Author*) Nothing to Disclose

Otto Ettala, Turku, Finland (*Abstract Co-Author*) Nothing to Disclose
Pekka Taimen, Turku, Finland (*Abstract Co-Author*) Nothing to Disclose
Esa Kahkonen, Turku, Finland (*Abstract Co-Author*) Nothing to Disclose
Kari Syvanen, Turku, Finland (*Abstract Co-Author*) Nothing to Disclose
Marjo Seppanen, Pori, Finland (*Abstract Co-Author*) Nothing to Disclose
Outi Oksanen, Helsinki, Finland (*Abstract Co-Author*) Nothing to Disclose
Antti Rannikko, Turku, Finland (*Abstract Co-Author*) Nothing to Disclose
Mika Matikainen, Helsinki, Finland (*Abstract Co-Author*) Nothing to Disclose
Jarno Riikonen, Tampere, Finland (*Abstract Co-Author*) Nothing to Disclose
Sanna-Mari Vimpeli, MD, Tampere, Finland (*Abstract Co-Author*) Nothing to Disclose
Ileana Montoya Perez, Turku, Finland (*Abstract Co-Author*) Nothing to Disclose
Markku Kallajoki, Turku, Finland (*Abstract Co-Author*) Nothing to Disclose
Hannu J. Aronen, MD, PhD, Kuopio, Finland (*Abstract Co-Author*) Nothing to Disclose
Peter Bostrom, Turku, Finland (*Abstract Co-Author*) Nothing to Disclose

PURPOSE

To evaluate negative predictive value of biparametric MRI (bpMRI) and bpMRI targeted TRUS-guided biopsy in patients with elevated PSA before their first biopsy in a multi-institutional prospective registered clinical trial.

METHOD AND MATERIALS

Between February 2015 and March 2016, 184 patients with elevated PSA (2.5 - 20.0 ng/ml) and/or abnormal digital rectal examination underwent bpMRI examination performed using surface array coils prior to a systematic 12 core biopsy (SB) at four centers. bpMRI was performed using surface array coils at 3 Tesla (3 centers) or 1.5 Tesla (1 center) and consisted of T2-weighted imaging (T2w) and three separate diffusion weighted imaging (DWI) acquisitions (5 b values 0-500 s/mm², 2 b values 0-1500 s/mm², 2 b values 0-2000 s/mm²). All bpMRI were reported centrally and approved by one reader before biopsy. If a suspicious lesion was present (Likert score 3-5), two cores of targeted biopsy (TB) were taken prior to the SB. A maximum of two lesions per patient were targeted. Clinically significant (SPCa) was defined as Gleason score 3+4 or higher.

RESULTS

Prostate cancer and SPCa were diagnosed in 108 (59%, 108/184) and 70 (43%, 70/184) patients, respectively. Fourteen (8%, 14/184), 22 (12%, 22/184), 36 (20%, 36/184), 34 (19%, 36/184), and 78 (43%, 78/184) patients presented with Likert score 1, 2, 3, 4, and 5, respectively. Performing biopsy only in patients with Likert score 3-5 or 4-5 would have resulted in a 20% (36/184) or 39% (72/184) reduction in the number of patients undergoing biopsy while missing only 0% or 2% (4/184) patients with SPCa, respectively. The corresponding negative predictive values are 100% and 94%. In patients with Likert score 3-5 (n=148), the addition of SB to TB resulted in the detection of SPCa in 7 (4%, 7/184) patients while SPCa was diagnosed only in the cores of TB in 8 (4%, 8/184) patients.

CONCLUSION

Biparametric MRI, consisting of T2w and DWI acquired using "low" and "high" b values, has high negative predictive value for SPCa and could be used to identify patients who would benefit from biopsy while limiting unnecessary biopsy procedures.

CLINICAL RELEVANCE/APPLICATION

Biparametric MRI, consisting of T2-weighted imaging and diffusion weighted imaging acquired using "low" and "high" b values, limits the number of unnecessary biopsy procedures.

SSG06

Science Session with Keynote: Health Service, Policy and Research (Quality)

Tuesday, Nov. 29 10:30AM - 12:00PM Room: S102D

HP

AMA PRA Category 1 Credits™: 1.50
ARRT Category A+ Credit: .50

Participants

Jonathan James, BMBS, Nottingham, United Kingdom (*Moderator*) Nothing to Disclose

Edward Y. Lee, MD, MPH, Boston, MA (*Moderator*) Nothing to Disclose

Sub-Events

SSG06-01 Improving Appropriateness in Medical Imaging of Low-Back Pain Patients in the Emergency Department Using Clinical Decision Support: A Choosing Wisely Initiative

Tuesday, Nov. 29 10:30AM - 10:40AM Room: S102D

Participants

Adam Min, Vancouver, BC (*Presenter*) Nothing to Disclose

Vivian Chan, MPH, PhD, Vancouver, BC (*Abstract Co-Author*) Nothing to Disclose

Ruben Aristizabal, MSc, Vancouver, BC (*Abstract Co-Author*) Nothing to Disclose

Bruce B. Forster, MD, Vancouver, BC (*Abstract Co-Author*) Nothing to Disclose

PURPOSE

To determine whether Electronic Health Record (EHR)-based clinical decision support (CDS) can effectively reduce inappropriate medical imaging (MI) of patients who present to the emergency department (ED) with low-back pain (LBP) without discouraging appropriate use of MI.

METHOD AND MATERIALS

This was a prospective, single-centre study of lumbar imaging referrals made by 25 ED physicians at a major acute-care centre. A point-of-care checklist of accepted red flag symptoms for LBP was embedded in the computerized order-entry for MI on 03/04/15. If physicians identified no red flags, they were required to enter their reason for imaging in a free-text box (medium stop). We compared the number of lumbar X-ray, CT, and MRI referrals of each physician before and after the implementation of the checklist (from 06/01/14 to 08/31/15). We then performed secondary pre- and post-intervention analysis to measure the potential harms of reduced imaging.

RESULTS

After intervention, the median proportion of LBP patients with an imaging order fell significantly (22.6% to 19.4%; $p=0.0043$; $CI=0.95$) compared to pre-intervention baseline, and variation in MI ordering rates across physicians decreased (interquartile range pre=16%; post=11%). There was no significant difference in the decrease in imaging across modalities. Further analysis showed no significant increase in harmful outcomes as a result of reduced MI. The percentage of patients without imaging who were later imaged at a hospital outpatient clinic within 30 days was 2.2% before intervention and 2.3% after. In addition, the proportion of patients discharged from the ED without MI who subsequently visited the same or another local ED within 30 days was 2.6% before intervention and 3.7% after, and 88% of returning patients were subsequently diagnosed on the second visit again with acute back pain or sciatica. One minor thoracic spine compression fracture was missed post-intervention; however, management was not impacted.

CONCLUSION

CDS integrated in electronic order-entry can safely and effectively reduce MI orders for LBP patients in the ED.

CLINICAL RELEVANCE/APPLICATION

Clinical decision support can reduce the number of inappropriate lumbar imaging studies ordered by emergency physicians who manage patients with acute, uncomplicated low-back pain.

SSG06-02 Epinephrine Auto-injector Versus Manual Intramuscular Delivery for Treatment of Moderate-Severity, Anaphylactoid Contrast Reactions: Comparison of Errors, Administration Times and Provider Preferences

Tuesday, Nov. 29 10:40AM - 10:50AM Room: S102D

Awards

Student Travel Stipend Award

Participants

Daniella Asch, MD, New Haven, CT (*Presenter*) Nothing to Disclose

Kyle E. Pfeifer, MD, New Haven, CT (*Abstract Co-Author*) Nothing to Disclose

Jennifer Arango, New Haven, CT (*Abstract Co-Author*) Nothing to Disclose

Lawrence H. Staib, PhD, New Haven, CT (*Abstract Co-Author*) Nothing to Disclose

Joseph Cavallo, MD, New Haven, CT (*Abstract Co-Author*) Nothing to Disclose

Jonathan D. Kirsch, MD, New Haven, CT (*Abstract Co-Author*) Nothing to Disclose

Melih Arici, MD, Branford, CT (*Abstract Co-Author*) Nothing to Disclose

Liana Kappus, New Haven, CT (*Abstract Co-Author*) Nothing to Disclose

Jay K. Pahade, MD, New Haven, CT (*Abstract Co-Author*) Consultant, Precision Imaging Metrics, LLC

PURPOSE

Given the rarity of contrast reactions in practice, most radiologists have little to no experience in management, and errors are common. We compared treatment of an anaphylactoid reaction in an adult without hypotension (moderate-severity) with 0.3 mg IM 1:1,000 epinephrine utilizing either the traditional manual method of drawing up and delivering epinephrine from a sealed 1 mg vial with needle/syringe or an epinephrine auto-injector (Auvi-Q). We hypothesized that use of an epinephrine auto-injector would result in decreased time to administration, fewer errors, and increased provider comfort.

METHOD AND MATERIALS

All non-interventional radiologists at our institution were requested to participate in our annual contrast reaction simulation program, which consisted of three simulation scenarios in a high-fidelity simulation lab. During the moderate-severity simulation scenario, the time to administer IM epinephrine and any errors in administration were recorded. Groups were randomized to use an auto-injector device or a manual method of drawing up and delivering IM epinephrine. All participants completed a survey assessing prior experience with epinephrine and comfort in treating a contrast reaction with a traditional manual approach vs. epinephrine auto-injector.

RESULTS

There were 188 participants in the contrast reaction simulation program over the course of 25 sessions, with 76 participating in the moderate-severity reaction simulation in groups of 2-5. Mean total time to administration was significantly longer (108.8 s) for manual delivery vs. the auto-injector (38.7 s), $p < 0.001$. There were 11 errors in the manual group and 1 error in the auto-injector group, $p = 0.005$. The most common error was administration of the wrong dose of IM epinephrine, which occurred in 5/13 (46%) simulation sessions. 94% of participants reported feeling "very comfortable" or "comfortable" with the auto-injector vs. 60% for manual delivery ($p < 0.001$). Overall, 96% of participants thought the auto-injector was easier to use.

CONCLUSION

Use of an epinephrine auto-injector for treatment of contrast reactions was associated with significantly increased provider comfort, shorter time to administration, and fewer errors.

CLINICAL RELEVANCE/APPLICATION

Our study demonstrates the benefit of IM epinephrine auto-injectors for the treatment of contrast-related anaphylactoid reactions and supports replacing epinephrine vials designed for IM use with auto-injectors.

SSG06-03 Use of Patient Questionnaires to Obtain Additional Clinical History: Impact on Abdominopelvic CT Interpretation

Tuesday, Nov. 29 10:50AM - 11:00AM Room: S102D

Participants

Ankur Doshi, MD, New York, NY (*Presenter*) Nothing to Disclose
Chenchan Huang, MD, New York, NY (*Abstract Co-Author*) Nothing to Disclose
Krishna Prasad Shanbhogue, MD, New York, NY (*Abstract Co-Author*) Nothing to Disclose
Luke A. Ginocchio, MD, New York, NY (*Abstract Co-Author*) Nothing to Disclose
Andrew B. Rosenkrantz, MD, New York, NY (*Abstract Co-Author*) Nothing to Disclose

PURPOSE

In our department, outpatients awaiting CT complete a written questionnaire with items pertaining to symptoms and medical history, which is subsequently scanned into the electronic medical record. The aim of this study was to evaluate if the questionnaires impact the interpretation of abdominopelvic CT performed for abdominal pain.

METHOD AND MATERIALS

100 adult outpatient contrast-enhanced abdominopelvic CT examinations performed for the evaluation of abdominal pain were included. The indication entered by the ordering physician and the patient questionnaire were compared in terms of specificity of the location of pain. An abdominal imaging fellow (R1) and abdominal radiologist with 5 years of experience (R2) independently interpreted the examinations in two separate reading sessions separated by 4 weeks. In the first session, readers were only provided with the exam indication entered by the ordering physician. In the second session, readers were also provided with the patient questionnaire. During each session, readers recorded any identified cause for abdominal pain and rated their confidence in interpretation (scale of 1 – 5; least to greatest). Paired Wilcoxon test was used to compare the two sessions.

RESULTS

The questionnaire contained a more specific location for pain than the exam indication entered by the ordering physician in 29% of cases. Among these, the pain was localized to a specific quadrant in 45%. In comparison with use of the provided history alone, use of the questionnaire resulted in identification of a cause for abdominal pain by the radiologist in an additional 7% of cases for R1 and 4% of cases for R2. For R1, additional identified causes of pain included diverticulitis, cystitis, peritoneal implants, epiploic appendagitis, and osseous metastatic disease. For R2, additional causes of pain included umbilical hernia, gastritis, SMA syndrome, and cystitis. Confidence in interpretation was significantly greater using the questionnaire (R1: 4.8 ± 0.6 vs. 4.0 ± 0.5 ; R2: 4.9 ± 0.3 vs. 4.7 ± 0.5 , $p < 0.001$).

CONCLUSION

Patient questionnaires provide additional relevant clinical history, increased diagnostic yield, and improve radiologists' confidence.

CLINICAL RELEVANCE/APPLICATION

Radiology practices are encouraged to implement patient questionnaires and to make these readily available to radiologists at the time of interpretation in order to improve exam interpretations.

Honored Educators

Presenters or authors on this event have been recognized as RSNA Honored Educators for participating in multiple qualifying educational activities. Honored Educators are invested in furthering the profession of radiology by delivering high-quality educational content in their field of study. Learn how you can become an honored educator by visiting the website at:

<https://www.rsna.org/Honored-Educator-Award/>

Krishna Prasad Shanbhogue, MD - 2012 Honored Educator
Krishna Prasad Shanbhogue, MD - 2013 Honored Educator

SSG06-04 How Satisfied are Patients with their Radiologists? Assessment Using a Patient Ratings Website

Tuesday, Nov. 29 11:00AM - 11:10AM Room: S102D

Participants

Luke A. Ginocchio, MD, New York, NY (*Presenter*) Nothing to Disclose
Richard Duszak JR, MD, Atlanta, GA (*Abstract Co-Author*) Nothing to Disclose
Andrew B. Rosenkrantz, MD, New York, NY (*Abstract Co-Author*) Nothing to Disclose

PURPOSE

To use a public patient ratings website to assess the performance of radiologists in patient satisfaction.

METHOD AND MATERIALS

Patient reviews were retrieved from www.RateMDs.com for all radiologists in the 297 U.S. cities with population $\geq 100,000$. Each review included ratings of 1-5 in four categories (staff, punctuality, knowledge, helpfulness). For Medicare-participating radiologists, group practice size and years in practice were obtained from the Physician Compare database. Common words in reviews' free-text comments were assessed. Statistical analysis included Spearman's rank coefficients, coefficients of variation (CV), ANOVA, and Kruskal-Wallis tests.

RESULTS

1,891 patient reviews for 1,259 unique radiologists were identified. For all four categories, the most common score was 5 (63-74%), and second most common score was 1 (14-20%); scores of 2-4 were less frequent (2%-12%). Scores for the four categories were all highly correlated with one another ($r=0.781-0.951$). Only 3% of reviews had a substantial discrepancy between average scores for radiologist factors (knowledge/helpfulness) and office factors (staff/punctuality). For 106 radiologists receiving ≥ 3 patient reviews (total of 572 reviews), average CV was 27%, indicating moderate reproducibility among different patients' reviews for a given radiologist; in addition, ANOVA demonstrated that the radiologist accounted for 30% of total variation in the average score across patient reviews. The Northeast scored significantly lower than other U.S. regions in average scores for staff ($p<0.001$) and punctuality ($p<0.001$); scores for helpfulness and knowledge were similar across regions. Radiologists' group practice size and years since graduation showed no correlation with satisfaction scores ($r=-0.140-0.021$). Common words in free-text comments included "caring", "knowledgeable", and "professional" for positive reviews, and "rude", "pain", and "unprofessional" for negative reviews.

CONCLUSION

Radiologists overall performed well, though patients posting online reviews tended to have strongly positive or negative views. Scores across categories were highly correlated, suggesting a halo effect influencing patients' global perceptions of radiologists.

CLINICAL RELEVANCE/APPLICATION

Given the observed halo effect, radiologists must recognize the importance of office/staff-related as well as radiologist-related factors in impacting patients' impressions and public ratings.

SSG06-05 Effectiveness of a Radiation Advisory Group (RAG) in CT Dose Reduction at a Tertiary Academic Medical Center

Tuesday, Nov. 29 11:10AM - 11:20AM Room: S102D

Awards

Student Travel Stipend Award

Participants

Neena Joseph, BS, BA, HERSHEY, PA (*Presenter*) Nothing to Disclose
Karen L. Brown, MPH, Hershey, PA (*Abstract Co-Author*) Nothing to Disclose
Erik Lehman, Hershey, PA (*Abstract Co-Author*) Nothing to Disclose
Nabeel I. Sarwani, MD, Hummelstown, PA (*Abstract Co-Author*) Nothing to Disclose

PURPOSE

To determine the effectiveness of a Radiation Advisory Group to reduce radiation dose in CT studies performed at a tertiary academic medical center.

METHOD AND MATERIALS

IRB approved retrospective study. A sample of patients who underwent specific CT examinations were selected following a search of the RIS. CT exam types described in the results. The Radiation Advisory Group (RAG) was functional in 2011. Studies from 2009 comprised the pre RAG group, and 2013 the post RAG group. Imaging protocols before and after the implementations of RAG were compared. Total mAs and DLP values were extracted from 50 CT dose sheets of each of the specified studies from 2009 and 2013 for data analysis. Wilcoxon Rank Sum test was used, with p-value of <0.05 .

RESULTS

798 cases were included for analysis. The median DLP for studies performed in 2009 compared to 2013 were as follows: CT abdomen/pelvis with contrast (854.5 vs. 720.2, $p=0.023$), abdomen/pelvis without contrast (837.5 vs. 675.0, $p=0.001$), chest with contrast (651.5 vs. 380.4, $p<0.001$), chest without contrast (646.5 vs. 492.9, $p<0.001$), head/neck perfusion (7248.5 vs. 3730.0, $p<0.001$), CT urogram (2111.0 vs. 1243.9, $p<0.001$), and triphasic abdomen with pelvis (1612.5 vs. 1297.9, $p=0.003$). The median DLP increased for CT head without contrast (832.5 vs. 1021.2, $p<0.001$). The total mAs was similarly significantly reduced for all studies with the exception of CT head, which showed significant increase.

CONCLUSION

Oversight of CT examinations by the multidisciplinary members of a Radiation Advisory Group can lead a multifaceted approach to radiation dose reduction in commonly performed CT examination. Failure to use tube current modulation in the x, y and z direction in head CT scans can lead to higher than expected CT doses.

CLINICAL RELEVANCE/APPLICATION

Effective CT dose reduction requires a multidisciplinary team approach. Dose reduction strategies include divisional standardization of CT protocols, specifying scan ranges, optimizing acquisition parameters (effective mAs, kV & pitch), and technologist education. Breast shields were eliminated and sampling rate for perfusion studies was reduced. Failure to apply built in dose reduction techniques in scanning protocols can increase radiation dose. A RAG should be a standard committee at any facility performing X-Ray examinations.

SSG06-06 Fluoroscopy Suites: A Lead Exposure Hazard?

Tuesday, Nov. 29 11:20AM - 11:30AM Room: S102D

Participants

Sukhraj S. Kahlon, MD, Sacramento, CA (*Presenter*) Nothing to Disclose
Morri Markowitz, MD, Bronx, NY (*Abstract Co-Author*) Nothing to Disclose
Benjamin Taragin, MD, Teaneck, NJ (*Abstract Co-Author*) Medical Advisory Board, Carestream Health, Inc
Kevin Burns, MD, Bronx, NY (*Abstract Co-Author*) Nothing to Disclose
Jamie Shoag, MD, Bronx, NY (*Abstract Co-Author*) Nothing to Disclose

PURPOSE

Dust containing lead (Pb) is a known source of exposure that can result in elevated blood lead levels (BLLs). We have reported previously that dust obtained from surfaces of radiation shields worn by medical workers often contains Pb, presumably due to seepage from the inner layers of Pb (RSNA 12/2015). This study was designed to achieve two aims: 1. to determine whether radiology room surfaces also contain Pb dust; 2. to assess whether these sources of Pb exposure result in hand and blood contamination of radiology workers.

METHOD AND MATERIALS

Surface dust samples were collected from 13 Radiology Department rooms: 9 fluoroscopy suites and 4 non-fluoroscopy control rooms; and from the dominant hand of 42 radiology workers. BLLs were collected from 58 radiology workers. Surface dust was collected from floors, walls and table tops. All samples were analyzed by atomic absorption spectrometry. For surface dust, data are expressed in micrograms per foot squared (ug/ft²), minimum detection limit (MDL) 5 ug/ft². Hand dust samples are reported in ug/wipe, MDL 3 ug/wipe. Venous BLLs are expressed in micrograms per deciliter (ug/dL), MDL 1 ug/dL.

RESULTS

Of fluoroscopy room samples 7 (78%) had detectable floor Pb; 2 (20%) detectable table Pb and 1 had measureable wall Pb. All control room samples except for one floor sample had values <5 ug/ft². Of note, an upward trend in fluoroscopy table samples was observed from <5 to 8 to 15 ug/ft² at morning, afternoon, and evening time points. Repeat fluoroscopy floor samples taken after floor surfaces were cleaned decreased from 20 to <5 ug/ft². All hand dust samples had values < 3 ug /wipe. 49 (84.5%) workers had BLLs ≤1 ug/dL, 8 (13.8%) had BLLs of 2 ug/dL, and 1 had a value of 3 ug/dL. There was no association between duration of shield use and BLLs.

CONCLUSION

Pb can be detected in dust obtained from surfaces in fluoroscopy rooms, with amounts increasing throughout the day and presumably originating in the use of Pb containing shields. BLLs were well below OSHA standards of concern for adults. However, low BLLs have been associated with lower cognitive scores in children, who may be at risk if undergoing multiple radiologic exams.

CLINICAL RELEVANCE/APPLICATION

Cleaning surfaces reduces dust Pb content to undetectable levels and sufficient hand hygiene may be reducing hand dust Pb to undetectable levels, which likely prevents elevated BLLs in workers.

SSG06-07 Authority Gradients in an Academic Radiology Department: A Safety Hazard?

Tuesday, Nov. 29 11:30AM - 11:40AM Room: S102D

Participants

Bettina Siewert, MD, Brookline, MA (*Presenter*) Nothing to Disclose
Olga R. Brook, MD, Boston, MA (*Abstract Co-Author*) Research Grant, Toshiba Medical Systems Corporation
Ronald L. Eisenberg, MD, JD, Boston, MA (*Abstract Co-Author*) Nothing to Disclose
Mary G. Hochman, MD, Boston, MA (*Abstract Co-Author*) Stockholder, General Electric Company; Stock options, Nomir Medical Technologies, Inc; Author, UpToDate, Inc

PURPOSE

To investigate barriers to reporting of safety events in an academic radiology department and to evaluate the role of authority gradients as a potential barrier to safety event reporting.

METHOD AND MATERIALS

A survey was sent out to the Radiology Department email list of a tertiary care institution in a major metropolitan area. The email addressed all Department staff (total number of staff N=648: 331 radiology technologists (51%), 80 attending physicians (12%), 70 residents and fellows (11%), 49 schedulers (8%), 43 nurses (7%), 37 administrative staff (6%), 23 image archive staff (3%) and 15 transport staff (2%) and included a link to a 10 point online questionnaire. Questions recorded respondent's frequency of speaking up about safety events, and respondent's perceived barriers to speaking up. Barriers listed included: high reporting threshold, challenging someone in authority, lack of being listened to, fear of disrespect being expressed, fear of retribution, individuals creating an uncomfortable work environment (toxic captain), responsibility within a team, shy personality, and lack of language skills. Respondents were asked to quantify the number of safety events they did not report annually (0, 1-5, 6-10, 11-20, >20

times).

RESULTS

363 of 648 (56%) of employees completed the survey. 182 of 363 (50%) employees reported always speaking up about safety concerns, 134 of 363 (37%) most of the time, 36 of 363 (10%) sometimes, 7 of 363 (2 %) rarely, and 4 of 363 (1%) never. Thus, 50% of employees do not speak up about safety concerns 100% of the time. Barriers to speaking up were: high reporting threshold 69%, challenging someone in authority 67%, fear of disrespect being expressed 53%, lack of being listened to 52%, fear of retribution 34%, lack of language skills 29%, individuals creating an uncomfortable work environment (toxic captain) 28%, and shy personality 25%.

CONCLUSION

50% of employees in a large academic radiology department do not attain 100% reporting of safety events. The most common barriers to speaking up are: high reporting threshold, not wanting to challenge authority and fear of disrespect. This suggests that existing authority gradients interfere with full reporting of safety events.

CLINICAL RELEVANCE/APPLICATION

To encourage full reporting of safety events, academic radiology departments need to focus on eliminating common barriers such as high reporting threshold, challenging authority and fear of disrespect.

Honored Educators

Presenters or authors on this event have been recognized as RSNA Honored Educators for participating in multiple qualifying educational activities. Honored Educators are invested in furthering the profession of radiology by delivering high-quality educational content in their field of study. Learn how you can become an honored educator by visiting the website at: <https://www.rsna.org/Honored-Educator-Award/>

Ronald L. Eisenberg, MD, JD - 2012 Honored Educator

Ronald L. Eisenberg, MD, JD - 2014 Honored Educator

SSG06-08 Patient Satisfaction and Quality Care in Radiology: Results from 6512 Patient Satisfaction Surveys over 2 Years

Tuesday, Nov. 29 11:40AM - 11:50AM Room: S102D

Participants

Elizabeth H. Dibble, MD, Providence, RI (*Presenter*) Nothing to Disclose

Grayson L. Baird, PhD, Providence, RI (*Abstract Co-Author*) Nothing to Disclose

Terrance T. Healey, MD, Providence, RI (*Abstract Co-Author*) Nothing to Disclose

PURPOSE

Identify factors that contribute to positive and negative patient satisfaction ratings so radiology practices can improve patient satisfaction, a component of quality care.

METHOD AND MATERIALS

This retrospective study examined web-based patient satisfaction surveys (Figure 1) collected at 5 outpatient imaging centers from 1/7/13-11/11/15. Construct validity was examined using factor analysis of the survey items using Promax rotation. Ratings were compared among sites, exam types, and survey questions. Optional free-text comments were grouped into categories (general, staff, wait time, facilities, convenience, cost, safety, and other) and compared by exam type.

RESULTS

6512 surveys were completed out of 137059 encounters (4.8% response). 3 factors were observed, as indicated by the scree plot, when using factor loading cutoffs of $>.3$. The factors were exam experience (Q8-10), intake experience (Q5-6), and facilities/convenience (Q3-4 and Q7). Good scale reliability was observed with a Cronbach's Coefficient Alpha value of .79. Though differences in survey responses were observed among sites, all ratings were above 95%, and differences were not large enough to be meaningful. Among survey questions, quality of care had the highest number of positive ratings (95.5%). Wait time had the highest number of negative/neutral ratings (19.9%) followed by preregistration process (11.9%); others $<10\%$. 1859 free-text comments (91.8%) were positive (60.0% pertained to staff, 28.2% to general experience, 11.9% to preregistration process, others $<10\%$), 155 (7.7%) were negative (31.6% pertained to convenience, 29.7% to facilities, 21.3% to staff, others $<10\%$), and 10 (0.5%) were neutral. Patients who had an MRI were most likely to write a negative comment (40.0% of negative comments vs. 26.0% of responder exams), most of which pertained to facilities (e.g., noisy machine, hard bed).

CONCLUSION

Patient satisfaction surveys should address exam experience, intake experience, and facilities/convenience. Wait-time and preregistration process were rated most negatively. Free-text negative comments pertained most frequently to convenience, facilities, and staff. Patients who underwent MRI were more likely to write a negative comment than patients who underwent other exams.

CLINICAL RELEVANCE/APPLICATION

Radiology practices may improve patient satisfaction by decreasing wait times, streamlining registration process, and improving patient comfort during MR exams.

SSG06-09 Health Service, Policy and Research Keynote Speaker: Duty of Candour-Impact on Disclosure of Audit

Tuesday, Nov. 29 11:50AM - 12:00PM Room: S102D

Participants

Eleanor Cornford, MBBS, Nottingham, United Kingdom (*Presenter*) Research Grant, General Electric Company

SSG07

Informatics (Results & Reporting)

Tuesday, Nov. 29 10:30AM - 12:00PM Room: S402AB

IN

AMA PRA Category 1 Credits™: 1.50
ARRT Category A+ Credits: 1.50

Participants

Amon Makori, MD, Chicago, IL (*Moderator*) Medical Advisory Board, Carestream Health, Inc
Tejas S. Mehta, MD, MPH, Boston, MA (*Moderator*) Nothing to Disclose

Sub-Events

SSG07-01 Radiology Examination Orders Lacking a Meaningful Reason for Exam Increases Suggestion for Clinical Correlation by Over 50%

Tuesday, Nov. 29 10:30AM - 10:40AM Room: S402AB

Participants

Pritesh Patel, MD, Chicago, IL (*Abstract Co-Author*) Nothing to Disclose
Merlijn Sevenster, PhD, Cambridge, MA (*Abstract Co-Author*) Employee, Koninklijke Philips NV
Igor Trilisky, MD, Chicago, IL (*Presenter*) Nothing to Disclose
Darren B. Van Beek, MD, Chicago, IL (*Abstract Co-Author*) Nothing to Disclose
Melvy S. Mathew, MD, Chicago, IL (*Abstract Co-Author*) Nothing to Disclose
Paul J. Chang, MD, Chicago, IL (*Abstract Co-Author*) Co-founder, Stentor/Koninklijke Philips NV; Researcher, Koninklijke Philips NV; Medical Advisory Board, lifeIMAGE Inc; Advisory Board, Bayer AG

PURPOSE

General consensus is that radiologist access to meaningful patient information improves diagnostic accuracy and report quality. Radiologists typically rely on the reason for exam (RFE) provided by the referring physician, which we have previously documented to be frequently sparse, especially when computerized order entry (CPOE) is used. We study the effect of lack of meaningful RFE on report quality, in particular on hedging language, in a large retrospective report corpus.

METHOD AND MATERIALS

A corpus of 44,162 anonymized reports and associated RFEs was obtained from an academic hospital. Three radiologists manually rated the 250 most frequent RFEs, accounting for > 10% of RFEs, as contextually meaningful (yes/no). Conflicting ratings were adjudicated by a senior radiologist. A natural language processing pipeline was used to detect sentences within the report impression suggesting the need for clinical correlation. A 2 x 2 matrix was created counting the number of reports with/without meaningful RFE and with/without at least one sentence suggesting the need for clinical correlation. We tested whether reports without meaningful RFE were more likely to suggest clinical correlation (Fisher's exact test).

RESULTS

Average inter-rater agreement for assessing RFE meaningfulness was kappa = 0.53. Of RFEs, 12.9% (5,716/44,162) were not meaningful. Of the reports, 0.8% (359/44,162) suggested clinical correlation. In reports with meaningful RFE, 0.8% suggested clinical correlation. In reports without meaningful RFE, 1.2% suggested clinical correlation. Thus, reports without meaningful RFE are 57.9% more likely to suggest clinical correlation than reports with meaningful RFE (P = 0.001).

CONCLUSION

Our study shows that in an uncontrolled environment, lack of meaningful RFE increases the prevalence of hedging language in radiology reports. This may be an unanticipated consequence of computerized physician order entry systems that focuses on data completeness for billing purposes rather than optimal information delivery to the radiologist. Novel software solutions that automatically synthesize patient history from the electronic medical record may assist the radiologist in producing high-quality reports.

CLINICAL RELEVANCE/APPLICATION

The clinical relevance of reason for examination ordering may impact the quality of radiology interpretation.

SSG07-02 Initial Effectiveness of a Monitoring System to Correctly Identify Inappropriate Lack of Follow-up for Abdominal Imaging Findings of Possible Cancer

Tuesday, Nov. 29 10:40AM - 10:50AM Room: S402AB

Participants

Hanna M. Zafar, MD, Philadelphia, PA (*Presenter*) Nothing to Disclose
Eilann Santo, MD, Philadelphia, PA (*Abstract Co-Author*) Nothing to Disclose
Peter Dunbar, MD, Philadelphia, PA (*Abstract Co-Author*) Nothing to Disclose
Caroline Sloan, Philadelphia, PA (*Abstract Co-Author*) Nothing to Disclose
Darco Lalevic, Philadelphia, PA (*Abstract Co-Author*) Nothing to Disclose
Tessa S. Cook, MD, PhD, Philadelphia, PA (*Abstract Co-Author*) Nothing to Disclose

PURPOSE

To explore the initial effectiveness of a monitoring system to correctly identify inappropriate lack of follow-up for abdominal imaging findings of possible cancer determined through direct provider contact.

METHOD AND MATERIALS

We identified 298 inpatients, emergency department (ED) patients and outpatients with standardized abdominal radiology reporting codes indicating possible cancer at our tertiary care hospital in July 2013; of these 67 had no documented pathology or imaging follow-up or clinical rationale for lack of follow-up on chart review. Miscoded cases were excluded and providers caring for these patients were e-mailed and telephoned to determine their awareness of the finding and whether follow-up was appropriate (i.e. clinically indicated and completed or not clinically indicated) or inappropriate (i.e. clinically indicated but incomplete). Patient and provider characteristics were collected.

RESULTS

The monitoring system overestimated inappropriate lack of follow-up for abdominal imaging findings of possible cancer in 63% of patients (42/67), mainly due to radiologist miscoding (34%, 23/67) and incomplete chart documentation of appropriate follow-up (24%, 16/67). One in ten patients (7/67) were correctly identified as inappropriately lacking follow-up. Only half of providers caring for correctly coded patients were successfully contacted (51%, 21/41); this was largely attributable to the absence of a documented outpatient provider among inpatient and ED patients (24%, 10/41) half of whom were uninsured or on Medicaid.

CONCLUSION

During the first month, the monitoring system overestimated inappropriate lack of follow-up for imaging findings of possible cancer in over half of patients. The two largest sources of error were incorrect coding of imaging findings and incomplete chart documentation of appropriate follow-up.

CLINICAL RELEVANCE/APPLICATION

Provider feedback is needed to select patients with true inappropriate lack of follow-up for imaging findings of possible cancer among all patients identified by the monitoring system. Thus, the system may increase disparities in inappropriate follow-up among patients with and without listed outpatient providers.

SSG07-03 Extraction of Acute Communicable Findings from Head CT Reports Using Natural Language Processing and Machine Learning: Inter-Reader Agreement and Accuracy of Three Methods

Tuesday, Nov. 29 10:50AM - 11:00AM Room: S402AB

Participants

Falgun H. Chokshi, MD, Marietta, GA (*Presenter*) Nothing to Disclose
Andrew B. Lemmon, MD, Atlanta, GA (*Abstract Co-Author*) Nothing to Disclose
Jinho D. Choi, PhD, Atlanta, GA (*Abstract Co-Author*) Nothing to Disclose

CONCLUSION

NLP and machine learning methods show promise for data mining radiology head CT reports. Further tailoring of methods, larger training annotated data sets, and continued comparisons of techniques should increase machine accuracy.

Background

Recent advances in natural language processing (NLP) using machine learning offer an opportunity to data mine radiology reports at a large scale. Our purpose was to test the accuracy of three document classification methods on a set of 500 head computed tomography (CT) reports for acute and communicable findings.

Evaluation

To analyze study feasibility & establish a human reference standard, two radiology attendings evaluated 20 head CT reports together to standardize annotation. Next, each reader annotated the same 500 head CT reports for 5 parameters: acute intracranial bleed, mass effect, acute stroke, hydrocephalus, and overall study severity using a scale of 0 to 2 (0=not present, 1=present but not new, 2=new or worsening). We then analyzed the inter-reader agreement (Cohen's kappa) and accuracy. Accuracy was measured by dividing agreed annotations by the total annotations. We then built three different baseline methods using NLP and machine learning techniques to determine how accurately the software could predict the values for these categories (using radiologists' rating as "truth"). Five-fold cross validation was used for evaluation. Method 1: bag-of-words, unweighted. Method 2: Bag-of-words, weighted by term frequencies. Method 3: Bag-of-words, weighted by term frequencies, regularized by dual averaging. Our open source NLP software is available at <https://github.com/emorynlp>.

Discussion

The two readers agreed 81-94% of the time and kappa scores were between 0.667 and 0.762, showing substantial agreement. Even with the small amount of pilot data and the minimalistic NLP and machine learning techniques, accuracies for the methods were as follows: Method 1, 78-89%, Method 2, 79-90%, and Method 3, 81-90%. More importantly, the results paralleled those of our radiologists (i.e., high for acute stroke and low for mass effect), suggesting the software is using similar information as humans.

SSG07-04 iWonder - Automated System to Notify Diagnostic Radiologists When Pathology Results are Available

Tuesday, Nov. 29 11:00AM - 11:10AM Room: S402AB

Participants

Thomas W. Loehfelm, MD, PhD, Palo Alto, CA (*Presenter*) Nothing to Disclose
Daniel L. Rubin, MD, MS, Stanford, CA (*Abstract Co-Author*) Nothing to Disclose

CONCLUSION

Annotating plain text reports using comprehensive structured ontologies can facilitate quality control and continuing medical education.

Background

Introduction: Following up on cases is cumbersome and requires periodic manual review of the medical record. An automated system that correlates pathology results with imaging studies can streamline follow-up and identify cases where pathology is discordant with radiology, facilitating continuing medical education. **Design:** We retrieved radiology and pathology reports along

with anonymized patient identifiers. Radiology impression and pathology specimen and diagnosis fields were annotated using the NCBO BioPortal Annotator to identify anatomy and pathology terms from the SNOMEDCT ontology. Reports were considered linked if the radiology report preceded the pathology report and if related anatomic terms were used in the impression and specimen description. Pathology terms in the impression were also mapped to anatomy using the "Finding site:" relationship in SNOMEDCT. For example, "cholecystitis" can be linked to "gallbladder" because the finding site of cholecystitis is defined as the gallbladder in SNOMEDCT.

Evaluation

Data: 36142 pathology reports between 2015-07-01 and 2016-04-01 had both a specimen and diagnosis indicated. 25020 were preceded by at least one radiology report. 103233 SNOMEDCT concepts were identified in 23955 pathology diagnoses, and 42911 concepts were identified in 17850 specimen descriptions. 70333 radiology reports preceded pathology reports. We have annotated 2400 report impressions, identifying 8182 SNOMEDCT anatomy concepts. Cross-referencing the anatomy terms from report impressions and pathology specimens using a transitive closure table yields 708 study matches. A web front end allows radiologists access to their personal list of radiology-pathology links. Users curate their list by acknowledging the pathology result, saving the study to a list, or discarding the match.

Discussion

In the future we plan to explore annotating other sections of the radiology report, remove negated statements before annotating pathology terms, and attempt to determine the degree of confidence in a particular diagnosis expressed by the radiologist.

Honored Educators

Presenters or authors on this event have been recognized as RSNA Honored Educators for participating in multiple qualifying educational activities. Honored Educators are invested in furthering the profession of radiology by delivering high-quality educational content in their field of study. Learn how you can become an honored educator by visiting the website at: <https://www.rsna.org/Honored-Educator-Award/>

Daniel L. Rubin, MD, MS - 2012 Honored Educator
Daniel L. Rubin, MD, MS - 2013 Honored Educator

SSG07-05 Using Artificial Intelligence to Improve Communication of Critical Results

Tuesday, Nov. 29 11:10AM - 11:20AM Room: S402AB

Participants

Luciano M. Prevedello, MD, MPH, Dublin, OH (*Presenter*) Nothing to Disclose
Barbaros S. Erdal, PhD, Columbus, OH (*Abstract Co-Author*) Nothing to Disclose
Richard D. White, MD, Columbus, OH (*Abstract Co-Author*) Nothing to Disclose

CONCLUSION

By expediting the initial recognition of critical imaging findings, Deep Learning has promise to positively impact patient care, improve adherence the local policies, and increase compliance to national regulations.

Background

Optimal communication of critical results is fundamental to clinical practice and is a National Patient Safety Goal proposed by the Joint Commission. In busy practices, a major source of delay in communicating a critical result relates to delays in recognizing the critical finding itself. This is especially true when a large number of competing high priority imaging studies are available. Short of having a radiologist screening every study, there has not been a practical solution; this is changing with the advent of Deep Learning. Deep Learning is a class of machine learning that has been successfully used in a variety of Artificial Intelligence applications including speech recognition, self-driving vehicles, and face recognition. We have evaluated the performance of a Deep Learning algorithm in recognizing critical imaging findings present in head CTs.

Evaluation

A total of 320 de-identified head CT images were utilized. The database was initially divided into 160 abnormal cases containing emergent intracranial findings (e.g. acute intracranial hemorrhage, cerebral contusions, tumors with mass effect, and occlusive venous sinus thrombosis), with the remaining 160 cases containing no emergent finding. Seventy five percent (75%) of the cases were randomly assigned to a training set and 25% to a validation set. The images were processed using a convolutional neural network using Caffe as the platform. The accuracy of the algorithm reached 87% after 30 iterations.

Discussion

This initial experience supports the deployment of the Deep Learning algorithm in clinical practice to screen head CT studies for potential critical findings. Once the algorithm detects a positive case, the study could be labeled as potentially critical and automatically receive a higher priority in the reading worklist (image); the application could then page the covering neuroradiologist for immediate review so the appropriate communication of the imaging findings could be accomplished more promptly.

SSG07-06 Radiology Report Terminology: Interpretive Differences between Patients and Radiologists

Tuesday, Nov. 29 11:20AM - 11:30AM Room: S402AB

Awards

Student Travel Stipend Award

Participants

Marina I. Mityul, MD, Saint Louis, MO (*Presenter*) Nothing to Disclose
Adam Searleman, BS, St. Louis, MO (*Abstract Co-Author*) Nothing to Disclose
Jennifer L. Demertzis, MD, Saint Louis, MO (*Abstract Co-Author*) Nothing to Disclose
Andrew J. Gunn, MD, St. Louis, MO (*Abstract Co-Author*) Nothing to Disclose

PURPOSE

Little is known about how patients interpret the terminology used by radiologists. Thus, we surveyed patients and radiologists to

Little is known about how patients interpret the terminology used by radiologists. Thus, we surveyed patients and radiologists to better understand how each group views commonly used phrases within the radiology report.

METHOD AND MATERIALS

138 patients and 113 radiologists were invited to participate in the anonymous survey. Respondents were asked to assign a statistical likelihood of the presence of cancer based upon the terminology used within a hypothetical radiology report. Common phrases such as "likely represents cancer," "compatible with cancer," "consistent with cancer," "concerning for cancer," "may represent cancer," "suspicious for cancer," "cannot exclude cancer," "diagnostic for cancer," "probably represents cancer," and "represents cancer" were evaluated. Potential responses for the statistical likelihoods included: 0-25%, 26-50%, 51-75%, 76-99%, and 100%. For statistical analysis, responses were given a numeric value by the authors on a 1-5 scale (1 = 0-25%; 2 = 26-50%; 3 = 51-75%; 4 = 76-99%; 5 = 100%).

RESULTS

115 patients (83.3% response rate) and 59 radiologists (52.2% response rate) participated. There was a significant difference in the assigned statistical likelihoods between the two groups for almost all phrases (Figure 1). The phrase "probably represents cancer" (mean: 4.16, 95%CI: 3.97-4.34) was selected by patients as conferring the highest statistical likelihood even though radiologists rated this phrase as conferring the sixth highest likelihood (mean: 3.64, 95%CI: 3.49-3.80) ($p < 0.0001$). Radiologists selected the phrase "diagnostic for cancer" as conveying the highest statistical likelihood (mean: 4.79; 95%CI: 4.69-4.90) while patients ranked this phrase as having the third highest statistical likelihood (mean: 3.33; 95%CI: 3.10-3.57) ($p < 0.0001$). The phrase "cannot exclude cancer" was assigned the lowest statistical likelihood by both groups; although patients assigned it a higher likelihood (mean: 2.23, 95%CI: 2.03-2.44) than radiologists (mean: 1.78, 95%CI: 1.56-2.00) ($p = 0.036$).

CONCLUSION

Patients' perceptions of terminology within the radiology report are not synonymous with those of radiologists. These differences could lead to confusion and dissatisfaction.

CLINICAL RELEVANCE/APPLICATION

Radiologists should consider that patients read their reports, and work to use unambiguous terms that communicate the results of an examination more clearly and effectively.

SSG07-07 Natural Language Processing to Automatically Categorize Recommendation Statements in Radiology Reports: Starting to Close the Loop

Tuesday, Nov. 29 11:30AM - 11:40AM Room: S402AB

Participants

Thomas W. Loehfelm, MD, PhD, Palo Alto, CA (*Presenter*) Nothing to Disclose
Andrew B. Lemmon, MD, Atlanta, GA (*Abstract Co-Author*) Nothing to Disclose
Daniel L. Rubin, MD, MS, Stanford, CA (*Abstract Co-Author*) Nothing to Disclose

PURPOSE

Radiologists often make recommendations ranging from clinical correlation to urgent action, but don't generally follow-up on them. An automated system that correctly classifies recommendations could be used to triage those statements that require closing the communication loop, without disrupting normal workflow.

METHOD AND MATERIALS

All CT, MRI, and US reports in a three month window ($n = 25039$) were analyzed for sentences in the impression containing the word "recommend" or "consider". Strings containing the identified sentence and the sentence preceding it were considered potential recommendation statement ($n = 3548$). Two radiologists reviewed 511 statements and categorized them as: Not a recommendation General preventative health recommendation Clinical correlation Routine follow-up Nonurgent action Urgent action A Random Forest classifier was applied to bag of words models of consensus statements using Weka Machine Learning Software. The classifier was tested using 10-fold cross validation of the training set. The F measure, which takes into account precision and recall, is used as the primary performance metric.

RESULTS

Interobserver Variability: Two radiologists agreed on categories for 458/511 (89.6%) potential recommendation statements, yielding the consensus data set with the following category distribution: 18 18 133 155 134 0 Only four statements in the original set of 511 were assigned to category 6 ("urgent action") by either of the reviewers, and in all four cases the reviewers disagreed, so none made it to the consensus data set. **Automatic Categorizer:** The Random Forest classifier correctly assigned 397/458 (86.6%, F measure = 0.862) of the consensus statements. Performance by category was (n , F measure): 6/18 (0.5) 18/18 (0.947) 119/133 (0.847) 147/155 (0.942) 107/134 (0.82)

CONCLUSION

Radiologists use imprecise and ambiguous language that impedes understanding. Two radiologists classifying recommendations from radiology reports only agreed 89.6% of the time. A Random Forest classifier correctly classified 86.7% of statements that the radiologists categorized. Such a classifier can be used to triage recommendations to facilitate closed-loop communication follow-up.

CLINICAL RELEVANCE/APPLICATION

Natural language processing tools can extract information from reports without disrupting the normal workflow of radiologists, facilitating the reporting and follow-up of findings and recommendations.

Honored Educators

Presenters or authors on this event have been recognized as RSNA Honored Educators for participating in multiple qualifying educational activities. Honored Educators are invested in furthering the profession of radiology by delivering high-quality educational content in their field of study. Learn how you can become an honored educator by visiting the website at: <https://www.rsna.org/Honored-Educator-Award/>

Daniel L. Rubin, MD, MS - 2012 Honored Educator
Daniel L. Rubin, MD, MS - 2013 Honored Educator

SSG07-08 Knowledge Representation of Prostatic Sector Anatomy from PI-RADS in Standard Lexicons

Tuesday, Nov. 29 11:40AM - 11:50AM Room: S402AB

Participants

David A. Clunie, MBBS, Bangor, PA (*Presenter*) Owner, PixelMed Publishing LLC; Consultant, Carestream Health, Inc; Consultant, CureMetrix, Inc; Consultant, MDDX Research & Informatics; Consultant, General Electric Company; ;
Andriy Fedorov, PhD, Boston, MA (*Abstract Co-Author*) Nothing to Disclose

CONCLUSION

Proactive incorporation of the PIRADS anatomical concepts in common lexicons assures interoperability, facilitates knowledge sharing, and enables communication of PIRADS results in DICOM SR. Supported by NCI U01 CA190819 - ITCR QIICR project.

Background

The PI-RADS Prostate Imaging - Reporting and Data System (PI-RADS v2) standardizes reporting of Multiparametric Magnetic Resonance Imaging (mpMRI). Communication of the precise localization of lesions is important clinically and for research. PI-RADS defines a sector map of the prostate anatomy but not a formal encoding or representation. Manual, semi-automated or automated annotations of lesion locations need to be labeled with pre-coordinated coded anatomical concepts for each sector. It is desirable to define the spatial relationships between these anatomic concepts to facilitate automated knowledge extraction. This abstract describes the definition of concepts corresponding to each of the 36 prostatic sectors defined in the PI-RADS Appendix II Sector Map in the form of an extension to existing medical anatomical ontologies, including the Foundational Model of Anatomy (FMA), SNOMED CT, the NCI Thesaurus and RadLex.

Evaluation

A survey of terminology sources evaluated the comprehensiveness of coverage of prostatic anatomy. None contained PIRADS v2 sector concepts. FMA contained the most detail, with concepts for peripheral, central and transition zones, and apical, middle and basal parts, but lacked subdivision into sectors, and concepts were not permuted with laterality.

Discussion

Using Protégé, FMA was extended with PIRADS sector classes, and OWL files and tabulated concepts submitted to FMA, SNOMED, NCI and RadLex for future inclusion. Added concepts were subdivisions of zones of the prostate; "regional part of" relationships were used for laterality and combined regions with more granular sectors. Concept were related to neighbors by "spatially related to" relationships, such as "anterior to". Practical use of the coded PIRADS v2 concepts was tested in DICOM Structured Reports using the Measurement Template (TID 1500) Finding Site, for single unifocal, multifocal and multiple lesions.

SSG07-09 Development and Evaluation of Natural Language Processing Software to Produce a Summary of Inpatient Radiographic Findings Identified for Follow-Up

Tuesday, Nov. 29 11:50AM - 12:00PM Room: S402AB

Awards

Student Travel Stipend Award

Participants

Ian R. Whiteside, MD, Stony Brook, NY (*Presenter*) Nothing to Disclose
Iv Ramakrishnan, PhD, Stony Brook, NY (*Abstract Co-Author*) Nothing to Disclose
Ritwik Banerjee, PhD, Stony Brook, NY (*Abstract Co-Author*) Nothing to Disclose
Vasudev Balasubramanian, Stony Brook, NY (*Abstract Co-Author*) Nothing to Disclose
Basava Raju Kanaparthi, Stony Brook, NY (*Abstract Co-Author*) Nothing to Disclose
Matthew A. Barish, MD, Stony Brook, NY (*Abstract Co-Author*) Nothing to Disclose

CONCLUSION

Manual and NLP searches for inpatient recommendations agree at a frequency sufficient to justify generation of an automated radiology discharge summary to avoid delayed or failed follow-up. NLP software accurately detects follow-up keywords in our test population of "long stay" inpatients. We are continuing to train, test and enhance the software to produce summaries containing pathologic findings, relevant anatomy, and recommendations.

Background

Hospital inpatients are subjected to multiple radiographic examinations during single admissions with frequent recommendations for follow-up of incidental findings. Urgent requirements of the patients' care may postpone follow-up during an inpatient stay and result in failure of follow-up. Inclusion of follow-up recommendations in the discharge summary may mitigate this risk. We are evaluating a natural language processing (NLP) software tool to produce a "radiology discharge summary" to facilitate follow-up of incidental findings.

Evaluation

We obtained 503 radiographic reports from our radiology report repository by randomly selecting 43 patients with at least 7 inpatient days. A physician manually annotated the reports by searching for expressions indicating the necessity for follow-up along with pertinent anatomy, details of pathologic findings and recommendations for follow-up. A list of keywords was extracted: recommend, correlate, follow-up, consider, advise, suggest, beneficial, could perform, further evaluation, can be obtained. We trained the NLP software using the annotated reports, keywords and keyword permutations.

Discussion

There were 32 multi-study reports, resulting in 471 unique reports. 106 instances of the keywords were found in 61(13%) reports resulting in 79(17%) unique recommendations. 71(90%) recommendations were addressed during the inpatient stay or in the

discharge summary. At this stage the NLP software identified 103(97%) keywords in the impression of the report. 3 keywords were not found as they were not included in the impression. NLP pattern recognition found relevant anatomy 28(53%) times in the keyword sentence, 12(23%) times in the sentence prior, and 9(17%) times prior to that. 4(8%) of relationships were misclassified.

SSG08

Science Session with Keynote: Molecular Imaging (Brain)

Tuesday, Nov. 29 10:30AM - 12:00PM Room: S504CD



AMA PRA Category 1 Credits™: 1.50
ARRT Category A+ Credits: 1.50

FDA Discussions may include off-label uses.

Participants

Jonathan E. McConathy, MD, PhD, Birmingham, AL (*Moderator*) Research Consultant, Eli Lilly and Company; Research Consultant, Blue Earth Diagnostics Ltd; Research Consultant, Siemens AG; Research Consultant, General Electric Company;
Satoshi Minoshima, MD, PhD, Salt Lake City, UT (*Moderator*) Royalties, General Electric Company; Research Consultant, Hamamatsu Photonics KK; Research Grant, Hitachi, Ltd; Research Grant, Nihon Medi-Physics Co, Ltd;

Sub-Events

SSG08-01 Molecular Imaging Keynote Speaker: A Short Overview on Relevant PET-Tracers for Brain Imaging

Tuesday, Nov. 29 10:30AM - 10:40AM Room: S504CD

Participants

Jonathan E. McConathy, MD, PhD, Birmingham, AL (*Presenter*) Research Consultant, Eli Lilly and Company; Research Consultant, Blue Earth Diagnostics Ltd; Research Consultant, Siemens AG; Research Consultant, General Electric Company;

SSG08-02 Radiogenomics Association and Comparison between Multiple Angiogenesis Imaging Surrogates derived from MR Perfusion Imaging and Molecular Genomic Biomarkers in Predicting Overall Survival in Patients with New Diagnosed Glioblastomas

Tuesday, Nov. 29 10:40AM - 10:50AM Room: S504CD

Participants

Xiang Liu, MD, Rochester, NY (*Presenter*) Nothing to Disclose
Wei Tian, MD, PhD, Rochester, NY (*Abstract Co-Author*) Nothing to Disclose

PURPOSE

Angiogenesis plays an important role in tumor proliferation and invasion, which is associated with poor survival outcome in glioblastomas. The purpose of this study is to investigate the genomic mechanism of MR perfusion abnormalities, and compared their prognostic value in predicting overall survival (OS) in glioblastoma patients.

METHOD AND MATERIALS

41 new diagnosed glioblastoma cases (mean age is 62.32±12.09) were enrolled. The molecular and genomics biomarkers of TP53, Ki-67 labelling index, isocitrate dehydrogenase (IDH), mammalian target of rapamycin (mTOR), and epidermal growth factor receptor (EGFR) were evaluated. Multiple relative cerebral blood volume (rCBV) parameters were measured based on ROI-based approach and voxel-based histogram analysis, including mean and maximal rCBV ratio, as well as 15%, 25%, 50%, 75%, 85% quantiles and the interquartile range (IQR) of rCBV ratio in the enhancing tumor, and maximal rCBV ratio of peri-enhancing tumor area (rCBVperi-tumor). The radiogenomics association analysis, Cox regression and Kaplan-Meier survival analysis were performed to compare the predictive value between imaging parameters, and molecular genomic biomarkers.

RESULTS

The rCBVmax, and 50%, 75%, 85% quantiles and IQR had significant association with mTOR, ($p=0.047$) without adjustment of age, gender and EGFR/mTOR. The rCBVperi-tumor showed significant correlation with mTOR and EGFR ($p=0.0183$ and 0.0047 separately). The Cox regression analysis showed that rCBVperi-tumor and age were the two strongest predictors of OS (hazard ratio= 1.29 and 1.063 separately). ROC analysis showed that the rCBVperi-tumor had better prognostic value than molecular genomic biomarkers, and the rCBVperi-tumor threshold of 3.13 could be used to predict shorter OS with specificity of 78.9% and sensitivity of 77.3%.

CONCLUSION

The difference of radiogenomic association in enhancing and peri-enhancing areas may suggest different moderation of angiogenesis by the mTOR-EGFR pathway in glioblastomas. The rCBVperi-tumor had better prognostic value. These findings will be useful for development of new targeting therapies aiming to tumor proliferation and vasculature infiltration, and future design of personalized multimodality treatment.

CLINICAL RELEVANCE/APPLICATION

The mTOR-EGFR pathway had different moderation on rCBV change within glioblastomas, the rCBVperi-tumor had better prognostic value than molecular genomic biomarkers alone.

SSG08-03 In Vivo MR Tacking of Labeled Adoptive T Cells with Ultrasmall Multi-Modal Nanoprobes in Orthotopic Glioma

Tuesday, Nov. 29 10:50AM - 11:00AM Room: S504CD

Participants

Hua Zhang, ShangHai, China (*Presenter*) Nothing to Disclose
Yue Wu, Shanghai, China (*Abstract Co-Author*) Nothing to Disclose
Zhenwei Yao, Shanghai, China (*Abstract Co-Author*) Nothing to Disclose

PURPOSE

To establish a novel T1MR-based multi-modal nanoparticles to effectively label adoptive T cells and achieve in vivo noninvasive tracking in orthotopic glioma.

METHOD AND MATERIALS

In vivo MR tracking was performed on a 3-T unit scanner (Signa, GE Medical Systems) with an 8-channel mouse coil. Orthotopic GL261 glioma were planted in C57/BL6 mice. HIV-1 transactivator (TAT) peptides were introduced into the surface of FITC-NaGdF4 to improve labeling efficiency. The effects of multi-modal nanoprobe on adoptive T cells viability, proliferation and functions were measured by CCK-8, enzyme-linked immunosorbent assay (ELISA) and flow cytometric analysis and compared with natural adoptive T cells. Axial T1 weighted images of mice brain were collected at different time points after intravenous infusion of 107 labeled T cells (experimental group) and unlabeled T cells (control group).

RESULTS

Ultra-small T1MR-based multi-modal nanoparticles (TAT/FITC-NaGdF4) were successfully developed with high longitudinal relaxivity ($8.93 \text{ s}^{-1}\text{mM}^{-1}$) and favorable stability. It can label adoptive T cells with over 95% efficacy, remarkably superior to FITC-NaGdF4 nanoparticles. Quantitative ICP analysis showed that internalization of Gd contents reached a plateau at five hours after co-incubation with adoptive T cells. The results of CCK-8 indicated that the optimal nanoparticle concentration of labeling was $500 \mu\text{g Gd/ml}$. There were no significant differences of the short and long-term viability, proliferative capacity, production of cytokines and expression levels of surface receptors between unlabeled and labeled T cells with TAT/FITC-NaGdF4 nanoprobe. Labeled T-cell clusters can be sensitively detected in C57/BL6 mouse orthotopic glioma at 24h by T1-weighted MR, which signal was distinctly higher than control group.

CONCLUSION

Adoptive T-lymphocytes can be efficiently labeled by novel multi-modal nanoparticles (TAT/FITC-NaGdF4) without measurable effects on their properties and be sensitively detected in vivo orthotopic glioma by T1MR.

CLINICAL RELEVANCE/APPLICATION

TAT/FITC-NaGdF4 nanoprobe acts as the novel and high-performance T1MR-based multi-modal contrast agent, which can label T cells with high efficacy and without any measurable effects on T cell properties.

SSG08-04 Noninvasive Tracking the Kinetic Phases of Distribution and Glioblastoma Targeting of EGFRvIII-specific Chimeric Antigen Receptor T Cells via MRI

Tuesday, Nov. 29 11:00AM - 11:10AM Room: S504CD

Participants

Xiao Chen, Chongqing, China (*Presenter*) Nothing to Disclose

Weiguo Zhang, Chongqing, China (*Abstract Co-Author*) Nothing to Disclose

Tian Xie, Chongqing, China (*Abstract Co-Author*) Nothing to Disclose

PURPOSE

Glioblastoma (GBM) is the most common primary malignant brain tumor in adults and is uniformly lethal. T-cell-based immunotherapy offers a promising platform for treatment given its potential to specifically target tumor tissue while sparing the normal brain. However, the challenge of monitoring the therapy in real time has been continually ignored. To address this issue, we developed MR imaging approaches to evaluate a recently reported novel CAR strategy for adoptive immunotherapy against glioma xenografts expressing EGFRvIII.

METHOD AND MATERIALS

T cells, isolated from the peripheral blood of healthy donors, were transduced by EGFRvIII-specific human CAR (EGFRvIII-CAR). Flow cytometry was used to detect CAR expression on transduced T cells. Elevated concentration of USPIO was labeled CAR T cells. The biological properties of these cells were detected. Cytotoxicity assay and cytokine production were analyzed in vitro. Then, USPIO-CAR T cells were transplanted into the nude mice bearing U87-EGFRvIII glioma. MRI and immunohistochemistry were performed.

RESULTS

We successfully labeled EGFRvIII-CAR T cells with USPIO without any influence on the biological properties and toxicity to tumor of these cells. After intravenous administration into glioma-bearing nude mice, the USPIO-EGFRvIII-CAR T cells specifically homed to gliomas and could be reliably tracked by 7.0 T MR as early as 1 day after transplantation, causing hypointensity on T2-weighted images. Prussian blue staining and CD3 immunohistochemistry staining confirmed the MRI findings. Infusion with EGFRvIII-CAR T cells led to cures in all mice with brain gliomas.

CONCLUSION

This therapeutic strategy offered efficient therapy effect to EGFRvIII+ glioma-bearing mice and implied that MR imaging is a highly useful tool in tracking the kinetic phases of CAR T cells distribution and monitoring its therapeutic effect.

CLINICAL RELEVANCE/APPLICATION

We will establish a new technological platform and evaluation system for in vivo tracking of CAR-T immunotherapy of GBM and other solid tumors to guide the design and improvement of new CAR with high penetration, proliferation and cytotoxicity in future, which will have great significance to the development of CAR-T immunotherapy and improvement of therapeutic efficacy in solid tumor.

SSG08-05 Imaging Aggregates, Fibrils, and Plaques using Small-Angle X-Ray Scattering: Initial Computational Modeling and Measurements Towards Designing an Anthropomorphic Phantom with Applications in Alzheimer's Disease

Tuesday, Nov. 29 11:10AM - 11:20AM Room: S504CD

Participants

Mina Choi, MS, Silver Spring, MD (*Abstract Co-Author*) Nothing to Disclose
Eshan Dahal, Silver Spring, MD (*Abstract Co-Author*) Nothing to Disclose
Nadia Alam, Silver Spring, MD (*Abstract Co-Author*) Nothing to Disclose
Bahaa Ghamraoui, Silver Spring, MD (*Abstract Co-Author*) Nothing to Disclose
Andreu Badal-Soler, Silver Spring, MD (*Abstract Co-Author*) Nothing to Disclose
Aldo Badano, PhD, Silver Spring, MD (*Presenter*) Research Grant, Barco nv

PURPOSE

Protein aggregates play significant roles in many biological processes and diseases. For instance, beta-amyloid plaques and tau tangles have been shown to have an effect in the development of Alzheimer's (AD), a neurodegenerative disease characterized by impaired memory, reduce cognitive skills, and diminished ability to perform everyday tasks affecting over 5 million Americans for which there is currently no cure or effective treatment. This work discusses computational modeling and physical phantom studies that show the potential of small-angle x-ray scattering (SAXS) imaging for detecting and characterizing aggregates, fibrils, and plaques of relevance for Alzheimer's and other neurological diseases.

METHOD AND MATERIALS

Optical imaging techniques for the characterization of the molecular AD hallmarks lack the ability to image deep tissue. PET imaging is used to locate beta-amyloid plaques in the brain but suffers from low spatial resolution and low specificity. SAXS can characterize and selectively image structures based on electron density maps without any additional contrast agents. We report SAXS measurements of beta-amyloid-42 aggregation in a 50% dimethyl sulfoxide solution and Bovine Serum Albumin (BSA) under various temperatures which form amyloid-like fibrils. We compare measured signals with theoretical estimates and use the measured and theoretical cross sections to perform simulations using a publicly available, GPU-accelerated, Monte Carlo radiation transport tool. This tool is modified for cross-section sampling at relevant small scattering angles allowing user-generated cross sections accounting for interference effects using uniform and anatomically accurate phantoms.

RESULTS

We obtained reconstructed scatter profiles for different target materials using experimentally measured cross sections showing increased contrast at peak scattering angles consistent with the structure of the BSA aggregates. Various phantom design approaches will be discussed including a flowing sample design and an encasing approach.

CONCLUSION

The findings of the study indicate that BSA aggregation states can be reproduced by controlling pH levels in solvents. A physical phantom for imaging aggregates might be feasible.

CLINICAL RELEVANCE/APPLICATION

These studies will contribute to assessing the feasibility and providing the tools needed for the design and optimization of SAXS imaging systems to measure AD biomarkers in vivo.

SSG08-06 Quantitative Analysis of Amide Proton Transfer (APT) and Nuclear Overhauser Enhancement (NOE) Contrasts in Rat Glioma

Tuesday, Nov. 29 11:20AM - 11:30AM Room: S504CD

Participants

Yuwen I. Zhou, PhD, Charlestown, MA (*Presenter*) Nothing to Disclose
Takahiro Takahiro, Charlestown, MA (*Abstract Co-Author*) Nothing to Disclose
Phillip Zhe Sun, PhD, Charlestown, MA (*Abstract Co-Author*) Nothing to Disclose

PURPOSE

Amide proton transfer (APT), a specific form of Chemical Exchange Saturation Transfer (CEST) MRI, detects endogenous amide protons and has been increasingly used for tumor detection and grading. However, the origin of APT CEST contrast in tumors has not been fully explained, because the routine asymmetry analysis (MTRAsym) is susceptible to confounding effects, such as spillover saturation and concomitant semisolid magnetization transfer (MT). In addition to APT, nuclear Overhauser enhancement (NOE) effects upfield from water also contributes to the observed CEST contrast. Here we combined analytic solution and numerical fitting to correct for spillover effect and decompose the contributions from APT, NOE and MT effects to CEST contrast in rat glioma.

METHOD AND MATERIALS

The non-infiltrating D74-rat glioma model was used. The animals (N=8) were imaged 11-13 days after tumor cell implantation using a 4.7T scanner. Multi-parametric MRI including T1, T2 mapping and CEST MRI was performed. CEST Z-spectrum were acquired with continuous-wave saturation pulses (0.75 μ T for 5 s) with 49 frequency offsets evenly distributed from -6 to 6 ppm relative to the water resonance.

RESULTS

The spillover corrected Z-spectrum was obtained by subtracting the experimental Z-spectrum from the Z-spectrum analytically derived from relaxation measurements (Fig1a). After corrections for spillover effect, multi-Lorentzian fitting of the corrected Z decoupled the contribution of different pools (Fig1b). The fitted APT, NOE and MT effects were further corrected for the influence of the longitudinal relaxation of the water pool (Fig2). Fig3 shows that corrected APT in tumors significantly increased in tumor tissues ($p < 0.005$, paired t-test), while corrected NOE and MT effects in tumors showed significant decreases compared with those in normal tissues ($p < 0.001$, paired t-test).

CONCLUSION

By combining analytic solution and numerical fitting, we were able to decouple individual contributions from APT, NOE and MT effects, providing better understanding of the CEST contrast in tumors and assisting in the development of improved APT and NOE measurements for cancer imaging.

CLINICAL RELEVANCE/APPLICATION

Relaxation-based correction of spillover effects simplifies quantitative analysis of APT and NOE contrasts in rat glioma, providing better understanding of the CEST contrast in tumors and assisting in the development of improved APT and NOE measurements for cancer imaging.

SSG08-07 Therapeutic Efficacy of Treg in Diabetic Stroke: Measurement with an Ultrafast MMP Activatable Probe

Tuesday, Nov. 29 11:30AM - 11:40AM Room: S504CD

Participants

Yu Cai, Nanjing, China (*Presenter*) Nothing to Disclose

Shenghong Ju, MD, PhD, Nanjing, China (*Abstract Co-Author*) Nothing to Disclose

PURPOSE

To measure the therapeutic efficacy of endogenous Treg cell in diabetic stroke by a novel and ultrafast MMP activatable probe.

METHOD AND MATERIALS

T2 diabetes mellitus was induced in C57BL/6(8-week-old) mice by administration of high-fat diet in combination with intraperitoneal injection of streptozotocin. CD28 superagonistic (200ug/mouse) was injected intraperitoneally 3-6 hours after photothrombotic stroke onset in wildtype mice and diabetic mellitus mice to boost the expression of endogenous regulatory T cells. Gelatin zymography assay, Immunofluorescent staining, T2-weighted MR scans and Near-infrared fluorescence (NIRF) imaging were performed on day 7 post stroke.

RESULTS

The group which was treated with CD28 SA, presented smaller infarct volume compared with control group, especially in diabetic mice (9.73%±2.25 vs.13.32%±2.24 in diabetic stroke group, p=0.16; 7.23%±0.45 vs. 9.29%±1.64 in wildtype stroke, p=0.014) (Figure 1).The results of Immunofluorescent staining and gelatin zymography assay demonstrated that the expression of MMP-9 were decreased in groups treated with CD28 SA (Figure 2). Here, we used a novel MMP activated optical imaging probe to visualize the MMP activity in vivo. Our preliminary results showed that TBR values were increased in diabetic stroke mice and significantly down regulated after treated with CD28 SA(2.05 vs.1.57 in diabetic stroke; 1.78 vs.1.40 in wildtype stroke)(Figure 3).

CONCLUSION

Amplification of regulatory T Cells using a CD28 SA improves outcome of diabetic stroke. Moreover, using MMP activatable probe, we successfully demonstrated the MMP activity and stroke outcome by non-invasive molecular imaging method.

CLINICAL RELEVANCE/APPLICATION

The results of our study is strongly suggest that the molecular imaging approach is valuable for measuring molecular-specific effects of treatment (CD28 SA induced Treg) in diabetic stroke and has great potential for clinical translation.

SSG08-09 Molecular Image-Guided Biopsy in Patients with Newly Diagnosed Gliomas Using Amide Proton Transfer-Weighted (APT_w) MR Imaging

Tuesday, Nov. 29 11:50AM - 12:00PM Room: S504CD

Awards

Student Travel Stipend Award

Participants

Shanshan Jiang, MD, Baltimore, MD (*Presenter*) Nothing to Disclose

Jinyuan Zhou, PhD, Baltimore, MD (*Abstract Co-Author*) License agreement, Koninklijke Philips NV

Charles Eberhart, MD, PhD, Baltimore, MD (*Abstract Co-Author*) Nothing to Disclose

Yi Zhang, Baltimore, MD (*Abstract Co-Author*) Nothing to Disclose

Hye-Young Heo, Baltimore, MD (*Abstract Co-Author*) Nothing to Disclose

Zhibo Wen, Guangzhou, China (*Abstract Co-Author*) Nothing to Disclose

Lindsay Blair, Baltimore, MD (*Abstract Co-Author*) Nothing to Disclose

Huamin Qin, Baltimore, MD (*Abstract Co-Author*) Nothing to Disclose

Michael Lim, Baltimore, MD (*Abstract Co-Author*) Nothing to Disclose

Alfredo Quinones-Hinojosa, Baltimore, MD (*Abstract Co-Author*) Nothing to Disclose

Peter B. Barker, DPhil, Baltimore, MD (*Abstract Co-Author*) Nothing to Disclose

Martin G. Pomper, MD, PhD, Baltimore, MD (*Abstract Co-Author*) Shareholder, CTS, Inc; Board Member, CTS, Inc; Research Grant, CTS, Inc; Advisor, CTS, Inc; Institutional license agreement, Progenics Pharmaceuticals, Inc; Institutional license agreement, Advanced Accelerator Applications SA; Institutional license agreement, LI-COR, Inc; Institutional license agreement, BIND Therapeutics, Inc

John Laterra, Baltimore, MD (*Abstract Co-Author*) Nothing to Disclose

Peter C. Van Zijl, PhD, Baltimore, MD (*Abstract Co-Author*) Speakers Bureau, Koninklijke Philips NV; License agreement, Koninklijke Philips NV

Jaishri Blakeley, Baltimore, MD (*Abstract Co-Author*) Nothing to Disclose

PURPOSE

Pathological diagnosis remains the gold standard for determining the treatment for malignant gliomas. However, the accuracy of diagnostic neurosurgical procedures is often limited by the heterogeneous characteristics of these tumors. APT imaging is a molecular imaging technique that generates MRI contrast based on endogenous cellular proteins in tissue. We explored APT_w image-guided neuro-navigation and radiopathologic correlation to assess the diagnostic accuracy of APT MRI in defining heterogeneous regions of malignant gliomas.

METHOD AND MATERIALS

Patients (n=24) with previously undiagnosed gliomas underwent a volumetric APT_w imaging sequence. Pre-determined regions of interest on the APT_w images were labeled on the co-registered clinical MR images in the BrainLab neuro-navigation system. The priority regions to sample included: (i) APT_w hyperintense, Gd enhancing; (ii) APT_w hyperintense, Gd non-enhancing; and (iii) APT_w

isointense, Gd enhancing. 70 APTw image-directed stereotactic biopsies were obtained from these 24 patients. Pathologic indices (tumor grade, cellularity, necrosis degree, and proliferation) were analyzed and correlated with corresponding APTw signal intensities.

RESULTS

Based on the histopathological analysis, 33 specimens were diagnosed as WHO grade-II pathology, 14 specimens grade-III, 15 specimens grade-IV, and eight specimens peritumoral edema. Multiple grades were found within a single tumor lesion in six patients. APTw signal intensities of the biopsied sites were significantly higher for high-grade specimens ($2.65 \pm 0.96\%$) than for low-grade specimens ($1.82 \pm 0.54\%$; $P < 0.001$), independent of Gd-enhancement patterns. APTw signal intensities of these biopsied sites showed strong positive correlations with cellularity and proliferation ($R = 0.751$ and 0.538 , respectively; both $P < 0.001$). Multiple linear regression showed that tumor cellularity and proliferation index were the two best predictors of APTw signal intensities ($R^2 = 0.540$; $P < 0.001$).

CONCLUSION

Areas with APTw hyperintensity displayed higher cellularity and higher proliferation suggesting that APTw imaging highlights the most active and aggressive portions of heterogeneous gliomas.

CLINICAL RELEVANCE/APPLICATION

APTw molecular image-guided biopsy procedure can increase precision of tumor sampling in patients with gliomas, particularly in lesions that show no Gd enhancement.

SSG09

Musculoskeletal (Arthritis and Inflammation)

Tuesday, Nov. 29 10:30AM - 12:00PM Room: E450B



AMA PRA Category 1 Credits™: 1.50
ARRT Category A+ Credits: 1.50

Participants

Andrew J. Grainger, MRCP, FRCR, Leeds, United Kingdom (*Moderator*) Speaker, General Electric Company; Equipment support, Siemens AG; Consultant, Medivir AB; Medical Advisor, Medivir AB
Daniel B. Nissman, MD, MPH, Raleigh, NC (*Moderator*) Royalties, John Wiley & Sons, Inc

Sub-Events

SSG09-01 The Atrophic Phenotype of Knee Osteoarthritis is not Associated with Faster Progression of Disease: The Multicenter Osteoarthritis (MOST) Study

Tuesday, Nov. 29 10:30AM - 10:40AM Room: E450B

Participants

Michel D. Crema, MD, Boston, MA (*Abstract Co-Author*) Shareholder, Boston Imaging Core Lab, LLC
Ali Guerhazi, MD, PhD, Boston, MA (*Abstract Co-Author*) President, Boston Imaging Core Lab, LLC Research Consultant, Merck KgaA Research Consultant, Sanofi-Aventis Group Research Consultant, TissueGene, Inc Research Consultant, OrthoTrophic Research Consultant, AstraZeneca PLC
David T. Felson, MD, MPH, Boston, MA (*Abstract Co-Author*) Consultant, Zimmer Biomet Holdings, Inc
Michael C. Nevitt, PhD, San Francisco, CA (*Abstract Co-Author*) Nothing to Disclose
Monica D. Marra, MD, Boston, MA (*Abstract Co-Author*) Shareholder, Boston Imaging Core Lab, LLC
Frank W. Roemer, MD, Boston, MA (*Presenter*) Chief Medical Officer, Boston Imaging Core Lab LLC; Research Director, Boston Imaging Core Lab LLC; Shareholder, Boston Imaging Core Lab LLC; ;

PURPOSE

In tibiofemoral compartments exhibiting fast progression of osteoarthritis (OA), osteophyte formation may lag behind cartilage loss, which might then manifest as an atrophic OA phenotype. The aim of this study was to assess the associations of atrophic tibiofemoral OA with progression of radiographic joint space narrowing (JSN) and magnetic resonance imaging (MRI)-defined progression of cartilage damage.

METHOD AND MATERIALS

Participants of the Multicenter Osteoarthritis (MOST) Study with available radiographic and 1.0T MRI assessments at baseline and 30 months follow-up (FU), were included. Radiographs were assessed according to the OARSI system for JSN and osteophytes (grades 0-3). Ten tibiofemoral regions were assessed on MRI for cartilage morphology (grades 0-6) and osteophytes (grades 0-7) using the WORMS system. On radiographs, atrophic OA was defined as OARSI grades 1 or 2 for JSN and grade 0 for osteophytes. On MRI, atrophic OA was defined as tibiofemoral cartilage damage grades ≥ 3 in at least 2 of 10 subregions with absent or equivocal osteophytes (grades 0 and 1) in all subregions. Progression of JSN and cartilage loss on MRI, was defined as 1) no, 2) slow, and 3) fast progression. Chi-square test and logistic regression with generalized estimated equations were performed to assess the association of atrophic knee OA with any progression, compared to non-atrophic OA knees (reference group).

RESULTS

A total of 476 knees from 432 participants were included. Using the radiographic definition, 50 (10.5%) had atrophic OA and 426 (89.5%) had non-atrophic OA knees at baseline. Using the MRI definition, there were 16 (3.4%) knees with atrophic OA and 460 (96.6%) with non-atrophic OA. Non-atrophic OA knees more commonly exhibited fast progression of JSN ($p=0.002$) and fast progression of MRI cartilage damage ($p=0.02$). Logistic regression showed that the atrophic phenotype of knee OA was modestly protective against progression of JSN and MRI when compared to non-atrophic OA knees.

CONCLUSION

In this sample of subjects with or at risk for knee OA the atrophic phenotype of knee OA did not predispose to more rapid progression compared to non-atrophic OA. Instead, the atrophic phenotype demonstrated a decreased risk for OA progression.

CLINICAL RELEVANCE/APPLICATION

Our results may potentially impact on subject selection in clinical trials of knee OA, as the atrophic phenotype is not associated with more progression of disease.

Honored Educators

Presenters or authors on this event have been recognized as RSNA Honored Educators for participating in multiple qualifying educational activities. Honored Educators are invested in furthering the profession of radiology by delivering high-quality educational content in their field of study. Learn how you can become an honored educator by visiting the website at: <https://www.rsna.org/Honored-Educator-Award/>

Ali Guerhazi, MD, PhD - 2012 Honored Educator

SSG09-02 Does Contrast-Enhanced MRI Sequence have Incremental Value in the Assessment of Active Sacroiliitis?

Tuesday, Nov. 29 10:40AM - 10:50AM Room: E450B

Participants

Siyoun Sung, MD, Seoul, Korea, Republic Of (*Abstract Co-Author*) Nothing to Disclose
Jong Won Kwon, MD, Seoul, Korea, Republic Of (*Presenter*) Nothing to Disclose

PURPOSE

To evaluate if contrast-enhanced MRI sequence increase the diagnostic value in the assessment of active sacroiliitis in patients with inflammatory back pain.

METHOD AND MATERIALS

Ninety-two patients with impression of inflammatory back pain were enrolled. All patients underwent MRI which contains coronal short tau inversion recovery (STIR) image, axial T2-weighted image with fat suppression (T2FS), and coronal and axial contrast-enhanced T1-weighted images with fat suppression (CET1FS). Two observers reviewed a set of coronal STIR with axial T2FS, and a set of coronal and axial CET1FS independently in two separate sessions. The presence and degree of bone marrow edema and osteitis were evaluated on each set. Each sacroiliac joint was divided into 4 quadrants and severity per quadrant was assigned a score of 0–4. Defining active sacroiliitis or not was made based on the findings of obvious subchondral bone marrow edema or osteitis (score 2 or more) in any quadrants. Presence of additional findings of active sacroiliitis such as synovitis, enthesitis, and capsulitis were evaluated. Cohen's kappa coefficients were used for the comparison of positivity of active sacroiliitis between two observers for same set, and between sets for each observer. Kendall's tau-b values were used for the comparison of scores of each quadrant between two observers for same set, and between sets for each observer. The z test for two population proportions was used to compare proportion of positive additional finding for between sets for same observer.

RESULTS

Cohen's kappa coefficients between two observers for same set were 0.956 and 0.978 for contrast-enhanced images and T2FS with STIR each. Cohen's kappa coefficients between two sets for each observer were 0.892 and 0.870. Kendall's tau-b value between two observers for same set and between sets for each observer was more than 0.783 in all quadrants, showing good agreement. There was no significant difference of proportion of positive cases for all additional findings for both observers.

CONCLUSION

The contrast-enhanced MRI sequences did not have an incremental value in the assessment of active sacroiliitis compared with the STIR and T2FS sequences

CLINICAL RELEVANCE/APPLICATION

With appropriate sequences and planes, unnecessary usage of contrast-enhanced sequences can be avoidable for the assessment of active sacroiliitis.

SSG09-03 Assessment of Spondyloarthritis using MR Spectroscopy: A Single Peak at 8ppm as a Potential Inflammatory Marker

Tuesday, Nov. 29 10:50AM - 11:00AM Room: E450B

Participants

Seunghun Lee, MD, Seoul, Korea, Republic Of (*Presenter*) Nothing to Disclose
Yoonah Song, MD, Seoul, Korea, Republic Of (*Abstract Co-Author*) Nothing to Disclose
Eun Ju Kim, BA, Seoul, Korea, Republic Of (*Abstract Co-Author*) Nothing to Disclose
Tae-Hwan Kim, Seoul, Korea, Republic Of (*Abstract Co-Author*) Nothing to Disclose

PURPOSE

To evaluate the potential role of magnetic resonance (MR) spectroscopy in patients with inflammatory arthritis, and correlation between active inflammation, C-reactive protein (CRP) and clinical concordance

METHOD AND MATERIALS

From May 2015 to March 2016, 130 consecutive patients with clinically suspected spondyloarthritis (77 men, 53 women; mean age, 30.3 years; range, 14-63 years) were assessed with 3.0-T MR imaging including single-voxel MR spectroscopy. We analyzed the presence of specific metabolite peak of active inflammation group compared them with those of inactive group. We draw two region of interest (ROI) in case of subchondral bone marrow edema and normal bone marrow. Two radiologists analyzed conventional MR findings by consensus: bone marrow edema, location, and presence/absence of active inflammation in sacroiliac joint. We use dedicated software for analyzing MR spectroscopy. Demographic data, MR findings, spectroscopic spectrum and concordance between active inflammation and CRP were compared using chi-square test.

RESULTS

There are 66 patients with active inflammation and the other 64 patients with inactive lesion in sacroiliac joint. All patients with active inflammation showed a single peak of carnosine (8 ppm). However, only 29 patients with active inflammation in sacroiliac joint showed elevated CRP values. In discordant group, 71.7% (33/46) cases showed carnosine peak although negative serologic results. Diagnostic concordance between CRP and MR finding had statistically significant ($p < 0.001$). Carnosine peak and active inflammation had also significant ($p < 0.001$). There was no statistically significant between other variables.

CONCLUSION

MR spectroscopy at 3.0-T with metabolite detection is a helpful method in spondyloarthritis. 8 ppm carnosine peak may be a promising inflammatory marker to detect and follow up active inflammation in spondyloarthritis.

CLINICAL RELEVANCE/APPLICATION

8 ppm carnosine peak add knowledge regarding inflammation. In the future, carnosine may be an inflammatory marker to evaluate activity

SSG09-04 Contribution of 18F-Fluoride PET/MRI for Assessment of Active Inflammation in Psoriatic Arthritis of the Hand

Tuesday, Nov. 29 11:00AM - 11:10AM Room: E450B

Participants

Nika Guberina, MD, Essen, Germany (*Presenter*) Nothing to Disclose
Michael Forsting, MD, Essen, Germany (*Abstract Co-Author*) Nothing to Disclose
Andreas Korber, Essen, Ghana (*Abstract Co-Author*) Nothing to Disclose
Thorsten D. Poeppel, Essen, Germany (*Abstract Co-Author*) Nothing to Disclose

PURPOSE

Psoriatic arthritis is a common comorbidity of Psoriasis vulgaris and affects approximately 25% of all patients with psoriasis. Occult clinical alterations of psoriatic arthritis might precede the onset of axial symptoms. Early and complete detection of Psoriatic arthritis is essential for a timely treatment initiation to prohibit joint destruction. The purpose of the study was to evaluate the contribution of 18F-Fluoride PET/MRI for assessment of active inflammation in psoriatic arthritis of the hand.

METHOD AND MATERIALS

Morphological features were differentiated according to early (synovitis, tendonitis, bone oedema, soft tissue oedema and effusion) and advanced changes observed in psoriatic arthritis (bone erosions, joint-space-narrowing, joint-subluxation, interphalangeal ankylosis, dactylitis). Altogether 357 joints of patients' hands with psoriatic arthritis were examined. Participants' hands were examined according to a dual time point protocol with the Magnetom Biograph mMR PET/MRI-scanner (SiemensHealthcare, Germany) 5 and 90min after injection of 150MBq18F. Inflammation was assessed based on MR images using a 3 pointed Likert scale (0 = not present, 1 = moderate, 2 = extensive) and based on 18F Fluoride PET images in terms of SUVmax.

RESULTS

In all 134/357 joints showed signs of inflammation in PET/MRI. The joint most often affected was the distal interphalangeal joint (47%), followed by the carpometacarpal (28%) and proximal interphalangeal joint (17%). Pearson's coefficient demonstrated significant correlation between SUVmax as well as early and advanced morphological changes ($p < 0.05$; $r = 0.525$).

CONCLUSION

Simultaneous 18F-PET/MRI bears substantial diagnostic potential for the assessment of inflammation and morphological changes in patients with early and advanced stage of psoriatic arthritis.

CLINICAL RELEVANCE/APPLICATION

Integrated PET/MRI provides information about both, inflammation activity and morphological features observed in early as well as in advanced stage of psoriatic arthritis.

SSG09-05 Prevalence of CPPD of the Temporomandibular Joint (TMJ) in Patients with CPPD in Other Joints

Tuesday, Nov. 29 11:10AM - 11:20AM Room: E450B

Participants

Hannes Devos, Brussels, Belgium (*Presenter*) Nothing to Disclose
Abd Alla Fares, Brussels, Belgium (*Abstract Co-Author*) Nothing to Disclose
Maryam Shahabpour, MD, Brussels, Belgium (*Abstract Co-Author*) Nothing to Disclose
Leon Lenchik, MD, Winston-Salem, NC (*Abstract Co-Author*) Nothing to Disclose
Inneke Willekens, MD, Brussels, Belgium (*Abstract Co-Author*) Nothing to Disclose
Michel O. De Maeseneer, MD, PhD, Jette, Belgium (*Abstract Co-Author*) Nothing to Disclose

PURPOSE

Calcium pyrophosphate disease (CPPD) is a common condition involving hyaline and fibrocartilage. It's potential for cartilage damage is now recognized. The aim of this study was to investigate the prevalence of CPPD of the temporomandibular joint (TMJ) in patients with CPPD in other joints.

METHOD AND MATERIALS

Medical record search over 1 year period revealed 227 patients who had a radiographic diagnosis of CPPD in the wrist, hand, or knee as well as a CT examination of the head. All radiographs and CT examinations were retrospectively reviewed by consensus of 2 PGY5 to confirm CPPD in the peripheral joints, and assess for presence of calcification in the TMJ. The cases of TMJ calcification were then reviewed by an experienced musculoskeletal radiologist for confirmation of their findings. The prevalence was determined and the association with gender and age were statistically tested.

RESULTS

There were 166 women, and 61 men (age range, 54-99 years). TMJ calcification was seen in 41 of 227 patients (18%). This included 3 men (7 %) and 38 women (93%) The involvement was bilateral in 34%, left sided in 46%, and right sided in 20%. There was a statistically significant increase with age, and the findings were significantly more common in women.

CONCLUSION

CPPD of the TMJ in patients with peripheral CPPD is common. The prevalence increases with age and is higher in women than men. Since CPPD may lead to cartilage damage in peripheral joints, it may play a similar role in the TMJ, resulting in TMJ pain and dysfunction.

CLINICAL RELEVANCE/APPLICATION

1. CPPD of the TMJ is very common in patients with CPPD in other joints. 2. Since CPPD may cause cartilage damage it could be involved in TMJ pain and dysfunction.

SSG09-06 Association of Baseline Meniscal Extrusion with Incident Knee Osteoarthritis after 6.6 Years in Overweight and Obese Women

Participants

Jan van der Voet, Rotterdam, Netherlands (*Presenter*) Nothing to Disclose
Jos Runhaar, PhD, Rotterdam, Netherlands (*Abstract Co-Author*) Nothing to Disclose
Bart Schouten, MSc, The Hague, Netherlands (*Abstract Co-Author*) Nothing to Disclose
Dammis Vroegindeweyj, Rotterdam, Netherlands (*Abstract Co-Author*) Nothing to Disclose
Edwin H. Oei, MD, PhD, Palo Alto, CA (*Abstract Co-Author*) Nothing to Disclose
Sita Bierma-Zeinstra, PhD, Rotterdam, Netherlands (*Abstract Co-Author*) Nothing to Disclose

PURPOSE

To evaluate whether there is an association between meniscal extrusion at baseline and the incidence of knee OA after 6.6 years in a high-risk population, free of clinical and radiological knee OA at baseline.

METHOD AND MATERIALS

For our analysis we used data of the PROOF study. This preventive RCT evaluated a high-risk population of 407 middle-aged overweight and obese women (BMI $\geq 27\text{kg/m}^2$) at baseline and after 2.5 and 6.6 years of follow-up. Meniscal extrusion at baseline was defined as having an extrusion of grade 2 or higher on MRI according to the MOAKS criteria ($\geq 3\text{mm}$), which is scored in the medial as well as the lateral meniscus centrally (coronal image) and anteriorly (sagittal image). The primary outcome measure was either incidence of clinical OA according to the ACR criteria or radiographic knee OA (Kellgren & Lawrence grade 2 or higher), determined after both 2.5 and 6.6 years. Using generalized estimating equations (GEE), we determined the association between knees with and without meniscal extrusion and both outcomes, corrected for the baseline differences between the two groups.

RESULTS

645 knees were available for statistical analysis at baseline. Due to a dropout percentage of 33%, 431 knees remained after 6.6 years. At baseline, the completers showed a small but significant difference compared to the dropouts regarding BMI ($p=0.013$), physical activity level ($p=0.048$) and maximum strength of the quadriceps muscle ($p<0.001$). 24% had meniscal extrusion at baseline of which 95% involved the medial meniscus and 8% the lateral meniscus. A significant higher incidence of clinical OA was found in knees with meniscal extrusion compared to the control group (25.2% vs. 13.5%, adjusted odds ratio (OR) 2.19, 95% CI 1.15, 4.16). The incidence of radiographic knee OA was more than three times higher, but after 6.6 years this finding was not significant (31.3% vs. 9.9%, OR 1.76, 95% CI 0.86, 3.59).

CONCLUSION

Meniscal extrusion was associated with a significantly higher incidence of clinical knee OA after 6.6 years in a high-risk population of middle-aged overweight and obese women. Over time meniscal extrusion also leads to a rising incidence of radiographic knee OA.

CLINICAL RELEVANCE/APPLICATION

The results demonstrate the independent effect of baseline meniscal extrusion on the development of knee OA and therefore it is important that radiologists report the presence of meniscal extrusion on MRI.

SSG09-07 Changes in Subchondral Bone Mineral Density of the Femur and Tibia in Knee Osteoarthritis

Participants

Patrick Omoumi, MD, Lausanne, Switzerland (*Presenter*) Nothing to Disclose
Julien Favre, Lausanne, Switzerland (*Abstract Co-Author*) Nothing to Disclose
Hugo Babel, Lausanne, Switzerland (*Abstract Co-Author*) Nothing to Disclose
Brigitte Jolles-Haeberli, Lausanne, Switzerland (*Abstract Co-Author*) Nothing to Disclose

PURPOSE

Knee osteoarthritis (OA) is a painful and incapacitating disease affecting about one third of the population above 65 years old. There is currently no efficient cure to OA, due to an incomplete understanding of its pathophysiology. Previous studies suggest that bone could play a central role in the pathogenesis of OA. Bone mineral density (BMD) is particularly interesting because it is related to loads transmission (Wolff's law) and thus to the mechanical constraints on cartilage. Traditionally, BMD has been assessed using two-dimensional dual-energy x-ray absorptiometry (DXA), thus allowing only crude evaluation of proximal BMD at the tibia. Recently, a method based on computed tomography (CT) was introduced, allowing 3D tibial and femoral assessment. This study aimed at characterizing the femoral and tibial subchondral BMD (sBMD) in non-OA and OA knees and determining the performance of sBMD at distinguishing healthy and OA knees.

METHOD AND MATERIALS

CT exams from 10 non-OA knees and 10 knees with severe medial OA, matched for age (60 ± 3 years old), gender (50% male) and bones size, were analyzed. Bones were segmented and three-dimensional models were reconstructed using custom software. Next, sBMD was calculated as three-dimensional maps based on the CT intensity in the most superficial 3mm of subchondral bone. Finally, average sBMD in the medial and lateral load-bearing regions were calculated to determine the tibial and femoral medial-to-lateral (M/L) sBMD ratios. Data were analyzed using unpaired t-tests and receiver operating characteristic (ROC).

RESULTS

The M/L sBMD ratios were significantly higher in OA compared to non-OA knees for the femoral condyles ($1.13\text{HU} \pm 0.08$ Vs. $1.06\text{HU} \pm 0.02$; $p=0.01$) and tibial plateaus ($1.14\text{HU} \pm 0.03$ Vs. $1.09\text{HU} \pm 0.06$; $p=0.01$). High classification performances were obtained for the femur and the tibia, with area under the ROC curve of 0.95 and 0.83, respectively. □

CONCLUSION

Femoral and tibial sBMD increase with knee OA, which could correspond to an adaptation of the bone to biomechanical changes, as supported by previous gait analyses. Our method is the first to allow the quantification of the femoral sBMD, which yielded to higher classification performance than the tibia.

CLINICAL RELEVANCE/APPLICATION

The analysis of sBMD following our technique based on clinical CT could improve our understanding of the pathophysiology of OA.

SSG09-08 Assessment of Metabolic and Structural Bone Abnormalities in Knee Osteoarthritis with Simultaneous PET and MR Imaging

Tuesday, Nov. 29 11:40AM - 11:50AM Room: E450B

Participants

Feliks Kogan, PhD, Stanford, CA (*Presenter*) Research Grant, General Electric Company
Audrey Fan, Stanford, CA (*Abstract Co-Author*) Nothing to Disclose
Emily McWalter, PhD, Stanford, CA (*Abstract Co-Author*) Research support, General Electric Company
Andrew Quon, MD, Los Angeles, CA (*Abstract Co-Author*) Nothing to Disclose
Edwin H. Oei, MD, PhD, Palo Alto, CA (*Abstract Co-Author*) Nothing to Disclose
Garry E. Gold, MD, Stanford, CA (*Abstract Co-Author*) Consultant, Boston Scientific Corporation Consultant, Olea Medical Research support, General Electric Company

PURPOSE

This study aims to investigate 18F-NaF PET-MR imaging to detect and characterize osseous metabolic abnormalities in patients with knee OA and correlate bony features of OA observed on MRI with 18F-NaF uptake on PET.

METHOD AND MATERIALS

Both knees of 12 subjects with radiographic knee OA were imaged on a 3T PET-MR hybrid system following injection of 2-5 mCi of 18F-NaF. Two MSK radiologists identified the following bony features of OA on MR images: Bone marrow lesions (BMLs) and osteophytes and subchondral sclerosis. The maximum pixel standardized uptake values (SUVmax) from volumes of interest (VOI) on PET images corresponding to bone pathology identified on MRI were compared. VOIs with SUV greater than 5 times the mean background bone SUV were identified (VOIhigh) on PET SUV maps.

RESULTS

BMLs observed on MRI consistently correlated with 18F-NaF PET VOIhigh (27/28). Further, SUVmax associated with BMLs was significantly higher than that of osteophytes or sclerosis ($p < 0.001$), suggesting that BMLs are significantly more metabolically active. Additionally, significant correlations were observed between SUVmax and BML grade based off MOAKS scoring ($p < 0.05$). Association between 18F-NaF VOIhigh and MRI findings of osteophytes (56/82) and sclerosis (6/11) was less consistent. However, there were significant correlations between SUVmax and osteophyte grade ($p < 0.05$). Further, many of the small osteophytes used as early signs of OA on radiographs did not show uptake on PET. The sensitivity of 18F-NaF PET-MR to bone remodeling may help us to better understand and characterize these lesions in subchondral bone. A lack of metabolic activity may signal that certain pathology play a reduced role in OA progression. Of significant interest, high 18F-NaF uptake in subchondral bone did not always correspond to structural damage detected on MRI (42/132 VOIhigh). Subchondral bone is associated with pain as well as cartilage degeneration, and 18F-NaF PET-MR data suggests that metabolic abnormalities in the bone may occur prior to structural changes are seen on MRI.

CONCLUSION

PET-MRI allows for better understanding of the role of bony changes in OA pathogenesis. Additionally, 18F-NaF PET-MR may detect knee abnormalities unseen on MRI alone and is a promising tool for detection of early metabolic changes in OA.

CLINICAL RELEVANCE/APPLICATION

This work demonstrates the potential of 18F-NaF PET-MR to evaluate metabolic bone activity in subchondral bone.

SSG09-09 To Evaluate the Role of 18F-FDG PET-CT in Evaluating the Lower Limb Prosthesis Implants Infection

Tuesday, Nov. 29 11:50AM - 12:00PM Room: E450B

Participants

Sikandar M. Shaikh, DMRD, Hyderabad, India (*Presenter*) Nothing to Disclose

PURPOSE

The purpose of this study was to evaluate the role of using 18F-FDG PET-CT for the detection of infection associated with lower limb prosthetic implants.

METHOD AND MATERIALS

Thirty seven prosthetic implants in 31 patients in whom infection was suspected after artificial hip or knee placement were evaluated with this technique. PET-CT images were obtained 60 -90min after an intravenous injection of FDG. The images were interpreted as positive for infection if tracer uptake was increased at the bone-prosthesis interface with or without CT structural abnormality. A final diagnosis was made by surgical exploration or clinical follow-up for 1 y. PET-CT results were compared with the follow-up outcome in all these patients.

RESULTS

The sensitivity, specificity, and accuracy of PET-CT for detecting infection associated with knee prostheses were 90.9%, 72.0%, and 77.8%, respectively. The sensitivity, specificity, and accuracy of PET-CT for detecting infection associated with hip prostheses were 90%, 89.3%, and 89.5%, respectively. Overall, the sensitivity was 90.5% and the specificity was 81.1% for detection of lower limb prosthesis infections.

CONCLUSION

Thus FDG PET-CT is a useful imaging modality for detecting infections associated with lower limb arthroplasty and is more accurate for detecting infections associated with hip and knee prostheses as compared to other imaging modalities.

CLINICAL RELEVANCE/APPLICATION

PET-CT is more sensitive compared with other modalities for evaluation of Prosthetic infection

SSG10

Neuroradiology (Movement Disorders)

Tuesday, Nov. 29 10:30AM - 12:00PM Room: N226



AMA PRA Category 1 Credits™: 1.50
ARRT Category A+ Credits: 1.50

FDA Discussions may include off-label uses.

Participants

Suyash Mohan, MD, Philadelphia, PA (*Moderator*) Grant, NovoCure Ltd; Grant, Galileo CDS, Inc
James R. Fink, MD, Seattle, WA (*Moderator*) Nothing to Disclose

Sub-Events

SSG10-01 Accuracy of Neuromelanin-Sensitive MRI to Diagnose Idiopathic Parkinson's Disease

Tuesday, Nov. 29 10:30AM - 10:40AM Room: N226

Awards

Student Travel Stipend Award

Participants

Nadya Pyatigorskaya, Paris, France (*Presenter*) Nothing to Disclose
Marie Mongin, Paris, France (*Abstract Co-Author*) Nothing to Disclose
Romain Valabregue, Paris, France (*Abstract Co-Author*) Nothing to Disclose
Claire Ewenczyk, Paris, France (*Abstract Co-Author*) Nothing to Disclose
Marie Vidailhet, Paris, France (*Abstract Co-Author*) Nothing to Disclose
Stephane Lehericy, MD, PhD, Paris, France (*Abstract Co-Author*) Nothing to Disclose

PURPOSE

Parkinson's disease (PD) is a neurodegenerative disease characterized by loss of dopaminergic neurons in the substantia nigra pars compacta (SNpc). These neurons contain a pigment, neuromelanin, which can be detected using neuromelanin-sensitive MRI. Recent MRI studies have reported quantitative reduction of the neuromelanin signal in patients with PD. The goal of the present study was to evaluate the accuracy of the visual assessment of neuromelanin signal in the SN to diagnose PD and to compare the visual evaluation with a quantitative analysis based on manual segmentation.

METHOD AND MATERIALS

Forty-four patients and 18 healthy volunteers (HV) were prospectively included. Neuromelanin-sensitive images were acquired at 3T using two-dimensional (2D) axial turbo spin-echo T1-weighted images (voxel size = 0.4*0.4*3 mm). The regions of interest in the SN area were drawn manually around the area of high signal intensity of the SNpc in the neuromelanin-sensitive images using the FreeSurfer software. Additionally, two raters performed visual analysis of SN signal intensity using a 2-point scale, a score of 1 and 2 indicated HV and PD, respectively. Intra- and inter-rater intraclass correlation coefficients (ICC) were calculated for quantitative data. The diagnosis accuracy was calculated using the ROC analysis and its sensibility and specificity were estimated. The inter- and intra-rater agreement for the qualitative measurements was estimated using Cohen's kappa coefficient.

RESULTS

ROC analysis for volume measurements showed high discrimination between PD patients and HV with AUC = 0.871, sensitivity =1, and specificity = 0.669 for cut-point =199.98 mm³. There was a good agreement between the two raters ($\kappa = 0.715$, 95% CI [0.532, 0.897], $p < 0.001$). For the visual assessment, the mean sensitivity across the two raters who performed the visual analysis for PD diagnosis was 0.81, the specificity was 0.89, the positive predictive value was 0.94 and the negative predictive value was 0.67.

CONCLUSION

Both visual rating and volume analysis using T1-weighted neuromelanin-sensitive images had good accuracy allowed to categorize PD patients. The results provided by visual rating of SNpc signal loss were similar to those obtained by manual segmentation, with good sensibility and better specificity.

CLINICAL RELEVANCE/APPLICATION

Neuromelanin-sensitive MRI appears to be promising in the clinical practice for PD diagnosis.

SSG10-02 Quantifying Progression of Parkinson's Disease using Dopaminergic Neuroimaging

Tuesday, Nov. 29 10:40AM - 10:50AM Room: N226

Participants

Hiroto Takahashi, MD, Suita, Japan (*Presenter*) Nothing to Disclose
Yoshiyuki Watanabe, MD, PhD, Suita, Japan (*Abstract Co-Author*) Nothing to Disclose
Hisashi Tanaka, MD, Suita, Japan (*Abstract Co-Author*) Nothing to Disclose
Hiroki Kato, Suita Osaka, Japan (*Abstract Co-Author*) Nothing to Disclose
Jun Hatazawa, MD, PhD, Osaka, Japan (*Abstract Co-Author*) Nothing to Disclose
Noriyuki Tomiyama, MD, PhD, Suita, Japan (*Abstract Co-Author*) Nothing to Disclose
Masahito Mihara, Suita, Japan (*Abstract Co-Author*) Nothing to Disclose
Hideki Mochizuki, Suita, Japan (*Abstract Co-Author*) Nothing to Disclose

PURPOSE

To evaluate disease progression in Parkinson's disease (PD) using neuromelanin (NM) and dopamine transporter (DAT) imaging in a quantitative and reproducible fashion.

METHOD AND MATERIALS

This study included 36 patients with PD (Hoehn and Yahr (HY) scale/patients: 1/2, 2/18, 3/8 4/6, 5/2) who underwent NM and three-dimensional (3D) T1-weighted imaging on a 3T-magnetic resonance imager, as well as DAT single-photon emission computed tomography imaging. The NM values of the substantia nigra pars compacta (SNpc) and the striatal DAT values were calculated using a volume of interest (VOI)-based automated segmentation system with a voxel-based morphometric technique. Images were preprocessed as follows (Figure): all NM and DAT images were coregistered with 3D T1-weighted structural images and were spatially normalized using statistical parametric mapping, thus allowing voxel-based measurements with automatic setting of the VOI. The spatially normalized images of all subjects were smoothed. Finally, the SNpc and striatal VOI were set on the images. The signal-to-noise ratio (SNR) of the SNpc in the NM images and the striatal specific binding ratio (SBR) in the DAT images were calculated based on the mean value of the background region (tegmentum in the midbrain for SNR and the occipital lobe for SBR). The significance of differences between the early-stage group (HY scale 1-2) and the advanced-stage group (HY scale 3-5) in each higher SNR of the SNpc and higher striatal SBR than that of each background region was tested using Mann-Whitney's U test. The correlation of each higher SNR of the SNpc and higher striatal SBR than that of each background region with HY scale was assessed.

RESULTS

The mean SNR of the SNpc and the striatal SBR were significantly larger in the early-stage group than in the advanced-stage group ($P < 0.05$). The coefficients of correlation were $r = -0.43$ (SNR of the SNpc - HY scale) and $r = -0.58$ (striatal SBR - HY scale).

CONCLUSION

Dopaminergic neuroimaging can reveal PD-related neurodegenerative changes, and DAT imaging in particular may be a useful method to record biomarkers for the quantitative evaluation of disease progression in PD.

CLINICAL RELEVANCE/APPLICATION

PD-related neurodegenerative changes with disease progression can be quantitatively and reproducibly assessed using dopaminergic neuroimaging with the voxel-based morphometric technique.

SSG10-03 Magnetic Resonance (MR) Fusion Imaging for Targeting in Transcranial MR-Guided Focused Ultrasound (TcMRgFUS) Thalamotomy in Patients with Essential Tremor

Tuesday, Nov. 29 10:50AM - 11:00AM Room: N226

Participants

Hiroki Hori, Kawasaki, Japan (*Presenter*) Nothing to Disclose
Toshio Yamaguchi, MD, PhD, Kawasaki, Japan (*Abstract Co-Author*) Nothing to Disclose
Keiichi Abe, Tokyo, Japan (*Abstract Co-Author*) Nothing to Disclose
Tomokatsu Hori, Kawasaki, Japan (*Abstract Co-Author*) Nothing to Disclose
Yoshihiro Muragaki, MD, PhD, Shinjuku-ku, Japan (*Abstract Co-Author*) Nothing to Disclose
Takaomi Taira, Tokyo, Japan (*Abstract Co-Author*) Nothing to Disclose
Yoshiyuki Konishi, PhD, Shinjuku-ku, Japan (*Abstract Co-Author*) Nothing to Disclose
Kazuo Watanabe, Koriyama, Japan (*Abstract Co-Author*) Nothing to Disclose
Jinichi Sasanuma, Kawasaki, Japan (*Abstract Co-Author*) Nothing to Disclose
Tsutomu Watanabe, Kawasaki, Japan (*Abstract Co-Author*) Nothing to Disclose
Youko Murakami, Kawasaki, Japan (*Abstract Co-Author*) Nothing to Disclose

PURPOSE

Although the ventral intermediate nucleus (VIM), the target area for essential tremor, cannot be directly visualized on MRI, it is located medial to the pyramidal tracts (PT). The purpose of this retrospective study is to identify the precise anatomic landmark for TcMRgFUS thalamotomy, using MR fusion imaging (short tau inversion recovery [STIR] - field-of-view optimized and constrained undistorted single shot-diffusion weighted imaging [FOCUS-DWI]) in patients with essential tremor.

METHOD AND MATERIALS

Eleven patients with essential tremor were treated by TcMRgFUS (InSightec). Magnetic resonance imaging (MRI) was performed using a 3.0T MRI machine (GE Healthcare) and fusion imaging was obtained using Advantage Workstation (GE Healthcare). In the pre-treatment fusion image, we identified a high-intensity area in the internal capsule as the PT on color-coded FOCUS-DWI, and determined the cross point X between the midline of the PT and the thalamus-internal capsule boundary on STIR. Subsequently, we measured the distance from the posterior commissure (PC) to the X (distance, a). In the post-treatment STIR, we measured the distance of the lesion center from the PC (distance, b), and measured the lesion size. We compared the relationship between the distances a and b. The clinical improvement and adverse events were compared in the clinical rating scale for tremor (CRST) and the post-treatment MRI.

RESULTS

Tremor improved in all patients. The X in pre-treatment fusion image was located 7.2 mm anterior and 19.0 mm lateral to the PC. In the post-treatment STIR image, the lesioning center was located 6.6 mm anterior and 16.5 mm lateral to the PC. In 2 patients with temporary paralysis, the lesion reached to the PT, and in 2 patients with numbness, it extended to the posterior thalamus.

CONCLUSION

MR fusion imaging can identify the precise anatomical landmark in TcMRgFUS thalamotomy in patients with essential tremor to avoid the adverse events.

CLINICAL RELEVANCE/APPLICATION

TcMRgFUS thalamotomy for essential tremor is performed with more safety and efficiency.

SSG10-04 Chemical Exchange Saturation Transfer MR Imaging of the Substantia Nigra in Parkinson's Disease

Patients with Unilateral Symptoms at 3 Tesla

Tuesday, Nov. 29 11:00AM - 11:10AM Room: N226

Participants

Chunmei Li, MD, Beijing, China (*Abstract Co-Author*) Nothing to Disclose
Min Chen, MD, PhD, Beijing, China (*Abstract Co-Author*) Nothing to Disclose
Na X. Zhao, PhD, Beijing, China (*Abstract Co-Author*) Nothing to Disclose
Jinyuan Zhou, PhD, Baltimore, MD (*Abstract Co-Author*) License agreement, Koninklijke Philips NV
Xiaojie Luo, MD, Beijing, China (*Presenter*) Nothing to Disclose

PURPOSE

To demonstrate the nigral characteristic of Parkinson's Disease (PD) patients with unilateral symptoms by chemical-exchange-saturation-transfer (CEST) imaging at 3 Tesla.

METHOD AND MATERIALS

21 PD patients with unilateral symptoms (Hoehn and Yahr (H&Y) scale = 1) and 24 age- and education-matched normal controls were scanned on a 3 Tesla MRI system. Magnetization transfer spectra with 31 different frequency offsets (-6 to 6 ppm) were acquired at the midbrain slice. For PD patients with unilateral symptoms, we defined the contralateral side of symptoms as the affected side and the ipsilateral side as the unaffected side. The measured CEST signal intensities (including amide proton transfer-weighted, or APTw, and total CEST, or CESTtotal) of the substantia nigra in normal controls, affected side and unaffected side of PD patients were acquired. ANOVA test was used to compare the differences in CEST imaging signals between the affected side and unaffected side of PD patients and normal controls.

RESULTS

The CEST/APT imaging intensities of the affected side and unaffected side are compared in Fig. 1. Compared to normal controls, both the APTw and CESTtotal values in the substantia nigra of the affected side were significantly lower (APTw: 1.10 ± 0.11 %; $P = 0.027$; CESTtotal: 2.43 ± 0.38 %; $P = 0.001$). The APTw and CESTtotal values in the substantia nigra of the unaffected side seemed to be lower than normal controls, but the differences were not significant (APTw: 1.20 ± 0.15 %; $P = 0.315$; CESTtotal: 2.86 ± 0.46 %; $P = 0.081$).

CONCLUSION

CEST imaging signals may reflect the different degree of dopamine neuron loss for the affected side and the unaffected side and may reveal the dopamine neuron loss in the progression of PD, from the preclinical stage to the clinical stage.

CLINICAL RELEVANCE/APPLICATION

CEST signal could provide information additional to conventional MR imaging and may reveal the dopamine neuron loss in the progression of PD, from the preclinical stage to the clinical stage.

SSG10-05 Determining Clinical Value of DaT Scan in Patients with Parkinson's and Parkinsonian-like Syndromes

Tuesday, Nov. 29 11:10AM - 11:20AM Room: N226

Awards

Student Travel Stipend Award

Participants

Varun Sethi, MD, Philadelphia, PA (*Presenter*) Nothing to Disclose
Simindokht Dadparvar, MD, Gladwyne, PA (*Abstract Co-Author*) Nothing to Disclose
Elizabeth Haberkamp, MD, Philadelphia, PA (*Abstract Co-Author*) Nothing to Disclose

PURPOSE

While diagnosis of idiopathic Parkinson's disease (PD) is typically clinical, it can be challenging when symptoms overlap with other disorders or are refractory to therapy. These disorders include essential tremor, dementia, drug induced and Parkinsonian-like syndromes, psychogenic Parkinsonism, and others. Anatomical imaging such as CT and MRI in patients with PD are typically normal, however can rule out other pathologies. I-123 ioflupane (DaT Scan) SPECT imaging is used for imaging PD. Ioflupane has high binding affinity for pre-synaptic dopamine transporters in the mammalian striatum – a subcortical region of the basal ganglia – where loss of dopaminergic neurons occurs in PD. We retrospectively reviewed patients who underwent DaT Scans to evaluate the efficacy of the DaT Scan and its impact on patient management.

METHOD AND MATERIALS

Retrospective review of 60 patient records (36 male, 24 female) with age range (38-80 yrs, mean age 68 yrs) were performed. Clinical and imaging data were collected. All patients underwent DaT Scan at one hour following intravenous injection of 5 mCi of I-123 ioflupane preceded by oral administration of Lugol's solution. DaT imaging results were reviewed and corroborated with Benamer's classification. Clinical follow up and changes in PD-related therapy were reviewed. Sensitivity, specificity, accuracy, positive predictive value (PPV) and negative predictive value (NPV) of DaT Scans was compared against final clinical diagnosis. Change in patient management were recorded.

RESULTS

Of the 60 patients, 24 were normal and 36 had positive scan. Of the positive studies, 21 were classified as G1, 15 as G2, and none as G3, by Benamer's classification. 11 patients were lost to follow up. Of the remaining 49 patients, the change in management was evaluated. Our study showed sensitivity 91%, specificity 92%, accuracy 92%, PPV 91%, NPV 92%. 16/49 (33%) of patients had alterations in their treatment after the scan.

CONCLUSION

DaT Scan is a highly effective tool in diagnosis of PD and differentiating it from Parkinsonian like syndromes with high sensitivity, specificity, accuracy, PPV and NPV. In our patient population, it altered the course of therapy for 33% of the patients. Prospective

study is recommended to validate the results in larger population.

CLINICAL RELEVANCE/APPLICATION

DaT Scan alters management of patients with suspected Parkinson's Disease.

SSG10-06 Iterative Metal Artifact Reduction in Computed Tomography Following Deep-Brain-Stimulation (DBS) Surgery

Tuesday, Nov. 29 11:20AM - 11:30AM Room: N226

Participants

Joel Aissa, Duesseldorf, Germany (*Presenter*) Nothing to Disclose
Johannes Boos, MD, Boston, MA (*Abstract Co-Author*) Nothing to Disclose
Christoph Schleich, MD, Dusseldorf, Germany (*Abstract Co-Author*) Nothing to Disclose
Patric Kroepil, MD, Duesseldorf, Germany (*Abstract Co-Author*) Nothing to Disclose
Gerald Antoch, MD, Duesseldorf, Germany (*Abstract Co-Author*) Nothing to Disclose
Christoph K. Thomas, MD, Dusseldorf, Germany (*Abstract Co-Author*) Nothing to Disclose
Rotem S. Lanzman, MD, Duesseldorf, Germany (*Abstract Co-Author*) Nothing to Disclose

PURPOSE

The purpose of this study was to assess the impact of the novel iterative MAR technique on image quality and diagnostic performance in the follow-up of patients with DBS-electrode implementation surgery. Our hypothesis was that artifact burden can be reduced and subjective image quality increased using the novel iterative MAR (iMAR) technique compared to the standard weighted filtered back projection (WFBP).

METHOD AND MATERIALS

Seventeen patients who had received routine intraoperative CT of the head following implantation of DBS electrodes between March 2015 and June 2015 were included in this retrospective study. Raw data of all patients were reconstructed with standard filtered back projection and additionally with a novel iMAR algorithm. We quantified frequencies of density changes to assess quantitative artifact reduction. For evaluation of qualitative image quality the visibility of numerous cerebral anatomic landmarks were scored first. Additionally, the exact intracerebral detectability of electrodes' localization/differentiation were evaluated as well as the artifact strength overall and adjacent to the electrodes.

RESULTS

Images reconstructed with iMAR contained significantly lower metal artifacts (overall low frequency values: 1608.6 ± 545.5 ; range 375.5-3417.2) compared to the WFBP (overall low frequency values: 4487.3 ± 875.4 ; range 2218.3-5783.5) ($p < 0.004$). Qualitative image analysis showed a significantly improved image quality for iMAR (overall anatomical landmarks: 2.49 ± 0.15 , range 2.31-2.66; overall electrode characteristics: 2.35 ± 0.16 , range 2.25-2.52; artifact characteristics: 2.16 ± 0.08 , range 2.11-2.22) compared to WFBP (overall anatomical landmarks: 1.21 ± 0.64 , range 0.58-2.11; overall electrode characteristics: 0.74 ± 0.37 , range 0.27-1.00; artifact characteristics: 0.51 ± 0.15 , range 0.39-0.63) ($p < 0.002$).

CONCLUSION

Reconstructions of cranial CT images with the novel iMAR algorithm in patients following DBS-implantation allows for an efficient reduction of metal artifacts near DBS electrodes compared to WFBP reconstructions. We demonstrated an improvement of quantitative and qualitative image quality of iMAR compared to WFBP in patients with DBS-electrodes.

CLINICAL RELEVANCE/APPLICATION

Iterative MAR allows an efficient artifact reduction following deep brain stimulation surgery compared to standard technique.

SSG10-07 Histogram Analysis of Quantitative Susceptibility Mapping for the Classification of Parkinson's Disease and Multiple System Atrophy with Predominant Parkinsonism

Tuesday, Nov. 29 11:30AM - 11:40AM Room: N226

Participants

Mi Sun Chung, MD, Seoul, Korea, Republic Of (*Presenter*) Nothing to Disclose
Sang Joon Kim, MD, Seoul, Korea, Republic Of (*Abstract Co-Author*) Nothing to Disclose
Woo Hyun Shim, Seoul, Korea, Republic Of (*Abstract Co-Author*) Nothing to Disclose
Ja Hwan Koo, Seoul, Korea, Republic Of (*Abstract Co-Author*) Nothing to Disclose
Seung Chai Jung, MD, Seoul, Korea, Republic Of (*Abstract Co-Author*) Nothing to Disclose
Ho Sung Kim, Seoul, Korea, Republic Of (*Abstract Co-Author*) Nothing to Disclose
Choong Gon Choi, MD, Seoul, Korea, Republic Of (*Abstract Co-Author*) Nothing to Disclose
Geon-Ho Jahng, PhD, Seoul, Korea, Republic Of (*Abstract Co-Author*) Nothing to Disclose

PURPOSE

We evaluated the usefulness of quantitative susceptibility mapping (QSM) value using histogram analysis to discriminate patients with Parkinson's disease (PD) and multiple system atrophy with predominant parkinsonism (MSA-P).

METHOD AND MATERIALS

Institutional review board approval was obtained and informed consent was waived for this retrospective study. 136 patients with PD and 18 patients with MSA-P were included. The QSM images were produced by implementing the Morphology Enabled Dipole Inversion (MEDI) method. After coregistration of QSM images and 3D T1-weighted images to the standard Montreal Neurologic Institution template using Freesurfer program, automatic brain tissue segmentation, motion correction and spatial normalization were conducted. The mean values of QSM were extracted in 4 brain structures (caudate nucleus, putamen, pallidum and thalamus) and cumulative histogram analyses were performed to determine optimal cut-off. Mann-Whitney U test were used to compare of mean QSM values and the results of histogram analysis. Area under the receiver operating characteristic curves (AUC) with bootstrapping method was conducted to evaluate accuracy of differentiating PD and MSA-P.

RESULTS

Mean and 75th to 95th percentile of QSM values of both putamina, pallidi and right thalamus were significantly different between PD and MSA-P group (all p-value <0.05). Cross-validated AUC and accuracy on the 95th percentile of histogram demonstrated the highest value (0.892 and 92.8%, respectively) and it was higher than those of mean QSM value (AUC, 0.793 and accuracy, 88.4%). The highest AUCs were demonstrated on 95th percentile in right putamen (AUC, 0.876; 95% confidential interval [CI], 0.813 to 0.923), left putamen (AUC, 0.815; CI, 0.722 to 0.873) and right pallidum (AUC, 0.775; CI, 0.700 to 0.838) and on 75th percentile in left pallidum (AUC, 0.772; CI, 0.697 to 0.836) and right thalamus (AUC, 0.764; CI, 0.689 to 0.829). All of the highest AUCs of histogram analyses were higher than AUCs of mean QSM values.

CONCLUSION

QSM values of both putamina, pallidi and right thalamus could be helpful to differentiate PD and MSA-P. Rather than mean QSM value, QSM values on 95th percentile cumulative histogram could be more helpful to discriminate PD and MSA-P.

CLINICAL RELEVANCE/APPLICATION

QSM values on 95th percentile cumulative histogram analysis could be helpful to differentiate PD and MSA-P.

SSG10-08 Diagnosis of Early-Stage Idiopathic Parkinson's Disease using High-Resolution Quantitative Mapping with Histogram Analysis in the Substantia Nigra at 3T

Tuesday, Nov. 29 11:40AM - 11:50AM Room: N226

Participants

Min Kyoung Lee, MD, Incheon, Korea, Republic Of (*Presenter*) Nothing to Disclose
Eung Yeop Kim, MD, Incheon, Korea, Republic Of (*Abstract Co-Author*) Nothing to Disclose
Yoonho Nam, Seoul, Korea, Republic Of (*Abstract Co-Author*) Nothing to Disclose
Jongho Lee, Seoul, Korea, Republic Of (*Abstract Co-Author*) Nothing to Disclose

PURPOSE

Conventional 2-mm or thicker quantitative susceptibility mapping (QSM) may be limited for the assessment of substantia nigra (SN) that contains small nigrosome 1. We hypothesized that higher-resolution QSM vertical to the axis of nigrosome 1 combined with a histogram analysis can improve diagnostic accuracy by reducing partial-volume effect between early-stage IPD patients and healthy subjects.

METHOD AND MATERIALS

We enrolled 29 patients with IPD (16 female; mean age, 68.9; symptom onset < 3 years), and 20 healthy subjects (10 female; mean age, 66.5). All participants underwent 3D multi-echo gradient-recalled echo imaging (number of echoes, 6; spatial resolution, 0.5 × 0.5 × 1.0 mm³) parallel to the plane from the posterior commissure and top of the pons at 3T. From unwrapped different echo-time phase images, normalized tissue frequency map was calculated after background field removal using the HARPERELLA method. After QSM reconstruction from the frequency map using the iLSQR method, 0.5-mm resliced QSM images were normalized by subtracting the value in the decussation of superior cerebellar peduncle. The regions of interest were semi-automatically drawn with a threshold of 80 ppb using Analyze version 12.0 with securing the areas of presumed nigrosome 1 below the red nucleus. Both the mean susceptibility and proportion less than 70 ppb on the side with lower values were compared between the two groups.

RESULTS

There was significant difference of the mean susceptibility (ppb) between the two groups (124.43 ± 12.67 [IPD] vs 99.10 ± 12.84 [normal subjects]; $P < 0.0001$; sensitivity of 96.6% and specificity of 75% [with a criterion > 105.91 ppb]). The proportion of the areas less than 70 ppb in the SN was significantly different between the two groups (median, 0; IQR, 0-0.34 [IPD] vs median, 10.34; IQR, 6.925-21.495 [normal subjects]; $P < 0.0001$), showing perfect sensitivity and specificity. The diagnostic accuracy with the threshold of 70 ppb was significantly higher than with the mean susceptibility values ($P = 0.0481$, pairwise comparison of ROC curves).

CONCLUSION

High-resolution QSM with histogram analysis can improve diagnostic accuracy of early-stage IPD at 3T.

CLINICAL RELEVANCE/APPLICATION

High-resolution QSM of the substantia nigra imaging at 3T can improve diagnostic accuracy of IPD, and its histogram analysis may serve as a novel imaging biomarker.

SSG10-09 Multi-Delay Multi-Parametric Arterial Spin Labeled Perfusion MRI in Early-Stage Parkinson's Disease and Mild Cognitive Impairment

Tuesday, Nov. 29 11:50AM - 12:00PM Room: N226

Participants

Xueling Suo, Chengdu, China (*Presenter*) Nothing to Disclose
Du Lei, Chengdu, China (*Abstract Co-Author*) Nothing to Disclose
Lei Li, Chengdu, China (*Abstract Co-Author*) Nothing to Disclose
Fuqin Chen, Chengdu, China (*Abstract Co-Author*) Nothing to Disclose
Lan Cheng, Chengdu, China (*Abstract Co-Author*) Nothing to Disclose
Nannan Li, Chengdu, China (*Abstract Co-Author*) Nothing to Disclose
Rong Peng, Chengdu, China (*Abstract Co-Author*) Nothing to Disclose
Qiyong Gong, MD, PhD, Chengdu, China (*Abstract Co-Author*) Nothing to Disclose

PURPOSE

Arterial spin labeling (ASL) offers a non-invasive MRI method for quantifying cerebral blood flow (CBF) and arterial transit time (ATT). However, existing ASL studies on Parkinson's disease (PD) generally employed a single post-labeling delay (PLD) time. It might result in underestimation of perfusion in brain tissue. The combination of multiple PLDs and single-shot 3D GRASE, background

suppression and pseudo-continuous ASL (pCASL) significantly improved the temporal stability. PD patients exhibiting mild cognitive impairment (PD_MCI) are at increased risk for developing dementia and are thus targets for disease-modifying intervention before irreversible changes. This study was to present a multi-delay multi-parametric pCASL protocol for perfusion in early-stage PD_MCI patients.

METHOD AND MATERIALS

PCASL data at 4 PLDs time were acquired at rest in 39 early-stage PD patients as (PD_MCI, N=22) and having normal cognition (PD_NMCI, N=17), and 36 age- and sex-matched healthy controls (HC) on a 3.0 T system. Image analysis was performed using a home-made protocol. ATT was estimated through the calculation of weighted delays across the 4 PLDs and included in the calculation of CBF, which were compared among the three groups using analysis of covariance (ANCOVA). For clusters identified in the ANCOVA, we performed follow-up between-group voxel-wise t tests to identify pair-wise group differences.

RESULTS

We identified prolonged ATT in right rolandic operculum and right thalamus in PD_MCI relative to both PD_NMCI and HC. PD_MCI showed prolonged ATT in left SFGorb relative to PD_NMCI. HC showed prolonged ATT in left SFGorb and right MFGorb relative to PD_NMCI. However, we did not find differences in CBF. Moreover, prolonged ATT in left SFGorb and right thalamus was positively and negatively correlated with Montreal Cognitive Assessment (MoCA) and Mini-Mental State Examination (MMSE) scores in the PD_MCI group, individually.

CONCLUSION

The results identify the true pattern of perfusion alterations in early PD_MCI. This could have an impact on our understanding of the pathological features of the disease cognitive impairment.

CLINICAL RELEVANCE/APPLICATION

ASL is completely noninvasive compared to nuclear imaging techniques and can, therefore, safely be used for repeated assessments, which may be an objective imaging markers of PD cognitive impairment.

SSG11

Neuroradiology (Stroke Imaging)

Tuesday, Nov. 29 10:30AM - 12:00PM Room: N227B



AMA PRA Category 1 Credits™: 1.50
ARRT Category A+ Credits: 1.50

Participants

Bharathidasan Jagadeesan, MD, Minneapolis, MN (*Moderator*) Consultant, Terumo Corporation; Consultant, Medtronic plc
Srinivasan Mukundan, MD, PhD, Boston, MA (*Moderator*) Institutional research support, Siemens AG Institutional research support,
Toshiba Corporation Consultant, Toshiba Corporation

Sub-Events

SSG11-01 Magnetization Transfer and Relaxation-normalized Amide Proton Transfer (MRAPT) MRI Enables Automatic Segmentation of Graded Tissue Acidification

Tuesday, Nov. 29 10:30AM - 10:40AM Room: N227B

Participants

Yuwen I. Zhou, PhD, Charlestown, MA (*Presenter*) Nothing to Disclose
Phillip Zhe Sun, PhD, Charlestown, MA (*Abstract Co-Author*) Nothing to Disclose
Ying-Kun Guo, MD, Chengdu, China (*Abstract Co-Author*) Nothing to Disclose
Lingyi Wen Jr, MD, Chengdu, China (*Abstract Co-Author*) Nothing to Disclose
Phoebe Chan, Charlestown, MA (*Abstract Co-Author*) Nothing to Disclose
Emiri T. Mandeville, Charlestown, MA (*Abstract Co-Author*) Nothing to Disclose
Eng Z. Lo, Charlestown, MA (*Abstract Co-Author*) Nothing to Disclose
Xunming Ji, Beijing, China (*Abstract Co-Author*) Nothing to Disclose

PURPOSE

pH-sensitive amide proton transfer (APT) MRI provides a surrogate metabolic biomarker that complements the widely-used perfusion and diffusion imaging. However, endogenous APT MRI relies on the asymmetry analysis (MTRasym), which is susceptible to an asymmetry shift due to concomitant semisolid magnetization transfer (MT) and nuclear overhauser (NOE) effects, resulting in intrinsic non-pH contrast between white and gray matters. Our study evaluated MT and relaxation-normalized APT (MRAPT) MRI in a rat model of acute ischemic stroke that enabled automatic segmentation of graded ischemic tissue injury.

METHOD AND MATERIALS

Normal and stroke rats (MCAO) were imaged at 4.7T. Multi-parametric MRI including diffusion, perfusion MRI, T1, T2 mapping and pH-weighted APT MRI was performed. Ischemic lesion was automatically defined using a K-means clustering-based algorithm.

RESULTS

We found that the heterogeneous MTRasym shift not related to pH highly correlates with mean MT ratio (MMTR) and longitudinal relaxation rate R1w, which can be largely corrected using the multiple regression analysis (Fig.1). We further evaluated MRAPT MRI in an animal model of acute stroke for lesion segmentation (Fig. 2). Given little MT and R1w change during acute stroke, the MRAPT analysis substantially increased its specificity to ischemia-induced acidosis than the routine MTRasym image, hence enabling automatic lesion segmentation of acidic lesion. We found significant differences in perfusion, pH and diffusion lesion volumes ($P < 0.001$, ANOVA). Furthermore, MRAPT MRI depicted heterogeneous ischemic acidosis, with the most severe acidosis in the diffusion lesion, moderate acidification within the pH/diffusion mismatch (metabolic penumbra) and little pH change in the perfusion/pH mismatch (benign oligemia), providing refined stratification of ischemic injury.

CONCLUSION

Multivariate regression analysis enables substantial reduction of intrinsic non-pH heterogeneity in pH-weighted APT MRI. The MRAPT approach enables automatic lesion segmentation, demonstrating graded tissue acidification in the acute stroke setting for refined tissue classification.

CLINICAL RELEVANCE/APPLICATION

Multivariate regression analysis substantially reduces intrinsic non-pH heterogeneity in pH-weighted APT MRI, enabling automatic segmentation of graded tissue acidification in acute stroke setting.

SSG11-02 The Importance of Differentiating Between Lacunes and Perivascular Spaces in Cerebral Small Vessel Disease

Tuesday, Nov. 29 10:40AM - 10:50AM Room: N227B

Participants

Philip Benjamin, MBBS, London, United Kingdom (*Presenter*) Nothing to Disclose

PURPOSE

Cerebral small vessel disease (SVD) is a major cause of cognitive impairment in the elderly. Perivascular spaces (PvS) are an important disease feature but their relationship to cognitive impairment remains controversial. One reason for this may be due to the difficulty in distinguishing between lacunes and PvS. We determined the relationship between baseline PvS score and PvS volume with change in cognition over a 5 year follow-up period. We compared this to the relationship between baseline lacune count and total lacune volume with cognition.

METHOD AND MATERIALS

Data from the prospective SCANS (St Georges Cognition And Neuroimaging in Stroke) study of patients with symptomatic lacunar stroke and confluent leukoaraiosis were used (n=121). Multimodal MRI and neuropsychological testing was performed annually over 5 years. Lacunes were manually identified and carefully distinguished from PvS. PvS were rated using a validated visual rating scale and PvS volumes calculated using T1-weighted images. Linear mixed effect models were used to determine the impact of baseline PvS and lacunes on cognition while adjusting for brain volume, T2 White Matter Hyperintensities (WMH) volume and microbleeds.

RESULTS

Baseline PvS showed no association with cognitive indices. Lacunes however, had a significant effect on all cognitive indices in the same cohort and were the only MRI marker in SVD at baseline which had an independent effect on cognitive decline over a 5 year follow-up period (p=0.007).

CONCLUSION

Lacunes were the only conventional MRI marker at baseline which were associated with a decline in cognition over a 5 year follow-up period. This study underlines the importance of carefully differentiating between lacunes and PvS in studies investigating vascular cognitive impairment.

CLINICAL RELEVANCE/APPLICATION

Lacunes although often overlooked, are the only conventional MRI marker at baseline which are associated with a longitudinal decline in cognition. Neuropathological studies also suggest that patients with subcortical lacunes have a higher prevalence of clinical dementia than those without. It is therefore important to develop treatment strategies aimed at preventing lacunar infarcts through clinical trials. This study underlines the importance of carefully differentiating between lacunes and PvS in studies investigating vascular cognitive impairment. PvS, although a feature of SVD are not associated with cognitive decline.

SSG11-03 Patient Outcomes and Recurrent Artery of Heubner Infarction after Ruptured Anterior Communicating Artery Aneurysm Treatment

Tuesday, Nov. 29 10:50AM - 11:00AM Room: N227B

Participants

Jeremy J. Heit, MD, PhD, Stanford, CA (*Presenter*) Consultant, Terumo Corporation
Nicholas Telischak, MD, MS, Boston, MA (*Abstract Co-Author*) Nothing to Disclose
Huy M. Do, MD, Stanford, CA (*Abstract Co-Author*) Nothing to Disclose
Robert Dodd, MD, PhD, Stanford, CA (*Abstract Co-Author*) Nothing to Disclose
Gary K. Steinberg, MD, PhD, Stanford, CA (*Abstract Co-Author*) Nothing to Disclose
Steven D. Chang, MD, Stanford, CA (*Abstract Co-Author*) Nothing to Disclose
Michael P. Marks, MD, Stanford, CA (*Abstract Co-Author*) Research Grant, Siemens AG

PURPOSE

Anterior communicating artery aneurysm (AcomA) rupture and treatment is associated with cognitive and behavioral deficits after recovery, but the cause of these deficits remains uncertain. Surgical clipping of AcomA has been associated with more severe cognitive and behavioral deficits when compared to endovascular coil embolization. We characterized patterns of cerebral ischemic injury and patient outcomes following treatment of ruptured AcomA by clipping or coiling.

METHOD AND MATERIALS

We retrospectively reviewed 100 consecutively treated patients with ruptured AcomA (50 clipped and 50 coiled) presenting to our neurovascular center. Patient demographic, treatment, and outcome data were determined by electronic medical record review. Neuroimaging was reviewed for aneurysm characteristics and associated hemorrhagic, ischemic, and vasospasm related cerebral injury.

RESULTS

Coiled patients were older (mean age 56 years versus 51; p=0.04) and presented with a worse clinical status (60% with Hunt and Hess Score >2 versus 34% in clipping group; p=0.009). Frontal lobe cerebral infarction (30% versus 4%; p=0.001) and cerebral infarction in the territory of the recurrent artery of Heubner (RAH) (33% versus 2%; p=0.0005) were more common in clipped patients. There was no difference in the frequency of frontal lobe hemorrhagic infarction, punctate embolic infarction, or infarction secondary to vasospasm between clipped and coiled patients. In a multivariate analysis, poor outcome (mRS greater than 2) was associated with diabetes mellitus (p=0.04), presentation with Hunt and Hess greater than 2 (p=0.02), age over 55 years (p=0.004), and the development of cerebral arterial vasospasm (p=0.0001). No differences in mortality, discharge modified Rankin score (mRS), or 3-month follow-up mRS were detected between the two groups.

CONCLUSION

Frontal lobe and RAH infarction were more common after surgical clipping of ruptured AcomA, but this increased infarct burden did not result in poorer outcomes as assessed by mortality or mRS.

CLINICAL RELEVANCE/APPLICATION

Further studies are warranted to determine if post-surgical frontal lobe and RAH infarctions contribute to cognitive and behavioral deficits after ruptured AcomA treatment.

SSG11-04 Disrupted Functional Connectivity within the Default-mode Network in Brainstem Ischemic Stroke Patients with Cognitive Impairment

Tuesday, Nov. 29 11:00AM - 11:10AM Room: N227B

Participants

Cheng-Yu Peng, Nanjing, China (*Presenter*) Nothing to Disclose
Shenghong Ju, MD, PhD, Nanjing, China (*Abstract Co-Author*) Nothing to Disclose
Gao-Jun Teng, MD, Nanjing, China (*Abstract Co-Author*) Nothing to Disclose

PURPOSE

The purpose of the current research is to explore the disrupted functional connectivity within the default-mode network (DMN) in brainstem ischemic stroke patients with cognitive impairment and whether the decreased connectivity is correlated with neurocognitive performance and the serum total homocysteine (tHcy) level.

METHOD AND MATERIALS

Thirty-two brainstem ischemic stroke patients and 34 well-matched healthy controls were included and underwent resting-state functional MRI. Independent component analysis was adopted to extract the DMN, including its anterior and posterior components. Z-maps of both sub-networks were compared between the two groups and correlated with each clinical variable.

RESULTS

Post-stroke patients showed decreased connectivity around the middle frontal cortex in the anterior sub-network and the posterior cingulate cortex in the posterior sub-network. The decreased connectivity in the posterior part was significantly correlated with the score on Auditory Verbal Learning Test -delay recall test ($r = 0.532$, $P = 0.006$), the Complex Figure Test-delay recall test ($r = 0.494$, $P = 0.012$), and the tHcy level ($r = -0.555$, $P = 0.007$).

CONCLUSION

Decreased connectivity within the DMN was found in brainstem ischemic stroke patients, which might provide powerful new insights into the neural mechanisms that underlie the post-stroke cognitive decline.

CLINICAL RELEVANCE/APPLICATION

The connectivity of the posterior cingulate cortex within the DMN revealed by the fMRI can be an indicator to assess the post-stroke cognitive impairment.

SSG11-05 Where Are the Cerebral Regions Saved by Successful Recanalization of M1 Occlusion?

Tuesday, Nov. 29 11:10AM - 11:20AM Room: N227B

Participants

Seyedmehdi Payabvash, MD, San Francisco, CA (*Presenter*) Nothing to Disclose
Shayandokht Taleb, Minneapolis, MN (*Abstract Co-Author*) Nothing to Disclose
Adnan I. Qureshi, MD, Minneapolis, MN (*Abstract Co-Author*) Nothing to Disclose

PURPOSE

To determine the distribution of cerebral regions that can potentially be saved by successful recanalization of acute M1 occlusion in stroke patients.

METHOD AND MATERIALS

47 patients with acute unilateral M1 occlusion who underwent endovascular treatment were included. Final infarct volumes were segmented on follow-up MRI/CT scans obtained 2-7 days post symptom onset, and then coregistered on standard brain map. Voxel-based analysis was performed to determine the topology of infarct lesions associated with successful versus unsuccessful recanalization, and disability/death. Successful recanalization was defined by a modified Thrombolysis in Cerebral Infarction (mTICI) score of 2b/3. Favorable outcome was defined by a 3-month modified Rankin Scale score ≤ 2 ; and disability/death by a score > 2 .

RESULTS

Successful recanalization of M1 was achieved in 26/47 (55%) patients, which was associated with higher rate of favorable outcome (54% versus 9%, $p=0.002$) and smaller final infarct volume (34.3 ± 43.7 mL versus 98.1 ± 47.7 mL, $p < 0.001$). Voxel-based analysis showed that patients with successful recanalization had lower rate of infarction in precentral gyrus and posterior insular ribbon compared to those with unsuccessful recanalization. Similarly, higher grades of recanalization were associated with lower rates of ischemic infarct in aforementioned regions. Favorable outcome was achieved in 16 (34%) patients, who were younger (62.2 ± 13.9 years versus 70.9 ± 13.9 years, $p=0.048$), had higher rate of successful recanalization (88% versus 39%, $p=0.002$), and smaller infarct volume (25.2 ± 23.6 mL versus 82.2 ± 57.1 mL, $p < 0.001$) compared to those with disability/death. In voxel-based analysis, infarction of the insular ribbon, precentral gyrus, middle centrum semiovale and corona radiata were associated with disability/death.

CONCLUSION

Successful recanalization of acute M1 occlusion tends to save the precentral gyrus and posterior insular ribbon from infarction in stroke patients; however, preservation of more anterior cerebral regions like anterior insular ribbon, middle centrum semiovale and coronal radiata can potentially further improve the outcome of endovascular treatment.

CLINICAL RELEVANCE/APPLICATION

Knowing the topographic distribution of salvageable cerebral regions with successful endovascular treatment can potentially guide patient selection based on the **location** of tissue at risk in acute phase stroke imaging.

SSG11-06 Stroke Assessment with Monoexponential, Biexponential, Stretched Exponential Diffusion Weighted MR Imaging and Diffusion Kurtosis MR Imaging

Tuesday, Nov. 29 11:20AM - 11:30AM Room: N227B

Participants

Chengxia Liu, Wuhan, China (*Presenter*) Nothing to Disclose
Shun Zhang, Wuhan, China (*Abstract Co-Author*) Nothing to Disclose
Wenjie Zhu, wuhan, China (*Abstract Co-Author*) Nothing to Disclose
Wenzhen Zhu, MD, PhD, Wuhan, China (*Abstract Co-Author*) Nothing to Disclose

PURPOSE

To investigate the concomitant change of multi model diffusion and kurtosis metrics in stroke patients and screen for difference among patients with different subtypes of potential etiology in all studied parameters.

METHOD AND MATERIALS

84 patients with acute stroke underwent multi b diffusion and kurtosis scan. ROI analysis was performed in metrics of monoexponential, biexponential, stretched exponential model and kurtosis imaging between ischemic tissue and contralateral hemisphere. Correlation between monoexponential apparent diffusion coefficient (mADC) and the other parameters was evaluated. Multiple comparisons of all parameters among patients with different potential etiologies were performed.

RESULTS

All 14 parameters exhibit significant difference between stroke and contralateral ROIs except pseudo-diffusion coefficient (Dfast) (P=0.342). Correlations between mADC and mean diffusion (MD), diffusion coefficient (Dslow), distributed diffusion coefficient (DDC) are fairly good in ischemic area (0.807, 0.698, 0.756, all P<0.05). Kurtosis metrics (mean kurtosis MK, axial kurtosis Ka, radial kurtosis Kr) are negatively correlated with mADC (rs =-0.505, -0.749, -0.430; all P<0.05). There is no significant correlation between mADC and perfusion metrics (Dfast, perfusion factor *f* and *f*·Dfast), neither between mADC and stretching parameter (α) (P=0.666, 0.232, 0.066, 0.871). Significant differences are observed between groups of cardioembolism and undetermined etiology in fractional anisotropy (FA), MK, Kr and α obtained from stroke tissue, while the differences also exist in contralateral MK and Kr (All P<0.05, SNK corrected). No significant difference is detected between groups of large artery atherosclerosis and cardioembolism or between groups of cardioembolism and undetermined etiology either in stroke or contralateral hemisphere (all P>0.05).

CONCLUSION

Diffusion and kurtosis change in stroke indicates disturbance of water microenvironment in different scales, together with diffusion derived perfusion information, yield a more comprehensive stroke assessment. In particular, inhomogeneity manifested by FA and α could potentially assist in clarifying stroke etiology despite its complexity, while kurtosis seems to be more relevant to stroke distribution.

CLINICAL RELEVANCE/APPLICATION

Multi model diffusion and kurtosis imaging provide biophysical and hemodynamic information in ischemic brain and thus a more comprehensive stroke assessment.

SSG11-07 Additional Value of Brain CT Perfusion in The Detection of Intracranial Vessel Occlusion in Acute Ischemic Stroke: A (Multi Experience Level) Inter-Observer Study

Tuesday, Nov. 29 11:30AM - 11:40AM Room: N227B

Participants

Ruud Becks, MD, Nijmegen, Netherlands (*Abstract Co-Author*) Nothing to Disclose
Midas Meijs, MSc, Nijmegen, Netherlands (*Presenter*) Research funded, Toshiba Corporation
Rashindra Manniesing, PhD, Nijmegen, Netherlands (*Abstract Co-Author*) Research funded, Toshiba Corporation
Jeroen Vister, MD, Nijmegen, Netherlands (*Abstract Co-Author*) Nothing to Disclose
Steven Schalekamp, MD, Nijmegen, Netherlands (*Abstract Co-Author*) Nothing to Disclose
Ritse M. Mann, MD, PhD, Nijmegen, Netherlands (*Abstract Co-Author*) Research agreement; Siemens AG; Research agreement, Seno Medical Instruments, Inc
Stefan Steens, MD, PhD, Leiden, Netherlands (*Abstract Co-Author*) Nothing to Disclose
Ewoud J. Smit, MD, Nijmegen, Netherlands (*Abstract Co-Author*) Speakers Bureau, Toshiba Corporation; Research Grant, Toshiba Corporation
Ewoud van Dijk, Nijmegen, Netherlands (*Abstract Co-Author*) Nothing to Disclose
Mathias Prokop, PhD, Nijmegen, Netherlands (*Abstract Co-Author*) Speakers Bureau, Bayer AG Speakers Bureau, Bracco Group
Speakers Bureau, Toshiba Corporation Speakers Bureau, Koninklijke Philips NV Research Grant, Toshiba Corporation
Frederick J. Meijer, MD, PhD, Nijmegen, Netherlands (*Abstract Co-Author*) Nothing to Disclose

PURPOSE

We aimed to evaluate the additional value of brain CT perfusion (CTP) for intracranial vessel occlusion detection in acute ischemic stroke for observers with different levels of experience.

METHOD AND MATERIALS

We retrospectively included all patients with symptoms of acute ischemic stroke (onset of less than 9 hours) who were scanned with non-enhanced CT (NECT), CT angiography (CTA) and CTP in the year 2015. Four observers with different levels of experience (neuroradiologist, non-neuroradiologist, two radiology residents) evaluated the imaging data with 2 imaging strategies. Method 1 included NECT and CTA. For method 2, additional CTP maps were provided for the evaluation of intracranial vessel occlusion on CTA. The observers were blinded to patient identity and clinical outcome. Receiver operating characteristic (ROC) was used for the evaluation of accuracy in intracranial vessel occlusion detection. The reference standard of vessel occlusion was set based on the evaluation by the four observers, and the judgment of an independent neuroradiologist serving as a referee in case of discrepancy.

RESULTS

In total 110 patients were included, preliminary analyses included 94 patients. There was an increase of AUC in the overall detection of intracranial vessel occlusion for observer 1, 3 and 4, though only for observer 1 the increase in AUC was statistically significant (p=0.041). Increase of intracranial vessel occlusion detection mainly concerned distal vessel occlusions. No significant added value of CTP was found for proximal vessel occlusions, with already a high accuracy based on NECT and CTA for all experience levels with sensitivity ranging between 86-94% and specificity between 92-100%.

CONCLUSION

Our study demonstrates that the use of CTP can aid in the detection of distal intracranial vessel occlusions on CTA in case CTP is integrated in the reading strategy. It is also demonstrated that CTP was not of added value for the detection of proximal intracranial vessel occlusions. Finally, there was no major difference in the diagnostic accuracy of intracranial vessel occlusion detection for the different levels in experience of the observers.

CLINICAL RELEVANCE/APPLICATION

Our study demonstrated that brain CT perfusion can aid in the detection of distal intracranial vessel occlusions, which is clinically relevant for optimizing the imaging strategy in acute ischemic stroke.

SSG11-08 Detection of Elevated Whole-Brain Oxygen Extraction Fraction (OEF) in Patients with Intracranial Stenosis Using Non-Invasive MRI

Tuesday, Nov. 29 11:40AM - 11:50AM Room: N227B

Awards

Trainee Research Prize - Medical Student

Participants

Jennifer M. Watchmaker, Nashville, TN (*Presenter*) Nothing to Disclose
Meher R. Juttukonda, PhD, Chapel Hill, NC (*Abstract Co-Author*) Nothing to Disclose
Lori Jordan, MD, Baltimore, MD (*Abstract Co-Author*) Nothing to Disclose
Larry T. Davis, MD, Nashville, TN (*Abstract Co-Author*) Nothing to Disclose
Melissa C. Gindville, Nashville, TN (*Abstract Co-Author*) Nothing to Disclose
Allison Scott, Nashville, TN (*Abstract Co-Author*) Nothing to Disclose
Manus Donahue, PhD, Nashville, TN (*Abstract Co-Author*) Nothing to Disclose

PURPOSE

The purpose of this work is to incorporate novel and noninvasive whole-brain MRI measures of cerebral oxygen extraction fraction (OEF; ratio of oxygen consumed to oxygen delivered) to test fundamental hypotheses regarding elevated OEF and its concordance with clinical radiological measures of impairment in patients with intracranial (IC) arterial stenosis at high risk of recurrent stroke. Elevated OEF is hypothesized to be driven by reduced oxygen carrying capacity, as in the case of hemoglobinopathies such as sickle cell anemia (SCA), or by reduced cerebral blood flow (CBF) as in the case of IC steno-occlusive disease. Unfortunately, tools capable of recording OEF routinely in clinical settings are limited. Here, we apply a novel whole-brain OEF MRI method in sequence with CBF and structural imaging.

METHOD AND MATERIALS

CBF and whole-brain OEF MRI were performed using pseudo-continuous arterial-spin labeling (pCASL) and T2-Relaxation-Under-Spin-Tagging (TRUST), respectively, in participants with IC stenosis (n=21), SCA (n=20), and age-matched (n=45) control participants. TRUST provided a venous blood water T2, which was converted to blood oxygenation level and OEF by utilizing the measured hematocrit and arterial oxygenation.

RESULTS

OEF was elevated in participants with IC stenosis (IQR = 0.38 - 0.45) and SCA (IQR = 0.37 - 0.45) compared to controls (IQR = 0.29 - 0.38). CBF was inversely correlated with OEF in IC stenosis participants (Spearman test; $r = -0.42, p = 0.03$), but not in control participants ($r = -0.07, p = 0.33$) or participants with SCA ($r = -0.28, p = 0.12$).

CONCLUSION

These results (i) are consistent with non-invasive MRI being able to quickly detect elevated OEF in multiple cases of reduced oxygen delivery to tissue, (ii) provide insights regarding differing pathological hemodynamic compensation mechanisms, and (iii) suggest that extreme hypoperfusion corresponds to elevated OEF in IC stenosis, which may be indicative of widespread, advanced disease and elevated stroke risk.

CLINICAL RELEVANCE/APPLICATION

Patients with symptomatic intracranial atherosclerotic stenosis have an unacceptably high 14-16% 1-year risk of recurrent stroke even on standard-of-care aggressive medical management; elevated cerebral oxygen extraction fraction (OEF), which can be quantified in approximately 1-minute with noninvasive MRI, may provide a new biomarker of stroke risk, which could guide personalized stroke prevention therapies.

SSG11-09 Collateral Assessment With Multi-Phase CTA In Thrombectomy Candidates in the Borderline ASPECTS Subgroup

Tuesday, Nov. 29 11:50AM - 12:00PM Room: N227B

Participants

Caitriona Logan, MBBCh, MRCP, Dublin, Ireland (*Presenter*) Nothing to Disclose
Aileen O'Shea, MBBCh, MRCS, Dublin, Ireland (*Abstract Co-Author*) Nothing to Disclose
Damien C. O'Neill, MBBCh, Cork, Ireland (*Abstract Co-Author*) Nothing to Disclose
John Thornton, Dublin, Ireland (*Abstract Co-Author*) Nothing to Disclose
Seamus Looby, FRCR, MBBCh, Dublin, Ireland (*Abstract Co-Author*) Nothing to Disclose
Paul Brennan, Dublin, Ireland (*Abstract Co-Author*) Nothing to Disclose
Hamed Asadi, MD, Dublin, Ireland (*Abstract Co-Author*) Nothing to Disclose

PURPOSE

Collateral blood supply an important factor in determining the extent of ischaemia in stroke (1). Good collaterals are an important predictor of good outcome from endovascular treatment of stroke (3). In cases of large vessel occlusion of the anterior circulation and early ischaemic changes or no established ischaemia, patients may be eligible for thrombectomy. CT is used to quantify established infarction according to the Alberta stroke score (4). Multiphase CT angiography is used for collateral assessment in our center (5). This study aims to assess if three-phase CTA assessment of collaterals is predictive of outcome in patients who had borderline ASPECTS scores and who subsequently went on to have mechanical thrombectomy.

METHOD AND MATERIALS

A retrospective analysis of 184 thrombectomy patients over a two year period with a proximal vessel occlusion in the anterior circulation was carried out. Patients with an ASPECTS score of 5/6/7, indicating early ischaemic change were selected. ASPECTS scores were assigned in the original report and subsequently by a neuroradiology interventionalist, blinded to the original report. Assessment of collaterals with three-phase CTA assigned a value of >50% or <50%. Success of mechanical thrombectomy and favourable outcome (as measured by a reduction in 90 day NIHSS or MRS).

RESULTS

184 patients had mechanical thrombectomy over a 12 month period. 26 patients were identified with ASPECTS score of 5/6/7, 19 with good collaterals, 7 with poor collaterals. In the good collaterals group there was an 84% recanalization rate, 85% in the poor collateral group. There was favourable 90 day outcome in 63% of the good collaterals group and 14% of the poor collateral group. Mortality in the good collateral group at 90 days was 31% and 57% in the poor collaterals group.

CONCLUSION

Linear regression analysis identified a statistically significant association between good collaterals and a reduction in disability at 90 days in the borderline ASPECTS subgroup with a P value = 0.012.

CLINICAL RELEVANCE/APPLICATION

Collateral assessment with three phase CT angiogram is an good predictor of outcome in thrombectomy candidates with large vessel occlusion who have evidence of early established ischemia and should be used as the standard imaging protocol in this group.

SSG12

Physics (CT Photon Counting)

Tuesday, Nov. 29 10:30AM - 12:00PM Room: S403B



AMA PRA Category 1 Credits™: 1.50
ARRT Category A+ Credits: 1.50

Participants

Willi A. Kalender, PhD, Erlangen, Germany (*Moderator*) Founder, CT Imaging GmbH; CEO, CT Imaging GmbH
Katsuyuki Taguchi, PhD, Baltimore, MD (*Moderator*) Research Grant, Siemens AG

Sub-Events

SSG12-01 Renal Imaging with Complimentary Contrast Materials Using A Whole Body Photon-Counting CT Scanner

Tuesday, Nov. 29 10:30AM - 10:40AM Room: S403B

Participants

Amir Pourmorteza, PhD, Bethesda, MD (*Presenter*) Researcher, Siemens AG
Rolf Symons, MD, Washington, DC (*Abstract Co-Author*) Nothing to Disclose
Manu N. Lakshmanan, PhD, Bethesda, MD (*Abstract Co-Author*) Research support, Siemens AG;
Tyler E. Cork, BS, Bethesda, MD (*Abstract Co-Author*) Nothing to Disclose
Kelly A. Rice, DVM, Bethesda, MD (*Abstract Co-Author*) Nothing to Disclose
Cynthia Davies-Venn, Bethesda, MD (*Abstract Co-Author*) Nothing to Disclose
Veit Sandfort, MD, Bethesda, MD (*Abstract Co-Author*) Nothing to Disclose
David A. Bluemke, MD, PhD, Bethesda, MD (*Abstract Co-Author*) Research support, Siemens AG

PURPOSE

To demonstrate the feasibility of using spectral photon-counting CT (PCCT) to differentiate the in vivo wash-in and wash-out dynamics of two contrast agents in the kidney for simultaneous visualization of different renal enhancement phases.

METHOD AND MATERIALS

This Institutional Animal Care and Use Committee-approved study used a canine model of chronic myocardial infarction. PCCT was performed during intravenous administration of 4.6 grams of gadolinium (Dotarem, Guerbet) followed after 3.5 minutes by 7.4 grams of iodine (Isovue 370, Bracco). PCCT images were acquired every 4 seconds for a total duration of 6 minutes at the level of the right renal pelvis to visualize the time course of contrast enhancement and excretion in the kidney for both contrast agents. After 1.5 minutes there was a 1 min pause in imaging to avoid system overheating. Scan parameters were 140 kVp tube voltage, 300 mAs tube current, 0.5 second rotation time and energy thresholds of 25, 50, 75, and 90 keV. Images were reconstructed with a quantitative soft tissue kernel (D30f), slice thickness of 1 mm, and increment of 1 mm. Least mean squares linear material decomposition—calibrated to gadolinium and iodine vials of known concentrations in the field-of-view—was used to calculate the concentrations of the contrast agents in the aorta, renal cortex, and renal pelvis.

RESULTS

Time-attenuation curves for gadolinium and iodine in the regions-of-interest (ROIs) were significantly different making contrast agent separation possible. Peak contrast concentration in the aorta and renal cortex were observed ~16 and 24 seconds after each injection. Contrast agent excretion in the renal pelvis started 60 seconds after injection and reached a plateau after ~2.5 minutes for both gadolinium and iodine. Co-registered arterial and equilibrium phase renal images can be reconstructed from a single PCCT scan.

CONCLUSION

PCCT can differentiate contrast agents in vivo. Therefore, multiple inherently co-registered phases of tissue enhancement can be acquired from a single PCCT scan, potentially obviating the need for multi-phase CT scans and reducing radiation dose.

CLINICAL RELEVANCE/APPLICATION

By differentiating contrast materials, PCCT can acquire multiple perfectly co-registered phases of tissue enhancement from a single PCCT scan, potentially obviating the need for multi-phase CT scans and reducing radiation dose.

SSG12-02 A Multi-Channel Block-Matching Denoising Algorithm for Spectral Photon-Counting CT Images

Tuesday, Nov. 29 10:40AM - 10:50AM Room: S403B

Awards

Trainee Research Prize - Fellow

Participants

Adam P. Harrison, PhD, Bethesda, MD (*Presenter*) Nothing to Disclose
Ziyue Xu, PhD, Bethesda, MD (*Abstract Co-Author*) Nothing to Disclose
Amir Pourmorteza, PhD, Bethesda, MD (*Abstract Co-Author*) Researcher, Siemens AG
David A. Bluemke, MD, PhD, Bethesda, MD (*Abstract Co-Author*) Research support, Siemens AG
Daniel J. Mollura, MD, Bethesda, MD (*Abstract Co-Author*) Nothing to Disclose

PURPOSE

We present a denoising algorithm designed for a new whole-body prototype photon-counting computed tomography (PCCT) scanner with up to 4 energy thresholds and associated energy-binned images.

METHOD AND MATERIALS

Spectral PCCT images can exhibit low signal to noise ratios (SNRs) due to the limited photon counts in each simultaneously-acquired energy bin. To correct this, denoising algorithms should exploit the correlation and exact alignment between energy bins. Our method follows this approach, modifying the highly-effective block-matching (BM3D) denoising algorithm for PCCT. The original single-channel BM3D algorithm operates patch-by-patch. For each small patch in the image, a grouping action (GA) collects similar patches from the rest of the image, which are then collaboratively filtered together. The resulting performance hinges on accurate GAs. Our improved multi-channel version, called BM3D_PCCT, calculates a shared GA based on the image reconstructed from photons detected in all 4 energy bins. As this image has higher SNR, its GA is more accurate. This shared and improved GA is then used to denoise each individual energy bin.

RESULTS

Preliminary results compare BM3D_PCCT against BM3D_Naive, which denoises each energy bin independently. Experiments used a three-contrast PCCT image of a canine abdomen. Within five regions of interest, selected from paraspinal muscle, liver, and visceral fat, BM3D_PCCT reduced the noise standard deviation by 73.4%, compared to 68.0% for BM3D_Naive. Attenuation values of the contrast agents in calibration vials also clustered much tighter to their respective lines of best fit. Mean angular differences (in degrees) from the line of fit for the original, BM3D_Naive, and BM3D_PCCT images, respectively, were 16.40, 5.98, and 5.11 (iodine); 13.09, 4.05, and 3.27 (gadolinium); and 17.81, 5.14, and 4.48 (bismuth).

CONCLUSION

We outlined a multi-channel denoising algorithm tailored for spectral PCCT images, demonstrating improved performance over an independent single-channel approach. Further advancement of this work in progress will include phantom and animal studies to determine the lowest possible mAs required for effective denoising.

CLINICAL RELEVANCE/APPLICATION

This algorithm can denoise PCCT images prior to tissue decomposition in order to produce a more detailed map of contrast-agent concentration.

SSG12-03 Dual-Contrast Spectral Photon-Counting CT: Feasibility for Myocardial Imaging

Tuesday, Nov. 29 10:50AM - 11:00AM Room: S403B

Participants

Amir Pourmorteza, PhD, Bethesda, MD (*Presenter*) Researcher, Siemens AG
Rolf Symons, MD, Washington, DC (*Abstract Co-Author*) Nothing to Disclose
Manu N. Lakshmanan, PhD, Bethesda, MD (*Abstract Co-Author*) Research support, Siemens AG;
Tyler E. Cork, BS, Bethesda, MD (*Abstract Co-Author*) Nothing to Disclose
Kelly A. Rice, DVM, Bethesda, MD (*Abstract Co-Author*) Nothing to Disclose
Cynthia Davies-Venn, Bethesda, MD (*Abstract Co-Author*) Nothing to Disclose
Mark A. Ahlman, MD, Bethesda, MD (*Abstract Co-Author*) Nothing to Disclose
Veit Sandfort, MD, Bethesda, MD (*Abstract Co-Author*) Nothing to Disclose
David A. Bluemke, MD, PhD, Bethesda, MD (*Abstract Co-Author*) Research support, Siemens AG

PURPOSE

To demonstrate the feasibility of using two contrast agents (CA) to enhance the myocardial scar and coronary vessels in a single scan using spectral photon-counting CT (PCCT). The first CA (gadolinium) may be injected 10-15 mins prior to scan to create delayed-enhanced images of the scar; the second CA (iodine) is injected at the time of scan to enhance the coronary arteries.

METHOD AND MATERIALS

This study was performed with the approval of ACUC. A canine model of chronic myocardial infarct was used. The animal received intravenous injections of gadoteric acid (60 mL, Dotarem, Guerbet). After 12 minutes, the animal was euthanized by an injection of KCL mixed with iodinated CA (20 mL, Isovue 370, Bracco). We acquired spiral spectral CT scans on a whole-body photon-counting CT scanner at tube voltage/current of 140 kVp, 300 mAs. The energy thresholds were set to 25/50/75/90 keV in order to create 4 spectral bins. Since the current prototype does not support ECG-gating, all cardiac scans were performed immediately after euthanasia. We calculated gadolinium and iodine concentration maps using a linear material decomposition technique calibrated to vials with known concentrations placed in the scan field-of-view. Ex-vivo magnetic resonance imaging was used as gold standard for scar characterization.

RESULTS

The concentration maps were compared in three regions selected based on the ex-vivo MRI: left ventricle (LV) blood pool, scar, and remote myocardium. Iodine concentration was significantly higher in the LV blood pool than in the scar or remote myocardium. In comparison, gadolinium concentrations in the LV blood pool and scar were significantly higher than those in the remote myocardium. By combining the iodine and gadolinium concentration maps, differentiation of blood pool, scar and remote myocardium was possible.

CONCLUSION

Dual contrast agent photon-counting CT may allow for combined assessment of coronary perfusion and delayed enhancement in one acquisition.

CLINICAL RELEVANCE/APPLICATION

Photon-counting CT has the potential for combined first-pass and delayed enhancement CT images, thereby potentially reducing radiation dose by half while providing registered images.

SSG12-04 Initial Experience in Improving Stent Analysis and Intra Stent Lumen Assessment using Spectral Photon Counting CT and K-edge Imaging

Tuesday, Nov. 29 11:00AM - 11:10AM Room: S403B

Participants

Monica Sigovan, PhD, Lyon, France (*Abstract Co-Author*) Nothing to Disclose
Daniel Bar-Ness, Bron, France (*Presenter*) Nothing to Disclose
Salim Si-Mohamed, Bron, France (*Abstract Co-Author*) Nothing to Disclose
Julia Mitchell, Bron, France (*Abstract Co-Author*) Nothing to Disclose
Jean-Baptiste Langlois, Bron, France (*Abstract Co-Author*) Nothing to Disclose
Philippe Coulon, PhD, Suresnes, France (*Abstract Co-Author*) Employee, Koninklijke Philips NV
Matthias Bartels, PhD, DIPLPHYS, Hamburg, Germany (*Abstract Co-Author*) Employee, Koninklijke Philips NV
Bernhard Brendel, Hamburg, Germany (*Abstract Co-Author*) Researcher, Koninklijke Philips NV
Heiner Daerr, DIPLPHYS, Hamburg, Germany (*Abstract Co-Author*) Employee, Koninklijke Philips NV
Axel Thran, Hamburg, Germany (*Abstract Co-Author*) Employee, Koninklijke Philips NV
Ewald Roessl, PhD, Hamburg, Germany (*Abstract Co-Author*) Employee, Koninklijke Philips NV
Ira Blevis, Haifa, Israel (*Abstract Co-Author*) Employee, Koninklijke Philips NV
Michal Rokni, PhD, Haifa, Israel (*Abstract Co-Author*) Employee, Koninklijke Philips NV
Philippe C. Douek, MD, PhD, Lyon, France (*Abstract Co-Author*) Nothing to Disclose
Loic Boussel, MD, Lyon, France (*Abstract Co-Author*) Nothing to Disclose

PURPOSE

Coronary stent analysis is still limited using standard CT. We assessed the capability of a spectral photon counting CT (SPCCT) to improve stent analysis and intra stent lumen assessment in comparison with standard CT

METHOD AND MATERIALS

In vitro and in vivo imaging using SPCCT (Philips, Haifa, Israel) and Brilliance 64 CT (B64, Philips, Cleveland, USA) were performed on a phantom consisting of plastic tubes (3.5 mm lumen diameter) and on the abdominal aorta of a NZW rabbit, using 3 types of stents: 1-Platinum (Pt)-Chromium, 2-Cobalt-Chromium, and 3-Stainless steel (true width of metallic struts between 60 to 80 μ m depending on the stent). Gadolinium (Gd) contrast agent was used both in vitro (\sim 0.05M) and in vivo (5mL of 0.5M injected for each stent imaging), all at 120 kV and 100 mAs. In plane pixel size of 0.2x0.2mm² was used for all image reconstructions: conventional HU images for B64, and conventional HU, and Gd and Pt K-edge specific images for SPCCT. Apparent width of the metallic struts was compared between the two systems using a Wilcoxon sign rank test to evaluate stent-related blooming artifact.

RESULTS

SPCCT HU images showed better visualization of the intra-stent lumen with Gd contrast agent due to improved spatial resolution and reduced blooming of the stent compared to B64. The apparent width of the metallic struts was significantly smaller on SPCCT than on B64 for all stents (mean values in mm: 0.68 \pm 0.01 vs 1.01 \pm 0.02 for Stent1, 0.71 \pm 0.01 vs 1.01 \pm 0.02 for Stent2, and 0.69 \pm 0.03 vs 1.00 \pm 0.09 for Stent3, p <0.05). Gd specific K-edge imaging enabled visualization of the aortic lumen itself. Finally, Pt specific K-edge imaging enabled exclusive visualization of the Pt only containing stent and removal of other backgrounds and contrast media.

CONCLUSION

SPCCT can allow significant reduction of stent blooming and better lumen assessment due to improved spatial resolution combined with sufficient energy resolution compared to conventional CT. K-edge specific images should allow precise validation of correct deployment of Pt containing stents.

CLINICAL RELEVANCE/APPLICATION

Reduction in blooming artifacts and improved visualization on the lumen of a stented vessel is expected to improve diagnosis of restenosis and stent malapposition.

SSG12-05 Advanced Spectral Analysis of Whole-Body Photon-Counting-Detector Computed Tomography Data

Tuesday, Nov. 29 11:10AM - 11:20AM Room: S403B

Participants

Ahmed Halaweish, PhD, Rochester, MN (*Presenter*) Employee, Siemens AG
Roy Marcus, MD, Rochester, MN (*Abstract Co-Author*) Institutional research agreement, Siemens AG; Research support, Siemens AG
Shuai Leng, PhD, Rochester, MN (*Abstract Co-Author*) Nothing to Disclose
Bernhard Krauss, PhD, Forchheim, Germany (*Abstract Co-Author*) Employee, Siemens AG
Martin U. Sedlmair, MS, Forchheim, Germany (*Abstract Co-Author*) Employee, Siemens AG
Thomas Allmendinger, Forchheim, Germany (*Abstract Co-Author*) Employee, Siemens AG
Steffen Kappler, Dipl Phys, Forchheim, Germany (*Abstract Co-Author*) Researcher, Siemens AG
Ralf Gutjahr, Munich, Germany (*Abstract Co-Author*) Grant, Siemens AG
Bernhard Schmidt, PhD, Forchheim, Germany (*Abstract Co-Author*) Employee, Siemens AG
Erik L. Ritman, MD, PhD, Rochester, MN (*Abstract Co-Author*) Nothing to Disclose
Cynthia H. McCollough, PhD, Rochester, MN (*Abstract Co-Author*) Research Grant, Siemens AG

PURPOSE

To investigate advanced spectral analysis of whole-body photon-counting-detector (PCD) CT data and compare it to 2nd generation dual-source (DS) dual energy (DE) imaging.

METHOD AND MATERIALS

A research, whole-body PCD CT scanner (Somatom Count, Siemens Healthcare) was utilized to acquire head/neck (H&N) and chest CTA data using 140kV at clinically equivalent doses, following iodine injections (Iohexol 350 @ 3cc/sec: Chest - 45 cc, H&N - 60 cc | Saline chaser - 30 cc) in a swine model. The PCD-CT scanner is based on the footprint of a 2nd generation DSCT scanner (Siemens Healthcare), where the "A" detector/source sub-system uses a conventional energy integrating detector (EID) and the

"B" detector/source sub-system uses a cadmium telluride PCD. PCD-CT acquisitions were performed using a 2-bin (Macro) and a 4-bin (Chess) mode, with energy thresholds set at 25/65 keV and 20/25/57/77 keV for the Macro and Chess modes, respectively. Dose matched DECT acquisitions were performed on a 2nd generation DSCT scanner using 80/Sn140 kV, with the same contrast injection protocol. Spectral post processing algorithms were calibrated for water and iodine and the energy thresholds set for each acquisition. The generated calibration tables were then utilized for the optimization of the PCD-CT analysis. Chess mode data was combined to generate 2 spectrally different datasets for input into the post processing algorithms.

RESULTS

Advanced spectral analysis of the PCD-CT data resulted in the generation of virtual non-contrast and iodine only maps, with qualitatively similar material separation as seen in clinically available techniques. Virtual monoenergetic images further improved upon the already-reported increased contrast-to-noise ratio achievable with PCD-CT. Other spectral analyses optimized for PCD-CT included, optimum contrast, pulmonary perfused blood volume and bone removal. Head and body bone removal algorithms demonstrated similar results as their clinically implemented counterparts.

CONCLUSION

The advanced spectral analysis of whole-body PCD-CT data provided qualitatively similar results to those attainable utilizing clinically available dual energy technologies, with improved image quality.

CLINICAL RELEVANCE/APPLICATION

Advanced spectral analysis of whole body PCD-CT allows the extraction of the quantitative spectral information needed to fully assess PCD-CT's capabilities and clinical potential.

SSG12-06 Spectral Performance of a Whole-Body Research Photon Counting Detector CT: Accuracy of Iodine Quantification

Tuesday, Nov. 29 11:20AM - 11:30AM Room: S403B

Participants

Shuai Leng, PhD, Rochester, MN (*Presenter*) Nothing to Disclose
Zhicong Yu, Rochester, MN (*Abstract Co-Author*) Nothing to Disclose
Ahmed Halaweish, PhD, Rochester, MN (*Abstract Co-Author*) Employee, Siemens AG
Bernhard Krauss, PhD, Forchheim, Germany (*Abstract Co-Author*) Employee, Siemens AG
Bernhard Schmidt, PhD, Forchheim, Germany (*Abstract Co-Author*) Employee, Siemens AG
Lifeng Yu, PhD, Chicago, IL (*Abstract Co-Author*) Nothing to Disclose
Steffen Kappler, Dipl Phys, Forchheim, Germany (*Abstract Co-Author*) Researcher, Siemens AG
Cynthia H. McCollough, PhD, Rochester, MN (*Abstract Co-Author*) Research Grant, Siemens AG
Michael R. Bruesewitz, Rochester, MN (*Abstract Co-Author*) Nothing to Disclose

PURPOSE

To assess the spectral performance of a research photon counting detector (PCD) CT scanner in terms of iodine quantification accuracy, and to compare the performance with that of dual-source (DS), dual-energy (DE) CT scanners with energy integrating detectors (EID).

METHOD AND MATERIALS

Vials containing iodine solutions at 5 concentrations (2, 5, 10, 15, and 20 mgI/cc) were placed in torso-shaped water phantoms (lateral widths 25 to 45 cm). Phantoms were scanned on the PCD-CT scanner using 140 kV, energy thresholds of 25 and 65 keV, 0.5 sec rotation time, and 0.6 helical pitch. Tube current was adjusted for each phantom size so that the CTDIvol matched that of clinical abdomen scans. For comparison, the same phantoms were also scanned on 2nd and 3rd generation DSDE scanners with matched CTDIvol. Material decomposition was performed using a 'virtual unenhanced' application on commercial software, and iodine concentration was measured in the 5 vials and the background water. Measurements were compared to known concentrations and the root-mean-square-errors (RMSE) were calculated for each phantom size, scanner and DE mode.

RESULTS

A linear relationship was observed between measured and true concentrations for PCD-CT and all DE modes on the EID scanners ($R^2 > 0.98$). For PCD-CT, iodine concentration errors ranged from -2.4 to +0.5 mgI/cc, with overall RMSE of 0.93 mgI/cc. Iodine quantification was more accurate for phantoms 35 cm and below (RMSE < 0.38 mgI/cc); accuracy decreased for 40 and 45 cm phantoms (RMSE of 1.21 and 1.59 mgI/cc, respectively). RMSE was 1.17 mgI/cc for the 80/Sn140 mode of the 2nd generation DSDE scanner, and 1.30 mgI/cc for the 70/Sn150 mode of the 3rd generation DSDE scanner. As the tube potential increased for the low energy beam, RMSE decreased substantially for EID scanners, with RMSE from 0.44 to 0.68 mgI/cc.

CONCLUSION

Phantom studies demonstrated high accuracy for iodine quantification using PCD-CT (RMSE of 0.93 mgI/cc), with slight degradation for larger size phantoms. The performance of iodine quantification is comparable to that of EID-based DSDE scanners.

CLINICAL RELEVANCE/APPLICATION

The spectral performance of a research PCD-CT scanner was comparable to that of EID-CT scanners, each of which provided accurate quantification of iodine concentrations, with RMSE of about 1 mgI/cc.

SSG12-07 Spectral Photon-counting CT for Imaging of Contrast Agents Based on lanthanides

Tuesday, Nov. 29 11:30AM - 11:40AM Room: S403B

Participants

Manu N. Lakshmanan, PhD, Bethesda, MD (*Abstract Co-Author*) Research support, Siemens AG;
William F. Pritchard JR, MD, PhD, Bethesda, MD (*Abstract Co-Author*) Nothing to Disclose
Tyler E. Cork, BS, Bethesda, MD (*Abstract Co-Author*) Nothing to Disclose
Pooyan Sahbaee, Durham, NC (*Presenter*) Employee, Siemens AG
Rolf Symons, MD, Washington, DC (*Abstract Co-Author*) Nothing to Disclose

Bradford J. Wood, MD, Bethesda, MD (*Abstract Co-Author*) Researcher, Koninklijke Philips NV; Researcher, Celsion Corporation; Researcher, BTG International Ltd; Researcher, W. L. Gore & Associates, Inc ; Researcher, Cook Group Incorporated; Patent agreement, VitalDyne, Inc; Intellectual property, Koninklijke Philips NV; Intellectual property, BTG International Ltd; ; ; ; David A. Bluemke, MD, PhD, Bethesda, MD (*Abstract Co-Author*) Research support, Siemens AG
Amir Pourmorteza, PhD, Bethesda, MD (*Abstract Co-Author*) Researcher, Siemens AG

PURPOSE

There are multiple techniques for dual-energy CT including fast-kV switching, dual-source, and dual-layer detectors. Here we demonstrate that photon-counting CT (PCCT) offers flexible threshold settings that can be tuned to optimize the differentiability of various contrast agents (CA) with high x-ray absorption k-edge.

METHOD AND MATERIALS

We used a hybrid (dual-source) whole-body prototype CT system (Siemens Healthcare, Germany), which consists of an energy integrating detector and a photon-counting detector. We imaged test tubes with soft tissue equivalent material, iodine (Isovue 300, Bracco), and known concentrations of salts of pentetic acid (DTPA) and 5 lanthanides: Samarium (Sm), Europium (Eu) Gadolinium (Gd), Terbium (Tb), and Lutetium (Lu) with k-edges ranging from 47 to 63 keV. Multiple PCCT scans were acquired with a tube voltage/current of 120kVp/300mA and 2 energy thresholds; one threshold was fixed at 22 keV and the second was swept from 47 to 65 keV, creating two energy bins. The angle between the attenuation coefficient vectors of the CAs and tissue equivalent sample was used as a metric for the spectral differentiability.

RESULTS

We could find a threshold setting that would yield a separation of at least 10° between the CA and tissue equivalent sample. Using different thresholds, for all lanthanide CAs angular separation of 10°-13° (CA vs tissue) and 8-20° (CA vs iodine) was achieved. As a reference, maximum iodine-soft tissue separation was 16°. Lanthanides with higher atomic number had higher angular separation; the highest angular separation was between lutetium and iodine at 65 keV threshold setting with tube voltage of 140 kVp.

CONCLUSION

We demonstrated the feasibility of tuning PCCT energy thresholds to differentiate CAs with various atomic numbers from soft tissue and iodinated contrast. Future work will include a wider and more detailed sweep of threshold settings, quantification of CA concentration mixed in tissue, and finding a 4-energy threshold setting that can differentiate three CA simultaneously.

CLINICAL RELEVANCE/APPLICATION

The improved ability to image contrast materials in PCCT allows for novel multi-contrast clinical protocols and for improved differentiation of contrast materials in existing protocols.

SSG12-08 Ultra-High-Resolution Imaging using a Photon-Counting-Detector CT System: Spatial Resolution, Image Quality and Dose Efficiency

Tuesday, Nov. 29 11:40AM - 11:50AM Room: S403B

Participants

Shuai Leng, PhD, Rochester, MN (*Presenter*) Nothing to Disclose
Zhicong Yu, Rochester, MN (*Abstract Co-Author*) Nothing to Disclose
Ahmed Halaweish, PhD, Rochester, MN (*Abstract Co-Author*) Employee, Siemens AG
Steffen Kappler, Dipl Phys, Forchheim, Germany (*Abstract Co-Author*) Researcher, Siemens AG
Katharina Hahn, DIPLPHYS, Forchheim, Germany (*Abstract Co-Author*) Nothing to Disclose
Andre Henning, MENG,MSc, Forchheim, Germany (*Abstract Co-Author*) Employee, Siemens AG
Zhoubo Li, Rochester, MN (*Abstract Co-Author*) Nothing to Disclose
John I. Lane, MD, Rochester, MN (*Abstract Co-Author*) Nothing to Disclose
David L. Levin, MD, PhD, Rochester, MN (*Abstract Co-Author*) Nothing to Disclose
Steven M. Jorgensen, Rochester, MN (*Abstract Co-Author*) Nothing to Disclose
Erik L. Ritman, MD, PhD, Rochester, MN (*Abstract Co-Author*) Nothing to Disclose
Cynthia H. McCollough, PhD, Rochester, MN (*Abstract Co-Author*) Research Grant, Siemens AG

PURPOSE

To evaluate ultra-high-resolution (UHR) imaging techniques on a photon counting detector (PCD) CT system by quantitatively and qualitatively assessing image quality and dose efficiency and by demonstrating the mode's clinical potential using phantoms and cadaveric specimens.

METHOD AND MATERIALS

A UHR data collection mode was enabled on a whole-body, research PCD-CT system that used 0.45 mm x 0.45 mm detector pixels, which corresponded to a pixel size of 0.25 mm x 0.25 mm at iso-center. There were z-axis two collimations: 32x0.25 or 48x0.25 mm, and two energy thresholds. Spatial resolution and image noise were quantitatively assessed for the PCD UHR scan mode, as well as for a commercially available UHR scan mode that uses an energy integrating detector (EID) and a set of comb filters to decrease the effective detector size. Spatial resolution was quantified by measuring the MTF from a scan of a 50-micron wire phantom and noise was quantified as the standard deviation of pixel values in a uniform region of interest. Images of an anthropomorphic lung phantom, cadaveric swine lung, swine heart specimen and cadaveric human temporal bone were assessed qualitatively by two experienced radiologists.

RESULTS

Nearly equivalent spatial resolution was demonstrated by the MTF measurements: 15.3 lp/cm and 20.3 lp/cm spatial frequencies were achieved at 10% and 2% modulation, respectively, for the PCD system, and 14.2 lp/cm and 18.6 lp/cm at 10% and 2% modulation, respectively, for the EID system. Noise was 29% lower in the PCD UHR images compared to the EID UHR images, representing a potential dose savings of 50% for equivalent image noise. PCD UHR images from the anthropomorphic phantom and cadaveric specimens showed clear delineation of small structures, such as lung vessels, lung nodules, temporal bone structures, and coronary arteries, with improvements in spatial resolution apparent in the PCD images.

CONCLUSION

Spatial resolution up to 20 lp/cm was achieved using the PCD UHR technique. This was achieved without the use of a dedicated comb attenuator, enabling 50% dose reduction. Phantom and cadaveric studies demonstrated the potential impact of this imaging mode in lung, temporal bone, and vascular imaging.

CLINICAL RELEVANCE/APPLICATION

The dose efficient PCD UHR mode enables the ultra-high spatial resolution that is needed to delineate fine anatomical structure and pathology in multiple clinical applications and has no dose penalty.

SSG12-09 Multi-Contrast Agent Quantitative Separation via K-Edge Imaging Using Spectral Photon-Counting Computed Tomography

Tuesday, Nov. 29 11:50AM - 12:00PM Room: S403B

Participants

Daniel Bar-Ness, Bron, France (*Presenter*) Nothing to Disclose
Salim Si-Mohamed, Bron, France (*Abstract Co-Author*) Nothing to Disclose
Monica Sigovan, PhD, Lyon, France (*Abstract Co-Author*) Nothing to Disclose
David P. Cormode, DPhil, MS, Philadelphia, PA (*Abstract Co-Author*) Research Grant, Koninklijke Philips NV;
Joelle Balegamire, Lyon, France (*Abstract Co-Author*) Nothing to Disclose
Franck Lavenne, Bron, France (*Abstract Co-Author*) Nothing to Disclose
Philippe Coulon, PhD, Suresnes, France (*Abstract Co-Author*) Employee, Koninklijke Philips NV
Matthias Bartels, PhD, DIPLPHYS, Hamburg, Germany (*Abstract Co-Author*) Employee, Koninklijke Philips NV
Bernhard Brendel, Hamburg, Germany (*Abstract Co-Author*) Researcher, Koninklijke Philips NV
Axel Thran, Hamburg, Germany (*Abstract Co-Author*) Employee, Koninklijke Philips NV
Heiner Daerr, DIPLPHYS, Hambrg, Germany (*Abstract Co-Author*) Employee, Koninklijke Philips NV
Ewald Roessl, PhD, Hamburg, Germany (*Abstract Co-Author*) Employee, Koninklijke Philips NV
Michal Rokni, PhD, Haifa, Israel (*Abstract Co-Author*) Employee, Koninklijke Philips NV
Ira Blevis, Haifa, Israel (*Abstract Co-Author*) Employee, Koninklijke Philips NV
Loic Bousset, MD, Lyon, France (*Abstract Co-Author*) Nothing to Disclose
Philippe C. Douek, MD, PhD, Lyon, France (*Abstract Co-Author*) Nothing to Disclose

PURPOSE

Conventional CT cannot discriminate between different contrast materials with similar attenuation using Hounsfield values. We herein report on the capability of spectral photon-counting computed tomography (SPCCT) to differentiate between multiple contrast materials in the same spatial location within a single scan.

METHOD AND MATERIALS

Two phantoms of 11 tubes (1 cm in diameter) were prepared with mixed dilution of two contrast agents (CA) in varying proportions. The CA used was either pegylated gold (Au-nano) nanoparticles (65mg/mL, size 18nm, synthesized in house) mixed with iodine (Iomeron 400 mg/mL, Bracco) or the same Au-nano mixed with gadolinium(Gd) (Multihance 0.5mmol/mL, Bracco). The proportions of CAs were adjusted so that the attenuation of each tube was about 280 HU for conventional CT images; with gd, Au-nano, iodine concentrations between 0 and 7.45 mg/mL, 0 and 10.4 mg/mL and 0 and 10 mg/mL respectively. Axial (1 second rotation time) scans were acquired at 120 kVp and 100 mAs with SPCCT (Philips, Haifa, Israel). Reconstructions were performed at a voxel size of 0.4x0.4x2mm and consisted of conventional HU images, Iodine material decomposition (MD), and Gd and Au K-edge specific images. Each CA was scanned on its own for calibration purposes. Linear regression was used to assess correlation between measured and expected concentrations.

RESULTS

As designed, different solutions of mixed contrast agents could not be differentiated on HU images as all showing the same attenuation of 279 ± 8 HU. Clear separations of the CAs were observed in the MD and K-edge images within the same tubes. The concentration measurements on K-edge images and MD images were in good correlation with the expected concentrations. For the Au-nano and iodine mixture, the Au image correlation had a slope of 1.02, offset -1.1 mg/mL and $R^2=0.98$; iodine correlation had a slope of 0.99, offset -0.1 mg/mL and $R^2=0.98$. Similar results were observed for the Au-nano and Gd mixture.

CONCLUSION

Multi-contrast agent quantitative separation via K-edge imaging is achievable using SPCCT as demonstrated by the accurate differentiation between multiple contrast materials within the same voxel using their spectral characteristics.

CLINICAL RELEVANCE/APPLICATION

SPCCT has the potential to provide a new form of functional imaging, opening the door for the use of two or more contrast agents with different pharmacokinetics.

SSG13

Physics (CT-Image Quality)

Tuesday, Nov. 29 10:30AM - 12:00PM Room: S404AB



AMA PRA Category 1 Credits™: 1.50
ARRT Category A+ Credits: 1.50

FDA Discussions may include off-label uses.

Participants

Jeffrey H. Siewerdsen, PhD, Baltimore, MD (*Moderator*) Research Grant, Siemens AG; Research Grant, Carestream Health, Inc; Advisory Board, Siemens AG; Advisory Board, Carestream Health, Inc; License agreement, Carestream Health, Inc; License agreement, Elekta AB; ;
Xiangyang Tang, PhD, Atlanta, GA (*Moderator*) Research Grant, SINOVISION Technologies Co, Ltd

Sub-Events

SSG13-01 Cloverleaf NPS in Clinical MDCT Systems: Physical Origin and Impact on Diagnostic Performance

Tuesday, Nov. 29 10:30AM - 10:40AM Room: S404AB

Awards

Trainee Research Prize - Resident

Participants

Daniel Gomez-Cardona, Madison, WI (*Presenter*) Nothing to Disclose
Juan Pablo Cruz Bastida, Madison, WI (*Abstract Co-Author*) Nothing to Disclose
Ke Li, PhD, Madison, WI (*Abstract Co-Author*) Nothing to Disclose
Adam Budde, MS, Madison, WI (*Abstract Co-Author*) Employee, General Electric Company
Jiang Hsieh, PhD, Waukesha, WI (*Abstract Co-Author*) Employee, General Electric Company
Guang-Hong Chen, PhD, Madison, WI (*Abstract Co-Author*) Research funded, General Electric Company Research funded, Siemens AG

PURPOSE

The noise power spectrum (NPS) is one of the most commonly used imaging performance metrics of CT. Aside from its rotational symmetry found in conventional QA routines, NPS with a peculiar cloverleaf or dumbbell shape was observed in clinical multi-detector CT (MDCT) systems. The purpose of this work is to study the physical origin of those peculiar NPS and the corresponding impact on diagnostic performance.

METHOD AND MATERIALS

A novel theoretical model for the NPS of real MDCT systems was developed to incorporate the impact of the bowtie filter, attenuation properties and position of the image object, and location of the region-of-interest (ROI) on the local NPS. Based on this model, the rotational symmetry of the NPS was found to depend greatly on all these factors. Numerical simulations and physical experiments were therefore performed under a wide variety of conditions to validate the theoretical predictions. The corresponding impact on detection performance was assessed via a human observer study using two CT imaging tasks and a visual grading characteristic (VGC) analysis.

RESULTS

The NPS predicted by the theoretical model matched closely those from simulations and physical experiments. The RMSE between theory and phantom experiments was < 0.12 in all cases. For a peripheral ROI inside a centered object with a small bowtie, a cloverleaf shaped NPS was observed; while, for a central ROI in an off-centered object, a dumbbell shaped NPS was obtained independently of the bowtie size. These peculiar cloverleaf or dumbbell shaped NPSs correspond to a highly oriented noise texture which can significantly influence image perception: depending on the orientation of the imaging task and noise texture, the sensitivity differed by up to 38% while specificity by 4%; the area under the curve (AUC) for VGC ranged between 0.61-0.89.

CONCLUSION

NPS with a peculiar cloverleaf or dumbbell shape was experimentally observed in clinical MDCT. The corresponding physical origin was successfully explained in terms of the bowtie filter and properties of the image object; the potential impact on diagnostic performance was also demonstrated. For certain CT applications, these nonconventional NPS properties need to be taken into account.

CLINICAL RELEVANCE/APPLICATION

The quality of CT images acquired under certain clinical scenarios (e.g. elbow CT scans), that lead to anisotropic NPS, should not be represented by conventional quality assurance procedures.

SSG13-02 Effect of Radiation Dose and Reconstruction Algorithm on Detectability of Subtle Hypo-Attenuating Liver Lesions in CT

Tuesday, Nov. 29 10:40AM - 10:50AM Room: S404AB

Participants

Justin B. Solomon, PhD, Durham, NC (*Presenter*) Nothing to Disclose
Daniele Marin, MD, Durham, NC (*Abstract Co-Author*) Research support, Siemens AG
Achille Mileto, MD, Durham, NC (*Abstract Co-Author*) Nothing to Disclose
Bhavik N. Patel, MD, MBA, Durham, NC (*Abstract Co-Author*) Nothing to Disclose
Ehsan Samei, PhD, Durham, NC (*Abstract Co-Author*) Research Grant, General Electric Company; Research Grant, Siemens AG

PURPOSE

To investigate the effect of radiation dose and reconstruction algorithm on noise, contrast, and observer-based detectability of subtle hypo-attenuating liver lesions.

METHOD AND MATERIALS

With IRB approval, a dual source CT system (Siemens SOMATOM Flash) enabling a partitioning of radiation dose from the two x-ray tubes was used to acquire raw CT projection data of a given patient (21 total patients in study) corresponding to six radiation dose levels (12.5, 25, 37.5, 50, 75, and 100%) using only two separate CT acquisitions. A series of anthropomorphic liver lesion models (5 per patient, 105 total) having an inherent (i.e., pre-reconstruction) contrast (lesion-to-liver-attenuation-difference) of -15 HU and average diameter of approximately 12 mm were virtually inserted into the raw CT projection data and images were reconstructed using FBP (filtered-backprojection, B31f) and SAFIRE (Sinogram-affirmed iterative reconstruction, I31f-5). Physical image properties of noise (pixel STD), lesion contrast (post-reconstruction), lesion edge blur (assessed visually), and contrast-to-noise ratio (CNR) were compared. Next, a two alternative forced choice (2AFC) perception experiment was performed (9 readers- 3 radiologists, 6 medical physicists) to estimate detection accuracy as a function of radiation dose and reconstruction algorithm. The results between FBP and SAFIRE were statistically compared using a McNemar binary outcomes test. The dose reduction potential of SAFIRE was estimated by fitting analytical functions of detection accuracy vs dose for FBP and SAFIRE and computing the reduced dose at which SAFIRE had equivalent performance compared to FBP at 100% reference dose.

RESULTS

Compared to FBP, SAFIRE reduced noise by 52% but due to a visually perceivable decrease in spatial resolution, the lesion contrast was also reduced by 12%. The net effect however was an increase in CNR by 87%. From the 2AFC experiment, detection accuracy was $3\pm 1\%$ higher on average in SAFIRE images compared to FBP ($P < .0001$). This increase in detection accuracy translated into a dose reduction potential of 23% for the SAFIRE algorithm.

CONCLUSION

The SAFIRE algorithm enables imaging at 23% reduced radiation dose while low-contrast detectability of very subtle liver lesions is preserved.

CLINICAL RELEVANCE/APPLICATION

The SAFIRE algorithm allows for reducing radiation dose without penalizing low-contrast detectability in body CT imaging.

SSG13-03 Objective and Subjective Image Quality Assessment of an Advanced Iterative Reconstruction Technique in Post Mortem CT Scans

Tuesday, Nov. 29 10:50AM - 11:00AM Room: S404AB

Participants

Marcel Van Straten, PhD, Rotterdam, Netherlands (*Presenter*) Research collaboration, Siemens AG
Mariska Rossius, MD, Rotterdam, Netherlands (*Abstract Co-Author*) Nothing to Disclose
Nomdo Stephan Renken, Rotterdam, Netherlands (*Abstract Co-Author*) Nothing to Disclose
Annick C. Weustink, MD, PhD, Rotterdam, Netherlands (*Abstract Co-Author*) Nothing to Disclose

PURPOSE

First, to quantify the noise reduction of an iterative reconstruction (IR) technique compared with a conventional filtered back projection (FBP) technique in images with anatomical textured backgrounds. Second, to assess whether or not IR is preferred over FBP by radiologists.

METHOD AND MATERIALS

Cadavers were scanned (SOMATOM Force, Siemens) at various anatomical positions (brain, abdomen, and thorax). Each axial scan was performed 20 times without table motion in between the scans. Images were reconstructed with both FBP and an Advanced Modeled IR technique (ADMIRE) at two strength settings. Slice thicknesses of 5 mm, 3 mm, and 1 mm, were used for the brain, abdomen, and thorax, respectively. Typical reconstruction kernels for the tissues scanned were used. Image noise for each individual pixel was defined as the standard deviation of the CT numbers in the 20 scans. The amount of noise reduction was defined as the median value of the noise reduction for pixels with a CT number > -800 HU. Two radiologists scored 192 image pairs on overall image quality. They were blinded for dose and reconstruction technique used. A 5-point scale (range, -2 to 2) was used to score the preferences. Half of the image pairs showed FBP and IR images at equal dose. The other half showed images at equal noise. Noise in the FBP images was reduced by averaging multiple scans.

RESULTS

Noise reduction at IR strength 3 was 9%, 25%, and 40% for the brain, abdomen, and thorax, respectively. At strength 5, the reduction was 14%, 43%, and 66% for the brain, abdomen, and thorax, respectively. In the observer study, virtually all mean scores were negative, i.e. showed a preference for the FBP technique. An exception was the mean score of 0 for the abdominal images at equal noise with IR strength 3. This allows for a dose reduction by a factor 2 when applying the IR technique. Interobserver agreement was excellent.

CONCLUSION

Mainly due to differences in anatomical texture and slice thickness, amount of noise reduction by ADMIRE varies widely (range 9-66%). For moderate levels of noise reduction only, IR can be fully applied to reduce the dose accordingly without affecting the radiologist's impression of the image quality.

CLINICAL RELEVANCE/APPLICATION

Scanning patients twice is unethical. Phantoms, however, lack realistic tissues. This cadaver study shows to what extent the dose can be reduced by applying IR techniques without affecting clinical image impression.

SSG13-04 Impact of Channel Filter Choices on Channelized Hotelling Observer Performance for a Low-contrast Detection Task in CT

Participants

Chi Ma, PhD, Rochester, MN (*Presenter*) Nothing to Disclose
Lifeng Yu, PhD, Chicago, IL (*Abstract Co-Author*) Nothing to Disclose
Christopher P. Favazza, PhD, Rochester, MN (*Abstract Co-Author*) Nothing to Disclose
Shuai Leng, PhD, Rochester, MN (*Abstract Co-Author*) Nothing to Disclose
Cynthia H. McCollough, PhD, Rochester, MN (*Abstract Co-Author*) Research Grant, Siemens AG

PURPOSE

Channelized Hotelling observers (CHO) with Gabor filters are popular for task-based CT image quality assessment. However, channel filter selection for a given clinical task remains unclear, despite being a critical component that affects correlation with human observer performance and image acquisition burden. This study aims to investigate reducing the number of channels without compromising the CHO's performance in a signal-known-exactly low-contrast detection task.

METHOD AND MATERIALS

A cylindrical phantom (Helical CT Phantom, CIRS Inc.) containing 21 low-contrast objects (3 contrast: -5, -10, and -20 HU, and 7 sizes: 10, 9.5, 6.3, 4.8, 4, 3.2, and 2.4 mm) was scanned on a 128-slice CT scanner (Definition Flash, Siemens) at 3 dose levels (CTDIvol of 16, 8, and 4 mGy). Scans at each dose level were repeated 100 times. A validated CHO model with 40 channels (4 frequency passbands, 5 orientations and 2 phases) was used to calculate the area under the receiver operating characteristic curve (Az) for each object and dose level. The Az values were also calculated for all objects with reduced number of channels by varying the number of frequency passbands, orientations, and phases. Correlation between the Az values obtained from images with reduced number of channels and the original 40 channel-images were determined.

RESULTS

When images were channelized with reduced number of filters— phases reduced from 2 to 1 or the number of orientations from 5 to 3, the CHO performance remained highly correlated with that with the original 40 channel-images (goodness-of-fit $r^2=0.99$ and 0.99). When the number of frequency passbands was reduced from 4 to 2, performance was well-correlated for the 2 smallest objects ($r^2=0.99$), less correlated for the 2 middle sizes ($r^2=0.96$), and poorly correlated for the three largest objects ($r^2=0.01$). Using as few as 12 filters (4 passbands x 3 orientations x 1 phase) to channelize the images demonstrated sufficient CHO performance correlation ($r^2=0.99$) for this low-contrast object detection task in the study.

CONCLUSION

The number of Gabor filters used to channelize image for a CHO can be empirically reduced based on performance correlation with a validated model.

CLINICAL RELEVANCE/APPLICATION

Channel reduction in a CHO can be achieved without sacrificing performance, thus improving statistical performance, reducing image acquisition burden, and facilitating practical implementation.

SSG13-05 Use of a Channelized Hotelling Observer Model to Guide Dose Reduction in Size-specific Acquisition Protocols with Iterative Reconstruction

Tuesday, Nov. 29 11:10AM - 11:20AM Room: S404AB

Participants

Christopher P. Favazza, PhD, Rochester, MN (*Presenter*) Nothing to Disclose
Andrea Ferrero, PhD, Rochester, MN (*Abstract Co-Author*) Nothing to Disclose
Kyle McMillan, Rochester, MN (*Abstract Co-Author*) Institutional research agreement, Siemens AG Research support, Siemens AG
Shuai Leng, PhD, Rochester, MN (*Abstract Co-Author*) Nothing to Disclose
Lifeng Yu, PhD, Chicago, IL (*Abstract Co-Author*) Nothing to Disclose
Michael R. Bruesewitz, Rochester, MN (*Abstract Co-Author*) Nothing to Disclose
Cynthia H. McCollough, PhD, Rochester, MN (*Abstract Co-Author*) Research Grant, Siemens AG

PURPOSE

Image quality improvements resulting from iterative reconstruction (IR) have been leveraged to lower patient dose in CT. However, overly aggressive dose reduction may lead to reduced low-contrast object conspicuity that cannot be restored by IR. Here, we apply an observer model to determine appropriate dose reduction for size-specific acquisition protocols that utilize IR.

METHOD AND MATERIALS

A validated channelized Hotelling observer (CHO) model was used to assess the detectability of a 4.8 mm diameter circular object possessing -25 HU contrast relative to background. A Toshiba Aquilion Prime 160 scanner was used to image the phantom (Spiral/Helical CT Phantom, CIRS) containing the object. The phantom was scanned 100 times at 8 different fixed tube current settings: 20, 30, 45, 60, 70, 90, 140, and 180 mA. Filtered back-projection (FBP) images acquired at 60, 90, and 180 mA were used as reference "full dose" FBP images for small, medium and large patient sizes, respectively. These settings yielded image noise values consistent with size-specific target values at our institution. Images were reconstructed with both FBP and IR (AIDR 3D) methods. Area under the receiver operator characteristic curve (AUC) was determined for each tube current setting using 100 signal present images and 100 signal absent images obtained at the same location in the phantom.

RESULTS

AUC measurements demonstrated that IR improves object detectability as compared to FBP for images acquired at the same dose level. This improvement enables moderate dose reduction without loss of low contrast object detectability. Specifically, IR images acquired with 22, 22, and 25% less dose yielded AUC values within measurement error of full dose FBP images for small, medium, and large patient sizes, respectively.

CONCLUSION

CHO-based image quality assessment can be used to guide dose reduction for size-specific acquisition protocols when using IR

CHO based image quality assessment can be used to guide dose reduction for size specific acquisition protocols when using it without compromising low contrast object detectability.

CLINICAL RELEVANCE/APPLICATION

Objective assessment of CT image quality with a CHO can help determine appropriate amounts of dose reduction for size specific acquisition protocols without loss of low contrast object detectability.

SSG13-06 CT X-Ray Spectrum Reconstruction with High Frequency Components

Tuesday, Nov. 29 11:20AM - 11:30AM Room: S404AB

Participants

Carsten Leinweber, Heidelberg, Germany (*Presenter*) Nothing to Disclose
Joscha Maier, Heidelberg, Germany (*Abstract Co-Author*) Nothing to Disclose
Marc Kachelriess, PhD, Heidelberg, Germany (*Abstract Co-Author*) Nothing to Disclose

PURPOSE

To provide an x-ray spectrum estimation method that is capable of reproducing high frequency components like characteristic radiation.

METHOD AND MATERIALS

The accurate knowledge of the x-ray spectrum is of importance for many CT applications and artifact correction methods (e.g. organ dose estimation, beam hardening correction, dual energy decomposition). To estimate the x-ray spectrum transmission measurements of different attenuators with known dimension and material decomposition are performed. The inverse problem of reconstructing the x-ray spectrum is solved in two steps. First a low frequency solution is calculated using truncated singular value decomposition (TSVD). In the second step a solution from nullspace is added to the TSVD solution to incorporate prior information of high frequency components. In this work information about the energy distribution of the characteristic peaks of the anode is used. The nullspace solution is found by minimizing a cost function that penalizes deviations from physical assumptions like non-negativity of the total spectrum and flatness of the bremsstrahlung fraction. The algorithm is applied to noise-free and noisy simulated as well as to measured CT data for tube voltages ranging from 80 kV to 150 kV. The resulting spectra are validated using attenuation measurements that are not included in the reconstruction process. We compare our method with the expectation-maximization (EM) approach widely used in literature.

RESULTS

Reconstructed spectra from simulated data show a high fidelity to the ground truth. In comparison to the EM method we found a reduction of the mean square error to a simulated spectrum by one order of magnitude. The proposed algorithm is less dependent on input parameters like the number of iterations or the incident peak height than the EM method. The estimated spectra from the measured data are capable of reproducing the incident attenuation curves as well as attenuation measurements from materials that are not involved in the reconstruction process while providing a physically reliable shape.

CONCLUSION

Our approach that uses minimal prior information accurately reconstructs x-ray spectra from transmission measurements. The method has been validated with help of simulated and measured data.

CLINICAL RELEVANCE/APPLICATION

Detailed x-ray spectra are required for accurate dose calculations in x-ray computed tomography and radiation therapy.

SSG13-07 Comparison on Image Quality and Radiation Dosage of Helical 4cm, Helical 8cm and Axial 16cm Scan Mode on Revolution CT for Whole Abdominal CT Scan

Tuesday, Nov. 29 11:30AM - 11:40AM Room: S404AB

Participants

Jin Wei, Fuzhou, China (*Presenter*) Nothing to Disclose
Yunjing Xue, MD, Fuzhou, China (*Abstract Co-Author*) Nothing to Disclose
Yuanfeng Liu, Fuzhou, China (*Abstract Co-Author*) Nothing to Disclose
Xuhui Chen, Fuzhou, China (*Abstract Co-Author*) Nothing to Disclose
Yu Xia, Fuzhou, China (*Abstract Co-Author*) Nothing to Disclose
Zhi-Yong Li, Fuzhou, China (*Abstract Co-Author*) Nothing to Disclose

PURPOSE

To compare three different scan mode on revolution CT: helical 4cm, helical 8cm and axial 16cm for whole abdominal CT scan and evaluate image quality and radiation dosage to provide the evidence to choose the reasonable abdominal CT scan mode.

METHOD AND MATERIALS

Totally 33 patients in our hospital referred to abdominal contrast-enhanced CT scans on GE Revolution CT were selected in this study. Plain CT scans were used helical 4cm helical mode, artery phase scans were used helical 8cm mode and portal phase scans were used axial 16cm mode. All scans were applied automatic mA modulation from 10-500mA and fixed tube voltage of 120kV, with noise index (NI) of 10. The SD value of fat as image noise in three different slices of the abdomen was measured in three locations: right branch of portal vein, left renal artery and navel. CT dose index volumes (CTDI vol), dose length product (DLP) were recorded from dose report, and effective dose (ED) was calculated. The image quality was evaluated by two experienced abdominal radiologists blindly and independently with a five-point scale (1 for poor and 5 for excellent). CTDI vol, ED, average image noise and average image score were compared with ANOVA.

RESULTS

There was no significant difference in terms of image noise (SD value, $F=0.31$, $P=0.73>0.05$) and subjective image quality (average image score, $F=0.47$, $P=0.63>0.05$) of the three scan modes during abdominal CT scans. 16cm axial scan produced highest radiation dosage (CTDI=11.74±3.81mGy, $F=5.04$, $P=0.01<0.05$; ED=8.45±3.03, $F=3.71$, $P=0.03<0.05$) than the helical 4cm and 8 cm scans,

while there was no statistically different between two helical scans.

CONCLUSION

The comparison of the three different scan modes showed that there was no statistical difference in objective and subjective image quality (SD value and average image score) during abdominal CT scans on Revolution CT. 16cm axial scan yielded higher radiation dosage than the other two helical scans because of wider coverage and mA modulation decreased less. The two helical scans had the similar image quality and radiation dosage.

CLINICAL RELEVANCE/APPLICATION

Helical 8cm scan mode on revolution CT is recommended to be a relatively optimal scan mode for whole abdominal CT scan because of short scan time and good image quality.

SSG13-08 CT Image Quality Assessment Using a 3D Model Observer for Lung Nodule Localization in the Presence of Anatomical Background

Tuesday, Nov. 29 11:40AM - 11:50AM Room: S404AB

Participants

Lifeng Yu, PhD, Chicago, IL (*Presenter*) Nothing to Disclose
Shane Dirks, Rochester, MN (*Abstract Co-Author*) Nothing to Disclose
Christopher P. Favazza, PhD, Rochester, MN (*Abstract Co-Author*) Nothing to Disclose
Shuai Leng, PhD, Rochester, MN (*Abstract Co-Author*) Nothing to Disclose
Matthew A. Kupinski, PhD, Chicago, IL (*Abstract Co-Author*) Nothing to Disclose
Baiyu Chen, Rochester, MN (*Abstract Co-Author*) Nothing to Disclose
Chi Wan Koo, MD, Rochester, MN (*Abstract Co-Author*) Nothing to Disclose
David L. Levin, MD, PhD, Rochester, MN (*Abstract Co-Author*) Nothing to Disclose
Joel G. Fletcher, MD, Rochester, MN (*Abstract Co-Author*) Grant, Siemens AG; ;
Cynthia H. McCollough, PhD, Rochester, MN (*Abstract Co-Author*) Research Grant, Siemens AG

PURPOSE

Objective assessment of nodule detection performance in chest CT using model observers is challenging since both a phantom with lung-mimicking anatomical background and the placement of the same set of nodules at numerous randomized locations are needed. The purpose of this work was to develop a 3D model that mimics the clinical task, without requiring randomized nodule placements, and to use this model to evaluate low-dose chest CT.

METHOD AND MATERIALS

The 3D nodule localization task was mimicked with an 8 cm segment of an anthropomorphic chest phantom (Lungman, Kyoto). Twelve spherical nodules at 3 brightness levels (100, -630, -800 HU) and 4 sizes (10, 8, 5, 3 mm) were attached to the pulmonary trees within the lower 4-cm segment. The phantom was scanned on a 192-slice scanner (Force, Siemens) at 5 low-dose settings (CTDIvol of 0.1, 0.2, 0.4, 0.8, 2.0 mGy) using 100 kV with a tin filter. Scans were repeated 100 times at each dose with each nodule at a fixed location. A 3D spatial-domain observer model, non-prewhitening matched filter with an eye filter (NPWE), was used to calculate a 3D map of test statistics for each scan. The test statistics at each location in the upper 4-cm segment, where nodules were actually absent, were compared to the test statistics at the true nodule locations (lower segment) in each scan to determine if a correct localization was achieved. This was repeated for all 100 scans to determine the localization accuracy for each nodule and dose level.

RESULTS

Localization accuracy improved as the dose level, nodule size, and nodule brightness increased. Using 90% accuracy as the acceptability criterion, dose could be reduced to 0.1, 0.1, 0.1, and 0.4 mGy for the 10, 8, 5, and 3 mm nodules, respectively, for the 100 HU solid nodules. For the -630 HU sub-solid nodules, the corresponding doses were 0.1, 0.1, 0.4, and 2.0 mGy. For the -800 HU nodules, dose could be dropped to 0.1, 0.2, and 0.4 mGy for the 10, 8, and 5 mm nodules, respectively.

CONCLUSION

The proposed phantom-based 3D model observer can be used for task-based image quality evaluation of chest CT without the need for nodule placements in random positions, which is typically needed to mimic a localization task.

CLINICAL RELEVANCE/APPLICATION

Objective assessment of CT image quality for 3D nodule localization in lung anatomical background has been a challenge. The proposed method may resolve this problem.

SSG14

Physics (MR Applications)

Tuesday, Nov. 29 10:30AM - 12:00PM Room: S405AB

MR PH

AMA PRA Category 1 Credits™: 1.50
ARRT Category A+ Credits: 1.50

FDA Discussions may include off-label uses.

Participants

Timothy J. Carroll, PhD, Chicago, IL (*Moderator*) Nothing to Disclose
Seth A. Smith, PhD, Nashville, TN (*Moderator*) Nothing to Disclose

Sub-Events

SSG14-01 Using 1H Spectrum as well as High Spectral and Spatial Resolution MRI to Characterize Water and Fat Variations in SV40 Mouse Mammary Gland Under Different Diet

Tuesday, Nov. 29 10:30AM - 10:40AM Room: S405AB

Participants

Dianning He, Chicago, IL (*Presenter*) Nothing to Disclose
Devkumar Mustafi, PhD, Chicago, IL (*Abstract Co-Author*) Nothing to Disclose
Sully Fernandez, Chicago, IL (*Abstract Co-Author*) Nothing to Disclose
Xiaobing Fan, PhD, Chicago, IL (*Abstract Co-Author*) Nothing to Disclose
Suzanne Conzen, MD, Chicago, IL (*Abstract Co-Author*) Nothing to Disclose
Gregory S. Karczmar, PhD, Chicago, IL (*Abstract Co-Author*) Nothing to Disclose
Erica Markiewicz, BA, Chicago, IL (*Abstract Co-Author*) Nothing to Disclose
Marta A. Zamora, BS, Chicago, IL (*Abstract Co-Author*) Nothing to Disclose
Matthew J Brady, Chicago, IL (*Abstract Co-Author*) Nothing to Disclose
Jeffrey Mueller, MD, Chicago, IL (*Abstract Co-Author*) Nothing to Disclose

PURPOSE

The influence of dietary animal fat on breast cancer risk is not well understood. In this study, we used MRI to investigate the effect of diet on the water – fat ratio in the mammary glands of SV40 mice.

METHOD AND MATERIALS

Female C3(1) SV40 Tag transgenic mice (n=12) were studied and divided into three different diet groups: control, high animal fat, and high fructose. Each diet was started when mice were 8 weeks old. MRI was performed on a 9.4T scanner when mice were 12 weeks old. After axial high resolution T2-weighted anatomic images, a 1H spectrum was acquired at two 1 mm³ point resolved spectroscopy (PRESS) boxes on each side of inguinal mammary gland. The boxes were placed to avoid cancer, lymph nodes, and lymph ducts. High spectral and spatial resolution (HiSS) images were acquired from nine 1 mm slices (2 mm gap). The PRESS spectra were analyzed by fitting with a combination of Gaussian and Lorentzian functions. The ratio of the integrals of the water and fat spectra (W/F) was calculated. Water and fat peak height images were generated from HiSS data. Then the percentage of fat in the mammary gland was calculated from fat peak height images. One-way ANOVA and Tukey's HSD tests were performed to determine whether there was a difference between the calculated parameters in the three groups of mice. A p-value less than 0.05 was considered significant.

RESULTS

On average the water-to-fat ratio (W/F) was 11.3±4.2, 5.8±3.8, and 7.7±2.3 for control, high animal fat and high fructose diet mice, respectively. W/F was significantly lower in mice on the high animal fat diet (p<0.05). The fat resonances at 1.3, 2.04, 2.77 and 5.31 ppm were significantly narrower (p<0.01) in mice on the high animal fat diet than in mice on the control diet. The fat peak height images showed that the fat occupied more than 90% of the mammary gland in mice on the high fat diet, which was significantly more than in control mice. All the calculated parameters for the high fructose diet mouse were in between control and fat diet mouse.

CONCLUSION

Although the mice on high animal fat diets did not gain significant weight compared to control diet mice, the water and fat composition in the mammary glands were dramatically changed by the high fat diet.

CLINICAL RELEVANCE/APPLICATION

The spectrum and HiSS MRI could be used to identify water and fat composition changes in the mammary gland or human breast due to diet.

SSG14-02 Quantifying Intracellular pH Changes in Breast Tumors during Administration of pH Modulating Agents using Chemical Exchange Saturation Transfer (CEST) Magnetic Resonance Imaging

Tuesday, Nov. 29 10:40AM - 10:50AM Room: S405AB

Awards

Student Travel Stipend Award

Participants

Matthew M. Miller, MD, PhD, Cary, NC (*Presenter*) Nothing to Disclose
Gopal Varma, PhD, Boston, MA (*Abstract Co-Author*) Nothing to Disclose
Xiaoen Wang, MD, Boston, MA (*Abstract Co-Author*) Nothing to Disclose

Han Xie, Boston, MA (*Abstract Co-Author*) Nothing to Disclose
Gerburg Wulf, MD, PhD, Boston, MA (*Abstract Co-Author*) Nothing to Disclose
Pankaj Seth, PhD, Boston, MA (*Abstract Co-Author*) Nothing to Disclose
David C. Alsop, PhD, Boston, MA (*Abstract Co-Author*) Research support, General Electric Company Royalties, General Electric Company
Aaron K. Grant, PhD, Boston, MA (*Abstract Co-Author*) Nothing to Disclose
Vikas Sukhatme, Boston, MA (*Abstract Co-Author*) Nothing to Disclose

PURPOSE

Tumors are dependent on proton transporters to remove excess protons derived from glycolysis, making them an attractive potential target for new adjunct agents that could be co-administered with traditional chemotherapy or immune therapies. Evaluation of the effectiveness of proton transport inhibitors in tumors has been limited by the lack of a non-invasive method of monitoring changes in pH. We investigated the ability of Chemical Exchange Saturation Transfer (CEST) MR, a quantitative imaging method, to non-invasively measure intracellular pH in vivo to characterize tumor response to pH modulating therapy.

METHOD AND MATERIALS

Experiments were performed using a well-established mouse model of BRCA1-related triple negative breast cancer. CEST MR imaging was performed at 9.4T using a 20mm RF surface coil placed over the tumor, before and after intraperitoneal injection of esomeprazole (40mg/kg) plus amiloride (5mg/kg) in 80uL DMSO or 80uL DMSO only as a control. Imaging acquisitions were performed at baseline and repeated at 15 minute intervals over 1 hour after injection. CEST spectra were analyzed using the previously described Amine/Amide Concentration Independent Detection (AACID) technique to calculate intracellular pH.

RESULTS

We imaged a total of 10 breast tumor-bearing mice. Eight mice were injected with esomeprazole and amiloride in DMSO and two mice were injected with DMSO only. There was a subtle shift in the relative amide and amine peak heights in tumors after drug administration but not with carrier only, corresponding to an approximate 0.2 pH unit decrease in intracellular pH. This effect on tumor pH appeared to peak during the first 15 minutes after injection before tapering back to baseline.

CONCLUSION

This early in vivo data suggests that our CEST imaging protocol may be able to detect a subtle shift in the intracellular pH in breast tumors after administration of esomeprazole and amiloride. Future studies will focus on using more potent proton modulating drugs with larger pH effects to further optimize our CEST imaging protocol. Further analysis of the CEST spectra already obtained will also be performed to identify any other peak changes that may reflect changes in pH.

CLINICAL RELEVANCE/APPLICATION

CEST MR imaging may be able to detect a subtle shift in intracellular pH in breast tumors after administration of esomeprazole and amiloride.

SSG14-03 Assessment of Interplatform Variability of T1 Quantification Methods Used for DCE-MRI in a Multicenter Phantom Study

Tuesday, Nov. 29 10:50AM - 11:00AM Room: S405AB

Participants

Octavia Bane, PhD, New York, NY (*Presenter*) Nothing to Disclose
Stefanie Hectors, PhD, New York, NY (*Abstract Co-Author*) Nothing to Disclose
Mathilde Wagner, MD, PhD, Paris, France (*Abstract Co-Author*) Consultant Olea Medical
Lori R. Arlinghaus, PhD, Nashville, TN (*Abstract Co-Author*) Nothing to Disclose
Michael Boss, PhD, Boulder, CO (*Abstract Co-Author*) Nothing to Disclose
Yue Cao, PhD, Ann Arbor, MI (*Abstract Co-Author*) Research Grant, Siemens AG Speaker, Siemens AG
Bachir Taouli, MD, New York, NY (*Abstract Co-Author*) Consultant, MEDIAN Technologies ; Grant, Guerbet SA

PURPOSE

The precision of pharmacokinetic parameters estimated from DCE-MRI contrast uptake curves is highly dependent on the conversion of T1-weighted signal to Gd concentration, and thus on the baseline T1 value. The objective of this study was to measure interplatform variability in T1 quantification in a multicenter study by testing common inversion-recovery spin-echo (IR-SE) and variable flip angle (VFA) protocols using a dedicated T1 phantom.

METHOD AND MATERIALS

A T1 phantom, produced by NIST, was scanned at 7 different sites on different platforms (eight 3.0T systems, one 1.5 T system) in duplicate (test-retest). The phantom consists of 14 spherical vials doped with varying concentration of NiCl₂. The T1 mapping protocols were standardized and consisted of an IR-SE and VFA sequence. T1 fitting was done on signal curves from ROIs drawn by a single observer in each vials. Test-retest and interplatform coefficients of variation (CV) were computed for each platform. The standardized VFA protocol was compared with the reference standard IR-SE protocol using Bland-Altman statistics.

RESULTS

T1 measurements in the 14 spheres ranged between 20 and 2000 ms at 3T, as expected, with greater spread in the distribution of T1 values observed between sites with the VFA sequence (CV range across platforms 18.7-45.6% vs 1.0-14.6% for IR-SE). The IR-SE protocol had high repeatability at both field strengths, with mean test-retest CV of 0.3% at 1.5T and <7% at 3T. The common VFA protocol had poorer repeatability, with test-retest CV <2% at 1.5T, and as high as 18% at 3T. The comparison of the common VFA protocol to the IR-SE reference standard protocol across eight 3T magnets showed absolute % difference bias in the range of 2%-36%.

CONCLUSION

Preliminary results show high interplatform variability in T1 values in test-retest scans and between different protocols. Future work will analyze accuracy of each T1 measurement method with respect to gold standard T1 values determined by NMR spectroscopy at NIST. The complete dataset will be analyzed with a generalized linear mixed statistical model, to compare accuracy of T1

measurements across field strength, scanner models, and sequences.

CLINICAL RELEVANCE/APPLICATION

Standardization of T1 mapping used for DCE-MRI quantification likely improves reliability of pharmacokinetic parameters and thereby potentially enhances the accuracy of e.g. treatment planning and monitoring based on these parameters.

SSG14-04 Classification of MRI Patterns of Multiple Myeloma (MM) Infiltration and Its Prognostic Value for Treatment Response Assessment

Tuesday, Nov. 29 11:00AM - 11:10AM Room: S405AB

Participants

Chuan Zhou, PhD, Ann Arbor, MI (*Presenter*) Nothing to Disclose
Qian Dong, MD, Ann Arbor, MI (*Abstract Co-Author*) Nothing to Disclose
Heang-Ping Chan, PhD, Ann Arbor, MI (*Abstract Co-Author*) Institutional research collaboration, General Electric Company
Lubomir M. Hadjiiski, PhD, Ann Arbor, MI (*Abstract Co-Author*) Nothing to Disclose
Jun Wei, PhD, Ann Arbor, MI (*Abstract Co-Author*) Nothing to Disclose
Attaphol Pawarode, Ann Arbor, MI (*Abstract Co-Author*) Nothing to Disclose

PURPOSE

Studies indicated that the patterns of MM infiltration manifested on MRI are associated with tumor burden and correlated with prognosis in patients with MM. This study investigated the feasibility of classifying the MRI patterns of MM infiltration and assessed the value of our developed pattern biomarker as a prognostic factor in MM patients after bone marrow transplant (BMT).

METHOD AND MATERIALS

With IRB approval, 63 pairs of spinal MRI scans performed pre- and post-BMT were collected retrospectively from 63 MM patients. An experienced musculoskeletal radiologist visually examined each vertebra and provided the descriptor of its pattern (normal, focal, variegated (salt-pepper), and diffuse) as reference standard. Thirty-seven texture features were extracted from each manually outlined vertebral body. Using leave-one-case out cross validation and ROC analysis, a logistic regression model (LRM) was built with stepwise feature selection for classifying the vertebrae into two groups: variegated and diffuse patterns (group 1) that tend to have higher tumor burden vs normal and focal patterns (group 2). Five effective features (1 gray level histogram feature, 3 run-length statistics, 1 gray tone spatial dependence feature) were selected. The percentage of analyzed vertebrae (pV) that were classified into group 1 by LRM for each patient was used as pattern biomarker to estimate progression-free survival. The prognosis was analyzed with the Cox proportional hazards regression model, with respect to the time to progression (TTP) censored at 3 years.

RESULTS

Of the 1244 vertebrae, 619 and 625 vertebrae were classified as group 1 and 2, respectively, by radiologist. The LRM achieved a test AUC of 0.81 ± 0.01 . The Cox model showed that, with an optimal cutoff point of $pV < 10\%$ determined by the maximally selected rank statistics, the patients had significantly longer TTP ($P < 0.001$; hazard ratio 5.7) compared to patients having $pV > 10\%$.

CONCLUSION

Our radiomic method classified MRI patterns between the high-grade diffuse or variegated patterns and the normal or focal patterns with high accuracy. The study demonstrated the feasibility of using the pattern biomarker (pV) as prognostic predictor for MM patients.

CLINICAL RELEVANCE/APPLICATION

MR-based radiomic biomarker with prognostic significance may improve the accuracy for staging and assessing treatment response for MM, allowing clinicians to optimize therapy for individual patients.

SSG14-06 Electrical Impedance Spectroscopy for Prompt Intracranial Hemorrhage Diagnosis

Tuesday, Nov. 29 11:20AM - 11:30AM Room: S405AB

Awards

Student Travel Stipend Award

Participants

Karen Buch, MD, Boston, MA (*Presenter*) Nothing to Disclose
Reza Atefi, PhD, Charlestown, MA (*Abstract Co-Author*) Nothing to Disclose
Shervin Kamalian, MD, MSc, Boston, MA (*Abstract Co-Author*) Nothing to Disclose
Eric S. Rosenthal, Boston, MA (*Abstract Co-Author*) Nothing to Disclose
Giorgio Bonmassar, PhD, Charlestown, MA (*Abstract Co-Author*) Nothing to Disclose
Michael H. Lev, MD, Boston, MA (*Abstract Co-Author*) Consultant, General Electric Company; Institutional Research Support, General Electric Company; Stockholder, General Electric Company; Consultant, MedyMatch Technology, Ltd; Consultant, Takeda Pharmaceutical Company Limited; Consultant, D-Pharm Ltd

PURPOSE

Emergent detection of intracranial haemorrhage (ICH) is crucial for the appropriate management to decrease the risk of permanent neurologic deficits or ensuring infarction. Typically, the diagnosis of ICH is made on CT or MR imaging, but these images only represent the brain at a single point in time. To date, there remains no clinical equipment for continuous monitoring expressly for the purpose of detecting ICH. The purpose of this study was to design and construct an Electrical Impedance Spectroscopy (EIS) platform to see if ICH could be detected.

METHOD AND MATERIALS

An in-house developed EIS platform was constructed to non-invasively detect the electrical properties of brain tissue. A conductive head phantom made of agarose gel was constructed to model the anatomic/geometric features of the human head with agarose simulating the native impedance of brain tissue. Stimulation electrodes were placed on scalp of the phantom in a montage

configuration similar to that for EEG recordings. Electrodes pairs were placed at F7, F8, C4, C3, P7 and P8 positions to detect changes in the electrical potential when exposed to Gaussian white noise stimulation pulse (range of 0-50 kHz). Baseline electrical potential recordings were obtained and normalized. A solution of 1 ml of saturated sodium chloride (NaCl) solution, simulating hemorrhage, was injected below the C4 electrode. Post-injection electrical potential measurements were obtained at each electrode position.

RESULTS

After the injection of saturated NaCl solution immediately deep to the C4 electrode an isolated decrease in the normalized C4 voltage of -0.33 volts was observed. Electrodes located anterior and posterior to the C4 electrode maintained their baseline voltage, prior to the injection of saline at the C4 electrode yielding an accurate localization of changes in electrical potential correlating with the site of simulated hemorrhage. Repeat simulation testing using this convention achieved similar results.

CONCLUSION

This study demonstrates proof of concept of using an EIS platform to detect changes in electrical potential within the brain parenchyma using an NaCl solution to simulate intracranial hemorrhage

CLINICAL RELEVANCE/APPLICATION

This study provides proof of concept in the development of a continuous electrical impedance recording device for the detection of intracranial hemorrhage.

SSG14-07 Arterial Input Functions Derived from Ultra-fast DCE MRI and Dynamic Contrast Computed Tomography in Prostate Cancer Patients

Tuesday, Nov. 29 11:30AM - 11:40AM Room: S405AB

Participants

Shiyang Wang, PhD, Chicago, IL (*Presenter*) Nothing to Disclose

Zheng Feng Lu, PhD, Chicago, IL (*Abstract Co-Author*) Nothing to Disclose

Xiaobing Fan, PhD, Chicago, IL (*Abstract Co-Author*) Nothing to Disclose

Milica Medved, PhD, Chicago, IL (*Abstract Co-Author*) Nothing to Disclose

Steffen Sammet, MD, PhD, Chicago, IL (*Abstract Co-Author*) Research Grant, Koninklijke Philips NV; Medical Advisory Board, Radiology Resources International LLC; Advisory Board, Guerbet SA

Aytekin Oto, MD, Chicago, IL (*Abstract Co-Author*) Research Grant, Koninklijke Philips NV

Ambereen Yousuf, MBBS, Chicago, IL (*Abstract Co-Author*) Nothing to Disclose

Gregory S. Karczmar, PhD, Chicago, IL (*Abstract Co-Author*) Nothing to Disclose

PURPOSE

The aim of this study is to evaluate the accuracy of arterial input functions (AIF) derived from ultra-high temporal resolution (Ufast) dynamic contrast enhanced (DCE) MRI following a low dose of Gadolinium (Gd) contrast media, using dynamic contrast enhanced (DCE) computed tomography (CT) as gold standard.

METHOD AND MATERIALS

Twenty-three men (46–72yo) who were scheduled for prostatectomy after MRI were enrolled in this IRB approved study. In all patients, DCE-CT scans (with 120mL Omnipaque350 injected at 4mL/s) were performed with 29 dynamics, a temporal resolution of 5s for the first 25 dynamics followed by 2 dynamic scans 1 min apart and 2 dynamic scans 2 min apart. Ufast DCE-MRI was performed ~3 hours after CT scans, 90 dynamic scans with 1.5s temporal, 1.5x2.8x3.5 mm³ in-plane resolution and a low dose injection (15% of conventional dose) Gd-based contrast agent (~3mL injected at 2mL/s). AIFs were extracted from an iliac artery on both Ufast DCE-MRI and DCE-CT images and were interpolated using empirical mathematical models (EMM) to match the temporal resolution. AIFs from Ufast DCE-MRI were convoluted with a rectangular function to adjust for differences in DCE-CT and MRI protocols. The resulting adjusted AIFs from MRI were compared to AIFs from DCE-CT. Goodness of fit R² was calculated between convoluted AIF from DCE-MRI and the AIF from DCE-CT.

RESULTS

The EMMs accurately fit both MRI and CT data. There was no significant difference ($p > 0.05$) between the maximum peak amplitude of AIFs from DCE-CT (mean=21.9kg/L) and convoluted AIFs from Ufast DCE-MRI (mean=25.5kg/L). The shapes of the AIFs from Ufast DCE-MRI and DCE-CT were very similar (mean R²=0.74).

CONCLUSION

AIFs derived from Ufast DCE-MRI correlated strongly with gold standard AIFs derived from DCE-CT. Contrast enhancement was measured in one of the iliac arteries in each patient. The low dose of contrast media in Ufast DCE-MRI minimized water exchange and T2* artifacts that cause underestimation of AIF peak magnitude when the conventional dose is used. The results demonstrate that the AIF directly measured by MRI following a low contrast media dose can be used to calculate accurate values of K[trans] and other pharmacokinetic parameters.

CLINICAL RELEVANCE/APPLICATION

A direct comparison of gold standard DCE-CT measurement with low dose Ufast DCE-MRI demonstrates that Ufast DCE-MRI can provide an accurate and reliable measure of the AIF for pharmacokinetic studies.

Honored Educators

Presenters or authors on this event have been recognized as RSNA Honored Educators for participating in multiple qualifying educational activities. Honored Educators are invested in furthering the profession of radiology by delivering high-quality educational content in their field of study. Learn how you can become an honored educator by visiting the website at: <https://www.rsna.org/Honored-Educator-Award/>

Aytekin Oto, MD - 2013 Honored Educator

SSG14-09 Cardiac MR-based 2D Strain Analysis as an Early Marker of Diastolic Dysfunction in the General

Population: A Reproducibility Study

Tuesday, Nov. 29 11:50AM - 12:00PM Room: S405AB

Participants

Tanja Zitzelsberger, MD, Tuebingen, Germany (*Presenter*) Nothing to Disclose
Roberto Lorbeer, Greifswald, Germany (*Abstract Co-Author*) Nothing to Disclose
Holger Hetterich, MD, Munich, Germany (*Abstract Co-Author*) Nothing to Disclose
Sigrid Auweter, Munich, Germany (*Abstract Co-Author*) Nothing to Disclose
Maximilian F. Reiser, MD, Munich, Germany (*Abstract Co-Author*) Nothing to Disclose
Fabian Bamberg, MD, MPH, Tuebingen, Germany (*Abstract Co-Author*) Speakers Bureau, Bayer AG; Speakers Bureau, Siemens AG; Research Grant, Bayer AG; Research Grant, Siemens AG;
Christa Meisinger, Neuherberg, Germany (*Abstract Co-Author*) Nothing to Disclose
Margit Heier, Neuherberg, Germany (*Abstract Co-Author*) Nothing to Disclose
Annette Peters, Neuherberg, Germany (*Abstract Co-Author*) Nothing to Disclose
Astrid Scholz, Tuebingen, Germany (*Abstract Co-Author*) Nothing to Disclose

PURPOSE

Initial data suggest that subtle alterations in LV function can also be assessed using SSFP MRI sequences, which may represent an early biomarker of increased risk in metabolic diseases of the general population, including pre-diabetes. However, the reproducibility of these measurements is unknown but critical for larger implementation.

METHOD AND MATERIALS

We included 30 random subjects from a larger prospective cohort study from the general population without prior cardiovascular disease or symptoms (KORA FF4 cohort) who underwent a 3T whole body MRI scan including Cine SSFP imaging (TR: 29.97ms, TE: 1.46ms, Flip Angle: 62°, Slice-Thickness: 8mm, Field of view: 297x360mm, Matrix: 240x160, Voxel size: 1.5x1.5mm², Segments: 25). Two independent observers determined image quality (5-point Likert scale) and measured radial, longitudinal and circumferential strain by using a semiautomatic segmentation algorithm (CVI42, Circle, Canada). Inter-reader and intra-reader variabilities were assessed using Bland-Altman plot analyses and intra-class-correlation coefficients (ICC) after one-way random-effects ANOVA.

RESULTS

Among all subjects (mean age: 56.3±9 years, 57.8% males) image quality was high (4.5±2) and all images were included in the analysis. Inter-reader reproducibility was excellent for longitudinal strain (relative difference: 0.2%±7.5%, ICC 0.50) whereas radial strain and circumferential strain showed a good inter-reader reproducibility (relative difference: 12.9%±9.7%, ICC 0.67 and 6.7%±6.1%, ICC 0.74; respectively). Intra-reader reproducibility was excellent for all strain directions (relative difference range: -0.6 to 1.4%, ICC from 0.67 to 0.84). All agreement was independent of image quality (p>0.05).

CONCLUSION

Cardiac MR-based 2D strain analysis is highly reproducible and may therefore be implemented in larger cohort studies to determine its value as a precursor of diastolic dysfunction in subjects at risk.

CLINICAL RELEVANCE/APPLICATION

Left ventricular 2D strain analysis may represent a reproducible marker for identifying subjects at risk for subclinical left ventricular dysfunction in the general population.

SSG15

Radiation Oncology (Genitourinary)

Tuesday, Nov. 29 10:30AM - 12:00PM Room: S104A



AMA PRA Category 1 Credits™: 1.50
ARRT Category A+ Credits: 1.50

FDA Discussions may include off-label uses.

Participants

Martin Colman, MD, Houston, TX (*Moderator*) Nothing to Disclose
Abhishek A. Solanki, MD, Maywood, IL (*Moderator*) Nothing to Disclose

Sub-Events

SSG15-01 **Margin-Positive (M+) Radical Prostatectomy (RP): Differential Risk of PSA Relapse by Extent of Margin Involvement**

Tuesday, Nov. 29 10:30AM - 10:40AM Room: S104A

Participants

James K. Russo II, MD, Charleston, SC (*Abstract Co-Author*) Nothing to Disclose
Michael Laszewski, MD, Bismarck, ND (*Abstract Co-Author*) Nothing to Disclose
Mark Rodacker, MD, Grand Forks, ND (*Abstract Co-Author*) Nothing to Disclose
Sarah Mott, MS, Iowa City, IA (*Abstract Co-Author*) Nothing to Disclose
John M. Watkins, MD, Bismarck, ND (*Presenter*) Nothing to Disclose

PURPOSE

M+ is an established risk factor for PSA failure following RP; however, often this is identified in the context of other high-risk feature(s). The objective of the current study was to expand upon our previous single-institution findings in the multi-institutional setting, with longer follow-up, in order to optimally delineate the margin extent (ME) for stratification by Gleason score (GS).

METHOD AND MATERIALS

Retrospective analysis of patient- and tumor-specific factor association with PSA relapse-free survival (bRFS). Eligible patients underwent RP at the study institutions for biopsy-proven prostate adenocarcinoma, without adjuvant radiotherapy (RT) or hormone therapy (HT). Patients with evidence of metastatic disease or PSA >30 at diagnosis, or pathologic involvement of seminal vesicles or lymph nodes at RP were excluded. RP specimen slides were reviewed by pathology, and M+ details (foci, ME) were recorded.

RESULTS

Between 2002 and 2010, 644 patients underwent RP at the study institutions, of whom 429 were eligible for the present analysis. The median age at diagnosis was 61 years (range 43-76), and pre-RP PSA was 5.6 (0.9-26). Of 154 patients with confirmed M+, 146 had slides available for review. At a median follow-up of 80 months (range 16-155), 100 patients had experienced PSA relapse at a median of 22 months post-RP (1-124), of whom 64 had involved surgical margins. On multivariate analysis, pre-RP PSA, pathologic GS, and margin status were significantly associated with bRFS. Subset evaluation by GS and ME identified a group at lower risk of failure: GS

CONCLUSION

Within the present study, GS/= \geq 7 with any extent M+ have poor early bRFS.

CLINICAL RELEVANCE/APPLICATION

Reporting of ME in RP pathology reports should be considered, as this may influence consideration of adjuvant therapy versus surveillance.

SSG15-02 **Stereotactic Body Radiotherapy (SBRT) for Primary Renal Cell Carcinoma (RCC): Intrafraction Target Movement and Patient Outcomes**

Tuesday, Nov. 29 10:40AM - 10:50AM Room: S104A

Participants

Orit Kaidar-Person, MD, Chapel Hill, NC (*Presenter*) Nothing to Disclose
Alex Price, Chapel Hill, NC (*Abstract Co-Author*) Nothing to Disclose
Eric C. Schreiber, Chapel Hill, NC (*Abstract Co-Author*) Nothing to Disclose
Timothy M. Zagar, MD, New York, NY (*Abstract Co-Author*) Nothing to Disclose
Ronald Chen, MD, Chapel Hill, NC (*Abstract Co-Author*) Nothing to Disclose

ABSTRACT

Purpose/Objective(s): Renal cell carcinoma (RCC) is traditionally considered to be radioresistant. The current standard treatment for clinically localized disease is partial or radical nephrectomy; in patients unfit for surgery, cryotherapy or HIFU are recommended. Little has been published on the use of SBRT for primary RCC. Materials/Methods: This is an IRB-approved retrospective study. All patients were treated using a robotic-arm stereotactic system with fiducial tracking; target motion during treatment was extracted from motion models from actual treatment sessions. Patient records were reviewed for toxicity and cancer control outcomes. Results: Between the years 2010 and 2016, 6 patients who were non-surgical candidates were treated with SBRT for primary RCC with curative intent; all were treated to 39 Gy in 3 fractions given daily. Median age was 68.5 years (range: 61-77). All patients had two kidneys, with one kidney involved with primary localized RCC with a mean size of 5 cm (range: 4.2-6.5) and a mean PTV 124 cc (range: 72-210). Mean intrafraction tumor motion available for 4 patients was: superior/inferior 4.2 mm, left/right

5.7 mm, anterior/posterior 3.0 mm. Median follow-up was 23 months (range 14-49). All patients were followed with imaging every 6 months after treatment. Acute toxicity (Conclusion: SBRT to 39 Gy in 3 fractions is well-tolerated and provided durable local control in patients with primary RCC who were not surgical candidates. Initial imaging after treatment can show slight tumor enlargement. Tumor motion is an important technical issue for this treatment.

SSG15-03 Intraprostatic Polymer Based Fiducial Marker (FM) Placement allows for Accurate Co-registration of mpMRI and Planning CT Images

Tuesday, Nov. 29 10:50AM - 11:00AM Room: S104A

Participants

Neilayan Sen, MD, Chicago, IL (*Presenter*) Nothing to Disclose
Dian Wang, MD, PhD, Columbus, OH (*Abstract Co-Author*) Nothing to Disclose
James C. Chu, PhD, Chicago, IL (*Abstract Co-Author*) Research Grant, Varian Medical Systems, Inc
Julius Turian, Chicago, IL (*Abstract Co-Author*) Nothing to Disclose

ABSTRACT

Purpose/Objective(s): Multiparametric magnetic resonance imaging (mpMRI) allows for reliable detection of adverse pathologic features (ie. high-grade tumor, extracapsular extension, and seminal vesicle involvement) which are indications for dose-escalated radiotherapy (RT). Accurate co-registration of the mpMRI and planning CT images using FMs is essential to enhance tumor target delineation and to deliver focal high-dose RT to intraprostatic lesions defined by mpMRI while sparing normal adjacent structures. However, it is unknown whether intraprostatic polymer based FMs may affect radiologic interpretation of the mpMRI. Additionally, it is unknown whether FMs can be reliably utilized for co-registration of the MRI with the planning CT images. To answer these questions, we have examined a cohort of patients with mpMRI and planning CT performed after FM placement. **Materials/Methods:** This analysis was limited to patients with histologically proven prostate cancer. All eligible patients had three polymer-based FMs (1 mm diameter and 3 mm in length, PolyMark™ Fiducial Markers, CIVCO Medical Solutions, Coralville IA), implanted into the prostate using transrectal ultrasound guidance (one FM placed to apex, one into base and a third one into contralateral lobe). Patients subsequently underwent mpMRI within 12-40 days (median 19) and CT simulation. **Results:** 18 patients met inclusion criteria. 8 had palpable disease by digital rectal examination (range T2a – T3a). Median PSA was 11.5 (range 5-144). Median Gleason sum was 8 (range 7-10), median % core involvement was 59 (range 8-100%), and 11 patients were high risk by NCCN criteria. 11 patients had at least one lesion identified on mpMRI (range 1-4) with median PI-RADS 4 (range 1-5). Of the patients with mpMRI positive lesions, 4 had pre-fiducial mpMRI available for comparison. According to expert radiology review, none of these patients had evidence of new lesions after FM placement. FMs were clearly identified in both mpMRI and planning CT, allowing for accurate co-registration. **Conclusion:** It is feasible to accurately co-register mpMRI and CT planning images using polymer based FMs implanted into the prostate. Furthermore, the placement of three intraprostatic FMs has not generated any false positives or otherwise altered mpMRI interpretation.

SSG15-04 Preliminary Evaluation of Seed Migration in Coated vs Non-coated Seeds for LDR Prostate Brachytherapy using the Mick Applicator Implant Technique

Tuesday, Nov. 29 11:00AM - 11:10AM Room: S104A

Participants

Bryan J. Traughber, MD, Cleveland Heights, OH (*Presenter*) Spouse, Employee, Koninklijke Philips NV
Tarun K. Podder, Greenville, NC (*Abstract Co-Author*) Nothing to Disclose
Yan Xing, Cleveland, OH (*Abstract Co-Author*) Nothing to Disclose
Valdir Colussi, PhD, Cleveland, OH (*Abstract Co-Author*) Nothing to Disclose
Elisha Fredman, MD, Cleveland, OH (*Abstract Co-Author*) Nothing to Disclose
Lee E. Ponsky, MD, Cleveland, OH (*Abstract Co-Author*) Nothing to Disclose
Rodney J. Ellis, MD, Pepper Pike, OH (*Abstract Co-Author*) Nothing to Disclose

PURPOSE

Low dose rate (LDR) brachytherapy is a highly effective modality for the treatment of prostate cancer. However, incorrect placement of seeds can lead to suboptimal outcomes and treatment related sequelae such as urethral and rectal toxicities. Even secondary lung cancers due to seed migration have been reported in the literature. The purpose of this study is to evaluate the incidence of seed migration and resultant dosimetric impact using coated vs. uncoated seeds with a Mick applicator implant technique.

METHOD AND MATERIALS

Twenty patients with prostate cancer treated at a high-volume single institution status post LDR brachytherapy were retrospectively analyzed and compared for seed slippage when using coated vs. uncoated seeds with a Mick applicator implant technique. All patients were planned with pre-treatment multi-parametric MRI and evaluated with intraoperative ultrasound, real-time intraoperative dosimetry, and a Day 0 CT-based dosimetric analysis. All dosimetric calculations were based on TG-43 formulation. The incidence of seed slippage was compared between patients treated with coated vs. uncoated seeds.

RESULTS

Eight patients were treated with coated seeds and twelve patients with uncoated seeds, representing 699 and 1099 total seeds placed respectively. The total migration rate was 3.2% vs. 10.2% for coated vs. uncoated seeds. Intra-prostatic migration was 1.2% for coated seeds, and 5.1% for uncoated seeds. Importantly, the seed non-visualization rate from intraoperative monitoring with ultrasound and Day 0 CT was 2.0% and 5.1% respectively, likely representing extra-prostatic seed migration. Dosimetric consequences were also evaluated but data not shown due to space limitations.

CONCLUSION

The use of coated seeds with a Mick applicator implant technique reduces seed migration by nearly ⅓ rds, including extra-prostatic slippage not identified on real-time intraoperative ultrasound or post-implant CT. Further sector based analyses including regional dosimetric impact relative to gross disease identified on multi-parametric MRI and adjacent organs-at-risk are warranted.

CLINICAL RELEVANCE/APPLICATION

Prostate seed migration following LDR brachytherapy can compromise local tumor control in addition to unintended consequences

such as extra-prostatic seed migration to the lungs and abdomen-pelvis.

SSG15-08 Comparison of Intraoperative MRI/US Fusion in Relation to Standard CT/US Based Planning for LDR Prostate Brachytherapy

Tuesday, Nov. 29 11:40AM - 11:50AM Room: S104A

Awards

Student Travel Stipend Award

Participants

Paul Renz, DO, Pittsburgh, PA (*Presenter*) Nothing to Disclose

Stephen Abel, BS, Pittsburgh, PA (*Abstract Co-Author*) Nothing to Disclose

Mark G. Trombetta, MD, Pittsburgh, PA (*Abstract Co-Author*) Nothing to Disclose

Olivier Gayou, PhD, Pittsburgh, PA (*Abstract Co-Author*) Nothing to Disclose

Jie Tang, MSc, Steubenville, OH (*Abstract Co-Author*) Nothing to Disclose

E. Day Werts, PhD, Pittsburgh, PA (*Abstract Co-Author*) Nothing to Disclose

PURPOSE

Intraoperative planning with transrectal ultrasound (US) is used for accurate seed placement and optimal dosimetry in prostate brachytherapy. However, prostate MRI has shown superiority in delineation of prostate anatomy. Accordingly, MRI/US fusion may be useful for accurate intraoperative planning. We analyzed planning with MRI/US fusion to compare differences in dosimetry to that derived from postoperative CT.

METHOD AND MATERIALS

Twenty patients underwent preoperative prostate MRI which was fused intraoperatively with US during prostate brachytherapy using a MIM Symphony treatment planning system (MIM Software; Cleveland, Ohio, USA). Following implantation, dose comparisons were made between data derived from MRI/US and that from post-operative CT scans. Plan parameters analyzed included the D90 (dose to 90% of the prostate), rectal D30, and the rectal V30 (volume of the rectum receiving 30 percent of dose), and the prostate V100.

RESULTS

The median number of seeds implanted per patient was 76 with mean activity of 0.381mCi per seed. The MRI measured prostate volume was on average 4.47cc smaller than the CT measured prostate volume. In 9 patients, the apex of the prostate was better identified under MRI and an average of 4 fewer seeds were required to be placed in the apex/urinary sphincter region. Both MRI and US individually showed reduced intraoperative prostate D90 in comparison to postoperative CT-based prostate D90 with a larger mean difference for MRI in comparison with US (9.71 vs. 4.31Gy, $p=0.007$). This was also true for the prostate V100 (5.18 vs. 2.73cc, $p=0.009$). Post-operative CT underestimated rectal D30 and V30 in comparison to both MRI and US with MRI showing a larger mean difference than US for D30 (40.64 vs. 35.92Gy, $p=0.04$) and V30 (50.20 vs. 44.38cc, $p=0.009$).

CONCLUSION

The MRI/US fusion demonstrated lower prostate volume compared with standard CT/US based planning likely due to the better resolution of the prostate apex. Furthermore, rectal dose was underestimated with CT vs. MRI based planning. Additional study is required to assess long term clinical implications of disease control and effects on the rectum and urinary sphincter.

CLINICAL RELEVANCE/APPLICATION

MRI/US intraoperative fusion may improve prostate dosimetry and sparing of the rectum, potentially impacting disease control and late toxicity.

SSG15-09 Impact Factors on Acute Hematologic Toxicity in Prostate Cancer Patients Treated with Radiation Therapy

Tuesday, Nov. 29 11:50AM - 12:00PM Room: S104A

Participants

Xiaoying Li, Beijing, China (*Abstract Co-Author*) Nothing to Disclose

Ke Wang, MD, Beijing, China (*Presenter*) Nothing to Disclose

ABSTRACT

Purpose/Objective(s): To determine factors predictive for hematologic toxicity (HT) in patients with prostate cancer treated with radiotherapy. **Materials/Methods:** The medical records of 47 men receiving radiation therapy for prostate cancer were reviewed. Hematologic toxicity was defined by use of Common Terminology Criteria for Adverse Events (version 4.0). Pelvic bone marrow (PBM) was contoured for each patient and divided into three subsites: lumbosacral spine (LSS), ilium (IBM), and lower pelvis (LP). The volume of each region receiving 5, 10, 15, 20, 25, 30, 35 and >40 Gy (V10, V15, V20, V25, V30, V35 and V40, respectively) was calculated. Endpoints included any grade hematologic event (HE). Logistic regression was used to test associations between HT and dosimetric/clinical parameters. **Results:** 24 (51.1%) patients experienced leukopenia, 20 (42.6%) were Grade I, 4 (8.5%) were Grade II. Pelvic radiation was associated with an increased worse leukopenia. No association was found with age, ADT therapy, radiation dose and other clinical factors. Multivariate logistic regression analysis shows PBM V5 (OR, 1.046; 95% CI, 1.006–1.088; $p=0.024$), IBM V10 (OR, 1.032; 95% CI, 1.006–1.059; $p=0.023$), ALS V25 (OR, 6.967; 95% CI, 1.336–36.338; $p=0.015$) was associated with an increased worse leukopenia. ROC curve shows, LS V25 is the best predictor of leukopenia (AUC 0.718 $p=0.01$). Patients with LS V25 $>71.38\%$, leukopenia significantly increased (65.7% Vs 8.3%, $P=0.001$). 21 patients experienced (44.7%) anemia during treatment. Univariate analysis shows age ($P=0.03$) and ADT therapy ($P=0.021$) was associated with incidence of anemia. Multivariate logistic regression analysis shows ADT therapy is the only factor associated with anemia (OR, 6.967; 95% CI, 1.336–36.338; $p=0.021$). ADT therapy increases by a factor (odds ratio) of 6.967. No association was found with ADT time, bone radiation dose and other clinical factors. No patient experienced thrombocytopenia. **Conclusion:** Leukopenia and anemia are the most common hematologic toxicity (HT) events happened during radiation therapy of prostate cancer patients. Pelvic radiation was associated with an increased worse leukopenia, LS V25 is the best predictor of leukopenia. When Patients' LS V25 is greater than 71.38%, leukopenia significantly increased. ADT therapy is the only factor associated with anemia during radiation therapy.

Area under the ROC curve variables area Std. error asymptotic sig asymptotic 95% confidence interval lower bound upper

boundLS250.718 0.076 0.01 0.569 0.868IBM100.674 0.08 0.041 0.517 0.831PBM50.665 0.08 0.053 0.508
0.821

SSG16

Vascular Interventional (Percutaneous Ablation: Basic Science)

Tuesday, Nov. 29 10:30AM - 12:00PM Room: E351

CT **IR** **PH**

AMA PRA Category 1 Credits™: 1.50
ARRT Category A+ Credits: 1.50

FDA Discussions may include off-label uses.

Participants

Gordon McLennan, MD, Chagrin Falls, OH (*Moderator*) Research Grant, Sirtex Medical Ltd; Research Grant, C. R. Bard, Inc; Consultant, Medtronic plc; Advisory Board, Siemens AG; Advisory Board, Surefire Medical, Inc; Stock Holder, Surefire Medical, Inc; Advisory Board, Medtronic plc; Advisory Board, Stealth Medical; Advisory Board, Rene Medical;
Himanshu Shah, MD, Zionsville, IN (*Moderator*) Consultant, IMARC Research Inc

Sub-Events

SSG16-01 Performance Evaluation of a Robotic Assistance Device Compared to Manual Fluoroscopy Procedure in Computed Tomography Guided Minimally Invasive Ablation Procedures and Diagnostic Punctures

Tuesday, Nov. 29 10:30AM - 10:40AM Room: E351

Participants

Arman Smakic, MD, Mannheim, Germany (*Presenter*) Nothing to Disclose
Nils Rathmann, MD, Mannheim, Germany (*Abstract Co-Author*) Nothing to Disclose
Michael Kostrzewa, MD, Mannheim, Germany (*Abstract Co-Author*) Institutional research agreement, Siemens AG
Stefan O. Schoenberg, MD, PhD, Mannheim, Germany (*Abstract Co-Author*) Institutional research agreement, Siemens AG
Steffen J. Diehl, MD, Mannheim, Germany (*Abstract Co-Author*) Nothing to Disclose

PURPOSE

To evaluate a novel commercially available robotic assistance device for computed tomography guided interventions compared to standard manually performed CT-scan guided interventions in terms of precision, radiation exposure and intervention time.

METHOD AND MATERIALS

Within 16 months 55 patients were treated using robotic assistance (group A) and compared to a control group of 102 patients previously treated with a standard CT-scan guided, manually performed, approach (group B). Evaluated parameters were precision (deviation from planned target and number of needle replacements), radiation exposure and intervention time. Evaluations were performed with regard to complexity (in plane vs. out of plane interventions) and anesthesia type (general vs. local anesthesia).

RESULTS

Parameters related to precision were in general significantly better in the robotic assistance group ($p < 0.01$) with a mean deviation of only 1.2mm (± 1.6 mm) compared to 2.6mm (± 1.1 mm) in the control group. Regarding the sub-groups, differences in deviation in both groups were smaller in procedures performed under general anesthesia compared to local anesthesia (Group A: 0.5mm (± 0.9 mm) vs. 2.1mm (± 1.9 mm) group B: 1.9mm (± 1.3 mm) vs. 3.4mm (± 1.1 mm) (both $p < 0.001$). Mean number of needle replacements necessary to reach the target was 0.3 (± 0.4) in the robotic assistance group compared to 1.8 (± 0.7) in the comparison group ($p < 0.001$). Compared to standard procedure mean intervention time was 15 minutes (± 5.4 min) shorter in complex out of plane punctures in the robotic group. There was no increase of radiation exposure to the patient while radiation exposure for the physician was reduced to zero when the navigation system was used.

CONCLUSION

Compared to manual placement the use of a robotic assistance device in complex out of plane CT guided interventions under general anesthesia allows probe placement with high precision, reduces intervention time with no increase of exposure to radiation to the patient and zero radiation for the physician. In less complex in plane punctures no advantages concerning intervention time and radiation dose were seen while precision analysis showed small advantages.

CLINICAL RELEVANCE/APPLICATION

Use of a robotic navigation system can improve the workflow of complex CT guided minimally invasive ablation procedures and diagnostic punctures in terms of precision, intervention time and eliminates radiation to the performing physician.

SSG16-02 Effect of Concentration of Perfusate and Power-Setting on Coagulated Size of Hydrochloric Acid-Infused Radiofrequency Ablation

Tuesday, Nov. 29 10:40AM - 10:50AM Room: E351

Awards

Trainee Research Prize - Resident

Participants

Tianqi Zhang, Guangzhou, China (*Presenter*) Nothing to Disclose
Kaiwen Huang, Taipei City, Taiwan (R.O.C.), Taiwan (*Abstract Co-Author*) Nothing to Disclose
Leyi Xu, Guangzhou, China (*Abstract Co-Author*) Nothing to Disclose
Yangkui Gu, Guangzhou, China (*Abstract Co-Author*) Nothing to Disclose
Rongqian Yang, Guangzhou, China (*Abstract Co-Author*) Nothing to Disclose
Ruhai Zou, Guangzhou, China (*Abstract Co-Author*) Nothing to Disclose
Jinhua Huang, Guangzhou, China (*Abstract Co-Author*) Nothing to Disclose

PURPOSE

To determine the optimal concentration of hydrochloric acid (HCl) applied in HCl-infused radiofrequency ablation (H-RFA) by investigating the H-RFA lesion sizes and the conductivities in different concentrations of HCl under different ablation powers.

METHOD AND MATERIALS

H-RFA procedure was conducted in 60 ex vivo porcine livers at 103°C within 30 minutes. To test four different concentrations of HCl (5%, 10%, 15%, 20%) as experimental groups and two control groups including distilled water and normal saline under two setting ablative powers (30 w, 60w), 12 subgroups were created, each with five specimens. For each ablation procedure, the power output was recorded every 2.5 minutes, the longitudinal and transverse diameters were measured, and ablation volumes were calculated. The average impedance, actual power output, longitudinal and transverse diameters, and volumes of the lesions in all eight groups were compared with analysis of variance. Alpha was set at 0.05.

RESULTS

The ablation zones of H-RFA were significantly larger than controls ($P < 0.001$). The largest mean lesion volume of H-RFA was 179.22 ± 24.79 cm³, with 10% HCl concentration at 60 w; the smallest was 93.97 ± 15.09 cm³, with 5% HCl at 30 w. The average power outputs at concentrations of 5% and 10% were significantly greater than those at 15% and 20% in the 30 w and 60 w groups, respectively ($P < 0.05$). In the 60 w groups, the longitudinal and transverse diameters and volume at 10% were significantly greater than those of the other three concentration groups ($P < 0.05$). Although the average power output of the 15% and 20% groups was smaller than that at 5% ($P > 0.05$), the lesion sizes were similar in 60 watt groups than those of the 5% group and were even larger in 30 watt groups.

CONCLUSION

An HCl concentration of 10% produced the largest lesion and is thus the optimal concentration for HRFA under the conditions tested.

CLINICAL RELEVANCE/APPLICATION

An HCl concentration of 10% is evaluated as the optimal concentration for hydrochloric acid infused radiofrequency ablation (HRFA). By applied 10% HCl, it could create large ablation zone by HRFA.

SSG16-03 Single Exponential Decay Voltage Profile for Non-thermal Tissue Ablation

Tuesday, Nov. 29 10:50AM - 11:00AM Room: E351

Participants

Michael K. Stehling, MD, PhD, Offenbach, Germany (*Presenter*) Investor, InterScience GmbH
Enric Guenther, Dipl Phys, Frankfurt, Germany (*Abstract Co-Author*) Investor, InterScience GmbH
Paul Mikus, DPhil, Coto De Caza, CA (*Abstract Co-Author*) Consultant, Interscience
Nina Klein, MSc, Offenbach am Main, Germany (*Abstract Co-Author*) Nothing to Disclose
Boris Rubinsky, PhD, Berkeley, CA (*Abstract Co-Author*) Consultant, InterScience GmbH

PURPOSE

Non-thermal irreversible electroporation (NTIRE) protocols are designed to maximize tissue ablation by irreversible electroporation while minimizing Joule heating; to spare vital structures such as blood vessels in the treated lesion. Due to muscle contractions, muscle relaxants are necessary. We designed a new technology for non-thermal tissue ablation, which employs a synergistic combination of electroporation and electrolysis (SEE) inducing electrical parameters. The voltage profile, delivered as a millisecond long exponential decay, generates products of electrolysis, which ablate cells by penetrating the interior of electroporation permeabilized cells.

METHOD AND MATERIALS

The liver of three pigs was exposed and treated with two custom-made, electrolysis promoting Ti based electrodes under ultrasound monitoring. We utilized a generator designed to simultaneously deliver electrolysis and electroporation. The initial voltage, the time constants of the exponential voltage profile and the number of pulses delivered were parameters of this study. Animals were sacrificed at 24 hours. For microscopic analysis, the liver samples were fixed in a 10% formalin solution, processed to wax blocks and stained with Masson's trichromatic stain for histologic examination.

RESULTS

Single SEE electric fields which decayed exponentially within milliseconds from field strengths of 750 and 1000 V/cm produced continuous ablation between electrodes with comparable ablation dimensions to that achieved with 70 typical NTIRE pulses, without the necessity of muscle relaxants. Animals tolerated the procedure without significant adverse events.

CONCLUSION

The SEE technology can reliably ablate liver tissue on a cellular level with single exponential decay voltage profiles. At the same time it reduces the muscle contraction to the extent that no muscle relaxants are needed. While other shapes of voltage potentials for SEE exist, an advantage of the exponential decay voltage shape is its technological simplicity. This non-thermal technology is therefore faster than comparable ablation modalities, with lower toxicity and lower requirements for anesthesia and muscle relaxation.

CLINICAL RELEVANCE/APPLICATION

SEE is a novel technology for non-thermal tissue ablation, which utilizes a synergistic combination of electroporation and electrolysis parameters, delivered as a single exponential decay voltage.

SSG16-04 Evaluation of A Novel Thermal Accelerant Agent to Augment Tissue Heating During Image-Guided Microwave Ablation

Tuesday, Nov. 29 11:00AM - 11:10AM Room: E351

Participants

William C. Park, PhD, Providence, RI (*Abstract Co-Author*) Nothing to Disclose
Damian E. Dupuy, MD, Providence, RI (*Presenter*) Research Grant, NeuWave Medical Inc Board of Directors, BSD Medical Corporation
Stockholder, BSD Medical Corporation Speaker, Educational Symposia
Aaron W. Maxwell, MD, Providence, RI (*Abstract Co-Author*) Nothing to Disclose
Shaolei Lu, MD, PhD, Providence, RI (*Abstract Co-Author*) Nothing to Disclose
Grayson L. Baird, PhD, Providence, RI (*Abstract Co-Author*) Nothing to Disclose
Edward G. Walsh, PhD, Providence, RI (*Abstract Co-Author*) Nothing to Disclose
Victoria Frank, Fall River, MA (*Abstract Co-Author*) Nothing to Disclose
Michael P. Primmer, Providence, RI (*Abstract Co-Author*) Nothing to Disclose
Kara A. Lombardo, BS, Providence, RI (*Abstract Co-Author*) Nothing to Disclose
Scott Collins, RT, Providence, RI (*Abstract Co-Author*) Nothing to Disclose

PURPOSE

The effectiveness of thermal ablation in solid tumors decreases with distance from the applicator tip (thermal diffusion) and with increased adjacent blood flow ("heat sink" effect). In this study, we describe our initial experience with a novel thermal accelerant (TA) agent designed to mitigate these factors and augment ablation zone volume.

METHOD AND MATERIALS

TA performance was evaluated with a commercially available microwave ablation system using *in vitro* agarose phantom, *ex vivo* bovine liver, and *in vivo* porcine liver, kidney, and muscle models. Microwave power, TA dose, and TA-to-tip distance were varied, and temperature readings compared with and without TA. Gross pathologic analysis was performed on *in vivo* specimens using triphenyl tetrazolium chloride (TTC) staining to calculate ablation zone volumes. Imaging characteristics were determined using ultrasound and CT.

RESULTS

Using the *in vitro* model, both the rate and magnitude of increase in ablation zone temperature were significantly greater with TA under all tested conditions ($p < 0.0001$). *Ex vivo*, the intrahepatic ablation zone temperature increase was directly proportional to dose, with 60°C reached in 180 second using 250 mg/mL at 60W. *In vivo*, liver, muscle, and kidney ablation zone volumes as determined by TTC staining were significantly increased with TA use ($p < 0.01$ for all). The compound exhibited biphasic gel properties, existing as a clear liquid at 25°C and an opaque gel at 37°C. On ultrasound imaging, the TA appeared hypoechoic when liquid and mildly echogenic as gel. On CT, TA density was proportional to dose, with average values ranging from 329 HU to 3071 HU at 10 mg/mL and 1,000mg/mL, respectively.

CONCLUSION

Our novel TA agent improved the performance of a commercially-available microwave ablation system and increased ablation zone volume in multiple tissue types. The agent is readily visible under both CT and ultrasound, and can be reliably placed within biologic tissues owing to its biphasic gel properties. Future studies evaluating optimal TA-to-target geometry and other organ-specific parameters are planned.

CLINICAL RELEVANCE/APPLICATION

Ablation volume is significantly augmented through the use of a novel thermal accelerant agent designed to mitigate thermal diffusion and heat sink effects.

Honored Educators

Presenters or authors on this event have been recognized as RSNA Honored Educators for participating in multiple qualifying educational activities. Honored Educators are invested in furthering the profession of radiology by delivering high-quality educational content in their field of study. Learn how you can become an honored educator by visiting the website at: <https://www.rsna.org/Honored-Educator-Award/>

Damian E. Dupuy, MD - 2012 Honored Educator

SSG16-05 Imaging-guided Spinal Radiofrequency, Microwave, and Cryoablation in a Sheep Model

Tuesday, Nov. 29 11:10AM - 11:20AM Room: E351

Participants

Adam N. Wallace, MD, Saint Louis, MO (*Abstract Co-Author*) In-kind support, DFINE, Inc ; In-kind support, Galil Medical Ltd; In-kind support, Medtronic plc
Travis J. Hillen, MD, Saint Louis, MO (*Abstract Co-Author*) Consultant, Biomedical Systems; Instructor, Dfine, Inc
Michael V. Friedman, MD, Saint Louis, MO (*Abstract Co-Author*) Nothing to Disclose
Zohny S. Zohny, MD, Saint Louis, MO (*Abstract Co-Author*) Nothing to Disclose
Bradley H. Stephens, MD, Saint Louis, MO (*Abstract Co-Author*) Nothing to Disclose
Suellen C. Greco, DVM, Saint Louis, MO (*Abstract Co-Author*) Nothing to Disclose
Michael R. Talcott, DVM, Saint Louis, MO (*Abstract Co-Author*) Nothing to Disclose
Jack W. Jennings, MD, Saint Louis, MO (*Presenter*) Speakers Bureau, DFINE, Inc Consultant, DFINE, Inc

PURPOSE

In this study, *in vivo* RFA, cryoablation, and MWA of healthy sheep vertebrae were performed to accomplish three objectives. First, the technical parameters of each modality were correlated with the diameter of the necrotic ablation zone on gross pathology. Second, ablations were performed that exceeded the dimensions of the vertebral bodies to determine whether the posterior vertebral body cortex acts as a protective barrier for the spinal cord. Third, post-ablation MRI and histologic findings were evaluated and correlated.

METHOD AND MATERIALS

Ten healthy sheep vertebrae were treated with radiofrequency ablation ($n = 3$), cryoablation ($n = 4$), or microwave ablation ($n = 3$). In the first sheep, the parameters of each ablation were chosen to produce an ablation volume with a 20-mm diameter orthogonal to the ablation probe based on preclinical data provided by the manufacturers. MRI was performed 48 hours (sheep 1) or 7 days (sheep 2, 3) after the ablation procedure. The vertebral bodies were then harvested for gross pathologic and histologic

evaluation.

RESULTS

Radiofrequency ablation zones on gross pathology were 5.9 ± 0.7 mm smaller than those expected based on previously derived correlations with technical parameters. Cryoablation and microwave ablation zones were within 2 and 1 mm, respectively, of those expected. Cryoablation and microwave ablation zones larger than the target vertebral bodies caused histologically confirmed spinal cord injury, but this was not observed with radiofrequency ablation. On MRI, all ablation modalities produced a non-enhancing ablation zone delineated by a thin rim of enhancement, which corresponded histologically to marrow necrosis and hemorrhagic congestion, respectively. Gross pathology ablation zones were larger than those measured on MRI by 0.6 ± 0.2 mm for radiofrequency ablation, 0.9 ± 0.3 mm for cryoablation, and 1.4 ± 0.8 mm for microwave ablation.

CONCLUSION

Estimations of ablation zone dimensions and the risk of ablation-induced spinal cord injury vary among modalities. Ablation zones are slightly larger on pathology than on MRI.

CLINICAL RELEVANCE/APPLICATION

Accurate estimation of spinal ablation zone dimensions derived from an in vivo sheep model, coupled with the knowledge of whether the cortex protects against ablation-induced spinal cord injury, will facilitate the adequate and safe ablation of spinal tumors.

SSG16-06 Use of CT Densitometry to Differentiate between Recurrence and Ablation Scar

Tuesday, Nov. 29 11:20AM - 11:30AM Room: E351

Awards

Student Travel Stipend Award

Participants

Lillian Xiong, MD, Providence, RI (*Presenter*) Nothing to Disclose

Erica S. Alexander, MD, Providence, RI (*Abstract Co-Author*) Nothing to Disclose

Grayson L. Baird, PhD, Providence, RI (*Abstract Co-Author*) Nothing to Disclose

Damian E. Dupuy, MD, Providence, RI (*Abstract Co-Author*) Research Grant, NeuWave Medical Inc Board of Directors, BSD Medical Corporation Stockholder, BSD Medical Corporation Speaker, Educational Symposia

PURPOSE

This study evaluates CT densitometry's ability to differentiate tumor from scar after radiofrequency ablation.

METHOD AND MATERIALS

Data used from a prospective, multicenter group trial approved by each institutional review board. 54 patients from 16 US sites were enrolled, of these, 50 patients (23 Men, 27 Women; mean age 75.3 ± 7.5 years) met eligibility requirements. Data from patients' pretreatment and multiple post treatment follow up multiphase CT scans (CT densitometry) at 3, 6, 9, and 12 months to evaluate recurrent tumor and scar enhancement at 0, 45, 90, 180, and 300 seconds.

RESULTS

Evaluation of the CT densitometry at times of recurrence showed kinetics that mimic the pretreatment densitometry. The average change in Hounsfield units (HU) from 0 to 45 seconds at time of recurrence was 48 HU CI 95% (29-67) and pretreatment, biopsy proven tumor, has an average change of 56 HU CI 95% (40-72) with a near identical slopes. After this initial increased uptake, the recurrences and biopsy proven tumor curves show plateau to slight washout of contrast. Conversely, the CT densitometry without recurrence showed kinetics that mimic the 3 month ablation scar densitometry curve with near identical slope. The average change in HU from 0 to 45 seconds with no recurrence was 13 HU CI 95% (1.2-24) and 28 HU CI 95% (14-41) in the 3 month ablation scar. At the 90 and 180 time points, these both show persistent uptake of contrast, consistent with the imaging findings of scar and fibrosis.

CONCLUSION

CT densitometry shows different kinetic curves in recurrent and primary tumor compared to scar. This may be a useful imaging biomarker of neovascularity in patients undergoing ablative therapies.

CLINICAL RELEVANCE/APPLICATION

Similar to the kinetic curves used in breast MRI to evaluate lesion physiology, CT densitometry's ability to differentiate tumor from scar makes it a viable alternative imaging method or adjunct method to evaluate post ablation patients.

Honored Educators

Presenters or authors on this event have been recognized as RSNA Honored Educators for participating in multiple qualifying educational activities. Honored Educators are invested in furthering the profession of radiology by delivering high-quality educational content in their field of study. Learn how you can become an honored educator by visiting the website at: <https://www.rsna.org/Honored-Educator-Award/>

Damian E. Dupuy, MD - 2012 Honored Educator

SSG16-07 Novel Needle-Attached Orientation Sensor to Correct for Respiratory Motion during Percutaneous Interventions: Accuracy of Lesion Position Estimation in the Liver

Tuesday, Nov. 29 11:30AM - 11:40AM Room: E351

Participants

Momen Abayazid, PhD, Boston, MA (*Abstract Co-Author*) Nothing to Disclose

Takahisa Kato, Boston, MA (*Abstract Co-Author*) Employee, Canon Inc

Stuart G. Silverman, MD, Brookline, MA (*Abstract Co-Author*) Author, Wolters Kluwer nv

Olutayo I. Olubiyi, MD, BOSTON, MA (*Abstract Co-Author*) Nothing to Disclose

Nobuhiko Hata, PhD, Boston, MA (*Presenter*) Research Grant, Canon USA Inc; Research Grant, Koh Young Technology Inc; Research Consultant, AZE, Ltd ; Research Consultant, Harmonus, Ltd ; Stockholder, Harmonus, Ltd

PURPOSE

Respiratory motion is the single-most important obstacle in targeting small lesions in the lung, liver and kidney. We assessed if the motion of an initially placed 'reference' needle coupled with an attached sensor could be used to accurately estimate the position of a simulated liver lesion motion in real-time at different proximities of the needle to the lesion.

METHOD AND MATERIALS

An experimental platform was developed to mimic liver motion during breathing using a 2-degrees-of-freedom (DOF) motorized stage. The motorized stage simulated the lesion motion; 10mm in the superior-inferior and 6mm in the anterior-posterior directions; during shallow breathing that includes inhalation (2s), exhalation (2s) and then a pause (2s). A custom made 9DOF inertial measurement unit (IMU) was attached to the hub of an 18-gauge standard 'reference' biopsy needle. Following 21 needle placements into the phantom, IMU collected the surrogate signals including 3D orientation, linear acceleration and angular velocity of the needle during synthetic motions of the phantom. A supervised learning algorithm based on Random k-Labelsets method was trained to create a correspondence model that correlated the surrogate signals to the lesion position over 20 seconds. The actual lesion position was measured using an electro-magnetic (EM) sensor at the lesion site and used as a gold standard. The IMU and EM sensor data were synchronized and split; 66% of the data was used for training and 34% was used for testing. The needle was placed with varying proximity to the lesion.

RESULTS

The errors to estimate lesion motion were 0.0, 1.0 and 0.0 mm in median value, and 0.63 ± 0.87 , 0.74 ± 0.79 , and 0.53 ± 0.81 mm in average value ($p=0.003$ by Kruskal-Wallis), for needle-to-lesion proximity range of 0-1cm, 1-2cm and 2-3cm respectively. The processing time for training and testing was 4-12 ms, which is sufficient for real-time lesion motion estimation using the proposed surrogate signal.

CONCLUSION

Motion of an initially placed 'reference' needle can be used as a surrogate signal to accurately estimate a lesion's position in real-time during percutaneous interventions. The needle proximity to lesion significantly affected the lesion position estimation error.

CLINICAL RELEVANCE/APPLICATION

As initially placed 'reference' needle with an attached sensor can be used to compensate for respiratory motion and improve targeting of small tumors in organs that move with respiration.

SSG16-08 In Vitro Artifact Assessment of a New MR-compatible Microwave Antenna Device for Tumor Ablation with Near-Realtime Fluoroscopic MRI-Sequences

Tuesday, Nov. 29 11:40AM - 11:50AM Room: E351

Participants

David-Emanuel Kessler, MD, Tübingen, Germany (*Presenter*) Nothing to Disclose

Jakob Weis, MD, Tübingen, Germany (*Abstract Co-Author*) Nothing to Disclose

Stephan Clasen, MD, Tübingen, Germany (*Abstract Co-Author*) Nothing to Disclose

Konstantin Nikolaou, MD, Tübingen, Germany (*Abstract Co-Author*) Speakers Bureau, Siemens AG; Speakers Bureau, Bracco Group; Speakers Bureau, Bayer AG

Rüdiger Hoffmann, Tübingen, Germany (*Abstract Co-Author*) Nothing to Disclose

PURPOSE

To evaluate artifact configuration and diameters of a new magnetic resonance (MR) compatible microwave (MW) applicator for percutaneous tumor ablation using two different near-realtime MR fluoroscopic sequences.

METHOD AND MATERIALS

Two new MW applicators (14 and 16 Gauge) were tested in a phantom study at 1.5T with two dedicated sequences optimized for MR fluoroscopic imaging: T1 weighted spoiled Gradient Echo (GRE) sequence and T1/T2 weighted Steady State Free Precession (SSFP) sequence. Applicator orientation to main magnetic field (B_0), slice orientation and phase encoding direction (PED) were varied in a systematic fashion. Needle tip location error (TLE) was assessed and artifact diameters were calculated for each needle, sequence, and position. Influence of imaging parameters on artifacts were assessed with ANOVA and post hoc testing.

RESULTS

The artifact was homogenous along the whole length of both antennas with all tested parameters. The tip artifact measured 7.7 ± 1.2 mm for the 14 G antenna and 6.9 ± 1.0 mm for the 16 G antenna, respectively. The shaft artifact diameter measured 9.6 ± 1.5 mm and 8.6 ± 1.2 mm, respectively. TLE was -1.6 ± 1.2 mm and -1.5 ± 1.2 mm, respectively. Orientation to B_0 had no statistically significant influence on the tip artifact diameter ($p=0.07$ and $p=0.55$, respectively) or the TLE ($p=0.26$ and $p=0.93$, respectively). GRE sequence produced statistically significant greater TLE ($p<0.0001$). Slice orientation had no statistically significant influence on the size of the tip artifact ($p=0.31$ and $p=0.93$, respectively) and on the TLE ($p=0.97$ and $p=0.35$, respectively). PED had no statistically significant influence on the TLE ($p=0.15$ and $p=0.68$, respectively)

CONCLUSION

The new MR-compatible MW applicator's artifact is adequately small and TLE seems small enough for safe applicator positioning during near-realtime fluoroscopic MR-guidance for percutaneous ablation procedures.

CLINICAL RELEVANCE/APPLICATION

The results of this study may help implementing MR-guided microwave ablation in clinical practice.

SSG16-09 Cardiac Safety of Irreversible Electroporation Evaluated by Biomarkers and Electrocardiographic Monitoring

Participants

Michael Kostrzewa, MD, Mannheim, Germany (*Presenter*) Institutional research agreement, Siemens AG

Erol Tueluemen, Mannheim, Germany (*Abstract Co-Author*) Nothing to Disclose

Volker Liebe, Mannheim, Germany (*Abstract Co-Author*) Nothing to Disclose

Nils Rathmann, MD, Mannheim, Germany (*Abstract Co-Author*) Nothing to Disclose

Thomas Henzler, MD, Mannheim, Germany (*Abstract Co-Author*) Research support, Siemens AG; Speaker, Siemens AG

Stefan O. Schoenberg, MD, PhD, Mannheim, Germany (*Abstract Co-Author*) Institutional research agreement, Siemens AG

Martin Borggreffe, Mannheim, Germany (*Abstract Co-Author*) Nothing to Disclose

Steffen J. Diehl, MD, Mannheim, Germany (*Abstract Co-Author*) Nothing to Disclose

PURPOSE

To systematically evaluate the safety of irreversible electroporation (IRE) in respect to cardiac safety, using cardiac biomarkers and electrocardiographic (ECG) monitoring.

METHOD AND MATERIALS

Computed tomography (CT) guided IRE ablation was conducted with intention to treat. All patients underwent 12-lead ECG and 24h Holter ECG recording on the day of the IRE procedure to detect procedure related conduction disturbances/arrhythmias. Venous blood samples (BNP, high sensitive Troponin I) were obtained before the procedure as baseline, and 4h and 16h after the procedure to detect cardiac injury. Findings were divided into normal, procedure related minor, procedure related major, procedure unrelated minor and procedure unrelated major.

RESULTS

In 25 patients (10 female, 15 male, mean age 63 years) IRE ablation was conducted in order to treat different malignancies at varying locations (liver: 9, kidney: 8, lung: 4, adrenal gland: 3, soft tissue: 1). A standard ablation protocol was used applying voltages from 2000 to 3000 Volts and currents from 20 to 30 Amperes. After ablation Troponin I elevation was found in 9 (36%), BNP elevation in 19 patients (76%). All patients except one with an elevation in Troponin I, also had a BNP elevation. The ECG and Holter results showed normal findings in 9 (36%) patients, procedure unrelated minor abnormalities in 5 (20%), procedure related minor abnormalities in 9 (36%) and procedure related major abnormalities in 2 (8%) patients (3rd grade AV block and non-sustained ventricular tachycardias). On follow up after three months patients had no residual arrhythmias, or signs of cardiac damage.

CONCLUSION

Our findings suggest that IRE might result in temporary cardiac injury. Thus we strongly recommend the implementation of a cardiac safety protocol consisting of ECG, biomarkers and cardiologic surveillance.

CLINICAL RELEVANCE/APPLICATION

Treatment of patients with IRE requires close collaboration between cardiology and radiology in order to assure patient's safety.

RCA33

Creating Vector-based Drawings for Presentations and Publications with Adobe Illustrator (Hands-on)

Tuesday, Nov. 29 12:30PM - 2:00PM Room: S401AB



AMA PRA Category 1 Credits™: 1.50
ARRT Category A+ Credits: 1.50

Participants

Sarah C. Abate, BS, Ann Arbor, MI, (sabate@med.umich.edu) (*Presenter*) Nothing to Disclose

Elise Van Holsbeeck, DO, Ann Arbor, MI (*Presenter*) Nothing to Disclose

LEARNING OBJECTIVES

1) Discuss why we use vector based programs. 2) Explain how to use the tools in Illustrator. 3) Demonstrate how to import and label an image. 4) Demonstrate how to make one's own line drawing. 5) Demonstrate how to color and shade drawing. 6) Demonstrate how to export an image for print, PowerPoint, and Internet

Active Handout: Sarah C. Abate

[http://abstract.rsna.org/uploads/2016/16005085/ACTIVE RCA33 Illustrator_FINAL.pdf](http://abstract.rsna.org/uploads/2016/16005085/ACTIVE_RCA33_Illustrator_FINAL.pdf)

Computer-Aided Diagnosis: Effective Use of Computer-Aided Diagnose in Clinical Practice

Tuesday, Nov. 29 12:30PM - 2:00PM Room: S501ABC

BR **CH** **GI** **IN**

AMA PRA Category 1 Credits™: 1.50
ARRT Category A+ Credits: 1.50

FDA Discussions may include off-label uses.

Participants

Hiroyuki Yoshida, PhD, Boston, MA, (yoshida.hiro@mgh.harvard.edu) (*Moderator*) Patent holder, Hologic, Inc; Patent holder, MEDIAN Technologies;

LEARNING OBJECTIVES

Learn about 1) the best uses of CAD in clinical practice, 2) current and upcoming reading paradigms for clinical use, 3) strengths and weaknesses of CAD systems, 4) characteristics and pitfalls of CAD prompts, 5) how to best incorporate CAD results into the diagnostic decision-making process.

ABSTRACT

Computer-aided diagnosis (CAD) has become a standard tool in diagnostic radiology. This refresher course will explain and demonstrate how to use three widely available CAD systems--breast CAD, lung CAD, and colon CAD--effectively in clinical practice. The purpose of CAD is to improve radiologists' diagnostic accuracy. A number of CAD systems have been made commercially available in the United States and worldwide, including CAD for the detection of breast cancer on mammograms and breast tomosynthesis, detection of lung nodules on chest radiographs and on thoracic CT, as well as detection of polyps on CT colonography. However, the use of CAD in clinical practice has not been well standardized, and its most effective use is not understood well by radiologists. Each CAD system has its own unique strengths and weaknesses depending on how it was developed and on the data that were used for its development. A good understanding of the intended use of CAD and its limitations in different modalities is important, because using CAD beyond its limitations can lead to ineffective or even harmful results. This course will provide the best CAD practices in clinical use, current and upcoming reader paradigms for clinical use, strengths and weaknesses of different CAD systems, characteristics of CAD prompts including pitfalls, and how to best incorporate CAD results into the diagnostic-decision making process.

Sub-Events

RCC33A Effective Use of Breast Computer-Aided Diagnosis in Clinical Practice

Participants

Robert M. Nishikawa, PhD, Pittsburgh, PA, (nishikawarm@upmc.edu) (*Presenter*) Royalties, Hologic, Inc; Research Consultant, iCAD, Inc;

LEARNING OBJECTIVES

1) Learn current state of computer-aided detection in screening mammography. 2) Learn new possible ways to implement computer-aided detection clinically. 3) Learn how computer-aided detection is used clinically affects its effectiveness.

ABSTRACT

RCC33B Effective Use of Lung Computer-Aided Diagnosis in Clinical Practice

Participants

Matthew T. Freedman, MD, MBA, Baltimore, MD (*Presenter*) Institutional research contract, Riverain Technologies, LLC

LEARNING OBJECTIVES

1) Be aware that CADe and image processing approaches are available to help them (a) detect lung nodules and lung cancer on chest radiographs and lung CTs, (b) the detection of change, the detection of tubes, lines and catheters on chest radiographs, and (c) to measure the extent of COPD, 2) Computer image processing approaches can suppress the visibility of ribs on chest radiographs and pulmonary blood vessels on CTs. 3) They will be informed that some CADe devices, in clinical tests, decrease the time for the detection of lung nodules and the localization of tubes, lines and catheters. 4) They will better understand a basic approach to start to select CADe software for their own clinical practices.

Active Handout: Matthew T. Freedman

http://abstract.rsna.org/uploads/2016/16005049/ACTIVE_RCC33B.pdf

RCC33C Effective Use of Colon Computer-Aided Diagnosis in Clinical Practice

Participants

Stuart A. Taylor, MBBS, London, United Kingdom, (stuart.taylor1@nhs.net) (*Presenter*) Research Consultant, Robarts Clinical Trials, Inc

LEARNING OBJECTIVES

1) To understand the rationale for CAD in CT colonography. 2) To appreciate the diagnostic accuracy of CAD in detecting colonic neoplasia according to lesion morphology. 3) To learn about the various CAD reading paradigms used in CT colonography, and the pros and cons of each. 4) To understand how colon CAD can be integrated into clinical practice.

MSRP32

RSNA Resident and Fellow Symposium: Career 102: Financial Planning (An Interactive Session)

Tuesday, Nov. 29 1:00PM - 3:00PM Room: E451B

ED

AMA PRA Category 1 Credits™: 2.00
ARRT Category A+ Credit: 0

Participants

Sub-Events

MSRP32A Personal Financial Planning

Participants

David C. Gimarc, MD, Denver, CO (*Presenter*) Nothing to Disclose
Ross Cameratta, Chicago, IL (*Presenter*)

MSRP32B Insurance

Participants

Courtney M. Tomblinson, MD, Phoenix, AZ (*Presenter*) Nothing to Disclose
David P. Feiler, Phoenix, AZ, (david@westmarkwealth.com) (*Presenter*) Nothing to Disclose

LEARNING OBJECTIVES

Attendees will be able to effectively identify, prioritize and evaluate risks to their financial household following this course. Attendees will have specific knowledge to be able to seek out resources to implement strategies and insurances to effectively manage risk in their personal finances.

Active Handout:David P. Feiler

http://abstract.rsna.org/uploads/2016/16019613/ACTIVE_MSRP32B.pdf

MSRP32C Rad-to-Rad on Personal Finance

Participants

Amy K. Janicek, MD, Tucson, AZ (*Presenter*) Nothing to Disclose
Wu S. Liu, DO, Tucson, AZ, (drwisemoney@gmail.com) (*Presenter*) Nothing to Disclose

LEARNING OBJECTIVES

1. Discuss student loan repayment options: IDR, PSLF*, refinance.2. Optimize a debt destruction plan: PSLF-Dometer Quiz.3. Direct cash flow to accelerate wealth accumulation.

ABSTRACT

MSRP32D What RSNA Has to Offer Members-In-Training

Participants

Nancy J. Benedetti, MD, Greenwood Village, CO (*Presenter*) Nothing to Disclose

Patient Centered Approach to Breast Imaging (Sponsored by the Associated Sciences Consortium) (An Interactive Session)

Tuesday, Nov. 29 1:30PM - 3:00PM Room: S105AB

BR

AMA PRA Category 1 Credits™: 1.50
ARRT Category A+ Credits: 1.50

Participants

Denise D. Collins, MD, Detroit, MI, (denisec@rad.hfh.edu) (*Moderator*) Nothing to Disclose
Kathleen Kath, Livonia, MI (*Moderator*) Nothing to Disclose
Denise D. Collins, MD, Detroit, MI, (denisec@rad.hfh.edu) (*Presenter*) Nothing to Disclose
Patricia A. Miller, MD, Bingham Farms, MI (*Presenter*) Nothing to Disclose
Lisa Brown, West Bloomfield, MI (*Presenter*) Nothing to Disclose

LEARNING OBJECTIVES

1) Assess collaborative reviews/relevant clinical practice regarding application to realign workflow. 2) Compare new electronic media designed for patient's needs. 3) Recommend technological innovations/advances that enhance timely diagnosis and reporting. 4) Apply principals of critical thinking from experts and peers. 5) Define new techniques for specific populations of breast patients.

ABSTRACT

Focus on a patient centered approach to healthcare delivery provided an opportunity to develop a new paradigm for delivery of breast imaging care. This course will review assessment of patient needs and our approach to the delivery of personalized healthcare. The program emphasizes screening based on personal and family history, diagnostic evaluation including core biopsy based on patient need, delivery of results to patients in an efficient, empathetic manner, and coordination of radiology care with surgery, oncology and primary care physicians.

MSCC33

Case-based Review of Nuclear Medicine: PET/CT Workshop-Cancers of the Abdomen and Pelvis (In Conjunction with SNMMI) (An Interactive Session)

Tuesday, Nov. 29 1:30PM - 3:00PM Room: S406A



AMA PRA Category 1 Credits™: 1.50
ARRT Category A+ Credits: 1.50

Participants

Janis P. O'Malley, MD, Birmingham, AL (*Moderator*) Nothing to Disclose

Katherine A. Zukotynski, MD, Hamilton, ON (*Presenter*) Nothing to Disclose

LEARNING OBJECTIVES

1) Recognize the role of PET/CT in the evaluation of abdominopelvic malignancies. 2) Describe how differences in tumor biology impact tumor assessment with PET. 3) Provide imaging examples specific to different abdominopelvic malignancies.

MSES33

Essentials of Neuro Imaging

Tuesday, Nov. 29 1:30PM - 3:00PM Room: S100AB



AMA PRA Category 1 Credits™: 1.50
ARRT Category A+ Credits: 1.50

Participants

David M. Yousem, MD, Baltimore, MD, (dyousem1@jhu.edu) (*Moderator*) Royalties, Reed Elsevier; Royalties, Oakstone Publishing, LLC

Sub-Events

MSES33A Sinonasal Carcinoma: What not to Miss

Participants

Patricia A. Hudgins, MD, Atlanta, GA, (phudgin@emory.edu) (*Presenter*) Nothing to Disclose

LEARNING OBJECTIVES

1) The attendee will become familiar with the characteristics of sino-nasal carcinoma that upstage the patient, or impact treatment. 2) The attendee will understand why both a CT and MRI are usually necessary when planning surgery or treatment for sino-nasal carcinoma. 3) The attendee will understand how each separate MR sequence is used to stage the tumor

ABSTRACT

Although sino-nasal carcinoma is relatively uncommon, all radiologists should be familiar with imaging characteristics. Many radiologists, even those who do not specialize in neuroradiology, will routinely interpret brain and sinus imaging. Sinus malignancies initially present clinically much like sinusitis or even allergic rhinitis, and delay to diagnosis is the rule. In this course the imaging findings that should alert the interpreting physician that the patient has a malignant process will be reviewed. The staging of sino-nasal tumors will be reviewed with an emphasis on why both a CT and MRI are usually needed to accurately plan treatment.

MSES33B Cranial Nerves: Perineural Spread and Primary Tumors

Participants

Ari M. Blitz, MD, Baltimore, MD (*Presenter*) Research Grant, Aesculab

LEARNING OBJECTIVES

1) List the segments of the cranial nerves and describe methods of visualization of each segment including high resolution 3D MR imaging. 2) Describe common tumors arising from the cranial nerves as well as tumors of the head and neck with a tendency for perineural spread. 3) Identify imaging features of primary tumors arising from the cranial nerves as well as perineural spread of disease on cross sectional imaging.

ABSTRACT

The cranial nerves (CNs) may be divided into segments based upon their anatomic context. Understanding the CN segments (a-nuclear, b-parenchymal fascicular, c-cisternal, d-dural cave, e-interdural, f-foraminal, g-extra-foraminal) provides a conceptual framework for understanding how best to image each portion of the CNs and allows for rapid and concise communication with referring clinicians when evaluating tumors arising from or adjacent to the CNs. The cranial nerves (CNs) span the central nervous system (CNS) and peripheral nervous system (PNS); the Obersteiner-Redlich (aka transition) zone occurs for most CNs in the cisternal (c) segment and demarcates the transition between the two. Primary tumors of the CNs differ in pathology depending upon whether they arise in the CNS or PNS. Proximal to the Obersteiner-Redlich zone gliomas may occur. Nerve sheath tumors (schwannomas and neurofibromas) on the other hand may arise at any point within the PNS. Unlike primary tumors, perineural involvement of the CNs originates uniformly within the extra-foraminal (g) segment. Perineural spread of disease occurs most frequently in skin malignancies, mucosal malignancies of the head and neck, and adenoid cystic carcinoma. Identification of perineural spread of malignancy is critical in assessing extent of disease and is often important in determining the treatment pathway.

Active Handout: Ari Meir Blitz

[http://abstract.rsna.org/uploads/2016/16000861/MSES33B Blitz RSNA 2016 Tuesday 29 November cranial nerve handout.pdf](http://abstract.rsna.org/uploads/2016/16000861/MSES33B%20Blitz%20RSNA%202016%20Tuesday%2029%20November%20cranial%20nerve%20handout.pdf)

MSES33C Multiparametric Imaging of Orbital Lesions

Participants

Minerva Becker, MD, PhD, Geneva, Switzerland, (Minerva.Becker@hcuge.ch) (*Presenter*) Nothing to Disclose

LEARNING OBJECTIVES

1) Provide a systematic approach for the evaluation of orbital masses. 2) Review key imaging features of benign and malignant lesions. 3) Discuss the importance of multimodality imaging for the differential diagnosis. 4) Summarize potential pitfalls of image interpretation and how to avoid them.

ABSTRACT

Tumors and tumor-like conditions involving the orbit represent a broad spectrum of lesions with a varying degree of malignant potential. As many orbital lesions are difficult to biopsy and to operate on, cross-sectional imaging and accurate image

interpretation are mandatory for patient management. In addition, as the orbit is routinely included in the field of view of brain or head and neck examinations, orbital lesions may be revealed incidentally. Knowledge of the clinical presentation, patient's age and characteristic imaging features is essential for the identification of those lesions, where biopsy is mandatory. This lecture focuses on multiparametric imaging of orbital tumors and tumor-like conditions. The clinical presentation, compartmental location, imaging characteristics and histological features will be discussed for each tumor type. First, lesions of the intraconal compartment arising from the globe (retinoblastoma, uveal melanoma), optic nerve sheath complex (glioma, meningioma) and intraconal vessels (hemangioma) will be presented followed by lesions arising in the extraconal compartment (dermoid, pleomorphic adenoma, lacrimal gland carcinoma, lymphoma, rhabdomyosarcoma), as well as bone and paranasal sinus compartment (fibrous dysplasia, osteoma). We will equally review multicompartiment lesions (vascular malformations, idiopathic orbital pseudotumor, IgG4 related disease, metastases) and we will discuss imaging pitfalls and how to avoid them. The role of advanced techniques including diffusion-weighted imaging (DWI), FDG positron emission tomography CT (FDG PET/CT) and FDG PET/MRI will be presented, in particular their added value for the evaluation of masses with non-specific CT and MRI findings.

Handout:Minerva Becker

http://abstract.rsna.org/uploads/2016/16000860/Becker-Orbit_RSNA2016-handout.pdf

MSES33D MRI Congenital and Inflammatory Disorders of Middle and Inner Ear

Participants

Jan W. Casselman, MD, PhD, Brugge, Belgium, (jan.casselmann@azsintjan.be) (*Presenter*) Equipment support, Koninklijke Philips NV; Equipment support, QR srl ;

LEARNING OBJECTIVES

1) Be familiar with the state of the art MR techniques to study congenital and inflammatory middle and inner ear pathology. 2) Recognize the most frequent congenital middle and inner ear pathology. 3) Know the most common inflammatory pathology affecting the middle and inner ear.

ABSTRACT

CT is still the technique of choice to study the middle ear. The value of MR in congenital middle ear malformations is restricted to the visualisation of congenital cholesteatomas, the detection and visualization of an abnormal course of arteries through the middle ear, the diagnosis of rare middle ear dermoids... However, the impact of non-EPI DWI imaging in imaging of the "non-aerated" middle ear cannot be underestimated. MR is able to distinguish fluid, fibrosis, cholesterol granuloma/protein rich collections and cholesteatoma from one another and CT is unable to provide this information. The confirmation of the presence of a cholesteatoma, the visualization of its extend and the screening for recurrent or residual disease with non-EPI DWI imaging has made life easier for the ear surgeons and has led to an important reduction in healthcare costs (MR replaces second look surgery). Inflammatory disorders of the inner ear are numerous including labyrinthitis, apicitis, osteomyelitis, tuberculosis, Wegener's disease, congenital cholesteatomas etc. Again MR, with the use of different sequences, is more sensitive and specific than CT. It is also becoming clear that gadolinium enhancement is much better seen on FLAIR images than on T1 images. The use of gadolinium is also crucial to detect the inflammatory disorders and also to detect the associated complications, especially towards the adjacent brain and veins. MR is the method of choice to study inner ear malformations. Semicircular canal, vestibule and cochlear malformations can all be detected by MR and even the subtle congenital intracochlear "incomplete partition" changes, as described by L. Sennaroglu, can easily be depicted. Moreover MR is also able to verify the presence of a normal cochleovesibular nerve, crucial in patients with congenital sensorineural deafness needing a cochlear implant. The most frequent inflammatory and congenital disorders of the middle and inner ear will be illustrated and discussed in this presentation.

Active Handout:Jan W. Casselman

http://abstract.rsna.org/uploads/2016/16000859/MSES33D_RSNA_ME_IE_2016.pdf

MSQI33

Quality Improvement Symposium: Quality and Value: Learning from Mistakes

Tuesday, Nov. 29 1:30PM - 3:00PM Room: S406B

SQ

AMA PRA Category 1 Credits™: 1.50
ARRT Category A+ Credits: 1.50

Participants

Olga R. Brook, MD, Boston, MA, (obrook@bidmc.harvard.edu) (*Moderator*) Research Grant, Toshiba Medical Systems Corporation

ABSTRACT

This session will focus on how to learn from our mistakes and how practice improvement efforts help us with that. We will hear three different perspectives from the national leaders in Radiology Quality. Dr Larson from Stanford will describe common mistakes in performance improvement and practical steps to prevent these mistakes. Dr Kazerooni from University of Michigan will introduce radiologists to a grass root service excellence program that aims to improve patient satisfaction. Dr Duncan from Mallinckrodt Institute of Radiology will try to predict how Radiology practice will look in 2025 and what do we need to get there in the best possible state.

Sub-Events

MSQI33A Common Mistakes in Performance Improvement and How to Avoid Them

Participants

David B. Larson, MD, MBA, Los Altos, CA (*Presenter*) License agreement, Bayer AG; Potential royalties, Bayer AG

LEARNING OBJECTIVES

1) Anticipate and avoid pitfalls and problems commonly encountered in performance improvement.

ABSTRACT

Performance improvement is a subspecialty of management. Like with many aspects of leadership and management, there are many ways to go wrong. Those who wish to lead organizational improvement should understand those pitfalls and take measures up front to avoid them.

Honored Educators

Presenters or authors on this event have been recognized as RSNA Honored Educators for participating in multiple qualifying educational activities. Honored Educators are invested in furthering the profession of radiology by delivering high-quality educational content in their field of study. Learn how you can become an honored educator by visiting the website at: <https://www.rsna.org/Honored-Educator-Award/>

David B. Larson, MD, MBA - 2014 Honored Educator

MSQI33B Uncommon Champions of Value

Participants

Ella A. Kazerooni, MD, Ann Arbor, MI, (ellakaz@umich.edu) (*Presenter*) Nothing to Disclose

LEARNING OBJECTIVES

1) Learn how a grass roots service excellence program can increase your patient satisfaction.

ABSTRACT

Honored Educators

Presenters or authors on this event have been recognized as RSNA Honored Educators for participating in multiple qualifying educational activities. Honored Educators are invested in furthering the profession of radiology by delivering high-quality educational content in their field of study. Learn how you can become an honored educator by visiting the website at: <https://www.rsna.org/Honored-Educator-Award/>

Ella A. Kazerooni, MD - 2014 Honored Educator

MSQI33C The Future of Value and Quality in Radiology: What Will Patients Demand in 2025?

Participants

James R. Duncan, MD, PhD, Saint Louis, MO, (jrduncan@wustl.edu) (*Presenter*) Stock options, Proteon Therapeutics, Inc; Scientific Advisory Board, Metactive Medical Inc; Scientific Advisory Board, Flow Forward Medical Inc

LEARNING OBJECTIVES

1) Describe what they (as consumers) will want from radiology in 2025. 2) Propose measures that could be used to track quality and value in 2025. 3) Predict how in 2025, data might be collected and transformed into quality and value metrics.

ABSTRACT

This presentation will look into a crystal ball and predict what the future of quality and value in radiology might look like in just

under a decade. Yogi Berra was absolutely right – predictions are difficult, especially when they involve the future. However the statistician George Box summed it up nicely when he observed that while every predictive model is flawed, some are useful. As a baseline, it seems reasonable to predict that diagnostic imaging and image-guided procedures will become an even more important component of healthcare. But what measures of radiology’s quality and value will be available to patients in the next decade? How will patients access this data? How might they use it? When making such predictions we should listen to physicist Michio Kaku who argued “that it is very dangerous to bet against the future”. So turn off your pager, pull out your smartphone and be ready to post your ideas to the cloud, #radiologyquality2025.

PS30

Tuesday Plenary Session

Tuesday, Nov. 29 1:30PM - 2:45PM Room: Arie Crown Theater



AMA PRA Category 1 Credits™: 1.25
ARRT Category A+ Credit: 1.00

Participants

Richard L. Baron, MD, Chicago, IL (*Presenter*) Nothing to Disclose

Sub-Events

PS30A Presentation of the Alexander R. Margulis Award for Scientific Excellence

Participants

PS30B Presentation of the Gold Medal of the Radiological Society of North America

Participants

Paul J. Chang, MD, Chicago, IL (*Presenter*) Co-founder, Stentor/Koninklijke Philips NV; Researcher, Koninklijke Philips NV; Medical Advisory Board, lifeIMAGE Inc; Advisory Board, Bayer AG
Burton P. Drayer, MD, New York, NY (*Presenter*) Advisor, Hologic, Inc
Robert J. Stanley, MD, Birmingham, AL (*Presenter*) Nothing to Disclose

PS30C Dedication of the New Horizons Lecture to the Memory of Gerald D. Dodd Jr., MD (1922-2015)

Participants

PS30D New Horizons Lecture: Beyond Imaging: Radiology of Tomorrow

Participants

Hedvig Hricak, MD, PhD, New York, NY (*Presenter*) Nothing to Disclose
Jon A. Jacobson, MD, Ann Arbor, MI (*Presenter*) Consultant, BioClinica, Inc; Royalties, Reed Elsevier; ;

Abstract

Cancer care—along with imaging—is on the brink of profound change. Over the last quarter century, researchers have been assembling the biological syntax and lexicon that are now starting to shape modern oncology. Shifting public expectations and technological innovations are also intensifying progress toward precision medicine. In the next ten years, radiologists will be able to take advantage of new molecular imaging probes and techniques as well as computer tools for pattern recognition, deep learning and artificial intelligence. These new techniques and tools will put us at the center of the evolving paradigm of precision oncology, giving us an unprecedented opportunity to once again reshape and enhance our specialty.

It is clear that cognitive computing will ultimately transform radiology. Rather than fear the changes it brings, we should understand and seize the opportunities. While cognitive computing may reduce the need for interpretation of today's routine imaging studies, it will also increase our efficiency and effectiveness, improving standards of care across the board and elevating radiology interpretation into the arena of quantitative science and precision medicine. It will allow us to focus on more complex diagnostic and clinical questions and become even more valuable consultants to patients and referring physicians.

The landscape of radiology is continuously expanding. Molecular imaging is gaining traction as more imaging probes, along with technologies such as hyperpolarized MRI and PET/MRI, enter clinical trials. Post-processing tools are enabling cross-sectional imaging studies to be converted into hundreds or even thousands of quantitative, "radiomics" features that, in combination with other sources of "big data," can be used to develop decision support. Furthermore, pilot studies have shown that radiogenomics can identify tumor phenotypes and provide prognostic and predictive imaging biomarkers.

The blossoming of all these new tools and approaches will alter and strengthen the roles of imaging. The dream of integrated diagnostics is already a reality, though not yet evenly distributed, and as we enrich our knowledge of disease-relevant molecular information, we will increasingly integrate information from imaging regarding morphology, function and metabolism into diagnostic and clinical decision-making algorithms. Though progress in precision medicine will continue to depend on tissue analysis, it will also depend on interventional radiology enabling precision biopsies based on morphologic and molecular information. In addition, imaging's role in treatment will continue expanding. Minimally invasive, image-guided treatments are becoming a mainstay of cancer care, and theranostic approaches that combine targeted molecular imaging with targeted therapies for precise treatment selection and treatment monitoring are being adopted.

Radiology is a specialty of technical innovations, and radiologists have always excelled in embracing new technologies. But we are more than technology users; we are key participants in patient-centered care. In the last 50 years, we have gone through a number of transformations, always emerging as more clinically essential than before. In the years ahead, we must and will continue to evolve—becoming not only stewards of the ever-increasing demand for imaging and image-guide therapies, but highly valued clinical consultants and innovators in the era of precision medicine.

Honored Educators

Presenters or authors on this event have been recognized as RSNA Honored Educators for participating in multiple qualifying educational activities. Honored Educators are invested in furthering the profession of radiology by delivering high-quality educational content in their field of study. Learn how you can become an honored educator by visiting the website at: <https://www.rsna.org/Honored-Educator-Award/>

Jon A. Jacobson, MD - 2012 Honored Educator

Interventional Oncology Series: Lung and Musculoskeletal

Tuesday, Nov. 29 1:30PM - 6:00PM Room: S405AB

AMA PRA Category 1 Credits™: 4.50
ARRT Category A+ Credits: 5.00

Discussions may include off-label uses.

Participants

Matthew R. Callstrom, MD, PhD, Rochester, MN, (Callstrom.matthew@mayo.edu) (*Moderator*) Research Grant, Thermedical, Inc
Research Grant, General Electric Company Research Grant, Siemens AG Research Grant, Galil Medical Ltd
Sean M. Tutton, MD, Milwaukee, WI (*Moderator*) Consultant, Benvenue Medical, Inc

LEARNING OBJECTIVES

1) Describe patients that are appropriate for ablation for lung and MSK tumors. 2) Describe the relative role of ablation with other treatments for lung and MSK tumors. 3) Describe outcome of the use of ablation for the treatment of lung and MSK tumors.

ABSTRACT**Sub-Events****VSIO31-01 Ablation Should Be First Option for Limited Metastatic Disease**

Tuesday, Nov. 29 1:30PM - 1:50PM Room: S405AB

Participants

Stephen B. Solomon, MD, New York, NY (*Presenter*) Research Grant, General Electric Company

VSIO31-02 Possibility of Pathological and Genetic Analysis of Percutaneous Needle Biopsy Performed Immediately after Lung Radiofrequency Ablation

Tuesday, Nov. 29 1:50PM - 2:00PM Room: S405AB

Participants

Takaaki Hasegawa, Nagoya, Japan (*Presenter*) Nothing to Disclose
Chiaki Kondo, Nagoya, Japan (*Abstract Co-Author*) Nothing to Disclose
Yoza Sato, MD, PhD, Nagoya, Japan (*Abstract Co-Author*) Nothing to Disclose
Yoshitaka Inaba, MD, Nagoya, Japan (*Abstract Co-Author*) Nothing to Disclose
Hidekazu Yamaura I, MD, Nagoya, Japan (*Abstract Co-Author*) Nothing to Disclose
Mina Kato, MD, Nagoya, Japan (*Abstract Co-Author*) Nothing to Disclose
Shinichi Murata, MD, Nagoya, Japan (*Abstract Co-Author*) Nothing to Disclose
Yui Onoda, MD, Shinagawa-ku, Japan (*Abstract Co-Author*) Nothing to Disclose
Yasushi Yatabe, MD, Nagoya, Japan (*Abstract Co-Author*) Nothing to Disclose

PURPOSE

To evaluate the possibility of pathological diagnosis and genetic mutation analysis for the specimen of percutaneous needle biopsy obtained immediately after lung radiofrequency ablation (RFA).

METHOD AND MATERIALS

During May 2013 to February 2016, 19 patients (8 male and 11 female; median age, 68 years; range, 52–88 years) underwent percutaneous needle biopsy immediately after RFA for 19 lung tumors of 0.5–2.6 cm (mean, 1.6±0.5 cm). Thirteen tumors were solid and 6 were consisted dominantly of ground-glass opacity (GGO). All specimens were pathologically classified using standard hematoxylin and eosin (H&E) staining and adding immunostaining as necessary. Genetic mutation of EGFR and KRAS was examined for the specimens containing tumor cells. The safety and technical success of the procedure and the possibility of pathological diagnosis and genetic mutation analysis were evaluated. Safety of the whole procedure was evaluated by using complication grading system of the Society of Interventional Radiology.

RESULTS

Nineteen patients were completed with both lung RFA and needle biopsy. Major complications occurred in 2 patients (11%, 2/19) (grade-D aseptic pleuritis (n=1) and grade-C pneumothorax with tube placement (n=1)) and minor complications occurred in 9 patients (47%, 9/19) (grade-B pneumothorax without tube placement (n=8) and self-limiting hemoptysis (n=1)). Tumor seeding was not seen during the median follow up of 9 months (range, 1-28 months). Tumor tissue was obtained in 16 patients, so technical success rate was 84% (16/19). Only normal pulmonary epithelium was obtained in 3 patients (16%, 3/19) with GGO dominant tumors. Pathological diagnosis was achieved in 14 patients, so pathological diagnosability rate was 74% (14/19). Although atypical cell was obtained, pathological diagnosis was not able to determine in 2 patients. Among 16 specimens containing tumor cell, both EGFR and KRAS mutation was able to analyze in 13 specimens (68%, 13/19). EGFR mutation could not be evaluated in 1 patient and KRAS mutation could not be in 2 patients, due to insufficient tumor cells.

CONCLUSION

Pathological diagnosis and genetic analysis were possible even for specimen obtained immediately after RFA for lung tumor.

CLINICAL RELEVANCE/APPLICATION

Percutaneous needle biopsy was feasibly performed immediately after lung RFA and the obtained specimen could be evaluated pathologically or genetically.

VSI031-03 Outcomes with SBRT in the Treatment of Metastatic Lung Tumors

Tuesday, Nov. 29 2:00PM - 2:20PM Room: S405AB

Participants

Kenneth R. Olivier, MD, Rochester, MN (*Presenter*) Nothing to Disclose

LEARNING OBJECTIVES

1) Review the technique and delivery of Lung SBRT. 2) Discuss the role of Lung SBRT in treatment of Oligometastatic Disease. 3) Compare SBRT to other modalities used in this context.

ABSTRACT

VSI031-04 VATS Resection with Radionuclide Localization - Effective Treatment for Small Lung Nodules

Tuesday, Nov. 29 2:20PM - 2:40PM Room: S405AB

Participants

Robert K. Shen, MD, Rochester, MN, (shen.krobert@mayo.edu) (*Presenter*) Nothing to Disclose

LEARNING OBJECTIVES

1) Develop an understanding of the technique using CT-guided placement of radionuclide to localize small indeterminate lung nodules to facilitate thoracoscopic resection. At the conclusion of the presentation the learner should have an understanding of the rationale for such an approach, the technical details of performing this technique, the indications for the technique and the outcomes of surgery performed using this technique.

ABSTRACT

VATS Resection with Radionuclide Localization-Effective Treatment for Small Indeterminate Lung Nodules K. Robert Shen, M.D. Mayo Clinic Division of General Thoracic Surgery The increased use of chest computed tomography (CT) in lung cancer screening programs and for various clinical applications has led to identification of significant numbers of indeterminate lung nodules. Improved CT technology allows diagnosis of not only more nodules, but also increasingly smaller nodules. Thoracic surgeons are now being called on to evaluate these lesions for the possibility of malignancy, often in the setting of high-risk patients with significant smoking histories. Although short-term follow-up imaging may often suggest either benignity or malignancy, caution should be exercised in accepting a benign diagnosis without tissue confirmation. Additionally, given evidence that tumor size directly impacts survival even within subgroups of stage IA tumors, it makes intuitive sense to attempt to treat potential cancers as early as possible.¹ We and others have found that small lung nodules, particularly subcentimeter nodules, cannot be reliably biopsied percutaneously. Often, the most expedient and direct path to definitive management of a suspicious indeterminate small pulmonary nodule is to proceed with surgical excisional biopsy. Thoracoscopic surgery carries less morbidity than diagnostic procedures performed through thoracotomy, but is limited by the frequent inability to see or palpate (digitally or instrumentally) small subpleural lesions. To overcome this limitation, several different thoracoscopic nodule localization techniques have been developed and have been reported to improve the ease and accuracy of thoracoscopic biopsy. These include the use of visual markers, such as methylene blue and hook wires, fluoroscopic localization using various radiopaque markers, radiotracer localization techniques, and more recently, thoracic endosonography. All of these techniques have their own advantages and disadvantages, as well as significant learning curves. Several years ago, we modified a technique utilizing CT-guided radiotracer injection followed by intraoperative thoracoscopic radioprobe localization as the preferred method for finding nodules that we anticipate preoperatively will be difficult to see or palpate. In this presentation, I will review our experience using this technique. References Stiles BM, Altes TA, Jones DR, Shen KR, Ailawadi G, Gay SB, Olazagasti J, Rehm PK, Daniel TM. Clinical experience with radiotracer-guided thoracoscopic biopsy of small, indeterminate lung nodules. *Ann Thorac Surg* 2006; 82:1191. Grogan EL, Jones DR, Kozower BD, Simons WD, Daniel TM. Identification of small nodules: technique of radio-tracer guided thoracoscopic biopsy. *Ann Thorac Surg* 2008; Feb 85(2): S772-7.

VSI031-05 Palliative Treatment of Painful Bone Metastases with MR Imaging-guided Focused Ultrasound Surgery: A Two-centre Study

Tuesday, Nov. 29 2:40PM - 2:50PM Room: S405AB

Participants

Alessandro Napoli, MD, Rome, Italy (*Presenter*) Nothing to Disclose
Andrea Leonardi, Roma, Italy (*Abstract Co-Author*) Nothing to Disclose
Fabrizio Andrani, Roma, Italy (*Abstract Co-Author*) Nothing to Disclose
Vincenzo Noce, MD, Rome, Italy (*Abstract Co-Author*) Nothing to Disclose
Carlo Catalano, MD, Rome, Italy (*Abstract Co-Author*) Nothing to Disclose
Alberto Bazzocchi, MD, Bologna, Italy (*Abstract Co-Author*) Nothing to Disclose

PURPOSE

To evaluate the efficacy of non-invasive high intensity MR guided focused Ultrasound Surgery (MRgFUS) for pain palliation of bone metastasis in patients over a large population.

METHOD AND MATERIALS

This prospective, single arm, two-centre study received IRB approval. 102 patients (female: 38, male: 64, mean age: 62,3) with painful bone metastases were enrolled. 121 non-spinal lesions underwent MRgFUS treatment using ExAblate 2100 system (InSightec). European Organization for Research and Treatment of Cancer QLQ- BM22 was used for clinical assessment additionally to Visual Analog Scale (VAS), at baseline and 1, 3 and 6 months after treatment. All patients underwent CT and MRI before treatment and 3-6 months afterward.

RESULTS

No treatment-related adverse events were recorded. 48/102 (47%) patients reported complete response to treatment and discontinued medications. 39/102 (38,2%) experienced a pain score reduction >2 points, consistent with partial response. Remaining 15 (14,7%) patients had recurrence after treatment. Statistically significant differences between baseline (6, 95%CI 5-

8) and follow-up (2, 95%CI 0-3) VAS values and medication intake were observed ($p < 0.05$). Similarly a significant difference was found for QLQ- BM22 between baseline and follow-up ($p < 0.05$).

CONCLUSION

MRgFUS can be safely and effectively be adopted for treatment of painful bone metastases.

CLINICAL RELEVANCE/APPLICATION

MRgFUS can be safely and effectively used as totally noninvasive treatment for pain palliation of acoustically accessible bone metastasis

VSIO31-06 Cryoablation is the Best Option for Ablation of Pulmonary Metastases

Tuesday, Nov. 29 2:50PM - 3:10PM Room: S405AB

Participants

Thierry Debaere, Villejuif, France (*Presenter*) Consultant, Terumo Corporation; Speaker, Terumo Corporation; Proctor, Galil Medical Ltd; Data Safety Monitoring Board, Medtronic plc

LEARNING OBJECTIVES

1) Select best candidate for lung cryoablation. 2) Apply adequate treatment algorithm for cryoablation in the lungs. 3) Understand pattern of imaging follow-up after lung cryoablation.

VSIO31-07 MW not RF Ablation is the Best Option for Ablation of Pulmonary Metastases

Tuesday, Nov. 29 3:10PM - 3:30PM Room: S405AB

Participants

Damian E. Dupuy, MD, Providence, RI (*Presenter*) Research Grant, NeuWave Medical Inc Board of Directors, BSD Medical Corporation Stockholder, BSD Medical Corporation Speaker, Educational Symposia

Honored Educators

Presenters or authors on this event have been recognized as RSNA Honored Educators for participating in multiple qualifying educational activities. Honored Educators are invested in furthering the profession of radiology by delivering high-quality educational content in their field of study. Learn how you can become an honored educator by visiting the website at: <https://www.rsna.org/Honored-Educator-Award/>

Damian E. Dupuy, MD - 2012 Honored Educator

VSIO31-08 Mid-Term Ablation Zone Evolution Following Microwave Ablation of Normal Swine Lung

Tuesday, Nov. 29 3:30PM - 3:40PM Room: S405AB

Participants

Hiroshi Kodama, MD, New York, NY (*Presenter*) Nothing to Disclose
Song Gao, New York, NY (*Abstract Co-Author*) Nothing to Disclose
Eisuke Ueshima, New York, NY (*Abstract Co-Author*) Nothing to Disclose
Kreg Howk, Mansfield, MA (*Abstract Co-Author*) Nothing to Disclose
Stephen B. Solomon, MD, New York, NY (*Abstract Co-Author*) Research Grant, General Electric Company
Govindarajan Srimathveeravalli, PhD, New York, NY (*Abstract Co-Author*) Support, Medtronic plc

PURPOSE

To compare CT images of microwave ablation (MWA) of lung in a porcine model with gross ablation zone measurements to understand evolution of treatment zone dimensions over 28 days.

METHOD AND MATERIALS

Twenty-two percutaneous microwave (Emprint™, Covidien) unilateral lung ablations were performed in 8 swine (2-3 ablations/animal). All sites were ablated at 100W for either 2 minutes (low; 14 ablations) or 10 minutes (high; 8 ablations, at least one/animal). Animals were sacrificed at 2 days (n=4) or 28 days (n=4) after the procedure. Non-contrast and dual-phase (30s and 90s) CECT imaging was performed post-treatment and prior to sacrifice in all animals. Animals sacrificed at 28 days were also imaged on days 7 and 14. Lungs and trachea were removed en-bloc after euthanasia, perfusion fixed with formalin, step sectioned at 3-5mm thickness and photographed at high resolution. CT and anatomical measurements were aggregated as mean \pm standard deviation, differences in measurements were evaluated with T-test, $p < 0.05$ was considered statistically significant.

RESULTS

In both treatment groups, ablation volume measured on CT was maximum at 7 days (high: 23.1 ± 11.1 cm³; low: 9.2 ± 5.2 cm³) and significantly larger compared to immediate post-ablation volume (high: 9.0 ± 3.5 cm³; low: 3.5 ± 1.8 cm³), $P = 0.004$. Two-axis measurements performed on the largest ablation cross section on CT corresponded well with gross ablation measurements for both high (CT: $3.5 \pm 0.5 \times 2.4 \pm 0.4$ cm vs. Gross: $3.3 \pm 0.6 \times 2.1 \pm 0.2$ cm at 2 days, CT: $2.7 \pm 1.0 \times 1.9 \pm 1.0$ cm vs. Gross: $2.7 \pm 0.9 \times 1.9 \pm 0.8$ cm at 28 days; no statistical difference) and low (CT: $2.3 \pm 0.5 \times 1.5 \pm 0.3$ cm vs. Gross: $1.9 \pm 0.5 \times 1.3 \pm 0.3$ cm at 2 days, CT: $1.4 \pm 0.5 \times 1.0 \pm 0.4$ cm vs. Gross: $1.2 \pm 0.5 \times 0.9 \pm 0.3$ cm; no statistical difference) dose ablations.

CONCLUSION

CT imaging correlates with the gross pathology size at 2 and 28 days following microwave ablation of normal swine lung. Volume of treatment zone can vary substantially, achieving largest size 7 days post-treatment.

CLINICAL RELEVANCE/APPLICATION

Follow-up imaging in patients must be performed within 2 or after 28 days after ablation to ensure accuracy.

VSIO31-09 Lung Tumor Board

Tuesday, Nov. 29 3:40PM - 3:55PM Room: S405AB

Participants

Matthew R. Callstrom, MD, PhD, Rochester, MN, (Callstrom.matthew@mayo.edu) (*Moderator*) Research Grant, Thermedical, Inc
Research Grant, General Electric Company Research Grant, Siemens AG Research Grant, Galil Medical Ltd

LEARNING OBJECTIVES

1) Describe patients that are appropriate for ablation for lung tumors. 2) Describe the relative role of ablation with other treatments for lung tumors. 3) Describe outcome of the use of ablation for the treatment of lung tumors.

VSIO31-10 Technical Approaches to Treatment of Metastatic Disease in the Pelvis

Tuesday, Nov. 29 3:55PM - 4:15PM Room: S405AB

Participants

Sean M. Tutton, MD, Milwaukee, WI (*Presenter*) Consultant, Benvenue Medical, Inc

VSIO31-11 Skeletal Metastases Treated by MR-guided Focused Ultrasound: Dynamic Contrast-Enhanced MRI (DCE-MRI) for Treatment Response Evaluation

Tuesday, Nov. 29 4:15PM - 4:25PM Room: S405AB

Participants

Vincenzo Noce, MD, Rome, Italy (*Presenter*) Nothing to Disclose
Carola Palla, MD, Rome, Italy (*Abstract Co-Author*) Nothing to Disclose
Susan Dababou, Rome, Italy (*Abstract Co-Author*) Nothing to Disclose
Cristina Marrocchio, Rome, Italy (*Abstract Co-Author*) Nothing to Disclose
Alessandro Napoli, MD, Rome, Italy (*Abstract Co-Author*) Nothing to Disclose
Carlo Catalano, MD, Rome, Italy (*Abstract Co-Author*) Nothing to Disclose

PURPOSE

To compare DCE-MRI findings in skeletal metastases treated with MR-guided Focused Ultrasound (MRgFUS) with clinical outcome assessed by visual analogue scale (VAS)

METHOD AND MATERIALS

Eighteen patients, enrolled for MRgFUS treatment for symptomatic skeletal metastases, underwent Dynamic Contrast-Enhanced MR exam (3T Discovery 750 scanner, GE; Gd-BOPTA, Bracco) before and 3 months after the ablative procedure. Perfusional parameters comprehended DCE transfer rate (Ktrans) and extravascular volume fraction (ve), calculated by dedicated analysis software. Every subject was monitored over the following three months to define clinical outcome in terms of pain relief

RESULTS

Fourteen of eighteen treated subjects demonstrated a clinical complete response (CR), with a VAS score mean reduction of 4,3 (47,8%. $p < 0,001$), whereas four patients showed a partial clinical response (PR) with incomplete relief according to VAS scale. Perfusional analysis demonstrated in CR population significant decrease of Gadolinium extraction (mean Ktrans reduction 2,14/min, $\Delta Kt = 52,65\%$. $p < 0,01$) and ve increase (5,6%. $p > 0,01$). Partial Responders showed no substantial modification in Ktrans value ($\Delta Kt = +0,042/\text{min}$, +11,39%. $p < 0,01$) or increase in extravascular volume. Spearman test revealed a significant relationship between Ktrans quantitative parameters and symptoms decrease evaluated by VAS scale ($p < 0,001$) in both CR and PR patients

CONCLUSION

Ktrans negative modifications ($-\Delta Kt$) may reflect effectiveness of ultrasound ablation procedure, as direct expression of decreased tumoral cells' metabolism, and positively correlate to clinical response

CLINICAL RELEVANCE/APPLICATION

DCE-MRI reflects clinical outcome in MRgFUS treated bone metastases. Perfusional data may be routinely included in imaging protocols for MRgFUS planning and follow-up

VSIO31-12 Surgical Management Using Cryoablation in MSK Tumors

Tuesday, Nov. 29 4:25PM - 4:45PM Room: S405AB

Participants

Bennie Lindeque, MD, PhD, Aurora, CO (*Presenter*) Research Grant, Endocare, Inc

LEARNING OBJECTIVES

Audience should be able to identify the problem tumors that need a multi-disciplinary approach. They should be able to identify the members of the multi-disciplinary treatment team. They should be able to note the indication for interventional action taken by the Orthopedic oncologist. They should be able to identify which interventional procedure (cryoablation, vascular embolization or RFA) would be most applicable for a specific case.

VSIO31-13 Preoperative Transcatheter Arterial Embolization of Bone Tumors

Tuesday, Nov. 29 4:45PM - 4:55PM Room: S405AB

Awards

Student Travel Stipend Award

Participants

Ashley Altman, MD, Chicago, IL (*Presenter*) Nothing to Disclose
Mikin V. Patel, MD, Chicago, IL (*Abstract Co-Author*) Nothing to Disclose
Steven M. Zangan, MD, Chicago, IL (*Abstract Co-Author*) Nothing to Disclose
Brian S. Funaki, MD, Riverside, IL (*Abstract Co-Author*) Data Safety Monitoring Board, Novate Medical Ltd

PURPOSE

To evaluate pre-operative embolization for surgical resection of primary and metastatic bone tumors.

METHOD AND MATERIALS

We retrospectively evaluated 58 patients (31 men, 19 women, 4 boys, 4 girls median age 56.5 years, age range 12-80 years) who underwent 52 preoperative transcatheter arterial embolizations between 2004 and 2015. Surgery was performed within 48 hours in 96.6% (57/59) of cases undergoing preoperative angiogram. Bone tumors included renal cell carcinoma (n=26), plasma cell (n=8), aneurysmal bone cyst (n=4), thyroid metastasis (n=2), giant cell tumor (n=2), chondroblastoma (n=2), melanoma metastasis (n=2), osteosarcoma (n=1), NSCLC (n=1), liposarcoma (n=1), malignant fibrous histiocytoma (n=1). Pathologic fractures were present in 32.7% (n=17) and impending in 38.5% (n=20) of patients. The majority of lesions (63.5%, n=33) were metastatic.

RESULTS

Technical success, on an intent-to-embolize basis, defined as complete or near-complete stasis on post-embolization angiogram, was achieved in 88% of patients (51/58). Seven patients (4 men, 3 women, median age 17, age range 11-70) had preoperative angiograms but embolization was not attempted due to lack of a suitable embolic target. One patient underwent embolization on two separate occasions for different bone tumors. Embolic agents included tris-acryl microspheres (Embospheres) (n=26), PVA (n=20), coils (n=8), and gelfoam (n=10). Surgeries included resection, curettage, ORIF, and spinal decompression. Average estimated blood loss for all surgeries was 774.5 cc. Twelve patients required blood transfusion following surgery during hospitalization, with mean overall transfusion 0.5 units per patient. Three minor complications were attributed to angiography: groin hematoma, suspected contrast induced nephropathy, and arterial branch dissection/thrombosis.

CONCLUSION

Preoperative transarterial embolization is safe and effective in a wide variety of bone tumors prior to resection, ORIF, curettage, biopsy, and spinal decompression. A small minority of patients with bone lesions that appear hypervascular on cross-sectional imaging have vascular anatomy that is not amenable to embolization.

CLINICAL RELEVANCE/APPLICATION

Preoperative embolization of primary and metastatic bone tumors is feasible in most patients and safe. Here we report the largest retrospective case series in existing literature.

VSIO31-14 Role of Ablation in MSK Oligometastatic Disease

Tuesday, Nov. 29 4:55PM - 5:15PM Room: S405AB

Participants

Anil N. Kurup, MD, Rochester, MN, (kurup.anil@mayo.edu) (*Presenter*) Research Grant, Galil Medical Ltd; Royalties, UpToDate, Inc

LEARNING OBJECTIVES

1) Identify indications and contraindications for ablation of MSK tumors in the setting of oligometastatic disease. 2) Triage patients to ablation and particular ablation modalities based on tumor characteristics. 3) Recognize lesions that require adjunctive techniques, such as cementoplasty.

VSIO31-15 Developing an Electroporation and Nanoparticle-based Therapeutic Platform for Bone Metastases

Tuesday, Nov. 29 5:15PM - 5:25PM Room: S405AB

Participants

Alda L. Tam, MD, Houston, TX (*Presenter*) Medical Monitor, Galil Medical Ltd; Research Grant, AngioDynamics, Inc; Travel support, Geurbet SA; Advisory Board, Geurbet SA

Marites P. Melancon, PhD, Houston, TX (*Abstract Co-Author*) Nothing to Disclose

Tomas Appleton Figueira, MD, Houston, TX (*Abstract Co-Author*) Nothing to Disclose

Li Tian, Houston, TX (*Abstract Co-Author*) Nothing to Disclose

Joe Ensor, Houston, TX (*Abstract Co-Author*) Consultant, Aetna, Inc

Kiersten Maldonado, Houston, TX (*Abstract Co-Author*) Nothing to Disclose

Katherine Dixon, RT, Houston, TX (*Abstract Co-Author*) Nothing to Disclose

Amanda McWatters, Houston, TX (*Abstract Co-Author*) Nothing to Disclose

Mark McArthur, Houston, TX (*Abstract Co-Author*) Nothing to Disclose

Sanjay Gupta, MD, Houston, TX (*Abstract Co-Author*) Nothing to Disclose

PURPOSE

To demonstrate the intratumoral uptake and antitumor effect of doxorubicin loaded superparamagnetic iron oxide nanoparticles (SPIO-DOX) when combined with irreversible electroporation (IRE).

METHOD AND MATERIALS

Fourteen rabbits with tibial VX2 tumors underwent one of three treatments: control (n=5); IRE (n=3); or injection of SPIO-DOX followed by IRE (SPIO-DOX+IRE) (n=6). Dynamic T2* weighted 4.7T MR images were obtained at t=0, 2 h, and 5 days after treatment to monitor the treatment effects mediated by SPIO-DOX. Elemental analysis was used to quantify iron concentration. Antitumor effect was expressed as a tumor growth ratio from T2* MR images and histological percent necrosis. A generalized linear model was used to analyze the data.

RESULTS

SPIO-DOX was clearly seen as a signal reduction in T2*-weighted images within the tumor up to 5 days after injection. Change in

T2* measurements show that there was a significant decrease in the signal intensity due to the presence of iron: 2.3 ms (control), 2.13 ms (IRE), and -8.94 ms (SPIO-DOX+IRE), $p < 0.0001$. Similarly, elemental analysis showed increased iron concentration in the tumor after SPIO-DOX: 30.8 ppm (control), 71.2 ppm (IRE), and 124 ppm (SPIO-DOX+IRE). Average volume of tumor prior to treatment was 157.3 ± 46.5 mm³ and not significantly different between groups ($p=0.29$). Average tumor growth ratios were calculated: control ($194.6 \pm 58\%$), IRE ($135.9 \pm 13.7\%$), and SPIO-DOX+IRE ($36.2 \pm 13.3\%$). While the difference between the average tumor growth ratio between the control and IRE groups was not significant ($p=0.15$), the group treated with SPIO-DOX+IRE shows a significant antitumor effect when compared to control ($p<0.0001$). Changes in tumor volume mirrored the histological calculation of percent necrosis: $59 \pm 20.4\%$ (control), 65% (IRE), and $79.2 \pm 11.1\%$ (SPIO-DOX+IRE). Percent necrosis was significantly different between the IRE and SPIO-DOX+IRE groups ($p=0.04$).

CONCLUSION

The intratumoral localization of SPIO-DOX can be successfully identified on MR imaging. Tibial VX2 tumors treated with combination therapy demonstrate enhanced antitumor effect when compared to control.

CLINICAL RELEVANCE/APPLICATION

Exploiting the synergy between electroporation and nanoparticle therapy is a viable strategy to surmounting the issue of incomplete tumor ablation in bone metastases.

VSI031-16 Avoiding Complications with Ablation in the Spine

Tuesday, Nov. 29 5:25PM - 5:45PM Room: S405AB

Participants

Afshin Gangi, MD, PhD, Strasbourg, France, (gangi@unistra.fr) (*Presenter*) Proctor, Gall Medical Ltd

LEARNING OBJECTIVES

1/Describe the complications which could occur during spinal tumor ablation 2/ Describe how to avoid these complications and reduce the risks 3/ Describe the limits of thermal ablation of spine

VSI031-17 Bone Metastases Tumor Board

Tuesday, Nov. 29 5:45PM - 6:00PM Room: S405AB

Participants

Sean M. Tutton, MD, Milwaukee, WI (*Moderator*) Consultant, Benvenue Medical, Inc

3D Printing Hands-on with Open Source Software Introduction (Hands-on)

Tuesday, Nov. 29 2:30PM - 4:00PM Room: S401AB



AMA PRA Category 1 Credits™: 1.50
ARRT Category A+ Credits: 1.50

Participants

Michael W. Itagaki, MD, MBA, Seattle, WA (*Moderator*) Owner, Embodi3D, LLC
Beth A. Ripley, MD, PhD, Seattle, WA, (bar23@uw.edu) (*Presenter*) Nothing to Disclose
Tatiana Kelil, MD, Brookline, MA, (Tkellil@partners.org) (*Presenter*) Nothing to Disclose
Anish Ghodadra, MD, Pittsburgh, PA, (aghodadramd@gmail.com) (*Presenter*) Nothing to Disclose
Hansol Kim, MD, Boston, MA (*Presenter*) Nothing to Disclose
Steve D. Pieper, PhD, Cambridge, MA (*Presenter*) CEO, Isomics, Inc; Employee, Isomics, Inc; Owner, Isomics, Inc; Research collaboration, Siemens AG; Research collaboration, Novartis AG; Consultant, Wright Medical Technology, Inc; Consultant, New Frontier Medical; Consultant, Harmonus; Consultant, Stryker Corporation; Research collaboration, gigmade;
Dmitry Levin, Seattle, WA (*Presenter*) Nothing to Disclose

LEARNING OBJECTIVES

1) To learn about basic 3D printing technologies and file formats used in 3D printing. 2) To learn how to segment a medical imaging scan with free and open-source software and export that anatomy of interest into a digital 3D printable model. 3) To perform basic customizations to the digital 3D printable model with smoothing, text, cuts, and sculpting prior to physical creation with a 3D printer.

ABSTRACT

"3D printing" refers to fabrication of a physical object from a digital file with layer-by-layer deposition instead of conventional machining, and allows for creation of complex geometries, including anatomical objects derived from medical scans. 3D printing is increasingly used in medicine for surgical planning, education, and device testing. The purpose of this hands-on course is to teach the learner to convert a standard Digital Imaging and Communications in Medicine (DICOM) data set from a medical scan into a physical 3D printed model through a series of simple steps using free and open-source software. Basic methods of 3D printing will be reviewed. Initial steps include viewing and segmenting the imaging scan with 3D Slicer, an open-source software package. The anatomy will then be exported into stereolithography (STL) file format, the standard engineering format that 3D printers use. Then, further editing and manipulation such as smoothing, cutting, and applying text will be demonstrated using MeshMixer and Blender, both free software programs. Methods described will work with Windows, Macintosh, and Linux computers. The learner will be given access to comprehensive resources for self-study before and after the meeting, including an extensive training manual and online video tutorials.

Active Handout: Michael Ward Itagaki

[http://abstract.rsna.org/uploads/2016/14003456/active RCA24-34 Intro to Open Source 3D Printing.pdf](http://abstract.rsna.org/uploads/2016/14003456/active_RCA24-34_Intro_to_Open_Source_3D_Printing.pdf)

RCB34

Intro to Texture Analysis (Hands-on)

Tuesday, Nov. 29 2:30PM - 4:00PM Room: S401CD



AMA PRA Category 1 Credits™: 1.50
ARRT Category A+ Credits: 1.50

Participants

Luciano M. Prevedello, MD, MPH, Dublin, OH (*Presenter*) Nothing to Disclose

Barbaros S. Erdal, PhD, Columbus, OH (*Presenter*) Nothing to Disclose

LEARNING OBJECTIVES

1) Learn what image texture analysis is and recognize some of its applications in Radiology through practical examples. 2) Understand how to extract imaging texture features from various imaging modalities. 3) Learn how to visualize and analyze results.

ABSTRACT

During this course, an introduction to image texture analysis will be provided through hands on examples. Participants will interact with open source as well as freely available commercial platforms in order to achieve tasks such as segmentation, registration and image feature extraction. Imaging samples will include both 2D and 3D datasets from a variety of anatomical regions and modalities (CT, MR). First, a brief generic introduction will be given and concepts related to algorithm development will be discussed. Participants will then be exposed to DICOM and various visible light based formats. After hands on exercises on texture extraction, visualization of results will be covered. Finally, various quantization methods for storage and analysis will be presented.

RCC34

3D Printing: Clinical Applications II

Tuesday, Nov. 29 2:30PM - 4:00PM Room: S501ABC

IN

AMA PRA Category 1 Credits™: 1.50
ARRT Category A+ Credits: 1.50

FDA

Discussions may include off-label uses.

Participants

Dimitris Mitsouras, PhD, Boston, MA, (dmitsouras@alum.mit.edu) (*Moderator*) Research Grant, Toshiba Corporation;
Adnan M. Sheikh, MD, Ottawa, ON, (asheikh@toh.on.ca) (*Moderator*) Nothing to Disclose

LEARNING OBJECTIVES

1. Review current clinical applications of 3D printing. 2. Review of 3D printing technologies 3. Review workflows for clinical 3D printing. 4. Quality assessment of medical 3D-printed models. 5. Future directions of 3D printing in medicine.

ABSTRACT

Sub-Events

RCC34A Introduction to 3D Printing

Participants

Dimitris Mitsouras, PhD, Boston, MA, (dmitsouras@alum.mit.edu) (*Presenter*) Research Grant, Toshiba Corporation;

LEARNING OBJECTIVES

1. Review current clinical applications of 3D printing. 2. Review of 3D printing technologies 3. Review workflows for clinical 3D printing. 4. Quality assessment of medical 3D-printed models. 5. Future directions of 3D printing in medicine.

ABSTRACT

Medical 3D printing is emerging as a clinically relevant imaging tool in directing preoperative and intraoperative planning in many surgical specialties. Data from standard imaging modalities such as CT, MRI, echocardiography and rotational angiography can be used to fabricate life-sized models of human anatomy and pathology, as well as patient-specific implants and surgical guides. 3D printed models can improve diagnosis and allow for advanced pre-operative planning. Printed models are suitable for planning both surgical and minimally invasive procedures. Added value has been reported toward improving outcomes, minimizing peri-operative risk, and helping develop new procedures such as transcatheter mitral valve replacements. Anatomic models enable surgeons and interventional radiologists to assimilate information more quickly than image review, choose the optimal surgical approach, and perform a procedure more safely and in a shorter time. Patient-specific 3D-printed implants are also beginning to appear and may have significant impact on cosmetic and life-saving procedures in the future. Finally, bioprinting of full replacement organs is a major research goal. In summary, medical 3D printing is rapidly evolving and may be a potential game-changer that radiologists are ideally-suited to deliver.

RCC34B 3D Printing Workflow

Participants

Carlos H. Torres, MD, FRCPC, Ottawa, ON, (catorres@toh.on.ca) (*Presenter*) Nothing to Disclose

LEARNING OBJECTIVES

1) Describe a 3D printing service. 2) Become familiar with common 3D printing software terminology and software capabilities. 3) Appreciate the implementation of 3D printing software in everyday clinical practice. 4) Illustrate current trends and future directions in 3D printing.

ABSTRACT

RCC34C 3D Printing in Interventional Radiology and Vascular Surgery

Participants

Matthew D. Tam, FRCR, Westcliff on Sea, United Kingdom (*Presenter*) Nothing to Disclose

LEARNING OBJECTIVES

1) Understand the potential roles of 3D printing in vascular surgery and interventional radiology 2) Gain an overview of the production of solid and hollow luminal models 3) See examples of use of 3D models in real cases in a vascular interventional service 4) Understand what is being done and delivered through a brief review of recent publications.

ABSTRACT

3D printing in medicine and radiology continues to be an interesting and developing field. Vascular surgery and interventional radiology procedures can benefit from 3D printing. It can be incorporated into daily practice through procedure planning and procedure execution. It can potentially advance the field through aiding implant design and development.

RCC34D Clinical Science Applications that Leverage the Use of 3D Printing

Participants

Justin R. Ryan, PhD, Phoenix, AZ (*Presenter*) Nothing to Disclose

LEARNING OBJECTIVES

1) List the necessary technologies for application-specific casting. 2) Describe the methods fundamental to lost-core casting. 3) Apply casting techniques to further leverage 3D printing for the purpose of low-cost simulation and clinical/research experimentation.

MSRO33

BOOST: Breast-Case-based Review (An Interactive Session)

Tuesday, Nov. 29 3:00PM - 4:15PM Room: S103AB



AMA PRA Category 1 Credits™: 1.25
ARRT Category A+ Credits: 1.50

Participants

Melissa L. Pilewskie, MD, New York, NY (*Presenter*) Nothing to Disclose
Shari Goldfarb, MD, New York, NY (*Presenter*) Nothing to Disclose
Karen Y. Oh, MD, Portland, OR (*Presenter*) Nothing to Disclose
Jean L. Wright, MD, New York, NY (*Presenter*) Nothing to Disclose

LEARNING OBJECTIVES

1) Improve basic knowledge and skills relevant to radiation therapy use in breast cancer patients. 2) Apply information learned from provided breast cancer case scenarios to clinical practice. 3) Assess technological innovations and advances which can enhance clinical practice and problem-solving in the breast cancer population. 4) Apply principles of critical thinking to ideas from breast oncology experts and peers in the radiologic sciences.

MSRO36

BOOST: Lung-Case-based Review (An Interactive Session)

Tuesday, Nov. 29 3:00PM - 4:15PM Room: S103CD

CH **RO**

AMA PRA Category 1 Credits™: 1.25
ARRT Category A+ Credits: 1.50

Participants

Simon S. Lo, MD, Seattle, WA, (simonslo@uw.edu) (*Moderator*) Research support, Elekta AB; Travel support, Accuray Incorporated; Speaker, Accuray Incorporated;
Jing Zeng, MD, Seattle, WA, (jzeng13@uw.edu) (*Presenter*) Nothing to Disclose
Jyoti D. Patel, MD, Chicago, IL (*Presenter*) Nothing to Disclose
Ben J. Slotman, MD, PhD, Amsterdam, Netherlands, (bj.slotman@vumc.nl) (*Presenter*) Research Grant, Varian Medical Systems, Inc; Speakers Bureau, Varian Medical Systems, Inc;
Philip A. Linden, Cleveland, OH, (Philip.linden@uhhospitals.org) (*Presenter*) Nothing to Disclose
Gregory Kicska, MD, PhD, Seattle, WA, (kicskag@uw.edu) (*Presenter*) Nothing to Disclose

LEARNING OBJECTIVES

1) Understand the role of radiation therapy in management of lung cancer, and areas of controversy.

ABSTRACT

Active Handout: Ben J. Slotman

[http://abstract.rsna.org/uploads/2016/16001275/Active MSRO36 Handout Slotman RSNA 2016.pdf](http://abstract.rsna.org/uploads/2016/16001275/Active_MSRO36_Handout_Slotman_RSNA_2016.pdf)

RC413

Pediatric Series: Abdomen

Tuesday, Nov. 29 3:00PM - 6:00PM Room: S102AB



AMA PRA Category 1 Credits™: 2.75
ARRT Category A+ Credits: 3.00

FDA Discussions may include off-label uses.

Participants

Young Hun Choi, MD, Seoul, Korea, Republic Of (*Moderator*) Nothing to Disclose
Geetika Khanna, MD, MS, Iowa City, IA (*Moderator*) Nothing to Disclose
Ethan A. Smith, MD, Saline, MI (*Moderator*) Nothing to Disclose
Shunsuke Nosaka, MD, Tokyo, Japan (*Moderator*) Nothing to Disclose
Jonathan R. Dillman, MD, Cincinnati, IA (*Moderator*) Research Grant, Siemens AG; Research Grant, Guerbet SA; Travel support, Koninklijke Philips NV; Research Grant, Toshiba

Sub-Events

RC413-01 Pediatric MR Urography Applications

Tuesday, Nov. 29 3:00PM - 3:15PM Room: S102AB

Participants

Jonathan R. Dillman, MD, Cincinnati, IA, (jonathan.dillman@cchmc.org) (*Presenter*) Research Grant, Siemens AG; Research Grant, Guerbet SA; Travel support, Koninklijke Philips NV; Research Grant, Toshiba

LEARNING OBJECTIVES

1) To understand state-of-the-art pediatric MR urography techniques. 2) To become familiar with common MRU applications in children and adolescents. 3) To comprehend how MRU can provide added value to the evaluation of the pediatric kidney and urinary tract.

ABSTRACT

LEARNING OBJECTIVES

1) Learn current state-of-the-art techniques for the performance of MR urography in children. 2) Learn the various typical clinical applications of MR urography in the pediatric population.

ABSTRACT

MRI of the kidneys and urinary tract, or MR urography (MRU), is a very useful imaging tool in a subset of the pediatric population when standard imaging evaluation (e.g., ultrasound, voiding cystourethrography, renal scintigraphy) is inadequate or unrevealing. This single imaging test can be used to thoroughly assess renal and urinary tract anatomy, differential renal function, and urinary tract drainage. This educational course will present state-of-the-art MRU techniques that can be used in children and adolescents. Additionally, common as well as uncommon clinical applications will be discussed using a case-based approach.

Honored Educators

Presenters or authors on this event have been recognized as RSNA Honored Educators for participating in multiple qualifying educational activities. Honored Educators are invested in furthering the profession of radiology by delivering high-quality educational content in their field of study. Learn how you can become an honored educator by visiting the website at: <https://www.rsna.org/Honored-Educator-Award/>

Jonathan R. Dillman, MD - 2016 Honored Educator

RC413-02 Non-Invasive MR Imaging Diagnosis of Pediatric Kidney Transplant Rejection

Tuesday, Nov. 29 3:15PM - 3:25PM Room: S102AB

Awards

Trainee Research Prize - Fellow

Participants

Maryam Aghighi, MD, Stanford, CA (*Presenter*) Nothing to Disclose
Laura J. Pisani, Stanford, CA (*Abstract Co-Author*) Nothing to Disclose
Anne Muehe, MD, Stanford, CA (*Abstract Co-Author*) Nothing to Disclose
Samantha Holdsworth, PhD, Palo Alto, CA (*Abstract Co-Author*) Nothing to Disclose
Neeraja Kambham, Stanford, CA (*Abstract Co-Author*) Nothing to Disclose
Waldo Concepcion, Stanford, CA (*Abstract Co-Author*) Nothing to Disclose
Paul Grimm, Stanford, CA (*Abstract Co-Author*) Nothing to Disclose
Heike E. Daldrup-Link, MD, Palo Alto, CA (*Abstract Co-Author*) Nothing to Disclose

PURPOSE

In children with kidney transplants, rejection is the major cause of allograft failure. There is currently no diagnostic tool capable of detecting rejection in vivo. The purpose of this study was to develop a non-invasive imaging test for detection of allograft rejection in pediatric patients.

METHOD AND MATERIALS

The approach relies on administration of the ultrasmall superparamagnetic iron oxide nanoparticle ferumoxytol, with long lasting blood half-life which is phagocytosed by macrophages causing significant signal effects on T2*-weighted MR images. In an IRB-approved single center prospective clinical trial, patients ranging between 10 to 26 years with acute transplant rejection (n = 4), non-rejecting allografts (n = 15) and normal native kidneys (n = 9) underwent multi-echo T2* fast spoiled gradient-echo (FSPGR) MR imaging at 1-14 days post intravenous injection (p.i.) of 5mg Fe/kg ferumoxytol. T2* relaxation times of renal allografts were correlated with the presence or absence of rejection using standard pathology criteria and macrophage semi-quantitative scoring by immunohistology.

RESULTS

Allografts with acute rejection showed prolonged T2* relaxation times compared to normal allografts at 1-24 p.i. (normal: T2* = 8.01 ms, rejection: T2* = 37.88 ms, $p < 0.001$) and, to a lesser extent, at 1-14 days p.i. (normal: 20.97 ms, rejection: 38.92 ms, $p = 0.005$). Histological analyses revealed edema and compressed microvessels of allografts undergoing rejection leading to decreased ferumoxytol enhancement. Allografts with or without acute rejection did not show significant differences in macrophage content on histopathology ($p = 0.44$).

CONCLUSION

A longer T2* on ferumoxytol-enhanced MR images was seen in patients with acute rejection compared with normal transplants. This may be attributable to reduced allograft perfusion and increased edema in rejected transplants as seen on histopathology. While further work is needed to decouple the confounding effects on MR imaging, this study suggests that a change in baseline MR imaging is a promising non-invasive tool for identifying allografts at high risk of rejection.

CLINICAL RELEVANCE/APPLICATION

A non-invasive diagnostic test enabling allograft rejection to be visualized and monitored directly and longitudinally *in vivo* could reduce anesthesia, invasive biopsies, and associated complications and costs. Further studies are ongoing to integrate this technique into clinical care.

RC413-03 Quantitative 3D Ultrasound Imaging in Pediatric Hydronephrosis

Tuesday, Nov. 29 3:25PM - 3:35PM Room: S102AB

Participants

Juan Cerrolaza, PhD, Washington, DC (*Abstract Co-Author*) Nothing to Disclose
Hansel J. Otero, MD, Silver Spring, MD (*Abstract Co-Author*) Nothing to Disclose
Elijah Biggs, BS, Washington, DC (*Abstract Co-Author*) Nothing to Disclose
Amanda M. George, RT, Springfield, VA (*Abstract Co-Author*) Nothing to Disclose
Peter H. Yao, BS, Washington, DC, DC (*Abstract Co-Author*) Nothing to Disclose
Roberto Ardon, Suresnes Cedex, France (*Abstract Co-Author*) Employee, Koninklijke Philips NV
James Jago, Bothell, WA (*Abstract Co-Author*) Employee, Koninklijke Philips NV
Craig A. Peters, MD, Washington, DC (*Abstract Co-Author*) Nothing to Disclose
Marius G. Linguraru, DPhil, MS, Washington, DC (*Presenter*) Nothing to Disclose

PURPOSE

After proof of concept in 2DUS, we create the first 3DUS-based computer-aided diagnostic (CAD) tool for the assessment of pediatric hydronephrosis (HN), aiming to identify 3D ultrasound (US)-based thresholds for hydronephrotic kidneys where diuretic nuclear renography (DR) could be safely avoided.

METHOD AND MATERIALS

The retrospective dataset (IRB approved) consists of 20 patients (mean age 10.93 months; range 0-84 months) of variable severity (grade 1 to 4 according to the Society for Fetal Urology HN scale) with concurrent renal 2D, 3DUS and DR (MAG-3) imaging. Mean washout half time (T1/2) was: 16 min. (range 2 to >100 min.). For each volume, segmentation of renal parenchyma (RP) and collecting system (CS) was obtained using a minimally-interactive segmentation tool. A set of 90 3D morphological parameters (including descriptors of the RP and CS size and shape) were automatically extracted using quantitative imaging (QI) analysis techniques. Machine learning theory was used to identify critical cases whose T1/2 was higher than clinically relevant thresholds (20 and 30 min). A best-fit model was derived for each threshold using optimal morphological parameters to categorize the kidneys and receiver operating characteristic curve analysis was performed. For comparison, a similar study was performed using 2DUS-based analysis.

RESULTS

Operating at the optimal point with 100% sensitivity, the accuracy, specificity and area under the curve for the 3DUS-based system were 100%, 100% and 100% for T1/2=20min, and 93%, 67% and 93% for T1/2=30min. This new 3DCAD tool significantly outperformed ($p < 0.05$ using McNemar's statistical test) the original 2D system, whose performance on the same data was 65%, 57%, and 86% for T1/2=20min, and 65%, 53% and 93% for T1/2=30min, respectively.

CONCLUSION

QI analysis of renal 3DUS provides accurate and reliable assessment of pediatric HN, identifying T1/2 thresholds non-invasively. This new 3DUS-based technology shows a higher diagnostic power than a previous 2DUS-based version.

CLINICAL RELEVANCE/APPLICATION

QI analysis of the 3D anatomy of the kidney has the potential to provide robust assessment of HN, avoiding unnecessary MAG-3 DR and its associated radiation and clinical cost.

RC413-04 Not Reported Limitations of Contrast-enhanced Voiding Urosonography Due to Premature Destruction of Second-generation Ultrasound Contrast Agents

Tuesday, Nov. 29 3:35PM - 3:45PM Room: S102AB

Participants

Dominik Swieton, MD, PhD, Gdansk, Poland (*Presenter*) Nothing to Disclose
Maciej Piskunowicz, MD, PhD, Gdansk, Poland (*Abstract Co-Author*) Nothing to Disclose
Dorota Rybczynska, Gdansk, Poland (*Abstract Co-Author*) Nothing to Disclose
Arkadiusz Szarmach, Gdansk, Poland (*Abstract Co-Author*) Nothing to Disclose
Edyta Szurowska, MD, PhD, Gdansk, Poland (*Abstract Co-Author*) Nothing to Disclose
Menno Pruijm, Lausanne, Switzerland (*Abstract Co-Author*) Nothing to Disclose

PURPOSE

Evaluation of contrast-enhanced voiding urosonography (ce-VUS) limitations due to premature destruction of second-generation ultrasound contrast agents (UCA).

METHOD AND MATERIALS

161 children were enrolled in the study (71 female and 90 male), the mean age of 3.5years (range 4 weeks - 16.0 years) who underwent ce-VUS examination between 2011 and 2015.

RESULTS

In 13 children (8%) who underwent ce-VUS we observed the premature destruction of the microbubbles in the urinary bladder, significant for examination efficiency. In all these cases the voiding phase of ce-VUS examination was impossible to be set correctly because of destroyed UCA microbubbles. The phenomenon occurred exclusively in anxious, crying infants and children with restricted voiding.

CONCLUSION

The premature destruction of ultrasound contrast agent is a major factor limiting the efficiency of ce-VUS since applicable voiding phase cannot be reached. Acknowledgments: The study was financed from the means of the National Science Centre granted on the basis of the decision No DEC-2012/05/B/NZ5/01554.

CLINICAL RELEVANCE/APPLICATION

The premature destruction of ultrasound contrast agent during ce-VUS is a significant limitation since it prevents applicable ce-VUS voiding phase evaluation and establishing the vesico-ureteric reflux (VUR) diagnosis. Therefore, the usefulness of ce-VUS with second generation UCA needs to be reevaluated, and special attention must be taken for anxious, constantly crying infants and children with possible voiding problems.

RC413-05 Feed-and-Sleep: Performing a Functional MR Urography (fMRU) in Infants Without Sedation

Tuesday, Nov. 29 3:45PM - 3:55PM Room: S102AB

Participants

Sebastian Werner, Stuttgart, Germany (*Presenter*) Nothing to Disclose
Ilias Tsiflikas, MD, Tuebingen, Germany (*Abstract Co-Author*) Nothing to Disclose
Matthias Teufel, Tuebingen, Germany (*Abstract Co-Author*) Nothing to Disclose
Florian Obermayr, Tuebingen, Germany (*Abstract Co-Author*) Nothing to Disclose
Konstantin Nikolaou, MD, Tuebingen, Germany (*Abstract Co-Author*) Speakers Bureau, Siemens AG; Speakers Bureau, Bracco Group; Speakers Bureau, Bayer AG
Juergen F. Schaefer, MD, Tuebingen, Germany (*Abstract Co-Author*) Nothing to Disclose

PURPOSE

Functional MR urography (fMRU) has established as a comprehensive imaging tool in evaluating malformations of kidneys and urinary tract. However, the utilization of fMRU is limited because of the need for sedation or even general anesthesia in infants, since there are great concerns regarding a possible injury of the developing brain by anesthesia. Therefore, we evaluated the feasibility of fMRU in feed-and-sleep technique.

METHOD AND MATERIALS

We performed feed-and-sleep fMRU in 25 infants (11 boys, median age 104 days, range 37-277 days) with a duplex kidney. Examinations were performed using an optimized MRI-protocol including T2-weighted Half-Fourier-acquisition single-shot turbo spin-echo (HASTE) sequences in transversal, coronal and sagittal plane for morphological imaging and a 15-min dynamic post-contrast scan (50 coronal 3-D-fat-saturated T1-weighted gradient recalled echo (GRE) volumetric interpolated breath-hold examination (VIBE) series. The image quality of examinations was analyzed by two raters in consensus regarding moving artifacts of morphological sequences (1=no; 2= moderate, 3=severe) and visualization of anatomical details of the kidneys and urinary tract (1=high; 2=reduced; 3= no). Further, we analyzed the evaluability of the dynamic urographic sequences with a free available software.

RESULTS

In 22 infants fMRU was performed successfully including evaluation of dynamic urography. Only in 3 infants abortion of examination was necessary due to a severe motion. In 8 infants there were no artifacts observed in transversal and sagittal planes. In the remaining patients, moderate artifacts were noted. Anatomical details of kidneys were visualized with high details in 20/23 infants, whereas only in 3 patients there was no visualization of ureters and ureter ostia possible.

CONCLUSION

We could demonstrate that the feed-and-sleep technique is feasible for fMRU in infants.

CLINICAL RELEVANCE/APPLICATION

Functional MR urography is an important diagnostic tool in CAKUT. Fast sequences offer the possibility of performing this examination in the feed-and-sleep technique.

RC413-06 Adnexal Torsion Revisit: Focused on the Initial CT Findings in Pediatric Patients

Tuesday, Nov. 29 3:55PM - 4:05PM Room: S102AB

Participants

Hyun-Hae Cho, MD, Seoul, Korea, Republic Of (*Presenter*) Nothing to Disclose
Sun Wha Lee, MD, Seoul, Korea, Republic Of (*Abstract Co-Author*) Nothing to Disclose
Somi Lee, Taegu, Korea, Republic Of (*Abstract Co-Author*) Nothing to Disclose
Sun Kyoung You, MD, Daejeon, Korea, Republic Of (*Abstract Co-Author*) Nothing to Disclose

PURPOSE

To evaluate the CT features of adnexal torsion in the pediatric patients and compared those features between two groups, whether hemorrhagic infarction exist or not.

METHOD AND MATERIALS

Total 31 consecutive pediatric patients (mean age, 12.1 years) were included. The presence of an abnormally located ovary, non-enhancement, hemorrhage, the string of pearls sign, protrusion, eccentric wall thickening, volume of the ipsi- and contralateral ovaries including the volume ratio, and the presence of preexisting lesions were evaluated. The presence of uterine deviation, fallopian tube thickening or dilatation, engorged vessels and vascular knots were evaluated for the CT features of the fallopian tube and uterus. The presence of ascites or hemoperitoneum and peritoneal fat infiltration were recorded for the peritoneal changes.

RESULTS

Among the parameters related with ovary itself, non-enhancement of the involved ovary, hemorrhage, string of pearls sign, protrusion of the torsed mass was noted significantly more frequent in hemorrhagic infarction group than non hemorrhagic infarction group (All $p < 0.05$). Mean volume of the ipsilateral ovary or contralateral ovary didn't show significant difference, but mean ratio of the volume of ovaries noted significantly larger in hemorrhagic infarction group (36.6, $p = 0.032$). The presence of uterine deviation toward the torsed side, fallopian tube thickening was noted significantly more frequent in hemorrhagic infarction group than non hemorrhagic infarction group (All $p < 0.05$).

CONCLUSION

Since the primary signs were not well visualized on the CT scan of pediatric patients, secondary signs including non-enhancement of the twisted ovary with hemorrhage, string of pearls sign, protrusion of the torsed mass, increased volume ratio, uterine deviation, fallopian tube thickening could be helpful enough for diagnosis the adnexal torsion in pediatric patients.

CLINICAL RELEVANCE/APPLICATION

Although CT is usually the initial diagnostic tool through which it may be possible to detect adnexal torsion, to our knowledge, only a few reports concerning the CT features of adnexal torsion have been published (and fewer still have been published on pediatric patients). And often misdiagnosis was made and misinterpretation of imaging results in adnexal torsion is commonplace. Therefore, this study might be helpful for improving the imaging diagnosis of adnexal torsion in pediatric patients.

RC413-07 MR Elastography in Children

Tuesday, Nov. 29 4:05PM - 4:20PM Room: S102AB

Participants

Andrew T. Trout, MD, Cincinnati, OH, (andrew.trout@cchmc.org) (*Presenter*) Advisory Board, Koninklijke Philips NV; Travel support, Koninklijke Philips NV; Author, Reed Elsevier; Research Grant, Siemens AG

LEARNING OBJECTIVES

1) Explain the basics of MR elastography technique. 2) Describe the current evidence for use of MR elastography in children and young adults. 3) Identify potential opportunities to apply MR elastography in clinical practice.

ABSTRACT

This activity will review the basics of performing and interpreting MR elastography (MRE) examinations in pediatric and young adult patients, in the context of disease processes relevant to these populations. Physics of MRE technique will be briefly reviewed and current evidence supporting use of MRE both in adult and pediatric and young adult patients will be discussed. Advanced and research MRE techniques will also be briefly reviewed in regard to potential advantages in the pediatric and young adult population.

RC413-08 Pediatric Hepatobiliary Imaging

Tuesday, Nov. 29 4:30PM - 4:45PM Room: S102AB

Participants

Shunsuke Nosaka, MD, Tokyo, Japan, (nosaka-s@ncchd.go.jp) (*Presenter*) Nothing to Disclose

LEARNING OBJECTIVES

1) Identify the imaging spectrum of hepatobiliary pathology in the pediatric population. 2) Discuss differential diagnosis based on imaging findings.

ABSTRACT

Diagnostic imaging of pediatric hepatobiliary system is usually started with ultrasound (US). US provides fine details of hepatobiliary system when precisely performed. Based on US findings, further imaging study such as hepatobiliary scintigraphy, MRCP, and/or CT will be indicated. An invasive procedure such as percutaneous transhepatic cholangiography is reserved for therapeutic purpose. This educational course will cover a variety of congenital as well as acquired diseases affecting the pediatric hepatobiliary system. In addition, imaging characteristics of common diseases with atypical presentations will be covered.

RC413-09 **Supersonic Shear-wave Elastography for Evaluation of the Liver Stiffness in Children: Reproducibility and Effect of Respiration on Measurements**

Tuesday, Nov. 29 4:45PM - 4:55PM Room: S102AB

Awards

Student Travel Stipend Award

Participants

Jeong Rye Kim, MD, Seoul, Korea, Republic Of (*Presenter*) Nothing to Disclose
Hee Mang Yoon, MD, Seoul, Korea, Republic Of (*Abstract Co-Author*) Nothing to Disclose
Young Ah Cho, Seoul, Korea, Republic Of (*Abstract Co-Author*) Nothing to Disclose
Jin Seong Lee, MD, Seoul, Korea, Republic Of (*Abstract Co-Author*) Nothing to Disclose
Ah Young Jung, MD, Seoul, Korea, Republic Of (*Abstract Co-Author*) Nothing to Disclose

PURPOSE

To evaluate interobserver variation in liver stiffness (LS) measurement by Shear-wave elastography (SWE) and to assess effect of respiration on LS measurement in children with liver diseases.

METHOD AND MATERIALS

This retrospective study was approved by our institutional review board, and written informed consent was waived. A total of 66 children who underwent SWE for LS measurement by two radiologists between April 2015 and August 2015 were included. Two operators (operator 1 and 2) were independently measured LS values from the same location of the liver more than three measurements in each patient. Operator 2 performed LS measurements during free breathing and breath-hold states in each patient. Median LS value of three measurements (LSMED3), four measurements (LSMED4), and five measurements (LSMED5) were calculated in two operators. Reproducibility of the LS measurement and interobserver agreement were determined by using 95% Bland-Altman limits of agreement and intraclass correlation coefficients (ICCs). The effect of the respiration on reproducibility of the LS values was assessed by using the paired t-test.

RESULTS

Interobserver agreement between LSMED3 performed by two radiologists showed ICC value of 0.909 (95 % confidence interval (CI), 0.859-0.943). The 95% limit of agreement between LSMED3 measured by two operators was 3.85 kPa (16.1% of mean LS value). ICC among LSMED3, LSMED4, and LSMED5 was 0.988 (95 % CI, 0.981-0.992) in the operator 1 and 0.990 (95 % CI, 0.985-0.994) in the operator 2. There was a significant difference between LS values measured during breath hold status and free breathing status ($P < .001$). The Bland-Altman plot for LS measurements showed mean differences between breath hold and free breathing of -13.1 kPa.

CONCLUSION

LS measured by SWE showed almost perfect agreement between two operators and the measurement error was ranged from 3.3-4.4 kPa. Free breathing technique significantly underestimated LS value compared with breath hold technique.

CLINICAL RELEVANCE/APPLICATION

When LS measurements are used for monitoring liver diseases, changes in median LS of 16% or greater should be considered to be beyond the range of measurement error and constant breathing technique should be applied.

RC413-10 **Optimal Acquisition Number for Ultrasonographic Shear Wave Velocity Measurements in Children**

Tuesday, Nov. 29 4:55PM - 5:05PM Room: S102AB

Participants

Hyun Joo Shin, MD, Seoul, Korea, Republic Of (*Presenter*) Nothing to Disclose
Myung-Joon Kim, MD, Seoul, Korea, Republic Of (*Abstract Co-Author*) Nothing to Disclose
Ha Yan Kim, Seoul, Korea, Republic Of (*Abstract Co-Author*) Nothing to Disclose
Yun Ho Roh, Seoul, Korea, Republic Of (*Abstract Co-Author*) Nothing to Disclose
Mi-Jung Lee, MD, PhD, Seoul, Korea, Republic Of (*Abstract Co-Author*) Nothing to Disclose

PURPOSE

To investigate the minimum optimal acquisition number of hepatic shear wave velocities (SWVs) on ultrasound elastography in children with free breathing.

METHOD AND MATERIALS

We prospectively performed hepatic ultrasound elastography (supersonic shear wave imaging, SSI) in healthy children with free breathing. SWVs were measured fifteen times for each child at 4 cm depth of the right lobe using a 1-6 MHz convex transducer. Mean SWVs from the three, five, and seven acquisitions were compared to the mean SWV from fifteen measurements, with the intraclass correlation coefficient (ICC) analyzed with the 1,000 times bootstrap method.

RESULTS

Twenty-two healthy children were included. Nine patients were boys and the age range was 5-10 years with a mean of 7 ± 1.3 years. The mean SWVs from the three (ICC 0.863), five (ICC 0.888) and seven (ICC 0.922) acquisitions demonstrated almost perfect agreement with the reference of fifteen acquisitions (mean, 6.2 ± 1.8 kPa). In m/sec units, the three (ICC 0.870), five (ICC 0.876) and seven (ICC 0.911) acquisitions also demonstrated almost perfect agreement with the fifteen acquisitions (mean, 1.4 ± 0.2 m/sec).

CONCLUSION

Three acquisitions can be enough to measure the hepatic SWVs in children with regular free breathing status using SSI.

CLINICAL RELEVANCE/APPLICATION

The reduced number of SWV acquisitions could shorten examination times and make examinations easier for children without the need for breath-holding, thus resulting in wider application of ultrasound elastography in children.

RC413-11 Magnetic Resonance Enterography (MRE) Surveillance of Asymptomatic Pediatric Crohn's Disease Patients

Tuesday, Nov. 29 5:05PM - 5:15PM Room: S102AB

Awards

Student Travel Stipend Award

Participants

Kaiming Wu, MD, Boston, MA (*Presenter*) Nothing to Disclose

Jess Kaplan, MD, Boston, MA (*Abstract Co-Author*) Nothing to Disclose

Christopher J. Moran, MD, Boston, MA (*Abstract Co-Author*) Research Grant, Allergan plc

Esther Israel, MD, Boston, MA (*Abstract Co-Author*) Nothing to Disclose

Harland S. Winter, MD, Boston, MA (*Abstract Co-Author*) Consultant, PAREXEL International Corporation Consultant, Johnson & Johnson Consultant, Shire plc Consultant, Salix Pharmaceuticals, Inc Institutional Grant support, Johnson & Johnson Institutional Grant support, AstraZeneca PLC Institutional Grant support, Shire plc

Michael S. Gee, MD, PhD, Jamaica Plain, MA (*Abstract Co-Author*) Nothing to Disclose

Aubrey Katz, MD, Boston, MA (*Abstract Co-Author*) Nothing to Disclose

Jeffrey Biller, MD, Boston, MA (*Abstract Co-Author*) Nothing to Disclose

PURPOSE

Magnetic resonance enterography (MRE) has become the primary imaging modality for evaluating disease activity in pediatric Crohn's disease (CD) patients. Typical standard of practice involves imaging patients when they become symptomatic; the significance of MRE for surveillance of asymptomatic CD patients is not known. The purpose of this study is to analyze MRE studies performed on asymptomatic young CD patients and to identify MRE imaging features associated with future clinical recurrence.

METHOD AND MATERIALS

A retrospective search was performed to identify patients 18 years of age or under with known CD who had MRE performed while asymptomatic on anti-TNF α therapy. All MRE studies were reviewed by an experienced pediatric radiologist blinded to clinical data for presence or absence of four imaging features of activity: wall thickening, T2 hyperintensity, mural hyperenhancement, and vasa recta engorgement (Comb sign), as well as overall assessment of presence or absence of active disease. Two pediatric gastroenterologists reviewed the electronic records of all patients to evaluate for future clinical recurrence, defined as CD-related hospital admission, surgery, or treatment escalation.

RESULTS

37 MRE studies performed in 36 asymptomatic patients were identified, with 10 patients demonstrating clinical recurrence within 6 months of MRE. Overall assessment of disease activity by MRE was observed in a higher proportion of patients with clinical recurrence within 6 months (80%) compared to patients without recurrence (29.6%), a statistically significant association ($p=0.01$, Fisher's Exact Test). Among individual MRE features, mural hyperenhancement demonstrated the highest accuracy (76%) and was observed in 80% of patients with 6 month clinical recurrence vs 26% without ($p<0.01$).

CONCLUSION

MRE evidence of active inflammation in asymptomatic CD patients on biologic therapy is associated with future clinical recurrence, with mural hyperenhancement having a statistically significant association with clinical recurrence within 6 months. These results suggest a role for imaging in routine surveillance of pediatric CD patients on treatment.

CLINICAL RELEVANCE/APPLICATION

Imaging may play a role in the routine surveillance of asymptomatic pediatric Crohn's disease patients in order to predict future recurrence and provide a temporal window for therapy modification before clinical symptoms recur.

RC413-12 Colonic Findings on MR Enterography Pre-Colectomy in Pediatric IBD-related Colitis

Tuesday, Nov. 29 5:15PM - 5:25PM Room: S102AB

Participants

Shilpa Radhakrishnan, MBBS, DMRD, Chennai, India (*Presenter*) Nothing to Disclose

Natashia M. Seeman, MD, Toronto, ON (*Abstract Co-Author*) Nothing to Disclose

Sebastian K. King, MBBS, PhD, Melbourne, Australia (*Abstract Co-Author*) Nothing to Disclose

Michelle Falkiner, Toronto, ON (*Abstract Co-Author*) Nothing to Disclose

Jacob C. Langer, Toronto, ON (*Abstract Co-Author*) Nothing to Disclose

Mary-Louise C. Greer, MBBS, FRANZCR, Toronto, ON (*Abstract Co-Author*) Nothing to Disclose

PURPOSE

Magnetic resonance enterography (MRE) is increasingly performed pre-colectomy in pediatric inflammatory bowel disease (PIBD)-related colitis, helping distinguish ulcerative colitis (UC) and Crohn's disease, aiding operative planning. While targeting small intestine, MRE provides opportunity to evaluate the colon. The purpose of the study was to assess the accuracy of MRE in detecting colonic disease in PIBD compared with post-colectomy histopathology.

METHOD AND MATERIALS

Research and ethics board approved, clinicopathologic data were captured by retrospective chart review of patients 2-18 years who underwent colectomy for PIBD from 2000-2014. Preoperative MRE were independently reviewed by two pediatric radiologists, with a consensus read, blinded to reports and clinicopathologic data. Subset colonic MRE findings recorded included: disease location and extent, wall thickness, wall T2 signal, enhancement degree and pattern, restricted diffusion, stricture presence and length. These were compared with post-colectomy histopathology reports and final diagnosis incorporating ileocolonoscopy data.

RESULTS

Colectomies were performed in 68 patients (36 male, 32 female), with median age at diagnosis 11 years (range 2-17) and 14 years (range 3-17) at colectomy. Preoperative MRE occurred in 23 patients, with average time to surgery < 1 year. Disease presence and location correlated well with histopathology in 16/23 (70%) MRE, was underestimated in 6 (26%) MRE, with 1 (4%) normal MRE showing UC on histopathology, surgery 1 year post-MRE. In 7 MRE, colonic strictures were reported in various locations, 4 (57%) with fibrotic strictures and 3 (43%) with severe active inflammation but no strictures/fibrosis on histopathology. Limitations related to time between MRE and surgery, and reliability localizing MRE findings with surgical and histopathology specimens, with presence or grade of fibrosis not always recorded on pathology.

CONCLUSION

MRE permits detection and localization of colonic IBD, delineating strictures variably. Minor modification such as rectally-instilled contrast may improve this. By correlating MRE with post-colectomy histopathology, there is opportunity to improve our understanding of PIBD on MRI.

CLINICAL RELEVANCE/APPLICATION

MRE allows us to assess the colon, with minor technique modification likely needed to optimize this, and correlation with post-colectomy histopathology improves our understanding of PIBD on MRI.

RC413-13 Effects of Adaptive Statistical Iterative Reconstruction-V Technique on Radiation Dose Reduction and Image Quality of Pediatric Abdominal CT

Tuesday, Nov. 29 5:25PM - 5:35PM Room: S102AB

Participants

Xin-Xian Zhang, Xu Zhou, China (*Presenter*) Nothing to Disclose
Chenglong Li, Xu Zhou, China (*Abstract Co-Author*) Nothing to Disclose
Tao Xin, Xuzhou, China (*Abstract Co-Author*) Nothing to Disclose
Jiong Li, Xuzhou, China (*Abstract Co-Author*) Nothing to Disclose
Yong Tang, Xuzhou, China (*Abstract Co-Author*) Nothing to Disclose
Qiancheng Li, Xuzhou, China (*Abstract Co-Author*) Nothing to Disclose

PURPOSE

To evaluate the effects of adaptive statistical iterative reconstruction V technique (ASIR-V) on radiation dose reduction and image quality in pediatric abdominal CT.

METHOD AND MATERIALS

Sixty children were randomized into three groups, 20 cases each. All children were scanned at 9HU (5mm slice thickness) noise index levels of automatic current modulation with 100 kV on 256-row CT scanner. The rotation time was 0.3s and detector width was 120-160mm. The presetting ASIR-V percentage was 30%, 50% and 70% in Group A, Group B and Group C, respectively. The CT number and standard deviation (SD) were measured on the upper abdominal slice, middle abdominal slice and lower abdominal slice. The dose-length product (DLP) was recorded and effective dose (ED) was computed. Statistical analyses were performed using independent sample t test and ANOVA

RESULTS

In Group A, B and C, SD was 10.28 ± 1.03 HU, 11.34 ± 0.82 HU and 9.34 ± 1.67 HU, respectively. And there was no statistically significant difference among three groups ($P > 0.05$); SD in the three groups was similar to presetting noise index. DLP (mGy·cm) was 3.69 ± 17.55 , 55.73 ± 10.62 and 37.65 ± 10.01 , respectively; ED (mSv) was 2.57 ± 0.43 , 1.78 ± 0.76 and 1.28 ± 0.75 , respectively. ED was declining with ASIR-V percentage increasing, and the difference between any two groups was statistically significant ($P < 0.01$).

CONCLUSION

ASIR-V technique can effectively reduce the radiation dose without increasing objective image noise, and is of important value in low-dose pediatric abdominal examination.

CLINICAL RELEVANCE/APPLICATION

Since children are more radio-sensitive than adults, there is a need to utilize adaptive statistical iterative reconstruction V to minimize radiation exposure without sacrificing image quality during CT exams.

RC413-14 Quantitative Analysis of Fatty Pancreas in Obese Children by Ultrasound: Its Correlation with Metabolic Syndrome and HOMA-IR

Tuesday, Nov. 29 5:35PM - 5:45PM Room: S102AB

Participants

Doo-ri Kim, Arail-Dong, Korea, Republic Of (*Presenter*) Nothing to Disclose
Mu Sook Lee, MD, Jeju-si, Korea, Republic Of (*Abstract Co-Author*) Nothing to Disclose
Guk Myung Choi, Jeju, Korea, Republic Of (*Abstract Co-Author*) Nothing to Disclose
Ki Soo Kang, Jeju-si, Korea, Republic Of (*Abstract Co-Author*) Nothing to Disclose

PURPOSE

To attempt a quantitative analysis of fatty pancreas by transabdominal ultrasound and evaluate its correlation with metabolic syndrome and insulin resistance (HOMA IR.)

METHOD AND MATERIALS

This retrospective study included 135 obese children who underwent transabdominal ultrasound between January and December 2015. Fatty pancreas was quantitatively analyzed by pancreato-perihepatic fat index (PPHFI) on transabdominal ultrasound. Associations between PPHFI and components of metabolic syndrome, and correlation between PPHFI and HOMA-IR were analyzed. Multivariate logistic regression analysis was used to identify factors independently correlated with metabolic syndrome. The optimal

cutoff value of PPHFI to predict metabolic syndrome was calculated

RESULTS

PPHFI and HOMA-IR were significantly higher in the group with metabolic syndrome than those in the group of non- metabolic syndrome ($p < 0.0001$). Each component of metabolic syndrome except fasting glucose level revealed a statistically significant association with PPHFI. PPHFI also showed a strong association with HOMA-IR ($r = 0.70$; $p < 0.0001$). PPHFI was an independent factor to predict metabolic syndrome (odds ratio, 3.322; $p = 0.023$), and the best cutoff value of PPHFI to predict metabolic syndrome was 2.34 with high sensitivity of 0.93

CONCLUSION

Sonographic fatty pancreas which was analyzed by PPHFI may represent a meaningful factor to predict metabolic syndrome and insulin resistance in obese children.

CLINICAL RELEVANCE/APPLICATION

Ultrasonographic quantitative analysis of fatty pancreas might be used as a predictor of metabolic syndrome in obese children.

RC413-15 Pancreatic Imaging in Children

Tuesday, Nov. 29 5:45PM - 6:00PM Room: S102AB

Participants

Michael S. Gee, MD, PhD, Jamaica Plain, MA (*Presenter*) Nothing to Disclose

LEARNING OBJECTIVES

1) Identify causes of pancreatitis and focal pancreatic lesions in children and adolescents. 2) Define the role of imaging in diagnosis and characterization of pancreatic pathology in the pediatric population.

ABSTRACT

SSJ01

Science Session with Keynote: Breast Imaging (Contrast Mammography/CT)

Tuesday, Nov. 29 3:00PM - 4:00PM Room: Arie Crown Theater



AMA PRA Category 1 Credit™: 1.00
ARRT Category A+ Credit: 1.00

Discussions may include off-label uses.

Participants

John M. Lewin, MD, Denver, CO (*Moderator*) Consultant, Hologic, Inc; Consultant, Novian Health Inc
Priscilla J. Slanetz, MD, MPH, Belmont, MA (*Moderator*) Nothing to Disclose

Sub-Events

SSJ01-01 Breast Imaging Keynote Speaker: Introduction to Contrast-enhanced Spectral Mammography

Tuesday, Nov. 29 3:00PM - 3:10PM Room: Arie Crown Theater

Participants

John M. Lewin, MD, Denver, CO (*Presenter*) Consultant, Hologic, Inc; Consultant, Novian Health Inc

SSJ01-02 Clinical Utility of CESM for Architectural Distortion without Mass: Retrospective Review of 49 Cases

Tuesday, Nov. 29 3:10PM - 3:20PM Room: Arie Crown Theater

Awards

Student Travel Stipend Award

Participants

Michelle E. Naylor, MD, Scottsdale, AZ (*Presenter*) Nothing to Disclose
Bhavika K. Patel, MD, Phoenix, AZ (*Abstract Co-Author*) Nothing to Disclose
Adrian M. Miller, MD, Memphis, TN (*Abstract Co-Author*) Nothing to Disclose
Victor J. Pizzitola, MD, MPH, Scottsdale, AZ (*Abstract Co-Author*) Nothing to Disclose

PURPOSE

Investigate whether CESM can be used to safely rule out or rule in malignancy in patients with suspicious architectural distortion seen on standard mammography or DBT.

METHOD AND MATERIALS

This IRB-approved retrospective study reviewed 410 consecutive CESM examinations from a 17-month period ending January 2016. Study cases included AD in patients with BIRADS 4 or 5 on mammograms and with available pathology. CESM was performed utilizing standard protocol. The AD descriptors, sonographic correlates and enhancement characteristics were recorded from the radiology reports. Pathology results were collected from the biopsy and/or surgical excision reports and divided into benign, radial scar, high-risk and malignant.

RESULTS

Final data set included 49 lesions in 45 patients (4 of the patients had 2 qualifying lesions). The histopathology demonstrated 29 invasive carcinomas and one case of DCIS, ranging in size from 0.4 cm to 4.7 cm (histologic measurements). There were 16 cases of invasive ductal carcinomas, 12 cases of invasive lobular carcinoma and 1 case of low-grade adenosquamous carcinoma. There were 9 radial scars and 10 benign lesions. Two of the radial scars also contained high-risk lesions (ADH and FEA). Thirty-seven of the 49 cases (75.5%) of AD were shown to enhance on CESM. Of these 29/37 were positive for carcinoma, with a PPV of enhancement of 78.4%. The sensitivity of enhancement on CESM for AD was 96.7% (29/30), the specificity was 57.9% (11/19) and the NPV was 91.7% (11/12). The false positive rate was 21.6% (8/37) and the false negative rate was 8.3% (1/12). Accuracy of enhancement on CESM for AD was 81.6% (40/49).

CONCLUSION

A PPV of enhancement on CESM of 78% leads us to conclude that any enhancing area of AD should be biopsied. Our small study included a sensitivity of 97% with one non-enhancing malignant lesion of 4 mm in a patient with significant background enhancement, potentially obscuring enhancement of the malignancy. Further research is needed on the importance of timing CESM with menstrual cycles. Within our data, 29 of the 30 malignancies (96.7%) associated with enhancement and architectural distortion were invasive, highlighting the significance of AD as a finding associated with invasion.

CLINICAL RELEVANCE/APPLICATION

The high sensitivity (97%) and high NPV (92%) of CESM in AD lesions is promising of CESM serving as an adjunct modality to diagnose malignancy and avoid biopsy, respectively.

SSJ01-03 Influence of Advanced Applications of Digital Mammogram Versus Magnetic Resonance Imaging on the Staging Evaluation of Breast Cancer

Tuesday, Nov. 29 3:20PM - 3:30PM Room: Arie Crown Theater

Participants

Maha H. Helal IV, MD, Cairo, Egypt (*Presenter*) Nothing to Disclose
Rasha M. Kamal, MD, Cairo, Egypt (*Abstract Co-Author*) Nothing to Disclose
Marwa A. Haggag, MD, Cairo, Egypt (*Abstract Co-Author*) Nothing to Disclose

Radwa Essam, MBCh, MBBS, Cairo, Egypt (*Abstract Co-Author*) Nothing to Disclose
Sahar Mansour, MD, Cairo, Egypt (*Abstract Co-Author*) Nothing to Disclose
Ahmed E. Hassan, MBCh, Cairo, Egypt (*Abstract Co-Author*) Nothing to Disclose
Asmaa I. Abdelaziz, MD, Cairo, Egypt (*Abstract Co-Author*) Nothing to Disclose

PURPOSE

For many years magnetic resonance imaging (MRI) being a multislice soft tissue focused and contrast based modality was considered the method of choice in staging of breast cancer. In the current work we compared the performance of advanced applications of digital mammogram: contrast-enhanced spectral mammography (CESM) and digital breast tomosynthesis (DBT) with that of MRI to detect the modality suitable for assessment of cancer extension.

METHOD AND MATERIALS

Our work is a prospective, ethics approved analysis that included 300 malignant proved breast pathologies. Evaluation methods included regular digital mammography, 3-D tomosynthesis and contrast enhanced spectral mammography. For acquisition the system acquires a traditional digital mammogram and a tomosynthesis scanning in the same compression. For contrast -enhanced images: low (22–33 kVp) and high (44–49 kVp) energy exposures were taken in the same projections after IV injection of contrast agent. Analysis considered lesions' extension, size, multiplicity and related calcifications. Operative data was the gold standard

RESULTS

CESM and MRI showed equal performance in estimating the accurate cancer size (accuracy: 95%). Tomosynthesis was superior in evaluating mass extension with an accuracy of 85% compared to 83% for MRI. Multiplicity was better demonstrated by CESM that showed an accuracy of 96% compared to 93% for that of MRI. The overall performance of digital mammogram aided by advanced applications (DBT and CESM) in staging of breast cancers was 95.7% sensitivity, 88% specificity and 93% total accuracy versus 95%, 76.5% and 91.3% respectively for MRI.

CONCLUSION

MRI breast was inferior to DBT in estimation of proper disease extend and to that of CESM in detection of multiplicity. The advanced applications of digital mamogram and MRI breast; both showed comparable estimation of the breast cancer size.

CLINICAL RELEVANCE/APPLICATION

Digital mammography aided by advanced applications: breast tomosynthesis and contrast-enhanced spectral mammogram provides an easy, fast and convenient breast imaging method that could be an alternative to MRI in breast cancer staging

SSJ01-04 Diagnostic Performance of Contrast-Enhanced Spectral Mammography(CESM) Compared Digital Mammography and Ultrasound in Screening

Tuesday, Nov. 29 3:30PM - 3:40PM Room: Arie Crown Theater

Awards

Student Travel Stipend Award

Participants

Vera Sorin, BMedSc, RAMAT GAN, Israel (*Presenter*) Nothing to Disclose
Miriam Sklair-Levy, MD, Tel -Hashomer, Israel (*Abstract Co-Author*) Nothing to Disclose
Yael Yagil, MD, Ramat Gan, Israel (*Abstract Co-Author*) Nothing to Disclose
Anat Shalmon, Ramat Gan, Israel (*Abstract Co-Author*) Nothing to Disclose
Arie Rudnstein, MD, TelHashomer, Israel (*Abstract Co-Author*) Nothing to Disclose
Yael Servadio, MD, ramat gan, Israel (*Abstract Co-Author*) Nothing to Disclose
Michael Gotlieb, MD, ramat gan, Israel (*Abstract Co-Author*) Nothing to Disclose

PURPOSE

Little is known regarding the use of contrast mammography in screening population. The purpose of this study is to evaluate and compare the diagnostic performance of contrast mammography compared to digital mammography and digital mammography combined with ultrasound (US) among women screened for breast cancer

METHOD AND MATERIALS

A retrospective cohort study of 438 consecutive women who underwent contrast mammography for screening indication between 2012 and 2016, sequentially followed by breast US. The BIRADS score of contrast mammography, digital mammography, and digital mammography and US was evaluated and compared with the actual disease status. Actual disease status was assessed by histopathology biopsy result, MRI or imaging follow-up. Diagnostic performance was assessed by the sensitivity, specificity, PPV and NPV for each screening method. Statistical analysis was performed using McNemar's test and ROC curve analysis.

RESULTS

438women were followed for 4years, mean follow up 18 moths, range 3-44months. A total of 23 carcinomas were detected. Contrast mammography detected 21/23 carcinomas, sensitivity 91.3% specificity 92.3% (PPV and NPV were 40%, 99.5%). Mammography detected 11/23 carcinomas , sensitivity 47.8%, specificity 93.7%. (PPV and NPV were 30%, 97%). Mammography combined with US detected 17/23 carcinomas, sensitivity of 73.9%%, specificity of 85.8% (PPV and NPV 22%, 98%). The differences in sensitivity and specificity were statistically significant (p=0.002). For the ROC curve, AUC was 0.926 for contrast mammography , 0.722 for digital mammography and 0.798 for digital mammography with US (p<0.0001).

CONCLUSION

Contrast enhanced spectral mammography significantly increased the diagnostic performance in the screening population of our study.

CLINICAL RELEVANCE/APPLICATION

Contrast enhanced spectral mammography may be a valuable screening tool for the early detection of breast carcinoma, providing anatomic and metabolic information It is feasible for screening in clinical practice with higher sensitivity compared to digital

mammography ..

SSJ01-05 Comparison of Contrast Enhanced Digital Mammography and Whole Breast Screening Ultrasound for Supplemental Breast Cancer Screening

Tuesday, Nov. 29 3:40PM - 3:50PM Room: Arie Crown Theater

Participants

Janice S. Sung, MD, New York, NY (*Presenter*) Nothing to Disclose
Maxine S. Jochelson, MD, New York, NY (*Abstract Co-Author*) Nothing to Disclose
Carol H. Lee, MD, New York, NY (*Abstract Co-Author*) Nothing to Disclose
Jonine L. Bernstein, New York, NY (*Abstract Co-Author*) Nothing to Disclose
Anne S. Reiner, MPH, New York, NY (*Abstract Co-Author*) Nothing to Disclose
Elizabeth A. Morris, MD, New York, NY (*Abstract Co-Author*) Nothing to Disclose
Christopher E. Comstock, MD, New York, NY (*Abstract Co-Author*) Nothing to Disclose

PURPOSE

To compare the performance of contrast enhanced digital mammography (CEDM) and whole breast screening ultrasound (WBUS) for supplemental breast cancer screening.

METHOD AND MATERIALS

This is a prospective IRB approved trial recruiting asymptomatic women scheduled for a screening mammogram and WBUS within 30 days of one another. Once accrued to the trial, a CEDM was performed in place of the screening mammogram. Between December, 2014 – March, 2016, 126 women enrolled. The CEDM and WBUS were performed at the same visit and interpreted independently by 2 radiologists blinded to the other modality. For the CEDM, the low dose 2D FFDM images were first interpreted alone prior to being given the contrast-enhanced images. Once final recommendations for each modality were recorded, the patient was managed per standard institutional practice after integrating findings of both studies. For indeterminate findings seen on the contrast-enhanced images of the CEDM but not the low dose 2D or targeted ultrasound, an MRI was performed for further evaluation. If no suspicious correlate was present on the MRI, a 6 month follow up CEDM was recommended. The cancer detection rate (CDR), number of work ups generated for findings seen only on the contrast-enhanced images alone, and the PPV3 of biopsy were determined. Risk factors (breast density, family history (FH), personal history (PH), BRCA status, prior high risk lesion) were recorded.

RESULTS

The mean patient age was 54 (range: 30-72). 106/126 (84%) of women had dense breasts. 5 (4%) women had no additional risk factors, 50 (40%) a PH of breast cancer, and 41 (33%) a FH in a 1st degree relative. 5 cancers (1 IDC, 1 invasive adenocarcinoma, 3 DCIS) were detected in 4 women for a CDR of 40/1000. Of the 5 cancers, 1 (DCIS) was seen on the 2D FFDM, 2 (1 IDC, 1 DCIS) on the WBUS, and all 5 cancers were detected on the CEDM. MRI was recommended for further evaluation of CEDM only findings in 9 (8%) of patients; of these 4 were negative. The PPV3 of biopsy was 42% of CEDM and 50% for WBUS.

CONCLUSION

The cancer detection rate of CEDM is higher than both 2D FFDM and WBUS. However, an MRI may be recommended in 8% of patients for further evaluation of CEDM only findings.

CLINICAL RELEVANCE/APPLICATION

Our early results suggest that CEDM has the potential to be a more sensitive alternative to WBUS for supplemental breast cancer screening.

SSJ01-06 Breast Cancer Characteristics and Shrinkage Patterns in Neo-Adjuvant Chemotherapy Monitoring: Comparison Between Contrast-Enhanced Spectral Mammography and Breast-MRI

Tuesday, Nov. 29 3:50PM - 4:00PM Room: Arie Crown Theater

Participants

Valentina Iotti, MD, Reggio Emilia, Italy (*Presenter*) Nothing to Disclose
Sara Ravaioli, Reggio Emilia, Italy (*Abstract Co-Author*) Nothing to Disclose
Gabriele Levrini, MD, Reggio E., Italy (*Abstract Co-Author*) Nothing to Disclose
Vanessa Marchesi, Villa Minozzo, Italy (*Abstract Co-Author*) Nothing to Disclose
Chiara Coriani, Reggio Emilia, Italy (*Abstract Co-Author*) Nothing to Disclose
Sabrina Caffari, Verona, Italy (*Abstract Co-Author*) Nothing to Disclose
Roberto Sghedoni, PhD, Reggio Emilia, Italy (*Abstract Co-Author*) Nothing to Disclose
Andrea Nitrosi, PhD, Reggio Emilia, Italy (*Abstract Co-Author*) Nothing to Disclose
Rita Vacondio, Reggio Emilia, Italy (*Abstract Co-Author*) Nothing to Disclose
Vladimiro Ginocchi, Reggio Emilia, Italy (*Abstract Co-Author*) Nothing to Disclose
Pierpaolo Pattacini, Reggio Emilia, Italy (*Abstract Co-Author*) Nothing to Disclose

PURPOSE

To compare Contrast-Enhanced Spectral Mammography (CESM) and contrast-enhanced Magnetic Resonance (MRI) in assessing response to neo-adjuvant chemotherapy (NAC) as a function of breast cancer histological and molecular characteristics. To evaluate if shrinkage patterns may influence measurements of residual tumor after NAC.

METHOD AND MATERIALS

Between October 2012 and December 2014, 54 consenting woman with breast cancer and indication of NAC were enrolled into this prospective study. 46 of them completed the study. Histological characteristics were: 40 Infiltrating Ductal Carcinoma (IDC), 4 Infiltrating Lobular Carcinoma (ILC) and 2 Metaplastic Carcinoma. Molecular characteristics were: 3 Luminal A, 16 Luminal B, 6 Luminal B HER+, 12 Triple Negative and 9 HER2+. Patients underwent CESM and MRI before, during and after the end of NAC. Shrinkage patterns were classified into: concentric (C), spotty (S), disappearance (D). Post-NAC CESM and MRI size measurements were compared to post-operative histopathology (gold standard) through correlation (Pearson's "r").

RESULTS

Overall correlation coefficients for CESM and MRI versus pathology post-NAC were $r=0.866$ and $r=0.728$, with mean underestimations in size of 4 mm and 8 mm, respectively. Main variances in correlation were seen in ILC ($r=0.628$ for CESM and $r=-0.298$ for MRI) and Luminal B ($r=0.750$ for CESM and $r=-0.003$ for MRI). Imaging shrinkage pattern overall were: 22 C, 15 S and 9 D. ILC presented 75% of S pattern and 25% of D; Luminal B presented 50% of C pattern, 44% of S and 6% of D. The mean underestimation in size versus histopathology differed between CESM and MRI only in S pattern both for ILC (30 mm on CESM vs 56 mm on MRI) and Luminal B (2 mm on CESM vs 18 mm on MRI). In D pattern it was respectively of 7 mm in ILC and of 5 mm in Lobular B for both CESM and MRI; in C pattern 3 mm in Lobular B for both CESM and MRI.

CONCLUSION

CESM may be more reliable than MRI in defining the response to NAC, in particular for challenging histological and molecular types of breast carcinomas as ILC and Luminal B. CESM is less influenced by the presence of the spotty shrinkage pattern, insidious to detect and define.

CLINICAL RELEVANCE/APPLICATION

Compared to MRI, CESM showed better results in defining the response after Neo-Adjuvant Chemotherapy in breast cancer, especially for challenging histological and molecular types like ILC and Luminal B.

SSJ02

Breast Imaging (Ultrasound Advanced Applications)

Tuesday, Nov. 29 3:00PM - 4:00PM Room: E450A



AMA PRA Category 1 Credit™: 1.00
ARRT Category A+ Credit: 1.00

Discussions may include off-label uses.

Participants

Sughra Raza, MD, Boston, MA (*Moderator*) Nothing to Disclose
Ellen B. Mendelson, MD, Chicago, IL (*Moderator*) Medical Advisory Board, Delphinus Medical Technologies, Inc; Research support, Siemens AG; Consultant, Siemens AG; Speaker, Siemens AG; ; ;

Sub-Events

SSJ02-01 Sub-Hertz Analysis of ViscoElasticity (SAVE) for Differentiation of Breast Masses

Tuesday, Nov. 29 3:00PM - 3:10PM Room: E450A

Participants

Mahdi Bayat, PhD, Rochester, MN (*Presenter*) Nothing to Disclose
Alireza Nabavizadehfransjani, Rochester, MN (*Abstract Co-Author*) Nothing to Disclose
Viksit Kumar, Rochester, MN (*Abstract Co-Author*) Nothing to Disclose
Adriana Gregory, Rochester, MN (*Abstract Co-Author*) Nothing to Disclose
Max Denis, Rochester, MN (*Abstract Co-Author*) Nothing to Disclose
Robert T. Fazzio, MD, PhD, Rochester, MN (*Abstract Co-Author*) Nothing to Disclose
Michael F. Insana, PhD, Davis, CA (*Abstract Co-Author*) Nothing to Disclose
Azra Alizad, MD, Rochester, MN (*Abstract Co-Author*) Nothing to Disclose
Mostafa Fatemi, PhD, Rochester, MN (*Abstract Co-Author*) Nothing to Disclose

PURPOSE

To evaluate the diagnostic performance of sub-Hertz analysis of viscoelasticity (SAVE) in differentiating breast masses.

METHOD AND MATERIALS

The study was conducted under a protocol approved by Institutional Review Board (IRB). Female patients with clinically suspicious breast masses participated in the study. HIPAA compliant written signed informed consent was obtained from each enrolled patient. The study included 42 women (mean age, 52.62 years; age range, 21–79 years) with 43 breast masses (18 benign, 25 malignant; mean mass size, 17.90mm); pathology results were available after the ultrasound test for all cases. Using a general purpose investigational ultrasound machine (Verasonics, Kirkland, WA) masses were first identified by an expert sonographer using conventional B-mode followed by acquiring SAVE data. This method consisted of applying a ramp-and-hold force on skin above the mass area for about 10 seconds using a custom-made automated compression device capable of ultrasound data acquisition. Sequences of raw ultrasound data obtained during the compression period were used for estimation of the strain-time curves. The resulting strain-time data were then used to calculate the viscoelastic properties of the tissue based on a general Kelvin-Voigt model. Using registered B-mode images, regions of interests (ROI) were selected from the mass and surrounding normal tissue. Diagnostic performance of each viscoelasticity measure, including “retardation time”, T1, was evaluated using a receiver operating characteristic analysis.

RESULTS

The lesion to normal retardation time contrast in benign lesions was significantly higher than malignant ($P < 0.0001$). Using retardation time contrast for diagnosis resulted in 88.9% specificity, 96.0% sensitivity and 96.9% negative predictive value (AUC: 0.98).

CONCLUSION

These results suggest that the SAVE method is a valuable diagnostic tool for differentiation of breast masses.

CLINICAL RELEVANCE/APPLICATION

The addition of viscoelasticity measures using SAVE method to ultrasound can greatly improve the specificity in differentiation of the breast masses; thus potentially can help reducing the number of unnecessary biopsies.

SSJ02-02 Effect of Calcifications on Shear Wave Elastography in Evaluating Breast Lesions

Tuesday, Nov. 29 3:10PM - 3:20PM Room: E450A

Participants

Seung Hee Choi, Seoul, Korea, Republic Of (*Presenter*) Nothing to Disclose
Eun Young Ko, MD, PhD, Seoul, Korea, Republic Of (*Abstract Co-Author*) Nothing to Disclose
Boo-Kyung Han, MD, PhD, Seoul, Korea, Republic Of (*Abstract Co-Author*) Nothing to Disclose
Eun Sook Ko, MD, Seoul, Korea, Republic Of (*Abstract Co-Author*) Nothing to Disclose
Ji Soo Choi, MD, PhD, Seoul, Korea, Republic Of (*Abstract Co-Author*) Nothing to Disclose
Jungmin Bae, Seoul, Korea, Republic Of (*Abstract Co-Author*) Nothing to Disclose
So Yoon Park, Seoul, Korea, Republic Of (*Abstract Co-Author*) Nothing to Disclose

PURPOSE

To investigate the effect of calcifications on shear wave elastography (SWE) in evaluating breast lesions.

METHOD AND MATERIALS

We retrospectively reviewed ultrasound (US) images of 807 consecutive patients who had breast US with SWE between October 2013 and March 2014. We excluded the patients who no mammography (n=54) or no measured Emean (n=51) or no follow up data (n=47), and the patients who had neoadjuvant chemotherapy before the US examination (n=24). Finally included 631 patients with 673 breast lesions were included in this study. We analyzed US findings of the lesions: type (mass or non-mass), size, Breast Imaging Reporting and Data System (BI-RADS) category and the elasticity score (E_{mean}) measured at the stiffest area of the lesions. And we compared the E_{mean} between breast lesions with calcifications and without calcifications in three subgroups: benign lesions, in situ carcinoma, and invasive carcinoma. We also analyzed the influence of other US factors on the E_{mean} of the breast lesions.

RESULTS

Breast lesions were confirmed by histologically (n=409) or by follow up images for more than 2 years (n=264). Calcifications were present in 25.3% (170/673) lesions and absent in 74.7% (503/673) lesions. E_{mean} was 33.9 kPa in overall benign lesions; 62.8 kPa in benign lesions with calcifications and 29.8 kPa in benign lesions without calcifications (p=0.000). In situ carcinoma showed 97.0 kPa; lesions with calcifications showed 114.6 kPa while lesions without calcifications showed 52.8 kPa (p=0.037). In invasive carcinoma, the overall E_{mean} was 157.6 kPa, and E_{mean} of lesions with calcifications and without calcifications were 146.4 kPa and 171.9 kPa (p=0.018). Other US factors such as lesion type (mass or non-mass), size, BI-RADS final category showed no statistically significant correlations with elasticity score in the lesions with same pathologic results.

CONCLUSION

The presence of calcifications significantly increased the E_{mean} of breast lesions. Elastography should be carefully interpreted considering the presence of calcifications within the lesions.

CLINICAL RELEVANCE/APPLICATION

The presence of calcifications significantly increased the elasticity score of breast lesions in shear wave elastography.

SSJ02-03 **Toward High Resolution Whole Breast Imaging using Ultrasound Tomography: A Comparison with MRI**

Tuesday, Nov. 29 3:20PM - 3:30PM Room: E450A

Participants

Neb Duric, PhD, Detroit, MI (*Presenter*) Officer, Delphinus Medical Technologies, Inc
Gursharan Sandhu, PhD, Plymouth, MI (*Abstract Co-Author*) Employee, Delphinus Medical Technologies, Inc
Olivier Roy, Plymouth, MI (*Abstract Co-Author*) Employee, Delphinus Medical Technologies, Inc
Cuiping Li, PhD, Plymouth, MI (*Abstract Co-Author*) Employee, Delphinus Medical Technologies, Inc
Peter J. Littrup, MD, Providence, RI (*Abstract Co-Author*) Founder, CryoMedix, LLC; Research Grant, Galil Medical Ltd; Research Grant, Endo International plc; Consultant, Delphinus Medical Technologies, Inc
Mark Sak, PhD, Plymouth, MI (*Abstract Co-Author*) Employee, Delphinus Medical Technologies, Inc
Rachel F. Brem, MD, Washington, DC (*Abstract Co-Author*) Board of Directors, iCAD, Inc; Board of Directors, Dilon Technologies LLC; Stock options, iCAD, Inc; Stockholder, Dilon Technologies LLC; Consultant, U-Systems, Inc; Consultant, Dilon Technologies LLC; Consultant, Dune Medical Devices Ltd

PURPOSE

A novel algorithm, based on the concept of waveform tomography has been applied to ultrasound tomography of the breast (UST) to create high resolution images of tissue sound speed. The purpose of this study is to compare, for the first time, the spatial resolution of the sound speed images with MRI.

METHOD AND MATERIALS

A HIPAA compliant, IRB approved study investigating Ultrasound Tomography (UST) to image the breast to compare the spatial resolution of UST reconstructions with contrast enhanced MRI due to its high sensitivity as well as the similar breast positioning, i.e. pendant, uncompressed breast, and both yielding true 3-D volumetric imaging. A total of 50 women had MR imaging performed during their workup as well as UST imaging. The UST coronal images are separated by 2mm increments and compared with MR images reconstructed in the coronal plane. The UST and MRI images were synchronized to allow slice-by slice comparisons. Images were compared by a single experienced radiologist. The spatial resolution of the UST sound speed images and the MR images were measured by creating profile cuts across sub-mm sized parenchymal features and using a Gaussian fit to model the width of such features. The full-width-half maximum measure was used to determine the spatial resolution in the coronal plane. 50 measurements were made for both the UST and MR images and the spatial resolution was determined by taking the average of the 50 measurements and determining the standard deviation.

RESULTS

The spatial resolution of the UST sound speed images was 0.7 +/- 0.1 mm. The MR resolution was 1.6 +/- 0.1 mm in the coronal plane. In the other planes, the resolution was 0.8 +/- 0.1 for MRI and 2.0 +/- 0.3 mm for UST sound speed. Examples of comparative images are shown in Figure 1.

CONCLUSION

A novel algorithm, based on waveform tomography, was applied to UST data to generate sound speed images that have comparable resolution to MRI.

CLINICAL RELEVANCE/APPLICATION

The similarity in spatial resolution between UST and MRI opens avenues to further develop high resolution 3D imaging using ultrasound for the detection of breast cancer. Waveform based UST imaging may become an important tool for future clinical use.

SSJ02-04 **Quantitative Analysis of Contrast-enhanced Ultrasound Imaging in Invasive Breast Cancer: A Novel Technique using Enhancement Area Ratio to Predict Histopathological Microvessel Density**

Tuesday, Nov. 29 3:30PM - 3:40PM Room: E450A

Participants

Naoko Mori, MD, PhD, Sendai, Japan (*Presenter*) Nothing to Disclose
Shunji Mugikura, MD, PhD, Sendai, Japan (*Abstract Co-Author*) Nothing to Disclose
Shoki Takahashi, MD, Aoba, Japan (*Abstract Co-Author*) Nothing to Disclose
Koichi Ito, PhD, Sendai, Japan (*Abstract Co-Author*) Nothing to Disclose
Chiaki Takasawa, Sendai, Japan (*Abstract Co-Author*) Nothing to Disclose
Li Li, MD, PhD, Sendai, Japan (*Abstract Co-Author*) Nothing to Disclose
Kei Takase, MD, PhD, Sendai, Japan (*Abstract Co-Author*) Nothing to Disclose

PURPOSE

To examine whether enhancement area ratios obtained by the new bubble-detection method correlate with histological microvessel density (MVD) in invasive breast cancer.

METHOD AND MATERIALS

The Institutional Review Board approved this retrospective study, and waived the requirement for informed consent. Between August 2014 and December 2015, consecutive 40 patients with invasive breast cancer lesions underwent contrast-enhanced ultrasound (US). Manual segmentation covering the entire tumor volume was made on precontrast US image. Ratios between enhanced areas and segmented tumor areas (enhancement area ratio) was obtained with the new method at peak and delayed phases (50–54, 55–59, 60–64, 65–69s). For each patient, we also analyzed time-intensity curves (TIC) in three regions of interest (ROI), with the supposed strongest enhancement, to obtain mean value of peak intensity (PI) and area under curve (AUC) of three ROIs. All parameters were measured by two observers independently and were correlated with histological MVD of surgical specimens.

RESULTS

Enhancement area ratios in both peak and delayed phases (50–54, 55–59, 60–64, 65–69s) were significantly correlated with histopathological MVD ($r=0.57, 0.62, 0.68, 0.61$ and 0.58 ; $P=0.0001, <0.0001, <0.0001, <0.0001$ and 0.0001 , respectively), and with almost perfect inter-observer reliability ($0.971, 0.972, 0.961, 0.952$ and 0.959 , respectively). In TIC analysis, PI was significantly correlated ($r=0.43$; $P=0.0073$) with substantial inter-observer reliability (0.782), whereas AUC was not ($r=0.29$; $P=0.0769$).

CONCLUSION

Enhancement area ratios obtained by the new method were reliably correlated with MVD in invasive breast cancer.

CLINICAL RELEVANCE/APPLICATION

MVD information might be obtainable for multiple lesions during one session of contrast-agent injection changing scanning planes during delayed phases by using our new method.

SSJ02-05 Using BI-RADS Mismatches to Assess Clinical Differences in Interpretation Between Whole-Breast Physician-performed Handheld Ultrasound (HHUS) and Supine Automated Ultrasound (AUS) Compared for Equivalence in Lesion Detection

Tuesday, Nov. 29 3:40PM - 3:50PM Room: E450A

Participants

Ellen B. Mendelson, MD, Chicago, IL (*Presenter*) Medical Advisory Board, Delphinus Medical Technologies, Inc; Research support, Siemens AG; Consultant, Siemens AG; Speaker, Siemens AG; ;
Marcela Bohm-Velez, MD, Pittsburgh, PA (*Abstract Co-Author*) Consultant, Koninklijke Philips NV Researcher, Siemens AG Researcher, Dilon Technologies, Inc
Thomas S. Chang, MD, Pittsburgh, PA (*Abstract Co-Author*) Consultant, iCad, Inc
Angela J. Fought, BS,MS, Chicago, IL (*Abstract Co-Author*) Nothing to Disclose
Erin I. Neuschler, MD, Chicago, IL (*Abstract Co-Author*) Research support, Seno Medical Instruments, Inc
Mariana Solari-Font, MD, River Forest, IL (*Abstract Co-Author*) Nothing to Disclose
Michelle R. Straka, MD, Pittsburgh, PA (*Abstract Co-Author*) Nothing to Disclose
Ingolf Karst, MD, Berlin, Germany (*Abstract Co-Author*) Nothing to Disclose
Sandra S. Rao, MD, Chicago, IL (*Abstract Co-Author*) Nothing to Disclose
Judith A. Wolfman, MD, River Forest, IL (*Abstract Co-Author*) Nothing to Disclose
Maria Kalata, Chicago, IL (*Abstract Co-Author*) Researcher, Siemens AG
Mickey Woodard, RT, Pittsburgh, PA (*Abstract Co-Author*) Nothing to Disclose
Alfred W. Rademaker, PhD, Chicago, IL (*Abstract Co-Author*) Nothing to Disclose
Andy Milkowski, MS, Issaquah, WA (*Abstract Co-Author*) Employee, Siemens AG

PURPOSE

With similar applications in clinical practice, whole breast HHUS and AUS may be regarded as 2 modalities because of major differences in image acquisition and display. To determine lesion detection equivalence of HHUS and AUS, we computed % agreement of BI-RADS assessments and categorized mismatches by their causes and clinical significance.

METHOD AND MATERIALS

This 2-site IRB-approved, HIPAA-compliant prospective study aimed to compare HHUS lesion detection with AUS in 500 women. Order of HHUS and technologist-performed AUS was randomized. Performance & interpretation times were recorded. Women ≥ 18 y with any indication for breast US were eligible, including screening & extent of disease. The 2 exams were interpreted by 2 different investigators, each blinded to the other US study. After data were recorded, studies were integrated with mammo and prior exams for management. Lesions were defined as non-cystic masses or other findings that might require recall for focused HHUS, the reference standard.

RESULTS

744 lesions were identified in 501 study participants between 2012-2014. 285/501 (56.9%) had screening US; one site's 251 studies were all screens, the other site with 34 screens had 216 for other indications e.g. palpable mass, BI-RADS 3 f/u, FFD,

DBT or MRI findings, 2nd look after MRI, extent of disease, and prebiopsy cases. Using a cut point of BI-RADS ≥ 3 for clinical significance of mismatches, HHUS had 24.2% and AUS 28.6%. Mismatches in non-screening cases were related to misinterpretation of artifacts as lesions, investigator assignment of category 3 when protocol required BI-RADS 2, and interpretive error, explanations that decreased during the second year of the study. Screening: 191 women had no lesions on AUS or HHUS. 94 women had 148 lesions, with 306 (90.3%) matching BI-RADS or BI-RADS ≤ 2 .

CONCLUSION

BI-RADS mismatches between automated and handheld scans are few and clinically insignificant for screening. Complexity of cases and inexperience with automated display may result in clinically significant BI-RADS mismatches that with training and case experience, as with other new breast imaging modalities should be reduced, promoting acceptance.

CLINICAL RELEVANCE/APPLICATION

Automated US can be used for US screening as an option to handheld; for diagnosis, advantages of whole breast US coronal display in demonstrating multiple bilateral masses when palpable mass is benign appearing can reduce BI-RADS assessment from BI-RADS 3 to 2.

SSJ02-06 Feasibility of Microbubble Contrast-Enhanced Ultrasound (CEUS) Sentinel Lymph Node Imaging with Guided Biopsy in Breast Cancer Patients

Tuesday, Nov. 29 3:50PM - 4:00PM Room: E450A

Participants

Basak E. Dogan, MD, Houston, TX (*Presenter*) Nothing to Disclose
Lumarie Santiago, MD, Houston, TX (*Abstract Co-Author*) Nothing to Disclose
Rosa Hwang, MD, Houston, TX (*Abstract Co-Author*) Nothing to Disclose
Elizabeth Mittendorf, MD, Houston, TX (*Abstract Co-Author*) Nothing to Disclose

PURPOSE

To determine the feasibility of using microbubble contrast-enhanced ultrasound (CEUS) with fine needle aspiration biopsy (FNAB) to identify and pre-operatively evaluate sentinel lymph nodes (SLN) in breast cancer patients.

METHOD AND MATERIALS

Twenty-one patients with newly-diagnosed early-stage (clinical T1-T2, N0) invasive breast cancer who had pre-operative axillary gray scale ultrasound (US) with or without US-guided FNAB revealing benign results were enrolled in an IRB-approved prospective, single-institutional clinical trial. All patients underwent ipsilateral subareolar microbubble contrast injection, followed by CEUS of the axilla. The first CEUS-visualized node was subjected to FNAB, followed by I-125 radioactive seed localization (RSL) of the node. Contrast dose, contrast travel length, travel time, side effects and FNA results were recorded. All patients underwent standard of care (SOC) SLN biopsy using Tc99m with or without blue dye. Correlation of the CEUS-identified node with surgical SLN was performed. Pre-operative FNAB result [benign or malignant] was compared with the final pathologic assessment of that node.

RESULTS

Median patient age was 61yrs (range 37-72). Median cancer size on pre-operative imaging was 12mm (range 6-27). In 20 of 21 (95.2%) patients, CEUS was technically successful. Median node contrast uptake time was 3 min (range 1-10), and travel length was 13cm (range 9-19). All (100%) biopsied and localized nodes correlated with a SLN identified surgically. In 18 (90%) patients, the CEUS-identified, localized node correlated with the hottest SLN. Pathologic evaluation of the SLN(s) revealed metastasis in a single lymph node in 2 (10%) patients, one of which was pre-operatively identified with CEUS-guided FNAB. No significant side effects were recorded in the immediate or 30 day follow up periods.

CONCLUSION

Pre-operative CEUS-guided SLNB is a minimally invasive technique that does not involve radiation exposure, and has no significant side effects. In a first North American experience, this feasibility study confirmed the ability of using microbubble CEUS to identify the SLN in early stage breast cancer patients, suggesting that further evaluation of the technology in larger cohorts is warranted.

CLINICAL RELEVANCE/APPLICATION

CEUS and guided FNAB of SNL is a minimally invasive procedure which may be useful as an alternative to surgical lymph node staging in breast cancer patients.

SSJ03

Cardiac (Cardiovascular Angiography/Intervention)

Tuesday, Nov. 29 3:00PM - 4:00PM Room: S502AB



AMA PRA Category 1 Credit™: 1.00
ARRT Category A+ Credit: 1.00

Participants

Antoinette S. Gomes, MD, Culver City, CA (*Moderator*) Nothing to Disclose

Gregory W. Gladish, MD, Houston, TX (*Moderator*) Nothing to Disclose

Sub-Events

SSJ03-01 **Influence of Contrast Material Density and kV Setting on Detectability of Calcified Plaques on Coronary CT Angiography in Patients with Suspected Coronary Artery Disease**

Tuesday, Nov. 29 3:00PM - 3:10PM Room: S502AB

Participants

Patricia Dewes, MD, Frankfurt, Germany (*Presenter*) Nothing to Disclose

Christophe Arendt, MD, Frankfurt am Main, Germany (*Abstract Co-Author*) Nothing to Disclose

Claudia Frellesen, Frankfurt, Germany (*Abstract Co-Author*) Nothing to Disclose

Thomas J. Vogl, MD, PhD, Frankfurt, Germany (*Abstract Co-Author*) Nothing to Disclose

Ralf W. Bauer, MD, Frankfurt, Germany (*Abstract Co-Author*) Speakers Bureau, Siemens Healthcare GmbH; Speakers Bureau, Bayer Healthcare; Speakers Bureau, GE Healthcare

PURPOSE

Calcified plaque may be missed on coronary CT angiography (cCTA) with highly concentrated iodinated contrast material (CM) at low kV settings. We analyzed the impact of different iodine density CM at varying tube potential for the assessment of calcified plaques on cCTA images.

METHOD AND MATERIALS

164 consecutive patients with suspected coronary artery disease underwent non-enhanced calcium scoring (CaSc) at 120 kV followed by cCTA with topogram-based automated kV selection on third- or second-generation dual-source CT. Based on prior observations 37 patients were injected diluted CM with a resulting iodine concentration of 280 mg/ml (group1) between September 2015 and March 2016 whereas 127 patients were injected undiluted CM with an concentration of 400 mgI/ml (group2). Amount (50 ml) and flow rate (5 ml/s) were kept constant. The sensitivity of cCTA for detecting calcified plaques was evaluated with CaSc at 120 kV serving as the reference.

RESULTS

97 patients (59%) had calcified plaques on CaSc, 78 patients of group 2 and 19 patients of group 1. The overall sensitivity of cCTA for detection of calcified plaques was 79% in group 1 and 73% in group 2. Sensitivity for patients examined at 70 kV was significantly higher with diluted CM (70% vs. 57%). There was no significant difference in sensitivity at 100 and 120 kV in both groups (100% and 82% in group 1 and 2, respectively). The overall median luminal contrast density was 389 HU with diluted CM and 503 HU with undiluted CM. At 70 kV, values were at 463 HU and 655 HU, at 100 kV they were at 197 HU and 365 HU with diluted vs. undiluted CM.

CONCLUSION

The combination of highly concentrated CM and 70 kV tube potential reduces the detectability of calcified plaques. In order to preserve reliable information on relevant calcifications, cCTA at 70 kV should be performed with CM with lower iodine concentration. If undiluted CM is used, 100 kV tube potential should preferably be chosen.

CLINICAL RELEVANCE/APPLICATION

Patients may benefit from both low radiation and contrast exposure when examined at 70 kV cCTA. However, 100 kV protocols yield higher sensitivity or reliable calcified plaque visualization.

SSJ03-02 **Comparison of Transcatheter Coronary Artery Fistula Closure Versus Surgery Closure**

Tuesday, Nov. 29 3:10PM - 3:20PM Room: S502AB

Participants

Junzhou Pu, Beijing, China (*Presenter*) Nothing to Disclose

Lianjun Huang, Beijing, China (*Abstract Co-Author*) Nothing to Disclose

Wenhui Wu, MD, Beijing, China (*Abstract Co-Author*) Nothing to Disclose

PURPOSE

The aim of this study was to compare transcatheter coronary artery fistula (CAF) closure (TC) with surgery closure (SC).

METHOD AND MATERIALS

From 2011 to 2015, 21 patients (age range from 18 to 76 years, 11 males) were diagnosed CAF in our center. Twelve of them were underwent transcatheter closure, 9 patients were attempted to closure in surgery. Hemodynamic evaluation and coronary artery angiography had been carried out before procedures.

RESULTS

Nine procedures in TC group were successful, 3 failures due to inability to cannulate the distal of lesion. There was no death in TC group. One patient in SC group had procedure related death. Procedure room time (103 ± 89 min vs. 305 ± 118 min, $p < 0.001$), intensive care unit time (0 hour vs. 24 hours, $p < 0.001$), length of stay (5 days \pm 15 days, $p < 0.001$) were significantly less in TC group. Two cases of residual shunts were detected in immediate angiography of TC group. One of them turned to a significant recanalization, and a second intervention was performed. No recanalization was found in SC during follow-ups. Follow-up was obtained in all the patients. At a median time of 17.5 months, there was no significant difference in survival (TC, 100% vs. SC, 94.4%, $p = 0.471$).

CONCLUSION

Both transcatheter and surgery closure can achieve satisfactory results of CAF. However, the procedure time, length of stay and resource use was significantly lower in TC group.

CLINICAL RELEVANCE/APPLICATION

Coronary artery fistula intervention is a safe and feasible method, and should be considered firstly if the anatomic condition was appropriate.

SSJ03-03 Improving Patient to Patient CT Value Uniformity in Coronary CT Angiography with an Individualized Contrast Injection Protocol Tailored to Fat Free Mass and kVp

Tuesday, Nov. 29 3:20PM - 3:30PM Room: S502AB

Participants

Laurence Delombaerde, MSc, Heverlee, Belgium (*Presenter*) Nothing to Disclose
Federica Zanca, PhD, Leuven, Belgium (*Abstract Co-Author*) Employee, General Electric Company
Gert Van Gompel, PhD, Brussel, Belgium (*Abstract Co-Author*) Nothing to Disclose
Kaoru Tanaka, MD, PhD, Brussels, Belgium (*Abstract Co-Author*) Nothing to Disclose
Nico Buls, DSc, PhD, Jette, Belgium (*Abstract Co-Author*) Nothing to Disclose
Johan De Mey, Jette, Belgium (*Abstract Co-Author*) Nothing to Disclose
Kristof De Smet, MD, MSc, Brussels, Belgium (*Abstract Co-Author*) Nothing to Disclose

PURPOSE

To achieve a consistent enhancement in coronary CT angiography (CCTA) by implementing a contrast injection protocol with adjusted iodine concentration based on patient habitus and kVp.

METHOD AND MATERIALS

Retrospective data from 80 consecutive patients (group 1) scanned on a Revolution CT (GE Healthcare) with one-heartbeat automated triggering, 100 kVp (N=74) or 120 kVp (N = 6), noise index = 25 and standard iodine dose (70 ml of 370 mg I / ml, 350 mg I / ml or 320 mg I / ml) was collected, using DoseWatch (GE Healthcare). The optimal correlation between arterial enhancement (HU) and body habitus normalized to total iodine dose (TID) was determined by considering following parameters: weight, Body Mass Index (BMI), Body Surface Area (BSA), Lean Body Mass (LBM) and Fat Free Mass (FFM). From the parameter giving the best correlation, a model for optimal contrast concentration to achieve a target enhancement value of 550 HUtarget was determined and prospectively applied to 62 patients (N=1 at 80 kVp, N=55 at 100 kVp and N=6 at 120 kVp) undergoing a CCTA exam (group 2). Personalized iodine concentration was administered by parallel mixing of iodine with saline on a dual-head power injector (Nemoto-Kyorindo, Japan). Enhancement was compared between group 1 and 2 (Mann-Whitney U- test) and homogeneity of variances was tested (Levene's test).

RESULTS

Compared to other body habitus parameters (R^2 range 0.1 – 0.5), Free Mass (FFM) showed the strongest correlation ($R^2 = 0.5$) with enhancement. Following contrast injection model was established for 100 kVp: $TID = (HU_{target} - 237) * FFM / 946$; for 120 and 80 kVp TID should be scaled by 1.22 and 0.77 respectively. With the modified protocol, variance (standard deviation) reduced from 102 HU to 67 HU ($p < 0.01$). The mean enhancement 506 HU was lower than the target 550 HU ($p < 0.01$).

CONCLUSION

An injection protocol with contrast concentration adapted to body habitus, iodine concentration and kVp improves patient-to-patient CT value uniformity.

CLINICAL RELEVANCE/APPLICATION

Personalizing the iodine injection protocol for CCTA homogenizes image quality in terms of contrast enhancement for an easier interpretation and correlation of images.

SSJ03-04 The Effect of Full Iterative Reconstruction on The Image Quality of Coronary Artery Stent at 320 Detector-Row CT Scanner

Tuesday, Nov. 29 3:30PM - 3:40PM Room: S502AB

Participants

Fuminari Tatsugami, Hiroshima, Japan (*Presenter*) Nothing to Disclose
Toru Higaki, PhD, Hiroshima, Japan (*Abstract Co-Author*) Nothing to Disclose
Chikako Fujioka, RT, Hiroshima, Japan (*Abstract Co-Author*) Nothing to Disclose
Wataru Fukumoto, Hiroshima, Japan (*Abstract Co-Author*) Nothing to Disclose
Yoko Kaichi, Hiroshima, Japan (*Abstract Co-Author*) Nothing to Disclose
Kazuo Awai, MD, Hiroshima, Japan (*Abstract Co-Author*) Research Grant, Toshiba Corporation; Research Grant, Hitachi, Ltd; Research Grant, Bayer AG; Research Grant, Eisai Co, Ltd; Medical Advisor, General Electric Company; ; ; ;
Makoto Iida, Hiroshima, Japan (*Abstract Co-Author*) Nothing to Disclose
Hiroaki Sakane, MD, Hiroshima, Japan (*Abstract Co-Author*) Nothing to Disclose

PURPOSE

Cardiac CT is an important and indispensable method for the assessment of coronary artery stent patency. However, when the CT

images are reconstructed with filtered back projection (FBP) or hybrid iterative reconstruction (IR) the diagnosis of in-stent restenosis is occasionally difficult due to blooming- and streak artifact. A new type of full IR algorithm (forward projected model-based iterative reconstruction solution; FIRST, Toshiba Medical Systems) improves the spatial resolution and decreases the artifacts. We compared the image quality of coronary artery stent between the CT images reconstructed with FIRST and with hybrid IR (AIDR 3D, Toshiba).

METHOD AND MATERIALS

We prospectively enrolled thirty patients (11 women, mean age 71.4 ± 8.6 years) who had 34 coronary stents. They underwent coronary CT angiography (CTA) using a 320-slice CT scanner. Images were reconstructed with AIDR 3D (standard setting) using a medium soft-tissue convolution kernel and with FIRST (cardiac setting). For each of the two reconstruction methods we generated attenuation profiles and measured the width of the 10-90% edge rise distance (ERD) at the boundary and determined a slope of linear function as follow: $\text{Slope} = (\text{CT}_{90\%} - \text{CT}_{10\%}) / \text{ERD}$. Two radiologists visually evaluated the image quality based on the blooming artifacts from the stent using a 4-point scale ranging from 1 = impaired diagnostic information to 4 = minimal or absent. The ERD and slope between the two reconstruction methods were compared using the paired t-test, image quality scores with the Wilcoxon signed-rank test.

RESULTS

There was no significant difference in the mean ERD between the two reconstruction methods (0.7 ± 0.2 mm vs. 0.6 ± 0.2 mm; $p = 0.14$). The mean slope on FIRST images was higher than AIDR 3D (378.7 ± 149.5 vs. 195.2 ± 116.6 ; $p < 0.001$). The mean image quality score for AIDR 3D and FIRST images were 2.7 and 3.6, respectively; the difference was also significant ($p < 0.05$).

CONCLUSION

As the use of the FIRST improved image quality of the coronary artery stent at coronary CTA, it may improve the detection of in-stent restenosis compared to the conventional method.

CLINICAL RELEVANCE/APPLICATION

The diagnostic performance could be improved when FIRST is used for the detection of in-stent restenosis compared to the conventional method.

SSJ03-05 How To Make Use of Coronary CT Angiography to Decrease Patient Dose in the Catheterization Laboratory

Tuesday, Nov. 29 3:40PM - 3:50PM Room: S502AB

Participants

Christophe Arendt, MD, Frankfurt am Main, Germany (*Presenter*) Nothing to Disclose

Patricia Dewes, MD, Frankfurt, Germany (*Abstract Co-Author*) Nothing to Disclose

Julian L. Wichmann, MD, Charleston, SC (*Abstract Co-Author*) Nothing to Disclose

Josef Matthias Kerl, MD, Frankfurt, Germany (*Abstract Co-Author*) Research Consultant, Siemens AG Speakers Bureau, Siemens AG

Thomas J. Vogl, MD, PhD, Frankfurt, Germany (*Abstract Co-Author*) Nothing to Disclose

Ralf W. Bauer, MD, Frankfurt, Germany (*Abstract Co-Author*) Speakers Bureau, Siemens Healthcare GmbH; Speakers Bureau, Bayer Healthcare; Speakers Bureau, GE Healthcare

PURPOSE

Cardiologists currently catheterize all three major coronary arteries as standard of care in patients with coronary artery disease (CAD), even though previously performed coronary CT angiography (cCTA) showed only one- or two-vessel disease with no or non-relevant atherosclerosis in the other vessels. We investigated the potential reduction of patient exposure during invasive coronary catheterization (ICA) if the procedure had only been directed to the vessel of interest by utilizing information of the CT report.

METHOD AND MATERIALS

Dose reports of 52 patients who were referred to ICA because of at least one moderate or severe stenosis on cCTA were retrospectively included. There was no selection of patients based on CT image quality. The dose-area product (DAP) was documented separately for the left (LAD, CX) and the right coronary artery (RCA) by summing up the single DAPs for each projection. The study population was further subdivided according to the procedure performed: coronary angioplasty/stent insertion of LCA (group 1) or RCA (group 2) only, or of both vessels (group 3), or no intervention (group 4). Furthermore, patients with no intervention but subsequent coronary artery bypass grafting were included (group 5).

RESULTS

All 36 arteries (LCA or RCA) classified as non-significantly diseased on cCTA out of 104 coronary arteries (35%) were confirmed by ICA with no further intervention. Half of the study population could have benefit from reduced exposure if catheterization had been directly guided to the vessel of interest as described on cCTA. Potential mean relative DAP reduction were as follows: group 1 ($n = 14$) 10.5%; group 2 ($n = 1$) 43.4%; group 3 ($n = 10$) 0%; group 4 ($n = 24$) 25.7%; group 5 ($n = 3$) 0%. However, calcium blooming artifacts caused overestimation of stenosis severity in 16/104 (15%) vessels on cCTA with subsequent need for diagnostic ICA.

CONCLUSION

Directing ICA to the vessel of disease as described on cCTA would be safe and reduce patient exposure in the cath lab substantially, especially for patients with one-vessel disease. Calcified plaques remain a limitation on cCTA leading to unnecessary ICA referrals.

CLINICAL RELEVANCE/APPLICATION

cCTA can guide cardiologists directly to the vessel of interest for coronary intervention with substantial dose reduction for the invasive procedure, making coronary catheterization safer and faster for patients.

SSJ03-06 Cardiac CT on the Third-generation Dual-source CT System: The Image Quality and Diagnostic Value of Single-phase Coronary Artery CT Angiography Image from Adenosine Triphosphate Stress Dynamic Myocardial CT Perfusion

Participants

Yan Yi, Beijing, China (*Presenter*) Nothing to Disclose
Yining Wang, MD, Beijing, China (*Abstract Co-Author*) Nothing to Disclose
Lu Lin, MD, Peking, China (*Abstract Co-Author*) Nothing to Disclose
Hao Qian, Beijing, China (*Abstract Co-Author*) Nothing to Disclose
Hongzhi Zhang, Beijing, China (*Abstract Co-Author*) Nothing to Disclose
Zheng Yu Jin, MD, Beijing, China (*Abstract Co-Author*) Nothing to Disclose

PURPOSE

To investigate the image quality (IQ) and diagnostic value of single-phase coronary artery CT angiography (CCTA) image from stress dynamic myocardial CT perfusion (CTP) scan on the third-generation dual-source CT (DSCT).

METHOD AND MATERIALS

Nineteen consecutive symptomatic patients (13men and 6women; 58.5 ± 10.3 years) who underwent CCTA and diagnosed with at least one moderate stenosis (degree $\geq 50\%$) lesion of the three main coronary arteries were recruited. The patients were scanned with prospective automatic CARE-kV selection ATP-stress dynamic myocardial CTP examination (44ml contrast media & 60ml saline at 5.5ml/s) on a third-generation DSCT with data acquisition window at the end systole. The single-phase CCTA image with the best enhancement of coronary arteries in the process of CTP was selected for reconstruction and measurement. The quantitative (CT value, background noise, signal-to-noise ratio [SNR] and contrast-to-noise ratio [CNR]) and qualitative (Likert four-point grading scale) IQ results as well as the diagnostic value (detection of coronary artery stenosis lesion) were compared with that of the former CCTA examination images.

RESULTS

There were no significant difference in quantitative (CT values, noise, SNR and CNR) IQ between the CTP-CCTA and former CCTA ($p>0.05$), except for the SNR of aorta root (14.70 ± 2.10 and 18.67 ± 4.85 , $p<0.05$). No significant difference in qualitative IQ has been found between CTP-CCTA and former CTA (score: 1.38 ± 0.60 and 1.47 ± 0.61 , $p>0.05$). CTP-CCTA detect stenosis in good correlation with former CCTA (97%, 99 of 102), especially for moderate-severe stenosis (100%, 53 of 53). The patients' mean heart rate (HR) during stress CTP (83.92 ± 11.03 bpm) was much higher than that of the former CCTA (68.91 ± 12.81 bpm) scan ($p=0.005$). The mean effective radiation dose (ED) of CTP is 4.48 ± 1.87 mSv.

CONCLUSION

The IQ and diagnostic value of single-phase CCTA image from stress dynamic myocardial CTP on the third-generation dual-source CT system was great and one myocardial CTP scan is potentially feasible to replace the CTP&CCTA examination.

CLINICAL RELEVANCE/APPLICATION

The single-phase CCTA image derived from CTP at the third-generation DSCT system is able to replace the CCTA scan for symptomatic patients with suspected or known CAD, which enable the greatly reduction of ED for patients and create highest possibilities for one-stop cardiac CT examination within one myocardial CTP scan.

Cardiac (Outcomes and Risk Stratification/Research Trials)

Tuesday, Nov. 29 3:00PM - 4:00PM Room: S504AB



AMA PRA Category 1 Credit™: 1.00
ARRT Category A+ Credit: 1.00

Participants

Karen G. Ordovas, MD, San Francisco, CA (*Moderator*) Nothing to Disclose
Pamela K. Woodard, MD, Saint Louis, MO (*Moderator*) Research Grant, Astellas Group; Research Grant, Bayer AG; Research agreement, Siemens AG; ; ; ;
Pal Maurovich-Horvat, MD, PhD, Pecs, Hungary (*Moderator*) Nothing to Disclose

Sub-Events**SSJ04-01 Recent Trends in Medicare Payments to Radiologists and Cardiologists: Who Has Been the Bigger Loser?**

Tuesday, Nov. 29 3:00PM - 3:10PM Room: S504AB

Participants

David C. Levin, MD, Philadelphia, PA (*Presenter*) Consultant, HealthHelp, LLC; Board of Directors, Outpatient Imaging Affiliates, LLC
Laurence Parker, PhD, Philadelphia, PA (*Abstract Co-Author*) Nothing to Disclose
Vijay M. Rao, MD, Philadelphia, PA (*Abstract Co-Author*) Nothing to Disclose

PURPOSE

Radiologists and cardiologists are the 2 highest users of imaging and receive the highest aggregate imaging payments from Medicare. But large cuts have been imposed on reimbursements in recent years. Our purpose was to compare trends between 2002 and 2014 in payments to the 2 specialties to determine which initially grew faster and which dropped further after peaking.

METHOD AND MATERIALS

The nationwide Medicare Part B Physician/Supplier Procedure Summary Master Files for 2002 through 2014 were the data source; these files provide total allowed payments for all noninvasive diagnostic imaging CPT codes to all specialties. Medicare specialty codes were used to identify payments to radiologists and cardiologists. Invasive procedures were not included. Payment amounts for all types of imaging to each specialty were tabulated each year and trends were ascertained.

RESULTS

Radiologists received \$3.714B for Medicare diagnostic imaging in 2002, increasing to a peak of \$5.300B in 2006 (+43%). In 2007, with the onset of the Deficit Reduction Act (DRA), radiologists' payments dropped by \$735M. Payments then remained relatively stable for the next 3 years but began a decline in 2011. By 2014, their payments had dropped to \$4.164B (-21% vs peak). Cardiologists received \$1.756B for Medicare diagnostic imaging in 2002, increasing to a peak of \$2.998B in 2006 (+71%). In 2007, with the onset of the DRA, their payments dropped by exactly \$300M. They then experienced even greater reductions in 2009 and 2010 as a result of code bundling in echocardiography (2009) and myocardial perfusion imaging (2010). Further reductions occurred in subsequent years. By 2014, their payments were \$1.673B (-44% vs peak).

CONCLUSION

Between 2002 and 2006, payments to cardiologists for noninvasive diagnostic imaging grew at a much faster rate than payments to radiologists. Both specialties were then adversely impacted by the DRA in 2007, but code bundling in echocardiography and myocardial perfusion imaging created additional losses for cardiologists. The result was that by 2014, cardiologists had proportionately lost over twice as much imaging reimbursement as radiologists.

CLINICAL RELEVANCE/APPLICATION

not applicable.

SSJ04-02 Cardiac Magnetic Resonance Imaging in Stroke Patients: A Prospective Substudy of the FIND-AF Multicenter Trial

Tuesday, Nov. 29 3:10PM - 3:20PM Room: S504AB

Awards**Student Travel Stipend Award****Participants**

Wieland Staab, MD, Goettingen, Germany (*Presenter*) Nothing to Disclose
Laura Wandelt, Goettingen, Germany (*Abstract Co-Author*) Nothing to Disclose
Rolf Wachter, Goettingen, Germany (*Abstract Co-Author*) Nothing to Disclose
Andreas Schuster, Goettingen, Germany (*Abstract Co-Author*) Nothing to Disclose
Michael Steinmetz, Goettingen, Germany (*Abstract Co-Author*) Nothing to Disclose
Christina Unterberg-Buchwald, Goettingen, Germany (*Abstract Co-Author*) Nothing to Disclose
Christian O. Ritter, MD, Wuerzburg, Germany (*Abstract Co-Author*) Nothing to Disclose
Jan Martin Sohns, MD, PhD, Goettingen, Germany (*Abstract Co-Author*) Nothing to Disclose
Johannes T. Kowallick, Gottingen, Germany (*Abstract Co-Author*) Nothing to Disclose
Joachim Lotz, MD, Gottingen, Germany (*Abstract Co-Author*) Research Cooperation, Siemens AG

PURPOSE

Atrial fibrillation (AF) is associated with an increased risk of stroke, but often remains undiagnosed in acute ischemic stroke

Atrial fibrillation (AF) is associated with an increased risk of stroke, but often remains undiagnosed in acute ischemic stroke patients. This prospective trial evaluates the role of delayed enhancement cardiac magnetic resonance (DE-CMR) imaging of the left atrium in acute stroke patients.

METHOD AND MATERIALS

Thirty- one patients ≥ 60 years with acute ischemic stroke (symptoms ≤ 7 days) presenting with sinus rhythm on admission and without a history of AF, irrespective of stroke etiology underwent DE – CMR. Distribution of left atrial fibrosis (LAF) was performed according to the Utah score. Evaluation of left atrial ejection fraction (LAEF), left atrial function, 3D left atrial volume, NIH stroke scale (NIHSS) and CHA2DS2-VASc-Score was performed.

RESULTS

The mean age of patients was 70.5 ± 6.2 years, 17 were female (54.9%). With enhanced rhythm electrocardiogram (ECG) monitoring. AF was not detected. Left atrial volume was 50.7 ± 12.7 ml/m², mean LAEF was 47.9 ± 7.8 % with a CHA2DS2-VASc-Score of 2.84 ± 1.6 . Mean LAF was 1.9 ± 0.9 % (Utah Score I group ≤ 10 % LA wall enhancement), demonstrating a perfect correlation with Utah I and no finding of AF in this study population. NIHSS was 2.84 ± 3 and positively correlated with LAF (Spearman rank correlation was 0.6, Ps <0.05).

CONCLUSION

In patients with acute ischemic stroke, left atrial fibrosis was associated with NIH stroke scale. Left atrial fibrosis with a Utah Score I correlated perfectly with no finding of AF.

CLINICAL RELEVANCE/APPLICATION

DE-CMR of the left atrium adds substantial information in patients with acute ischemic stroke.

SSJ04-03 Myocardial Tissue Phase Mapping in Mice using Cine Phase-Contrast MRI

Tuesday, Nov. 29 3:20PM - 3:30PM Room: S504AB

Participants

Nivedita Naresh, Chicago, IL (*Presenter*) Nothing to Disclose

Cynthia Yang, Chicago, IL (*Abstract Co-Author*) Nothing to Disclose

Bradley D. Allen, MD, Chicago, IL (*Abstract Co-Author*) Nothing to Disclose

Sol Misener, Chicago, IL (*Abstract Co-Author*) Nothing to Disclose

Michael Markl, PhD, Chicago, IL (*Abstract Co-Author*) Institutional research support, Siemens AG; Consultant, Circle Cardiovascular Imaging Inc;

James C. Carr, MD, Chicago, IL (*Abstract Co-Author*) Research Grant, Astellas Group Research support, Siemens AG Speaker, Siemens AG Advisory Board, Guerbet SA

Daniele Proccisi, MS, PhD, Pasadena, CA (*Abstract Co-Author*) Nothing to Disclose

PURPOSE

Mouse models can help investigate the molecular mechanisms underlying complex cardiovascular diseases. Assessment of myocardial regional wall motion plays a very important role in the diagnosis and management of several cardiovascular diseases and can be linked to many underlying biological processes. Our purpose was to develop a mouse tissue phase mapping method as a quantitative imaging biomarker to study myocardial regional wall motion.

METHOD AND MATERIALS

10 week old female C57Bl/6 mice (n=5) were imaged at 7T. Mice were maintained at 1.25% isoflurane and 36 ± 1 C during MRI. 2D cine phase-contrast MRI with prospective ECG and respiratory triggering of the mouse heart was performed at basal, mid-ventricular, and apical locations. Imaging parameters included: TE/TR = 3.6/6 ms, FOV=30x30 mm, phase resolution=50%, image resolution = 117x117 μ m, flip angle=15 degrees, slice thickness=1 mm, averages=2, in-plane VENC= 4 cm/s and through-plane VENC= 4cm/s. A segmented acquisition (1 line per heartbeat) was used and the velocity-encoded scans were acquired in consecutive heartbeats to perform imaging at a high temporal resolution. The scan time was 6-7 min per slice depending on the heart and respiratory rates. For all mice, radial, tangential and longitudinal velocity-time curves were measured at base, mid, and apex. Global peak and time-to-peak (TTP) radial and longitudinal velocities were also quantified for all mice.

RESULTS

Peak radial velocity was 0.99 ± 0.15 cm/s at systole and -1.06 ± 0.11 cm/s at diastole. Peak longitudinal velocity was 0.94 ± 0.11 cm/s at systole and -1.16 ± 0.26 cm/s at diastole. Systolic TTP radial velocity was 22 ± 2 ms and diastolic TTP radial velocity was 78 ± 3 ms. Systolic TTP longitudinal velocity was 43 ± 5 ms and diastolic TTP longitudinal velocity was 84 ± 5 ms.

CONCLUSION

2D cine myocardial tissue phase mapping in mice can be used to comprehensively analyze regional myocardial wall motion in mice with a total scan time of less than 20 minutes. Future cardiac MRI studies exploiting this technique in genetically modified mice will help track progression of cardiovascular disease and shed light into the underlying biological processes that characterize it.

CLINICAL RELEVANCE/APPLICATION

In the present study, we demonstrated the feasibility of performing myocardial tissue phase mapping in mice to comprehensively evaluate regional wall motion.

SSJ04-04 Prospective Evaluation of Left Atrial Function and Gadolinium Delayed Enhancement with MRI in Patients with Atrial Fibrillation Before and After Catheter Ablation

Tuesday, Nov. 29 3:30PM - 3:40PM Room: S504AB

Participants

Adrian Curta, MD, Munich, Germany (*Presenter*) Nothing to Disclose

Stephanie Fichtner, Munchen, Germany (*Abstract Co-Author*) Nothing to Disclose

Reza Wakili, Munich, Germany (*Abstract Co-Author*) Nothing to Disclose

Heidi Estner, Munich, Germany (*Abstract Co-Author*) Nothing to Disclose
Harald Kramer, MD, Munich, Germany (*Abstract Co-Author*) Nothing to Disclose

PURPOSE

An improvement in left atrial (LA) functional parameters post catheter ablation (CA) with pulmonary vein isolation and ablation of the anterior mitral line in patients with persistent atrial fibrillation (AF) has been demonstrated through echocardiography. Successful CA should lead to scarring of the left atrium along the ablation pathways. We intended to confirm the improvement in left atrial function and to correlate it with the presence of gadolinium late enhancement (GLE) along the ablation pathways with cardiac MRI (cMRI).

METHOD AND MATERIALS

Functional imaging of the LA was performed via steady-state-free-precession (SSFP) cine sequences. GLE was visualised with 3D-fast low-angle shot (FLASH) inversion recovery sequences 15 minutes post i.v. administration of GBCA. Imaging was performed on a 3 Tesla MRI system (MAGNETOM Verio, Siemens Medical) before and after CA. For statistical analysis, pre- and post-CA functional parameters were recorded. GLE was evaluated blinded and randomized in terms of pre/post ablation in consensus by a cardiologist and a radiologist with expertise in cMRI. Patients were grouped in a) subjects with successful CA, i.e. sinus rhythm, and b) subjects without sinus rhythm at the time of follow-up-MRI. Results were evaluated with a paired t-test; a p value of .05 was set as the significance level.

RESULTS

72 patients were included in the study. Pre- and post-CA MRI was performed in 44 patients. The mean time before CA and follow-up-cMRI was 111 days (76-313). 8 patients were excluded due to poor image quality. 30 patients were allotted to group a), 6 to group b). Group a) showed a significant difference in ejection fraction (23,5±6,9% vs. 28,7±4,6%; p<.001; CI=95%), end-systolic volume (107±47ml vs. 96±37ml; p=.012; CI=95%), stroke volume (32±13ml vs. 38±12ml; p=.002; CI=95%) and GLE (80% vs. 10%; p<.001; CI=95%) in the follow-up cMRI. Group b) showed no significant changes in LA functional parameters and in GLE in the follow-up cMRI.

CONCLUSION

Scarring along the ablation pathways could be visualized with GLE and was significantly present only in patients with successful CA. These patients also showed a significant improvement in LA function.

CLINICAL RELEVANCE/APPLICATION

cMRI is a reliable and objective method to assess left atrial function post catheter ablation. The presence of delayed enhancement along the ablation pathways shows a correlation with short term success and could be of prognostic value.

SSJ04-05 Ventricular Myocardial Fat: An Unexpected Biomarker for Long-term Survival

Tuesday, Nov. 29 3:40PM - 3:50PM Room: S504AB

Awards

Student Travel Stipend Award

Participants

Anna S. Bader, MD, Bronx, NY (*Presenter*) Nothing to Disclose
Jeffrey M. Levsky, MD, PhD, Bronx, NY (*Abstract Co-Author*) Nothing to Disclose
Benjamin Zalta, MD, New York, NY (*Abstract Co-Author*) Nothing to Disclose
Anna Shmukler, MD, Brooklyn, NY (*Abstract Co-Author*) Nothing to Disclose
Arash Gohari, MD, Brooklyn, NY (*Abstract Co-Author*) Nothing to Disclose
Vineet R. Jain, MD, New York, NY (*Abstract Co-Author*) Nothing to Disclose
Victoria Chernyak, MD, Bronx, NY (*Abstract Co-Author*) Nothing to Disclose
Eran Bellin, Bronx, NY (*Abstract Co-Author*) Nothing to Disclose
Linda B. Haramati, MD, MS, Bronx, NY (*Abstract Co-Author*) Spouse, Board Member, Bio Protect Ltd; Spouse, Board Member, OrthoSpace Ltd; Spouse, Board Member, Kryon Systems Ltd

PURPOSE

Left ventricular (LV) myocardial fat has been described on CT as a sign of chronic myocardial infarction (MI). Right ventricular (RV) fat is usually considered a sign of aging. We postulated that presence of LV fat in patients without history of MI indicates silent MI and portends higher mortality. The purpose of this study is to determine the relationship between myocardial fat and all-cause mortality.

METHOD AND MATERIALS

We identified all patients with chronic MI (≥3 years prior) and 3 age- and time-matched patients without MI who underwent non-contrast chest CT between 1/1/2005-12/31/2008. Patients with cancer were excluded. All CTs were reviewed for myocardial fat by two cardiothoracic radiologists blinded to history and outcome. LV fat, RV fat, and fat in either ventricle were each classified as dichotomous variables. Electronic health records were surveyed for variables related to mortality. Death was verified by in-hospital events and the National Death Index. Logistic regression was used to identify factors associated with myocardial fat. Kaplan-Meier and Cox proportional hazard analyses were used to determine the association between myocardial fat and all-cause mortality.

RESULTS

The study population comprised 690 patients without MI and 265 patients with prior MI, mean age 73.7±10.6 years. There were 277 and 190 deaths, respectively (median follow-up 6.8 years [IQR 2.5, 8.4]). In the no MI group, 25.7% had LV and 49.9% had RV fat. In the MI group, 32.8% had LV and 42.3% had RV fat. LV and RV fat were highly associated (OR 5.3, p<0.001). The presence of fat in either ventricle was not associated with common cardiovascular risk factors and comorbid conditions, such as age, sex, hypertension, diabetes, stroke, obesity, and dyslipidemia. In the no MI group, those with myocardial fat had a 25% reduction in hazard of death, adjusting for age, sex, setting, ordinal calcium score and heart failure (p=0.04). In the MI group, those with myocardial fat had a 31% reduction in hazard of death, adjusting for age, setting, heart failure and kidney disease (p=0.018).

CONCLUSION

Patients with myocardial fat have improved survival, suggesting that myocardial fat is either protective or is a biomarker of a beneficial physiologic process, even for patients with prior MI.

CLINICAL RELEVANCE/APPLICATION

Myocardial fat is a marker of enhanced survival and has the potential to improve patient risk stratification beyond traditional risk factors.

SSJ04-06 Atorvastatin Reduces Aortic Plaque Volume in HIV: A Randomized Placebo-Controlled Trial

Tuesday, Nov. 29 3:50PM - 4:00PM Room: S504AB

Awards

Student Travel Stipend Award

Participants

Balint Szilveszter, MD, Boston, MA (*Presenter*) Nothing to Disclose
Janet Lo, Boston, MA (*Abstract Co-Author*) Nothing to Disclose
Kathleen Fitch, Boston, MA (*Abstract Co-Author*) Nothing to Disclose
Steven Grinspoon, Boston, MA (*Abstract Co-Author*) Nothing to Disclose
Udo Hoffmann, MD, Boston, MA (*Abstract Co-Author*) Nothing to Disclose
Michael T. Lu, MD, Boston, MA (*Abstract Co-Author*) Nothing to Disclose

PURPOSE

HIV confers substantial risk of cardiovascular disease, including myocardial infarction (MI) and stroke. HIV is also associated with aortic inflammation; however whether statins reduce aortic plaque in HIV is not known.

METHOD AND MATERIALS

Forty persons with subclinical coronary atherosclerosis, LDL cholesterol <130 mg/dL, and treated HIV participated in a 12-month randomized, double blind trial of atorvastatin vs. placebo. Participants had ECG-gated CT angiography (CTA) of the thoracic aorta and coronary arteries at enrollment and after 12 months of treatment. The primary outcome was change in ascending aortic plaque volume, quantified by an independent reader blinded to scan order and treatment allocation. Change in plaque volume was compared between statin and placebo arms with the Wilcoxon rank sum test. Intra-reader reliability for plaque volume was assessed in 14 CTAs using intra-class correlation (ICC). We previously reported change in coronary plaque volume – correlation with aortic plaque volume was assessed with Spearman's correlation coefficient.

RESULTS

Thirty-seven completed the trial (17 atorvastatin, 20 placebo). Twelve months of atorvastatin reduced aortic plaque volume relative to placebo: median change in aortic plaque volume was -107.0 mm³ [-441.0, 177.5] for atorvastatin vs. +151 mm³ [-34.3, 551.5] for placebo (p=0.015). The percent change in aortic plaque volume was -4.1% [-16.7, 7.9] for statin vs. +7.9% [-3.8, 17.6] for placebo (p=0.026). Excellent intra-reader reliability was found for aortic plaque volume (ICC: 0.90). There was not significant correlation between change in aortic and coronary plaque in individuals (rs=0.14, p=0.42).

CONCLUSION

In persons with HIV and subclinical atherosclerosis, 12 months of atorvastatin reduced aortic plaque. Absent correlation between changes in coronary and aortic plaque in individual subjects suggest possible distinct underlying pathophysiology.

CLINICAL RELEVANCE/APPLICATION

Further investigation is necessary to determine the association between changes in aortic plaque and cardiovascular events, including MI and stroke.

Honored Educators

Presenters or authors on this event have been recognized as RSNA Honored Educators for participating in multiple qualifying educational activities. Honored Educators are invested in furthering the profession of radiology by delivering high-quality educational content in their field of study. Learn how you can become an honored educator by visiting the website at: <https://www.rsna.org/Honored-Educator-Award/>

Udo Hoffmann, MD - 2015 Honored Educator

SSJ05

Chest (Functional)

Tuesday, Nov. 29 3:00PM - 4:00PM Room: S404CD

CH MR

AMA PRA Category 1 Credit™: 1.00
ARRT Category A+ Credit: 1.00

FDA Discussions may include off-label uses.

Participants

Hiroto Hatabu, MD, PhD, Boston, MA (*Moderator*) Research Grant, Toshiba Corporation; Research Grant, AZE, Ltd; Research Grant, Canon Inc; Research Grant, Konica Minolta Group
Katherine R. Birchard, MD, Chapel Hill, NC (*Moderator*) Nothing to Disclose

Sub-Events

SSJ05-01 **Fourier Decomposition Based Non-Contrast Enhanced Functional Lung MRI for Quantitative Ventilation Assessment in Patients with Cystic Fibrosis**

Tuesday, Nov. 29 3:00PM - 3:10PM Room: S404CD

Participants

Simon Veldhoen, MD, Wurzburg, Germany (*Presenter*) Nothing to Disclose
Andreas M. Weng, Wurzburg, Germany (*Abstract Co-Author*) Nothing to Disclose
Janine Knapp, Wurzburg, Germany (*Abstract Co-Author*) Nothing to Disclose
Andreas Kunz, MD, Wurzburg, Germany (*Abstract Co-Author*) Nothing to Disclose
Daniel Stab, St Lucia, Australia (*Abstract Co-Author*) Nothing to Disclose
Clemens Wirth, MD, Wurzburg, Germany (*Abstract Co-Author*) Nothing to Disclose
Florian Segerer, Wurzburg, Germany (*Abstract Co-Author*) Nothing to Disclose
Helge Hebestreit, MD, Wurzburg, Germany (*Abstract Co-Author*) Nothing to Disclose
Uwe Malzahn, PhD, Wurzburg, Germany (*Abstract Co-Author*) Nothing to Disclose
Herbert Koestler, PhD, Wurzburg, Germany (*Abstract Co-Author*) Nothing to Disclose
Thorsten A. Bley, MD, Hamburg, Germany (*Abstract Co-Author*) Nothing to Disclose

PURPOSE

To assess the clinical feasibility of Fourier decomposition-based SENCEUL-MRI (Self-gated Non-Contrast-Enhanced Functional Lung imaging) for quantitative ventilation imaging in patients with cystic fibrosis (CF).

METHOD AND MATERIALS

Following review board approval and informed consent of all participants, 20 CF patients and 20 matched healthy volunteers underwent Fourier decomposition-based MRI on a 1.5T scanner using the SENCEFUL approach, which utilizes a 2D-FLASH sequence with quasi-random sampling for data acquisition. The lungs were manually segmented from the ventilation-weighted images for automatic measurements of the quantitative ventilation (QV) indicated in ml gas per ml lung parenchyma per respiratory cycle (ml/ml). QV was compared for CF patients and volunteers and QV values of the CF patients were correlated to results of pulmonary function testing. Three radiologists rated the functional images for presence of ventilation deficits.

RESULTS

QV of the lungs was lower for CF patients (0.09 vs. 0.11 ml/ml, $p < 0.01$, Figure 1). In accordance with the known predominate affection of upper parts of the lungs in CF, QV ratios of upper to lower lung quadrants were lower in CF patients expressing less ventilation of the upper parts (right, 0.84 vs. 1.16, $p < 0.001$; left, 0.88 vs. 1.11, $p = 0.02$). Accordingly, ventilation differences between the groups were larger in the upper quadrants (mean difference 0.04 ml/ml, $p < 0.01$). Mean breathing frequency was significantly higher in CF patients with 20 respiratory cycles per minute vs. 16 in the controls ($p < 0.01$). QV values of CF patients correlated with vital capacity ($r = 0.7$, $p = 0.01$), with residual volume (marker for static hyperinflation, $r = -0.8$, $p < 0.01$) and with FEV1 (marker for airway obstruction, $r = 0.7$, $p = 0.02$). A pattern of widely distributed small ventilation deficits was found in 40% of the patient's maps vs. 8% of the volunteers. Unimpaired ventilation was found in 28% vs. 67%, respectively ($p < 0.001$).

CONCLUSION

SENCEFUL-MRI is feasible for contrast-free quantitative ventilation assessment. CF patients show less ventilation of upper lung parts and lower overall QV values, which correlate with vital capacity and with markers for hyperinflation and airway obstruction.

CLINICAL RELEVANCE/APPLICATION

Fourier decomposition-based SENCEFUL-MRI allows for site-resolved assessment of lung ventilation in cystic fibrosis without the necessity for contrast application or breath-holds.

SSJ05-02 **Acinar Scale Relative Regional Air Volume Change Maps Reflecting Mechanics of LAAs in COPD Patients**

Tuesday, Nov. 29 3:10PM - 3:20PM Room: S404CD

Participants

Kum Ju Chae, MD, Seoul, Korea, Republic Of (*Presenter*) Nothing to Disclose
Chang Hyun Lee, MD, PhD, Seoul, Korea, Republic Of (*Abstract Co-Author*) Nothing to Disclose
Ji Woong Choi, Iowa city, IA (*Abstract Co-Author*) Nothing to Disclose
Gong Yong Jin, MD, PhD, Jeonju, Korea, Republic Of (*Abstract Co-Author*) Nothing to Disclose
Margaret Park, Seoul, Korea, Republic Of (*Abstract Co-Author*) Nothing to Disclose

Ching-Long Lin, PhD, Iowa City, IA (*Abstract Co-Author*) Nothing to Disclose
Eric A. Hoffman, PhD, Iowa City, IA (*Abstract Co-Author*) Founder, VIDA Diagnostics, Inc Shareholder, VIDA Diagnostics, Inc
Advisory Board, Siemens AG
Hyun-Ju Lee, MD, PhD, Seoul, Korea, Republic Of (*Abstract Co-Author*) Nothing to Disclose

PURPOSE

Low attenuation areas (LAAs) on CT scans have been used to evaluate emphysema and air trapping. However, the regional ventilation changes of LAAs while breathing may vary due to the various causes of emphysema or air trapping. Therefore, the purpose of this study was to investigate regional air volume change at acinar scale of the lung using mass preserving image registration technique and compare with the $-950HU_{insp}$, $-856HU_{exp}$ and PFTs in COPD.

METHOD AND MATERIALS

18 emphysema patients (12 centriacinar, 6 distal acinar emphysema) and 10 normal subjects were included in the study. VIDA Apollo software (Coralville, IA) and mass preserving image registration technique were used to compute relative regional air volume change (RRAVC) between inspiration and expiration CT scans. Then, low ventilation area (LVA) was defined as percent lung volume of RRAVC < 0.8. $-950HU_{insp}$, $-856HU_{exp}$ and LVA0.8 in total lung were correlated with FEV₁, FEV₁/FVC and compared between normal and emphysema patients.

RESULTS

LVA0.8 and $-856HU_{exp}$ showed positive correlation with FEV₁ ($r=-0.89$ and $p=0.016$, $r=-0.91$, $p=0.014$) while $-950HU_{insp}$ did not show a correlation with FEV₁ in distal acinar emphysema patients. $-950HU_{insp}$ and $-856HU_{exp}$ correlated well with FEV₁/FVC in centriacinar emphysema ($r=-0.61$, $p=0.036$; $r=-0.65$, $p=0.021$). In the RRAVC map, LVA0.8 (colored blue) was well-matched with low attenuation (emphysema) regions, demonstrating decreased ventilation (air volume change) when compared with adjacent normal lung.

CONCLUSION

RRAVC map correlates well with FEV₁ and demonstrates various ventilation patterns in the LAAs on CT in COPD and the proposed LVA0.8 may provide additional functional information at an acinar scale, supplementing LAAs in quantitative CT scans.

CLINICAL RELEVANCE/APPLICATION

Relative regional air volume change map using mass preserving registration technique may be useful for the explanation of different pathophysiology of the LAAs in COPD.

SSJ05-03 DCE-MRI versus 18F FDG PET/CT: Which is Better in Differentiation Between Malignant and Benign Solitary Pulmonary Nodules?

Tuesday, Nov. 29 3:20PM - 3:30PM Room: S404CD

Participants

Feng Feng, Nan Tong, China (*Presenter*) Nothing to Disclose
Peng Cao, Shanghai, China (*Abstract Co-Author*) Nothing to Disclose
Ganlin Xia, nantong, China (*Abstract Co-Author*) Nothing to Disclose

PURPOSE

To prospectively compare the diagnosis efficacy of dynamic contrast enhanced-MRI (DCE-MRI) with that of PET/CT for differentiation between malignant and benign solitary pulmonary nodules (SPN). To find out the correlations between the quantitative MR pharmacokinetic parameters including K_{trans}, K_{ep}, V_e, and PET/CT parameter maximum standardized uptake value (SUV_{max}).

METHOD AND MATERIALS

49 consecutive patients (29 males and 20 females; Age range: 44 -78 years; Mean value: 62 years) with SPNs were included in this prospective study. 32 SPNs were malignant, the other 17 were benign. All these patients underwent DCE-MRI and PET/CT. The quantitative MR pharmacokinetic parameters including K_{trans}, K_{ep}, and V_e were calculated using Extended-Tofts Linear two-compartment model. SUV_{max} was also measured. Inter- and intraobserver agreement was analyzed by Bland and Altman plots. Metabolic and perfusion parameters of benign and malignant lesions were compared using the Mann-Whitney U test. The sensitivity, specificity for differentiating malignant from benign lung lesions were calculated for PET-CT and MRI parameters. ROC curve was used to find the optimal cut-off.

RESULTS

1. Good intra- and interobserver reproducibility was obtained for K_{trans}, K_{ep}, V_e and SUV_{max}. 2. There were significant differences between malignant and benign nodules in K_{trans}, K_{ep} ($P < 0.05$). There was a statistical difference between malignant and benign nodules in SUV_{max} ($P < 0.05$). There were no significant differences between malignant and benign nodules in V_e ($P > 0.05$). 3. The AUC of K_{trans}, K_{ep}, and SUV_{max} between malignant and benign nodules were 0.909, 0.838, and 0.759, respectively. The sensitivity of these parameters were 90.6%, 87.5%, and 75.0% and specificity were 82.4%, 76.5%, and 70.6% for the differential diagnosis of solitary pulmonary nodule if taken the maximum Youden's index as cut-off. There were no significant differences of AUC between K_{trans} and SUV_{max}, as well as K_{ep} and SUV_{max} for differential diagnosis of solitary pulmonary nodule ($P > 0.05$).

CONCLUSION

The sensitivity and specificity of K_{trans} and K_{ep} in diagnostic performance for the differentiation of malignant from benign nodules were higher than those of SUV_{max} but had no significant difference between them.

CLINICAL RELEVANCE/APPLICATION

MRI has the following advantages over FDG-PET: (1) no radiation; (2) less time; (3) economic.

SSJ05-04 Time-Resolved Hyperpolarised Xenon Lung Imaging (HP 129Xe-MRI) for Evaluation of Collateral Ventilation in Chronic Obstructive Pulmonary Disease (COPD)

Awards

Student Travel Stipend Award

Participants

Tahreema N. Matin, MBBS, Oxford, United Kingdom (*Presenter*) Nothing to Disclose
Mitchell Chen, DPhil, MBBS, Oxford, United Kingdom (*Abstract Co-Author*) Nothing to Disclose
Ozkan Doganay, PhD, Oxford, United Kingdom (*Abstract Co-Author*) Nothing to Disclose
Xiaojun Xu, MSc, DPhil, Oxford, United Kingdom (*Abstract Co-Author*) Employee, Perspectum Diagnostics
Tom Doel, DPhil, Oxford, United Kingdom (*Abstract Co-Author*) Nothing to Disclose
Najib Rahman, MSc, DPhil, Oxford, United Kingdom (*Abstract Co-Author*) Nothing to Disclose
Vicente Grau, PhD, Oxford, United Kingdom (*Abstract Co-Author*) Nothing to Disclose
Annabel Nickol, Oxford, United Kingdom (*Abstract Co-Author*) Nothing to Disclose
Fergus V. Gleeson, MBBS, Oxford, United Kingdom (*Abstract Co-Author*) Consultant, Alliance Medical Limited Consultant, Blue Earth Diagnostics Limited Consultant, Polarean, Inc

PURPOSE

To demonstrate the feasibility of time-resolved hyperpolarised xenon lung imaging (HP 129Xe-MRI) for evaluation of delayed and collateral ventilation in patients with chronic obstructive pulmonary disease (COPD).

METHOD AND MATERIALS

Fourteen patients with COPD (stage II – IV GOLD criteria classification) underwent HP 129Xe-MRI at 1.5T, combined nuclear medicine ventilation and computed tomography (NM-V SPECT/CT) at a single time point. Time-resolved HP 129Xe-MRI involved repeat acquisition of coronal image slices at 3-second intervals up to five times during a single breath-hold. In house software was used to quantify the ventilation level per pulmonary lobe at each time point. Delayed ventilation (DV) was defined increased ventilation in a lobe showing ventilation defects at baseline. Corresponding co-registered coronal image slices acquired with NM-V SPECT/CT were reviewed for any discernable differences that may contribute to collateral ventilation. Interlobar fissure completeness was evaluated on CT by the presence of >90% fissure in at least one plane. The McNemar's test was used to determine the association between CT predicted collateral ventilation from fissure integrity and observed HP 129Xe-MR DV in each lobe.

RESULTS

DV was demonstrated in 13 of the 14 patients involving a total of 42 pulmonary lobes. No differences in pulmonary parenchyma were visible on CT between lobes that did and did not show DV. Furthermore, DV demonstrated with HP 129Xe-MRI was not observed on co-registered NM-V image slices. There was a statistically significant association between CT predicted collateral ventilation from fissure integrity and HP 129Xe-MRI delayed ventilation in the left upper and lower lobes ($\chi^2 = 6.13$, $p = 0.01$ and $\chi^2 = 6.13$, $p = 0.01$).

CONCLUSION

Time-resolved breath-hold HP 129Xe-MR ventilation imaging is a feasible technique to demonstrate DV in patients with COPD. Future work may confirm that the observed DV represents collateral ventilation and subsequently identify a potential role for HP 129Xe-MRI to improve patient selection for regional treatments including lung volume reduction surgery and endobronchial valve placement.

CLINICAL RELEVANCE/APPLICATION

Delayed ventilation detection with HP 129Xe-MRI is superior to NM-V SPECT/CT detection. It may be of clinical value in patients considered for lung volume reduction therapy.

SSJ05-05 Application of Image Registration Based Local Displacement Measurement (Lung Motionography) for the Assessment of Lung Fibrosis

Tuesday, Nov. 29 3:40PM - 3:50PM Room: S404CD

Participants

Jiwoong Choi, PhD, Seoul, Korea, Republic Of (*Presenter*) Nothing to Disclose
Chang Hyun Lee, MD, PhD, Seoul, Korea, Republic Of (*Abstract Co-Author*) Nothing to Disclose
Kum Ju Chae, MD, Seoul, Korea, Republic Of (*Abstract Co-Author*) Nothing to Disclose
Gong Yong Jin, MD, PhD, Jeonju, Korea, Republic Of (*Abstract Co-Author*) Nothing to Disclose
Ching-Long Lin, PhD, Iowa City, IA (*Abstract Co-Author*) Nothing to Disclose
Eric A. Hoffman, PhD, Iowa City, IA (*Abstract Co-Author*) Founder, VIDA Diagnostics, Inc Shareholder, VIDA Diagnostics, Inc Advisory Board, Siemens AG
Hyun-Ju Lee, MD, PhD, Seoul, Korea, Republic Of (*Abstract Co-Author*) Nothing to Disclose
Jin Mo Goo, MD, PhD, Seoul, Korea, Republic Of (*Abstract Co-Author*) Nothing to Disclose

PURPOSE

Elastography has been used for the assessment of fibrosis in the liver and breast. However, ultrasonography is not easy to be applied for the fibrosis in the lung parenchyma due to the air. In this study, we applied image registration based local displacement information from expiration to inspiration to grade the degree of fibrosis in the idiopathic interstitial lung disease such as usual interstitial pneumonia and nonspecific interstitial pneumonia.

METHOD AND MATERIALS

10 normal and 18 idiopathic interstitial lung disease (13 IPF and 5 NSIP) subjects were included in our study. VIDA Apollo software (Coralville, Iowa) and mass preserving image registration technique were used to compute displacement vectors of local lung regions at an acinar scale. Three-dimensional displacements and dorsal basal displacements were normalized by the cubic root of global lung volume change from expiration to inspiration CT scans. Displacements and volume changes in the upper and lower lobes and the whole lung are compared between three groups using analysis of variance test (ANOVA).

RESULTS

IPF and NSIP were not differentiated by volume changes of the whole lung or upper and lower lobes, whereas lower lobe air volume change were smaller in both IPF and NSIP than normal subjects ($p=0.02$, $p=0.001$). In the whole lung, dorsal basal displacement was smaller in ILD and normal subjects ($p=0.035$), while three-dimensional displacement was not different between the groups. Three-dimensional and dorsal basal displacement was smaller in the lower lobes of IPF subjects than NSIP ($p=0.044$) and normal ($p=0.006$) subjects.

CONCLUSION

Lung motionography using image registration based dorsal basal displacement in the lower lobe may be used for the understanding of the structure-function relationships in fibrotic lung disease.

CLINICAL RELEVANCE/APPLICATION

Image registration based local displacement information may help us to assess the degree of lung fibrosis and to make a diagnosis in the fibrotic lung disease.

SSJ05-06 Deep Convolutional Neural Network Approaches in Making a Diagnosis with Chest Radiographs: Initial Experience

Tuesday, Nov. 29 3:50PM - 4:00PM Room: S404CD

Participants

Chang Min Park, MD, PhD, Seoul, Korea, Republic Of (*Presenter*) Nothing to Disclose
Jong Hyuk Lee, MD, Seoul, Korea, Republic Of (*Abstract Co-Author*) Nothing to Disclose
Anthony S. Paek, PhD, Seoul, Korea, Republic Of (*Abstract Co-Author*) CEO, Lunit Inc
Sangheum Hwang, Seoul, Korea, Republic Of (*Abstract Co-Author*) Employee, Lunit Inc
Meejin Cho, MD,JD, Seoul, Korea, Republic Of (*Abstract Co-Author*) Employee, Lunit Inc
Su Suk Oh, Seoul, Korea, Republic Of (*Abstract Co-Author*) Nothing to Disclose
Jin Mo Goo, MD, PhD, Seoul, Korea, Republic Of (*Abstract Co-Author*) Nothing to Disclose

PURPOSE

Chest radiograph (CR) is the first-line and most common method for the diagnosis of pulmonary diseases. The purpose of this study was to develop a deep convolutional neural network model for the purposes of making a diagnosis with CRs and to evaluate its diagnostic performance in 102,885 CRs.

METHOD AND MATERIALS

From 2010 to 2015, 102,885 CRs were taken at our hospital in 24,105 individuals which were then subcategorized into normal and abnormal CRs based on radiologists' reports (37,247 normal CRs from 4,572 individuals (M:F=1,831:2,741; mean age, 53.3years) and 65,638 abnormal CRs from 19,533 individuals (M:F=11,127:8,406; mean age, 58.6years)). Abnormal CRs were those in which lung diseases such as pneumonia, emphysema, diffuse interstitial lung disease, tuberculosis, lung cancer, and pulmonary metastasis were present. All CRs were randomly divided into group 1 (27,224 normal and 55,638 abnormal), group 2 (5,021 normal and 4,995 abnormal), and group 3 (5,002 normal and 5,005 abnormal). Thereafter, a diagnostic model based on a deep convolutional neural network was developed using a 25-layer deep residual network and trained with the group 1 dataset, validated through the group 2 dataset, and tested for diagnostic performance using the group 3 dataset. The diagnostic performance of the model was evaluated using receiver-operating characteristics (ROC) curve analysis.

RESULTS

In the validation dataset, the trained deep neural network model showed an area under the ROC curve (AUC) of 0.944, with an accuracy, sensitivity and specificity of 86.6%, 87.8% and 85.4%, respectively. When tested with the group 3 dataset, the AUC of the established algorithm was 0.948 (accuracy, 88.0%; sensitivity, 88.8%; specificity, 87.2%). When specificity was set at 99% and 95%, the algorithm showed sensitivities of 60.1% and 79.6%, respectively. There were no significant differences in the diagnostic performance of the trained model between the validation setting and the test setting ($p=0.165$).

CONCLUSION

A data-driven diagnostic model based on a deep neural network demonstrated high diagnostic performance in differentiating normal from abnormal CR findings.

CLINICAL RELEVANCE/APPLICATION

A diagnostic system based on a deep convolutional neural network has high diagnostic performance in differentiating normal and abnormal CRs, and thus helps radiologists read CRs with high accuracy.

SSJ06

Emergency Radiology (Dual Energy CT)

Tuesday, Nov. 29 3:00PM - 4:00PM Room: N227B



AMA PRA Category 1 Credit™: 1.00
ARRT Category A+ Credit: 1.00

FDA Discussions may include off-label uses.

Participants

Martin L. Gunn, MBChB, Seattle, WA (*Moderator*) Research Grant, Koninklijke Philips NV; Royalties, Cambridge University Press; Spouse, Consultant, Reed Elsevier; Spouse, Consultant, athenahealth, Inc; ;
Aaron D. Sodickson, MD, PhD, Boston, MA (*Moderator*) Research Grant, Siemens AG; Consultant, Bayer AG

Sub-Events

SSJ06-01 Role of a Novel Material Decomposition Algorithm in Detection of Acute Infarction

Tuesday, Nov. 29 3:00PM - 3:10PM Room: N227B

Awards

Student Travel Stipend Award

Participants

Mohammed F. Mohammed, MBBS, Vancouver, BC (*Presenter*) Nothing to Disclose
Faisal Khosa, FFR(RCSI), FRCPC, Atlanta, GA (*Abstract Co-Author*) Nothing to Disclose
David J. Ferguson, MBBCh, FRCR, Vancouver, BC (*Abstract Co-Author*) Nothing to Disclose
Reem S. Zakzouk, MD, Riyadh, Saudi Arabia (*Abstract Co-Author*) Nothing to Disclose
Olivia Marais, BEng, Vancouver, BC (*Abstract Co-Author*) Nothing to Disclose
Tim O'Connell, MD, Meng, Vancouver, BC (*Abstract Co-Author*) President, Resolve Radiologic Ltd Speake, Siemens AG
Heiko Schmiedeskamp, PhD, Malvern, PA (*Abstract Co-Author*) Employee, Siemens AG
Bernhard Krauss, PhD, Forchheim, Germany (*Abstract Co-Author*) Employee, Siemens AG
Michael E. O'Keefe, MBBCh, Vancouver, BC (*Abstract Co-Author*) Speaker, Siemens AG
Axel C. Rohr, MD, Kiel, Germany (*Abstract Co-Author*) Nothing to Disclose
Patrick D. McLaughlin, FFRCSI, Vancouver, BC (*Abstract Co-Author*) Speaker, Siemens AG
Savvas Nicolaou, MD, Vancouver, BC (*Abstract Co-Author*) Institutional research agreement, Siemens AG

PURPOSE

The role of the non-enhanced CT in the setting of acute stroke has always been that of a quick rule-out tool to exclude haemorrhage, with low accuracy in detecting acute infarcts and reported accuracy of 61%.DECT with material decomposition (MD) has shown promise in post post intra-arterial revascularization. We present a novel material decomposition algorithm which improves detection of acute infarcts on non-enhanced DECT by subtracting grey and white matter, accentuating cytotoxic edema.

METHOD AND MATERIALS

A retrospective study was conducted on consecutive patients that presented to the Emergency Department (ED) at our institution between January, 2016 and March, 2016, with clinical suspicion of stroke within the last 4 hours and underwent non-enhanced Dual Energy CT (DECT) of the head (N = 26). Informed consent was waived for this retrospective study. Follow up CT, MRI or catheter angiography served as the reference standard.DECT images were acquired on a 3rd generation Dual Source DECT scanner at 100 kV and 150 kV. Material decomposition (MD) images were reconstructed on the Syngo.Via platform, allowing subtraction of Grey Matter (GM) from White Matter (WM).The images were reviewed by 2 neuroradiology fellowship trained radiologists, blinded to outcomes, and independently rated concordance of 120 kV images and MD images with the reference standard.

RESULTS

15 of 26(57.7 %) patients presented with confirmed acute infarcts. 120 kV images had a sensitivity, specificity, PPV and NPV of 80% (95% CI = 51.9%-95.7%), 72.7% (95% CI = 39%-94%), 80% (95% CI = 51.9%-95.7%) and 72.73% (95% CI 51.91%-95.67%) respectively.MD images provided greater sensitivity, specificity, PPV and NPV of 93.33% (95% CI = 68.05%-99.83%), 100% (95% CI = 71.51%-100%), 100% (95% CI = 76.84%-100%) and 91.67% (95% CI = 61.52%-99.79%) respectively when assessed in conjunction with the conventional images. MD images improved confidence by 30.77% and were found useful in 85% of studies.

CONCLUSION

Head DECT with MD images reconstructed to subtract GM from WM improve the PPV and NPV of non-enhanced CT in the setting of acute infarction, up to 100% and 91.67% respectively while boosting confidence by 30.77% when read in conjugation with conventional 120 kV blended images.

CLINICAL RELEVANCE/APPLICATION

MD images provide a novel tool in assessment of acute stroke on the non-enhanced CT of the head.

SSJ06-02 Advanced Virtual Monoenergetic Imaging in Low-dose Dual-energy Unenhanced Head CT: Evaluation of Image Quality, Delineation of Intracranial Hemorrhage and Radiation Exposure

Tuesday, Nov. 29 3:10PM - 3:20PM Room: N227B

Participants

Christoph Polkowski, MD, Frankfurt, Germany (*Presenter*) Nothing to Disclose
Moritz Kaup, Frankfurt, Germany (*Abstract Co-Author*) Nothing to Disclose
Doris Leithner, MD, Frankfurt am Main, Germany (*Abstract Co-Author*) Nothing to Disclose

Moritz H. Albrecht, MD, Charleston, SC (*Abstract Co-Author*) Nothing to Disclose
Julian L. Wichmann, MD, Charleston, SC (*Abstract Co-Author*) Nothing to Disclose
Claudia Frellesen, Frankfurt, Germany (*Abstract Co-Author*) Nothing to Disclose
Thomas J. Vogl, MD, PhD, Frankfurt, Germany (*Abstract Co-Author*) Nothing to Disclose
Jan-Erik Scholtz, MD, Boston, MA (*Abstract Co-Author*) Nothing to Disclose

PURPOSE

To evaluate quantitative image quality parameters of advanced monoenergetic imaging algorithm (VMI+) in low-tube-current dual-energy unenhanced head CT and diagnostic accuracy for the detection of intracranial hemorrhage (ICH) compared to standard 120-kVp.

METHOD AND MATERIALS

In this retrospective IRB-approved study with a waiver for written consent, 94 patients underwent unenhanced head CT to detect or rule out ICH on a third-generation dual-source CT. Standard 120-kVp CT (n=44; CTDIvol, 39.5±0.4mGy) was compared with low-tube-current dual-energy CT (DECT, 80/140-kVp; n=50, CTDIvol, 23.7±2.7mGy) with post-processing VMI+ algorithm. Gray matter (GM) signal-to-noise ratio (SNR), white matter (WM) SNR, GM-WM contrast-to-noise ratio (CNR), ICH-GM CNR, and posterior fossa artifact index (PFAI) were calculated. Measurements in VMI+ were performed at energy levels from 40-190-keV with 5-keV increment. Image series with highest GM-WM CNR and ICH-GM CNR in VMI+ were reconstructed for subjective image analysis. Three radiologists performed diagnostic evaluation for ICH for both protocols, "gold standard" for ICH evaluation was the medical report.

RESULTS

GM SNR (18.5±3.5 vs. 11.7±1.9) and WM SNR (15.5±2.5 vs. 8.2±1.2) were significantly better at 110-keV VMI+ compared to 120-kVp. GM-WM CNR was highest at 40-keV with no significant difference compared to 120-kVp (2.3±0.6 vs 2.2±0.6). ICH-GM CNR was significantly higher in 140-keV compared to 120-kVp (7.7±3.7 vs. 3.4±2.7, p<0.001). 110-keV VMI+ showed slightly, but not significantly lower values for ICH-GM CNR compared to 140-keV. PFAI was significantly lower at 110-keV compared to 120-kVp (2.1±0.3 vs 4.9±0.5HU, p<0.001). All examinations were sufficient for evaluation of ICH in 120-kVp and 110-keV VMI+ with no non-diagnostic cases. 40-keV VMI+ with best values for GM-WM CNR was inadequate for evaluation of ICH non-diagnostic to poor ratings. Diagnostic accuracy for detection of ICH was excellent in both 110-keV VMI+ (n=14) and 120-kVp (n=11) with no significant difference and almost perfect interobserver agreement (ICC, 0.88).

CONCLUSION

110-keV VMI+ low-dose dual-energy unenhanced head CT provides increased CNR between ICH and GM with excellent diagnostic accuracy of ICH while radiation dose is significantly reduced compared to 120-kVp.

CLINICAL RELEVANCE/APPLICATION

110-keV VMI+ allows low-dose unenhanced head dual-energy CT with superior ICH to GM contrast compared to 120-kVp.

SSJ06-03 The Dual Energy Hot Gallbladder and Rim Signs: Evaluation of DECT Iodine Content in Acute Cholecystitis

Tuesday, Nov. 29 3:20PM - 3:30PM Room: N227B

Participants

Jennifer W. Uyeda, MD, Boston, MA (*Presenter*) Nothing to Disclose
Tony W. Trinh, MD, Salt Lake City, UT (*Abstract Co-Author*) Nothing to Disclose
Jeremy R. Wortman, MD, Boston, MA (*Abstract Co-Author*) Nothing to Disclose
Aaron D. Sodickson, MD, PhD, Boston, MA (*Abstract Co-Author*) Research Grant, Siemens AG; Consultant, Bayer AG

PURPOSE

ED patients often undergo abdominal CT as the initial imaging examination for nonspecific abdominal pain. The purpose of this study was to assess differences in the dual energy CT (DECT) iodine content of pericholecystic hepatic parenchyma and of the gallbladder wall in acute cholecystitis compared with controls.

METHOD AND MATERIALS

17 patients (10M, 7F) who underwent cholecystectomy with pathology confirmed acute cholecystitis were included in this IRB approved, HIPAA compliant study. All patients underwent contrast enhanced DECT on a dual-source 128x2 slice scanner (Siemens FLASH) with either 80/Sn140 or 100/Sn140 kV pairs depending on patient size. Within 3 mm reconstructed slices, the following regions of interest (ROI) were placed on iodine overlay images to measure dual energy iodine concentration derived from three material decomposition: 1 cm² hepatic parenchyma around the gallbladder fossa, 1 cm² hepatic parenchyma in a different hepatic segment, and 5 mm² on the gallbladder wall. These values were normalized to the iodine concentration in a main portal vein ROI to calculate a normalized iodine concentration. Measurements were compared to 20 control patients who underwent DECT without gallbladder pathology. Normalized iodine content in each of the three ROI locations was compared between the two groups using a t-test.

RESULTS

There was no significant difference between cholecystitis and control patients in normalized iodine content within the hepatic parenchyma remote from the gallbladder fossa (p=0.72). However, compared with controls, acute cholecystitis patients demonstrated higher normalized iodine concentration values within the hepatic parenchyma of the gallbladder fossa and within the gallbladder wall (p<0.001 for both comparisons).

CONCLUSION

DECT can detect increased pericholecystic hepatic parenchymal and gallbladder wall iodine content in patients with acute cholecystitis. Further work is needed to determine appropriate threshold values of iodine content that may aid in the diagnosis of acute cholecystitis.

CLINICAL RELEVANCE/APPLICATION

Cholecystitis patients demonstrate increased iodine content within the gallbladder wall and pericholecystic hepatic parenchyma by

Dual Energy CT. This may prove helpful in improving CT diagnosis of acute cholecystitis.

Honored Educators

Presenters or authors on this event have been recognized as RSNA Honored Educators for participating in multiple qualifying educational activities. Honored Educators are invested in furthering the profession of radiology by delivering high-quality educational content in their field of study. Learn how you can become an honored educator by visiting the website at: <https://www.rsna.org/Honored-Educator-Award/>

Aaron D. Sodickson, MD, PhD - 2014 Honored Educator

SSJ06-04 Detection of Isodense Gallstones using Monoenergetic Dual Energy CT: Evaluation of Stone Size Thresholds

Tuesday, Nov. 29 3:30PM - 3:40PM Room: N227B

Awards

Student Travel Stipend Award

Participants

Jun Wang, MD, Vancouver, BC (*Presenter*) Nothing to Disclose

Yuhao Wu, Vancouver, BC (*Abstract Co-Author*) Nothing to Disclose

Faisal Khosa, FFR(RCSI), FRCPC, Atlanta, GA (*Abstract Co-Author*) Nothing to Disclose

Savvas Nicolaou, MD, Vancouver, BC (*Abstract Co-Author*) Institutional research agreement, Siemens AG

Tim O'Connell, MD, Meng, Vancouver, BC (*Abstract Co-Author*) President, Resolve Radiologic Ltd Speake, Siemens AG

Luck J. Louis, MD, Vancouver, BC (*Abstract Co-Author*) Nothing to Disclose

Patrick D. McLaughlin, FFRCSI, Vancouver, BC (*Abstract Co-Author*) Speaker, Siemens AG

PURPOSE

To establish the size threshold for identifying previously undetectable isodense gallstones using monoenergeticDual Energy CT (DECT)

METHOD AND MATERIALS

A retrospective review was performed on 3464 consecutive DECT scans of the abdomen acquired using a dual-source 128-slice CT (Definition FLASH; Siemens Healthcare, Forchheim, Germany) between the dates January 2013-June 2015. These patients were cross-referenced using our Picture Archival and Communication System (Impax; Agfa Healthcare, Mortsel, Belgium) to select those who had undergone an ultrasound of the gallbladder, MRCP or ERCP within six weeks of the DECT scan. Inclusion criteria were patients who had a DECT scan that did not demonstrate cholelithiasis, but a subsequent investigation (US, MRCP, or ERCP) that did demonstrate gallstones. Monoenergetic reconstructions were then performed at 40 keV and 190 keV using the DECT raw data from these patients with gallstone disease that was missed on conventional CT. Overall sensitivity for using monoenergetic reconstructions to detect isodense gallstones was calculated. Attenuation measurements were made using 1cm² regions of interest in the gallbladder as well as the gallstones at 190 keV and 40 keV.

RESULTS

Monoenergetic reconstructions at 40 keV and 190 keV were performed on a total of 31 patients who fit the inclusion criteria and reviewed for the presence of gallstones. Eight patients had identifiable gallstones. Using a size threshold of <10mm, the sensitivity of monoenergetic imaging to detect previously missed isodense gallstones was 25.8%. When a threshold size of >10mm was used, the sensitivity of monoenergetic reconstructions to identify previously missed isodense gallstones increased to 88.9%. ROI measurements of the gallbladder at 190 keV (mean attenuation 7.77±5.80 HU) were significantly different from gallstone ROI attenuation (44.9±14.5 HU, p<0.001.). ROI measurements of the gallstones and gallbladder at 40 keV did not differ significantly (3.70±47.6 HU vs. 23.9±22.5 HU).

CONCLUSION

Monoenergetic dual energy CT acquisitions of the abdomen at 190 keV can identify gallstones that appear iso-dense on conventional CT with a sensitivity of 88.9% at a size threshold of 10mm.

CLINICAL RELEVANCE/APPLICATION

The use of monoenergetic dual energy CT imaging allows identification of previously undetectable isodense gallstones at a size threshold of 10mm and improves the sensitivity of CT in the investigation of gallstone disease.

SSJ06-05 Improved Signal and Image Quality at the Cervicothoracic Junction Utilizing Third Generation Dual Source CT Technology

Tuesday, Nov. 29 3:40PM - 3:50PM Room: N227B

Participants

Sudha R. Muly, MBBS, FRCR, Vancouver, BC (*Presenter*) Nothing to Disclose

Savvas Nicolaou, MD, Vancouver, BC (*Abstract Co-Author*) Institutional research agreement, Siemens AG

Luck J. Louis, MD, Vancouver, BC (*Abstract Co-Author*) Nothing to Disclose

Tim O'Connell, MD, Meng, Vancouver, BC (*Abstract Co-Author*) President, Resolve Radiologic Ltd Speake, Siemens AG

Patrick D. McLaughlin, FFRCSI, Vancouver, BC (*Abstract Co-Author*) Speaker, Siemens AG

Faisal Khosa, FFR(RCSI), FRCPC, Atlanta, GA (*Abstract Co-Author*) Nothing to Disclose

Nizar Bhulani, MD, Houston, TX (*Abstract Co-Author*) Nothing to Disclose

Heiko Schmiedeskamp, PhD, Malvern, PA (*Abstract Co-Author*) Employee, Siemens AG

Bernhard Krauss, PhD, Forchheim, Germany (*Abstract Co-Author*) Employee, Siemens AG

PURPOSE

Evaluation of the cervicothoracic junction is frequently limited by beam hardening and scatter radiation artifacts. Previous studies have shown the usage of dual energy CT (DECT) to reduce this artifact and improve image quality utilizing Monoenergetic algorithm (Mono +). The purpose of our study is to determine if the artifacts at the cervicothoracic junction can be further reduced and

image quality can be improved using the third generation dual source CT scanner.

METHOD AND MATERIALS

In this retrospective study, 20 consecutive trauma patients who underwent cervical spine DECT using a third generation dual source CT scanner (Definition FORCE, Siemens Health care, Germany) between February to April 2016. The DECT data sets (100 and 150 sn kv) were reconstructed using Mono + algorithm at energy levels ranging from 70 to 190 Kev. Attenuation of the spinal cord at each energy level was compared to the values on the simulated 120kv scan images obtained from the mixed DECT data sets. Subjective analysis of image quality was conducted on a semi-objective 4 point scoring scheme by 2 radiologists.

RESULTS

Our data demonstrates reduction of noise on the images of 110-130keV range, when compared to the mixed data set images of 120 kvp. We found that the optimal energy level for reduction of artifacts and noise is around 130Kev. The attenuation values of the spinal cord at C2 and at the cervico-thoracic level are most stable between 110 and 130Kev reconstruction. Semi-quantitative analysis showed improvement of visualization of the soft tissue structures at 130Kev (p value of 0.002). The diagnostic confidence of the reader in identifying bone and soft tissue abnormality at the cervico-thoracic junction was significantly increased at the higher energy levels 130 Kev (p value 0.001 compared to 70 Kev

CONCLUSION

DECT assessment using Mono + algorithm shows significantly reduced artifact at the cervicothoracic junction with increased reader confidence of assessing structures. Our study demonstrates that reconstruction of images on mono+ at energy levels closer to 130 Kev provide the best image quality with reduced beam hardening artifact reduction and noise levels.

CLINICAL RELEVANCE/APPLICATION

Due to its superior image quality, third generation dual source CT images using Mono + algorithm can provide a significant benefit by reducing artifact and improving assessment of cervicothoracic junction without increasing the radiation dose.

SSJ07

Gastrointestinal (Hepatocellular Carcinoma)

Tuesday, Nov. 29 3:00PM - 4:00PM Room: E350

GI CT MR OI US

AMA PRA Category 1 Credit™: 1.00
ARRT Category A+ Credit: 1.00

FDA Discussions may include off-label uses.

Participants

Hero K. Hussain, MD, Ann Arbor, MI (*Moderator*) Nothing to Disclose
Steven S. Raman, MD, Santa Monica, CA (*Moderator*) Nothing to Disclose

Sub-Events

SSJ07-01 **Prospective Intraindividual Comparison of Non-Contrast MRI and US as a Surveillance Tool for HCC in Patients with Cirrhosis at High Risk of HCC**

Tuesday, Nov. 29 3:00PM - 3:10PM Room: E350

Participants

Hye Young Jang, Seoul, Korea, Republic Of (*Presenter*) Nothing to Disclose
So Yeon Kim, MD, Seoul, Korea, Republic Of (*Abstract Co-Author*) Nothing to Disclose
Jae Ho Byun, MD, Seoul, Korea, Republic Of (*Abstract Co-Author*) Nothing to Disclose
So Jung Lee, Seoul, Korea, Republic Of (*Abstract Co-Author*) Nothing to Disclose
Hyung Jin Won, MD, Seoul, Korea, Republic Of (*Abstract Co-Author*) Nothing to Disclose
Jihyun An, Seoul, Korea, Republic Of (*Abstract Co-Author*) Nothing to Disclose
Young-Suk Lim, Seoul, Korea, Republic Of (*Abstract Co-Author*) Nothing to Disclose
Seong Ho Park, MD, Seoul, Korea, Republic Of (*Abstract Co-Author*) Research Grant, DONGKOOK Pharmaceutical Co, Ltd

PURPOSE

To prospectively compare the diagnostic yield of non-contrast MRI including diffusion-weighted imaging (DWI) and US as a surveillance tool for detecting HCCs in patients with cirrhosis at high risk of HCC.

METHOD AND MATERIALS

A prospective surveillance study included 407 consecutive cirrhosis patients with an estimated annual risk of HCC > 5% who underwent one to three, biannual screening examinations with paired liver MRI and US between November 2011 and August 2014. The referral criteria for HCC on non-contrast MRI were defined as a nodule showing one of the following criteria: the presence of intralesion fat, mild to moderate hyperintensity on T2-weighted imaging, or hyperintensity on DWI at b-500 s/mm². On US, a discrete focal lesion equal or more than 1cm in diameter or suspicious tumor thrombosis was referred for a further work-up for HCC. During image interpretation, radiologists were blinded to the results of the other imaging modality. The confirmation of HCC was based on the results of a histologic examination and/or typical CT images of HCC. Per-lesion sensitivity of HCC and per-exam specificity were compared between non-contrast MRI and US.

RESULTS

In 1100 screening rounds of paired MRI and US, 48 HCCs were diagnosed in 43 patients. Among the 48 HCCs, intralesional fat was detected in 4 HCCs (8.3%), 31 HCCs (64.6%) showed mild to moderate hyperintensity on T2-weighted imaging, and 37 HCC (77.1%) appeared hyperintensity on DWI. Among the 71 positive cases on US, 12 patients were confirmed to have HCC. Using the diagnostic criteria, per lesion sensitivity of non-contrast MRI was 81.3 % (39/48), which was significantly higher than that of 25% (12/48) (P<0.001). Non-contrast MRI showed a significantly higher per-exam specificity than US [98.0% (1036/1057) vs. 94.4% (998/1057), P<0.001].

CONCLUSION

In this prospective intraindividual comparison study, non-contrast MRI including DWI outperformed US as a surveillance test for HCC in patients with cirrhosis at high risk of HCC.

CLINICAL RELEVANCE/APPLICATION

In patients with cirrhosis at high risk of HCC, the non-contrast MRI including DWI can be considered to an alternative surveillance tool to US.

SSJ07-02 **Diagnostic Accuracy of Prospective Applications of Liver Imaging Reporting and Data System (LI-RADS) on Gadoteric Acid-Enhanced MRI**

Tuesday, Nov. 29 3:10PM - 3:20PM Room: E350

Participants

Yeun Yoon Kim, MD, Seoul, Korea, Republic Of (*Presenter*) Nothing to Disclose
Chansik An, MD, Seoul, Korea, Republic Of (*Abstract Co-Author*) Nothing to Disclose
Sungwon Kim, MD, Seoul, Korea, Republic Of (*Abstract Co-Author*) Nothing to Disclose
Myeong-Jin Kim, MD, PhD, Seoul, Korea, Republic Of (*Abstract Co-Author*) Research Grant, Bayer AG

PURPOSE

To evaluate the diagnostic accuracy of prospectively applied Liver Imaging Reporting and Data System (LI-RADS, v2014) for hepatocellular carcinoma (HCC) on gadoteric acid-enhanced liver MRI.

METHOD AND MATERIALS

This study included 528 hepatic observations from 268 patients who met the following criteria: 1) at high risk for HCC, 2) underwent gadoxetic acid-enhanced liver MRI in 2014 at our institution, 3) not previously treated for HCC, and 4) whose radiologic reports were prospectively reported using LI-RADS. Final diagnoses were determined histologically for all non-HCC malignancies (two cholangiocarcinomas [CCs] and four combined HCC-CCs), 110 of 122 HCCs, seven regenerative or dysplastic nodules, and one hemangioma. Fifty benign lesions and 12 HCCs were clinically diagnosed with follow-up imaging. The sensitivities and specificities of LI-RADS categories were calculated with 95% confidence intervals (CIs).

RESULTS

None of the nine (0%) LR-1, one of 22 (4.5%) LR-2, 14 of 35 (40.0%) LR-3, 19 of 27 (70.4%) LR-4, 73 of 75 (97.3%) LR-5, and all of the five (100%) LR-5V observations were HCCs. Two of 75 (2.7%) LR-5 observations were combined HCC-CCs. Of 13 LR-M lesions, only three (23.1%) were non-HCC malignancies and the remainder were HCCs. Three of six (50%) non-HCC malignancies were categorized as LR-4 or LR-5. When LR-5 and LR-5V were considered positive diagnosis for HCC, the sensitivity and specificity were 63.9% (95% CI, 54.8–72.4) and 96.9% (95% CI, 89.2–99.6), respectively. When LR-4, LR-5, and LR-5V were considered positive, the sensitivity and specificity were 79.5% (95% CI, 71.3–86.3) and 84.4% (95% CI, 73.1–92.2), respectively.

CONCLUSION

In high-risk patients for HCC, LR-5 and LR-5V showed a high specificity for diagnosing HCC. However, a significant portion of non-HCC malignancies were categorized as LR-4 or LR-5 and a majority of LR-M lesions were HCCs, which suggests the necessity for modification of criteria for the LR-M category.

CLINICAL RELEVANCE/APPLICATION

LR-M category of LI-RADS v2014 needs improvement to better exclude non-HCC malignancies in high risk patients for HCC and to decrease the misdiagnosis rate of HCCs as non-HCC malignancies.

SSJ07-03 Abdominal Ultrasound Compared to Cross-Sectional Imaging for Surveillance of Hepatocellular Carcinoma in High Risk Patients: Results of 5-year Cohort Follow-up

Tuesday, Nov. 29 3:20PM - 3:30PM Room: E350

Participants

Francois Willemsen, MD, Hoogstraten, Belgium (*Presenter*) Nothing to Disclose
Lievay van Dam, MSc, MD, Rotterdam, Netherlands (*Abstract Co-Author*) Nothing to Disclose
Roy S. Dwarkasing, MD, PhD, Rotterdam, Netherlands (*Abstract Co-Author*) Nothing to Disclose

PURPOSE

Hepatocellular carcinoma (HCC) is the most common primary malignant tumor of the liver and is the third leading cancer-related cause of death. Major risk factors are identified including cirrhosis caused by viral hepatitis B and C infection, and hereditary hemochromatosis. According to European guidelines patients at risk for HCC should be surveyed with abdominal ultrasound (US) every 6 months.

METHOD AND MATERIALS

In our tertiary referral institute, we selected all patients between October 2005-October 2010 from our HCC database. Inclusion criteria were: pathological or histochemical confirmed HCC, abdominal ultrasound and contrast-enhanced computed tomography (CT) or magnetic resonance imaging (MRI) within three months. Number and size of the detected lesions were compared.

RESULTS

In 88 patients included, 83 HCC lesions were described at US evaluation compared to 181 lesions detected using CT or MRI. Lesions found on US had a mean diameter of 60mm (range 5-135mm, median 45mm), on cross-sectional imaging the mean diameter was 56mm (range 5-160mm, median 45mm). In 30 of the 88 (34%) patients US was negative, while cross-sectional imaging detected HCC lesions. In 18 of those 30 cases all lesions were smaller than 25mm (60%). Of all the patients (n=25) with lesions smaller than 25mm, 18 ultrasound examinations were false negative (72%).

CONCLUSION

Surveillance for HCC in high-risk patients using US is inadequate. A significant number of HCC lesions are missed using US surveillance, especially small lesions, resulting in a false negative examination in a third of the cases.

CLINICAL RELEVANCE/APPLICATION

This warrants the question if surveillance for HCC should be performed with advanced cross sectional imaging modalities.

SSJ07-04 Effect of Threshold Growth on Liver Imaging Reporting and Data System Categorization

Tuesday, Nov. 29 3:30PM - 3:40PM Room: E350

Participants

Victoria Chernyak, MD, Bronx, NY (*Presenter*) Nothing to Disclose
Mariya Kobi, MD, New York, NY (*Abstract Co-Author*) Nothing to Disclose
Kate Fruitman, Bronx, NY (*Abstract Co-Author*) Nothing to Disclose
Alla M. Rozenblit, MD, Bronx, NY (*Abstract Co-Author*) Nothing to Disclose
Claude B. Sirlin, MD, San Diego, CA (*Abstract Co-Author*) Research Grant, General Electric Company; Research Grant, Siemens AG; Research Grant, Guerbet SA; ;

PURPOSE

Liver Imaging Reporting and Data System (LI-RADS, LR) uses major features (arterial phase hyperenhancement [APHE], "washout" [WO], "capsule", diameter, threshold growth [TG]) to codify probability of an observation being hepatocellular carcinoma. Inclusion of TG in the LI-RADS algorithm was based on expert opinion rather than scientific evidence. The goal of this study was to assess the effect of TG on LR categorization.

METHOD AND MATERIALS

All MR and CT reports created using a standardized LR v2014 template at one tertiary care center between 4/15–2/16 were identified. For each LR3, LR4, and LR5 reported observation, the presence of every LR major feature was recorded retrospectively. Two LR categories were then assigned: one using all LR-v2014 major features and one using a revised system that disregards TG (LR-revised). Categories assigned using LR-v2014 and LR-revised were compared. Some analyses were repeated excluding patients without prior exams (TG not applicable).

RESULTS

136 patients (85 [62%] male, mean age 62 [\pm 10] years) with 297 observations (median diameter 13mm, IQR 9–20mm) were included. Of 297 observations, 204 (69%) had APHE, 186 (63%) had WO, 49 (16%) had "capsule" and 40 (14%) had TG. Of 40 observations with TG, 26 (65%) were new observations \geq 10mm, 8 (20%) had diameter increase \geq 50% in \leq 6 months and 6 (15%) had diameter increase \geq 100% in $>$ 6 months. LR-v2014 categories were LR3 in 131/297 (44%), LR4 in 87/297 (29%) and LR5 in 79/297 (27%). LR-revised categories were LR3 in 147/297 (50%), LR4 in 78/297 (26%) and LR5 in 72/297 (24%). Assigned categories were discrepant in 22/297 (7%) observations. 7/79 (9%) observations categorized LR5 with LR-v2014 were recategorized LR4 with LR-revised. Of these, all 7 were 10–19 mm and had APHE; 5/7 (71%) were new observations and 2/7 (29%) had diameter increase \geq 50% in \leq 6 months. When excluding 70 observations without prior exams, 22/227 (10%) categories were discrepant; 7/50 (14%) observations categorized LR5 with LR-v2014 were recategorized LR4 with LR-revised.

CONCLUSION

TG affects LI-RADS category in the minority of cases. Disregarding TG causes a small but meaningful proportion of LR5 observations to be downgraded to LR4.

CLINICAL RELEVANCE/APPLICATION

Removing threshold growth as a major feature to simplify LI-RADS algorithm would not affect final LI-RADS category in most cases but would cause downgrading of a meaningful proportion of LR5 observations.

SSJ07-05 Risk Assessment for Hepatocellular Carcinoma by Using Magnetic Resonance Elastography during Follow-up

Tuesday, Nov. 29 3:40PM - 3:50PM Room: E350

Participants

Shintaro Ichikawa, MD, Chuo-Shi, Japan (*Presenter*) Nothing to Disclose
Utaroh Motosugi, MD, Yamanashi, Japan (*Abstract Co-Author*) Nothing to Disclose
Tetsuya Wakayama, PhD, Hino-shi, Japan (*Abstract Co-Author*) Employee, General Electric Company
Hiroshi Onishi, MD, Yamanashi, Japan (*Abstract Co-Author*) Nothing to Disclose

PURPOSE

To evaluate magnetic resonance elastography (MRE) as a means for predicting the development of hepatocellular carcinoma (HCC) in chronic liver disease.

METHOD AND MATERIALS

We reviewed data from 161 patients with chronic liver disease with the following inclusion criteria: had 2 MRE examinations between days 365–1424 with $>$ 12 month interval, no prior history of or development of HCC between the two exams, and available laboratory results. Liver stiffness was classified as low ($<$ 3 kPa), moderate (3–4.7 kPa), and high ($>$ 4.7 kPa). The classification for change in stiffness between the two MREs is as follows: high on both or high on the first and moderate on the second (group A, $n=61$), low on both (group C, $n=39$), and other combinations (group B, $n=61$). We used Cox analyses and Kaplan-Meier methods to determine the risk of developing HCC.

RESULTS

Forty-seven patients (29.2%) developed HCC during the follow-up period (45.9% (28/61) of group A, 27.9% (17/61) of group B; 5.1% (2/39) of group C). There was a significant difference in the disease-free survival rates between groups A (54.9%), B (73.9%), and C (87.6%) at 3-years ($p=0.0001$). The independent risk factors for development of HCC included: belonging to Group A (hazard ratio [HR] versus group C=6.0, $P=0.0028$; versus group B=2.16, $P=0.0268$), age (HR = 1.04, $P=0.0154$), and alanine aminotransferase level (HR=1.02, $P=0.0196$).

CONCLUSION

Results from MRE can stratify the risk of developing HCC during the follow-up of patients with chronic liver disease.

CLINICAL RELEVANCE/APPLICATION

Patients with chronic liver disease with high liver stiffness ($>$ 4.7 kPa) on their first MR elastography are at high risk for developing an HCC, regardless of the results of their second MR elastography. Thus, they should have meticulous follow-up and be screened for HCC development.

SSJ07-06 Evaluation of Texture Analysis Parameters for Response Prediction and Monitoring in Patients with Hepatocellular Carcinoma Undergoing Transarterial Chemoembolization Using Biphasic Contrast-Enhanced CT Image Data: Correlation with Results of Liver Pe

Tuesday, Nov. 29 3:50PM - 4:00PM Room: E350

Participants

Christopher Kloth, Tuebingen, Germany (*Presenter*) Nothing to Disclose
Wolfgang M. Thaiss, MD, Tuebingen, Germany (*Abstract Co-Author*) Nothing to Disclose
Rainer Kargel, Forchheim, Germany (*Abstract Co-Author*) Employee, Siemens AG
Rainer Grimmer, Forchheim, Germany (*Abstract Co-Author*) Employee, Siemens AG
Gerd Grozinger, MD, Tubingen, Germany (*Abstract Co-Author*) Nothing to Disclose
Roland Syha, Tuebingen, Germany (*Abstract Co-Author*) Nothing to Disclose

Dominik Ketelsen, MD, Tuebingen, Germany (*Abstract Co-Author*) Nothing to Disclose
Konstantin Nikolaou, MD, Tuebingen, Germany (*Abstract Co-Author*) Speakers Bureau, Siemens AG; Speakers Bureau, Bracco Group; Speakers Bureau, Bayer AG
Marius Horger, MD, Tuebingen, Germany (*Abstract Co-Author*) Nothing to Disclose

PURPOSE

To analyze the value of different parameters derived from CT texture analysis (CTTA) image data in hepatocellular carcinoma (HCC) for prediction of response and response evaluation to transarterial chemoembolization (TACE).

METHOD AND MATERIALS

The study group consisted of 56 HCC in 28 patients (27 male; mean age 67.2±10.4) who underwent CECT examinations before and after TACE therapy. The study was approved by the local ethic committee. Mean time between the two CT examinations was 39.93 ± 62.21 days. Standard of reference was perfusion-CT of the liver additionally to arterial and portal-venous post-contrast phases. Patients were assigned into subgroups: no response-NR (n=9), partial response-PR (n=34) and complete response-CR (n=13). CTTA parameters were: heterogeneity/intensity/average/deviation/skewness/contrast of NGTDM (Neighborhood Grey-Tone Difference Matrix). For each parameter mean, entropy and uniformity were calculated. Blood flow (BF), blood volume (BV), arterial liver perfusion (ALP), portal-venous perfusion (PVP) and hepatic perfusion index (HPI) were calculated in the pre- and post-TACE settings by liver perfusion-CT.

RESULTS

Patients with CR showed higher tumor perfusion parameters before TACE and a significant decrease in BF/BV/ALP/HPI after TACE ($p=0.002/0.002/0.002/0.003$). Patients with PR showed similar results, but only in responding tumor parts. ROC analysis of CTTA parameters yielded predictive cut-off values for CR in the arterial CECT-phase (sensitivity/specificity) for mean intensity (88.9%/69.8%), mean average (88.9%/69.8%) and skewness (90.0%/58.1%). In the portal-venous CECT-phase similar for uniformity of heterogeneity, uniformity of skewness and mean contrast (92.3%/81.8%/92.3%/54.5%/92.3%/95.2%). Significant correlations were registered between changes in mean heterogeneity and BF ($p=0.004$, $r=-0.815$), BV ($p=0.002$, $r=-0.851$) and ALP ($p=0.002$, $r=-0.851$) in the arterial phase in CR and PR.

CONCLUSION

Significant correlations exist between CTTA parameters and those derived from perfusion-CT both in the pre- and post-TACE setting with predictive value for TACE outcome.

CLINICAL RELEVANCE/APPLICATION

Prediction of response to local therapy (TACE) by means of CTTA can be implemented for choosing the best treatment strategy. Improved response monitoring by CTTA is beneficial for optimal patient management and could be a substitute for more sophisticated imaging techniques like perfusion-CT or MRI.

SSJ08

Gastrointestinal (New Ultrasound Techniques)

Tuesday, Nov. 29 3:00PM - 4:00PM Room: E353A



AMA PRA Category 1 Credit™: 1.00
ARRT Category A+ Credit: 1.00

FDA Discussions may include off-label uses.

Participants

Anthony E. Samir, MD, Boston, MA (*Moderator*) Consultant, Pfizer Inc Consultant, General Electric Company Consultant, PAREXEL International Corporation Research Grant, Koninklijke Philips NV Research Grant, Siemens AG Research Grant, Toshiba Corporation Research Grant, General Electric Company Research Grant, Samsung Electronics Co, Ltd Research Grant, Analogic Corporation Research support, SuperSonic Imagine Research support, Hitachi, Ltd
Jessica B. Robbins, MD, Madison, WI (*Moderator*) Nothing to Disclose

Sub-Events

SSJ08-01 Characterization of Malignant versus Benign Focal Liver Lesions with Lumason-Enhanced Ultrasound Imaging

Tuesday, Nov. 29 3:00PM - 3:10PM Room: E353A

Participants

Richard G. Barr, MD, PhD, Youngstown, OH (*Presenter*) Consultant, Siemens AG; Consultant, Koninklijke Philips NV; Research Grant, Siemens AG; Research Grant, SuperSonic Imagine; Speakers Bureau, Koninklijke Philips NV; Research Grant, Bracco Group; Speakers Bureau, Siemens AG; Consultant, Toshiba Corporation; Research Grant, Esaote SpA; Research Grant, B and K Ultrasound; Research Grant, Hitachi Aloka Ultrasound
Edward G. Grant, MD, Los Angeles, CA (*Abstract Co-Author*) Research Grant, General Electric Company ; Medical Advisory Board, Nuance Communications, Inc
Dirk-Andre Clevert, MD, Muenchen, Germany (*Abstract Co-Author*) Speaker, Siemens AG; Speaker, Koninklijke Philips NV; Speaker, Bracco Group;
Barry B. Goldberg, MD, Philadelphia, PA (*Abstract Co-Author*) Nothing to Disclose
Michelle L. Robbin, MD, Birmingham, AL (*Abstract Co-Author*) Consultant, Koninklijke Philips NV;
Andrew De la Torre, MD, Newark, NJ (*Abstract Co-Author*) Nothing to Disclose
Wui K. Chong, MD, Chapel Hill, NC (*Abstract Co-Author*) Advisory Board, Bracco Group;
Deike H. Strobel, MD, Erlangen, Germany (*Abstract Co-Author*) Nothing to Disclose

PURPOSE

To compare the diagnostic performance of contrast-enhanced ultrasound (CEUS) with Lumason (sulfur hexafluoride lipid-type A microspheres) to that of unenhanced ultrasound (UEUS) for characterization of malignant versus benign focal liver lesions (FLLs).

METHOD AND MATERIALS

Two multicenter clinical trials of identical design were conducted in adult subjects with at least one FLL requiring work-up for characterization; subjects underwent UEUS followed by CEUS with 2.4 mL Lumason. UEUS and CEUS images were evaluated by on-site investigators and 3 off-site, blinded readers unaffiliated with the enrolment centers and blinded to any clinical data. Diagnostic performance of UEUS and CEUS for FLL characterization was determined using tissue pathology/histology (when FLL biopsy could be performed), or 6-month follow-up with contrast-enhanced CT or MRI as truth standard.

RESULTS

A total of 499 subjects were included in the 2 trials. Per truth standard, 256 lesions were benign (n=116 hemangioma, n=64 focal nodular hyperplasia, n=76 other) and 243 were malignant (n=131 hepatocellular carcinoma, n=78 metastases, n=34 other). For the off-site reads, the pooled sensitivity, specificity, and accuracy were 43.6%, 34.0%, 38.7%, respectively for UEUS and 72.4%, 80.5%, 76.6%, respectively for CEUS (p<.05). For on-site reads, sensitivity, specificity, and accuracy were 37.0%, 21.5%, 29.1%, respectively for UEUS and 89.3%, 84.0%, 86.6%, respectively for CEUS (p<.05). No serious adverse events related to Lumason administration were reported.

CONCLUSION

Overall, Lumason-enhanced ultrasound imaging provided an improvement from UEUS for characterization of FLLs.

CLINICAL RELEVANCE/APPLICATION

The results suggest that CEUS with 2.4 mL of Lumason is safe and may be useful to improve characterization of focal liver lesions when UEUS is inconclusive.

SSJ08-02 Characterization of Focal Liver Masses: A Multicentre Study Comparing Contrast Enhanced Ultrasound (CEUS) to Grayscale/Doppler Ultrasound, Computed Tomography and Magnetic Resonance Imaging

Tuesday, Nov. 29 3:10PM - 3:20PM Room: E353A

Awards

Student Travel Stipend Award

Participants

David P. Burrowes, MD, Calgary, AB (*Presenter*) Nothing to Disclose
Alexandra Medellin-Kowalewski, MD, Calgary, AB (*Abstract Co-Author*) Nothing to Disclose
Alison C. Harris, MBChB, Vancouver, BC (*Abstract Co-Author*) Nothing to Disclose

Laurent Milot, Lyon, France (*Abstract Co-Author*) Nothing to Disclose

Stephanie R. Wilson, MD, Calgary, AB (*Abstract Co-Author*) Equipment support, Siemens AG; Equipment support, Koninklijke Philips NV

PURPOSE

In light of recent FDA approval of a microbubble for liver CEUS in the USA, we propose that CEUS is superior to grayscale ultrasound and equivalent to institutional CT and MR for characterization of focal liver masses.

METHOD AND MATERIALS

This prospective study comprises 224 patients, from 5 geographically separate centres, presenting for evaluation of a focal liver mass (12 adenoma, 8 cholangiocarcinoma, 55 FNH, 41 hemangioma, 71 HCC, 25 metastasis, 12 other). All had US/CEUS and CT and/or MR. CEUS was performed with Definity (Lantheus, Billerica MA) on standard US systems. They included a continuous cine of wash-in to peak enhancement, and still portal venous and delayed images to 5 minutes. CT and MR were performed as standard care with institutional protocols. Pre-contrast, arterial phase and portal venous phase images were included. Three separate electronic blind read files; one for each of CEUS (including grayscale and Doppler images), CT and MR were created and read blindly by four radiologists, two for CEUS and two for CT/MR utilizing a Microsoft Access based questionnaire regarding the arterial, portal venous and delayed phase enhancement of each lesion. Readers also provided a preference for malignancy or benignancy, a final diagnosis as well as a confidence level. Results of the blind read were compared with the truth standard from pathology, long-term stability or expert consensus.

RESULTS

Our results show that CEUS is superior to grayscale/Doppler ultrasound and at least equivalent to CT and MR both in determining the malignancy of a lesion and in diagnostic accuracy, with an increase in confidence from a mean of 1.6 for grayscale/Doppler to 3.9 on CEUS on a 5 point scale. Sensitivity, specificity and accuracy of CEUS are 95%, 82%, 67%, of grayscale/Doppler are 81%, 56% 40%, of CT are 89%, 75%, 62% and of MR are 85%, 79%, 62% respectively.

CONCLUSION

CEUS is superior to grayscale ultrasound both for determination of malignancy and when assigning a final diagnosis for a focal liver mass. Additionally, CEUS is equivalent, and in select cases performs better, in the characterization of focal liver lesions than institutional CT and MRI.

CLINICAL RELEVANCE/APPLICATION

In the evaluation of a focal liver mass, CEUS is a necessary adjuvant to grayscale/Doppler ultrasound and is equivalent to CT and MR in its ability to predict malignancy and provide a diagnosis.

SSJ08-03 Relationship between Liver Tissue Stiffness and Histopathological Findings Analyzed by Shear Wave Elastography in Patients with Non-alcoholic Fatty Liver Disease

Tuesday, Nov. 29 3:20PM - 3:30PM Room: E353A

Participants

HIROHITO TAKEUCHI, Tokyo, Japan (*Presenter*) Nothing to Disclose

Katsutoshi Sugimoto, MD, PhD, Tokyo, Japan (*Abstract Co-Author*) Nothing to Disclose

Yoshiyuki Kobayashi, Toyo, Japan (*Abstract Co-Author*) Nothing to Disclose

Fuminori Moriyasu, MD, Kyoto, Japan (*Abstract Co-Author*) Nothing to Disclose

Takao Itoi, Tokyo, Japan (*Abstract Co-Author*) Nothing to Disclose

PURPOSE

Shear wave elastography (SWE) is validated in chronic hepatitis C and B; however, limited data are available in Non-Alcoholic Fatty Liver Disease (NAFLD). This study is aimed to assess the accuracy and the efficacy of SWE for the detection of fibrosis in patients with NAFLD and to evaluate the effect of other histologic parameters on SWE measurement.

METHOD AND MATERIALS

Written informed consent was obtained from all subjects, and the local ethics committee approved the study. Seventy-one patients with histologically proven NAFLD (mean age, 50.8 years \pm 15.7) were examined. All patients underwent SWE (AixplorerTM; SuperSonic Imagine) and FIB4 index (based on age, aspartate aminotransferase [AST] and alanine aminotransferase [ALT] levels, and platelet counts). SWE measurements were compared to the histologic features based on of NAFLD activity score and FIB4 index.

RESULTS

The area under the ROC curve (AUC) for the diagnosis of hepatic fibrosis stages 3 or higher was 0.821 (optimal cutoff value, 13.1 kPa; sensitivity, 62.5%; specificity, 57.4%) for SWE, as was 0.822 (optimal cutoff value, 1.41; sensitivity, 71.9%; specificity, 53.9%) for FIB4 index, respectively. Median liver stiffness values measured using SWE showed a stepwise increase with increasing hepatic fibrosis stage ($P < 0.001$), inflammation score ($P = 0.018$), and ballooning score ($P < 0.001$), and showed a stepwise decrease with increase hepatic steatosis stage ($P = 0.046$).

CONCLUSION

SWE is a promising imaging modality for assessing the presence or absence of advanced fibrosis in patients with NAFLD. The effect of steatosis on SWE measurements may be controversial.

CLINICAL RELEVANCE/APPLICATION

SWE is a rapid and noninvasive method of detecting fibrosis in patients with nonalcoholic fatty liver disease.

SSJ08-04 Noninvasive Evaluation of Liver Fibrosis using Two-dimensional Shear Wave Elastography: A Comparison with Different Serum Fibrosis Indices in Chronic Hepatitis B

Tuesday, Nov. 29 3:30PM - 3:40PM Room: E353A

Participants

Hong Ding, MD, Shanghai, China (*Presenter*) Nothing to Disclose
Yuan Zhuang, Shanghai, China (*Abstract Co-Author*) Nothing to Disclose
Hong Han, Shanghai, China (*Abstract Co-Author*) Nothing to Disclose
Wenping Wang, MD, PhD, Shanghai, China (*Abstract Co-Author*) Nothing to Disclose

PURPOSE

To explore the value of 2D-SWE in assessing the extent of liver fibrosis with chronic hepatitis B (CHB) and to compare its diagnostic accuracy with different fibrosis indices involving aminotransferase/platelet ratio index (APRI), fibrosis index based on the 4 factors (FIB-4), King's score and Forns index.

METHOD AND MATERIALS

A total of 384 subjects (304 with CHB and 80 controls) who underwent partial hepatectomy were enrolled and divided into five groups (S0~S4) according to Scheuer scoring system histologically. All patients were examined with 2D-SWE to obtain liver stiffness measurements (LSMs), which were compared with the histological findings and analyzed with factors including age, gender and several blood markers that might influence the value of LSMs.

RESULTS

The intraclass correlation coefficient of five LSMs with 2D-SWE was 0.948. The average LSMs were 5.74±1.10 kPa for fibrosis S0 (n=10), 6.53±0.96 kPa for S1 (n=30), 7.94±0.89 kPa for S2 (n=50), 9.40±1.31 kPa for S3 (n=47), and 14.52±3.55 kPa for S4 (n=167). The multiple comparisons of LSMs showed significant statistical difference between every two fibrotic groups except between S0 and S1 groups. For the prediction of S≥2 and S=4, the optimal cut-off values of LSMs were 7.6 kPa and 10.4 kPa, with a sensitivity of 92.0% and 94.6% and a specificity of 90.0% and 94.9%, respectively. All these methods correlated with fibrosis stages statistically (p<0.05) and the correlation coefficients between pathological stages with LSMs, APRI, FIB-4, King's score and Forns index were 0.875, 0.409, 0.397, 0.428 and 0.452, respectively. The AUROC in diagnosing fibrosis S≥2 were 0.970, 0.771, 0.727, 0.787, and 0.765, respectively; and the AUROC were 0.986, 0.703, 0.712, 0.716, and 0.740 for diagnosing S=4, respectively. Liver fibrosis stages, inflammatory activity grades and the level of gamma glutamyltranspeptidase (GGT), albalanine aminotransferase (ALT), and aspartate aminotransferase (AST) significantly correlated with LSMs (β=0.618, 0.015, 0.079, -0.083 and 0.146, respectively; p<0.05).

CONCLUSION

2D-SWE could be used to predict significant fibrosis (S≥2) and cirrhosis (S=4) in CHB patients with notable higher diagnostic accuracy than serum fibrosis models. In terms of LSM associated with hepatic fibrosis, the confounding factors including inflammatory activity, and the level of GGT, ALT, and AST that independently influence the value of LSMs with 2D-SWE.

CLINICAL RELEVANCE/APPLICATION

N/A

SSJ08-05 Initial Experience Using a Telerobotic Ultrasound System to Perform Adult Abdominal Examinations

Tuesday, Nov. 29 3:40PM - 3:50PM Room: E353A

Awards

Student Travel Stipend Award

Participants

Scott J. Adams, Saskatoon, SK (*Presenter*) Nothing to Disclose
Brent E. Burbridge, MD, FRCPC, Saskatoon, SK (*Abstract Co-Author*) Nothing to Disclose
Ivar Mendez, MD, PhD, Saskatoon, SK (*Abstract Co-Author*) Nothing to Disclose
Paul S. Babyn, MD, Saskatoon, SK (*Abstract Co-Author*) Nothing to Disclose
Leanne Langford, Saskatoon, SK (*Abstract Co-Author*) Nothing to Disclose
Vincent Vergara, MD, Saskatoon, SK (*Abstract Co-Author*) Nothing to Disclose
Andreea Badea, BSC, Saskatoon, SK (*Abstract Co-Author*) Nothing to Disclose
Rhonda Bryce, MD, Saskatoon, SK (*Abstract Co-Author*) Nothing to Disclose
Luis Bustamante, Saskatoon, SK (*Abstract Co-Author*) Nothing to Disclose

PURPOSE

To assess the feasibility of performing adult abdominal examinations using a telerobotic ultrasound system in which radiologists/sonographers can control fine movements of a transducer and all ultrasound settings from a remote location.

METHOD AND MATERIALS

Eighteen patients prospectively underwent a conventional sonography examination (using EPIQ 5, Philips or LOGIQ E9, GE Healthcare) followed by a telerobotic sonography examination (using the MELODY System, AdEchoTech; SonixTablet, BK Ultrasound; and TE30 All-in-One HD Videoconferencing Endpoint, Huawei Technologies) according to a standardized abdominal imaging protocol. For telerobotic examinations, patients located at an imaging clinic were scanned remotely by a sonographer 2.75 km away. Conventional examinations were read independently from telerobotic examinations. We assessed the ability of the system to generate images of diagnostic quality and acceptability of the system to patients and sonographers.

RESULTS

92% of organs visualized on conventional examinations were sufficiently visualized on telerobotic examinations. Five pathological findings were identified on both telerobotic and conventional examinations, three findings were identified using only conventional sonography and two findings were identified using only telerobotic sonography. A paired sample t-test showed no significant difference between the two modalities in measurements of the liver, spleen, and diameter of the proximal aorta; however, telerobotic assessments overestimated distal aorta and common bile duct diameters and underestimated kidney lengths (p-values <0.05). All patients strongly agreed or somewhat agreed that they would be willing to have another telerobotic examination.

CONCLUSION

A telerobotic ultrasound system is feasible for performing abdominal ultrasound examinations at a distant location with minimal training and set-up requirements and a moderate learning curve. Telerobotic sonography may open up the possibility of establishing remote ultrasound clinics for communities which lack skilled sonographers and radiologists, thereby improving access to care.

CLINICAL RELEVANCE/APPLICATION

A telerobotic ultrasound system is feasible for performing abdominal ultrasound examinations at a distant location with minimal training and set-up requirements and may improve access to care.

Honored Educators

Presenters or authors on this event have been recognized as RSNA Honored Educators for participating in multiple qualifying educational activities. Honored Educators are invested in furthering the profession of radiology by delivering high-quality educational content in their field of study. Learn how you can become an honored educator by visiting the website at: <https://www.rsna.org/Honored-Educator-Award/>

Paul S. Babyn, MD - 2012 Honored Educator

SSJ08-06 Differentiation of Inflammatory from Fibrotic Bowel Strictures Among Patients with Crohn's Disease through Analysis of Time-intensity Curves Obtained after Microbubble Contrast Agent Injection

Tuesday, Nov. 29 3:50PM - 4:00PM Room: E353A

Participants

Emilio Quaia, MD, Edinburgh, United Kingdom (*Presenter*) Nothing to Disclose
Antonio Giulio Gennari, MD, Trieste, Italy (*Abstract Co-Author*) Nothing to Disclose
Michele Pontello, Trieste, Italy (*Abstract Co-Author*) Nothing to Disclose
Federica Arban, Trieste, Italy (*Abstract Co-Author*) Nothing to Disclose
Maria A. Cova, MD, Trieste, Italy (*Abstract Co-Author*) Nothing to Disclose

PURPOSE

To assess whether the analysis of time-intensity curves obtained after sulphur hexafluoride-filled microbubble contrast agent injection could differentiate inflammatory from fibrotic strictures among patients with Crohn's disease (CD).

METHOD AND MATERIALS

Sixty-five consecutive patients (40 male and 25 female; mean age \pm SD, 42.2 years \pm 12.22) with a diagnosis of CD were included. Inclusion criteria were: (1) CD involving the terminal ileal loop as shown by endoscopy with serial deep mucosal biopsies or cross sectional imaging with a thickness of the terminal ileal loop $>$ 3mm; (2) availability of the histologic score based on mucosal ulceration (grade 0-3), edema (grade 0-3), and quantity (grade 0-3) and depth (grade 0-4) of neutrophilic infiltration; (3) availability of mural fibrosis diagnosis when abnormal depositions of collagens were identified in the edges of mucosal ulceration; (4) at least 12 weeks of clinical follow-up in CD diagnosed no more than 2 years before the study. In each patient the terminal ileal loop was scanned by a convex-array probe (2-5 MHz) before and after sulfur hexafluoride-filled microbubble injection. The digital cine-clips registered after microbubble injection during the first-pass dynamic enhancement was quantified in lineary units by a dedicated software through manually-drawn regions of interest (ROIs) encompassing the anterior bowel wall. Time-intensity curves from patients with inflammatory and fibrotic stenosis were compared. The peak enhancement, rise time, time to peak, area under the time-intensity curve (AUC), AUC during wash-in (AUCWI), and AUC during wash-out (AUCWO) were compared between patients with inflammatory or fibrotic strictures.

RESULTS

Inflammatory (n=40) vs fibrotic stenoses (n=25) differed in the AUC (234274 ± 293293 vs 89787 ± 53819 ; $P = <0.05$), AUCWI (53256 ± 53871 vs 30993 ± 19454 ; $P = <0.05$), AUCWO (150910 ± 177859 vs 61930 ± 36181 ; $P = <0.05$) and peak enhancement (11556 ± 11298 vs 6252 ± 5504 ; $P < .05$).

CONCLUSION

The quantitative analysis of small bowel wall contrast enhancement after microbubble contrast agent injection may differentiate inflammatory from fibrotic ileal stenosis in patients with CD.

CLINICAL RELEVANCE/APPLICATION

Contrast-enhanced ultrasound provides an early identification of those patients with a fibrotic ileal stricture who deserve surgical resection from those patients with an inflammatory stricture who deserve pharmacologic treatment.

SSJ09

Gastrointestinal (Diffuse Liver Disease and HCC)

Tuesday, Nov. 29 3:00PM - 4:00PM Room: E353C

CT **GI** **MR**

AMA PRA Category 1 Credit™: 1.00
ARRT Category A+ Credit: 1.00

FDA Discussions may include off-label uses.

Participants

Shahid M. Hussain, MD, PhD, Omaha, NE (*Moderator*) Nothing to Disclose
Myeong-Jin Kim, MD, PhD, Seoul, Korea, Republic Of (*Moderator*) Research Grant, Bayer AG

Sub-Events

SSJ09-01 The Optimal Measurement Number of Shear Wave Elastography(SWE) for Different Liver Fibrosis Stages

Tuesday, Nov. 29 3:00PM - 3:10PM Room: E353C

Participants

Qian Li, MD, PhD, Boston, MA (*Presenter*) Nothing to Disclose
Manish Dhyani, MBBS, Boston, MA (*Abstract Co-Author*) Nothing to Disclose
Atul K. Bhan, MD, Boston, MA (*Abstract Co-Author*) Nothing to Disclose
Xi Zhang, PhD, Indianapolis, IN (*Abstract Co-Author*) Nothing to Disclose
Anthony E. Samir, MD, Boston, MA (*Abstract Co-Author*) Consultant, Pfizer Inc Consultant, General Electric Company Consultant, PAREXEL International Corporation Research Grant, Koninklijke Philips NV Research Grant, Siemens AG Research Grant, Toshiba Corporation Research Grant, General Electric Company Research Grant, Samsung Electronics Co, Ltd Research Grant, Analogic Corporation Research support, SuperSonic Imagine Research support, Hitachi, Ltd

PURPOSE

To explore the optimal minimum number of SWE measurements in liver fibrosis with different stages.

METHOD AND MATERIALS

218 consecutive patients who underwent SWE before their scheduled liver biopsy (age 18–78 years; mean 48 years; men 96, women 122) were enrolled in this study between August 2013 and January 2015. Ten SWE values were obtained at the right upper lobe of the liver through an intercostal approach in suspended respiration. A single sub-special pathologist reviewed all biopsy specimens as per the METAVIR criteria. Median values using a different number of measurements (2-9) were chosen from the ten measurements randomly for each subject. Receiver operating characteristic (ROC) curves were constructed for distinguishing $\geq F2$ fibrosis for 10 measurements, and then sequentially, for measurement numbers below 10. The variability in intra-subject SWE measurements was calculated by comparing difference of individual measurements from the median value for each subject, and its relationship with measurement numbers was analyzed.

RESULTS

Study population fibrosis stages were F0=86, F1=80, F2=22, F3=22, F4=8. For all subjects, the areas under the ROC curve (AUROC) of the 10 measurements in differentiation of stage F2 or greater and stage F4 were 0.81 (95%CI: 0.69-0.94) and 0.847 (95%CI: 0.72-0.96) respectively. The minimum measurement numbers in differentiation of corresponding fibrosis stages were 7 (AUC=0.79, 95%CI: 0.67-0.916, P=0.17) and 6 (AUC=0.82, 95%CI: 0.71-0.94, P=0.53) respectively. As shown in Figure 1, in both groups (F0 or 1 vs. $\geq F2$), the variability of measurements did not change much with the increase of the measurement number ($r=0.53$, $P=0.14$), especially between 6-10, but the variability is much higher in stage F2 or greater.

CONCLUSION

Our study indicates that, in the patients with variety of hepatic diseases, the optimal minimum numbers of SWE measurements were 7 for differentiation of $\geq F2$ fibrosis and 6 for F4. There was no statistically significant variability in intra-subject SWE measurements using 6-10 measurement numbers, which implies the optimal measurement numbers obtained in this study are reliable.

CLINICAL RELEVANCE/APPLICATION

Standardization of number of measurements needed for SWE assessment of fibrosis stage is essential for SWE clinical workflow. More measurements will decrease variability on a per subject basis, however time, labor, cost-effectiveness and reliability are very important factors.

SSJ09-02 Gd-EOB-DTPA-Enhanced MR Relaxometry for the Detection and Staging of Liver Fibrosis

Tuesday, Nov. 29 3:10PM - 3:20PM Room: E353C

Awards

Trainee Research Prize - Resident

Participants

Michael Haimerl, Regensburg, Germany (*Presenter*) Nothing to Disclose
Kirsten Utpatel, Regensburg, Germany (*Abstract Co-Author*) Nothing to Disclose
Claudia Fellner, MD, PhD, Regensburg, Germany (*Abstract Co-Author*) Nothing to Disclose
Marcel D. Nickel, Erlangen, Germany (*Abstract Co-Author*) Employee, Siemens AG
Christian R. Stroszczyński, MD, Regensburg, Germany (*Abstract Co-Author*) Nothing to Disclose
Philipp Wiggermann, Regensburg, Germany (*Abstract Co-Author*) Nothing to Disclose

PURPOSE

To examine the diagnostic performance of gadoteric-acid (Gd-EOB-DTPA)-enhanced T1 relaxometry in the staging of hepatic fibrosis using histopathologic examination as the reference standard.

METHOD AND MATERIALS

Sixty-five patients (41 men and 24 women; mean age, 55.9 +/- 14.8) with histologically proven liver fibrosis (LF) who underwent Gd-EOB-DTPA-enhanced MR including T1 MR-relaxometry were analyzed. The fibrosis stage was assessed according to the METAVIR score (fibrosis scores range: F0, no fibrosis to F4, cirrhosis). For the T1 relaxometry, a transverse 3D VIBE sequence (TR 5.79 ms, TE 2.46 ms, α 1°, 7°, 14°) with inline T1 calculation was acquired prior to and 20 minutes after Gd-EOB-DTPA administration following the acquisition of a B1 map for inline correction of the B1 inhomogeneities. The reduction rates of the T1 relaxation time (rT1) between the pre- and postcontrast images were calculated, and the optimal cutoff values for the fibrosis stages were determined with receiver operating characteristic (ROC) curve analyses.

RESULTS

The rT1 decreased with the severity of liver fibrosis with the following mean values (%): stage F0, 69.4±2.6; stage F1, 59.1±3.7; stage F2, 55.3±4.6; stage F3, 42.2±0.10; and stage F4, 28.8±8.2. Regression analysis revealed a significant correlation of the rT1 with the stage of liver fibrosis ($r=-0.906$, $p<0.001$). T1 relaxometry performed well in the staging of liver fibrosis with AUCs of 1.0 for the stages of F1 and greater, 0.92 for the stages of F2 and greater, 0.98 for the stages of F3 and greater, and 0.96 for stage F4.

CONCLUSION

Gd-EOB-DTPA-enhanced T1 relaxometry is a reliable tool for the staging of hepatic fibrosis. The results of the ROC analyses demonstrated the high accuracy in the detection of the initial stages of hepatic fibrosis.

CLINICAL RELEVANCE/APPLICATION

Our study supports the conclusion that measuring T1 relaxation times via Gd-EOB-DTPA-enhanced MRI may be incorporated into the clinical routine as a liver imaging screening test for the detection of silent disease and the non-invasive definition of the stage of liver fibrosis.

SSJ09-03 Role of Shear Wave Sono-Elastography of Liver in Monitoring Patients of Non-Alcoholic Fatty Liver Disease (NAFLD): Comparison with Magnetic Resonance Imaging- A Prospective Study

Tuesday, Nov. 29 3:20PM - 3:30PM Room: E353C

Awards

Student Travel Stipend Award

Participants

Nikhil Makhija, MBBS, New Delhi, India (*Presenter*) Nothing to Disclose
Madhusudhan Kumble Seetharama, MD, FRCR, New Delhi, India (*Abstract Co-Author*) Nothing to Disclose
Deepnarayan Srivastava, Delhi, India (*Abstract Co-Author*) Nothing to Disclose
Raju Sharma, MD, New Delhi, India (*Abstract Co-Author*) Nothing to Disclose
Shivanand R. Gamanagatti, MBBS, MD, New Delhi, India (*Abstract Co-Author*) Nothing to Disclose
Naval K. Vikram, New Delhi, India (*Abstract Co-Author*) Nothing to Disclose

PURPOSE

To measure liver stiffness (LS) by Shear-wave sono-elastography (SWE) in patients of non-alcoholic fatty liver disease (NAFLD) before and after intervention and to compare it with hepatic fat fraction (FF) measured by Magnetic Resonance Spectroscopy (MRS)

METHOD AND MATERIALS

41 adult treatment-naive patients (mean age: 39yrs, male:female=22:19 of NAFLD) were included in this prospective study after obtaining approval from Institutional Ethics Committee and informed patient consent. Known diabetics, alcohol users (>20g/day) and patients on chronic drug intake were excluded. After initial clinical (body mass index-BMI) and biochemical (liver function tests-LFT, lipid profile) evaluation, MRS and SWE were done for all patients and mean hepatic fat fraction (FF) and mean liver stiffness (LS) were obtained. Following dietary and lifestyle changes and oral Vitamin E for six months repeat clinico-biochemical tests, MRI and SWE were done. Based on compliance to intervention, patients were categorized into good compliance and poor compliance groups. The FF and LS before and after treatment in both groups were compared.

RESULTS

30 patients had good and 11 had poor compliance to intervention. Baseline mean LS did not show significant correlation with mean MRS FF ($r=0.19$, $p>0.05$). After intervention, in both the groups, mean LS and mean MRS FF did not show significant correlation. In the group with good compliance, there was significant reduction in BMI which showed moderate correlation ($r=0.45$, $p<0.05$) with change in MRS FF. LS also showed significant reduction ($p<0.05$). In the group with poor compliance, there was significant increase in BMI which showed good correlation ($r=0.79$, $p<0.05$) with increase in mean MRS. LS did not show significant change ($p>0.05$). The change in mean LS showed no correlation either with mean MRS FF ($p>0.05$) or with BMI after treatment.

CONCLUSION

LS measured by SWE does not show correlation with MRS FF and is not useful in monitoring of NAFLD.

CLINICAL RELEVANCE/APPLICATION

Change in gray scale USG, BMI and biochemical parameters do not accurately represent change in liver fat content. Although MRI is useful as a non-invasive modality to diagnose and quantify liver fat as well as its monitoring, its use in follow-up is expensive. SWE, however, cannot be used in monitoring changes in liver fat content after interventional regimens.

SSJ09-04 Maximum Value Measured by Two-Dimensional Shear Wave Elastography Helps in Differentiating Malignancy From Benign Focal Liver Lesions

Tuesday, Nov. 29 3:30PM - 3:40PM Room: E353C

Participants

Wenshuo Tian, Guangzhou, China (*Presenter*) Nothing to Disclose
Xiaoyan Xie, Guangzhou, China (*Abstract Co-Author*) Nothing to Disclose
Lu-Yao Zhou, MD, Guangzhou, China (*Abstract Co-Author*) Nothing to Disclose
Manxia Lin, Guangzhou, China (*Abstract Co-Author*) Nothing to Disclose
Fu-Shun Pan, Guangzhou, China (*Abstract Co-Author*) Nothing to Disclose

PURPOSE

To evaluate the diagnostic efficacy of two-dimensional shear wave elastography (2D SWE) in differentiating malignancy from benign focal liver lesions (FLL).

METHOD AND MATERIALS

Institutional review board approval and written informed consent was obtained. The maximum, minimum, mean, and the standard deviation of 2D SWE measurements, expressed in kPa (E_{max}, E_{min}, E_{mean}, E_{sd}), were underwent in 221 patients with 229 FLLs. Receiver operating characteristic (ROC) curve analysis was performed to evaluate the diagnostic performance of 2D SWE. Mann-Whitney U test was used to assess the inter-group differences.

RESULTS

E_{max}, E_{min}, E_{mean}, E_{sd} was significantly higher in 164 malignant lesions than that in 65 benign lesions (P<0.001). For identification of malignant FLL, the area under ROC curves for E_{max} was 0.920 (E_{min} 0.710, E_{mean} 0.879, E_{sd} 0.915). E_{max} was 96.21±35.40 for 19 intrahepatic cholangiocarcinomas (ICC) and 90.32±54.71 for 35 liver metastatic lesions, which was significantly higher than 61.83±28.87 for 103 hepatocellular carcinomas (HCC), respectively (P<0.0001, P=0.0237). E_{max} was 38.72±18.65 for 15 focal nodular hyperplasias, which was significantly higher than 20.56±10.74 for 37 hemangiomas (P=0.0009). E_{max} of adjacent liver parenchyma of HCC and ICC were significantly higher than that of the other three lesion types (P<0.005).

CONCLUSION

E_{max} of FLL and adjacent liver parenchyma could help in differentiating malignancy from benign FLLs.

CLINICAL RELEVANCE/APPLICATION

Maximum value measured by two-dimensional shear wave elastography of focal liver lesion and adjacent liver parenchyma may be considered for differential malignant from benign lesions.

SSJ09-05 Lack of Standardized Terminology and Definitions for Major Imaging Features of HCC among Clinical Practice Guidelines Released by Medical Societies

Tuesday, Nov. 29 3:40PM - 3:50PM Room: E353C

Participants

Adrija Mamidipalli, MBBS, San Diego, CA (*Presenter*) Nothing to Disclose
Saya Igarashi, San Diego, CA (*Abstract Co-Author*) Nothing to Disclose
Ryan L. Brunsing, MD, San Diego, CA (*Abstract Co-Author*) Nothing to Disclose
Claude B. Sirlin, MD, San Diego, CA (*Abstract Co-Author*) Research Grant, General Electric Company; Research Grant, Siemens AG; Research Grant, Guerbet SA; ;

PURPOSE

Multiple medical societies have published clinical practice guidelines that include algorithms for non-invasive imaging-based diagnosis of HCC in patients with cirrhosis using multiphasic contrast-enhanced MRI/CT. The purpose of this structured review of the literature was to extract and compare the terminology and definitions endorsed by these guidelines for the following major imaging features of HCC: arterial phase hyperenhancement (APHE), "washout"(WO), "capsule" (C), and diameter (D). Liver Imaging Reporting and Data System (LI-RADS) was not included in this review

METHOD AND MATERIALS

We identified 38 guidelines published since 1995, cited in PubMed, and containing imaging criteria for HCC. Each guideline was reviewed by 2 independent readers. Terms and definitions describing APHE, WO, C, and D were recorded. If for a given feature no term was used, "term not used" was recorded and the next feature assessed. If a term was used but no definition provided, all citations supporting that term were similarly reviewed and all definitions relating to the term were recorded. If no definition was provided within either the guideline or citations, "no definition used" was recorded

RESULTS

There was >95% inter-reader agreement in identifying terms and definitions. Of 38 guidelines reviewed; 78%, 68%, 13%, and 42% contained terms while only 8%, 13%, 3%, and 3% contained definitions for APHE, WO, C, and D, respectively. Terms used for APHE and WO were variable with only 53% incorporating the language "arterial-phase enhancement" or "washout". There were 43 unique citations supporting undefined terms, yielding an additional 13 definitions each for APHE/WO and 4 each for C/D. While both APHE and WO were usually described using lesion signal/attenuation relative to the surrounding liver parenchyma, details on contrast phase and measurement technique were inconsistent. The few definitions for C and D used ambiguous language and clear definitions could not be extracted

CONCLUSION

Imaging guidelines for the non-invasive diagnosis of HCC use variable terms for key imaging features. Definitions usually are not provided. When provided, definitions are inconsistent between guidelines and/or ambiguous

CLINICAL RELEVANCE/APPLICATION

Lack of standardized and defined terminology for imaging features used in the non-invasive diagnosis of HCC complicates the interpretation and comparison of the HCC literature

SSJ09-06 Prediction of Microvascular Invasion in Hepatocellular Carcinoma: Preoperative Gd-EOB-DTPA-Dynamic Enhanced MRI and Histopathologic Correlation

Tuesday, Nov. 29 3:50PM - 4:00PM Room: E353C

Awards

Student Travel Stipend Award

Participants

Mengqi Huang, MD, Guang zhou, China (*Presenter*) Nothing to Disclose
Zhi Dong, Guangzhou, China (*Abstract Co-Author*) Nothing to Disclose
Keguo Zheng, MD, Guangzhou, China (*Abstract Co-Author*) Nothing to Disclose
Ping Xu, BMedSc, GuangZhou, China (*Abstract Co-Author*) Nothing to Disclose
Shiting Feng, MD, Guangzhou, China (*Abstract Co-Author*) Nothing to Disclose

PURPOSE

We aimed to prospectively investigate the imaging features on the preoperative Gd-EOB-DTPA-dynamic enhanced MRI correlate with the present of microvascular invasion(MVI) in hepatocellular carcinoma(HCC).

METHOD AND MATERIALS

A total of 66 HCC lesions in 60 patients with preoperative Gd-EOB-DTPA-dynamic enhanced MRI were prospectively analyzed. Tumor size, signal homogeneity, tumor capsule, tumor margin, peritumor enhancement in mid-arterial phase, peritumor hypointense in hepatobiliary phase, signal intensity ratio on DWI and apparent diffusion coefficients (ADCs), T1 relaxation times and the reduction rate between pre- and post-contrast enhancement images were assessed. Correlation between these factors and presence of MVI were determined and the prediction model was established.

RESULTS

Histopathologic findings revealed 17 of 66 HCC had MVI. The univariate analysis showed the tumor size($p=0.003$), margin($p=0.013$),peritumor enhancement($p=0.001$)and hypointense in hepatobiliary phase($p=0.004$) were associated with MVI. However,the multiple logistic regression indicated that the tumor size, margin and peritumor enhancement were predictors of present of MVI($\alpha=0.01$). The R^2 of this prediction model was 0.353,and the sensitivity and specificity were 52.9% and 93.0%,respectively.

CONCLUSION

Tumor size, margin and peritumor enhancement in the preoperative Gd-EOB-DTPA-dynamic enhanced MRI can predict MVI of HCC with low sensitivity but high specificity.

CLINICAL RELEVANCE/APPLICATION

Preoperative Gd-EOB-DTPA- dynamic enhanced MRI can help to predict MVI of HCC, though are not sensitive but have high specificity.

SSJ10

Genitourinary (Imaging Renal Stones)

Tuesday, Nov. 29 3:00PM - 4:00PM Room: E351

CT **GU**

AMA PRA Category 1 Credit™: 1.00
ARRT Category A+ Credit: 1.00

FDA Discussions may include off-label uses.

Participants

Daniele Marin, MD, Durham, NC (*Moderator*) Research support, Siemens AG
Hilton M. Leao Filho, MD, Sao Paulo, Brazil (*Moderator*) Nothing to Disclose

Sub-Events

SSJ10-01 **Detecting Urinary Stones by Using Low-Dose Non-Enhanced Abdominopelvic CT with Tin Filtration Technique**

Tuesday, Nov. 29 3:00PM - 3:10PM Room: E351

Participants

Gu Mu Yang Zhang, MD, Beijing, China (*Presenter*) Nothing to Disclose
Bing Shi, Beijing, China (*Abstract Co-Author*) Nothing to Disclose
Hao Sun, MD, Beijing, China (*Abstract Co-Author*) Nothing to Disclose
Huadan Xue, MD, Beijing, China (*Abstract Co-Author*) Nothing to Disclose
Zheng Yu Jin, MD, Beijing, China (*Abstract Co-Author*) Nothing to Disclose

PURPOSE

To evaluate stone detection, radiation exposure and image quality by utilizing non-enhanced abdominopelvic CT with a novel tin filter

METHOD AND MATERIALS

This IRB-approved prospective study enrolled 80 consecutive patients with suspected urolithiasis. Consenting subjects underwent both regular-(120kV) and low-dose (150kV Sn) abdominopelvic examinations on a third-generation dual-source CT. Low-dose CT (LDCT) scans were read by radiologists blinded to regular-dose interpretations. Scans were interpreted for stone characteristics, image noise (SD) and signal-to-noise-ratio (SNR). Volume based CT weighted Dose Index (CTDIvol) and Dose-Length-Product (DLP) were recorded, effective dose (ED) was calculated. Stone detection, dose and image quality measurements were compared between regular-dose CT (RDCT) and LDCT

RESULTS

Seventeen patients had no urinary stones. A total of 157 stones from the rest of 63 patients were detected by RDCT. LDCT correctly identified 154 of 157 stones with an overall detection rate of 98.1%. Average stone size had no difference between RDCT and LDCT (5.37±4.45 vs. 5.22±4.39mm, P>0.05). Detection rates of LDCT for stones ≥ 2mm and < 2mm were, respectively, 100.0% (138/138) and 84.2% (16/19). CTDIvol and ED of LDCT were significantly lower in comparison to RDCT by 56.6% and 55.6% (3.12 vs. 7.19 mGy, P<0.001; 2.33 vs. 5.25 mSv, P<0.001). There was no significant difference in SD or SNR between LDCT and RDCT (P<0.05)

CONCLUSION

Non-enhanced abdominopelvic CT with 150kV Sn substantially reduces radiation exposure of patients while maintaining image quality and an excellent detection of urinary stones

CLINICAL RELEVANCE/APPLICATION

Non-enhanced abdominopelvic CT with 150kV Sn lowers radiation exposure while maintaining stone detection. It should be considered as the standard examination for detecting urinary stones in clinical practice

SSJ10-02 **Detection and Characterization of Urinary Stones using Photon-Counting-Detector CT in a Clinical Setting**

Tuesday, Nov. 29 3:10PM - 3:20PM Room: E351

Participants

Roy Marcus, MD, Rochester, MN (*Presenter*) Institutional research agreement, Siemens AG; Research support, Siemens AG
Joel G. Fletcher, MD, Rochester, MN (*Abstract Co-Author*) Grant, Siemens AG; ;
Terri J. Vrtiska, MD, Rochester, MN (*Abstract Co-Author*) Nothing to Disclose
Michael L. Wells, MD, Rochester, MN (*Abstract Co-Author*) Nothing to Disclose
Andrea Ferrero, PhD, Rochester, MN (*Abstract Co-Author*) Nothing to Disclose
Juan Montoya, Rochester, MN (*Abstract Co-Author*) Nothing to Disclose
Alice Huang, Rochester, MN (*Abstract Co-Author*) Nothing to Disclose
Ahmed Halaweish, PhD, Rochester, MN (*Abstract Co-Author*) Employee, Siemens AG
Felicity Enders, Rochester, MN (*Abstract Co-Author*) Nothing to Disclose
Shuai Leng, PhD, Rochester, MN (*Abstract Co-Author*) Nothing to Disclose
Cynthia H. McCollough, PhD, Rochester, MN (*Abstract Co-Author*) Research Grant, Siemens AG

PURPOSE

To compare in patients the detection and characterization of urinary stones between dual-source, dual-energy CT (DECT) and

preclinical photon-counting-detector CT (PCCT).

METHOD AND MATERIALS

Thirty patients underwent a clinical non-contrast-enhanced DECT stone characterization exam using a 2nd generation dual-source CT system (SOMATOM Flash, Siemens) using 80/140Sn kVp or 100/140Sn kVp, depending on patient size. Patients subsequently underwent an identical exam on a preclinical PCCT system, with images acquired at 140 kV in macro-mode with energy thresholds set at 25 and 75 keV. CTDIvol values were matched between exams. 1 and 5 mm images were reconstructed using filtered backprojection and a D30 kernel. Two radiologists in consensus examined DECT mixed and low kV images, and PCCT threshold 1 (25 – 140 keV) and bin 1 (25-75 keV) images, in a blinded fashion to determine confidence in stone presence (1= definitely present, 2 =probably present, lower confidence, 3=questionable if present, 4=not seen) and identify artifacts affecting diagnostic confidence in the region of each stone. Stone type was determined using commercial software (Syngo DE, Siemens) based on low and high kV, or bin 1 and bin 2 images (25-75 and 75-140 keV).

RESULTS

There were 161 stones (5.4±9.3 mm), with 72 stones ≤3mm. There was no difference in confidence for stone presence between 1 mm configurations for both modalities (p= 0.38 to 0.81), even for small stones (≤ 3mm). There were few artifacts affecting confidence with PCCT (2 for threshold 1 and 3 for bin 1 out of 161 readings). Stones were much more likely to be considered definitely present with 1 mm slices compared to 5 mm slices (p < .0001). Automatic stone characterization was more successful in PCCT than DECT (113 vs. 88 stones), and especially for small stones (37 vs.19). Agreement in stone composition between scanners (κ = .65) was substantial, with all uric acid stones detected in DECT classified similarly with PCCT.

CONCLUSION

Detection confidence for small stones was identical between PCCT and DECT. The primary advantage was the improved automatic characterization for small (≤ 3 mm) stones.

CLINICAL RELEVANCE/APPLICATION

PCCT's can display small stones as well as DECT, but allows more robust automated stone classification. Further, 1 mm images are far superior than 5 mm images for stone detection.

Honored Educators

Presenters or authors on this event have been recognized as RSNA Honored Educators for participating in multiple qualifying educational activities. Honored Educators are invested in furthering the profession of radiology by delivering high-quality educational content in their field of study. Learn how you can become an honored educator by visiting the website at: <https://www.rsna.org/Honored-Educator-Award/>

Terri J. Vrtiska, MD - 2016 Honored Educator

SSJ10-03 Assessment of Radiation Dose of Renal Colic CT Protocol with Dose Management Software: Comparison of an Academic Center with the ACR Dose Index Registry

Tuesday, Nov. 29 3:20PM - 3:30PM Room: E351

Participants

Markus M. Obmann, Basel, Switzerland (*Presenter*) Nothing to Disclose

Anushri Parakh, MBBS, MD, Basel, Switzerland (*Abstract Co-Author*) Consultant, Bayer AG

Andre Euler, MD, Basel, Switzerland (*Abstract Co-Author*) Nothing to Disclose

Sebastian T. Schindera, MD, Basel, Switzerland (*Abstract Co-Author*) Research Grant, Siemens AG; Research Grant, Ulrich GmbH & Co KG; Research Grant, Bayer AG; Speakers Bureau, Bayer AG

PURPOSE

To report the radiation dose for a renal colic CT protocol of an academic institution over a four year period and to compare those data with the published data from the ACR Dose Index Registry.

METHOD AND MATERIALS

The radiation dose of adult patients who underwent a renal colic CT protocol at an academic institution was tracked over a 4-year period (January 1st, 2012 to December 31st, 2015) with a radiation dose management software (Radimetrics, Bayer Healthcare). A total of 2760 CT scans were acquired with four CT scanners (one dual-source and three single-source CT scanners (16 to 128 slices)). The 25th, 50th and 75th percentile for the size-specific dose estimate (SSDE) and dose-length product (DLP) was recorded. The 50th percentile for the SSDE and DLP was used for comparison with the recent published ACR data (July to December 2015).

RESULTS

The 25th, 50th and 75th percentile for the SSDE of the academic center measured 5.8/7.1/8.7 mGy for 2012, 4.1/5.1/6.1 mGy for 2013, 4.1/5.1/6.0 mGy for 2014 and 4.5/5.3/6.2 mGy for 2015. The 25th, 50th and 75th percentile for the DLP of the academic center measured 167/289/474 mGy*cm for 2012, 143/177/236 mGy*cm for 2013, 142/170/217 mGy*cm for 2014 and 141/172/221 mGy*cm for 2015. The published ACR data was 145% higher for the 50th percentile of the SSDE (5.3 vs 13 mGy, respectively) and 256% higher for the 50th percentile of the DLP (172 vs 612 mGy*cm, respectively) compared with the academic center.

CONCLUSION

Over a 4-year period, a continuous radiation dose reduction was achieved by an academic institution (25% reduction for the 50th percentile SSDE and 41% reduction for the 50th percentile DLP). Dose-optimized renal colic CT protocols are not generally used in the institutions participating in the ACR dose registry.

CLINICAL RELEVANCE/APPLICATION

Substantial effort is required to increase the awareness and acceptance of dose-optimized CT protocols for urolithiasis in US radiology practices in order to increase patient safety.

SSJ10-04 Urinary Stone Characterization Using Single-Source and Dual-Source Dual Energy CT in Patients with Large Body Habitus

Tuesday, Nov. 29 3:30PM - 3:40PM Room: E351

Participants

Vinit Baliyan, MBBS, MD, Boston, MA (*Presenter*) Nothing to Disclose
Hamed Kordbacheh, MD, Boston, MA (*Abstract Co-Author*) Nothing to Disclose
Raul N. Uppot, MD, Boston, MA (*Abstract Co-Author*) Nothing to Disclose
Brian H. Eisner, MD, Boston, MA (*Abstract Co-Author*) Nothing to Disclose
Dushyant V. Sahani, MD, Boston, MA (*Abstract Co-Author*) Research support, General Electric Company; Medical Advisory Board, Allena Pharmaceuticals, Inc
Avinash R. Kambadakone, MD, Boston, MA (*Abstract Co-Author*) Nothing to Disclose

PURPOSE

The purpose of this study was to investigate the role of single-source and dual-source dual energy CT in the characterization of urinary stones in patients with large body habitus with emphasis on image quality and stone composition determination.

METHOD AND MATERIALS

In this retrospective study, we included patients with large body habitus (>90 kg) who underwent DECT (single-source and dual-source DECT) scans for evaluation of urolithiasis between February 2015 to February 2016. Qualitative and quantitative evaluation of the post processed DECT data sets was performed by independent reviewers for determination of stone composition (uric acid vs non-uric acid) and assessment of image quality based on European Quality Criteria for CT (image quality: score 1-4, artifact: score 1-4).

RESULTS

A total of 116 urinary tract calculi (mean size-4.7mm, range 1.8-19mm) were detected in 76 patients (ssDECT, n=36 and dsDECT, n=40). The mean patient body weight was 103.9± 13.5 kg (range 91-163 kg). Stone detection rate on standard blended(140/80kVp), quality control 140kVp and virtual monochromatic images was 100%. Image quality score of standard image data sets was acceptable (score:3.9). Characterization of stone composition into uric acid/non-uric acid stones was achieved in 74% (86/116) of calculi (mean size 5.1mm, range 2-19mm) while 20/116 stones could not be characterized (mean size: 3mm, range 1.8-6 mm)(p<0.001). Most common reason for non-characterization was image quality deterioration of the material specific iodine images due to severe photon starvation artifacts. Determination of stone composition was particularly limited in patients weighing >106kg and in stones <5mm. Effective DE field of view limitation did not hamper characterization of stone composition.

CONCLUSION

In patients with large body habitus, single source and dual-source DECT allow accurate characterization of urinary stone composition in 74% of calculi with limited role in characterization of small stones (<5mm) and in patients weighing >106 kg.

CLINICAL RELEVANCE/APPLICATION

DECT allows accurate differentiation of stone composition in patients with body habitus however characterization of small stones is limited and therefore careful patient selection is imperative.

Honored Educators

Presenters or authors on this event have been recognized as RSNA Honored Educators for participating in multiple qualifying educational activities. Honored Educators are invested in furthering the profession of radiology by delivering high-quality educational content in their field of study. Learn how you can become an honored educator by visiting the website at: <https://www.rsna.org/Honored-Educator-Award/>

Dushyant V. Sahani, MD - 2012 Honored Educator
Dushyant V. Sahani, MD - 2015 Honored Educator
Dushyant V. Sahani, MD - 2016 Honored Educator

SSJ10-05 Textural Features of Kidney Stone Fragility from Routine Single and Dual Energy CT

Tuesday, Nov. 29 3:40PM - 3:50PM Room: E351

Participants

Andrea Ferrero, PhD, Rochester, MN (*Presenter*) Nothing to Disclose
Juan Montoya, Rochester, MN (*Abstract Co-Author*) Nothing to Disclose
Alice Huang, Rochester, MN (*Abstract Co-Author*) Nothing to Disclose
Felicity Enders, Rochester, MN (*Abstract Co-Author*) Nothing to Disclose
Cynthia H. McCollough, PhD, Rochester, MN (*Abstract Co-Author*) Research Grant, Siemens AG

PURPOSE

Computed tomography (CT) is the recommended method for non-invasively imaging symptomatic urinary stones as it provides accurate sub-mm details of the size and location of stones within the urinary system. Previous studies have demonstrated a qualitative relationship between stone fragility and internal stone morphology. The goal of this study was to quantify morphological features from single and dual energy CT (SECT and DECT, respectively) images and assess their relationship to stone fragility.

METHOD AND MATERIALS

Thirty-three urinary stones of known composition (primarily calcium oxalate and calcium phosphate) were scanned with the routine DECT stone protocol in use at our institution (90/Sn150, 350/219 quality reference mAs, pitch = 0.6). Data were reconstructed both with the clinical 30 cm field of view (FOV) and with a smaller FOV (12 cm) centered on the stones using a quantitative kernel, 1 mm slice thickness and 0.8 mm slice interval. In addition to volume and surface morphology, 12 metrics describing internal morphology were computed using the co-occurrence matrix of each stone. Subsequent to stone imaging, stone fragility was measured by disintegrating each stone in a controlled ex vivo experiment using an ultrasonic lithotripter and recording the comminution time. A multivariable linear regression model was developed to predict time to comminution based on the measured

morphology and DECT metrics. A second model, which excluded DECT information, was developed to predict comminution time for SECT.

RESULTS

Using the routine scan protocol from our clinical practice, the DECT-derived metrics of volume, CT number ratio and surface shape index were found to have the best combined predictive ability to estimate comminution time (adjusted $R^2=0.58$). Similarly, a model that used only variables available with SECT data resulted in a predictive estimation of comminution time with $R^2=0.54$.

CONCLUSION

Volumetric and morphological metrics derived from routine SECT or DECT in vivo images can be used to estimate time to comminution time during lithotripsy performed ex vivo. 58% and 54% of all variation observed in stone comminution time was explained by our DECT and SECT models, respectively.

CLINICAL RELEVANCE/APPLICATION

If validated in vivo, the predictive models for stone fragility developed in this study would provide valuable information for the urologic surgeon and the patient to better evaluate treatment options.

SSJ10-06 Characterization of Urinary Calculi by Dark-field X-ray Radiography

Tuesday, Nov. 29 3:50PM - 4:00PM Room: E351

Participants

Iwan Jerjen, Villigen PSI, Switzerland (*Presenter*) Departmental Research Grant, Koninklijke Philips NV
Tilo Niemann, MD, Lille, France (*Abstract Co-Author*) Nothing to Disclose
Lukas Hefermehl, MD, Baden, Switzerland (*Abstract Co-Author*) Nothing to Disclose
Zhentian Wang, PhD, Villigen, Switzerland (*Abstract Co-Author*) Nothing to Disclose
Rahel A. Kubik-Huch, MD, Baden, Switzerland (*Abstract Co-Author*) Nothing to Disclose
Marco Stambanoni, PhD, Zurich, Switzerland (*Abstract Co-Author*) Nothing to Disclose

PURPOSE

The objective of our study was to evaluate the feasibility of in vitro characterization of stone composition of urinary calculi using grating-based x-ray interferometry.

METHOD AND MATERIALS

We prospectively evaluate sensitivity and specificity of a combination of attenuation and dark field contrast for stone characterization compared to dual energy computed tomography measurements. According to power analysis, a total of 100 stones is analysed with regard to material specific attenuation and scattering ratios. We use the combination of x-ray interferometric signals to estimate composition-related differences for different stone types. Results are compared with laboratory based infrared spectroscopy as reference standard.

RESULTS

For each calculus, the material specific attenuation to scattering ratio is determined. First results for the mean and sigma values are 0.13/0.04 for Uricite, 0.26/0.03 for Weddellite, 0.38/0.11 for Whewellite and 0.45/0.05 for Apatite stones. Depending on the heterogeneity of stone material composition there is a moderate to high correlation with laboratory characterization. Dense but compact calculi (e.g. Whewellite and Apatite) generally exhibit a higher attenuation to scattering ratio than light and structured calculi (e.g. Uricite) which have a lot of scattering centres and attenuate X-rays less. The variations between samples of the same type are huge and a lot of stones have mixed composition which may impede a clear classification of the calculi, but the same is true for dual energy X-ray imaging.

CONCLUSION

In vitro characterization of urinary stone composition is feasible using dark-field imaging. The variations between samples of the same type are huge and a lot of stones have mixed composition which may impede a clear classification of the calculi. Still there is high correlation with standard laboratory work-up.

CLINICAL RELEVANCE/APPLICATION

Today CT allows for diagnosis of urinary calculi as well as for determination of composition using dual energy acquisitions. Grating-based x-ray interferometry may have the potential to assess stone disease at lower doses than CT.

SSJ11

Genitourinary (Intervention of the Genitourinary Tract: Non-Prostate)

Tuesday, Nov. 29 3:00PM - 4:00PM Room: E353B



AMA PRA Category 1 Credit™: 1.00
ARRT Category A+ Credit: 1.00

Participants

David D. Childs, MD, Clemmons, NC (*Moderator*) Nothing to Disclose
Steven S. Raman, MD, Santa Monica, CA (*Moderator*) Nothing to Disclose

Sub-Events

SSJ11-01 Disposition after Percutaneous Thermal Ablation of localized RCC: Risk Factors Associated with Need for Hospitalization

Tuesday, Nov. 29 3:00PM - 3:10PM Room: E353B

Participants

Shane A. Wells, MD, Madison, WI (*Presenter*) Nothing to Disclose
J. Louis Hinshaw, MD, Middleton, WI (*Abstract Co-Author*) Stockholder, NeuWave Medical Inc; Stockholder, Collectar Biosciences, Inc
Timothy J. Ziemlewicz, MD, Madison, WI (*Abstract Co-Author*) Consultant, NeuWave Medical, Inc
Sarah Best, Madison, WI (*Abstract Co-Author*) Nothing to Disclose
Meghan G. Lubner, MD, Madison, WI (*Abstract Co-Author*) Grant, Koninklijke Philips NV; Grant, Johnson & Johnson;
Fred T. Lee JR, MD, Madison, WI (*Abstract Co-Author*) Nothing to Disclose
Jason Abel, Madison, WI (*Abstract Co-Author*) Nothing to Disclose

PURPOSE

To identify patient and tumor characteristics predictive of early procedure related complications in patients undergoing thermal ablation of localized renal cell carcinoma.

METHOD AND MATERIALS

Retrospective review of 235 consecutive patients who underwent percutaneous thermal ablation for localized RCC from 2001-2015. Patient demographics, comorbidities, pathology, tumor size, RENAL score, procedure and hospital course details, and 30 day complications were recorded. We used an inclusive retrospective assessment to determine which patients benefited from overnight hospitalization. This included patients experiencing a complication, those who stayed >24 hours and those readmitted within 72 hours from discharge. Fischer's exact, Wilcoxon rank sum, and univariate logistic regression tests were used as appropriate.

RESULTS

High-grade complications (3.4%) were rare. Six patients (2.5%) had a bleeding complication. These patients had a higher BMI (39.4 vs 31.3, $p=0.047$), larger tumors (median 4.0 vs 2.6cm, $p=0.04$), higher RENAL score (9 vs 7, $p=0.056$) and were more likely to have a hematoma on immediate post-procedure CT (67% vs 12%, $p=0.004$). Patients with a hematoma were 14.3x more likely to have a bleeding complication ($p=0.0028$). The use of ≥ 3 ablation applicators was associated with an 18.9x risk of bleeding ($p=0.008$). In retrospect, 14 patients (6%) were judged to benefit from hospital admission. Factors associated with this include tumor ≥ 3 cm (OR 4.4, $p=0.152$), RENAL score >8 (OR 7.2, $p=0.0012$), post-procedure hematoma (OR 5.6, $p=0.0029$), and using ≥ 3 ablation applicators (OR 7.2, $p=0.0007$).

CONCLUSION

High-grade complications, including significant bleeding, are rare following thermal ablation of localized RCC. Larger tumors, higher tumor complexity, post-procedure hematoma, and higher BMI increase the risk for complications. These patients may benefit from overnight hospital admission.

CLINICAL RELEVANCE/APPLICATION

The majority of patients who undergo percutaneous thermal ablation of renal cell carcinoma can be safely discharged on the day of the procedure and avoid the cost and inconvenience of hospitalization.

Honored Educators

Presenters or authors on this event have been recognized as RSNA Honored Educators for participating in multiple qualifying educational activities. Honored Educators are invested in furthering the profession of radiology by delivering high-quality educational content in their field of study. Learn how you can become an honored educator by visiting the website at: <https://www.rsna.org/Honored-Educator-Award/>

Meghan G. Lubner, MD - 2014 Honored Educator
Meghan G. Lubner, MD - 2015 Honored Educator

SSJ11-02 Single Institutional Review of 15 Years of Renal Mass Biopsy

Tuesday, Nov. 29 3:10PM - 3:20PM Room: E353B

Participants

Rosaleen B. Parsons, MD, Philadelphia, PA (*Presenter*) Nothing to Disclose
David B. Cahn, DO, Philadelphia, PA (*Abstract Co-Author*) Nothing to Disclose
Alexander Kutikov, Philadelphia, PA (*Abstract Co-Author*) Nothing to Disclose
David Y. Chen, MD, Philadelphia, PA (*Abstract Co-Author*) Nothing to Disclose

Richard E. Greenberg, Philadelphia, PA (*Abstract Co-Author*) Nothing to Disclose
Rosalie Viterbo, MD, Philadelphia, PA (*Abstract Co-Author*) Nothing to Disclose
Marc Smaldone, Philadelphia, PA (*Abstract Co-Author*) Nothing to Disclose
Robert Uzzo, MD, Philadelphia, PA (*Abstract Co-Author*) Nothing to Disclose

PURPOSE

The purpose of this study was to review our 15 yr institutional experience with renal mass biopsy

METHOD AND MATERIALS

Using our prospectively maintained database we identified patients who underwent renal mass biopsy and reviewed our institutional experience and assessed pathologic and histologic features and concordance rates.

RESULTS

A total of 374 renal biopsies were performed from 1999-2015. Core(+/- FNA) was performed in 65.2% of the cases and 41% underwent surgical resection. Core was nondiagnostic in 9% of surgical cases and subsequently diagnosed with RCC. 11% of biopsies were benign and no surgery was performed. Of the benign lesions 69% were oncocytoma and 2.5% angiomyolipoma. RCC diagnosed on core sampling that underwent resection demonstrated histological/grade concordance of 94.3%/62.5%. All discordant grades were upgraded at surgery. FNA was performed on 22.7% of cases and at final pathology histologic concordance was 72.5% and 5% were upgraded from benign to malignant.

CONCLUSION

Renal lesion biopsy is effective in the evaluation of renal masses and our data is consistent with previously published data. This underscores that although biopsy harbors clinical uncertainties diagnostic accuracy may assist in clinical management. Pathways incorporating renal biopsy may decrease over treatment but may also risk under treatment based on poor grade concordance.

CLINICAL RELEVANCE/APPLICATION

Renal mass biopsy is becoming increasingly important in the patient management and as radiologists we should anticipate that requests for biopsy of renal masses will continue

SSJ11-03 Evaluation of Complications from Ultrasound-Guided Percutaneous Transplant Kidney Biopsies

Tuesday, Nov. 29 3:20PM - 3:30PM Room: E353B

Awards

Student Travel Stipend Award

Participants

Neema J. Patel, MD, Jacksonville, FL (*Presenter*) Nothing to Disclose
Jacob Lewis, MD, Jacksonville, FL (*Abstract Co-Author*) Nothing to Disclose
Andrew Bowman, MD, PhD, Jacksonville, FL (*Abstract Co-Author*) Nothing to Disclose

PURPOSE

To determine the prevalence and type of complications that occur during ultrasound-guided transplant kidney biopsies in order to discern whether routine pre-procedure intravenous (IV) access is necessary for potential resuscitation efforts.

METHOD AND MATERIALS

A retrospective review of medical records was performed in patients who underwent an ultrasound-guided kidney biopsy performed between 7/2/2013 and 6/30/2015. Procedures performed on inpatients, native kidneys, renal lesions, and those performed by services other than Radiology were excluded. Biopsy information was recorded and analyzed, including the following: any intervention or treatment (other than pain control), unexpected complications, and hospital admissions or return visits to the emergency department (ED) within 7 days of the biopsy.

RESULTS

After exclusion criteria were applied, there were 1318 transplant kidney biopsies in 601 patients. There were five (0.38%) serious complications/unexpected adverse events requiring treatment. These complications included bleeding/hematuria, hypotension, hypertensive urgency, syncope, and pain. Only 1 (0.07%) of the cases was taken to angiography to evaluate for active bleeding, which did not occur until several hours after the biopsy, and no bleeding was found thus no intervention was performed. There were 8 (0.62%) minor complications requiring hospital admission for observation and/or a return visit to the ED for additional evaluation. These included perinephric hematoma (0.38%), hematuria (0.15%), and pain (0.07%).

CONCLUSION

The prevalence of renal transplant biopsy complications at our institution is low (1.0%), with only 0.38% of biopsies requiring IV access for treatment, which suggests that IV access is not routinely required prior to renal transplant biopsy.

CLINICAL RELEVANCE/APPLICATION

Routine pre-procedure IV placement may be safely discontinued without negatively affecting patient outcomes, and this should improve both departmental efficiency and patient satisfaction.

SSJ11-04 MRgFUS as Minimally Invasive Alternative Therapy in the Treatment of Submucosal Fibroids: Effectiveness and Safety

Tuesday, Nov. 29 3:30PM - 3:40PM Room: E353B

Participants

Fabiana Ferrari, MD, L'Aquila, Italy (*Abstract Co-Author*) Nothing to Disclose
Fernando Smaldone, MD, L'Aquila, Italy (*Presenter*) Nothing to Disclose
Francesco Arrigoni, Coppito, Italy (*Abstract Co-Author*) Nothing to Disclose

Anna Miccoli, MD, L'Aquila, Italy (*Abstract Co-Author*) Nothing to Disclose
Eva Fascetti, MD, L'Aquila, Italy (*Abstract Co-Author*) Nothing to Disclose
Carlo Masciocchi, MD, L'Aquila, Italy (*Abstract Co-Author*) Nothing to Disclose

PURPOSE

To evaluate the effectiveness of MRgFUS as mini-invasive alternative therapy in the treatment of submucosal fibroids and to discuss about its safety and feasibility.

METHOD AND MATERIALS

From July 2012 to June 2014, 13 patients (mean age 48 years), affected by submucosal uterine fibroids, were treated using MRgFUS. The patients were submitted to preliminary MRI to classify the sub-mucosal fibroids (FIGO classification) and to measure the pre-treatment fibroid volumes. Sub-mucosal fibroids of type 0, 1 and 2 (measuring between 1.5 and 4 cm) were treated using MRgFUS. Five out of 13 patients presented only a single submucosal fibroid (2 of type 1, 2 of type 2 and 1 of type 0). Eight out of 13 patients were simultaneously affected by sub-mucosal fibroids (6 of type 2, 3 of type 1 and 2 of type 0) and other fibroids (type 3-6). The patients were submitted to one treatment alone. Immediately after treatment, the patients were submitted to c.e. MRI to evaluate the Non Perfused Volume (NPV) on the c.e. T1-weighted sequences and measure the radicalization of the treatment in comparison to the pre-treatment volume and after 2-4 years from the treatment.

RESULTS

All treated patients presented a mean extension of the NPV of 90% with a significant radicalization of the treatment without complications or side effects. After 2-4 years from the treatment, 7/13 (54%) showed progressive reduction of the volume with a regularization of the uterine wall. Five out of 13 patients (38%) showed significant reduction of fibroid volume (about 80%.) In one patient (8%), the fibroids of type 0 were partially eliminated from inside the uterine cavity. In this case, the patient was submitted to close MRI follow-up, which showed progressive elimination of the necrotic product. A poor vaginal bleeding lasted 15 days without necessity of hysteroscopy.

CONCLUSION

MRgFUS represent a valid miniminvasive and radical approach in the treatment of submucosal fibroids. It allows treatment of the intramural part of the fibroid that cannot be completely treated with hysteroscopy.

CLINICAL RELEVANCE/APPLICATION

MRgFUS is promising technique in submucosal fibroids without significant risks and complications.

SSJ11-05 Uterine Fibroids treated with MR guided High Intensity Focused Ultrasound (MRgFUS): Clinical Outcome in Comparison to Current Therapeutic Strategies

Tuesday, Nov. 29 3:40PM - 3:50PM Room: E353B

Participants

Fabrizio Andrani, Roma, Italy (*Presenter*) Nothing to Disclose
Carola Palla, MD, Rome, Italy (*Abstract Co-Author*) Nothing to Disclose
Federica Ciolina, MD, Rome, Italy (*Abstract Co-Author*) Nothing to Disclose
Michele Anzidei, MD, Rome, Italy (*Abstract Co-Author*) Nothing to Disclose
Alessandro Napoli, MD, Rome, Italy (*Abstract Co-Author*) Nothing to Disclose

PURPOSE

To prospectively evaluate clinical outcome of patients affected by uterine leiomyoma and treated using Magnetic Resonance Focused Ultrasound (MRgFUS), Uterine Artery Embolization (UAE) or Surgery.

METHOD AND MATERIALS

570 women affected by symptomatic uterine leiomyoma referred our department for treatment of uterine fibroids with MRgFUS. Pre-treatment evaluation assessed fibroids MR characteristics and MRgFUS eligibility. 166 of 182 eligible patients (group A) were treated with MRgFUS, while 388 women resulted ineligible. 33/388 patients underwent UAE (group B), 140/388 myomectomy (group C) and 58/388 hysterectomy (group D). Clinical efficacy for each treatment was determined by Symptoms Severity Score (SSS) pre-treatment and at 3- and 12-month follow-up intervals. Further data concerning number and type of complications, days of hospitalization and days of convalescence were also collected and compared.

RESULTS

MRgFUS group showed a mean decrease in SSS of 24,6% at 3 months and 55,8% at 12 months. SSS drop in UAE group was 51,2% and 57,4%, respectively. SSS reduction in myomectomy was 71,5% and 66,0%. After hysterectomy SSS decrease was 96,6% and 94,5%. MRgFUS group demonstrated the least number of adverse events (3 patients, 1,8 %), while the major adverse events rate was experienced in UAE group (37 patients, 26,4 %). MRgFUS patients were treated in outpatient setting, while mean days for hospitalisation and convalescence for other groups were respectively 3,1±2 and 12,4±9 days for group B; 4,5±2 and 17,2±12 days for group C; 4±1 and 26,3±14 days for group D.

CONCLUSION

MRgFUS clinical efficacy for uterine fibroids treatment is comparable to UAE and only slightly lower than myomectomy. However, MRgFUS is feasible in an outpatient setting and complications rate is significantly lower than other therapeutic strategies.

CLINICAL RELEVANCE/APPLICATION

MRgFUS added a new therapeutic strategy for uterine fibroids, being validated as a non-invasive, safe and effective option for selected patients.

SSJ11-06 Post Ablation Tubal Sterilization Syndrome (PATSS), A Complication of Endometrial Ablation and Surgical Sterilization: New Entity Under-Diagnosed by Radiologists

Tuesday, Nov. 29 3:50PM - 4:00PM Room: E353B

Awards

Student Travel Stipend Award

Participants

Sumin S. Lee, MD, Winston-Salem, NC (*Presenter*) Nothing to Disclose

Keyanoosh Hosseinzadeh, MD, Winston Salem, NC (*Abstract Co-Author*) Nothing to Disclose

James J. Perumpillichira, MD, Winston-Salem, NC (*Abstract Co-Author*) Nothing to Disclose

Pooja H. Doshi, MD, Winston Salem, NC (*Abstract Co-Author*) Nothing to Disclose

PURPOSE

PATSS is a debilitating condition, an under-recognized complication of combined endometrial ablation and surgical sterilization. The aim is to determine imaging features of PATSS in symptomatic women.

METHOD AND MATERIALS

Retrospective chart review revealed 104 women who had endometrial ablation (EA) and surgical sterilization (SS). Inclusion criteria consisted of symptomatic women with imaging studies. 38 patients with total of 55 studies were included. Two radiologists independently reviewed randomized studies in a blinded fashion for presence or absence of: cornual hematometra, central hematometra, hematosalpinx or fluid filled fallopian tube, adhesions, endometriosis, and adenomyosis. Discordances were resolved by a third radiologist. Interobserver agreement was assessed by kappa statistics for the imaging features and diagnosis of PATSS (fluid filled fallopian tube and either central or cornual hematometra).

RESULTS

18 CT, 34 ultrasound, and 3 MRI studies were performed. Kappa values for CT and US were: cornual hematometra (0.77 vs 0.59), central hematometra (0.43 vs 0.15), fluid filled fallopian tube (0.63 vs 0.69), PATSS (0.68 vs 0.64), adhesions (0.15 vs 0.42), adenomyosis (0.55 vs 0.39), and endometriosis (1.0 vs 0.65). Interobserver analysis on MRI was excluded due to the small number. PATSS was diagnosed in 6/34 (18%) US, 5/18 (28%) CT, and 3/3 (100%) MRI. Concordance rates for PATSS with final radiology reports were: 4/6 (67%) US, 2/5 (40%) CT, and 3/3 (100%) MRI. 4 out of 11 (36%) women diagnosed with PATSS underwent hysterectomies, often without salpingectomies, with pathology report demonstrating changes consistent with only endometrial ablation.

CONCLUSION

PATSS is under-diagnosed in symptomatic women with history of endometrial ablation and surgical sterilization, with fair to good agreement by US and CT. Limited hysterectomy pathologies are not diagnostic for PATSS. Rather, given the data above, radiologic studies should be considered diagnostic in evaluation of this new entity given management considerations.

CLINICAL RELEVANCE/APPLICATION

Radiologists need to recognize imaging features related to complications of EA and SS procedure with increasing awareness of PATSS.

Science Session with Keynote: Health Service, Policy and Research (Miscellaneous)

Tuesday, Nov. 29 3:00PM - 4:00PM Room: S102D

HPAMA PRA Category 1 Credit™: 1.00
ARRT Category A+ Credit: 0**Participants**

Christopher P. Hess, MD, PhD, San Francisco, CA (*Moderator*) Research Grant, General Electric Company; Research Grant, Quest Diagnostics Incorporated; Research Grant, Cerebrotech Medical Systems, Inc; Speaker, Siemens AG;
Pari Pandharipande, MD, MPH, Boston, MA (*Moderator*) Nothing to Disclose

Sub-Events**SSJ12-01 Do We Agree to Disagree? Patterns of Radiologist Reporting of Indeterminate and Suspicious Findings on Abdominal Imaging**

Tuesday, Nov. 29 3:00PM - 3:10PM Room: S102D

Participants

Tessa S. Cook, MD, PhD, Philadelphia, PA (*Presenter*) Nothing to Disclose
Rebecca Hubbard, Philadelphia, PA (*Abstract Co-Author*) Nothing to Disclose
Darco Lalevic, Philadelphia, PA (*Abstract Co-Author*) Nothing to Disclose
Christopher Pizzurro, Philadelphia, PA (*Abstract Co-Author*) Nothing to Disclose
Mitchell D. Schnall, MD, PhD, Philadelphia, PA (*Abstract Co-Author*) Nothing to Disclose
Hanna M. Zafar, MD, Philadelphia, PA (*Abstract Co-Author*) Nothing to Disclose

PURPOSE

Using structured reporting to characterize imaging findings indeterminate or suspicious for cancer in the abdomen enables the study of the patterns of radiologist reporting of these lesions.

METHOD AND MATERIALS

A coding system analogous to BI-RADS® was developed for focal lesions in the liver, pancreas, kidneys and adrenal glands at our main hospital. Lesions were categorized as benign (category 1, 2 or 7), indeterminate (category 0 or 3) and suspicious (category 4 or 5); category 99 was used for technically inadequate imaging, and category 6 for known cancer. The system was incorporated into a structured template required for all abdominal CT, MR and US exams, and mined using a recommendation-tracking engine. Data collected by the engine for the first 2 years were reviewed to characterize the variability in assigning degrees of suspicion for malignancy between radiologists.

RESULTS

A total of 57,500 abdominal CT, MR and US exams were reported by 29 radiologists using the system between 7/1/2013 and 6/30/2015. Radiologists identified indeterminate findings in the liver at a similar frequency, with interquartile ranges (IQRs) between 1.7% and 2.7% for all modalities. Both indeterminate and suspicious findings in the kidneys and adrenal glands were also identified on CT and MR with low variability among radiologists (IQRs 0.4-1.7%) By contrast, identification of indeterminate findings in the pancreas on MR demonstrated high inter-radiologist variability, with an IQR of nearly 10% and one radiologist reporting such findings nearly 25% of the time. Wider inter-radiologist variability was also noted for suspicious liver findings, particularly when identified on MR (IQR 3.5%); one radiologist reported such findings nearly 11% of the time.

CONCLUSION

Radiologists variably report indeterminate and suspicious findings on abdominal imaging depending on organ and modality. Understanding this variability can lead to more consistent reporting and potentially reduce unnecessary follow-up imaging.

CLINICAL RELEVANCE/APPLICATION

Structured radiology reporting can be used to characterize radiologists' reporting patterns for indeterminate and suspicious findings of cancer on abdominal imaging.

Honored Educators

Presenters or authors on this event have been recognized as RSNA Honored Educators for participating in multiple qualifying educational activities. Honored Educators are invested in furthering the profession of radiology by delivering high-quality educational content in their field of study. Learn how you can become an honored educator by visiting the website at: <https://www.rsna.org/Honored-Educator-Award/>

Mitchell D. Schnall, MD, PhD - 2013 Honored Educator

SSJ12-02 Cadaver-Specific CT Scans Visualized at the Dissection Table Combined with Virtual Dissection Tables Improve Learning Performance in General Gross Anatomy

Tuesday, Nov. 29 3:10PM - 3:20PM Room: S102D

Awards**Trainee Research Prize - Resident****Participants**

Daniel Paech, MD, Heidelberg, Germany (*Presenter*) Nothing to Disclose
Sara Doll, Heidelberg, Germany (*Abstract Co-Author*) Nothing to Disclose

Thomas Kuner, Heidelberg, Germany (*Abstract Co-Author*) Nothing to Disclose
Heinz-Peter W. Schlemmer, MD, Heidelberg, Germany (*Abstract Co-Author*) Nothing to Disclose
Roland Unterhinninghofen, PhD, Karlsruhe, Germany (*Abstract Co-Author*) Nothing to Disclose
Frederik L. Giesel, MD, MBA, Heidelberg, Germany (*Abstract Co-Author*) Patent application for F18-PSMA-1007

PURPOSE

To quantify the benefit of the incorporation of radiologic anatomy (RA), in terms of student training in RA-seminars, cadaver CT scans and life size virtual dissection tables on the learning success in general anatomy.

METHOD AND MATERIALS

Three groups of a total of 238 students were compared in a multiple choice general anatomy examination. The intervention group (year 2015, n1=50) with training in radiologic image interpretation (RA-seminar) and additional access to cadaver CT scans was compared to a group that was trained in the RA-seminar only (2011, n2=90) and a control group without any radiologic image interpretation training (2011, n3=98). All participants took a test of 40 highly discriminating questions, comprising of 10 questions each on head & neck, abdomen, thorax and extremities derived from the 10% most difficult questions of the National Board Examinations (2005-2010). Furthermore, the students' perception was assessed qualitatively through a survey (12 questions; 5 item Lickert-scale).

RESULTS

The average test score of the intervention group (21.8 ± 5.0) was significantly higher both compared to the group that was trained in the RA-seminar only (18.3 ± 5.0) and to the control group (17.1 ± 4.7) (p<0.001). The intervention group showed highly significant improvements compared to the other two groups in the subcategories head & neck (p<0.001) and extremities (p<0.001, p=0.002). In the category of thorax small but significant differences were detectable between the students of the intervention and the control group. Significant differences between the RA-seminar and the control group were only found in the category of thorax (p=0.025). 87.8% of the students agreed that teaching with radiologic imaging modalities was a good supplement to first year gross anatomy and a large majority of 85.4% stated that it was sensible to learn how to read CT scans at the beginning of their medical studies.

CONCLUSION

The incorporation of cadaver CT scans and life size virtual dissection tables significantly improved the performance of medical students in general gross anatomy. Medical imaging and virtual dissection tables should therefore be considered to be part of the standard curriculum of gross anatomy.

CLINICAL RELEVANCE/APPLICATION

Training in radiologic image interpretation on cadaver CT-scans and virtual dissection tables improves general anatomical knowledge and facilitates a smooth transition into the clinical work.

SSJ12-03 Conflict of Interest Disclosure in Medical Journals: Comparing Imaging Journal to Non-imaging Journals and Radiologists to other Specialists

Tuesday, Nov. 29 3:20PM - 3:30PM Room: S102D

Participants

Nasrin Fatemi, MD, Stony Brook, NY (*Presenter*) Nothing to Disclose
Danielle Kruse, BA, Stony Brook, NY (*Abstract Co-Author*) Nothing to Disclose
Mark E. Schweitzer, MD, Stony Brook, NY (*Abstract Co-Author*) Consultant, MMI Munich Medical International GmbH Data Safety Monitoring Board, Histogenics Corporation

PURPOSE

To determine authors' compliance with the conflict of interest (COI) policies published in specific medical journals, and to see if this compliance is different for imaging oriented journals and for radiologists as opposed to other specialists.

METHOD AND MATERIALS

COI reports submitted by authors to 15 medical journals for a three month period, from July to September of 2015, were collected. The journals were chosen to be able to compare imaging journals with clinical medicine and surgical ones. These journals included Radiology, AJR, AJNR, JVIR, JBJS, CORR, Spine, JCO, Cancer Research, JACS, Neurosurgery, Arthritis and Rheumatology, Clinical Rheumatology, JVS and JAMA Surgery. Physician authors who are required by law to report their payments and other transfer values to the government, were identified. The data were compared with the open payment data available at the government CMS (Center for Medicare and Medicaid Services) website. Data was stratified by journal type (imaging vs non imaging), and physician specialty (radiologists vs other specialists).

RESULTS

1336 articles were analyzed with 2368 contributing authors qualified. Review of the COI policies of 15 journals showed that 3 required a full unconditional report, with 12 having less rigorous disclosure policies. Overall only 0.3%-7% of authors fully reported their COI. Three journals studied had robust COI disclosure, nonetheless 30%, 61% and 62% of authors denied any COI in contradistinction to the financial data published on the CMS website. Similar false denial rates ranged from 27% to 83% in the journal with looser policies. The rate of incomplete disclosures was 11%-19% in journals with strict policies as opposed to 3%-29% in journals laxer disclosure requirements. In imaging journals 30% (220) of radiologists falsely denied COI as compared to a much higher rate (57% (1081)) of other specialists writing in non imaging journals (p<0.0002). However, 34% (253) of radiologists writing in imaging journals correctly denied COIs, as opposed to 22% (431) of other specialists writing in non imaging journals (p<0.0002).

CONCLUSION

A surprisingly small percent of scientific authors acknowledge their financial support. Radiologists seems more compliant with these published policies.

CLINICAL RELEVANCE/APPLICATION

This study can bring a discussion about COI in clinical research.

SSJ12-04 Structured Reporting of Focal Abdominal Masses Suspicious for Cancer: Lessons Learned from a Two-Year Initiative at a Multi-Hospital Academic Medical Center

Tuesday, Nov. 29 3:30PM - 3:40PM Room: S102D

Participants

Tessa S. Cook, MD, PhD, Philadelphia, PA (*Presenter*) Nothing to Disclose
Darco Lalevic, Philadelphia, PA (*Abstract Co-Author*) Nothing to Disclose
Seetharam C. Chadalavada, MD, MS, Cincinnati, OH (*Abstract Co-Author*) Nothing to Disclose
Caroline Sloan, Philadelphia, PA (*Abstract Co-Author*) Nothing to Disclose
Curtis P. Langlotz, MD, PhD, Menlo Park, CA (*Abstract Co-Author*) Shareholder, Montage Healthcare Solutions, Inc; Spouse, Consultant, Novartis AG;
Rebecca Hubbard, Philadelphia, PA (*Abstract Co-Author*) Nothing to Disclose
Mitchell D. Schnall, MD, PhD, Philadelphia, PA (*Abstract Co-Author*) Nothing to Disclose
Charles E. Kahn JR, MD, MS, Philadelphia, PA (*Abstract Co-Author*) Nothing to Disclose
Hanna M. Zafar, MD, Philadelphia, PA (*Abstract Co-Author*) Nothing to Disclose

PURPOSE

Using structured reporting to characterize imaging findings suspicious for cancer in the abdomen allows radiologists to quantify the types of lesions identified within four solid abdominal organs and monitor patients who require follow-up evaluation.

METHOD AND MATERIALS

Our main hospital developed a coding system analogous to BI-RADS® for focal lesions in the liver, pancreas, kidneys and adrenal glands. Lesions were categorized as benign (category 1, 2 or 7), indeterminate (category 0 or 3) and suspicious (category 4 or 5); category 99 was used for technically inadequate imaging, and category 6 for known cancer. The system was incorporated into a structured template used for CT, MR and US imaging in the abdomen, and a recommendation-tracking engine was built. The first 2 years' worth of data from the system were reviewed, to study the types of studies performed and the distribution of lesion types across the reported organs and modalities.

RESULTS

A total of 57,778 abdominal imaging exams (34,991 CT; 10,751 MR; and 12,036 US) were performed at our main hospital between 7/1/2013 and 6/30/2015. 61% exams were performed in the outpatient setting, 22% in the inpatient setting, and 16% in the emergency department; patient location could not be determined for 1% of exams. Abdominal imaging was ordered by physicians (79%), advanced practice nurses (14%) and physician assistants (4%); ordering provider type could not be determined for 3% of exams. The majority of cases were coded as benign. 16% of all exam reports identified indeterminate (9%) or suspicious (7%) findings. Most of these findings were identified in the liver using CT (4.6% of exams) or MR (2.1%). In the kidneys, 2.7% were identified using CT and 1% using MR. Only 2.1% and 1.8% of all exams revealed either indeterminate or suspicious findings in the pancreas and adrenal glands, respectively.

CONCLUSION

In a 2-year period, 16% of abdominal imaging reports identified findings indeterminate or suspicious for malignancy. Most such findings were identified in the liver and kidneys.

CLINICAL RELEVANCE/APPLICATION

Combining structured reporting with a standardized nomenclature and an informatics solution enables identification and monitoring of patients at risk for missed follow-up and adverse outcomes.

Honored Educators

Presenters or authors on this event have been recognized as RSNA Honored Educators for participating in multiple qualifying educational activities. Honored Educators are invested in furthering the profession of radiology by delivering high-quality educational content in their field of study. Learn how you can become an honored educator by visiting the website at: <https://www.rsna.org/Honored-Educator-Award/>

Charles E. Kahn JR, MD, MS - 2012 Honored Educator
Mitchell D. Schnall, MD, PhD - 2013 Honored Educator

SSJ12-05 Prevalence of Burnout Among Practitioners of a Radiology Subspecialty

Tuesday, Nov. 29 3:40PM - 3:50PM Room: S102D

Participants

Felix S. Chew, MD, Seattle, WA (*Presenter*) Nothing to Disclose
Michael J. Mulcahy, PhD, Ellensburg, WA (*Abstract Co-Author*) Nothing to Disclose
Jack A. Porriño Jr, MD, Seattle, WA (*Abstract Co-Author*) Nothing to Disclose
Hyojeong Mulcahy, MD, Seattle, WA (*Abstract Co-Author*) Nothing to Disclose
Annemarie Relyea-Chew, JD,MS, Seattle, WA (*Abstract Co-Author*) Nothing to Disclose

PURPOSE

According to Maslach, burnout is a job-related psychological syndrome with three aspects: emotional exhaustion, depersonalization, and perceived lack of personal accomplishment. Burnout has been associated with deleterious effects on both the workers and the quality of their work. When burnout affects physicians, their well-being and longevity and the care of their patients may be at risk. Recent reports concerning burnout among physicians tend to treat specialists such as radiologists as a single group. We sought to explore the prevalence of burnout in a sample of musculoskeletal (MSK) radiologists.

METHOD AND MATERIALS

An IRB waiver was obtained. During Jan 2016, the 1,100 members of a society of MSK radiologists were invited to take an

An IRB waiver was obtained. During Jan 2010, the 1,170 members of a Society of MSK radiologists were invited to take an anonymous survey that included questions adapted from the Maslach Burnout Inventory (MBI). The MBI evokes responses on a seven-point scale along the three dimensions of burnout: emotional exhaustion, depersonalization, and perceived lack of personal accomplishment. Maslach's normative categorization of MBI scores divided occupational subgroups into thirds, representing low, average, and high levels of burnout. We considered a manifestation of burnout to be present if the specific MBI subscore for that manifestation would have placed the respondent into the high burnout level for the medicine occupational subgroup. There were 433 respondents (36% response rate). Not every respondent completed every question.

RESULTS

In our sample, the prevalence of emotional exhaustion was 62%, of depersonalization 53%, and of perceived lack of accomplishment 40%. Only 20% reported no manifestations of burnout, while 80% reported manifestations along at least one dimension of burnout, 52% along at least two, and 22% along all three. Between men and women, the overall prevalence of burnout was similar. In private practice, emotional exhaustion and depersonalization was worse than in academics, but in academics, lack of accomplishment was worse than in private practice.

CONCLUSION

Among MSK radiologists, the prevalence and severity of burnout was worse than previously reported for radiologists. There were differences between genders and practice settings.

CLINICAL RELEVANCE/APPLICATION

The high prevalence of burnout among MSK radiologists suggests that ameliorating burnout should be a priority. Doing so may help address manpower needs and quality of care concerns.

Honored Educators

Presenters or authors on this event have been recognized as RSNA Honored Educators for participating in multiple qualifying educational activities. Honored Educators are invested in furthering the profession of radiology by delivering high-quality educational content in their field of study. Learn how you can become an honored educator by visiting the website at: <https://www.rsna.org/Honored-Educator-Award/>

Felix S. Chew, MD - 2012 Honored Educator

Felix S. Chew, MD - 2016 Honored Educator

SSJ12-06 Health Service, Policy and Research Keynote Speaker: Recent Trends Suggest Private Office Imaging May Be in Jeopardy

Tuesday, Nov. 29 3:50PM - 4:00PM Room: S102D

Participants

David C. Levin, MD, Philadelphia, PA (*Presenter*) Consultant, HealthHelp, LLC; Board of Directors, Outpatient Imaging Affiliates, LLC

Informatics (Enterprise Integration and Business Analytics)

Tuesday, Nov. 29 3:00PM - 4:00PM Room: S402AB



AMA PRA Category 1 Credit™: 1.00
ARRT Category A+ Credit: 0

Participants

Rasu B. Shrestha, MD, MBA, Pittsburgh, PA (*Moderator*) Advisory Board, General Electric Company; Editorial Advisory Board, Anderson Publishing, Ltd; Advisory Board, KLAS Enterprises LLC; Advisory Board, Peer60; Board, Pittsburgh Dataworks; Board, Omnyx, LLC;
Jonelle M. Petscavage-Thomas, MD, MPH, Hummelstown, PA (*Moderator*) Consultant, Medical Metrics, Inc

Sub-Events

SSJ13-01 Report Turnaround Time after Mobile Dictation System Implementation - An Initial Assessment

Tuesday, Nov. 29 3:00PM - 3:10PM Room: S402AB

Participants

Raja Gali, MS, Philadelphia, PA (*Presenter*) Nothing to Disclose
Jaydev K. Dave, PhD, MS, Philadelphia, PA (*Abstract Co-Author*) Nothing to Disclose
Vijay M. Rao, MD, Philadelphia, PA (*Abstract Co-Author*) Nothing to Disclose
Paras Lakhani, MD, Philadelphia, PA (*Abstract Co-Author*) Nothing to Disclose
Adam E. Flanders, MD, Narberth, PA (*Abstract Co-Author*) Nothing to Disclose
Yeeting Young, Philadelphia, PA (*Abstract Co-Author*) Nothing to Disclose

CONCLUSION

The introduction of mobile app that lets the attending radiologist finalize a report shows a marked improvement in the turnaround time.

Background

Report turnaround time is one of the critical quality metric used in radiology and is important for patient care. This study was performed to evaluate the impact of a mobile app, designed for attending radiologist to sign-off and finalize a report, on the report turnaround time in an academic radiology department of a tertiary care center.

Evaluation

Report turnaround time data was collected 60 days before and 30 days immediately after the implementation of the mobile app (PowerScribe 360 Mobile Radiologist, Nuance Communications, Inc.) from RIS (Centricity, GE Healthcare). Data from the attending radiologists with less than 30 cases either before or after the implementation was not included in the analysis. The outcome variable tested was the average time taken from initial dictation (D) to final sign-off (F) of the report (D – F). Pre and post mobile app implementation data were compared for the entire data set and then comparisons were repeated split by modality (MRI, CT, and US) and by patient type (Emergency, Outpatient and Inpatient) Paired t-test with Bonferroni corrections for multiple comparisons was used for analysis.

Discussion

Data from 102,084 reports read by 59 attending radiologist was obtained. Aggregate data analysis showed a significant mean reduction in D – F by 3.9 hours (95% CI: 2.9 to 5.0 hours; $p < 0.05$) post mobile app implementation. Analysis split by modality also showed a significant mean reduction in D – F for CT by 2.9 hours (95% CI: 1.9 to 3.9 hours; $p < 0.05$), for MRI by 5.4 hours (95% CI: 3.8 to 7.0 hours; $p < 0.05$), and for US by 6.2 hours (95% CI: 2.2 to 10.1 hours; $p < 0.05$). Analysis was repeated split by patient type; no significant difference was noted for emergency patients ($p = 1$), while outpatients and inpatients reports showed significant reductions in D – F by 58.6% and 52.5% ($p < 0.05$), respectively.

SSJ13-02 Effect of Medical Provider Sentiment on Intensive Care Unit Diagnostic Imaging Utilization

Tuesday, Nov. 29 3:10PM - 3:20PM Room: S402AB

Participants

Mohammad Ghassemi, MSc, Cambridge, MA (*Abstract Co-Author*) Nothing to Disclose
Tuka Al-Hanai, MSc, Cambridge, MA (*Abstract Co-Author*) Nothing to Disclose
Jesse Raffa, PhD, Cambridge, MA (*Abstract Co-Author*) Nothing to Disclose
Shamim Nemati, PhD, Atlanta, GA (*Abstract Co-Author*) Nothing to Disclose
Falgun H. Chokshi, MD, Marietta, GA (*Presenter*) Nothing to Disclose

PURPOSE

The contribution of medical provider judgment to diagnostic imaging utilization is unclear. Our purpose was to investigate the effects of intensive care unit (ICU) provider sentiment in medical notes as a proxy for such judgment.

METHOD AND MATERIALS

Using the Multiparameter Intelligent Monitoring In Critical Care database (MIMIC-III), we included all adult ICU patients admitted for up to 5 days (2001-2012). Provider note sentiment was converted to positive & negative sentiment scores using SentiWordNet. Using a Poisson Generalized Estimating Equation (GEE) regression model, we performed three analyses, each with primary outcome as number of imaging exams. We adjusted for age, gender, ethnicity, illness severity, multiple comorbidities, and ICU type. First analysis: we investigated the linear association between sentiment and imaging utilization. Second analysis was identical to the first, but included quadratic terms for the sentiment features in the model. Third analysis, we estimated the effect of time on the

associations found in the first two parts of the analysis by including dummy encoded ICU stay day terms, and day x sentiment interaction terms in the models.

RESULTS

We analyzed 272,879 distinct medical provider notes, from 18,607 distinct ICU stays, with 45,699 distinct days of data. There was statistically significant association between provider sentiment and imaging utilization ($p < 0.01$); negative sentiment was associated with an increase in imaging utilization. Also, the nature of the provider sentiment-imaging utilization relationship is not strictly linear, and changed over time. Sentiment's effects are most pronounced at the beginning of the stay, and grow weaker over subsequent days. We found that the presence of any form of sentiment may increase imaging utilization up until a critical threshold, beyond which utilization is reduced.

CONCLUSION

Even with a simplistic sentiment analysis method, we have shown that ICU medical provider sentiment has a non-linear (quadratic) effect on diagnostic imaging utilization that evolves over time; this likely reflects complexities in provider decision-making and medical notes that were not captured by our simplistic method.

CLINICAL RELEVANCE/APPLICATION

Provider sentiment adds a dimension to clinical decisions that has not been evaluated. Sophisticated methods may lead to decision support that incorporate sentiment to guide resource utilization.

SSJ13-04 **The Patient Engagement for Equity in Radiology (PEER) project: Big-Data Driven Predictive Analytics Model to Identify Social Determinants of Health Negatively Impacting Access to Radiology Care and Develop Culturally Sensitive Healthcare Solution**

Tuesday, Nov. 29 3:30PM - 3:40PM Room: S402AB

Participants

Efren J. Flores, MD, Boston, MA (*Presenter*) Nothing to Disclose
Thomas J. Bollerman, Boston, MA (*Abstract Co-Author*) Nothing to Disclose
Christina Jaworsky, Boston, MA (*Abstract Co-Author*) Nothing to Disclose
Jing Ai, Boston, MA (*Abstract Co-Author*) Nothing to Disclose
Oleg S. Pinykh, Newton Highlands, MA (*Abstract Co-Author*) Nothing to Disclose

CONCLUSION

The **PEER** project embraces the opportunity to mitigate the negative impact of social determinants of health and develop patient-centered, socially sensitive solutions to improve patient engagement and healthcare access.

Background

Healthcare disparities negatively affect patients and occur across many medical conditions, socioeconomic and demographic factors. The term "non-compliance" places the responsibility of attending a medical appointment solely on the patient. "Missed Care Opportunities" (MCO) reflect the responsibility of the healthcare system to improve patient engagement. Big-data predictive analytics provide an opportunity to address these factors.

Evaluation

Data obtained from radiology scheduling system and electronic medical record included age, gender, religion, race, ethnicity, address, veteran status, education level, employment, type insurance, religion, address, physical limitations, absence at clinical appointments, medical conditions and homelessness, among others. External sources, including Census data, were utilized to obtain factors such as weather conditions, median household income, public transportation access, distance to appointment, among others. Multivariate logistic regression identified factors significantly associated with MCOs. Preliminary analysis of 1.1 million outpatient exams from February 2014- March 2016 that languages other than English (OR: 1.7), certain ethnic groups compared to Caucasian (OR= 1.8) and lower education level (OR:1.3) were significantly associated ($p < 0.001$) with MCOs. Among the pediatric population, obesity (OR: 2.69), ICD codes including child abuse or neglect (OR= 1.8, $p < 0.001$), failure to thrive (OR: 1.6), and missed clinical visit appointments (OR: 1.7) were significantly associated with MCOs ($p < 0.001$). In breast imaging, medical conditions such as congestive heart failure (OR: 2.3) and COPD (OR: 2.0) were significantly associated with MCOs ($p < 0.001$).

Discussion

The predictive analytics model leverages technology to identify socioeconomic, demographic and medical factors that are strongly associated with MCOs. Identifying these factors is paramount to understand our patient's needs beyond radiology in order to bridge the healthcare gap and provide equitable care.

SSJ13-05 **Contextualized Prioritization of Problem Lists for Efficient Radiologist Consumption: Algorithm Development and Evaluation**

Tuesday, Nov. 29 3:40PM - 3:50PM Room: S402AB

Participants

Pritesh Patel, MD, Chicago, IL (*Abstract Co-Author*) Nothing to Disclose
Merlijn Sevenster, PhD, Cambridge, MA (*Abstract Co-Author*) Employee, Koninklijke Philips NV
Ranjith Tellis, Cambridge, MA (*Abstract Co-Author*) Nothing to Disclose
Richard J. Gorniak, MD, Philadelphia, PA (*Abstract Co-Author*) Nothing to Disclose
Adam E. Flanders, MD, Narberth, PA (*Abstract Co-Author*) Nothing to Disclose
Igor Trilisky, MD, Chicago, IL (*Presenter*) Nothing to Disclose
Melvy S. Mathew, MD, Chicago, IL (*Abstract Co-Author*) Nothing to Disclose
Paul J. Chang, MD, Chicago, IL (*Abstract Co-Author*) Co-founder, Stentor/Koninklijke Philips NV; Researcher, Koninklijke Philips NV; Medical Advisory Board, lifeIMAGE Inc; Advisory Board, Bayer AG

PURPOSE

The electronic medical record (EMR) problem list (PL) contains the patient's historical and current information in the form of ICD10

code that may be valuable to radiological interpretation. However, PLs can be lengthy and cumbersome to review as most codes are irrelevant for image interpretation (e.g., nail fungus). We developed and evaluated a data-driven algorithm that prioritizes PLs based on contextual radiological relevance.

METHOD AND MATERIALS

Development: A code relevance metric was introduced that rank ordered ICD10 codes more frequent in history sections of radiology reports (thus assumed relevant normalized by frequency in a set of PLs). To determine frequency, MetaMap detected code occurrences in a de-identified corpus of 243,374 reports; PLs of 20,148 patients were used for frequency normalization. The relevance metric was contextualized for neuroimaging exams by filtering for neuro reports and relevant PLs of patients with neuro exams. A similar process was used for abdomen, MSK, cardiac and chest examinations. **Evaluation:** Via survey, radiologists from two academic hospitals indicated preferred order for 20 randomly selected PLs with > 9 codes displayed in: (1) chronological, (2) indifferent or (3) decreasing relevance. Neuro-radiologists were presented the neuro-contextualized rankings, and so on. A significance level of 0.05 was used.

RESULTS

39 radiologists completed the survey (response: 20%) yielding 780 votes. The relevance order was preferred by radiologists in 40% of all PLs and chronological order preferred in 22%. Abdomen (avg score 2.3), chest (2.3) and neuro respondents (2.2) significantly preferred the relevance order; MSK readers favored the chronological order (1.7). Cardiac readers had no significant preference (2.0). There were no significant differences in the preferences between institutions.

CONCLUSION

An algorithmically determined contextual prioritization of PLs is preferred over the EMR's chronological order. The technology can be integrated in a software solution that automatically synthesizes an "executive summary" of the patient's history, signs, symptoms and problems thereby assisting the radiologist in the efficient and accurate correlation of image findings and improving the value added by the exam interpretation.

CLINICAL RELEVANCE/APPLICATION

A prioritization option can be included in problem list viewers assisting the radiologists in propagating more relevant codes to the top of the list.

SSJ13-06 MRI Schedule Optimization through Discrete Event Simulation and Neural Networks as a means of Increasing Scanner Productivity

Tuesday, Nov. 29 3:50PM - 4:00PM Room: S402AB

Awards

Student Travel Stipend Award

Participants

Michael Muelly, MD, Stanford, CA (*Presenter*) Nothing to Disclose

Shreyas S. Vasanawala, MD, PhD, Stanford, CA (*Abstract Co-Author*) Research collaboration, General Electric Company; Consultant, Arterys Inc; Research Grant, Bayer AG;

CONCLUSION

Scanner productivity can be increased by up to 60% with optimized exam slot length. Further, neural networks can be used to reliably estimate exam length on the basis of individual patient and study characteristics.

Background

Despite advantages of MRI, CT remains the preferred modality in many clinical settings due to the higher cost of MRI. Scanner productivity may be increased with shortened scan time or improved scheduling efficiency. Most MRI facilities use fixed block lengths for scheduling. However, exams are variable in length leading to significant dead time. Our aim was to devise the optimal slot length and estimate individual scan times based on a priori data.

Evaluation

We ran a discrete event simulation using Mathworks Matlab to test different scheduling strategies for a one-month period using historical data from MR scanners used in both the in- and outpatient setting. The average exam length in July 2015 was found to be 34.9 min with a standard deviation of 11.1 min. Studies were randomly inserted into slots in repeated fashion, 1000 times each for exam slot lengths ranging from 10 to 60 minutes. Using this method, the optimal slot length to maximize productive scan time was determined to be 28.8min (CI 27.5-30.1min) resulting in an increase in the studies performed compared to 60min slots (614/month vs 355/month, $p < 0.01$). Next, we used a feed-forward type neural network, trained using the same data, to predict study length with a priori information: scan protocol, patient age, contrast usage, and protocol mean of unplanned sequence repeats. On testing, the correlation coefficient was $r = 0.90$ with a mean squared error of 8.6.

Discussion

A barrier to the use of MRI is cost. One way to reduce cost per exam is through reducing inefficiencies in scheduling thus increasing the number of exams performed per scanner. For convenience, exams are usually scheduled using fixed time slots often resulting in dead time. Using discrete event simulation, we have determined the slot length to maximize scheduling efficiency. To further increase efficiency fixed slot times could be completely abandoned and slot length estimated using data available a priori.

SSJ14

Molecular Imaging (Inflammation/Metabolism/Musculoskeletal)

Tuesday, Nov. 29 3:00PM - 4:00PM Room: S504CD



AMA PRA Category 1 Credit™: 1.00
ARRT Category A+ Credit: 1.00

FDA Discussions may include off-label uses.

Participants

Tomio Inoue, MD, PhD, Yokohama, Japan (*Moderator*) Nothing to Disclose
Michael S. Gee, MD, PhD, Jamaica Plain, MA (*Moderator*) Nothing to Disclose

Sub-Events

SSJ14-01 Whole-body Assessment of Fat Content and Insulin Sensitivity in Different Tissues of Healthy Volunteers and T2D Patients using a Fully Integrated PET/MR System

Tuesday, Nov. 29 3:00PM - 3:10PM Room: S504CD

Participants

Hakan Ahlstrom, Uppsala, Sweden (*Presenter*) Research funded, AstraZeneca PLC
Emil Johansson, Uppsala, Sweden (*Abstract Co-Author*) Nothing to Disclose
Mark Lubberink, Uppsala, Sweden (*Abstract Co-Author*) Nothing to Disclose
Greta Boersma, Uppsala, Sweden (*Abstract Co-Author*) Nothing to Disclose
Stanko Skrtic, Molndal, Sweden (*Abstract Co-Author*) Employee, AstraZeneca PLC
Jan Eriksson, Uppsala, Sweden (*Abstract Co-Author*) Nothing to Disclose
Joel Kullberg, DiplPhys, Uppsala, Sweden (*Abstract Co-Author*) Nothing to Disclose

PURPOSE

Parameters that are important for development of Type 2 Diabetes (T2D) are whole-body fat content and insulin sensitivity of all tissues in the body (expressed with the M-value). These parameters can be studied on a tissue level with a 18F-FDG PET/MR investigation. The main objective was to apply an integrated whole-body PET/MR protocol for assessment of glucose uptake using 18F-FDG, during euglycemic clamp conditions, and fat content of various tissues, of healthy volunteers and T2D patients, using a whole-body fully integrated PET/MR equipment.

METHOD AND MATERIALS

10 subjects (5 healthy, 5 T2D) were imaged using 18F-FDG and an integrated PET/MR system under steady state clamp conditions. PET: 1 dynamic acquisition (thorax, 10 min) with simultaneous administration of 18F-FDG (average 330 MBq/subject), followed by 6 serial whole body scans (5 min/scan). MRI: 6 point Dixon for quantitative fat, water separated images were acquired after the PET scans. Standard Patlak model using image derived input function (IDIF) from ascending aorta (manually derived region of interest from dynamic PET series) was used for kinetic modelling of tissue specific glucose uptake. Tissue specific glucose uptake [μmol glucose/100 g tissue min] from PET was manually segmented from the fused MRI and PET-Patlak volumes. The M-value [$\text{mg}/\text{kg min}$] expressing the whole-body insulin sensitivity of the subject was determined during PET/MRI acquisition with the clamp-method, where a constant infusion of insulin ($56 \text{ mU}/\text{m}^2/\text{min}$) and variable infusion of glucose to the subject was set to maintain a steady state level of $5.6 \text{ mmol}/\text{l}$ (plasma glucose) during imaging. The M-value was normalized to fat-free mass.

RESULTS

The M-value showed positive correlation with the fat fraction of the liver, whole body fat volume and the tissue specific uptake rate of 18F-FDG in skeletal muscle, subcutaneous adipose tissue and liver and a negative correlation in the brain. No correlation was seen for pancreas' fat fraction and the uptake rate of 18F-FDG in heart (left ventricle) and pancreas.

CONCLUSION

The applied whole-body FDG PET/MRI protocol, during euglycemic clamp, is feasible for studies of fat content and insulin sensitivity in various tissue, parameters relevant for development of T2D.

CLINICAL RELEVANCE/APPLICATION

FDG-PET/MR data generated at different stages of T2DM development, integrated with non-imaging data, can give important information for future more individualized therapy and improved outcomes.

SSJ14-02 Molecular MRI Targeting Myeloperoxidase Detects Inflammation in Human Non-Alcoholic Steatohepatitis

Tuesday, Nov. 29 3:10PM - 3:20PM Room: S504CD

Awards

Student Travel Stipend Award

Participants

Benjamin Pulli, MD, Boston, MA (*Presenter*) Nothing to Disclose
Gregory R. Wojtkiewicz, MSc, Boston, MA (*Abstract Co-Author*) Nothing to Disclose
Yoshiko Iwamoto, Boston, MA (*Abstract Co-Author*) Nothing to Disclose
Muhammad Ali, MBBS, Boston, MA (*Abstract Co-Author*) Nothing to Disclose
Matthias Zeller, MD, 02114, MA (*Abstract Co-Author*) Nothing to Disclose
Lionel A. Bure, MD, Boston, MA (*Abstract Co-Author*) Nothing to Disclose
Cuihua Wang, PhD, Boston, MA (*Abstract Co-Author*) Nothing to Disclose

Yuri Choi, Boston, MA (*Abstract Co-Author*) Nothing to Disclose
Ricard Masia, MD, PhD, Boston, MA (*Abstract Co-Author*) Nothing to Disclose
Alexander R. Guimaraes, MD, PhD, Portland, OR (*Abstract Co-Author*) Speakers Bureau, Siemens AG;
Kathleen Corey, MD, Boston, MA (*Abstract Co-Author*) Advisory Board, Gilead Sciences, Inc
John W. Chen, MD, PhD, Boston, MA (*Abstract Co-Author*) Research Grant, Pfizer Inc

PURPOSE

Only a subset of patients with non-alcoholic fatty liver disease will progress to non-alcoholic steatohepatitis (NASH) and subsequently cirrhosis. Inflammation and oxidative stress are key facilitators for progression. Myeloperoxidase (MPO) is a pro-inflammatory and oxidative enzyme expressed by myeloid cells. We hypothesized that MPO-Gd, an MRI probe specific for MPO, could detect MPO activity in human biopsy samples.

METHOD AND MATERIALS

A total of 11 liver biopsy samples from obese patients undergoing clinical evaluation for NASH were obtained. A waiver was granted by our institution's IRB. Samples were incubated in cell culture medium, and T1 fat-sat pre-contrast MR imaging was performed on a 4.7 T MRI (Bruker). MPO-Gd (1 mg/ml) was added, and samples were incubated for 2 hours. Samples were washed. Post-contrast MR images were then acquired, and MPO-specific signal was calculated as CNR_{post}/CNR_{pre} . After imaging, samples were cut to 5 μ m thickness, and stained with H&E and MPO for histopathological evaluation. The NAFLD activity score (NAS) was calculated; NASH was defined as $NAS > 5$.

RESULTS

5 of 11 patients fulfilled criteria for NASH ($NAS > 5$), the remaining 6 were used as controls. There was no difference in age (49.2 ± 13.2 in NASH vs. 40.3 ± 9.2 in control, $P = 0.35$) or BMI (44.4 ± 8.7 vs. 45.1 ± 6.8 , $P = 0.87$). As expected, NASH patients had higher NAS sub-scores in steatosis (3 [interquartile range IQR 1.5–3], vs. 0 [0–0.5]), inflammation (1 [1.5–3] vs. 0 [0–0]), fibrosis (1 [1–2] vs. 0 [0–0]), hepatocyte ballooning (2 [2–2] vs. 0 [0–0]), and a higher total NAS score (6 [5.5–6] vs. 0 [0–0.5]). Molecular MRI with MPO-Gd demonstrated an increase in CNR in samples from NASH patients (Fig., A) versus control (Fig., B) (CNR_{post}/CNR_{pre} 2.61 ± 0.91 vs. 1.29 ± 0.22 , $P = 0.004$). Correlating with these results, we found more clusters of MPO-positive cells on histology in NASH versus control patients (Fig., C, 5.60 ± 1.52 vs. 1.00 ± 0.89 , $P = 0.002$).

CONCLUSION

In liver core biopsy samples of patients undergoing evaluation for NASH, MPO-Gd enhanced molecular MRI can reliably and non-invasively detect MPO activity in NASH patients.

CLINICAL RELEVANCE/APPLICATION

Molecular MRI with MPO-Gd could non-invasively assess for liver inflammation. This could allow for noninvasive identification of patients with NASH who are at high risk for developing cirrhosis.

SSJ14-03 Investigation of Aquaporin by DWI MRI with Multiple B Values in a Rat Model of Diabetic Nephropathy

Tuesday, Nov. 29 3:20PM - 3:30PM Room: S504CD

Participants

Yu Wang, BDS, Chengdu, China (*Presenter*) Nothing to Disclose
Rongbo Liu, MD, Prof, Chendu, China (*Abstract Co-Author*) Nothing to Disclose
Heng Zhang, BDS, Luzhou, China (*Abstract Co-Author*) Nothing to Disclose
Ruzhi Zhang, BSC, Chengdu, China (*Abstract Co-Author*) Nothing to Disclose
Zhouzhe Zhao, Beijing, China (*Abstract Co-Author*) Nothing to Disclose
Fabao Gao, MD, PhD, Chengdu, China (*Abstract Co-Author*) Nothing to Disclose
Lei Wang, BA, Chengdu, China (*Abstract Co-Author*) Nothing to Disclose

PURPOSE

To assess the correlation between renal apparent diffusion coefficient (ADC) obtained from ultra-high b-values and the change of aquaporins (AQPs) in a rat model of type 2 diabetic nephropathy.

METHOD AND MATERIALS

Twenty-four male Sprague-Dawley rats were divided into 2 groups: (1) untreated controls, (2) diabetes (DM). Forty days after diabetes induction with streptozotocin, MR imaging was performed in a 7.0-T scanner. All rats received diffusion-weighted imaging (DWI) with 18 b-values (0–4500 s/mm²). Renal apparent diffusion coefficient values were calculated for each of the different anatomical layers of the kidney and maps of low ADC (ADCl) maps were calculated from low b-values (0–200), maps of standard ADC (ADCst) maps were calculated from standard b-values (300–1500) and maps of ultra-high ADC (ADCuh) were calculated from the ultra-high b-values (1700–4500). The expression of proteins involved in renal water transport in diabetic rats were then studied by immunohistochemistry microscopy and the mean value of integral optical density (IOD) of aquaporins positive signals were measured by applying immune tissue chemistry method. Imaging result, laboratory parameters of diabetic and kidney function, and renal histopathological changes were compared between groups.

RESULTS

All diabetic animals developed hyperglycemia. ultra-high ADC was significantly increased in DM animals in the cortex (CO) ($1.40 \pm 0.10 \times 10^{-3} \text{mm}^2/\text{s}$; $P < 0.001$), outer stripe of the outer medulla (OS) ($1.42 \pm 0.10 \times 10^{-3} \text{mm}^2/\text{s}$; $P < 0.001$), inner stripe of the outer medulla (IS) ($1.32 \pm 0.14 \times 10^{-3} \text{mm}^2/\text{s}$; $P = 0.010$) and inner medulla (IM) ($1.60 \pm 0.12 \times 10^{-3} \text{mm}^2/\text{s}$; $P = 0.041$) compared with control animals (CO, $1.20 \pm 0.14 \times 10^{-3} \text{mm}^2/\text{s}$; OS, $1.22 \pm 0.14 \times 10^{-3} \text{mm}^2/\text{s}$; IS, $1.19 \pm 0.41 \times 10^{-3} \text{mm}^2/\text{s}$; IM, $1.51 \pm 0.15 \times 10^{-3} \text{mm}^2/\text{s}$). While, between groups, ADCl and ADCst values were not different. DM rats had an increased IOD of AQP2 in the CO (0.035 ± 0.010 ; $P = 0.008$), OS (0.06 ± 0.019 ; $P = 0.011$), IM (0.058 ± 0.016 ; $P = 0.001$), and IM (0.040 ± 0.012 ; $P = 0.009$) compared with control animals (CO, 0.023 ± 0.010 ; OS, 0.043 ± 0.009 ; IS, 0.036 ± 0.010 ; IM, 0.026 ± 0.011). In contrast, there were no major changes in the abundance of AQP1 and AQP4.

CONCLUSION

ADCuh may be a useful measurement for noninvasive evaluating kidney damage in diabetic nephropathy, and these changes in

ADCuh may be a useful measurement for noninvasive evaluating kidney damage in diabetic nephropathy, and these changes in ADCuh may reflect function of the AQP.

CLINICAL RELEVANCE/APPLICATION

ADCuh may be a promising biomarker in differential diagnosis of diabetic nephropathy patients.

SSJ14-04 Facet Tropism and Facet Joint Orientation: Risk Factors For the Development of Early Biochemical Alterations of Lumbar Intervertebral Discs

Tuesday, Nov. 29 3:30PM - 3:40PM Room: S504CD

Awards

Student Travel Stipend Award

Participants

Christoph Schleich, MD, Dusseldorf, Germany (*Presenter*) Nothing to Disclose
Anja Lutz, Dusseldorf, Germany (*Abstract Co-Author*) Nothing to Disclose
Joel Aissa, Duesseldorf, Germany (*Abstract Co-Author*) Nothing to Disclose
Benjamin Schmitt, Vienna, Austria (*Abstract Co-Author*) Nothing to Disclose
Bernd Bittersohl, MD, Bern, Switzerland (*Abstract Co-Author*) Nothing to Disclose
Gerald Antoch, MD, Duesseldorf, Germany (*Abstract Co-Author*) Nothing to Disclose
Hans-Joerg Wittsack, PhD, Duesseldorf, Germany (*Abstract Co-Author*) Nothing to Disclose
Johannes Boos, MD, Boston, MA (*Abstract Co-Author*) Nothing to Disclose
Katrin S. Blum, MD, Dusseldorf, Germany (*Abstract Co-Author*) Nothing to Disclose
Falk R. Miese, MD, Dusseldorf, Germany (*Abstract Co-Author*) Nothing to Disclose

PURPOSE

To assess the glycosaminoglycan (GAG) content of lumbar intervertebral discs (IVD) in healthy volunteers with facet tropism (FT) and sagittal facet joint (FJ) orientation using glycosaminoglycan chemical exchange saturation transfer imaging (gagCEST).

METHOD AND MATERIALS

Seventy-five lumbar IVDs of twenty-five young, healthy volunteers without any history of lumbar spine pathologies (13 female; 12 male; mean age: 28.0 ± 4.4 years; range: 21 - 35 years) were examined with a 3T MRI scanner. Orientation of FT and FJ were assessed for L3/4, L4/5 and L5/S1 using standard T2 weighted images. Biochemical gagCEST imaging was used to determine the GAG content of each nucleus pulposus (NP) and annulus fibrosus (AF).

RESULTS

Significantly higher gagCEST values of NP were found in volunteers without FT and normal FJ orientation compared to volunteers with FT and sagittal FJ orientation $> 45^\circ$ ($p < 0.0001$). GagCEST values were significantly higher in volunteers without FT compared to volunteers with moderate or severe FT (moderate FT: $p < 0.0001$; severe FT: $p = 0.0033$). Volunteers with normal FJ orientation showed significantly higher gagCEST values compared to those with sagittal FJ orientation $> 45^\circ$ ($p < 0.001$). We found a significant, negative correlation between gagCEST values and higher angles in sagittal FJ orientation ($\rho = -0.459$; $p < 0.0001$).

CONCLUSION

GagCEST analysis demonstrated significantly lower GAG values of NP in young volunteers with FT and sagittal orientated FJ, indicating that FT and sagittal orientation of the FJ represent risk factors for the development of early biochemical alterations of lumbar IVDs.

CLINICAL RELEVANCE/APPLICATION

gagCEST imaging may be an additional feature in the evaluation of the biochemical composition in lumbar intervertebral discs on a clinical 3T MRI system and may be a powerful, non-invasive tool to investigate early disc degeneration processes.

SSJ14-05 Dynamic Creatine CEST MRI for Measuring Muscle Fatigability Post Exercise

Tuesday, Nov. 29 3:40PM - 3:50PM Room: S504CD

Participants

Alessandro Scotti, Chicago, IL (*Presenter*) Nothing to Disclose
Rongwen Tain, PhD, Chicago, IL (*Abstract Co-Author*) Nothing to Disclose
Xiaohong J. Zhou, PhD, Chicago, IL (*Abstract Co-Author*) Nothing to Disclose
Kejia Cai, PhD, Chicago, IL (*Abstract Co-Author*) Nothing to Disclose

PURPOSE

Chronic fatigability is a pathological condition associated with abnormally fast exhaustion and slow energy restoration. Muscular fatigability prevents people from exercising, leading to obesity and progressive mobility impairment. Many studies investigated the rate of phosphocreatine (PCr) re-synthesis after exercise as a measure of energetic restoration rate. However, the detection of PCr by ^{31}P -MRS is associated with long scan times and poor spatial resolution. Creatine (Cr), a key metabolites in cellular energy system, can be imaged with high resolution using an emerging method, Cr Chemical Exchange Saturation Transfer (CrCEST) MRI. Herein, we demonstrate a quantitative method for mapping energy restoration rate, an index for muscular fatigability, by fitting the post-exercise dynamic CrCEST data.

METHOD AND MATERIALS

Six healthy subjects underwent MRI at a 3T scanner while performing a physical exercise consisting of repeated pushes (1Hz rate) on a mildly loaded pedal (16 lbs) for 3 minutes. After B_0 and B_1 mapping, the calf muscles were imaged at rest and for 12 minutes following the workout by a series of fast CrCEST sequences with two pairs of offsets around 2ppm. Assuming a linear signal variation in the range between the two offsets, the B_0 -corrected CrCEST map at 2ppm was determined according to the deviation in the B_0 map.

RESULTS

CrCEST maps were created at each time point, showing spatial variation in muscle activation. The time constant of the CrCEST contrast decay during the recovery phase was quantified pixelwise with a mono-exponential function. Our preliminary results demonstrate that subjects with high maximum voluntary strength showed much shorter energy restoration time (<5 minutes) compared to subjects with lower strength (>25 minutes) in the working muscles.

CONCLUSION

The design of the dynamic CEST sequence with only 2 offsets allows for fast acquisitions, and thus to distinguish Cr expression in different working muscles with unprecedented spatial and temporal resolution. Mapping the post-exercise energy restoration rate by our technique may have broad clinical impacts on the management of chronic fatigability.

CLINICAL RELEVANCE/APPLICATION

Dynamic bionergetic MRI based on creatine CEST contrast can have broad clinical impacts on the monitoring and management of chronic fatigability.

SSJ14-06 Non-Invasive Imaging of Human Intestinal Perfusion and Oxygenation of Hemoglobin in Patients with Crohn's Disease Using Multispectral Optoacoustic Tomography

Tuesday, Nov. 29 3:50PM - 4:00PM Room: S504CD

Participants

Ferdinand Knieling, Erlangen, Germany (*Presenter*) Nothing to Disclose
Cornelia Egger, Erlangen, Germany (*Abstract Co-Author*) Nothing to Disclose
Jing Claussen, Munich, Germany (*Abstract Co-Author*) Employee, iThera Medical GmbH
Alexander Ulrich, Munchen, Germany (*Abstract Co-Author*) Nothing to Disclose
Stefan Morscher, Munchen, Germany (*Abstract Co-Author*) Employee, iThera Medical GmbH
Marcel Vetter, Erlangen, Germany (*Abstract Co-Author*) Nothing to Disclose
Christian Kielisch, Erlangen, Germany (*Abstract Co-Author*) Nothing to Disclose
Sarah Fischer, MD, Erlangen, Germany (*Abstract Co-Author*) Nothing to Disclose
Alexander Hagel, Erlangen, Germany (*Abstract Co-Author*) Nothing to Disclose
Rudiger Gortz, Erlangen, Germany (*Abstract Co-Author*) Nothing to Disclose
Dane Wildner, Erlangen, Germany (*Abstract Co-Author*) Speaker, Bracco Group
Raja Atreya, Erlangen, Germany (*Abstract Co-Author*) Nothing to Disclose
Deike H. Strobel, MD, Erlangen, Germany (*Abstract Co-Author*) Nothing to Disclose
Markus F. Neurath, Erlangen, Germany (*Abstract Co-Author*) Nothing to Disclose
Maximilian J. Waldner, Erlangen, Germany (*Abstract Co-Author*) Nothing to Disclose

PURPOSE

Multispectral Optoacoustic Tomography (MSOT) is a physical imaging approach to examine tissue by utilizing the photoacoustic effect to detect molecules based on their characteristic absorption spectra. The aim of the study was to non-invasively image human intestinal perfusion and oxygenation status of hemoglobin (hb) in patients with Crohn's disease (CD) and compare the results to clinical parameters of disease activity.

METHOD AND MATERIALS

The trial was registered (ClinicalTrials.gov ID: NCT02622139), ethical board approval was provided, and informed consent was obtained. n=60 patients (32♀/28♂) were included, mean age: 34.2±13.5; n=27 in remission, n=15 with mild, and n=13 with moderate disease according to Harvey Bradshaw Index (HBI). The handheld optoacoustic detector (MSOT Acuity, iThera Medical GmbH, Munich, probe: 3-4MHz, 256 elements) was positioned on the skin of the abdomen. MSOT signals were acquired at 700/730/760/800/850/900nm. From all patients HBI, B-mode&Doppler ultrasound/endoscopic/histologic score, C-reactive protein and total leukocyte count was assessed and compared to MSOT signals.

METHOD AND MATERIALS

The clinical trial was registered (ClinicalTrials.gov Identifier: NCT02622139), ethical board approval was provided, and informed consent was obtained. n=60 patients (32♀/28♂) were included, mean age: 34.2±13.5; n=27 in remission, n=15 with mild, and n=13 with moderate disease according to HBI. The used device (MSOT EIP 100, iThera Medical GmbH, Munich, probe: 4MHz, 256 elements) comprises as handheld detector that was positioned on the skin of the abdominal wall (Figure 1). Spectra were performed at 700, 730, 760, 800, 850, and 900nm. The region of interest was placed in the colon and 5mm above in the abdominal wall. From all patients Harvey Bradshaw Index (HBI) for disease activity, B-mode&Doppler ultrasound/endoscopic/histologic score, C-reactive protein and total leukocyte count was assessed and compared to MSOT signals.

RESULTS

Using B-Mode imaging, inflamed parts of the intestine were located and MSOT signals were acquired within only about 5 minutes per patient. Bowel wall thickness was 4.9±2.7mm, imaged at a depth of 19.1±7.2mm (terminal ileum) or 18.9mm±6.9mm (sigma). Using the MSOT system, deoxy- and oxyhemoglobin content in the intestinal wall could be quantified. An increase in oxygenated and deoxygenated hb from histologic grade 0 to 2 (oxy:15.5±3.8 vs. 23.8±7.1; P =.03; deoxy: 19.9±5.0 vs. 27.5±3.6; P =.01) with a further rise in grade 3 (26.7±5.1; P =.004; 26.3±4.5; P =.02) was observed. Total hb increased from grade 0 to 2 (35.4±6.6 vs. 51.3±9.1; P =.005) also followed by a further rise in grade 3 (53.0±9.0; P =.001). Ultrasound showed moderate correlation with histology (R²=.51, P<.0001); laboratory assessments did not show significant correlations with disease activity.

CONCLUSION

MSOT is a promising clinical translatable real-time, non-invasive modality to visualize inflammation in patients with CD. Further human studies are needed to define absolute cut-off parameters.

CLINICAL RELEVANCE/APPLICATION

This is a clinical feasibility study showing that MSOT enables physicians to quickly and non-invasively assess the disease activity of CD in order to personalize therapeutic decisions.

SSJ15

Musculoskeletal (Quantitative Techniques)

Tuesday, Nov. 29 3:00PM - 4:00PM Room: E450B



AMA PRA Category 1 Credit™: 1.00
ARRT Category A+ Credit: 1.00

Participants

Thomas M. Link, MD, PhD, San Francisco, CA (*Moderator*) Research Grant, General Electric Company; Research Consultant, General Electric Company; Research Consultant, InSightec, Ltd; Research Grant, InSightec Ltd; Royalties, Springer Science+Business Media Deutschland GmbH; Consultant, Springer Science+Business Media Deutschland GmbH; Research Consultant, Pfizer Inc;
Jean-Francois Budzik, MD, PhD, Lille, France (*Moderator*) Nothing to Disclose

Sub-Events

SSJ15-01 MRI-Based Bone Models in the Knee: An Analysis of Manual and Automated Modeling Techniques

Tuesday, Nov. 29 3:00PM - 3:10PM Room: E450B

Participants

Ales Neubert, Herston, Australia (*Abstract Co-Author*) Nothing to Disclose
Katharine Wilson, MS, Vail, CO (*Presenter*) Nothing to Disclose
Craig Engstrom, Herston, Australia (*Abstract Co-Author*) Nothing to Disclose
Rachel K. Surowiec, MSc, Vail, CO (*Abstract Co-Author*) Nothing to Disclose
Anthony Paproki, Herston, Australia (*Abstract Co-Author*) Nothing to Disclose
Nicholas S. Johnson, MD, Milwaukee, WI (*Abstract Co-Author*) Nothing to Disclose
Stuart Crozier, Herston, Australia (*Abstract Co-Author*) Nothing to Disclose
Jurgen Fripp, Herston, Australia (*Abstract Co-Author*) Nothing to Disclose
Charles P. Ho, MD, PhD, Vail, CO (*Abstract Co-Author*) Research funded, Siemens AG Research funded, Smith & Nephew plc
Research funded, Arthrex, Inc Research funded, Ossur HF Scientific Advisory Board, Rotation Medical, Inc

PURPOSE

Bone modeling with magnetic resonance imaging (MRI) rather than computed tomography (CT) would offer clinical advantages in reducing patient exposure to the ionizing radiation of CT and potential evaluation of hard and soft tissues within the same joint model. We evaluated the feasibility of MRI-based bone modeling of the knee with 3 sequences compared to a gold standard CT-based model, using both manual and automated segmentation techniques.

METHOD AND MATERIALS

An in-vitro left knee specimen was imaged using CT (axial, 2.0mm slice thickness, 0.49x0.49 in-plane resolution) and three MRI sequences (PDFS SPACE, T1 VIBE, T2 TRUFISP; sagittal, 0.7mm slice thickness, up to 0.63x0.63 resolution) at 3.0 T. For each dataset the distal femur, proximal tibia and patella were manually segmented using imaging software and automatically segmented using custom-designed and published software. 3D mesh models of each bone were reconstructed. Two comparisons were made of the models: i) manually segmented MRI vs. manually segmented CT, and ii) automatically segmented MRI vs manually segmented CT. For each comparison the bone models were registered using an iterative closest points algorithm and the mean distance between the models was calculated.

RESULTS

Sub-millimeter agreement was found for all manually segmented MRI-based bone models when compared to the manually segmented CT models. MRI models tended to be slightly smaller than CT models, particularly within concave regions, i.e. depressions of the tibial plateau. The automated software was capable of sub-millimeter agreement in creating MRI-based models from the SPACE and VIBE sequences, with slightly less agreement for the TRUFISP sequence. (Figure 1)

CONCLUSION

MRI-based bone models of the knee demonstrated sub-millimeter agreement with manually segmented CT bone models. This was true for the manually segmented MRI models of all 3 sequences tested (SPACE, VIBE, TRUFISP), as well as for the automatically segmented MRI models of the SPACE and VIBE sequences. The current study indicates that MRI can be used for successful 3D bone modeling and may offer clinical advantages for comprehensive evaluation and automated modeling of the knee joint.

CLINICAL RELEVANCE/APPLICATION

MRI-based bone models are a feasible alternative to CT, avoiding unneeded radiation to patients. Automated modelling techniques would allow for direct application into the standard clinical workflow.

SSJ15-02 Quantitative Dual-energy Computed Tomography-based Molecular Imaging of Hemosiderin in Pigmented Villonodular Synovitis

Tuesday, Nov. 29 3:10PM - 3:20PM Room: E450B

Participants

Steven D. Hajdu, MD, Lausanne, Switzerland (*Presenter*) Nothing to Disclose
Stephane Cherix, Lausanne, Switzerland (*Abstract Co-Author*) Nothing to Disclose
Patrick Omoumi, MD, Lausanne, Switzerland (*Abstract Co-Author*) Nothing to Disclose
Igor Letovanec, MD, Lausanne, Switzerland (*Abstract Co-Author*) Nothing to Disclose
Laurent Guiral, BSC, Buc, France (*Abstract Co-Author*) Employee, General Electric Company
Francis R. Verdun, PhD, Lausanne, Switzerland (*Abstract Co-Author*) Nothing to Disclose
Hannes A. Rudiger, MD, Lausanne, Switzerland (*Abstract Co-Author*) Nothing to Disclose

Fabio Becce, MD, Lausanne, Switzerland (*Abstract Co-Author*) Nothing to Disclose

PURPOSE

To assess the feasibility of dual-energy computed tomography (DECT) in the detection and quantification of hemosiderin deposits in patients with known intra-articular knee masses detected on previous magnetic resonance imaging (MRI) examinations. To quantify the iron content of the two types of pigmented villonodular synovitis (PVNS).

METHOD AND MATERIALS

Twelve consecutive patients (seven males, mean age of 38 years) with single or multiple intra-articular knee masses previously detected on MRI underwent single-source DECT scans using a rapid tube-voltage-switching technique. Semi-automated volumetric tumor segmentation was performed using proprietary post-processing software. A specific color-coding protocol with two-material differentiation was applied using a pre-defined threshold of 4 to 10 mg/cm³ based on a previous phantom study with various known iron concentrations. Tumor volume and iron content were quantified. Iron/tumor volume ratio was subsequently calculated. Histopathological analysis from all 12 surgically resected masses was used as the reference standard.

RESULTS

All 12 masses showed hemosiderin deposits on color-coded DECT images, and all contained iron foci at histopathology. Seven lesions were giant cell tumors of tendon sheath (localized-type PVNS), two were diffuse-type giant cell tumors, and three were classified as other: two arteriovenous malformations and one tendon sheath fibroma. Among both PVNS types, mass volumes ranged from 2.9cm³ to 26.6cm³ with a mean of 8.7cm³ for the localized types, and from 51.2cm³ to 128.2cm³ with a mean of 89.7cm³ for the diffuse types, respectively. Iron volume ranged from 0.6cm³ to 3.8cm³ with a mean of 2cm³ (corresponding to approximately 10mg) for the localized types, and from 14.6cm³ to 34cm³ with a mean of 24.3cm³ (corresponding to approximately 121.5mg) for the diffuse types, respectively (p=0.055). The iron/tumor volume ratio ranged from 0.14 to 0.49 with a mean of 0.28 for the localized types, and from 0.26 to 0.28 with a mean of 0.27 for the diffuse types, respectively (p=0.72).

CONCLUSION

Dual-energy computed tomography is a feasible technique that allows the detection and quantification of hemosiderin deposits in patients with intra-articular knee masses. Hemosiderin volume is greater in diffuse-type PVNS compared with localized-type PVNS.

CLINICAL RELEVANCE/APPLICATION

DECT can be used as a novel imaging technique to quantify iron content in soft-tissue masses.

SSJ15-03 Detection of Myeloma Infiltration of Bone Marrow using Texture Analysis of Apparent Diffusion Coefficient Maps: A Feasibility Study

Tuesday, Nov. 29 3:20PM - 3:30PM Room: E450B

Awards

Student Travel Stipend Award

Participants

Qin Wang, MD, Beijing, China (*Presenter*) Nothing to Disclose
Huadan Xue, MD, Beijing, China (*Abstract Co-Author*) Nothing to Disclose
Shuo Li, MD, Beijing, China (*Abstract Co-Author*) Nothing to Disclose
Zheng Yu Jin, MD, Beijing, China (*Abstract Co-Author*) Nothing to Disclose

PURPOSE

To evaluate the feasibility of using texture analysis of apparent diffusion coefficient maps for the detection of myeloma infiltration of bone marrow.

METHOD AND MATERIALS

17 consecutive patients with plasma disorder was recruited prospectively, including 8 clinically diagnosed multiple myeloma (MM) and 9 patients with monoclonal gammopathy of undetermined significance (MGUS). All patients received whole-body DWI MRI. A hyperintense appearance on high-b-value DWI images was considered as myeloma infiltration. Texture Analysis of ADC maps on lumbar vertebral bodies in each patient were performed using TexRAD commercially available research software (TexRAD Ltd, Cambridge, UK) by manually delineating a round region of interest covering the middle cross-sectional area of each vertebra. Vertebrae with focal lesions or compression fracture were excluded from the analysis. The technique selectively filters and extracts textures at different size scales (fine, medium and coarse) followed by quantification of the histogram using 6 parameters: mean, standard-deviation (SD), kurtosis, entropy, skewness, and mean value of positive pixels (MPP). Students' t test was performed to compare the texture analysis parameters between myeloma-infiltrated vertebrae and non-infiltrated vertebrae. ROC analysis was performed to assess the diagnostic performance of these parameters to detect myeloma infiltration.

RESULTS

A total of 22 myeloma-infiltrated vertebrae and 27 non-infiltrated vertebrae were evaluated. At fine texture scale, most of the parameters (ie. mean, kurtosis, entropy, skewness, and MPP) except SD were significantly different between the two groups (P<0.05). ROC analysis identified three texture parameters (at fine texture scale) with highest AUCs, including mean (0.974), entropy (0.998) and MPP (0.974). The sensitivity of mean, entropy and MPP was 90.9%, 100% and 90.9% respectively. The specificity of mean, entropy and MPP was equal (96.2%).

CONCLUSION

It is feasible to use texture analysis of ADC Maps for the differentiation between myeloma-infiltrated from non-infiltrated bone marrow.

CLINICAL RELEVANCE/APPLICATION

Texture analysis of ADC Maps may complement conventional DWI MRI to differentiate myeloma-infiltrated from non-infiltrated bone marrow.

SSJ15-04 Fat Fraction Map Reconstructed from Two-point Dixon Technique in Quantification of Early Fatty Infiltration in Multiple Myeloma Patients: Comparison and Correlation with Single-voxel Magnetic Resonance Spectroscopy

Tuesday, Nov. 29 3:30PM - 3:40PM Room: E450B

Participants

Xiao-Jiao Pei, MD, Beijing, China (*Presenter*) Nothing to Disclose
Zhen-Yu Pan, MD, Beijing, China (*Abstract Co-Author*) Nothing to Disclose
Yufei Lian, MA, MA, Beijing, China (*Abstract Co-Author*) Nothing to Disclose
Shurong Jin, MA, MA, Beijing, China (*Abstract Co-Author*) Nothing to Disclose
Yuchang Yan, MD, Beijing, China (*Abstract Co-Author*) Nothing to Disclose
Kun Li, Beijing, China (*Abstract Co-Author*) Nothing to Disclose
Qinglei Shi, Beijing, China (*Abstract Co-Author*) Nothing to Disclose
Xiaoye Wang, MD, MD, Beijing, China (*Abstract Co-Author*) Nothing to Disclose

PURPOSE

To test whether fat fraction map (FFM) reconstructed from two-point Dixon technique can be used to quantify fat content of vertebral bone marrow in multiple myeloma patients by comparing the results with single voxel Magnetic Resonance Spectroscopy (MRS) and to evaluate the correlation between these quantitative parameters.

METHOD AND MATERIALS

Twenty patients with different pathological patterns of multiple myeloma (MM) and twenty healthy volunteers were enrolled and underwent three volume two-point T1-Dixon and single voxel MRS imaging. The FFM were reconstructed from Dixon images using the equation $FFM = Lip/In$ where Lip represented fat images and In represented in-phase images. The quantitative parameters were measured by placing the region of interest (ROI) in certain regions that corresponding to the MR-spectroscopy voxel. The fat fraction of MRS (MRS-FF) was calculated by using the integral area of lip peak divided by the sum of integral area of lip peak and water peak. The paired samples t test was used to compare the difference among quantitative parameters. The relationship about FF between T1-Dixon and MRS was assessed by using the Pearson correlation test. Receiver operating characteristic (ROC) analysis of discrimination between normal and MM were performed to determine the optimal cut-off value.

RESULTS

FF values were significantly correlated between T1-dixon and MRS: $r = 0.775$ ($P = 0.001$). ROC analysis demonstrated that no significance difference were found between area under the curve of T1-Dixon ($[0.805 \pm 0.087, (0.646 \text{ to } 0.986)]$ (normal vs MM)) and MRS ($[0.768 \pm 0.119, (0.478 \text{ to } 0.932)]$ ($P = 0.478$)), with optimal cutoff values of 16.627 and 10.216, respectively.

CONCLUSION

Both two-point T1-Dixon and single-voxel MRS may be reliable method to examine the bone marrow fat of vertebral bone, and good correlations are existed between two-point T1-dixon and MRS.

CLINICAL RELEVANCE/APPLICATION

Because the two-point T1-Dixon technique and MRS can be used for the detection of fat content, and bone marrow fat content is more sensitive to change in patients with multiple myeloma fat, the two technique may provide vital information for identification and diagnosis of multiple myeloma.

SSJ15-05 Quantifying and Optimizing Metal Artefact Reduction using Virtual Monochromatic Dual-Source CT in different Metal Implants

Tuesday, Nov. 29 3:40PM - 3:50PM Room: E450B

Participants

Ruud H. Wellenberg, MSc, Amsterdam, Netherlands (*Presenter*) Nothing to Disclose
Emilie C. Donders, Amsterdam, Netherlands (*Abstract Co-Author*) Nothing to Disclose
Peter Kloen, Amsterdam, Netherlands (*Abstract Co-Author*) Nothing to Disclose
Geert J. Streekstra, PhD, Amsterdam, Netherlands (*Abstract Co-Author*) Nothing to Disclose
Cornelis Slump, Enschede, Netherlands (*Abstract Co-Author*) Nothing to Disclose
Mario Maas, MD, PhD, Utrecht, Netherlands (*Abstract Co-Author*) Nothing to Disclose
Martijn F. Boomsma, MD, Zwolle, New Caledonia (*Abstract Co-Author*) Nothing to Disclose
Roeland P. Kleipool, Amsterdam, Netherlands (*Abstract Co-Author*) Nothing to Disclose
Ludo F. Beenen, MD, Amsterdam, Netherlands (*Abstract Co-Author*) Nothing to Disclose
Nick H. Lobe, Amsterdam, Netherlands (*Abstract Co-Author*) Nothing to Disclose

PURPOSE

To quantify and optimize metal artifact reduction using virtual monochromatic Dual-Source CT in different metal implants compared to non-metal reference scans. Region-of-interest (ROI) measurements were used to determine fluctuations and inaccuracies in soft tissues and bone due to metal artifacts.

METHOD AND MATERIALS

A human cadaver was scanned on a Dual-Source CT scanner with 80kVp/150kVp and 100kVp/150kVp. Scans without osteosynthetic implants, served as a reference. Thereafter scans were made after implanting a titanium plate, a stainless-steel plate and a titanium intramedullary pen in the left lower leg respectively. Scans were reconstructed with three different reconstruction filters. Virtual monochromatic images were analyzed from 70 to 190 keV, with steps of 10 keV, where 70 keV served as a reference. ROIs were placed in muscle, fat, cortical bone, implant and in the tibial medulla where CT numbers and standard deviation (SD) were measured. Optimal keVs regarding CT number accuracy and SDs were determined by searching for minimal absolute differences between the reference and implant scans.

RESULTS

Based on visual assessment, 100kVp/150kVp and the sharpest filter were chosen with less metal artifacts and sharper edges

respectively. The stainless-steel implant resulted in more severe artifacts. The titanium pen resulted in the least severe metal artifacts. CT number inaccuracies in 70keV images were decreased with 96%, 87% and 73% at optimal keVs of 130keV, 180keV and 190keV for the titanium plate, stainless-steel plate and titanium pen ($p < 0.001$) respectively. SDs decreased with 73%, 66% and 35% at optimal keVs of 130keV, 150keV and 140keV for the titanium plate, stainless-steel plate and titanium pen respectively ($p < 0.001$).

CONCLUSION

When optimizing metal artifact reduction by virtual monochromatic imaging a metal specific tailoring is advised in order to minimize fluctuations and inaccuracies in soft tissues and bone due to metal artifacts.

CLINICAL RELEVANCE/APPLICATION

In DECT, tailoring monochromatic energies for different metal implants is essential order to minimize fluctuations and inaccuracies in soft tissues and bone due to metal artifacts.

SSJ15-06 MRI in Forensic Medicine - A Unique Approach using 31P Magnetic Resonance Spectroscopy of the Skeletal Muscle

Tuesday, Nov. 29 3:50PM - 4:00PM Room: E450B

Participants

Jin Yamamura, MD, Hamburg, Germany (*Presenter*) Nothing to Disclose
Sarah Keller, MD, Hamburg, Germany (*Abstract Co-Author*) Nothing to Disclose
Tony Schmidt, Hamburg, Germany (*Abstract Co-Author*) Nothing to Disclose
Gerhard B. Adam, MD, Hamburg, Germany (*Abstract Co-Author*) Nothing to Disclose
Roland Fischer Sr, DiplPhys, Hamburg, Germany (*Abstract Co-Author*) Nothing to Disclose

PURPOSE

The aim of this study was to investigate the temporal pattern of phosphor metabolites in the adductor magnus muscle post mortem and to check the value of 31P-MRS as a forensic tool especially for the determination of the time of death.

METHOD AND MATERIALS

21 corpses, died of natural cause, were examined (13 male, 8 female; age: 70.5 ± 8.7 y, weight 74 ± 18 kg). A control group of 3 male subjects (mean age: 38.7 ± 24.5 y, range: 2 -67 y, mean body weight: 81 ± 17 kg) was examined at a single time point as well. 31P MRS was performed on a 1.5 T MRI (TR 700 ms, TE 0.35 ms, averages 256, flip angle 90°). A standard 31P surface coil in the patient table, placed under the thigh, was employed. To measure the concentration of the phosphor metabolites scans were repeated in intervals of one hour over a period from 2 to 24 h post mortem (p.m.). The core temperature was rectally measured throughout the MRI examination.

RESULTS

The mean core temperature decreased from 36.0°C to 25.7°C . The comparison of ex vivo and in vivo spectra of the adductor magnus muscle showed characteristic differences. In opposite to in vivo spectra, the ex vivo spectra were dominated by the inorganic phosphate (Pi) peak which was used for further analyses. The ex vivo phosphocreatine (PCr) signal was either very small or even not detectable depending on the time post mortem. During the investigated period, the ex vivo peaks showed similar chemical shifts compared to the in vivo spectra (PCr, γ -ATP, α -ATP, β -ATP: 0.34 ± 0.11 , -2.01 ± 0.12 , -7.08 ± 0.16 , -15.43 ± 0.37 ppm). However, the Pi peak shifted from 5.18 ± 0.13 ppm (in vivo) by about 1.0 ppm and 1.5 ppm after 5 and 10 hours p. m., respectively. The α -, β -, γ -ATP/Pi and the PCr/Pi ex vivo ratios decrease from the beginning of the measurement to the end, while the PME/ β -ATP ratio is exponentially increasing with a slope of $0.39 \pm 0.02 \text{ h}^{-1}$ ($r^2 = 0.54$). The α -ATP/Pi ratio decreased exponentially from 0.445 to 0.032 ($r^2 = 0.997$, $p < 0.001$).

RESULTS

The mean core temperature decreased from 36.0°C to 25.7°C . The comparison of ex vivo and in vivo spectra of the adductor magnus muscle showed characteristic differences. In opposite to in vivo spectra, the ex vivo spectra were dominated by the inorganic phosphate (Pi) peak which was used for further analyses. The ex vivo phosphocreatine (PCr) signal was either very small or even not detectable depending on the time post mortem. During the investigated period, the ex vivo peaks showed similar chemical shifts compared to the in vivo spectra (PCr, γ -ATP, α -ATP, β -ATP: 0.34 ± 0.11 , -2.01 ± 0.12 , -7.08 ± 0.16 , -15.43 ± 0.37 ppm). However, the Pi peak shifted from 5.18 ± 0.13 ppm (in vivo) by about 1.0 ppm and 1.5 ppm after 5 and 10 hours p. m., respectively. The α -, β -, γ -ATP/Pi and the PCr/Pi ex vivo ratios decrease from the beginning of the measurement to the end, while the PME/ β -ATP ratio is exponentially increasing with a slope of $0.39 \pm 0.02 \text{ h}^{-1}$ ($r^2 = 0.54$). The α -ATP/Pi ratio decreased exponentially from 0.445 to 0.032 ($r^2 = 0.997$, $p < 0.001$).

CONCLUSION

There is a characteristic postmortal time pattern of the phosphor metabolites. Especially the α -ATP/Pi ratio could be useful as a forensic tool because of its significant exponential postmortal time course.

CLINICAL RELEVANCE/APPLICATION

The phosphor magnetic resonance spectroscopy (31P MRS) could be used as an important tool in the forensic medicine.

Science Session with Keynote: Musculoskeletal (Muscle and Tendon)

Tuesday, Nov. 29 3:00PM - 4:00PM Room: E451A

MKAMA PRA Category 1 Credit™: 1.00
ARRT Category A+ Credit: 1.00**Participants**Jeffrey J. Peterson, MD, Neptune Beach, FL (*Moderator*) Nothing to DiscloseCraig W. Walker, MD, Omaha, NE (*Moderator*) Nothing to Disclose**Sub-Events****SSJ16-01 Musculoskeletal Keynote Speaker: Muscle Evaluation-Imaging Value Added**

Tuesday, Nov. 29 3:00PM - 3:20PM Room: E451A

ParticipantsRobert D. Boutin, MD, Davis, CA (*Presenter*) Nothing to Disclose**SSJ16-03 Diffusion Tensor Imaging based Tractography of the Myopathic and Dystrophic Skeletal Muscle**

Tuesday, Nov. 29 3:20PM - 3:30PM Room: E451A

Awards**Trainee Research Prize - Resident****Participants**Sarah Keller, MD, Hamburg, Germany (*Presenter*) Nothing to DiscloseZhiyue J. Wang, PhD, Dallas, TX (*Abstract Co-Author*) Nothing to DiscloseAmir Golsari, MD, Hamburg, Germany (*Abstract Co-Author*) Nothing to DiscloseHendrik Kooijman, Hamburg, Germany (*Abstract Co-Author*) Nothing to DiscloseJonathan Chia, Highland Heights, OH (*Abstract Co-Author*) Employee, Koninklijke Philips NVRyota Inai, MD, Hamburg, Germany (*Abstract Co-Author*) Nothing to DiscloseMathias Gelderblom, Hamburg, Germany (*Abstract Co-Author*) Nothing to DiscloseGerhard B. Adam, MD, Hamburg, Germany (*Abstract Co-Author*) Nothing to DiscloseJin Yamamura, MD, Hamburg, Germany (*Abstract Co-Author*) Nothing to Disclose**PURPOSE**

Diffusion tensor imaging (DTI) of the skeletal muscle remains challenging in muscular dystrophies as these conditions are frequently associated with an increase of the percent muscle fat fraction (MFF%) lowering the signal to noise ratio (SNR). The goal of this study was to assess the DTI metrics in a pixel-based and ROI-based quantification method using unselective and muscle-tissue selective ROIs in patients and controls.

METHOD AND MATERIALS

In this prospective study, ten patients (42±18.7y; m:f 5:5) with various muscular dystrophies and ten controls (32±3.0y; m:f 6:4) were included. MRI-scans were performed on a 3.0T system. A fat-suppressed DTI echo planar imaging (EPI) of the thigh was performed. Regions of interest (ROIs) were drawn in a muscle tissue selective and unselective approach using the manufacturers and IDL software. Quantitative ADC and FA-values were generated. The MFF% was obtained using two-point Dixon-based MRI and the following algorithm: $MFF\% = \frac{\text{meanSIFAT}}{\text{meanSIFAT} + \text{meanSIWATER}} \times 100$. Statistical analysis was performed using GraphPad Prism 6.0f. Correlation and significance of DTI values from controls and patients was tested by the Student's T-test and parametric Pearson correlation and considered significant with an $\alpha=0.05$.

RESULTS

The MFF% of the thigh muscles ranged from 15%-89% in patients compared to controls with 3-9%. Using the pixel-based quantification the patients' ADC was significantly decreased corresponding to a FA increase in all muscle groups (rectus femoris (RF): ADC: $1.32 \pm 0.50 \cdot 10^{-3}$ mm²/s, FA: 0.45 ± 0.16 , $p < 0.01$). The ADC and FA correlated inversely to one each other ($r = -0.91$; $p < 0.001$) and to the MFF% (FA $r = 0.53$; ADC $r = -0.56$; $p < 0.001$). The muscle-selective ROI-based quantification revealed no significant alterations of the ADC.

CONCLUSION

The biasing effect of fatty infiltration in muscular dystrophy is diminished by a ROI-based muscle tissue selective quantification of DTI-metrics. Using a muscle tissue selective ROI-localization, aberrations of DTI-metrics in patients are less shifted, indicating no obvious changes of the remaining muscle preceding the muscle cell decay.

CLINICAL RELEVANCE/APPLICATION

A muscle-tissue selective DTI quantification technique enables a more sensitive evaluation of the remaining muscle microstructure as this method is more resistant to the biasing effect a low SNR, causing an artificial shift of the diffusion parameters.

SSJ16-04 Psoas Muscle Atrophy Post Unilateral Hip Implant

Tuesday, Nov. 29 3:30PM - 3:40PM Room: E451A

ParticipantsDavina Mak, MBBS, BSC, Middlesex, United Kingdom (*Presenter*) Nothing to DiscloseCassandra Chisholm, MBBCh, Birmingham, United Kingdom (*Abstract Co-Author*) Nothing to Disclose

Rajesh Botchu, MBBS, Kettering, United Kingdom (*Abstract Co-Author*) Nothing to Disclose
Mark Davies, MBChB, Birmingham, United Kingdom (*Abstract Co-Author*) Nothing to Disclose
Steven L. James, Birmingham, United Kingdom (*Abstract Co-Author*) Nothing to Disclose

PURPOSE

We performed this study to determine if there was significant psoas muscle atrophy and fatty infiltration following unilateral hip implant. As the psoas muscle is one of the major hip flexors, if there is statistically significant atrophy and/or fat infiltration post-operatively this may contribute to sub-optimal post-operative rehabilitation.

METHOD AND MATERIALS

A retrospective study was conducted on all patients who had a unilateral hip implant and then subsequently had an MRI lumbar spine scan between September 2007 and March 2015. The transverse cross sectional area (CSA) of the psoas muscle on T1 axial image was measured at the L3/4 disc level. Psoas CSA on the normal (non-operative) side was used as control to compare psoas CSA on the implant side. The degree of fat infiltration was also measured based on the Goutallier grading. The degree of osteoarthritis of the normal hip was also measured. Statistical analysis with the paired t-test was performed.

RESULTS

In total 412 scans were included in the study (68% female, 32% male) with a mean age 65.8 years at time of MRI scan, and a mean time between operation and MRI scan of 4.21 years. The mean psoas CSA of the implant side was 9.70cm² (SD 3.1) and the normal side 10.31cm² (SD 3.2) with a mean difference between the two sides of 0.61cm² (SD 1.74), P-value <0.0001. In both the implant and normal sides the majority of patients had no evidence of fat infiltration (62.9% and 75.5% respectively). However, when severe fatty atrophy (grade 3 and 4) was seen it was only ever on the implant side and not the normal side. The majority of patients had normal or mild osteoarthritis in their normal hip (35.2% and 37.6% respectively).

CONCLUSION

Our results demonstrate a statistically significant difference in psoas CSA between the implant and normal side post-operatively with the same results when analyzing individual types of implants. There was no significant difference in the degree of psoas fat infiltration between the implant and normal side. The results of statistically significant reduction in psoas CSA on the implant side could be translated into a post-operative rehabilitation that focuses on psoas strengthening exercises.

CLINICAL RELEVANCE/APPLICATION

Post-operative hip implant rehabilitation may benefit from more focused psoas (hip flexor) strengthening exercise to improve functional outcome.

SSJ16-05 Tendon Involvement at the Myo-tendinous Junction in Acute Hamstring Injuries Assessed on MRI and Relationship with Clinical Features at Baseline

Tuesday, Nov. 29 3:40PM - 3:50PM Room: E451A

Participants

Michel D. Crema, MD, Boston, MA (*Abstract Co-Author*) Shareholder, Boston Imaging Core Lab, LLC
Johannes Tol, MD, PhD, Doha, Qatar (*Abstract Co-Author*) Nothing to Disclose
Frank W. Roemer, MD, Boston, MA (*Abstract Co-Author*) Chief Medical Officer, Boston Imaging Core Lab LLC; Research Director, Boston Imaging Core Lab LLC; Shareholder, Boston Imaging Core Lab LLC; ;
Mario Maas, MD, PhD, Utrecht, Netherlands (*Abstract Co-Author*) Nothing to Disclose
Gustaaf Reurink, Rotterdam, Netherlands (*Abstract Co-Author*) Research Grant, Arthrex, Inc
Ali Guermazi, MD, PhD, Boston, MA (*Presenter*) President, Boston Imaging Core Lab, LLC Research Consultant, Merck KgaA Research Consultant, Sanofi-Aventis Group Research Consultant, TissueGene, Inc Research Consultant, OrthoTrophic Research Consultant, AstraZeneca PLC

PURPOSE

Myotendinous junction (MTJ)'s tendon involvement has been reported by some to increase recovery times in athletes with acute hamstring injuries. In order to confirm the clinical relevance of tendon involvement, we aimed to assess the relationship between tendon involvement at the MTJ in acute hamstring injuries evaluated on MRI and baseline clinical features.

METHOD AND MATERIALS

Athletes included in a multicentre randomized controlled trial on the effect of platelet rich plasma in acute hamstring injuries participated in this study. 1.5T MRI was performed at inclusion, within 5 days of injury. One experienced musculoskeletal radiologist assessed the MRIs and evaluated the presence of injuries at the MTJ as grade 0 (no morphological or signal changes around the MTJ), 1 (edema around the MTJ with normal tendon), 2 (thickening and signal changes of the tendon without discontinuity), 3 (partial-thickness discontinuity of the tendon), and 4 (complete discontinuity of the tendon). The following clinical parameters were assessed on the same day as MRI: active knee extension (AKE) and passive straight leg raise (PSLR) for hamstring flexibility, and isometric dynamometer knee flexion force with 15° (F15) and 90° (F90) flexion. One-way analysis of variance (ANOVA) was used to determine if there were significant differences in clinical parameters assessed between the various grades of MTJ involvement on MRI.

RESULTS

Seventy-four acute hamstring injuries were included, with 52 (70.3%) injuries affecting the MTJ on MRI assessment. There was a linear relationship between MRI grade and AKE, with the increase on MRI grade related to a decrease in hamstring flexibility (p=0.03). Injuries exhibiting tendon discontinuity at the MTJ (grades 3 and 4) had a significantly decreased hamstring flexibility for the AKE test (20.4° ± 14.9 vs. 10.7° ± 9.0; p=0.01) and a significant decreased strength (F15) (62.2 ± 26.7 vs. 76.6 ± 22.5; p=0.05) when compared to injuries without tendon discontinuity (grades 1 and 2).

CONCLUSION

Tendon involvement at the MTJ in acute hamstring injuries assessed on MRI is related to decreased hamstring flexibility and strength at the time of injury, especially in hamstring injuries exhibiting discontinuity of the tendon.

CLINICAL RELEVANCE/APPLICATION

Clinically, when flexibility and strength are reduced in acute hamstring injuries, tendon involvement at the MTJ may be present, which may ultimately lead to longer recovery times.

Honored Educators

Presenters or authors on this event have been recognized as RSNA Honored Educators for participating in multiple qualifying educational activities. Honored Educators are invested in furthering the profession of radiology by delivering high-quality educational content in their field of study. Learn how you can become an honored educator by visiting the website at: <https://www.rsna.org/Honored-Educator-Award/>

Ali Guermazi, MD, PhD - 2012 Honored Educator

SSJ16-06 Achilles Tendon Diffusion Tensor Imaging and Tendon Fiber Tracking by Stimulated Echo Resolve (ste-RESOLVE)

Tuesday, Nov. 29 3:50PM - 4:00PM Room: E451A

Participants

Xiang He, PhD, Stony Brook, NY (*Abstract Co-Author*) Nothing to Disclose
Kenneth T. Wengler, MS, Stony Brook, NY (*Abstract Co-Author*) Nothing to Disclose
Chien-Hung Lin, MD, Stony Brook, NY (*Abstract Co-Author*) Nothing to Disclose
Marco A. Oriundo Verastegui, MD, Lima, Peru (*Abstract Co-Author*) Nothing to Disclose
Alex Sacher, BSC, Binghamton, NY (*Abstract Co-Author*) Nothing to Disclose
Kevin S. Baker, MD, Stony Brook, NY (*Abstract Co-Author*) Nothing to Disclose
Mingqian Huang, MD, Syosset, NY (*Abstract Co-Author*) Nothing to Disclose
Elaine S. Gould, MD, Stony Brook, NY (*Abstract Co-Author*) Nothing to Disclose
Mark E. Schweitzer, MD, Stony Brook, NY (*Abstract Co-Author*) Consultant, MMI Munich Medical International GmbH Data Safety Monitoring Board, Histogenics Corporation
Dharmesh Tank, MD, Stony Brook, NY (*Presenter*) Nothing to Disclose

PURPOSE

Approximately 75% of Achilles tendon (AT) rupture is related to athletic activities. These disorder usually begin as subclinical Achilles tendinosis, characterized by injury-induced disruption to the tendon microstructure integrity and degeneration, which may progress into rupture. Diffusion tensor imaging (DTI) provided a sensitive tool to non-invasively detect changes on AT micro-architecture. However, normal AT has an effective T2/T2* of ~5-10 ms such that clinical DTI protocol (TE ~60-80 ms) has poor SNR. In this pilot, a new DTI protocol with short TE (~20 ms) was developed and assessed.

METHOD AND MATERIALS

Six healthy subjects were recruited for this IRB approved study on a Siemens Prisma 3T magnet. A novel approach of combining stimulated-echo DTI and readout-segmented multi-shot EPI (ste-RESOLVE) was developed. To further boost tendon MR signal, magic angle effect was adopted by positioning AT ~55 degrees w.r.t. B0 direction. The tendon fractional anisotropy (FA), apparent diffusion coefficient (ADC), DTI tensor and fiber tractography were generated from DTI Studio. T2* maps were calculated using a mono-exponential on multi-echo GRE signal.

RESULTS

The measured ADC and FA were $1.16 \pm 0.17 \times 10^{-3}$ mm²/s and 0.34 ± 0.03 respectively. The AT fiber tractography provides a visual description of microstructure integrity, with spatial distribution and orientation of DTI fiber tract following the parallel collagen fiber bundles running along the major axis. The relative angle of the AT (w.r.t. B0) was $47.5 \pm 7.5^\circ$ in this study, resulting in a T2* of 14.8 ± 2.0 ms.

CONCLUSION

This study evaluated the feasibility and robustness of a ste-RESOLVE-based DTI protocol that can be used on Achilles tendinosis patients to assess the risk of tendon rupture. Combining the magic angle effect with short TE ste-RESOLVE sequence, DTI of the AT can be accomplished in healthy subjects with no history of AT injury. The estimated ADC, FA and fiber tractography in control subject may serve as a baseline for subsequent studies on patients with clinical and subclinical Achilles tendinosis.

CLINICAL RELEVANCE/APPLICATION

This study evaluated the feasibility and robustness of a novel stimulated echo based RESOLVE DTI protocol that can be used on Achilles tendinosis patients to assess the risk of tendon rupture.

Nuclear Medicine (Musculoskeletal Imaging)

Tuesday, Nov. 29 3:00PM - 4:00PM Room: S505AB



AMA PRA Category 1 Credit™: 1.00
ARRT Category A+ Credit: 1.00

Participants

Yonglin Pu, MD, PhD, Chicago, IL (*Moderator*) Nothing to Disclose
Andrew C. Homb, MD, Louisville, KY (*Moderator*) Nothing to Disclose

Sub-Events**SSJ17-01 Pilot Evaluation of Two-Phase Hybrid 18F-Fluoride PET/MRI of the Sacroiliac Joints in Patients with Ankylosing Spondylitis**

Tuesday, Nov. 29 3:00PM - 3:10PM Room: S505AB

Participants

Lino Sawicki, MD, Dusseldorf, Germany (*Abstract Co-Author*) Nothing to Disclose
Susanne Luetje, Essen, Germany (*Abstract Co-Author*) Nothing to Disclose
Julian Kirchner, Dusseldorf, Germany (*Presenter*) Nothing to Disclose
Verena Ruhlmann, Essen, Germany (*Abstract Co-Author*) Nothing to Disclose
Gerald Antoch, MD, Duesseldorf, Germany (*Abstract Co-Author*) Nothing to Disclose
Christian Buchbender, Duesseldorf, Germany (*Abstract Co-Author*) Nothing to Disclose

PURPOSE

To evaluate the feasibility of blood-pool phase 18F-Fluoride positron emission tomography/magnetic resonance imaging (18F-F PET/MRI) of the sacroiliac joints (SIJ) in patients with active ankylosing spondylitis (AS) and to compare blood-pool and standard mineralization-phase 18F-F PET/MRI in different AS lesions.

METHOD AND MATERIALS

13 patients with active AS were prospectively enrolled. Early 18F-F PET was acquired in the blood-pool phase 6 min after injection of 158±8 MBq 18F-F. Then, a standard 18F-F PET was acquired in the mineralization phase 40 min after injection. PET and MR images were analyzed in consensus regarding image quality (IQ) (four-point Likert scale: 0=non-diagnostic, 3=excellent image quality). The iliac and the sacral part of each SIJ was subdivided in an upper and a lower part, resulting in 4 SIJ quadrants (SQ) per side. All SQ were then evaluated regarding the presence of bone marrow edema (BME), fatty deposits (FD), sclerosis, ankylosis, and focal 18F-F uptake on blood-pool and mineralization phase PET. Additionally, PET/MR images were reviewed for extraosseous 18F-F uptake.

RESULTS

Mean IQ was 3.0±0 for MRI, 3.0±0 for mineralization phase, and 2.2±0.4 for blood-pool phase 18F-F PET. 66 SQ (63.4%) showed FD, 44 SQ (42.3 %) BME, and 28 SQ (26.9%) erosions. Sclerosis was found in 27 SQ (26%), and ankylosis in 11 SQ (10.6%). On mineralization phase 18F-F PET/MRI focal uptake was seen in 45 SQ (43.3%), whereas on blood-pool phase 18F-F PET/MRI focal uptake was found in only 25 SQ (24.0%, p<0.001). There was no focal 18F-F uptake detectable on blood-pool phase PET/MRI without a corresponding uptake on mineralization phase PET/MRI. Moreover, blood-pool phase 18F-F PET/MRI revealed no additional extraosseous PET-positive lesions. On mineralization phase 18F-F PET/MRI, SQ showing BME alone or a combination of BME with other AS lesions had a significantly higher (p<0.001) percentage of focal uptake (38/44 SQ; 86.4%) than on blood-pool phase 18F-F PET/MRI (21/44 SQ; 47.7%).

CONCLUSION

Two-phase 18-F PET/MRI of the SIJ is feasible. However, the blood-pool phase 18F-F PET offered no added diagnostic value as compared with standard mineralization phase 18F-F PET/MRI in patients with active AS.

CLINICAL RELEVANCE/APPLICATION

According to our data, there seems to be no relevance of a blood-pool phase PET scan as part of a two-phase 18F-F PET/MRI protocol for the assessment of SIJ involvement in AS.

SSJ17-02 Diagnostic Performance of 18F-Fluorodeoxyglucose (18F-FDG) Positron Emission Tomography/Computed Tomography (PET/CT) for Detection and Localization of Infective Spondylodiscitis

Tuesday, Nov. 29 3:10PM - 3:20PM Room: S505AB

Participants

Christoph Weber, MD, Hamburg, Germany (*Presenter*) Nothing to Disclose
Silvia Muenster, Hamburg, Germany (*Abstract Co-Author*) Nothing to Disclose
Gerhard B. Adam, MD, Hamburg, Germany (*Abstract Co-Author*) Nothing to Disclose
Thorsten Derlin, MD, Hannover, Germany (*Abstract Co-Author*) Nothing to Disclose

PURPOSE

The aim of this study was to assess the diagnostic performance of 18F-fluorodeoxyglucose (18F-FDG) positron emission tomography/computed tomography (PET/CT) for detection and localization of infective spondylodiscitis.

METHOD AND MATERIALS

18F-FDG PET/CT was performed in 23 consecutive patients (13 men; 10 women; mean age 67.4 ± 11.1 years, range, 40.7 to 88.8 years). All PET/CT scans were analyzed by two independent readers both visually and semiquantitatively by measurement of the maximum standardized uptake value (SUVmax) in areas of visually increased spinal tracer uptake. Laboratory parameters of infection/inflammation including C-reactive protein (CRP), procalcitonin (PCT) and leucocyte count were recorded. Histopathological evaluation and microbiological pathogen detection by either intraoperative material collection and/or blood cultures served as the reference standard. Nonparametric Spearman's rho was used for correlation analysis. Cohen's kappa was used for assessment of intra- and interrater agreement.

RESULTS

36 foci of increased tracer uptake within the spine were detected in 21 study patients. Staphylococcus aureus was the predominant pathogen. Mean SUVmax of lesions was 5.6 ± 2.2 (range, 2.6 to 13.0). SUVmax did neither correlate with CRP ($p = 0.29$), nor with PCT ($p = 0.91$) nor with leucocyte count ($p = 0.82$). 18F-FDG PET/CT had a sensitivity of 100%, a specificity of 66.7%, a positive predictive value of 95.2 %, a negative predictive value of 100%, and an overall accuracy of 95.7%. The interrater Cohen's kappa was 0.62 (95% CI 0.16 - 1.09), whereas the intrarater Cohen's kappa was 0.78 (95% CI 0.36-1.20).

CONCLUSION

18F-FDG PET/CT is a reliable and highly sensitive imaging modality for detection of pyogenic spondylodiscitis. Whole-body evaluation by PET may contribute to the detection of additional sites of inflammation. Particularly high uptake values (SUVmax) may be observed in Staphylococcus aureus infection; however, SUVmax cannot reliably predict the causing pathogen. Tracer uptake did not correlate with the level of inflammatory serum markers in this study, questioning the role of PET for grading the strength of inflammatory reaction.

CLINICAL RELEVANCE/APPLICATION

18F-FDG PET/CT is a reliable and highly sensitive imaging modality for detection and localization of pyogenic spondylodiscitis and may contribute to the detection of additional sites of inflammation.

SSJ17-03 Do Meniscal Pathologies Correlate with Increased Bone Tracer Uptake Using SPECT/CT?

Tuesday, Nov. 29 3:20PM - 3:30PM Room: S505AB

Participants

Anna Hirschmann, MD, Basel, Switzerland (*Presenter*) Nothing to Disclose
Anna L. Falkowski, Basel, Switzerland (*Abstract Co-Author*) Nothing to Disclose
Milos Dordevic, Bruderholz, Switzerland (*Abstract Co-Author*) Nothing to Disclose
Jan Rechsteiner, Bruderholz, Switzerland (*Abstract Co-Author*) Nothing to Disclose
Felix Amsler, Basel, Switzerland (*Abstract Co-Author*) Nothing to Disclose
Michael T. Hirschmann, MD, Bruderholz, Switzerland (*Abstract Co-Author*) Nothing to Disclose

PURPOSE

To assess the correlation of subchondral bone tracer uptake (BTU) of the knee joint using single photon emission computed tomography (SPECT)/computed tomography (CT) and meniscal pathologies using magnetic resonance (MR) imaging.

METHOD AND MATERIALS

Twenty-five consecutive patients (mean age 45.5 ± 11.5 years) with MR and SPECT/CT within three months were prospectively collected and retrospectively included. Patients with previous knee surgery as well as with grade 3 and 4 cartilage lesions were excluded. For analysis and comparison of MR and SPECT/CT a specific localisation scheme was used. Maximum values of each subchondral femorotibial area were quantified and a ratio was calculated in relation to a reference region in the femoral shaft, which represented the BTU background activity. Meniscal pathologies on MR were graded (non, degeneration, tear) by two experienced musculoskeletal radiologists blinded to the SPECT/CT findings. Extrusion of the meniscus was assessed. ANOVA and Chi-Square ($p < 0.05$) served for statistics.

RESULTS

Meniscal degeneration showed a significantly higher mean relative BTU compared to an intact meniscus on the femoral side ($p = 0.018$; tibial side $p = 0.072$). Meniscal tear showed significantly higher mean relative BTU compared to an intact meniscus ($p < 0.01$ femoral and tibial side) as well to degeneration ($p = 0.006$, respectively). Meniscal extrusion showed significantly higher mean relative BTU compared to non-extruded meniscus ($p < 0.02$). Medial meniscal pathologies (0.52) showed higher correlation with BTU than on the lateral side (0.23).

CONCLUSION

Subchondral BTU in SPECT/CT of the knee with preserved cartilage was significantly higher with meniscal degeneration or tear as well as meniscal extrusion. SPECT/CT is able to identify patients with an increased risk for development of osteoarthritis.

CLINICAL RELEVANCE/APPLICATION

The present results demonstrate the need for a valid tool, which is able to diagnose osteoarthritis in its earliest stages, in order to create specialized treatments in a timely manner avoiding outcomes caused by osteoarthritis progression.

SSJ17-04 Variability in Sodium Fluoride PET Imaging Observed in Multicenter Clinical Trials

Tuesday, Nov. 29 3:30PM - 3:40PM Room: S505AB

Participants

Prayna Bhatia, BS, Columbus, OH (*Presenter*) Nothing to Disclose
David Poon, BS, Columbus, OH (*Abstract Co-Author*) Nothing to Disclose
Jun Zhang, PhD, Columbus, OH (*Abstract Co-Author*) Nothing to Disclose
Chadwick L. Wright, MD, PhD, Lewis Center, OH (*Abstract Co-Author*) Nothing to Disclose
Lawrence H. Schwartz, MD, New York, NY (*Abstract Co-Author*) Committee member, Celgene Corporation Committee member, Novartis AG Committee member, ICON plc Committee member, BioClinica, Inc
Michael V. Knopp, MD, PhD, Columbus, OH (*Abstract Co-Author*) Nothing to Disclose

PURPOSE

To identify areas of variability or non-compliance and critical challenges in NaF PET/CT imaging by analyzing de-identified imaging examinations from a multi-center oncology trial that included bone imaging in comparison to the SNMMI standard NaF PET/CT acquisition guidelines.

METHOD AND MATERIALS

30 patients with 80 NaF PET/CT examination from over 14 credentialed institutions within the USA were included in this assessment. A standardized quality control (QC) process was utilized pulling key information from the DICOM tags including NaF dosage and uptake time. Trial-specific data compliance was evaluated. The utilized dosage and uptake time was compared to the SNMMI standard NaF guidelines. A standard QC scoring system for NaF PET was developed and implemented to determine the variability of the exams.

RESULTS

The SNMMI guidelines on NaF PET/CT imaging recommend imaging 45-60 minutes post-injection. We found that only 33% fell within those guidelines while 66% were outside that range. The average uptake time for the trial studies was 58 ± 17 min, with a range of 20 to 103 minutes (median: 61 minutes). Compared to the recommended dose for adults of 185-370 MBq (5-10 mCi), only 39% of the studies fell within the protocol range. The average dose for the trial studies was 358 ± 66 MBq (9.7 ± 1.8 mCi) with a median of 375 MBq (10.1 mCi). 6% of the dose activity were below the protocol minimal dose and 55% were above.

CONCLUSION

Currently, only a few publications summarize recommendations for Sodium Fluoride PET acquisition and the SNMMI imaging protocol includes several considerations for patient acquisition. There is no evidence that higher than recommended dose are diagnostically beneficial nor imaging outside the recommend p.i. time frame. It is thus evident, that clinical practice is currently in 2/3 of the scans outside current recommendations and that based on ALARA dose reductions should be considered. While most of the variability does not impact the visual accessibility of NaF PET, safety and potential quantitative assessment considerations necessitate a substantial improvement in community practice within clinical trials.

CLINICAL RELEVANCE/APPLICATION

As osseous disease burden are increasingly decision points for adaptive clinical trials, quality assurance standards for NaF PET/CT must be monitored, as current procedural variability is excessive.

SSJ17-05 18F-FDG Super Bone Marrow Uptake: A PET Presentation of Bone Marrow Malignant Infiltration?

Tuesday, Nov. 29 3:40PM - 3:50PM Room: S505AB

Awards

Student Travel Stipend Award

Participants

Mohammed Shah Alam, MBBS, Guangzhou, China (*Presenter*) Nothing to Disclose
Hu Bing Wu, PhD,MD, Guangzhou, China (*Abstract Co-Author*) Nothing to Disclose
Lilan Fu, MBBS, Guangzhou, China (*Abstract Co-Author*) Nothing to Disclose
Wen-Lan Zhou, MD, Guangzhou, China (*Abstract Co-Author*) Nothing to Disclose
Wang Quan-Shi Wang, PhD,MD, Guangzhou, China (*Abstract Co-Author*) Nothing to Disclose

PURPOSE

It has not been illuminated what causes the super 18F-FDG uptake in bone marrow (SBMU), which presents as particular high diffuse 18F-FDG uptake in bone marrow similar to or higher than that in the brain. The present study was performed to investigate its origins and clinical significance.

METHOD AND MATERIALS

31 newly diagnosed patients with SBMU were retrospectively reviewed from April 2008 to December 2015. Twenty normal subjects were selected as the control group. The SUVmax of bone marrow was measured and the bone marrow to cerebellum (BM/C) ratio was calculated. Blood parameters as well as fever were also been collected and analyzed.

RESULTS

Of 31 patients with SBMU, 29 (93.6%) were diagnosed to have malignancies including 14 lymphoma, 11 leukemia, 3 multiple myeloma and 1 bone metastasis. BM malignant infiltration (BMI) was confirmed in all these patients. SUVmax and BM/C ratios of the SBMU were significantly higher than that of control subjects (SUVmax, 11.30 ± 3.95 vs. 2.43 ± 0.51 , $t=9.936$, $P=0.000$; BM/C ratios, 1.24 ± 0.36 vs. 0.23 ± 0.02 , $t=12.463$, $P=0.000$; respectively). Extra-bone marrow lesions were found in 15 patients with malignancies. Decrease of leukocyte count (WBC) count, hemoglobin (HB) and platelet count (PLT) were noted in 48.4% , 86.2% and 51.5% of the patients with BMI respectively . HB, PLT, lactic dehydrogenase (LDH), C-reactive protein (CRP) and the fever incidence were observed to be helpless for the differentiation of lymphoma and leukemia (all $P>0.05$). However, increase of WBC counts and extra-BM involvement found on PET were useful for differentiation, especially the liver and nasal cavity involvements ($P=0.020$ and $P=0.046$, respectively).

CONCLUSION

Most of the SBMU was caused by the malignant infiltration which often accompany with decrease of hematopoietic function. 18F-FDG PET/CT is useful for detection of extra-BM involvements and for differentiation of lymphoma and leukemia

CLINICAL RELEVANCE/APPLICATION

Study revealed that super BMU was a highly potent indicator for the malignant BMI which mostly originated from lymphoma and leukemia.

SSJ17-06 The Prognostic and Diagnostic Value of FDG PET/CT for Assessment of Symptomatic Osteoarthritis

Tuesday, Nov. 29 3:50PM - 4:00PM Room: S505AB

Awards

Trainee Research Prize - Medical Student

Participants

Brian J. Nguyen, BA, San Diego, CA (*Presenter*) Nothing to Disclose
Ashley Burt, MD, San Diego, CA (*Abstract Co-Author*) Nothing to Disclose
Randall L. Baldassarre, MD, San Diego, CA (*Abstract Co-Author*) Nothing to Disclose
Edward Smitaman, MD, West Hartford, CT (*Abstract Co-Author*) Nothing to Disclose
Maud M. Morshedi, MD, PhD, San Diego, CA (*Abstract Co-Author*) Nothing to Disclose
Steven Kao, MD, Los Angeles, CA (*Abstract Co-Author*) Nothing to Disclose
Sebastian Obrzut, MD, San Diego, CA (*Abstract Co-Author*) Nothing to Disclose

PURPOSE

The purpose of this study was to assess the clinical significance of increased FDG uptake on PET/CT in the joints for evaluation of symptomatic osteoarthritis (OA) and for prediction of OA progression.

METHOD AND MATERIALS

In this prospective study, shoulder, hip and knee joints were imaged in 79 patients undergoing routine FDG PET/CT imaging. Subsequently, patients completed Western Ontario and McMaster Universities Osteoarthritis Index (WOMAC) questionnaire to assess for joint pain, stiffness, and physical function. SUVs were measured in acromioclavicular, glenohumeral, hip and knee joints. Scout images were reviewed and joints were evaluated for OA using the The Kellgren and Lawrence (KL) system. Patients were followed for 2 years to determine progression of OA based on follow up imaging or surgical intervention.

RESULTS

In the knees ROC AUCs for SUV were 0.737 (WOMAC Total), 0.784 (WOMAC Pain) and 0.743 (WOMAC Function). ROC AUCs in the knees for KL score were 0.794 (WOMAC Total), 0.859 (WOMAC Pain), 0.795 (WOMAC Stiffness) and 0.805 (WOMAC Function). In the hips ROC AUCs for SUV were 0.703 (WOMAC Pain) and 0.764 (WOMAC Function). In the glenohumeral and acromionclavicular joints ROC AUCs for SUV were 0.716 and 0.916 (WOMAC Pain) respectively. Follow-up imaging was available for 19 knee joints. OA progressed in 6 knee joints and was stable in 13. SUV ($p = 0.0229$), KL score ($p = 0.5324$), Age ($p = 0.8978$) and WOMAC score ($p = 0.1265$) variables were entered simultaneously into the Cox proportional hazards model and only SUV was found to be an independent predictor of OA progression in the knees.

CONCLUSION

SUV measurement on FDG PET/CT may be helpful for assessment of symptomatic OA in the knees and hips, and pain in the shoulders. Increased FDG uptake on PET/CT in the knees may be predictive of progression of OA. KL score of the scout images can aid in identification of symptomatic OA in the knees.

CLINICAL RELEVANCE/APPLICATION

SUV measurement on FDG PET/CT may be helpful for assessment of symptomatic OA in the knees and hips, and pain in the shoulders.

Neuroradiology/Head and Neck (Head and Neck Vascular Diseases)

Tuesday, Nov. 29 3:00PM - 4:00PM Room: N226



AMA PRA Category 1 Credit™: 1.00
ARRT Category A+ Credit: 1.00

FDA Discussions may include off-label uses.

Participants

Yoshimi Anzai, MD, Salt Lake Cty, UT (*Moderator*) Nothing to Disclose
Ronald L. Wolf, MD, PhD, Philadelphia, PA (*Moderator*) Nothing to Disclose

Sub-Events**SSJ18-01 The Association of CT Angiographic Plaque Features with Symptomatic Atherosclerotic Carotid Artery Disease: A Systematic Review and Meta-Analysis**

Tuesday, Nov. 29 3:00PM - 3:10PM Room: N226

Participants

Khalid Al-Dasuqi, New York, NY (*Presenter*) Nothing to Disclose
Hediyeh Baradaran, MD, New York, NY (*Abstract Co-Author*) Nothing to Disclose
Diana Delgado, MS, New York, NY (*Abstract Co-Author*) Nothing to Disclose
Ajay Gupta, MD, New York, NY (*Abstract Co-Author*) Consultant, Biomedical Systems;

PURPOSE

CT Angiography (CTA) is a commonly acquired imaging modality which provides a detailed examination of the carotid plaque, but has been limited in its use for risk stratification because of the lack of prospective studies to support the link between cerebrovascular ischemia and certain plaque features. We performed this systematic review and meta-analysis to assess the association between carotid plaque features on CTA and cerebrovascular ischemia.

METHOD AND MATERIALS

A medical librarian performed a literature search to identify published English-language studies that evaluated the link between carotid plaque features and ischemic events. The selection criteria included studies that: (1) evaluated internal carotid artery (ICA) plaque features on CTA of the extracranial carotid arteries, (2) involved patients with symptomatic correlation (transient ischemic attack/stroke) with plaque features, and (3) included asymptomatic controls, either the contralateral carotid artery, asymptomatic subjects or both. Four meta-analyses were performed and the combined Odds Ratios (ORs) were obtained using a random-effects model (Figure 1).

RESULTS

The literature search yielded 12,557 articles from which 14 studies, with a total of 2028 patients and 3194 arteries, were included for review. We found significant associations between both soft plaque and increased carotid artery wall thickness (CAWT) and higher occurrence of ipsilateral ischemic events with ORs of 3.633 (95% CI 1.087-12.142, $p=0.036$) and 6.204 (95% CI 2.485 - 15.493, $p<0.001$), respectively. In addition, we found a significant relationship between calcified plaque and decreased likelihood of ipsilateral ischemic events (OR 0.544; 95% CI 0.320-0.923, $p=0.024$). There was no statistically significant relationship between plaque ulceration and ipsilateral symptoms (OR 1.898; 95% CI 0.914-3.942, $p=0.086$).

CONCLUSION

Our meta-analysis demonstrates that soft plaques and increased CAWT measurements are highly associated with ipsilateral ischemic events, while calcified plaques are linked to lower occurrence of ipsilateral ischemia. These results warrant future prospective studies to validate the use of these plaque features in stroke risk stratification.

CLINICAL RELEVANCE/APPLICATION

CTA may be used to detect high-risk plaques that could aid in identifying patients at an increased risk of stroke who may be potential candidates for surgical revascularization.

SSJ18-02 Atherosclerotic Plaque Characterization in Humans with Acoustic Radiation Force Impulse (ARFI) Imaging

Tuesday, Nov. 29 3:10PM - 3:20PM Room: N226

Participants

Tomasz Czernuszewicz, PhD, Chapel Hill, NC (*Abstract Co-Author*) Nothing to Disclose
Jonathon Homeister, MD, PhD, Chapel Hill, NC (*Abstract Co-Author*) Nothing to Disclose
Melissa Caughey, PhD, Chapel Hill, NC (*Abstract Co-Author*) Nothing to Disclose
Benjamin Y. Huang, MD, MPH, Chapel Hill, NC (*Abstract Co-Author*) Consultant, LQ3 Pharmaceuticals, Inc
Ellie R. Lee, MD, Chapel Hill, NC (*Abstract Co-Author*) Nothing to Disclose
Carlos Zamora, MD, PhD, Chapel Hill, NC (*Abstract Co-Author*) Nothing to Disclose
Mark Farber, MD, Chapel Hill, NC (*Abstract Co-Author*) Nothing to Disclose
Joseph Fulton, MD, Chapel Hill, NC (*Abstract Co-Author*) Nothing to Disclose
Peter Ford, MD, Chapel Hill, NC (*Abstract Co-Author*) Nothing to Disclose
William Marston, MD, Chapel Hill, NC (*Abstract Co-Author*) Nothing to Disclose
Raghu Vallabhaneni, Chapel Hill, NC (*Abstract Co-Author*) Nothing to Disclose
Timothy C. Nichols, MD, Chapel Hill, NC (*Abstract Co-Author*) Nothing to Disclose

Caterina Gallippi, PhD, Chapel Hill, NC (*Presenter*) Nothing to Disclose

PURPOSE

Stroke is commonly caused by thromboembolic events originating from vulnerable atherosclerotic plaques in the carotid vasculature. To improve carotid plaque characterization with ultrasound, we have been investigating ARFI imaging, a novel elasticity imaging technique, that has shown promise for discriminating soft from stiff plaque. In this study, in vivo carotid ARFI imaging is implemented in patients undergoing carotid endarterectomy (CEA) and compared against matched histology with blinded reader assessment to validate performance.

METHOD AND MATERIALS

Patients (N = 25) undergoing CEA were recruited and imaged transcutaneously with ARFI. After surgery, the extracted specimens were sectioned and aligned to the ultrasound plane. 2D ARFI images of peak displacement were rendered and evaluated by 3 radiologists blinded to histology. Receiver operating characteristic (ROC) curve analysis was performed and area under the curve (AUC) was taken as a metric of performance for detecting features such as necrotic core (NC), intraplaque hemorrhage (IPH), collagen (COL), and calcium (CAL). Also, readers were asked to measure fibrous cap thickness (FCT) from ARFI images, and their results were compared against FCT from histology by Spearman correlation (ρ), regression (R²), and Bland-Altman (BA) analysis.

RESULTS

Median AUC performance for plaque features were as follows: NC, 0.809; COL, 0.696; IPH, 0.639; CAL, 0.612. Grouping the stiff (COL/CAL) and soft (NC/IPH) features together resulted in marked improvement in performance, with median AUCs of 0.859 for COL/CAL and 0.887 for NC/IPH (Fig. 1). For FCT measurements, two of the three radiologists achieved good agreement with histologic measurements. The first reader identified 11 FCs (out of 16) with moderately high agreement with histology (R² = 0.64, ρ = 0.81). The second reader identified 7 FCs with high agreement with histology (R² = 0.89, ρ = 0.75). The third reader identified 11 FCs, but had weak agreement to histology (R² = 0.27, ρ = 0.56).

CONCLUSION

This study suggests that ARFI may be capable of distinguishing soft from stiff features of atherosclerotic plaques and that ARFI may also be relevant to measuring FCT, an important indicator of plaque vulnerability.

CLINICAL RELEVANCE/APPLICATION

ARFI ultrasound imaging is capable of discriminating between soft from stiff carotid plaque, representing a novel approach to detecting vulnerable lesions, which may help predict stroke risk.

SSJ18-03 Evaluation of Restenosis After Carotid Artery Stenting: Comparison on CT Images Reconstructed with Full Iterative Reconstruction and Ultrasound Images

Tuesday, Nov. 29 3:20PM - 3:30PM Room: N226

Participants

Kazushi Yokomachi, RT, Hiroshima, Japan (*Presenter*) Nothing to Disclose

Shinji Kume, Hiroshima, Japan (*Abstract Co-Author*) Nothing to Disclose

Fuminari Tatsugami, Hiroshima, Japan (*Abstract Co-Author*) Nothing to Disclose

Chikako Fujioka, RT, Hiroshima, Japan (*Abstract Co-Author*) Nothing to Disclose

Eiji Nishimaru, RT, Hiroshima, Japan (*Abstract Co-Author*) Nothing to Disclose

Kazuo Awai, MD, Hiroshima, Japan (*Abstract Co-Author*) Research Grant, Toshiba Corporation; Research Grant, Hitachi, Ltd; Research Grant, Bayer AG; Research Grant, Eisai Co, Ltd; Medical Advisor, General Electric Company; ; ; ;

Masao Kiguchi, RT, Hiroshima, Japan (*Abstract Co-Author*) Nothing to Disclose

Yoshinori Funama, PhD, Kumamoto, Japan (*Abstract Co-Author*) Nothing to Disclose

PURPOSE

Carotid artery stenting (CAS) has been widely used to treat carotid artery stenosis. To evaluate restenosis after CAS, patients undergo ultrasound (US) studies, however, their interpretation varies with the operators. CT angiography (CTA) is also used for the evaluation of restenosis after CAS. However, when the images are reconstructed with conventional filtered back projection (FBP), blooming artifacts from the stent structure render the detection of restenosis difficult. The new full iterative reconstruction algorithm (forward projected model-based iterative reconstruction solution: FIRST algorithm) increases spatial resolution and reduces artifacts. We compared the detectability of restenosis after CAS on CT images reconstructed with full IR and on US images.

METHOD AND MATERIALS

We enrolled 15 patients who underwent CTA and US studies for stent patency. All CT and US examinations were performed within one month. We generated CT images with conventional filtered back projection (FBP), hybrid IR (AIDR 3D, Toshiba), and FIRST. To minimize measurement errors, all US studies were performed by one operator. We compared the thickness of intimal thickening (IT) on axial CT- and US images and calculated the change rate (CR) on CT and US images as $CR(\%) = (\text{echo-IT} - \text{CT-IT}) / \text{echo-IT} \times 100$.

RESULTS

US studies detected restenosis in 9 of 15 patients. On FBP-, AIDR 3D-, and FIRST images 4, 4, and 9 cases, respectively, were identified. The mean CR from US images on FBP-, AIDR 3D-, and FIRST images was 66.0%, 62.9%, and 11.9%, respectively. The FIRST algorithm made it possible to detect all IT and the mean CR was smaller than on images subjected to the other two reconstruction methods.

CONCLUSION

After carotid artery stenting, the detectability of restenosis was similar on FIRST- and US images.

CLINICAL RELEVANCE/APPLICATION

FIRST is recommended for the precise evaluation of restenosis after carotid artery stenting.

SSJ18-04 Carotid Intraplaque Hemorrhage Imaging using MRI: Comparison of the Diagnostic Performance Between MATCH and MPRAGE Sequences at 3T

Tuesday, Nov. 29 3:30PM - 3:40PM Room: N226

Participants

Yanni Du, MMed,MMed, Beijing, China (*Presenter*) Nothing to Disclose
Wei Yu, MD, Beijing, China (*Abstract Co-Author*) Nothing to Disclose
Zhaoyang Fan, Los Angeles, CA (*Abstract Co-Author*) Nothing to Disclose
Zhanhong Wang, Beijing, China (*Abstract Co-Author*) Nothing to Disclose
Xiaoming Bi, PhD, Chicago, IL (*Abstract Co-Author*) Nothing to Disclose
Jing An, Beijing, China (*Abstract Co-Author*) Research collaboration, Siemens AG
Tianjing Zhang, Beijing, China (*Abstract Co-Author*) Employee, Siemens AG
Debiao Li, PhD, Chicago, IL (*Abstract Co-Author*) Nothing to Disclose
Lixin Yang, MMed,MMed, Beijing, China (*Abstract Co-Author*) Nothing to Disclose

PURPOSE

3D magnetization-prepared rapid acquisition gradient-echo (MPRAGE) sequence has been validated to detect IPH with high sensitivity and specificity. Recently, a new 3D plaque imaging sequence, Multicontrast Atherosclerosis Characterization (MATCH) developed for the characterization of carotid plaque IPH, calcification and overall plaque morphology can be depicted in three interleaved image sets of a single scan, allowing complete image registration. The purpose of the work is to compare the diagnostic performance of MATCH and MPRAGE for the detection of IPH, with histologic analysis as the reference standard.

METHOD AND MATERIALS

Thirty-five individuals scheduled for carotid endarterectomy underwent 3 T carotid MR imaging using MPRAGE and MATCH. Imaging parameters for MATCH and MPRAGE are listed in Table 1. All image data sets were processed on commercial plaque analysis software (MRI-Plaque View, VPDiagnostics, US). Two reviewers blinded to the histologic results assessed the presence and signal intensity of IPH for each sequence. Images were matched to histology results using morphological features of the lumen, vessel wall and the distance from the carotid bifurcation. Sensitivity, specificity and cohen kappa (K) were computed to quantify the agreement in the detection of IPH among the two MRI protocols with reference to the pathology results.

RESULTS

Among 35 patients, a total of 664 available sections and 71 matching histology specimens were included for the analysis. MATCH yielded good agreement with MPRAGE ($\kappa=0.702$) on detecting the presence of IPH for 664 available sections. With pathological specimens as the gold standard, moderate to good agreement was shown between MATCH and MPRAGE ($\kappa=0.785$ vs. 0.637). Sensitivity for the detection of IPH was 92.5% vs. 83.0%, respectively, for MATCH and MPRAGE. Specificity was 88.9% for both protocols.

CONCLUSION

Compared to the MPRAGE sequence, MATCH technique demonstrates similar diagnostic performance for the detection of IPH. Excellent suppression of background tissues in MATCH images greatly simplifies the visualization of IPH. Furthermore, two additional image contrasts are acquired from the same 5 min MATCH scan that can be used to characterize other plaque compositions. MATCH is a promising CMR imaging method for assessing the vulnerable plaque in a clinical workup.

CLINICAL RELEVANCE/APPLICATION

MATCH is a promising CMR technique for assessing the vulnerable plaque in a clinical workup.

SSJ18-05 Evaluating the Impact of Ice Collar on the Blood Flow of the Internal and External Carotid Arteries

Tuesday, Nov. 29 3:40PM - 3:50PM Room: N226

Awards

Student Travel Stipend Award

Participants

Maryam Mohammad Zadeh, MD, Laguna Niguel, CA (*Presenter*) Nothing to Disclose
Ali Mohammadzadeh Koupareh, MD, Los Angeles, CA (*Abstract Co-Author*) Nothing to Disclose
Vahid Mohammadzadeh, Tehran, Iran (*Abstract Co-Author*) Nothing to Disclose
Reza Erfanian, tehran, Iran (*Abstract Co-Author*) Nothing to Disclose
Abolfazl K. Shiravi, MD, Tehran, Iran (*Abstract Co-Author*) Nothing to Disclose
Pouya Entezari, tehran, Iran (*Abstract Co-Author*) Nothing to Disclose
Ali Borhani, MD, Tehran, Iran (*Abstract Co-Author*) Nothing to Disclose
Mojtaba Mohammadi Ardehali, tehran, Iran (*Abstract Co-Author*) Nothing to Disclose
Mahtab Rabbani Anari, tehran, Iran (*Abstract Co-Author*) Nothing to Disclose
Sakineh Kadivar, tehran, Iran (*Abstract Co-Author*) Nothing to Disclose

PURPOSE

To assess the impact of ice collar on the blood flow (BF) of the internal (ICA) and external carotid (ECA), facial (FA) and temporalis (TA) arteries

METHOD AND MATERIALS

The Study consists of three separate phases conducted on 10 men and 2 women (mean age of 29.8 ± 3 yrs) (1) Cervical and tympanic temperatures, systolic (SBP), diastolic blood pressure (DBP) and heart rate (HR) were measured at the baseline and every 5 minutes for 25 minutes once with ice collar (-6°C) in place and then after it was removed. (2) Blood flow of ICA, ECA, FA and TA were assessed before applying regular collar (25°C), promptly after removing it and 10 minutes after collar removal using Doppler US. Facial and temporal BF was measured 5 and 15 minutes after applying regular collar as well. (3) Second phase was repeated this time using an ice collar.

RESULTS

Applying ice collar was significantly associated with tympanic and cervical temperatures ($P=0.002$ and <0.0001 , respectively) while it had no significant impact on the HR ($P=0.1$), SBP ($P=0.5$) and DBP ($P=0.3$). Applying regular collar did not significantly affect BF of the internal and external carotid, facial and temporalis arteries ($P=0.9$, 0.1 , 0.5 and 0.06 respectively). Pearson's correlation coefficients for flow assessment of ICA, ECA, FA and TA by Doppler US before collar use and after collar removal were 0.73 , 0.96 , 0.76 and 0.90 respectively ($P=0.01$, <0.001 , 0.02 , <0.0001 respectively). Ice collar use did not alter BF to ICA ($P=0.1$) but significantly decreased BF to ECA, FA and TA ($P=0.0002$, <0.0001 and <0.0001 ; respectively)

CONCLUSION

Obtained test-retest-reliability coefficient indicated that Doppler US is a reliable method for BF assessment of the ICA, ECA, facial and temporalis arteries. Cold application on neck can decrease the BF of the ECA, FA and TA while BF to ICA remains unchanged. This method can potentially be used to control ECA bleeding without compromising brain's blood supply.

CLINICAL RELEVANCE/APPLICATION

We proved the positive impact of ice collar on decreasing BF to cervical arteries, which can serve as an effective, non-invasive method to control the head and neck bleeding.

SSJ18-06 Simultaneous Measurement of in-vivo ADC and T2* in Atherosclerotic Plaque using a 3D Multiple Echo Diffusion Weighted Driven Equilibrium Stack of Stars (3D ME-DW-DE SOS) Sequence

Tuesday, Nov. 29 3:50PM - 4:00PM Room: N226

Participants

Seong-Eun Kim, PhD, Salt Lake City, UT (*Presenter*) Nothing to Disclose
Bradley D. Bolster Jr, PhD, Salt Lake City, UT (*Abstract Co-Author*) Nothing to Disclose
Dennis L. Parker, Salt Lake City, UT (*Abstract Co-Author*) Nothing to Disclose
Gerald S. Treiman, Salt Lake City, UT (*Abstract Co-Author*) Nothing to Disclose
Scott McNally, Salt Lake City, UT (*Abstract Co-Author*) Nothing to Disclose

PURPOSE

The purpose of this work was to develop and evaluate the 3D carotid wall imaging technique for simultaneous measurement of in-vivo ADC and T2* in Atherosclerotic plaque to increase the quantification of high risk plaque components.

METHOD AND MATERIALS

We have developed a motion insensitive high resolution 3D multiple echo diffusion weighted driven equilibrium Stack of Stars (3D ME-DW-DE SOS) sequence that can simultaneously measure ADC and T2* of water proton in a single scan. To test technique feasibility, MRI studies of twelve symptomatic and eight asymptomatic patients with atherosclerosis were performed on a 3T MRI scanner with a home built phased array coils. The parameters were: FOV=152x152 mm², 2 mm slice thickness, TE/TR = 2.05/8.0ms, 32 slices/slab, b =20, 450 s/mm². The resultant in-plane spatial resolution was 0.6x0.6 mm². The total imaging time was 3 min 20 sec. Mean and standard deviation values were computed using all pixels identified by ROI for T2* and ADC. Quantitative statistical comparison of ADC values from symptomatic and asymptomatic groups was conducted using ANOVA.

RESULTS

Symptomatic plaque had significantly lower both of T2* and ADC than asymptomatic plaque (25 ± 7.5 vs. 45 ± 9.8 ms, or 0.74 ± 0.23 vs. 1.29 ± 0.51 x10¹¹.29±0.51x10⁻³mm²/sec, respectively, $p<0.002$). This value is close to the values reported previously.

CONCLUSION

The 3D ME-DW-DE SOS can provide high resolution T2* and ADC values simultaneously, which may provide important clinical information to detect plaque progression.

CLINICAL RELEVANCE/APPLICATION

DWI has the potential to provide information that will allow better discrimination of plaque components such as lipid core. Iron has consistently been found in higher concentrations in plaque compared to vessel tissue. In previous studies, intraplaque T2* distinguished symptomatic from asymptomatic plaques in patients with carotid atherosclerosis. This technique can provide high resolution T2* and ADC values simultaneously, which may provide important clinical information to detect plaque progression.

SSJ19

Neuroradiology (Imaging of Neurotrauma)

Tuesday, Nov. 29 3:00PM - 4:00PM Room: N228



AMA PRA Category 1 Credit™: 1.00
ARRT Category A+ Credit: 1.00

Participants

Pia C. Maly Sundgren, MD, PhD, Ann Arbor, MI (*Moderator*) Nothing to Disclose
Tabassum A. Kennedy, MD, Madison, WI (*Moderator*) Nothing to Disclose

Sub-Events

SSJ19-02 Transport-Based Morphometry of Diffusion Tensor Images for Assessment of Postconcussive Reaction Time

Tuesday, Nov. 29 3:10PM - 3:20PM Room: N228

Participants

Shinjini Kundu, PhD, Pittsburgh, PA (*Presenter*) Nothing to Disclose
Anish Ghodadra, MD, Pittsburgh, PA (*Abstract Co-Author*) Nothing to Disclose
Saeed Fakhran, MD, Pittsburgh, PA (*Abstract Co-Author*) Nothing to Disclose
Lea M. Alhilali, MD, Pittsburgh, PA (*Abstract Co-Author*) Nothing to Disclose
Gustavo Rohde, PhD, Pittsburgh, PA (*Abstract Co-Author*) Nothing to Disclose

PURPOSE

Although cognitive changes are common post-concussion, the structural basis is poorly assessed with traditional image analysis. The goal of this study was to assess structural correlates of reaction time in brains of post-concussive patients. Transport-Based Morphometry is used to statistically model and evaluate dependent image morphology features on MRI, enabling patterns of white matter injury to be visualized.

METHOD AND MATERIALS

Diffusion tensor imaging was performed on 64 patients with mild traumatic brain injury (mTBI). Patients were imaged at a mean 65 ± 124 days after mTBI. Patients underwent neurocognitive testing with the Immediate Post-Concussion Assessment. Transport-Based Morphometry was performed on coregistered fractional anisotropy (FA) maps, resulting in a transport map for each patient characterizing spatial distribution of FA compared to a common reference image. The direction in feature space most correlated with reaction time percentile² is computed, correcting for age as a covariate and significance assessed. The direction is inverted to visualize patterns of white matter injury as radiologically interpretable images.

RESULTS

The direction in feature space most correlated with the reaction time percentile², corrected for age as a covariate had a Pearson correlation coefficient of 0.3940 and p value of 0.0150. The direction in the feature space represents increases in FA of the corpus callosum and decreased FA within the optic radiations, corticospinal tracts and the anterior thalamic radiations. These changes correlated with decreased reaction time percentile. The latter changes are consistent with the visual-spatial interpretation and response selection aspects of reaction time.

CONCLUSION

Transport-Based Morphometry applied to FA maps of post-concussive patients can identify patterns of change in the corpus callosum, visual tracts, corticospinal tracts, and anterior thalamic radiations that correlate with decreasing reaction time percentile.

CLINICAL RELEVANCE/APPLICATION

The knowledge gap between brain structure and clinical outcomes in mTBI can be bridged by Transport-Based Morphometry. Unique patterns of injury can be identified to guide prognosis and treatment.

SSJ19-03 Aberrant Brain Networks Efficiency in Mild Traumatic Brain Injury Patients with Depression Symptom - A Multimodal Study

Tuesday, Nov. 29 3:20PM - 3:30PM Room: N228

Participants

Ping-Hong Yeh, Bethesda, MD (*Presenter*) Nothing to Disclose
John Graner, Bethesda, MD (*Abstract Co-Author*) Nothing to Disclose
Cheng Guan Koay, Bethesda, MD (*Abstract Co-Author*) Nothing to Disclose
Gerard Riedy, Bethesda, MD (*Abstract Co-Author*) Nothing to Disclose
Grant Bonavia, MD, PhD, Bethesda, MD (*Abstract Co-Author*) Nothing to Disclose
John Ollinger, Bethesda, MD (*Abstract Co-Author*) Nothing to Disclose

PURPOSE

Comorbid psychiatric disorders, such as anxiety disorders and major depressive disorders (MDD), are very common among military personnel with traumatic brain injury (TBI). The goal of this study is to identify relationships between brain microstructural changes and network connectivity in military mild TBI (mTBI) patients.

METHOD AND MATERIALS

Participants included 130 male active service members diagnosed with mTBI (age 34.7 ± 7.8 years old) and 53 non-TBI male controls

(age 31.9 ± 8.3 years old) who underwent structural MRI, diffusion weighted imaging (DWI) and resting state fMRI (rsfMRI) exams on a 3T MRI scanner. Depression symptoms were rated based on the Beck Depression Inventory (BDI). Subjects with a BDI score greater than 20 are considered to have moderate to severe depression symptoms, and less than 19 is considered mild or minimal. Global probabilistic tractography was performed to reconstruct major white matter tracts followed by extraction of diffusion tensor imaging metrics (Fig A). Normalized Z-score of correlation coefficients of rsfMRI temporal dynamics were reconstructed for statistical analyses. Probabilistic ICA (FSL MELODIC) was applied to identify the functional networks.

RESULTS

Among 130 mTBI participants, 75 of them were classified as having moderate to severe depression symptoms. The moderate to severe MDD TBI group had lower FA than mild depressed mTBI group over the hippocampal branch of the right cingulum bundle, and both of the temporal and parietal branches of the right superior longitudinal fasciculus. For functional connectivity, the moderate to severe MDD mTBI had decreased connectivity within the anterior default mode network (Fig. B) and executive control network, but increased thalamo-striatal connectivity than the non-TBI and/or mild depressed mTBI, suggesting reduced DMN suppression and increased rumination in symptomatic depressed mTBI (Fig. C).

CONCLUSION

Our results suggest that disrupted neurocircuitry, particularly the cognitive-emotional pathways, e.g. cingulum bundle interconnecting frontal cortex, parietal cortex and limbic system, play an important role in the comorbidity of MDD-TBI spectrum disorders.

CLINICAL RELEVANCE/APPLICATION

Aberrant WM tracts and changed functional connectivity interconnecting the fronto-cingulate-temporal regions and the limbic system suggest poor top-down emotional processing and greater maladaptive rumination in symptomatic depressed mTBI patients.

SSJ19-04 Intracellular Volume Fraction Image on NODDI (Neurite Orientation Dispersion and Density Imaging) in Diffuse Axonal Injury

Tuesday, Nov. 29 3:30PM - 3:40PM Room: N228

Participants

Toshiaki Taoka, MD, PhD, Nagoya, Japan (*Presenter*) Nothing to Disclose
Hisashi Kawai, Nagoya, Japan (*Abstract Co-Author*) Nothing to Disclose
Toshiki Nakane, Nagoya, Japan (*Abstract Co-Author*) Nothing to Disclose
Kazuo Okuchi, Kashihara, Japan (*Abstract Co-Author*) Nothing to Disclose
Kimihiko Kichikawa, MD, Kashihara, Japan (*Abstract Co-Author*) Nothing to Disclose
Shinji Naganawa, MD, Nagoya, Japan (*Abstract Co-Author*) Nothing to Disclose
Toshiteru Miyasaka, MD, Kashihara, Japan (*Abstract Co-Author*) Nothing to Disclose

PURPOSE

NODDI (neurite orientation dispersion and density imaging) is an advanced diffusion imaging technique that provides detailed information on tissue microstructure. Intracellular volume fraction (ICVF) image is one of the products of NODDI, and is a marker of neurite density. In the current study, we evaluated the changes in ICVF image in the cases of diffuse axonal injury (DAI) after high energy traumatic brain damage, and compared the findings with fluid attenuated inversion recovery (FLAIR) and conventional diffusion weighted images (DWI).

METHOD AND MATERIALS

We acquired images for NODDI including ICVF as well as FLAIR and DWI by using a 3T scanner in consecutive 22 cases after 10 to 20 days from high energy traumatic brain injury. In the 17 DAI lesions detected on FLAIR image out of 13 cases, area (mm²) of abnormal signal were measured in ICVF, FLAIR and DWI. Existence of hemorrhage within the lesions were evaluated by susceptibility weighted image (SWI), and lesions with and without hemorrhage were separately evaluated for ICVF/FLAIR area ratio and DWI/FLAIR area ratio.

RESULTS

In the 6 lesions without hemorrhage, areas with abnormal signal were larger on ICVF images compared to FLAIR images in all cases, and mean ICVF/FLAIR area ratio were 2.40 (SD=1.23), while, in the 11 lesions with hemorrhage, mean value was 1.06 (SD=0.79). Mean DWI/FLAIR area ratio was 0.45 (SD=0.34) in the cases without hemorrhage and 0.61 (SD=0.39) in the cases with hemorrhage.

CONCLUSION

In the lesion of DAI without hemorrhage, ICVF images showed larger area of abnormal signal compared to FLAIR images and DWI in all lesions, indicating that ICVF can delineate the pathological changes of DAI with higher sensitivity. On the other hand, for the lesion of DAI with hemorrhage, the ICVF image did not showed larger area of abnormal signal. This difference may be just because of susceptibility effect by hemorrhage, however, potential difference in tissue character between DAI with and without hemorrhage should also be taken into consideration.

CLINICAL RELEVANCE/APPLICATION

ICVF image on NODDI showed high sensitivity in the DAI lesions without hemorrhage. NODDI might help evaluation of the DAI lesions with subtle changes on other images including FLAIR and DWI.

SSJ19-05 The Influence of Cerebral Microbleeds in Working Memory Functional Activation after Mild Traumatic Brain Injury

Tuesday, Nov. 29 3:40PM - 3:50PM Room: N228

Awards

Student Travel Stipend Award

Participants

Yi-Tien Li, MSc, New Taipei, Taiwan (*Presenter*) Nothing to Disclose

PURPOSE

Alterations in working memory (WM) circuitry are observed in several studies after mild traumatic brain injury (mTBI). The presence of cerebral microbleeds were associated poorer memory function has been reported recently. The aim of this study was to evaluate the influence of the presence of cerebral microbleeds in WM functional activation pattern after mTBI.

METHOD AND MATERIALS

Brain activation patterns in response to a WM task (n-back; 0, 1 and 2-back conditions) were assessed with fMRI on a 3T MR system in 52 patients within one month after mTBI and 26 healthy controls. The patients were divided in to two groups: one with cerebral microbleeds (N=26) and one without cerebral microbleeds (N=26) based on the susceptibility weighted angiography (SWAN). The post-concussion syndrome (PCS) score was recorded and digit span test and continuous persistence test were performed in all patients.

RESULTS

The patient with cerebral microbleeds had more activation than controls in bi-frontal and bi-parietal regions (in 2b > 1b condition, p-value < 0.001 cluster36). However, the patients without cerebral microbleeds had less activation than controls. There were no between group difference in PCS score, digit span score and CPT test.

CONCLUSION

Distinct different WM cerebral activation pattern was found in the patient with and without cerebral microbleeds which may affect the memory function after mTBI. WM n-back task may be a more sensitive method to reveal the impact of cerebral microbleeds in the mTBI patients.

CLINICAL RELEVANCE/APPLICATION

Presence of cerebral microbleeds in MTBI patients may represent a more severe brain injury. Cerebral microbleeds in SWAN MRI may be a sensitive indicator of severity of MTBI, especially in CT negative patients.

SSJ19-06 Soccer Heading and Diffusion Tensor Imaging (DTI): The Effects of Subconcussive Head Injury on White Matter Microstructure

Tuesday, Nov. 29 3:50PM - 4:00PM Room: N228

Awards

Student Travel Stipend Award

Participants

Sara B. Rosenbaum, MD, Bronx, NY (*Presenter*) Nothing to Disclose
Roman Fleysheer, PhD, Bronx, NY (*Abstract Co-Author*) Nothing to Disclose
Namhee Kim, PhD, Bronx, NY (*Abstract Co-Author*) Nothing to Disclose
Mark E. Wagshul, PhD, Bronx, NY (*Abstract Co-Author*) Nothing to Disclose
Kyle Friedman, Bronx, NY (*Abstract Co-Author*) Nothing to Disclose
Naomi Wakschlag, Bronx, NY (*Abstract Co-Author*) Nothing to Disclose
Chloe Ifrah, Bronx, NY (*Abstract Co-Author*) Nothing to Disclose
Susan Sotardi, MD, MS, Bronx, NY (*Abstract Co-Author*) Nothing to Disclose
Michael L. Lipton, MD, PhD, Bronx, NY (*Abstract Co-Author*) Nothing to Disclose

PURPOSE

Concussion results in microstructural brain injury, associated with persistent neurobehavioral dysfunction in a significant minority of patients. Though an area of increasing concern, less is known about the potential deleterious effects of repeated subconcussive head impacts. DTI is frequently used in the study of head injury, and low fractional anisotropy (FA) is thought to reflect white matter injury. A previous study of a small group of soccer players (n=37) demonstrated significantly lower FA as a function of heading in three temporal-occipital white matter regions. The purpose of this study was to explore the generalizability of the previously demonstrated relationship between heading and FA in a larger, more demographically heterogeneous sample of adult amateur soccer players.

METHOD AND MATERIALS

This study was conducted with IRB approval and written, informed consent, and was HIPAA compliant. 192 amateur soccer players, ages 18-55, were recruited via print and online advertising and social media. 3T DTI was performed at time of enrollment, and subjects completed a standardized questionnaire assessing one year cumulative heading and heading parameters such as impact, context (practice vs. competition) and player position. Voxelwise analysis was used to identify clusters of voxels demonstrating a significant association between FA and heading (p(individual voxel)<0.01,67 voxel minimum per cluster). Covariates include age, gender, years of education, total years of soccer play, and concussion history.

RESULTS

We identified 11 white matter regions where lower FA was associated with more heading. Locations included frontal, parietal, temporal and occipital white matter and the cingulum and corpus callosum.

CONCLUSION

In this large sample of active adult amateur soccer players, we reproduce and extend previously published findings from a much smaller sample. Similar to the prior study, we identified an association of lower FA in temporo-occipital white matter with more heading over the prior year, an effect not accounted by history of recognized concussion or a number of relevant covariates. Possibly due to our much larger sample, we also identify a similar relationship at multiple additional white matter locations.

CLINICAL RELEVANCE/APPLICATION

These preliminary findings suggest that soccer heading may result in detectable alterations of white matter microstructure, which

are not explained by recognized concussions.

SSJ20

Neuroradiology (Epilepsy and Metabolic Disorders)

Tuesday, Nov. 29 3:00PM - 4:00PM Room: N229



AMA PRA Category 1 Credit™: 1.00
ARRT Category A+ Credit: 1.00

Participants

Tina Y. Poussaint, MD, Boston, MA (*Moderator*) Nothing to Disclose
Andrew P. Klein, MD, Pewaukee, WI (*Moderator*) Nothing to Disclose

Sub-Events

SSJ20-01 Image Processing to Improve Visualization of Mesial Temporal Sclerosis on MRI

Tuesday, Nov. 29 3:00PM - 3:10PM Room: N229

Participants

Matthew S. Parsons, MD, Saint Louis, MO (*Abstract Co-Author*) Nothing to Disclose
Aseem Sharma, MBBS, Saint Louis, MO (*Presenter*) Stockholder, General Electric Company Consultant, BioMedical Systems Co-Founder, Correlative Enhancement, LLC
Rishi Mhapsekar, MD, Saint Louis, MO (*Abstract Co-Author*) Nothing to Disclose
Charles F. Hildebolt, DDS, PhD, Saint Louis, MO (*Abstract Co-Author*) Nothing to Disclose

PURPOSE

Mesial Temporal Sclerosis (MTS) may be difficult to detect on MRI if associated volume loss and signal alteration are minimal. Aim of this study was to test whether an image-processing algorithm can aid in detection of MTS by increasing the contrast between abnormal hippocampus and normal brain.

METHOD AND MATERIALS

We selected coronal FLAIR Images across hippocampi of 18 adult patients (10 females, 8 males; mean age 41.2 years) with proven MTS. One investigator who did not participate in patient selection, image analysis or statistical analysis processed these images in MATLAB using an algorithm (patent pending, Correlative Enhancement LLC) that aimed to selectively increase intensity of abnormal hippocampus. Another investigator recorded signal intensity of hippocampi, gray matter, and white matter for baseline and enhanced images placing equivalent ROIs. Standard deviation in air signal was used as a measure of noise. Using these measurements, we calculate average (Hmean) and maximum (Hmax) contrast-to-noise ratio (CNR) between abnormal hippocampus and white matter. We also calculated CNR for normal extralimbic gray matter (GM). In separate sessions, a neuroradiologist rated signal intensity of hippocampi on baseline and enhanced images on a 5-point scale ranging from 1 (definitely abnormal) to 5 (definitely normal). Differences in Hmean, Hmax, GM, and SI ratings for baseline and enhanced images were assessed for statistical significance.

RESULTS

At baseline, both Hmean (mean 30.0, 95% CI 24.5-35.5) and Hmax (mean 33.5, 95% CI 27.3-39.6) were higher than GM (mean 20.5, 95% CI 15.0 -24.9, $p < 0.0001$). Image processing resulted in significant increase in Hmean (mean 40.4, 95% CI 33.3-47.5; $p < 0.0001$) and Hmax (mean 50.9, 95% CI 41.6 - 60.3; $p < 0.0001$) without affecting GM (mean 20.5, 95% CI 16.3-24.7; $p = 0.9375$). SI ratings showed a more confident identification of abnormality on enhanced images ($p=0.0001$).

CONCLUSION

In an experimental setting, image-processing algorithm resulted in selective improvement in CNR of abnormal hippocampus with associated improved visual conspicuity of hippocampal signal alteration.

CLINICAL RELEVANCE/APPLICATION

It may be feasible to improve MRI detection of MTS using image-processing algorithms that selectively enhance CNR of abnormal hippocampus.

SSJ20-02 Can FreeSurfer Detect Focal Cortical Dysplasia?

Tuesday, Nov. 29 3:10PM - 3:20PM Room: N229

Awards

Student Travel Stipend Award

Participants

Maria M. Serra, MD, Buenos Aires, Argentina (*Presenter*) Nothing to Disclose
Hernan Chaves, MD, Ciudad de Buenos Aires, Argentina (*Abstract Co-Author*) Nothing to Disclose
Pablo M. Pfister, MD, Buenos Aires, Argentina (*Abstract Co-Author*) Nothing to Disclose
Fernando Ventrice Jr, PhD, Capital Federal, Argentina (*Abstract Co-Author*) Nothing to Disclose
Jorge Calvar, PhD, Buenos Aires, Argentina (*Abstract Co-Author*) Nothing to Disclose
Paulina Yanez, MD, Autonomous City of Buenos Aires, Argentina (*Abstract Co-Author*) Nothing to Disclose

PURPOSE

Focal cortical dysplasia (FCD) represents one of the first causes of drug resistant epilepsy in children and adults. These subtle lesions remain a challenging diagnosis. The purpose of this study is to evaluate the findings of automated surface-based analysis software in magnetic resonance images (MRI) of patients with known FCD.

METHOD AND MATERIALS

We retrospectively searched patients with anatomic-pathologic diagnosis of FCD. Patients with isolated hippocampal affection were excluded. 16 patients between 4 and 50 years (y) of age were selected (mean: 19.25y; median 14.5y). Male/female distribution was 8/8. FCD was localized in frontal (10), temporal (4), parietal (1) and occipital (1) lobes. All patients had presurgical MRI in 3.0T scanner (Signa HDxt 3.0T, GE Healthcare) with an 8-channel head coil. MRI were evaluated by an experienced radiologist; FCD was identified in all cases. Cortical reconstruction and volumetric segmentation was performed with Freesurfer image analysis suite v5.3. We visually evaluated color maps of surface based data including cortical thickness (C-T), grey-white matter contrast (G-WM) and sulcal depth (S-D) in the inflated model. Findings in MRI and Freesurfer were compared. Patients were classified according to the number of surface based parameters that showed significant changes in the dysplastic focus when compared to the homologous contralateral region.

RESULTS

In 8 patients (50%) 2 to 3 parameters detected the FCD; in 3 patients (18.75%) 1 parameter, and in 5 patients (31.25%) the FCD was not identified. FCD was identified in C-T maps in 9 patients (56.25%), G-WM contrast maps in 7 patients (43.75%) and S-D maps in 6 patients (37.5%). In 4 of 5 patients where FCD was not identified, cortical surface delimitation errors were recognized.

CONCLUSION

Surface-based software analysis detected FCD in 68.75% of the patients. C-T was the most sensitive parameter. Further research should be done to define if this tool could increase sensitivity and specificity of MRI in the detection FCD. When dysplasia was not detected, this was mostly due to errors in cortical surface delimitation; improvement in software and MRI technology should help to get better results in these cases.

CLINICAL RELEVANCE/APPLICATION

Surface-based software analysis could help radiologist detect and increase confidence in the diagnosis of focal cortical dysplasia which remains a challenging diagnosis.

SSJ20-03 Diagnostic Value of Hybrid [(18) FDG] - PET/MRI in Patients with Epilepsy

Tuesday, Nov. 29 3:20PM - 3:30PM Room: N229

Participants

Cornelius Deuschl, Essen, Germany (*Presenter*) Nothing to Disclose
Theodor Ruber, Bonn, Germany (*Abstract Co-Author*) Nothing to Disclose
Sophia Goericke, Essen, Germany (*Abstract Co-Author*) Nothing to Disclose
Verena Ruhlmann, Essen, Germany (*Abstract Co-Author*) Nothing to Disclose
Thorsten D. Poeppel, Essen, Germany (*Abstract Co-Author*) Nothing to Disclose
Michael Forsting, MD, Essen, Germany (*Abstract Co-Author*) Nothing to Disclose
Christian Elger, Bonn, Germany (*Abstract Co-Author*) Nothing to Disclose
Lale Umutlu, MD, Essen, Germany (*Abstract Co-Author*) Consultant, Bayer AG

PURPOSE

While epilepsy is a rather common disease in developing countries, the etiology of most cases of epilepsy remains unknown despite a thorough diagnostic work-up. Hence, the aim of this was to assess the diagnostic value of simultaneous 18F-FDG PET/MRI (18F-fluorodesoxyglucose positron emission tomography/magnetic resonance imaging) of the brain for patients with drug resistant epilepsy.

METHOD AND MATERIALS

Six patients with drug resistant epilepsy were enrolled in this ongoing prospective study (mean age: 42,6 years, range: 25-65 years, 2 female, 4 male). All patients underwent a simultaneous 18F-FDG PET/MRI of the brain, comprising the following sequences: (1) non-enhanced MPRAGE, (2) 3D FLAIR, (3) STIR cor, (4) T2 ax, (5) SWI. Image analysis was performed by a neuroradiologist and a nuclear medicine specialist during consensus reading with subsequent reading of the (1)MRI, (2)PET and (3) fused PET/MR datasets regarding (a) lesion detection and (b) diagnostic confidence.

RESULTS

All examinations were obtained successfully without any relevant (misregistration) artifacts. Based on morphologic MR readings, 2 out of the 6 patients were found to show subtle swelling of the Corpus amygdaloideum in the right / left hemisphere, respectively (Figure 1). Based on the fused image analysis the diagnostic confidence was rated higher (mean 2.8) when compared to sole morphologic reading (2.4). 4/6 patients did not show any pathologic findings in MRI and / or PET(MRI).

CONCLUSION

Our preliminary study results indicate the added diagnostic value of hybrid [(18) FDG] PET/MRI in improving the diagnostic confidence for detection of epileptogenic lesions.

CLINICAL RELEVANCE/APPLICATION

Simultaneous 18F-FDG PET/MRI may serve as a valuable imaging tool for the diagnostic work-up of drug resistant epilepsy patients.

SSJ20-04 Cortical Venous Disease Severity in MELAS Syndrome Correlates with Brain Lesion Development

Tuesday, Nov. 29 3:30PM - 3:40PM Room: N229

Participants

Matt Whitehead, MD, Washington, DC (*Presenter*) Nothing to Disclose
Michael Wien, MD, Cleveland, OH (*Abstract Co-Author*) Nothing to Disclose
Bonmyong Lee, MD, Baltimore, MD (*Abstract Co-Author*) Nothing to Disclose
Andrea L. Gropman, MD, Washington, DC (*Abstract Co-Author*) Nothing to Disclose

PURPOSE

MELAS syndrome is a mitochondrial disorder typified by recurrent stroke-like episodes and seizures that cause progressive brain injury. Abnormal mitochondria have been found in arterial walls implicating a vasculogenic etiology. However, the pattern of brain injury is not often confined to arterial territories, and is more typical of venous ischemic injury. We have observed abnormal T2 FLAIR signal within and along multiple cerebral cortical veins in MELAS patients. We believe this represents cortical venous wall thickening and sluggish flow. We sought to examine the relationship of T2 FLAIR hyperintense cortical veins, symptoms and brain lesions in patients with MELAS syndrome.

METHOD AND MATERIALS

The imaging database at a single academic hospital was searched for all brain MR exams from patients with MELAS syndrome. Motion artifact, sedated exams, and lack of T2FLAIR sequences were exclusion criteria. Two neuroradiologists counted and categorized T2FLAIR hyperintense cortical veins in consensus. Each exam was assigned a venous score based on number of hyperintense veins (1=fewer than ten, 2=ten-twenty, 3=more than twenty). MELAS and aged-matched normal exams were compared by Mann-Whitney test. $P < 0.05$ was considered significant.

RESULTS

Seventy-three exams from 7 different MELAS patients (15 +/- 4 years) and 30 exams from normal aged-matched patients (15 +/- 3 years) were evaluated and compared. Median venous score between MELAS and control patients significantly differed (3 versus 1; $p < 0.001$). In the MELAS group, venous score correlated with presence (median=3) or absence (median=1) of cumulative focal brain lesions. In all 5 MELAS patients that developed focal brain lesions, venous signal abnormality was present prior to, during, and after lesion onset. Venous score did not correlate with acuity of symptoms.

CONCLUSION

Abnormal venous signal correlates with brain lesion severity in MELAS syndrome. Cortical venous stenosis, congestion, and venous ischemia may be a mechanism of brain injury in MELAS syndrome.

CLINICAL RELEVANCE/APPLICATION

Identification of cortical venous pathology may aid in diagnosis and could be predictive of lesion development and disease severity in patients with MELAS syndrome.

SSJ20-05 Semi-Quantitative Analysis of Dynamic Contrast Enhanced MRI Can Be Used to Diagnosis of Adult-onset Hypopituitarism?

Tuesday, Nov. 29 3:40PM - 3:50PM Room: N229

Participants

Shiyun Tian, MD, Dalian, China (*Presenter*) Nothing to Disclose
Bingbing Gao, Dalian, China (*Abstract Co-Author*) Nothing to Disclose
Yanwei Miao, Dalian, China (*Abstract Co-Author*) Nothing to Disclose

PURPOSE

To analysis the pituitary imaging characteristics of patients with adult-onset hypopituitarism confirmed by clinical diagnosis, who had no significant change in the plain MRI and dynamic contrast enhanced MRI (DCE-MRI). The aim of our study was to evaluate the usefulness of semi-quantitative analysis of the time intensity curve (TIC) by DCE-MRI distinguish adult-onset hypopituitarism from normal pituitary.

METHOD AND MATERIALS

Nineteen patients with adult-onset hypopituitarism and nineteen controls with normal pituitary form and function were analyzed in this retrospective pilot study. The TIC was extracted from DCE-MRI, and semi-quantitative analysis included: maximum intensity (SI_{max}), time to peak (T_{max}), the enhancement rate (E1-7) and peak enhancement rate (PER). The mean values of ten semi-quantitative parameters were compared between hypopituitarism and normal pituitary group. Receiver operating characteristic (ROC) curves were used to evaluate the parameters.

RESULTS

Normal pituitary gland showed a fast upward plat curve, while adult-onset hypopituitarism showed a slow upward curve. The signal values of adult-onset hypopituitarism were lower than normal ones in seven time phases. Compared with normal pituitary, SI_{max}, E3-7 and PER in adult-onset hypopituitarism had statistical difference ($p = 0.035, 0.010, 0.019, 0.010, 0.003, 0.000, 0.010$). The AUC (0.889) of combined features was the best one to identify adult-onset hypopituitarism and normal pituitary, the best diagnostic value was 0.650, the sensitivity was 0.696, and the specificity was 0.955. No significant difference in T_{max}, E1 and E2 were found between the two groups .

CONCLUSION

Semi-quantitative parameters of the time intensity curve (TIC) from DCE-MRI can distinguish adult-onset hypopituitarism from normal pituitary.

CLINICAL RELEVANCE/APPLICATION

DCE-MRI could provide additional information helpful in diagnosis adult-onset hypopituitarism.

SSJ20-06 Brain Iron Measurement in Patients with Liver Cirrhosis using Quantitative Susceptibility Mapping: Relationship with Pallidal T1 Hyperintensity

Tuesday, Nov. 29 3:50PM - 4:00PM Room: N229

Participants

Song Lee, Seoul, Korea, Republic Of (*Presenter*) Nothing to Disclose
Yoonho Nam, Seoul, Korea, Republic Of (*Abstract Co-Author*) Nothing to Disclose
Jinhee Jang, Seoul, Korea, Republic Of (*Abstract Co-Author*) Nothing to Disclose
Gun Hyung Na, Seoul, Korea, Republic Of (*Abstract Co-Author*) Nothing to Disclose

Dong Goo Kim, Seoul, Korea, Republic Of (*Abstract Co-Author*) Nothing to Disclose
Hyun Seok Choi, MD, Seoul, Korea, Republic Of (*Abstract Co-Author*) Nothing to Disclose
So Lyung Jung, Seoul, Korea, Republic Of (*Abstract Co-Author*) Nothing to Disclose
Kookjin Ahn, MD, PhD, Seoul, Korea, Republic Of (*Abstract Co-Author*) Nothing to Disclose
Bum-Soo Kim, MD, PhD, Seoul, Korea, Republic Of (*Abstract Co-Author*) Nothing to Disclose

PURPOSE

To elucidate the relationship between pallidal T1 hyperintensity and iron deposition in deep gray matters in liver cirrhosis patients, using quantitative susceptibility mapping (QSM).

METHOD AND MATERIALS

From 2015 March to 2016 March, we identified 34 consecutive patients who were preparing liver transplantation and performed brain MRI at 3T unit. Brain MRI was done as a part of pre-surgical evaluation. Patient demographics and liver function test results were collected. Patients were divided into two groups according to the presence of pallidal T1 hyperintensity (T1h group and T1n group). QSM was reconstructed using the iLSQR method from (multi-echo) phase images after background phase removal. After susceptibility values were acquired for bilateral caudate nucleus heads (CN), putamina (Put), globus pallidi (GP), thalami (Tha), and dentate nuclei (DN), mean values from each side were calculated for the 5 deep gray matter structures. QSM measures, demographics and laboratory findings were compared between T1h group and T1n group.

RESULTS

Twenty-two patients showed pallidal T1 hyperintensity and 12 did not. Susceptibility of GP of T1h group (121.9 ± 41.4 ppb) was significantly lower than that of T1n group (151.9 ± 32.7 , $P=.038$). Susceptibility of DN of T1h group (86.5 ± 32.1) was significantly lower than that of T1n group (126.9 ± 28.9 , $P=.001$). Susceptibility of CN, Put, and Tha was not significantly different. MELD score was higher in T1h group (13.7, IQR 10.5-19.5) than T1n group (5.9, IQR 4.7-7.6 $P=.029$). In addition, Total iron binding capacity was significantly lower in T1h group ($190.5 \mu\text{g/dL}$, IQR 152.0-261.0) than T1n group (293.5 , IQR 216.0-321.5, $P=.007$). Serum iron was higher in T1h group than T1n group, without statistical significance.

CONCLUSION

Liver cirrhosis patients with T1 pallidal hyperintensity had less iron deposition in GP and DN than those without.

CLINICAL RELEVANCE/APPLICATION

QSM might be used to discover iron metabolism of the brain in liver cirrhosis patients.

SSJ21

Physics (Ultrasound)

Tuesday, Nov. 29 3:00PM - 4:00PM Room: S403A

US PH

AMA PRA Category 1 Credit™: 1.00
ARRT Category A+ Credit: 1.00

FDA Discussions may include off-label uses.

Participants

Zheng Feng Lu, PhD, Chicago, IL (*Moderator*) Nothing to Disclose
R. Jason Stafford, PhD, Houston, TX (*Moderator*) Nothing to Disclose

Sub-Events

SSJ21-01 **Monitoring Neoadjuvant Chemotherapy Response of Breast Cancer using 4D Subharmonic Aided Pressure Estimation and Imaging with Ultrasound Contrast Agents**

Tuesday, Nov. 29 3:00PM - 3:10PM Room: S403A

Participants

Kibo Nam, PhD, Philadelphia, PA (*Abstract Co-Author*) Nothing to Disclose
Maria Stanczak, MS, Philadelphia, PA (*Abstract Co-Author*) Nothing to Disclose
Anush Sridharan, Philadelphia, PA (*Abstract Co-Author*) Nothing to Disclose
Adam Berger, MD, Philadelphia, PA (*Abstract Co-Author*) Nothing to Disclose
Tiffany Avery, Philadelphia, PA (*Abstract Co-Author*) Nothing to Disclose
John R. Eisenbrey, PhD, Philadelphia, PA (*Abstract Co-Author*) Support, General Electric Company; Support, Lantheus Medical Imaging, Inc
Flemming Forsberg, PhD, Philadelphia, PA (*Presenter*) Equipment support, Toshiba Corporation; Research Grant, Toshiba Corporation; Equipment support, Siemens AG; In-kind support, General Electric Company; In-kind support, Lantheus Medical Imaging, Inc

PURPOSE

To determine if 4D subharmonic aided pressure estimation (SHAPE) and imaging (SHI) can predict the response of breast cancer to neoadjuvant chemotherapy based on changes in interstitial fluid pressures and breast tumor vascularity.

METHOD AND MATERIALS

Seventeen patients scheduled for neoadjuvant therapy of a localized breast cancer underwent 4 ultrasound exams: immediately prior to therapy, at 10%, 60%, and 100% completion of chemotherapy. The exams were performed using a modified Logiq 9 scanner with a 4D10L probe (GE Healthcare, Milwaukee, WI). Modified software enabled RF data collection from 4D subharmonic imaging (transmitting pulses at 5.8 MHz and receiving at 2.9 MHz) before and during infusion of the contrast agent Definity (Lantheus Medical Imaging, N Billerica, MA) at acoustic settings optimized for SHAPE and SHI separately. The maximum subharmonic frequency magnitude and mean subharmonic intensity were calculated from the RF data of SHAPE and SHI, respectively, for all 4 exams. The relative signal differences in the tumor relatively to the surrounding area were then compared according to the final tumor treatment response.

RESULTS

Four patients left the study and 2 patients' data were discarded due to technical problems. Patients' clinical outcomes consisted of 6 complete responders (final tumor size < 10% of the original) and 5 partial/non responders. The results from 10% completion of the therapy showed the subharmonic signal increased more in the tumor than in the surrounding area for complete responders compared to partial/non responders (3.23 ± 1.41 dB vs. -0.88 ± 1.46 dB; $p = 0.001$ from SHAPE and 1.32 ± 0.73 dB vs. -0.82 ± 0.88 dB; $p = 0.002$ from SHI). Also the relative subharmonic signal in the tumor increased for complete responders, but decreased for partial/non responders after 10% completion of the therapy relatively to that before the therapy. Moreover, 3 patients whose tumor size increased after 10% completion of the therapy were predicted by SHAPE and SHI to be complete responders.

CONCLUSION

4D SHAPE and SHI have the potential to predict neoadjuvant chemotherapy response of breast cancer as early as at 10% completion of the therapy; albeit based on a small sample size.

CLINICAL RELEVANCE/APPLICATION

It may be possible to predict neoadjuvant chemotherapy treatment response of breast cancers prior to changes in tumor size using contrast-enhanced SHI or SHAPE.

SSJ21-02 **Shear Wave Speed Measurement with Point Shear-Wave Elastography and MR Elastography: A Phantom Study Compared with Rheometer Measurement**

Tuesday, Nov. 29 3:10PM - 3:20PM Room: S403A

Participants

Riwa Kishimoto, MD, PhD, Chiba, Japan (*Presenter*) Nothing to Disclose
Mikio Suga, PhD, Chiba, Japan (*Abstract Co-Author*) Nothing to Disclose
Tokuhiko Omatsu, MD, PhD, Chiba-Shi, Japan (*Abstract Co-Author*) Nothing to Disclose
Yasuhiko Tachibana, MD, PhD, Chiba, Japan (*Abstract Co-Author*) Nothing to Disclose
Daniel K. Ebner, Chiba, Japan (*Abstract Co-Author*) Nothing to Disclose
Takayuki Obata, MD, PhD, Chiba, Japan (*Abstract Co-Author*) Nothing to Disclose

PURPOSE

To compare shear-wave speed (SWS) measured by US-based point shear-wave elastography (pSWE) using acoustic radiation force impulse (ARFI) technology and magnetic resonance elastography (MRE) on phantoms with known shear modulus, and to assess the method validity and variability.

METHOD AND MATERIALS

Five homogeneous phantoms of different stiffness were made for this study. Their shear modulus was physically measured by rheometer, and this value used as standard. Ten SWS measurements were obtained with 1.0 – 4.5 MHz convex (4C1) and 4.0 – 9.0 MHz linear (9L4) transducers using pSWE, at four different depths each (2, 4, 6, 8cm for 4C1 transducer and 1, 2, 3, 4 cm for 9L4). Spin-echo echo planar imaging (SE-EPI) MRE was carried out once per phantom, and SWS at five different depths (2, 3, 4, 5, 6 cm) was obtained. These SWS were then compared with those obtained by rheometer using linear regression analyses. Repeatability of the 10-repeat pSWE measurement was assessed with single-measure intraclass correlation coefficient (ICC).

RESULTS

From rheometer measurement, the SWS of each phantom was 1.41, 2.23, 3.01, 3.56, and 4.86 m/s. In pSWE, measurement error occurred more than 50% at a depth of 1 cm with the 9L4 and at 2 cm with the 4C1 transducer. Therefore, the data at these depths were abandoned. SWS' obtained with both pSWE as well as MRE had strong correlation with these obtained using a rheometer ($R^2 > 0.97$). ICC of SWS measurement with pSWE was more than 0.93 for all measurements with the 9L4 and 4C1 transducers. The relative difference in SWS between those procedures was from -25.2% to 25.6% for all phantoms, and from -8.1 to 6.9% when the softest and hardest phantoms were excluded. Depth-dependent bias was found in the 9L4 transducer of pSWE and MRE.

CONCLUSION

SWS' from pSWE and MRE showed a strong correlation with rheometer-determined SWS. Although based on phantom studies SWS' obtained with these methods are not always equivalent, the measurement can be thought of as reliable and these SWS' were reasonably close to each other for the middle range of stiffness within the measurable range.

CLINICAL RELEVANCE/APPLICATION

pSWE and MRE gave similar SWS for the middle range of stiffness within the measurable range, on the other hand, SWS' obtained with these modalities were not equivalent for the extremes of the total measurement range.

SSJ21-03 Improved Measurement of Portal Pressures Using Subharmonic Contrast Imaging and Pulse Shaping

Tuesday, Nov. 29 3:20PM - 3:30PM Room: S403A

Participants

Ipshita Gupta, MS, Philadelphia, PA (*Abstract Co-Author*) Nothing to Disclose

Flemming Forsberg, PhD, Philadelphia, PA (*Presenter*) Equipment support, Toshiba Corporation; Research Grant, Toshiba Corporation; Equipment support, Siemens AG; In-kind support, General Electric Company; In-kind support, Lantheus Medical Imaging, Inc

Maria Stanczak, MS, Philadelphia, PA (*Abstract Co-Author*) Nothing to Disclose

Anush Sridharan, Philadelphia, PA (*Abstract Co-Author*) Nothing to Disclose

Jaydev K. Dave, PhD, MS, Philadelphia, PA (*Abstract Co-Author*) Nothing to Disclose

Ji-Bin Liu, MD, Philadelphia, PA (*Abstract Co-Author*) Nothing to Disclose

Christopher Hazard, PhD, Oak Brook, IL (*Abstract Co-Author*) Employee, General Electric Company

Colette Shaw, MBBCh, Philadelphia, PA (*Abstract Co-Author*) Nothing to Disclose

Susan Shamimi-Noori, MD, Philadelphia, PA (*Abstract Co-Author*) Nothing to Disclose

Jonathan Fenkel, Philadelphia, PA (*Abstract Co-Author*) Consultant, Gilead Sciences, Inc Consultant, Johnson & Johnson Consultant, Bristol-Myers Squibb Company

Michael C. Soulen, MD, Philadelphia, PA (*Abstract Co-Author*) Royalties, Cambridge University Press; Consultant, Guerbet SA; Research support, Guerbet SA; Consultant, BTG International Ltd; Research support, BTG International Ltd; Consultant, Merit Medical Systems, Inc; Speaker, Sirtex Medical Ltd; Consultant, Terumo Corporation; Consultant, Bayer AG

Chandra Sehgal, PhD, Philadelphia, PA (*Abstract Co-Author*) Nothing to Disclose

Kirk Wallace, PhD, Niskayuna, NY (*Abstract Co-Author*) Employee, General Electric Company

John R. Eisenbrey, PhD, Philadelphia, PA (*Abstract Co-Author*) Support, General Electric Company; Support, Lantheus Medical Imaging, Inc

PURPOSE

To analyze the effect of pulse shape on the sensitivity of subharmonic aided pressure estimation (SHAPE) *in vitro* and *in vivo*, and using SHAPE to estimate portal pressures in patients undergoing a transjugular liver biopsy compared to the hepatic venous pressure gradient (HVPG).

METHOD AND MATERIALS

A Logiq 9 ultrasound scanner with a 4C curvi-linear probe (GE, Milwaukee, WI) was used to acquire radio frequency data. The SHAPE mode was set to transmit 4 cycle pulses at 2.5 MHz and receive subharmonic signals at 1.25 MHz. The contrast agent Sonazoid (GE, Oslo, Norway) was infused at a rate of 0.024 $\mu\text{L}/\text{kg}/\text{min}$. Eight different pulse waveforms (3 narrowband and 5 broadband) were implemented and tested *in vitro* and *in vivo* in 3 canines. Sensitivity of the pulses for SHAPE was based on the decrease in the subharmonic signal amplitude with increasing ambient pressure and correlation coefficients. Next, 43 transjugular liver biopsy subjects were enrolled as part of an ongoing IRB approved protocol. Post biopsy, patients received an infusion of Sonazoid. An ROI within the portal vein was selected and an automated power control algorithm was initiated to determine the optimal acoustic output power for maximum SHAPE sensitivity. Cine loops were collected in triplicate, averaged and compared to the HVPG.

RESULTS

A linear decrease in subharmonic amplitude with increased pressure was observed for all waveforms (r from -0.77 to -0.93; $p < 0.001$) *in vitro*. Data from 1 of the 3 canines was eliminated for technical reasons, while the other 2 produced similar results to

those obtained *in vitro* (r from -0.72 to -0.98; $p < 0.01$). Overall, the broadband pulses performed better ($p < 0.05$). Within the broadband group, the Gaussian windowed binomial filtered square wave was the most sensitive. The linear relationship between the SHAPE gradient (obtained with the new pulse) and HVPG over the patient dataset showed a good correlation ($r = 0.72$).

CONCLUSION

Pulse shaping can greatly improve the sensitivity of SHAPE. A Gaussian windowed binomial filtered square wave gives the highest correlation between changes in subharmonic amplitude of the microbubbles and ambient pressure changes. Results in patients indicate SHAPE may be useful for estimation of portal pressures.

CLINICAL RELEVANCE/APPLICATION

It may be possible to noninvasively quantify portal vein pressures and accurately diagnose portal hypertension using SHAPE.

SSJ21-04 A Novel Wearable Fluorescence Surgical Navigation System for Segmentectomy

Tuesday, Nov. 29 3:30PM - 3:40PM Room: S403A

Participants

Kunshan He, Beijing, China (*Abstract Co-Author*) Nothing to Disclose
Chongwei Chi, Beijing, China (*Abstract Co-Author*) Nothing to Disclose
Yamin Mao, Beijing, China (*Abstract Co-Author*) Nothing to Disclose
Jie Tian, PhD, Beijing, China (*Abstract Co-Author*) Nothing to Disclose
Kun Wang, Beijing, China (*Presenter*) Nothing to Disclose

PURPOSE

Recently, segmentectomy has become a secure and effective treatment for certain small, early-stage lung cancer, especially in patients with emphysema. To achieve complete segmentectomy, it is critical to precisely identify adjacent lung segments, which is difficult for surgeons without suitable interventions. Thus, a novel technique by transbronchial or intravenous injection of indocyanine green (ICG) has been developed, which can efficiently avert needless resection, lower the costs and reduce complications. However, lack of intraoperative fluorescence imaging systems has seriously impeded the further development of this method. So, we developed a novel wireless wearable fluorescence surgical navigation system (WFNS).

METHOD AND MATERIALS

WFNS is composed of a laptop, Google glass, light source and handle, which consists of a filter, C mount lens and CCD camera. Firstly, NIR light excited by the light source transmitted through the filter, illuminated the target and then was collected by the NIR camera installed in the handle. An application was written to capture real-time images. Finally, the result was displayed simultaneously on the Google glass in real-time mode at video-rate capacity of 20 frames per second, which was achieved by synchronizing the Google glass with the laptop.

RESULTS

Twelve swine were equally divided into two groups. Group A was injected with 0.2mg/kg ICG into the marginal ear vein and Group B was injected with 0.6mg/kg ICG. Five seconds later after injection, the black-and-white transition borders among the targeted segment and the non-targeted segments were easily recognized visually in all swine. Real-time videos were displayed on the prism screen of the Google glass during the surgery. Using ImageJ (Image Processing and Analysis Application in Java), the corresponding SBR of the two groups (Group A and Group B) were 9.00 ± 0.70 and 8.96 ± 1.23 respectively. The NIR fluorescent images of Group A lasted ten minutes and those of Group B lasted up to fourteen minutes until the SBR was 1. Besides, the surgical field was 200 mm x 200 mm.

CONCLUSION

This study demonstrates our system has major advantages in identifying intersegmental planes and potentials in determining the margin of tumors.

CLINICAL RELEVANCE/APPLICATION

(dealing with segmentectomy)"A novel wearable fluorescence surgical navigation system can be used to conduct segmentectomy for certain small, early-stage lung cancer, especially in patients with emphysema."

SSJ21-05 Clinical Evaluation of Real-Time Optical Tracking to Provide Feedback During Blinded Contrast-Enhanced Ultrasound Imaging

Tuesday, Nov. 29 3:40PM - 3:50PM Room: S403A

Participants

Ahmed El Kaffas, PhD, Palo Alto, CA (*Presenter*) Co-founder, Oncoustics
Renhui Gong, Palo Alto, CA (*Abstract Co-Author*) Nothing to Disclose
Rosa Maria Silveira Sigrist, MD, Palo Alto, CA (*Abstract Co-Author*) Nothing to Disclose
Juergen K. Willmann, MD, Stanford, CA (*Abstract Co-Author*) Research Consultant, Bracco Group; Research Grant, Siemens AG; Research Grant, Bracco Group; Research Grant, Koninklijke Philips NV; Research Grant, General Electric Company; Advisory Board, Lantheus Medical Imaging, Inc; Advisory Board, Bracco Group
Dimitre Hristov, PhD, Stanford, CA (*Abstract Co-Author*) Research Grant, Koninklijke Philips NV Partner, SoniTrack Systems, Inc

CONCLUSION

To the best of our knowledge, this study is the first to demonstrate the feasibility of tracking for 3D DCE-US to provide feedback during lengthy scan sessions.

Background

Current commercial matrix transducers for 3D Dynamic Contrast-Enhanced Ultrasound (3D DCE-US) do not display side-by-side B-mode and contrast-mode images, thus leaving the operator with no position feedback during lengthy acquisitions. The purpose of this study was to demonstrate the feasibility of using tracking to provide positioning feedback and to assess resulting improvements

in maintaining imaging position.

Evaluation

A tracking system was developed in house using infrared camera (Polaris, NDI, Canada) and a 3D-printed tracking target attached to a X6-1 matrix transducer. Cameras were connected to a PC, enabling real-time streaming of transducer coordinates and display of virtual probe on a separate screen. The tracking system captures a reference position to provide operators positioning feedback when no B-mode image is available. To test this set-up, five experienced operators were asked to locate an image landmark within a healthy volunteer liver in B-mode images using the X6-1 connected to an EPIQ7 system (Philips, Bothell, WA). Operators were then asked to maintain the transducer position for 4 min under three feedback methods: i) B-mode, ii) display of real-time virtual transducer, iii) blind. The magnitude of displacement of a voxel over the cine was computed relative to the reference position as an estimate of the imaging position error.

Discussion

Results suggest that tracking can assist operators maintain a position during a lengthy acquisition. An average displacement of 3.75 mm with standard deviation (S.D.) of 3.31 mm and displacement histogram skewness of -0.18 was noted when using B-mode feedback. When blinded, an average displacement of 4.58 mm (S.D. 2.65 mm; skewness 6.19) was noted. In contrast, the average displacement for tracking-feedback was comparable to that from B-mode at 3.48 mm (S.D. 0.8 mm; skewness 0.09). One operator performed better with tracking than B-mode; one operator performed better blinded than with tracking and B-Mode.

SSJ21-06 An Experimental Study for the Evaluation of the Photoacoustic Effect of Pectin-melanin Admixture in the Subcutaneous Muscle Layer and Liver of Rat as a Long-retaining Inoculating Photoacoustic Contrast Agent

Tuesday, Nov. 29 3:50PM - 4:00PM Room: S403A

Participants

Won Jae Lee, MD, Seoul, Korea, Republic Of (*Presenter*) Research Grant, Samsung Electronics Co, Ltd
Hyo Keun Lim, MD, Seoul, Korea, Republic Of (*Abstract Co-Author*) Nothing to Disclose

PURPOSE

To evaluate the feasibility of biocompatible pectin-melanin admixture to be used as a long-retaining, inoculating photoacoustic (PA) contrast agent by comparing the sustainability for the PA effect of melanin alone and pectin-melanin admixture in the subcutaneous muscle layer and liver of rat.

METHOD AND MATERIALS

Two types of biocompatible PA contrast agents, i.e., the 'melanin alone' (3% melanin) and 'pectin-melanin admixture' (2% pectin and 3% melanin) were inoculated into two organs, i.e., the subcutaneous muscle (hypovascular) and liver (hypervascular) of 40 rats so that each contrast agent was inoculated into ten of each organ. PA imaging was obtained every week after the contrast inoculation for four weeks, and analyzed qualitatively (the presence of PA signal) and quantitatively (the measurement of relative PA signal intensity). PA imaging was performed with a L5-13 linear array transducer (Accuvix A30, Samsung Medison, Seoul, Korea) combined with a Nd:YAG laser (Phocusmobile, Optek, USA).

RESULTS

Both 'melanin alone' and 'pectin-melanin admixture' groups showed persistent PA signals during four weeks when inoculated into the subcutaneous layer, while only 'pectin-melanin admixture' group showed persistent PA signals during four weeks when inoculated into the liver.

CONCLUSION

The biocompatible 'pectin-melanin admixture' can be used as a long-retaining, inoculating PA contrast agent, regardless of the organ vascularity.

CLINICAL RELEVANCE/APPLICATION

If this biocompatible PA contrast agent becomes available clinically, PA imaging combined with this contrast agent can be used for pre- or intra-operative localization of various cancers such as breast cancer and liver metastasis after chemotherapy.

SSJ22

Physics (Nuclear Medicine, SPECT and PET)

Tuesday, Nov. 29 3:00PM - 4:00PM Room: S403B

NM PH

AMA PRA Category 1 Credit™: 1.00
ARRT Category A+ Credit: 1.00

Participants

Paul E. Kinahan, PhD, Seattle, WA (*Moderator*) Research Grant, General Electric Company; Co-founder, PET/X LLC
Chien-Min Kao, PhD, Chicago, IL (*Moderator*) Stockholder, Walgreens Boots Alliance, Inc

Sub-Events

SSJ22-01 Coincidence Imaging of In-111: A Monte Carlo Simulation

Tuesday, Nov. 29 3:00PM - 3:10PM Room: S403B

Participants

Raymond B. Pahlka, PhD, Houston, TX (*Presenter*) Nothing to Disclose
Srinivas C. Kappadath, PhD, Houston, TX (*Abstract Co-Author*) Research Grant, General Electric Company
Osama R. Mawlawi, PhD, Houston, TX (*Abstract Co-Author*) Research Grant, General Electric Company; Research Grant, Siemens AG

CONCLUSION

This work demonstrates that coincident imaging of In-111 using a clinical gamma camera is possible. Further work to determine optimal clinical applications and conducting measurements on a physical scanner is ongoing.

Background

The decay of In-111 results in a gamma-ray cascade of two photons. Because the gamma-rays are emitted in succession, we consider the concept of employing the gamma-ray coincidence to provide additional information about the decay and its environment. Gamma cameras operated in coincidence mode have been used successfully to image PET tracers, however the concept of producing images from gamma cameras using cascaded gamma-rays in coincidence from In-111 has not been previously explored. Coincidence images can provide three-dimensional (3D) information in planar gamma camera studies, and can complement information obtained in tomographic acquisitions. This work provides the foundation for exploring coincidence imaging with In-111 by producing some simple images and evaluating some important basic considerations including the source activity and timing window resolution, for future studies.

Evaluation

GEANT4 was used to model a gamma camera and to simulate the decay of the In-111 nucleus. A point source of In-111 was simulated to evaluate the true coincidence efficiency. We use a simple reconstruction algorithm to produce images when the detector heads are positioned at 90°. The decay vertex is computed by projecting a ray from each interaction point, normal to each detector face, then finding the point of minimum separation. To test the algorithm, images are produced from reconstructed coincident events from point sources positioned at the camera isocenter at several source-to-detector distances. To determine the optimal timing window and activity concentration, we compute the noise equivalent count rate as a function of timing window resolution for different activities.

Discussion

We found the coincidence detection efficiency to be around 5 events/mCi-s, independent of source-to-detector distance. We found that point source activities ranging from 10 uCi to 5 mCi could be imaged with spatial resolutions of ~1 cm. Optimal time window resolutions ranged between 200 and 500 ns.

SSJ22-02 Initial Evaluation of a Novel General Purpose CZT based Digital SPECT Camera: Significant Improvement of Resolution and Contrast Compared to Standard Analog SPECT

Tuesday, Nov. 29 3:10PM - 3:20PM Room: S403B

Participants

Simona Ben-Haim, MD, DSc, Ramat Gan, Israel (*Presenter*) Consultant, Spectrum Dynamics Ltd; Consultant, Molecular Dynamics; Spouse, Stockholder, Molecular Dynamics
Elinor Goshen, MD, Ramat Gan, Israel (*Abstract Co-Author*) Nothing to Disclose
Ronen Goldkorn, MD, Ramat Gan, Israel (*Abstract Co-Author*) Research support, Molecular Dynamics
Leonid Beilin, PhD, Caesarea, Israel (*Abstract Co-Author*) Employee, Molecular Dynamics Ltd

PURPOSE

We have assessed the performance of a novel digital SPECT camera with multiple pixelated cadmium zinc telluride (CZT) detectors and high sensitivity collimators (Digital SPECT; Valiance X12 prototype, Molecular Dynamics). The system's architecture enables gantry rotation, as well as radial and swivel detector motion, providing multiple degrees of freedom for the scanning pattern. These features are used to minimize the patient-detector distance, providing patient-tailored imaging.

METHOD AND MATERIALS

Images of Tc-99m filled Jaszczak phantom with cold rod and solid sphere inserts (rod diameter 4.8-12.7 mm, spheres 9.5-31.8 mm) were compared to images acquired on a standard NaI based analog (Anger) SPECT system with high resolution collimators (Discovery NM/CT 670, GE). All images (analog and digital SPECT) were iteratively reconstructed and evaluated visually for resolution. Contrast was calculated using standard methodology.

RESULTS

Digital SPECT demonstrated cold rods in reconstructed transaxial slices of 5 segments with rod diameters of 12.7, 11.1, 9.5, 7.9, 6.4 mm, and in five external rows in the sixth segment (diameter 4.8 mm). Analog SPECT demonstrated rods in 4 segments and in part of the 5th (down to 6.4mm). Spheres were resolved on digital SPECT with contrast of 92.9%, 87.8%, 82.7%, 68.2%, 66.3% and 51.7% (for sphere diameters measuring 31.8, 25.4, 19.1, 15.9, 12.7 and 9.5 mm, respectively). These results are a significant improvement compared to analog SPECT, with 63.5%, 52.8%, 44.4%, 39.3%, 26.4%, and 18.6% for the same spheres respectively. See figure: Transaxial slices of Jaszczak phantom cold rods section: Left - Valiance X12 prototype; Right - NaI based analog SPECT system.

CONCLUSION

Contrast and resolution of digital SPECT consistently surpassed standard analog SPECT performance in the phantom studies reported.

CLINICAL RELEVANCE/APPLICATION

The superior image quality will likely prove useful in clinical settings.

SSJ22-03 Best in Class Time of Flight PET Performance - What is the Clinical Benefit?

Tuesday, Nov. 29 3:20PM - 3:30PM Room: S403B

Participants

Jun Zhang, PhD, Columbus, OH (*Presenter*) Nothing to Disclose
Ajay Siva, Columbus, OH (*Abstract Co-Author*) Nothing to Disclose
Prayna Bhatia, BS, Columbus, OH (*Abstract Co-Author*) Nothing to Disclose
Katherine Binzel, PhD, Columbus, OH (*Abstract Co-Author*) Nothing to Disclose
Chadwick L. Wright, MD, PhD, Lewis Center, OH (*Abstract Co-Author*) Nothing to Disclose
Michael V. Knopp, MD, PhD, Columbus, OH (*Abstract Co-Author*) Nothing to Disclose
Chuanyong Bai, Cleveland, OH (*Abstract Co-Author*) Employee, Koninklijke Philips NV;

PURPOSE

As the benefits of time-of-flight (TOF) in PET has been increasing recognized, we wanted to assess if there are clinical benefits by using best in class TOF timing resolution, which is enabled by next generation, solid state digital photon counting PET detectors.

METHOD AND MATERIALS

30 patients receiving a whole body oncologic FDG PET participated in an intra-individual comparison study to detect and assess potential differences due to different timing resolution of TOF. Patients were sequentially imaged using a 325 ps TOF next generation digital dPET (Vereos) and a conventional 550 ps TOF cPET (Gemini). A dose of 13mCi FDG and 90s/bed were used. Listmode data sets were reconstructed with and without TOF using optimized 3D OSEM algorithms. ROI's of liver background and lesions were placed with SUV and SNR compared between all data sets. Blinded image reviews were performed comparing the 4 image data sets. Additionally, phantoms with hot spheres and cold rods of varying sizes were acquired and assessed.

RESULTS

109 assessable lesions were identified and analyzed. The 325ps TOF dPET images were ranked best in all categories with best signal-to-noise, contrast, recovery coefficient, visual quality and lesion delineation. Comparing the two generation systems, 325ps TOF dPET presented SNR of $\sim 2x$ vs non TOF, 550ps TOF cPET a SNR of $\sim 1.6x$ vs non TOF. On SUV analysis, 325ps presented with $20\% \pm 27\%$ higher SUV vs non TOF, 550ps with $15\% \pm 18\%$ vs non TOF. No significant SUV differences in the liver background ROI were found ($p > 0.05$). 10% of the lesions confidentially classifiable on 325ps TOF were not assessable on 550 ps TOF, while 25% were non assessable on non-TOF.

CONCLUSION

325ps TOF PET was found to consistently present with the best performance in all categories, especially SNR. The clinical benefit appears to come from the more precise localization of metabolic activity which translates to higher SUV peak value, sharper lesion delineation and overall better visualization with an improved lesion detection of 10% compared to current generation TOF timing resolution.

CLINICAL RELEVANCE/APPLICATION

SNR, lesion uptake and visual quality all benefit from improved timing resolution with the more precise event localization that appears to be able to improve clinically relevant lesion detectability.

SSJ22-04 System Physics Characteristics and Stability of Next Generation Digital Photon Counting PET

Tuesday, Nov. 29 3:30PM - 3:40PM Room: S403B

Participants

Jun Zhang, PhD, Columbus, OH (*Presenter*) Nothing to Disclose
Michael Miller, Highland Heights, OH (*Abstract Co-Author*) Nothing to Disclose
Katherine Binzel, PhD, Columbus, OH (*Abstract Co-Author*) Nothing to Disclose
Michael V. Knopp, MD, PhD, Columbus, OH (*Abstract Co-Author*) Nothing to Disclose

PURPOSE

To measure and assess the system physics characteristics and stability of a next generation solid state, digital PET and its potential to advance clinical PET.

METHOD AND MATERIALS

Physical characteristics of timing resolution and energy resolution as well as NEMA 2012 based spatial resolution, sensitivity, count loss and image quality of the next generation digital photon counting (DPC) PET/CT system (Vereos) was performed. System stability in timing and energy were monitored over a year, and complete NEMA testing was done at the beginning and the end of the 1-yr window since system installation. CQIE PET uniformity was measured in a quarterly manner. The observed system

characteristics were compared to current technology systems and its potentials impact for clinical oncologic PET imaging assessed.

RESULTS

The DPC PET/CT system demonstrated robust system physics characteristics with <2% variability in timing resolution, $\pm 0.4\%$ change in energy resolution, <2% change in spatial resolution, <10% variations in detector temperature and humidity as well as <5% change of SUV/uniformity profile through a > one year monitoring period. NEMA 2012 testing found a spatial resolution (in mm FWHM) from 4.10 / 3.96 at 1 cm to 5.79 / 6.20 at 20 cm in the transverse and axial plane. 325 ps timing resolution and 11.1 % energy resolution were consistently obtained. We measured a 5.7 kcps/MBq system sensitivity and 24.1 kcps/MBq effective sensitivity with TOF gain. For count loss testing, ~ 171 kcps peak NECR and > 680 kcps peak true rate were obtained at 50 kBq/mL, and the scatter fraction is about 30%. NEMA IQ demonstrated hot sphere contrast ranging from $\sim 62\% \pm 2\%$ (10 mm) to $\sim 88\% \pm 2\%$ (22 mm), cold sphere contrasts of $\sim 86\% \pm 2\%$ (28 mm) and $\sim 89\% \pm 3\%$ (37 mm) and excellent image uniformity. These characteristics led to excellent image quality of clinical oncologic PET imaging.

CONCLUSION

The system physics performance characteristics were found to be robust over an one year period and of excellent specifications, overall considerably more preferential than current conventional benchmark systems.

CLINICAL RELEVANCE/APPLICATION

The next generation solid state, high TOF temporal resolution PET technology is robust and with excellent imaging physics characteristics promising substantial improvements for clinical PET imaging.

SSJ22-05 Are Camera Measurements Alone Sufficient in Determining I-131 Thyroid Cancer Therapy Maximum Permissible Blood Dose?

Tuesday, Nov. 29 3:40PM - 3:50PM Room: S403B

Participants

Kenneth Nichols, PhD, New Hyde Park, NY (*Presenter*) Royalties, Syntermed, Inc;
Fitzgerald Leveque, New Hyde Park, NY (*Abstract Co-Author*) Nothing to Disclose
Miyuki Yoshida-Hay, BS, New Hyde Park, NY (*Abstract Co-Author*) Nothing to Disclose
William Robeson, MSC, New Hyde Park, NY (*Abstract Co-Author*) Nothing to Disclose
Christopher J. Palestro, MD, New Hyde Park, NY (*Abstract Co-Author*) Nothing to Disclose

PURPOSE

Our study was undertaken to determine the validity of recent suggestions that I-131 thyroid cancer therapy dose to blood can be estimated by camera measurements alone (Health Phys 2015;108:53-58eHH), rather than the conventional approach of combining camera count measurements with blood assays (Am J Roentgenol Radium Ther Nucl Med 1962;87:171-182).

METHOD AND MATERIALS

Data were examined retrospectively for 74 pts undergoing I-131 therapy for thyroid cancer ablation, divided into first & second half groups of 37 pts each (Groups 1&2). Following the conventional approach, anterior & posterior pt counts were obtained by an uncollimated gamma camera, & blood withdrawn & assayed in vitro by a well counter 1, 4, 24, 48, 72-96, & 96-144 hrs after ingestion of I-131 to compute the whole body γ & in vivo β dose contributions to blood. Linear regression for Group1 established predictions of total blood dose by in vitro-only and by camera-only measurements. Predictions were compared to conventional total blood dose for Group1, Group2 & for all pts by the paired t-test and by Pearson correlation.

RESULTS

Mean doses were similar for total blood dose by conventional, in vitro-only & camera-only methods ($p > 0.40$) for Group1 (0.75 ± 0.50 , 0.76 ± 0.50 & 0.74 ± 0.47 rad/mCi, respectively), Group2 (0.77 ± 0.56 , 0.76 ± 0.54 & 0.80 ± 0.55 rad/mCi, respectively), & all pts (0.76 ± 0.52 , 0.77 ± 0.51 & 0.76 ± 0.51 rad/mCi, respectively). However, correlation was significantly stronger between conventional & in vitro-only than between conventional & camera-only estimates for Group1 ($r = 0.98$ versus $r = 0.94$, $p = 0.02$), Group2 ($r = 0.98$ versus $r = 0.94$, $p = 0.02$) & for all pts ($r = 0.98$ versus $r = 0.94$, $p = 0.0004$).

CONCLUSION

While it is possible to simplify I-131 dose estimation using camera measurements alone, estimating blood dose by blood work alone is the more statistically robust approach.

CLINICAL RELEVANCE/APPLICATION

For cases in which camera measurements are compromised by technical errors, it is justifiable to rely on blood measurements alone in estimating I-131 thyroid cancer therapy maximum permissible blood dose.

SSJ22-06 Evaluation of Different Strategies to Improve CT-based PeT Attenuation Correction Close to Metal Impants: A Phantom Study

Tuesday, Nov. 29 3:50PM - 4:00PM Room: S403B

Participants

Christoph Schabel, MD, Tübingen, Germany (*Presenter*) Nothing to Disclose
Sergios Gatidis, MD, Tübingen, Germany (*Abstract Co-Author*) Nothing to Disclose
Malte N. Bongers, MD, Tübingen, Germany (*Abstract Co-Author*) Nothing to Disclose
Juergen Kupferschlaeger, Tübingen, Germany (*Abstract Co-Author*) Nothing to Disclose
Georg Bier, MD, Tübingen, Germany (*Abstract Co-Author*) Nothing to Disclose
Fabian Bamberg, MD, MPH, Tübingen, Germany (*Abstract Co-Author*) Speakers Bureau, Bayer AG; Speakers Bureau, Siemens AG;
Research Grant, Bayer AG; Research Grant, Siemens AG;
Christian la Fougere, Munich, Germany (*Abstract Co-Author*) Nothing to Disclose
Konstantin Nikolaou, MD, Tübingen, Germany (*Abstract Co-Author*) Speakers Bureau, Siemens AG; Speakers Bureau, Bracco Group;
Speakers Bureau, Bayer AG
Christina Pfannenber, MD, Tübingen, Germany (*Abstract Co-Author*) Nothing to Disclose

PURPOSE

To compare different strategies of metal artifact (MA) reduction in CT for the improvement of CT-based PET attenuation correction close to metal implants.

METHOD AND MATERIALS

A phantom was studied consisting of a cylindrical tube filled with [¹⁸F]FDG solution containing two artificial jaws with metal containing dental work. CT datasets were acquired using a 3rd generation dual-source CT (Somatom Definition Flash, Siemens Healthcare, Germany). Two datasets were obtained with a CTDI of 15mGy using single energy (SE) mode at 120kV and dual energy mode at 100/Sn140kV. Single energy datasets were reconstructed using filtered back projection without (NOMAR) and with iterative MA reduction (IMAR, Siemens Healthcare, Germany). Dual energy datasets were reconstructed using linear blending (Mix) and mono energetic extrapolation (ME) at 150 and 190 keV without IMAR. PET measurements of the phantom were performed on a state-of-art PET/CT scanner. Afterwards PET/CT datasets were co-registered with the CT only datasets and PET data were reconstructed with the previously reconstructed CT only data sets. Relative PET quantification errors were quantified by 16 regions of interest (ROI).

RESULTS

MA were present in all CT datasets. MA reduction strategies were able to reduce these artifacts to different extend, with IMAR showing best capabilities followed by ME190keV and ME150keV. SE and Mix images depicted strongest artifacts. In general, activity concentrations were overestimated / underestimated in areas of high/low-density metal, artifacts respectively. Relative errors in PET quantification ranged between -71 and 70% for Mix, -63 and 49% for SE, -67 and 42% for ME150keV, -66 and 39% for ME190keV and -37 and 13% for IMAR images. Averaged absolute values were 34±22%, 29±17%, 24±18%, 23±18%, 8±9%, respectively (p<0.001).

CONCLUSION

CT-based PET-attenuation correction was improved significantly using dual energy based metal artifact reduction strategies; nevertheless iterative metal artifact reduction strategy was superior. Further clinical studies are necessary in order to assess the clinical performance of this algorithm in patients.

CLINICAL RELEVANCE/APPLICATION

CT-based PET attenuation is susceptible for errors in regions with CT artifacts. Metal artifact reduction is essential to optimize attenuation correction. This study compares different and novel strategies.

SSJ23

Physics (Diagnostic X-Rays II)

Tuesday, Nov. 29 3:00PM - 4:00PM Room: S404AB

PH

AMA PRA Category 1 Credit™: 1.00
ARRT Category A+ Credit: 1.00

FDA

Discussions may include off-label uses.

Participants

Stephen Rudin, PhD, Buffalo, NY (*Moderator*) Research Grant, Toshiba Corporation
Ioannis Sechopoulos, PhD, Atlanta, GA (*Moderator*) Research agreement, Siemens AG; Research agreement, Toshiba Medical Systems Corporation; Speaking agreement, Siemens AG

Sub-Events

SSJ23-01 Validation of Model Observers: Required Number of Radiologists and Cases

Tuesday, Nov. 29 3:00PM - 3:10PM Room: S404AB

Participants

Robert M. Nishikawa, PhD, Pittsburgh, PA (*Presenter*) Royalties, Hologic, Inc; Research Consultant, iCAD, Inc;

PURPOSE

It has been well established that inter-reader variability is high amongst radiologists. The purpose of this study was to determine the minimum of radiologists and cases required to validate a model observer for screening mammography.

METHOD AND MATERIALS

We examined the performance of 208 radiologists who attended one of five American College of Radiology Breast Imaging Boot Camps, which are three-day intensive courses designed to provide practicing radiologists with an intensive hands-on experience in breast imaging. Each radiologist read up to 240 cases under direct supervision from the course instructors. We examined data from 108 radiologists who read the same 102 digital screening mammograms. We randomly selected a predetermined number of radiologists and cases and computed the overall sensitivity. This was repeated 1000 times. From this resampling, we computed the 95% confidence intervals (CI) for the measured sensitivity as a function of number of cases and the number of radiologists. Calculations were done per view and the radiologist needed to specify the correct location of the cancer to be considered correct.

RESULTS

The average sensitivity for all 108 readers reading 102 cases was 0.643. There was a strong dependence of the 95%CI range on the number of readers. Estimating sensitivity based on 10 radiologists gave a 95% CI range of 0.109. This decreased to 0.015 with 90 readers. We found a weaker dependence on the number of cases. For 30 radiologists, the 95% CI range decreased from 0.080 to 0.055, as the number of cases increased from 10 to 102 cases. For a +/-5% error in sensitivity based on the 95% CI (i.e., a 95% CI range of 0.064) required at least 30 radiologists and 30 cancer cases. Thirty radiologists far exceed the typical number of radiologists participating in an observer study and will present a challenge when validating model observers.

CONCLUSION

To perform an observer study to validate a model of observer for screening mammography can be done with a relatively small number of cases, but requires a large number of radiologists to reduce the inter-reader variability.

CLINICAL RELEVANCE/APPLICATION

Proper validation of observer models is needed to ensure that predictions based on model observers will be clinically relevant and correct. Our study indicates that a large number of radiologists is needed for proper validation.

SSJ23-02 Optimizing Neonatal Techniques After Replacing a Computed Radiography with a Digital Radiography Portable

Tuesday, Nov. 29 3:10PM - 3:20PM Room: S404AB

Participants

Loretta Johnson, PhD, Birmingham, AL (*Presenter*) Nothing to Disclose

CONCLUSION

Our newly-programmed techniques have made it easier for technologists to achieve good neonate image quality at a low and appropriate dose every time.

Background

Our neonatal ward recently replaced their portable computed radiography (CR) unit with a Carestream Revolution DRX digital radiography (DR) portable. Since DR can achieve comparable image quality with less radiation, we took this opportunity to optimize techniques for the DRX. Data from two types of phantoms (Lucite and Cornish hen) as well as neonates was used. The DICOM headers of the DRX provide the deviation index (DI) and relative x-ray exposure, which were used to determine whether sufficient radiation reached the detector. As a quantitative measure of image quality (IQ), a region of interest was drawn over a uniform area (e.g. neonate liver), and the standard deviation (SD) was recorded. Radiologist reports were checked for references to IQ problems.

Evaluation

100 neonate examinations performed and 100 had acceptable IQ and dose metrics. Repeat survey data was used to estimate the

180 neonate exams were reviewed and 138 had acceptable IQ and dose metrics. Recent survey data was used to estimate the patient entrance exposure for the neonates and phantoms. For each 500 g increment in neonate weight, the lowest dose technique with acceptable IQ was determined from phantom images. These techniques were then compared to the techniques recently used for neonates; half the new techniques were consistent with (though on the low-dose side) the neonate exams that had acceptable image quality and appropriate DI, while 1/6 were higher-dose and 1/3 were lower-dose techniques.

Discussion

Since our new portable arrived, technologists have had to dial in the technique for each neonate, and as a result, the techniques used have varied widely. Having each technologist think about patient size for each neonate and dial in the kVp and mAs is both wasteful of the technologists' time and opens doors to potential errors. Neonate radiography is already challenging for plenty of patient-related reasons that cannot be easily addressed. Developing an optimal technique chart and programming in the techniques by neonate weight is an achievable and useful goal for a medical physicist.

SSJ23-03 Can Solid-State Meters Reliably Measure Fluoroscopic Air-Kerma Rates?

Tuesday, Nov. 29 3:20PM - 3:30PM Room: S404AB

Participants

Janet Ching-Mei Feng, PhD, MSc, Houston, TX (*Presenter*) Nothing to Disclose

Bahadir Ozus, PhD, Houston, TX (*Abstract Co-Author*) Nothing to Disclose

Luong Thai, Houston, TX (*Abstract Co-Author*) Nothing to Disclose

Louis K. Wagner, PhD, Houston, TX (*Abstract Co-Author*) Partner, Partners in Radiation Management Ltd Company

CONCLUSION

Air-kerma rates can be measured favorably well using solid-state devices, but users must be aware of the possibility that readings can be grossly in error with no discernible indication for the deviation.

Background

Ionization chambers remain the standard for calibration of air-kerma rate measuring devices. Despite their strong energy-dependent response, solid state radiation detectors are increasingly used, primarily due to their efficiency in making standardized measurements. To test the reliability of these devices in measuring air-kerma rates, we compared ion chambers measurements with solid-state measurements for various mobile fluoroscopes operated at different beam qualities and air-kerma rates.

Evaluation

Six mobile fluoroscopes (GE OEC models 9800 and 9900) were used to generate test beams. Using various field sizes and dose rate controls, copper attenuators and a lead attenuator were placed at the image receptor in varying combinations to generate a range of air-kerma rates. Air-kerma rates at 30 centimeters from the image receptors were measured using two 6-cm³ ion chambers with monitors (Radcal, models 1015 and 9015) and two with solid state detectors (Unfors Xi and Raysafe X2). No error messages occurred during measurements. However, about two months later, one solid-state device stopped working and was replaced by the manufacturer. Two out of six mobile fluoroscopic units were retested with the replacement unit.

Discussion

Generally, solid state and ionization chambers agreed favorably well, with two exceptions. Before replacement of the detector, the Xi meter when set in the "RF High" mode deviated from ion chamber readings by factors of 2 and 10 with no message indicating error in measurement. When set in the "RF Low" mode, readings were within -4% to +3%. The replacement Xi detector displayed messages alerting the user when settings were not compatible with air-kerma rates.

SSJ23-04 Tomosynthesis Reconstruction Based on Principal Component Analysis (PCA)

Tuesday, Nov. 29 3:30PM - 3:40PM Room: S404AB

Participants

Lucas R. Borges, Philadelphia, PA (*Presenter*) Nothing to Disclose

Eileen Hwuang, Philadelphia, PA (*Abstract Co-Author*) Nothing to Disclose

Raymond Acciavatti, Philadelphia, PA (*Abstract Co-Author*) Nothing to Disclose

Marcelo A. Vieira, PhD, Sao Carlos, Brazil (*Abstract Co-Author*) Nothing to Disclose

Andrew D. Maidment, PhD, Philadelphia, PA (*Abstract Co-Author*) Research support, Hologic, Inc; Research support, Barco nv; Research support, Analogic Corporation; Spouse, Employee, Real-Time Tomography, LLC; Spouse, Stockholder, Real-Time Tomography, LLC; Scientific Advisory Board, Real-Time Tomography, LLC; Scientific Advisory Board, Gamma Medica, Inc

PURPOSE

To explore whether digital breast tomosynthesis reconstruction can be recast as a denoising problem to be addressed with principal component analysis (PCA).

METHOD AND MATERIALS

Tomosynthesis projection images were acquired on an anthropomorphic phantom and a geometry phantom. Commercial reconstruction software (Real Time Tomography, Villanova, PA) was used to compute backprojections. Conventionally, the backprojections are averaged in filtered backprojection reconstructions; in this work, PCA was investigated as an alternative to redistribute the backprojection data into independent components ranked by variance. PCA was performed treating the image as a whole and in patches. Three PCA algorithms were investigated. Images were evaluated qualitatively to look at the impact on artifacts and quantitatively to assess noise and artifact spread function.

RESULTS

Our hypothesis was confirmed that the first principal component (PC1 map) is the reconstructed image, and the remaining higher order components predominantly contain artifacts and noise. When PCA was performed on the image as a whole, the PC1 map demonstrated reduced artifacts compared to conventional reconstruction; the PC1 map corresponds to >99.97% of variance. Successively higher order components contain banded features at locations of out-of-plane artifacts. The artifact spread function showed no significant difference between the commercial reconstruction and PCA reconstruction. When PCA was performed in

patches, smaller kernel sizes produced PC1 maps with fewer discernible structures, increased noise, and discontinuities that we attribute to variations in the order of principal components; larger kernel sizes yielded superior PC1 maps. Singular value decomposition and eigenvalue decomposition produce similar results.

CONCLUSION

PCA produces tomosynthesis reconstructions that are comparable to current methods and may have the advantage of removing out-of-plane artifacts. Further work needs to be performed to understand the mechanism of PCA in reconstruction and develop an appropriate mathematical framework.

CLINICAL RELEVANCE/APPLICATION

Digital breast tomosynthesis is still in its infancy. As such, there is a need for reconstruction methods that more effectively remove artifacts and noise than current methods.

SSJ23-05 Characterizing Noise Sources for Image Receptors of Digital Radiography Systems using the Pixel Variance Technique

Tuesday, Nov. 29 3:40PM - 3:50PM Room: S404AB

Participants

Caitlin Finley, Wynnewood, PA (*Presenter*) Nothing to Disclose

Prakruti Talreja, Philadelphia, PA (*Abstract Co-Author*) Nothing to Disclose

Jaydev K. Dave, PhD, MS, Philadelphia, PA (*Abstract Co-Author*) Nothing to Disclose

CONCLUSION

Pixel variance technique characterizes noise sources which may affect image quality. This technique may be integrated during periodic quality assessments of digital image receptors.

Background

Images acquired using digital radiography systems may be affected by structured, quantum or electronic noise. For an optimal performing clinical system, quantum noise is the dominant noise source. Characterizing the noise sources for image receptors of digital radiography systems is therefore useful. The purpose of this work was to evaluate the use of pixel variance technique to characterize the noise sources for image receptors of digital radiography systems.

Evaluation

Nine portable digital radiography systems (Carestream Health, Inc., Rochester, NY) equipped with 11 calibrated image receptors (9: 35x43 cm; 2: 25x30 cm) were used to acquire noise only images. Thirteen images per image receptor using RQA5 beam conditions and with input detector air kerma ranging from 0 to 110 mGy were acquired. Linearized 'For Processing' images were extracted for analysis. Square ROIs with varying dimensions (2.5 to 20 mm) were used to obtain mean pixel value (MPV), standard deviation (SD), and relative noise (SD/MPV) from each image. Variance (SD^2) and relative noise were fitted as a function of input detector air kerma, using least-squares approach, to determine structured, quantum, and electronic noise coefficients and the overall contribution of quantum noise.

Discussion

There was no effect of the ROI size on the analysis (coefficient of variation < 1%). All fitting functions showed correlation values above 0.9. The structured, quantum, and electronic noise coefficients were 0.6 ± 0.3 , 5.6 ± 3.7 , and 3.4 ± 1.4 (mean \pm standard deviation). One image receptor showed electronic noise to be dominant, but for all other image receptors quantum noise was the dominant noise source. The noise coefficients with 35x43 cm sized image receptor (0.4 ± 0.1 , 4.0 ± 3.7 , and 2.9 ± 0.7) were lower relative to 25x30 cm sized image receptor (1.2 ± 0.3 , 13.1 ± 0.3 , and 5.9 ± 0.5). The power parameter from the relative noise fitting equation was 0.47 ± 0.02 indicating minor contributions from other noise sources (a value of 0.50 indicates purely quantum noise).

SSJ23-06 Comparison of 3 Performance Metrics for the Assessment of Microcalcification Detection in 2D Digital Mammography

Tuesday, Nov. 29 3:50PM - 4:00PM Room: S404AB

Participants

Kristina Wigati, Leuven, Belgium (*Presenter*) Nothing to Disclose

Lesley Cockmartin, Leuven, Belgium (*Abstract Co-Author*) Nothing to Disclose

Joke Binst, Leuven, Belgium (*Abstract Co-Author*) Nothing to Disclose

Nelis Van Peteghem, Leuven, Belgium (*Abstract Co-Author*) Nothing to Disclose

Liesbeth Vancoillie, Leuven, Belgium (*Abstract Co-Author*) Nothing to Disclose

Nicholas Marshall, Leuven, Belgium (*Abstract Co-Author*) Research Grant, Siemens AG

Hilde Bosmans, PhD, Leuven, Belgium (*Abstract Co-Author*) Co-founder, Qaelum NV Research Grant, Siemens AG

PURPOSE

To compare 3 different types of performance metrics for microcalcification detection in 2D mammography.

METHOD AND MATERIALS

The 3 metrics tested were: (1) Contrast-detail analysis with CDMAM phantom and automatic read-out with cdcom software (www.euref.org). Threshold gold thickness (T) for the 0.1 mm diameter disk was obtained. (2) A detectability index d' for a 0.1 mm diameter disk was calculated from modulation transfer function, noise power spectrum, contrast and visual transfer function. (3) Detectability was tested with a 3D structured phantom including different size groups of calcifications on a background of beads in water. The percent correct (PC) response for the 0.119 mm calcification group was assessed based on a four-alternative forced-choice task performed by 5 readers. The 3 metrics were tested on 24 2D digital mammography (DM) systems, including recently introduced systems such as Siemens PRIME, GE PRISTINA and Giotto CLASS, and all types of digital detectors (flat panel, computed radiography and photon counting), under automatic exposure control (AEC) settings. Four systems were also tested at a dose of half and double the AEC level.

RESULTS

A logarithmic relation between d' and T was found with R^2 equal to 0.65. Detectability indices of 1.6 and 0.95 were found equivalent to the achievable and acceptable European limits of T (1.10 μm and 1.68 μm resp.). These limits for d' were close to previously published limiting values i.e. 1.7 and 1.05 resp. Detection results of the structured phantom correlated with T (Spearman correlation $r=-0.64$) and with d' ($r=0.70$). The achievable and acceptable threshold of $d'=1.6$ and $d'=0.95$ resulted in PC limits of 85% and 56% for the 0.119 mm microcalcifications.

CONCLUSION

Performance results of the three investigated metrics correlated well. Next to this, the phantoms are intrinsically complementary, with method (1) a detection task performed on for processing data and homogenous background, (2) a Fourier-based approach that allows analysis of the impact of the different system components, (3) detection task for a group of microcalcifications within a 3D structured background.

CLINICAL RELEVANCE/APPLICATION

Calcification detection remains a critical task in DM. The correlation between 3 different test metrics shows the validity of each of them for system benchmarking.

Radiation Oncology (Breast)

Tuesday, Nov. 29 3:00PM - 4:00PM Room: S104A



AMA PRA Category 1 Credit™: 1.00
ARRT Category A+ Credit: 1.00

Participants

L. Christine Fang, MD, Seattle, WA (*Moderator*) Nothing to Disclose
Tracy M. Sherertz, MD, San Francisco, CA (*Moderator*) Nothing to Disclose

Sub-Events**SSJ24-01 Cosmesis after Early Stage Breast Cancer Treatment with Breast Conserving Surgery and Radiotherapy: Experience of Patients Treated In A Chilean Radiotherapy Center**

Tuesday, Nov. 29 3:00PM - 3:10PM Room: S104A

Participants

Lorena Vargas, Oak Brook, IL (*Presenter*) Nothing to Disclose

ABSTRACT

Purpose/Objective(s): The aim of this study is to analyze the overall cosmetic outcome according to patient self assessment and evaluate differences according to the fractionation received. **Materials/Methods:** A questionnaire was drawn up on the basis of subjective rating scales of cosmesis and it was applied at the start of treatment, at discharge and/or at follow-up visits to patients with early stage breast cancer who received radiotherapy (RT) with tangential fields between June/2014 and July/2015. Self-perception of cosmesis, pain, changes in the treated breast, and fractionation used (hypofractionation (HF) or conventional fractionation (CF)) were evaluated. Surgical bed boost and use of field in field technique (FIF) were also recorded. A descriptive analysis was performed to calculate proportions, frequencies and medians. Chi square and Kruskal Wallis tests were use when appropriate. **Results:** 352 questionnaires were obtained: 71 at enrollment, 80 at discharge and 201 at follow up visits (281 were considered as evaluation of RT effect). Median age was 58 yo. Forty five percent (126/279) of patients reported "excellent" cosmesis, 53% (147/279) "acceptable", and 2% (6/279) "poor" cosmesis. Cosmesis was considered "acceptable/excellent" by 98% (273/279) of patients. According to fractionation received, no statistically significant difference was found in overall cosmesis ($p = 0.6$), pain ($p=0.9$), boost use or FIF. The alteration that occurred more frequently was "difference between the two breasts" (77%), followed by "alteration in shape of the breast" (56%) and then for "induration" (53%). Change in breast normal color was reported in 48%. Fifteen percent of patients younger than 58 yo reported change of normal breast color affecting cosmesis compared to 9% of patients older than 58 yo ($p = 0.04$). Patients under 58 yo had a greater frequency of breast induration (61% versus 49%, $p=0.03$). Nine percent of patients with stage I-II reported complications affecting breast cosmesis compared with 2% with cancer in situ (DCIS) ($p = 0.04$). Fourteen percent in stage I-II referred color change affecting cosmesis compared with 6% of those with DCIS ($p = 0.03$). Pain was reported by 68% of patients, and in most of them it was occasional (62%), whereas only 6.4% reported permanent pain. When considering only the questionnaires before the start of RT and at the end of it, in both times the most frequent response was acceptable cosmesis (53.5% and 63.8% respectively), while 3% and 4% reported poor cosmesis at the beginning and at discharge respectively. Ninety-four percent of patients stated that they would accept treatment again. **Conclusion:** No difference was found between HF and CF in our patients in terms of cosmetic results. Great satisfaction regarding cosmetic outcome of cancer treatment is reported, given by 98% of excellent/acceptable cosmesis, and 94% of patients who would receive treatment again.

SSJ24-02 Cost Minimizing Analysis of Intraoperative Radiotherapy (IORT) in Conservatively Treated Early Breast Cancer

Tuesday, Nov. 29 3:10PM - 3:20PM Room: S104A

Participants

Pedro Lara, Oak Brook, IL (*Presenter*) Nothing to Disclose

ABSTRACT

Purpose/Objective(s): Accelerated Partial Breast Irradiation (APBI) by IORT is becoming an attracting alternative to external beam radiotherapy (EBRT) in early breast cancer treated by conservative surgery (BCS). One of the mayor issues for implementing a new treatment is the cost related to health results. **Materials/Methods:** The Breast IORT programme started in our center in January 2013. Since then, 195 patients received BCS for early breast cancer until December 2014. The cost analysis was performed after the completion of the treatment of every patient. The full cost of the surgical procedure included: Operating Room (OR), physicians and other personnel, pharmacy, pathology, nuclear medicine, recovery and days in bed at hospital. Cost of the IORT administration were also calculated and included in the analysis: first consultation, preplanning CT scan, disposables, time of radiation oncologist, physicist, technician, annual equipment cost per number of patients treated. EBRT treatment included the whole (consultation, simulation, planning and treatment delivery) process for 25 fractions. **Results:** Two patients were treated of bilateral cancer with IORT and were excluded from the analysis. Of the 193 remaining cases, 108 were referred to IORT although only 81 received the treatment. 27 cases do not fit for IORT due to the big size of the cavity after removal of the tumor (24 cases) or device technical problems at OR (3 patients). The mean cost of surgery for the whole 193 cases was 4,610.31±1,591.67€ (median 4,346.91€). Surgery was slightly more expensive for those cases that received IORT treatment (4,777.75±1,650.78€; median: 4,430.86€) compared with those not referred to IORT (4,376.54±1,443.90€; median: 4,206.11€) (5,2% incremental cost; p The total cost of the BCT for the whole series of patients was 9,091.09±2,016.28€ per case. Cost comparison of BCS+IORT (6,800.79±1,658.17€; median: 6,463.98€) vs BCS+EBRT (10,090.97±1,443.70€; median 9,920.54€) showed a strong advantage in total cost for IORT treatment (incremental cost 53,47%; p Health results showed a 100% actuarial local control at 3 years for IORT (follow-up closed at Feb 2016) and no CTACAE 4.0 toxicity score over 2 were observed. Results non-inferior to those observed in the EBRT arm for BCT. **Conclusion:** IORT slightly increases the cost of the surgical procedure of BCS (5,2%) but saves up to a 53,47% of the total cost of a Breast Conserving Treatment, when compared with standard EBRT in 25 fractions, showing equivalent health results in terms of clinical outcome and toxicity. Indirect cost and patient convenience are further advantages to be taking into account.

SSJ24-03 VMAT as Treatment Technique in Complex Radiotherapy Breast including IMC, L3 and L4 Nodes

Tuesday, Nov. 29 3:20PM - 3:30PM Room: S104A

Participants

Antonia Lavorato, Oxford, United Kingdom (*Presenter*) Nothing to Disclose
Asadulla Khan, Oxford, United Kingdom (*Abstract Co-Author*) Nothing to Disclose
Sileida Oliveros, Oxford, United Kingdom (*Abstract Co-Author*) Nothing to Disclose

ABSTRACT

Purpose/Objective(s): The aim of the present study is to demonstrate the validity of the volumetric modulated arc therapy technique (VMAT) for the whole breast, internal mammary nodal chain (IMC) and medial supraclavicular fossa (SCF) in deep inspiration and compare its dosimetric results to the standard tangential field-in-field (FinF) combined with an anterior beam technique. **Materials/Methods:** A complex case was chosen for this study. A 31 years old lady presented with a self-detected lesion in the medial aspect of the left breast. She was diagnosed with an invasive ductal carcinoma of the left breast grade 3, ER 3/8, PR negative (0/8), HER-2 negative. BRCA 1 and 2 negative as well as panel gene testing negative. CT showed no evidence of metastatic disease or enlarged internal mammary nodes. The patient had undergone a total of six cycles of chemotherapy and left breast wide local excision with complete pathological response. Adjuvant breast radiotherapy and boost to the tumour bed was recommended (Px 40Gy/15#, 16Gy in 8#). Risks versus benefits of irradiating the IMC and SCF were evaluated by the oncologist who concluded that in this clinical case the benefits would outweigh the risks providing an optimised plan could be achieved minimising, as much as possible, the dose to the ipsilateral lung and to the heart. The oncologist delineated the relevant CTVs following the ESTRO consensus guideline. The patient central lung dose for tangential beams was 4.5cm. A total of three plans were generated for this patient: two VMAT partial arcs with different gantry angles and a standard tangential FinF with a combined anterior beam. The plans were created with Pinnacle, treatment planning system. **Results:** Treatment Technique Left Lung V20 Left Lung V10 Left Lung V5 Heart V25 Heart V10 Heart Mean Gy Spinal Canal Max Gy Tangential FinF + Ant Beam 34.9% 43.6% 54.3% 00.6% 2.238.4 VMAT Gantry 150-300 degrees 23% 42.2% 64.3% 08.1% 5.229.9 VMAT Gantry 178-300 degrees 25% 43.3% 57% 04.6% 4.426.9 In Both VMAT plans better V20 and V10 to the Left (Ipsilateral) Lung was achieved; also better coverage and dose homogeneity were achieved with VMAT when compared with FinF techniques. There was no significant difference to the mean contralateral breast between the two VMAT techniques. The dose coverage (V38Gy) to the breast and L3 and L4 nodes was quite comparable across the techniques but IMC coverage using tangential beams was inferior. **Conclusion:** The results support the hypothesis that VMAT technique is feasible and in this specific case perhaps the only solution. The results showed that the dose to the ipsilateral lung can be reduced and the dose homogeneity can be improved without increasing the dose to the contralateral breast or lung.

SSJ24-04 Effect of Adjuvant Radiotherapy on Survival in Male Breast Cancer: A Population-Based Analysis

Tuesday, Nov. 29 3:30PM - 3:40PM Room: S104A

Awards

Trainee Research Prize - Resident

Participants

Matthew J. Abrams, MD, Boston, MA (*Presenter*) Nothing to Disclose
Paul Koffer, MD, Boston, MA (*Abstract Co-Author*) Nothing to Disclose
Jaroslaw Hepel, MD, Providence, RI (*Abstract Co-Author*) Nothing to Disclose

PURPOSE

There are no randomized trials providing evidence for or against adjuvant radiation for male breast cancer because of its rarity. This study examines the impact of post-lumpectomy (PLRT) and post-mastectomy radiation (PMRT) in male breast cancer patients in the National Cancer Institute's Surveillance Epidemiology and End Results (SEER) database.

METHOD AND MATERIALS

The SEER database 8.3.1 was queried for men ages 20+ diagnosed with localized or regional non-metastatic grade I-III invasive ductal/lobular carcinoma from 1998-2011. Included patients were treated with a lumpectomy or modified radical mastectomy (MRM) with or without post-surgical external beam radiation. Univariate and multivariate analyses evaluated predictors for PMRT use after MRM. Overall survival (OS) curves were calculated by the Kaplan-Meier method and compared by the log-rank test. Cox-regression was used for multivariate survival analyses.

RESULTS

A total of 1,980 patients were followed for a maximum of 10 yrs (median follow up = 56 months). 349 patients underwent lumpectomy while 1,631 underwent MRM. Of those who underwent lumpectomy, PLRT improved 10 yr OS (68% vs. 57% p=0.001). Of those who underwent MRM, PMRT had no impact on neither the entire group 10 yr OS (54% PMRT vs. 53% no PMRT) p=0.585 nor on the subset of node negative patients 10 yr OS (60% PMRT vs. 62% no PMRT) p=0.736. However, there was a benefit in 10 yr OS for 1-3 nodes positive (55% PMRT vs. 46% no PMRT, p=0.033) and for 4+ nodes positive (49% vs. 21%, p=0.001). Using cox-regression analysis, increasing number of nodes positive, larger size and older age were all associated (p<0.001) with a survival detriment while the use of PMRT (p<0.001) was associated with improved survival (HR=0.62 [0.49-0.77]). Using binary logistic regression, predictors for the use of PMRT were unknown/borderline ER status, grade III disease, increasing nodes positive, and larger primary tumor size.

CONCLUSION

The use of post-lumpectomy radiation is associated with a survival benefit. After a modified radical mastectomy, PMRT improves survival in those with positive nodes. There may be a subset of node negative patients who derive a survival benefit and more study of this group is needed.

CLINICAL RELEVANCE/APPLICATION

After a diagnosis of male breast cancer, post-lumpectomy radiation should be considered for all patients and post-mastectomy radiation should be considered for node positive patients.

SSJ24-05 Assessment of Cosmetic Outcome Following Intra-operative Radiation Therapy during Breast

Conserving Surgery as Treatment for Early Breast Cancer

Tuesday, Nov. 29 3:40PM - 3:50PM Room: S104A

Participants

Norman S. Williams, London, United Kingdom (*Presenter*) Travel support, Carl Zeiss AG

ABSTRACT

Purpose/Objective(s): Intra-operative radiation therapy during breast-conserving surgery is increasingly being used as a treatment for early breast cancer. A variety of techniques are used, and many have been shown to be safe and effective. Another important aspect is the long-term cosmetic (aesthetic) results of treatment, as most women will survive for decades. In order to determine the variety and extent of methods currently being used to assess cosmetic outcome, a review of the literature was performed. In particular, the results obtained from objective assessment methods were sought. **Materials/Methods:** PubMed was searched using the terms (ioert[All Fields] OR IORT[All Fields] OR intraoperative[All Fields]) AND ("breast"[MeSH Terms] OR "breast"[All Fields]) AND (cosmesis[All Fields] OR cosmetic[All Fields] OR ("esthetics"[MeSH Terms] OR "esthetics"[All Fields] OR "aesthetic"[All Fields]) OR ("esthetics"[MeSH Terms] OR "esthetics"[All Fields] OR "esthetic"[All Fields])). Abstracts of all articles were read to eliminate those not relevant to this study. Review articles were read in their entirety to determine if any articles were missed from the initial PubMed search. From the final set of articles, the methods used for intra-operative radiation therapy cosmetic assessment, and results obtained from the assessment, were tabulated. The proportion of patients determined to have Excellent or Good outcome (EG), and the 95% confidence intervals, were calculated. **Results:** A total of 184 items were identified by the search, of which 145 were determined from the abstract to be not relevant. 39 publications were read in detail, and included 10 reviews and editorials, 2 studies where either no assessment was made or no radiation therapy given. Of the remaining studies, only 4 reported the use of an objective method of assessment of cosmetic outcome, the others using either subjective or poorly specified methods. One study used a LINAC-based method of delivering the intra-operative radiation therapy, the other three used Intrabeam (the TARGIT technique). Results are shown in the Table. **Conclusion:** A minority of reports assessing cosmetic outcomes following intra-operative radiation therapy use objective methods. Such methods should be required as they provide unbiased estimates of outcome. **Publication Method n Proportion EG (95%CI)** Cracco et al (2015) LINAC-IORT 8184 (8) % EBRT 10588 (6) % Keshtgar et al (2013) Intrabeam-IORT 17186 (5) % EBRT 15175 (7) % Grobmyer et al (2013) Intrabeam-IORT 1788 (15) % Kraus-Tiefenbacher et al (2006) Intrabeam-IORT (as boost) plus EBRT 7393 (6) %

SSJ24-06 Evaluation of Axillary Dose Coverage following Whole Breast Radiotherapy: Variation with the Different Radiotherapy Field

Tuesday, Nov. 29 3:50PM - 4:00PM Room: S104A

Participants

Rong Cai, Oak Brook, IL (*Presenter*) Nothing to Disclose

ABSTRACT

Purpose/Objective(s): To evaluate dose distribution and coverage of the axilla levels I-III, superior axillary vein lymph nodes (Sup-AV) and inferior axillary vein lymph nodes (infer-AV) area, according to AMAROS field (A), high tangent field (HT), standard tangent field (ST). **Materials/Methods:** We retrospectively delineated the axillary levels I-III, Sup-AV and Infer-AV on planning CT-images of 10 patients who treated with breast conservation and whole breast radiotherapy along 2015 in our institution. Every patients were treated using the AMAROS (A), high tangent field (HT), standard tangent field (ST). Mean dose levels and V90 (volume receiving at least 90% of the prescribed dose) of every axillary lymph nodes, Su-AV and In-AV were evaluated. **Results:** The median dose delivered to level I using A, HT and ST were 42.96Gy, 37.3Gy, 27.9Gy. The median dose delivered to level II using A, HT and ST were 46.4Gy, 26.6Gy, 18.5Gy. The median dose delivered to level III using A, HT and ST were 50.9Gy, 19.1Gy, 10.3Gy. The median dose delivered to Sup-AV using A, HT and ST were 47.3Gy, 19.4Gy, 6.16Gy. The median dose delivered to Inf-AV using A, HT and ST were 43.8Gy, 41.4Gy, 33.4Gy. The dose of lung V20% using A, HT and ST were 38.8Gy, 16.74Gy and 16.14Gy. **Conclusion:** AMAROS provide high coverage of axilla I-III but high lung dose coverage. For level I, A and HT had similar dose distribution higher than ST; For level II, AMAROS and HT provide high dose coverage than ST.

SSJ25

Vascular Interventional (Aortic Imaging and Intervention)

Tuesday, Nov. 29 3:00PM - 4:00PM Room: E352



AMA PRA Category 1 Credit™: 1.00
ARRT Category A+ Credit: 1.00

FDA Discussions may include off-label uses.

Participants

Graham J. Robinson, MBBCh, Hull, United Kingdom (*Moderator*) Proctor, W. L. Gore & Associates, Inc; Proctor, Cook Group Incorporated;
Kenneth J. Kolbeck, MD, PhD, Portland, OR (*Moderator*) Nothing to Disclose

Sub-Events

SSJ25-01 Abdominal Aortic Aneurysm Screening Practices: Impact of the 2014 United States Preventive Services Task Force Recommendations

Tuesday, Nov. 29 3:00PM - 3:10PM Room: E352

Awards

Student Travel Stipend Award

Participants

Evan J. Zucker, MD, Boston, MA (*Presenter*) Nothing to Disclose
Alexander S. Misono, MD, MBA, Boston, MA (*Abstract Co-Author*) Nothing to Disclose
George R. Oliveira, MD, East Boston, MA (*Abstract Co-Author*) Nothing to Disclose
Anand M. Prabhakar, MD, Somerville, MA (*Abstract Co-Author*) Nothing to Disclose

PURPOSE

On 6/24/2014, the U.S. Preventive Services Task Force (USPSTF) released updated abdominal aortic aneurysm (AAA) ultrasound (US) screening recommendations, more inclusive of screening selected male never-smokers and female ever-smokers compared to 2005 guidelines. We sought to determine if the new guidelines have been associated with changes in screening practices.

METHOD AND MATERIALS

All AAA screening US exams performed in our radiology dept. in the 15 months before and after the new guideline release (3/1/2013 through 9/11/2015) were retrospectively reviewed to assess changes in exam volume and appropriateness, patient demographics, aneurysm incidence and size at diagnosis, frequency and type of incidental findings, and radiologist recommendations. Appropriateness was based on patient age, gender, and smoking status. Exams were considered "definitely appropriate" in male ever-smokers ages 65-75 and "possibly appropriate" in other men in this age range. Exams after the new guidelines were additionally considered "possibly appropriate" in female ever-smokers ages 65-75. The t-test was used to compare means.

RESULTS

831 AAA screening US exams were reviewed, 417 (50.2%) performed before and 414 (49.8%) after the new guidelines. Overall mean (SD) age was 67.9 (6.8) years, 89.2% male. The fraction of definitely or possibly appropriate exams increased from 289/417 (69.3%) before to 327/414 (79.0%) after the guideline release ($p = 0.001$), mostly due to definitely appropriate exams (253/417 or 60.1% before vs. 286/414 or 69.1% after the guidelines). Aneurysm incidence increased from 23/417 (5.5%) exams before to 39/414 (9.4%) exams after the revisions ($p = 0.03$). Mean (SD) aneurysm size (cm) at diagnosis was smaller after (3.3 [0.6]) compared to before (3.8 [0.7]) the revisions ($p = 0.01$). Exam volume, demographics, and rates of incidentals and recommendations remained similar. Incidentals arose in 15.6% of all exams, often iliac artery aneurysms or renal masses. Recommendations were made in 4.9%, generally for imaging follow-up of AAA or further mass characterization.

CONCLUSION

The revised USPSTF guidelines have been associated with an increase in AAA screening appropriateness and aneurysm detection yield in our practice, with smaller aneurysm size at diagnosis.

CLINICAL RELEVANCE/APPLICATION

The revised 2014 USPSTF guidelines for AAA US screening are associated with more appropriate exam referrals and greater diagnostic yield of exams performed.

SSJ25-02 Endoleaks after Endovascular Aortic Aneurysm Repair: Detection with Noise-Optimized Virtual Monochromatic Dual-Energy Computed Tomography

Tuesday, Nov. 29 3:10PM - 3:20PM Room: E352

Participants

Simon S. Martin, MD, Frankfurt, Germany (*Presenter*) Nothing to Disclose
Julian L. Wichmann, MD, Charleston, SC (*Abstract Co-Author*) Nothing to Disclose
Jan-Erik Scholtz, MD, Boston, MA (*Abstract Co-Author*) Nothing to Disclose
Doris Leithner, MD, Frankfurt am Main, Germany (*Abstract Co-Author*) Nothing to Disclose
Volkmar Jacobi, MD, Frankfurt, Germany (*Abstract Co-Author*) Nothing to Disclose
Thomas J. Vogl, MD, PhD, Frankfurt, Germany (*Abstract Co-Author*) Nothing to Disclose
Moritz H. Albrecht, MD, Charleston, SC (*Abstract Co-Author*) Nothing to Disclose

PURPOSE

To assess image quality and diagnostic performance of a noise-optimized algorithm for reconstruction of virtual monoenergetic images (VMI+) regarding detection and localization of endoleaks after endovascular abdominal aortic aneurysm repair (EVAR) in dual-energy CT angiography (DE-CTA).

METHOD AND MATERIALS

Sixty-nine patients (42 men; 65.9±14.1 years) underwent DE-CTA following EVAR. Arterial phase images were acquired in dual-energy mode for reconstruction of standard linear blended (F_0.5, 50% low-keV spectrum), VMI+ and traditional monoenergetic (VMI) images in 10-keV intervals from 40 to 100 keV. Attenuation measurements were performed in the descending aorta, the iliofemoral arteries and the area of leakage for objective signal-to-noise (SNR) and contrast-to-noise ratio (CNR) calculation in patients with findings of endoleaks. Based on objective image quality results, best series for each reconstruction technique were chosen (F_0.5, 40-keV VMI+, 70-keV VMI) for further analysis. Five-point scales were used to evaluate contrast enhancement, overall image quality, and suitability for endoleak detection. Diagnostic accuracy for the diagnosis of arterial hemorrhage of these series was assessed and receiver operating characteristics (ROC) curve analysis was performed.

RESULTS

Thirty-two patients showed findings of endoleak subsequent to EVAR. Objective image quality metrics were highest in 40-keV VMI+ compared to VMI series, which showed highest values at 70-keV, and F_0.5 images (CNR: 20.8±11.6, 10.4±9.5, and 13.3±9.8, respectively; all P<0.001). 40-keV VMI+ series were found most suitable for endoleak detection (P<0.001). Sensitivity and specificity for detection of endoleaks were 98% and 68% for 40-keV VMI+, 96% and 57% for 70-keV for VMI, and 96% and 64% for F_0.5 reconstructions. Area under the curve (AUC) was significantly superior (P≤0.005) for 40-keV VMI+ (0.98) compared to 70-keV VMI (0.81) and F_0.5 series (0.84).

CONCLUSION

Diagnostic accuracy in the assessment of endoleaks after EVAR can be significantly increased using 40-keV VMI+ reconstructions compared with standard linearly blending and traditional VMI technique in arterial phase DE-CTA.

CLINICAL RELEVANCE/APPLICATION

Diagnostic performance for detection and localization of endoleaks after EVAR can be significantly improved with 40-keV VMI+ reconstructions.

SSJ25-03 Dual Source Dual Energy CTA for the Detection of Endoleaks after (Thoracic) Endovascular Aneurysm Repair

Tuesday, Nov. 29 3:20PM - 3:30PM Room: E352

Participants

Lydia Maaskant, Rotterdam, Netherlands (*Presenter*) Nothing to Disclose

Ronald Booiij, RT, Rotterdam, Netherlands (*Abstract Co-Author*) Nothing to Disclose

Marcel L. Dijkshoorn, RT, Rotterdam, Netherlands (*Abstract Co-Author*) Consultant, Siemens AG

Jasper Florie, Rotterdam, Netherlands (*Abstract Co-Author*) Nothing to Disclose

Adriaan Moelker, MD, Rotterdam, Netherlands (*Abstract Co-Author*) Nothing to Disclose

Mohamed Ouhous, MD, PhD, Rotterdam, Netherlands (*Abstract Co-Author*) Nothing to Disclose

PURPOSE

The purpose of this study was to evaluate the diagnostic value of Dual Source Dual Energy CTA (DS DECTA) in the detection of endoleaks after (thoracic) endovascular aneurysm repair ((T)EVAR).

METHOD AND MATERIALS

In total, 52 patients scanned with a dual contrast phase DECTA on a 2nd generation DS DECT-scanner (n=30) and on a 3rd generation DS DECT-scanner (n=22) were included in this retrospective study. These patients were compared with patients scanned on a single source CT (n=53). The virtual non-contrast (VNC) and DECTA images were analysed by two observers for overall quality, endoleak detection, and VNC calculation errors. Additional Hounsfield Units (HU), noise (measured by SD), and iodine measurements were performed, by drawing ROI's in the "true" lumen and the thrombus of the aorta. In addition, differences in radiation dose between the scanners were assessed by calculating the effective dose as DLP * conversion factor.

RESULTS

The median overall quality and calcium subtraction of the VNC images were according to both reviewers 'good' or 'excellent' in all images. In addition, there were no missing or additional structures in 84.4-93.3% of the VNC images. Also the noise was significantly higher in the true unenhanced CT than in the VNC images. Observer 1 detected thirteen endoleaks and observer 2 eleven endoleaks (agreement kappa = 0.78). Consensus was achieved for all cases after individual detection. In addition, the diagnostic certainty based on the DECTA and VNC images was 88.5-94.2%, with no diagnostic changes by observer 1 and two diagnostic changes by observer 2. Furthermore, the iodine measurement for the detection of endoleaks had a sensitivity and specificity of 100% and 92.1%, respectively. Finally, replacing the true unenhanced CT with VNC images resulted in a radiation dose reduction of 26.5-45.8% in the 2nd generation DS DECT-scanner and 6.8-9.3% in the 3rd generation DS DECT-scanner.

CONCLUSION

DS DECTA with the use of iodine measurements increases the detection of endoleaks. Furthermore, replacing the true unenhanced CT with VNC images results in a radiation dose reduction.

CLINICAL RELEVANCE/APPLICATION

Dual Energy CTA can replace the single-energy CTA with additional true unenhanced CT in post-(T)EVAR patients. Better endoleak detection and radiation dose reduction can be achieved.

SSJ25-04 Can Arterial Phase CTA Be Replaced with a Virtual Arterial Phase Reconstruction From a Venous Phase CT During a Triple Phase CT in the Evaluation of Postoperative Aorta using a Detector-Based Spectral CT

Awards

Student Travel Stipend Award

Participants

Anish A. Patel, MD, Dallas, TX (*Presenter*) Nothing to Disclose
Ali Alian, MD, Dallas, TX (*Abstract Co-Author*) Nothing to Disclose
Yin Xi, Dallas, TX (*Abstract Co-Author*) Nothing to Disclose
Patrick D. Sutphin, MD, PhD, Dallas, TX (*Abstract Co-Author*) Nothing to Disclose
Sanjeeva P. Kalva, MD, Dallas, TX (*Abstract Co-Author*) Consultant, CeloNova BioSciences, Inc

PURPOSE

Detector-based spectral CT allows for the utilization of virtual monoenergetic (VME) images to approximate the attenuation (HU) of polyenergetic grayscale images from conventional CT while reducing artifacts such as beam hardening. Spectral CT also allows for the retrospective augmentation of vascular enhancement to further interrogate a region of interest. The purpose of this study is to compare the signal-to-noise ratios (SNR) of true arterial phase CT data with virtual arterial phase monoenergetic data reconstructed from the venous phase of a triple phase CT during the evaluation of the aorta after endovascular repair.

METHOD AND MATERIALS

The arterial phase CT was compared to VME data from venous phase CT in 16 patients using the same acquisition parameters on a detector-based spectral CT (IQon, Philips Healthcare) at various anatomic locations (sagittal aorta, aorta at celiac axis and renal arteries, common iliac arteries, femoral arteries). VME images were reconstructed at various energy levels ranging from 42-58 keV in 2 keV increments. ROIs were drawn and average attenuation (HU) and standard deviations were obtained. The equivalent test with tolerance margin 15 and 10 was used for signal and noise, respectively. The SNR was defined as the ratio of mean HU attenuation to standard deviation on ROIs. Approximation of arterial images by virtual venous images was defined as a difference in mean SNR within 5.

RESULTS

Statistically significant ($p < 0.05$) arterial approximations at measured locations were seen at the following energies: sagittal aorta (42-58 keV), celiac aorta (42-58 keV), renal aorta (42-58 keV), right common iliac (48-58 keV), left common iliac (54-58 keV), right femoral (56-58 keV), left femoral (58 keV).

CONCLUSION

A nearly identical reconstruction of virtual arterial phase CT angiography based on the SNR is feasible using spectral CT reconstruction of the venous phase CTA, allowing only a single phase CTA to routinely evaluate post-operative aortas. Central arterial vessels can utilize monochromatic energies from 42-58 keV to best approximate the arterial phase while more peripheral vessels required energies around 54-58 keV for the same effect, likely due to contrast dilution.

CLINICAL RELEVANCE/APPLICATION

The retrospective simulation of arterial enhancement using only a single venous phase will limit both the contrast and radiation dose to patients undergoing routine evaluation of postoperative aortas.

SSJ25-05 Aortic Bulge Sign: Predicting Aortoenteric Fistula before Catastrophe

Tuesday, Nov. 29 3:40PM - 3:50PM Room: E352

Awards

Student Travel Stipend Award

Participants

Patrick J. Kennedy, MD, Hamilton, ON (*Presenter*) Nothing to Disclose
Michelle Kuang, Hamilton, ON (*Abstract Co-Author*) Nothing to Disclose
Fernando Gastaldo, MD, Dundas, ON (*Abstract Co-Author*) Nothing to Disclose

PURPOSE

Aortoenteric fistula (AEF) is typically interpreted on computed tomography (CT) in the context of clinical gastrointestinal (GI) bleeding or graft infection. The purpose of this study is to introduce the aortic bulge sign, a novel finding observed retrospectively on CT prior to the acute presentation of AEF, and determine its diagnostic value.

METHOD AND MATERIALS

Following research ethics board approval, a retrospective chart review was undertaken to isolate all cases of AEF at our institution from 2011 to 2015. CTs on presentation and operative reports were reviewed to confirm the presence of AEF. Comparison was made to available previous abdominal CTs, regardless of indication or protocol. Demographics, known pre-morbid conditions, and clinical outcomes were documented from clinical notes. The previous CTs of patients who eventually presented with AEF were combined with age and gender matched control CTs into a case bank. Seven radiology residents and staff were instructed in observing the aortic bulge sign: a focal anterior outpouching in the aorta or aortic graft extending toward a nearby bowel loop. These observers then reviewed the case bank as part of a blinded analysis to determine the interobserver reliability and diagnostic value of the aortic bulge sign.

RESULTS

Fourteen cases of AEF were identified. Nine patients died within 30 days of presentation, yielding a mortality rate of 64.3%. All 14 patients had CTs on presentation, with direct signs of AEF present in nine cases. Eleven patients had previous CTs available for review. The time intervals between these CTs and the onset of GI bleeding ranged from eight to 2096 days (mean 417.3 days). Blinded analysis of the previous CTs yielded the following mean values for the aortic bulge sign: sensitivity 68.8%, specificity 96.4%, positive predictive value 98.0%, negative predictive value 55.1%, and accuracy 76.2%. Substantial interobserver reliability was demonstrated ($k = 0.61$).

CONCLUSION

The aortic bulge sign has been retrospectively identified as a reliable CT finding of eventual AEF prior to the acute presentation.

CLINICAL RELEVANCE/APPLICATION

Impending AEF may be predicted on CT prior to the acute presentation by identifying an anterior bulge in the abdominal aorta.

SSJ25-06 Feasibility of Shear Wave Elasticity Imaging to Detect Endoleak and Evaluate Thrombus Organization after Endovascular Repair of Abdominal Aortic Aneurysm

Tuesday, Nov. 29 3:50PM - 4:00PM Room: E352

Participants

Antony Bertrand-Grenier, Montreal, QC (*Abstract Co-Author*) Nothing to Disclose
Nicolas Voizard, Montreal, QC (*Presenter*) Nothing to Disclose
Husain M. Alturkistani, MD, Montreal, QC (*Abstract Co-Author*) Nothing to Disclose
Eric Therasse, MD, Montreal, QC (*Abstract Co-Author*) Nothing to Disclose
An Tang, MD, Montreal, QC (*Abstract Co-Author*) Advisory Board, Imagia Cybernetics Inc
Stephane Elkouri, MD, Montreal, QC (*Abstract Co-Author*) Nothing to Disclose
Claude Kauffmann, PhD, Montreal, QC (*Abstract Co-Author*) Nothing to Disclose
Guy Cloutier, PhD, Montreal, QC (*Abstract Co-Author*) Nothing to Disclose
Gilles P. Soulez, MD, Montreal, QC (*Abstract Co-Author*) Speaker, Bracco Group Speaker, Siemens AG Research Grant, Siemens AG Research Grant, Bracco Group Research Grant, Cook Group Incorporated Research Grant, Object Research Systems Inc

PURPOSE

To investigate the feasibility of shear wave elasticity imaging (SWI) for detection of endoleaks and characterization of abdominal aortic aneurysms (AAAs) healing after endovascular aneurysm repair (EVAR), using a combination of duplex ultrasound (DUS) and CT-scan as the reference standard.

METHOD AND MATERIALS

Endoleaks areas were detected on SWI by 2 readers and compared with DUS and CT in 25 patients. Elasticity values of endoleaks and thrombus were calculated and compared. Analysis included: a) Correlation between thrombus elasticity and AAA diameter and volume and their variation over time and b) Correlation between endoleak and fresh thrombus areas and aneurysm diameter and volume.

RESULTS

Endoleaks were present in 6 patients. SWI, DUS and CT respectively detected 5 (83%), 3 (50%) and 4 (67%) of these endoleaks. SWI detected 2 endoleaks not seen on DUS and two others not seen on CT. SWI reported 6 false positives (specificity of 76%). Elasticity moduli in endoleaks and thrombi regions were estimated at 0.08 ± 0.13 kilopascal (kPa) and 17.9 ± 11.4 kPa, respectively ($P < 0.001$). Thrombus elasticity of AAA with and without endoleaks were not significantly different ($P = 0.792$). No significant correlations were found between thrombus elasticity moduli and AAA diameter and volume and their variation over time. The surface of fresh thrombi (less rigid and non-organized thrombi; 3-19 kPa) or fresh thrombi and endoleak was associated with larger AAA diameters and volumes ($P < 0.001$).

CONCLUSION

This clinical study evaluated SWI as a biomarker of endoleak and thrombus stiffness in 25 patients with AAA after EVAR. AAAs were evaluated and correlated with SWI, DUS and CT-scan. SWI provides real time mechanical information on AAA sac content that is complementary to B-mode and DUS assessments. Our results suggest that not only SWI may help detecting endoleak but it may also detect aneurysm likely to grow by identifying the amount of fresh thrombus that is likely to be associated with post EVAR aneurysm enlargement.

CLINICAL RELEVANCE/APPLICATION

SWI has the potential to identify endoleaks and to detect aneurysms that are likely to grow after EVAR. As both techniques are implemented on the same imaging modality, SWI may be combined with DUS in post-EVAR surveillance of endoleak. SWI could reduce costs, exposure to ionizing radiation and nephrotoxic contrast agents associated with CT-scan follow-up.

Vascular Interventional (Venous Interventions)

Tuesday, Nov. 29 3:00PM - 4:00PM Room: N230B



AMA PRA Category 1 Credit™: 1.00
ARRT Category A+ Credit: 1.00

Participants

Nael E. Saad, MBBCh, Saint Louis, MO (*Moderator*) Research Consultant, Veran Medical Technologies, Inc; Proctor, Sirtex Medical Ltd
Charles T. Burke, MD, Chapel Hill, NC (*Moderator*) Nothing to Disclose

Sub-Events

SSJ26-01 Extracellular Matrix Remodeling in Venous Hypertension

Tuesday, Nov. 29 3:00PM - 3:10PM Room: N230B

Participants

Rahmi Oklu, MD, PhD, Scottsdale, AZ (*Presenter*) Nothing to Disclose
Sanjay Misra, MD, Rochester, MN (*Abstract Co-Author*) Data Safety Monitoring Board, Flexible Stenting Solutions, Inc
Hassan Albadawi, MD, Boston, MA (*Abstract Co-Author*) Nothing to Disclose

PURPOSE

Extracellular matrix remodeling has been implicated in a number of vascular conditions, including venous hypertension and varicose veins. However, to date no systematic analysis of matrix remodeling in human veins has been performed.

METHOD AND MATERIALS

Following IRB approval, normal and varicose venous tissues were processed for cell culture, histology, protein purification and gene expression assays. For mass spectrometry analysis, tryptic peptides from processed NaCl and GuHCl extracts were separated on a nanoflow LC system. Gel and in-solution LC-MS/MS analysis were performed. LC-MS/MS analysis was also performed in normal veins following chymase and trypsin digestion. Mass spectrometry data was subsequently confirmed by Western blot analysis, RT-QPCR and immunohistochemistry. A p-value of <0.05 was considered significant for all tests used.

RESULTS

The proteomics analysis revealed the presence of more than 150 extracellular matrix proteins, of which 48 had not been previously detected in venous tissue. Extracellular matrix remodeling in varicose veins was characterised by a loss of aggrecan and several small leucine-rich proteoglycans and a compensatory increase in collagen I and laminins. Gene expression analysis of the same tissues suggested that the remodeling process associated with venous hypertension predominantly occurs at the protein rather than the transcript level. Loss of aggrecan in varicose veins was paralleled by a reduced expression of aggrecanases. Chymase and trypsin β 1 were among the upregulated proteases. The effect of these serine proteases on the venous extracellular matrix was further explored by incubating normal saphenous veins with recombinant enzymes. Proteomics analysis revealed extensive extracellular matrix degradation after digestion with trypsin β 1. In comparison, chymase was less potent and degraded predominantly basement membrane-associated proteins.

CONCLUSION

The present proteomics study provides unprecedented insight into the expression and degradation of structural and regulatory components of the vascular extracellular matrix in varicosis.

CLINICAL RELEVANCE/APPLICATION

In conclusion, varicosis is intimately related to dynamic changes in the vascular ECM and its associated proteins. Our findings may lead to newer targeted therapies for venous hypertension as well as hypertension in general.

SSJ26-02 Incidence of Infection in Patients undergoing Chest Port Placement: A Cohort Study Utilizing Pooled, Multi-institutional Electronic Health Record Data

Tuesday, Nov. 29 3:10PM - 3:20PM Room: N230B

Participants

Stephanie Soriano, MD, Cleveland, OH (*Abstract Co-Author*) Nothing to Disclose
Indravadan J. Patel, MD, Cleveland, OH (*Presenter*) Nothing to Disclose
Jon Davidson, MD, Cleveland, OH (*Abstract Co-Author*) Nothing to Disclose

PURPOSE

To determine the effectiveness of the use of antibiotic prophylaxis for chest port placement, and examine the incidence of infection at the 16- and 30-day post-procedure interval.

METHOD AND MATERIALS

A retrospective cohort analysis was performed utilizing a HIPAA-compliant, patient de-identified clinical database from a large multi-institution electronic health records data web application EPM:Explore (Explorys Inc, Cleveland, Ohio), identifying patients who underwent port placement. Cohorts were created based on patients who underwent initial port placement, and further divided into those who received antibiotic prophylaxis prior to the procedure, specifically cefazolin, vancomycin, or clindamycin, and those who did not. We then evaluated the incidence of central line infections within 16 and 30 days of the procedure. Statistical analysis was performed utilizing IBM SPSS version 23.

RESULTS

There were 110,250 patients who underwent initial chest port placement. The infection rates within 16 and 30 days of the procedure, with antibiotics, were 1.8% and 2.2%, respectively. The infection rates within 16 and 30 days of the procedure, without antibiotics, were 1.2% and 1.4%, respectively. Of the patients that were diagnosed with infection, 83.7% and 84.6% were diagnosed in the first 16 days, in the population prophylactically treated with and without antibiotics, respectively.

CONCLUSION

Our analysis showed no benefit of prophylactic antibiotic use for port placement. Of the population that was diagnosed with central line infection, the majority were diagnosed within the first 16 days post procedure.

CLINICAL RELEVANCE/APPLICATION

Due to the large population sample this is likely to have a profound impact on the judicious use of peri-procedural antibiotic in regards to chest port placement.

SSJ26-03 Adrenal Venous Sampling in Primary Aldosteronism: External Validation of Multinomial Regression Modelling to Detect Aldosterone Hypersecretion Lateralization When the Right Adrenal Vein Sampling is Missing

Tuesday, Nov. 29 3:20PM - 3:30PM Room: N230B

Participants

Florence Perrault, Montreal, QC (*Presenter*) Nothing to Disclose

Gregory Kline, Calgary, AB (*Abstract Co-Author*) Nothing to Disclose

Gilles P. Soulez, MD, Montreal, QC (*Abstract Co-Author*) Speaker, Bracco Group Speaker, Siemens AG Research Grant, Siemens AG Research Grant, Bracco Group Research Grant, Cook Group Incorporated Research Grant, Object Research Systems Inc

Miguel Chagnon, Montreal, QC (*Abstract Co-Author*) Nothing to Disclose

Patrick Gilbert, MD, Montreal, QC (*Abstract Co-Author*) Nothing to Disclose

Vincent L. Oliva, MD, Montreal, QC (*Abstract Co-Author*) Nothing to Disclose

Marie-France Giroux, MD, Montreal, QC (*Abstract Co-Author*) Research Grant, Johnson & Johnson Research Grant, BIOTRONIK GmbH & Co KG Stockholder, Abbott Laboratories

Isabelle Bourdeau, MD, Montreal, QC (*Abstract Co-Author*) Nothing to Disclose

Andre Lacroix, MD, Montreal, QC (*Abstract Co-Author*) Nothing to Disclose

Eric Therasse, MD, Montreal, QC (*Abstract Co-Author*) Nothing to Disclose

PURPOSE

To assess the external validity of multinomial regression modelling (MRM) of adrenal venous sampling (AVS) to detect lateralization of aldosterone secretion (LAS) when the right AVS is missing.

METHOD AND MATERIALS

All consecutive AVS from 2 university medical centers were included from 1990 (center #1) and 2005 (center #2) to 2015. Non selective AVS and AVS with missing data were excluded. Bilateral simultaneous AVS were performed before (basal) and after intravenous injection of 250 ug of cosyntropin in both centers. LAS was defined as an adrenal vein aldosterone /cortisol ratio >2 the opposite side for basal AVS and >4 after cosyntropin. MRMs of AVS from center #1 were built to detect LAS without the right AVS. Sensitivity and specificity to predict LAS with MRM were compared between both centers at a specificity cut off useful for clinical decision making. This specificity was set at 95% from the receiver operating characteristic curve of MRM of AVS from center #1.

RESULTS

AVS of 174/197 patients (69.5% men, mean age 53.3 years) from center #1 and 122/133 patients (60.2% men, mean age 51.4 years) from center #2 were analyzed. In center #1 and #2, basal LAS was found respectively in 142/180 (78.9%) and 86/122 (70.5%) AVS ($p=0.096$), while after cosyntropin LAS was found respectively in 107/176 (60.8%) and 60/122% (49.2%) AVS ($p=0.047$). In center #2, specificity for right and left LAS detection was respectively 91.8 % and 93.2% for basal AVS and 93.8% and 95.3% after cosyntropin ($p>0.30$ for all comparisons with 95% set in center #1). Sensitivity to detect LAS in center #1 and #2 was respectively 65.5% (93/142) and 59.3% (51/86) ($p=0.35$) for basal AVS, and respectively 72.9% (78/107) and 61.7% (37/60) ($p=0.13$) after cosyntropin. With basal AVS, there were 4 (3 in center #1, 1 in center #2) false positives that showed contralateral LAS. Post-cosyntropin, there was no false positives that showed contralateral LAS in both centers.

CONCLUSION

Minimal changes in diagnostic accuracy from one center to another validate the use of MRM of AVS to predict LAS when the right adrenal vein sampling is missing.

CLINICAL RELEVANCE/APPLICATION

External validation of MRM of AVS to predict LAS could allow its use in any centers plagued by low AVS diagnostic performance due to failure to cannulate the right adrenal vein.

SSJ26-04 Totally Implantable Venous Access Port Placement via The axillary Vein in Patients with Head and Neck Cancer

Tuesday, Nov. 29 3:30PM - 3:40PM Room: N230B

Participants

Sun Hong, Seoul, Korea, Republic Of (*Presenter*) Nothing to Disclose

Tae Seok Seo, MD, PhD, Seoul, Korea, Republic Of (*Abstract Co-Author*) Nothing to Disclose

Myung Gyu Song, MD, Seoul, Korea, Republic Of (*Abstract Co-Author*) Nothing to Disclose

PURPOSE

To evaluate clinical outcomes and complications of totally implantable venous access ports (TIVAPs) implantation via the axillary

vein in patients with head and neck cancer.

METHOD AND MATERIALS

A total 133 TIVAPs were placed via the axillary vein in 131 head and neck cancer patients between May 2012 and June 2015. All cases were placed under fluoroscopic guidance in the intervention suite. The patients were 108 men and 23 women with the mean age of 58.5 years (range: 19 ~79 years). TIVAPs were implanted by right and left axillary vein access in 89 (66.9%) and 44 cases (33.1%), respectively. Medical records were retrospectively reviewed for patient's demographics, procedure related complications, catheter related infections and reasons of TIVAPs removal. The presence of central vein stenosis, catheter related thrombus and catheter migration were evaluated on neck CT images.

RESULTS

The total TIVAPs indwelling time was 59742 catheter days and the mean indwelling time was 449 catheter days (range of 4 to 1207 days). Of 133 implanted TIVAPs, complications developed in 10 cases (10/133, 7.5%) and incidence was 0.017 events/1000 catheter days. Complication related axillary vein access was developed in 4 cases (4/133, 3%) and incidence was 0.167 events/1000 catheter days. All patients presented thrombus in axillary or subclavian vein. Other complications were 3 cases (3/133, 2.3%) of catheter related blood stream infection, 2 cases (2/133, 1.5%) of central vein stenosis and 1 case (1/133, 0.8%) of tissue hypertrophy on needling site. There was no procedure related complication or catheter migration. Among 10 complication cases, 7 TIVAPs were removed except 3 cases which were one case of left brachiocephalic vein stenosis and two cases of axillary vein thrombosis.

CONCLUSION

TIVAPs implantation via the axillary vein in patients with head and neck cancer seems to be safe and feasible with low complication rate related with axillary vein access.

CLINICAL RELEVANCE/APPLICATION

The axillary vein would be a good access route for TIVAPs implantation in the patients with head and neck cancer instead of the internal jugular vein.

SSJ26-05 Vascular Imaging in the Asymptomatic High Risk Cancer Population: A Role for Thrombosis Screening and Therapy Management

Tuesday, Nov. 29 3:40PM - 3:50PM Room: N230B

Awards

Student Travel Stipend Award

Participants

Zhongxia Hu, MD, Rochester, NY (*Presenter*) Nothing to Disclose
Katherine A. Kaproth-Joslin, MD, PhD, Rochester, NY (*Abstract Co-Author*) Nothing to Disclose
Burke Morin, DO, Rochester, NY (*Abstract Co-Author*) Nothing to Disclose
Susan K. Hobbs, MD, PhD, Pittsford, NY (*Abstract Co-Author*) Nothing to Disclose
Charles Francis, MD, Rochester, NY (*Abstract Co-Author*) Nothing to Disclose
Alok Khorana, Cleveland, OH (*Abstract Co-Author*) Nothing to Disclose
Deborah J. Rubens, MD, Rochester, NY (*Abstract Co-Author*) Nothing to Disclose

PURPOSE

We will discuss the utility of screening for venous thromboembolism events (VTE) with lower extremity venous US and chest CTs as a secondary endpoint in a study designed to evaluate the benefit of thromboprophylaxis in a prospective cohort of initially asymptomatic cancer patients with a Khorana score ≥ 3 initiating outpatient chemotherapy.

METHOD AND MATERIALS

117 asymptomatic cancer patients starting new therapy and found to be high-risk for VTE with a predictive risk model were enrolled in a prospective cohort study. Initial US and CTs excluded patients with VTEs from the intervention phase. Subsequently, patients were randomly sorted into observation only or dalteparin prophylaxis groups and were screened with serial US for up to 12 weeks and chest CT at 12 weeks. Additional imaging performed for restaging or for symptomatic events was also evaluated for VTE.

RESULTS

All PE and DVT events recorded were non-fatal. 10 patients were found to have VTE on baseline exam (9%). In the observation only group (48 patients), 10 developed VTE (21%). Screening detected 7 asymptomatic patients (15%) with VTE: 7 with DVT (15%), 2 with PE (4%), and 1 with PE and DVT (2%). In the dalteparin group (50 patients), 6 developed VTE (12%). Screening detected 4 asymptomatic patients with VTE (8%): 2 with DVT (4%) and 2 with PE (4%). 2 developed symptomatic PE (4%). 8 out of 98 patients developed major or clinically significant bleeding, which 7 were in the dalteparin group. Overall, screening exams identified 21 of the 26 patients with VTE in this study (81%). In addition, of the 28 VTE events, 18 were DVTs (64%), of which 13 occurred in the lower extremities (72%).

CONCLUSION

This study confirms validity of the Khorana risk score as 9% of the high risk patients had asymptomatic VTE on initial screening and a total of 22% of patients developed VTE during the study. All cases of detection changed management, which suggests utility in screening for asymptomatic VTEs. More than half of the VTEs detected were DVTs and a majority of them in the lower extremities. As lower extremity veins are not typically examined as part of cancer staging, routine screening lower extremity US may be useful in high risk asymptomatic patients.

CLINICAL RELEVANCE/APPLICATION

This study finds screening CT/US often discover DVT/PEs in some asymptomatic cancer patients that change management, suggesting that screening maybe warranted for a subset of high risk patients.

SSJ26-06 Dynamic Effects of Therapy - Induced Changes in Microcirculation after Percutaneous Treatment of

Vascular Malformations using Contrast-Enhanced Ultrasound (CEUS) and Time Intensity Curve (TIC) analyses

Tuesday, Nov. 29 3:50PM - 4:00PM Room: N230B

Participants

Isabel Wiesinger, Regensburg, Germany (*Presenter*) Nothing to Disclose

Christian R. Stroszczynski, MD, Regensburg, Germany (*Abstract Co-Author*) Nothing to Disclose

Ernst Michael Jung, MD, Regensburg, Germany (*Abstract Co-Author*) Nothing to Disclose

PURPOSE

Quantification of dynamic micro-vascularization differences of peripheral vascular malformations with CEUS and TIC.

METHOD AND MATERIALS

After general examination with B-Scan, and Doppler imaging CEUS was performed after injection of 1-2.4 ml of sulfur hexafluoride microbubbles using a 6-9 MHz linear probe. Digitally stored cine loops up to 1 minute after the injection were analysed by an independent reader. Regions of interest (10x 30 mm) were defined in the centre, and at the margins of the malformation as well as in the healthy tissue. TIC with Time to Peak (TTP), and Area under the Curve (AUC) were calculated using special software.

RESULTS

Evaluation of the capillary micro-vascularization in all cases was only possible by using CEUS. There were no complications after the i.v. contrast injection. Retrospective analysis of 197 patients (136 female; 61 male; 3-86 years) with 135 venous (VM), 39 arterio-venous (AVM), and 23 combined peripheral vascular malformations before and after percutaneous treatment. After the treatment there was a significant decrease in AUC for VM in the centre down to 337.7 rU ($p=0.043$) and in the surrounding tissue to 139.9 rU ($p=0.022$). After the treatment TTP for AVM increased to 17.7 sec in the centre and to 23.2 sec in the surrounding tissue. After the treatment the AUC for AVM in the centre decreased to 518.9 rU at the margins 417.6 rU, and in the surrounding tissue 181.1 rU.

CONCLUSION

By recording capillary perfusion CEUS and TIC analysis offer a possibility of monitoring therapy-induced changes of vascular malformations and help planning interventional procedures by displaying feeder vessels.

CLINICAL RELEVANCE/APPLICATION

CEUS and TIC before and after percutaneous treatment help to plan and control the success of interventional procedures.

MSAS34

The Business of Radiology: Updates and Issues (Sponsored by the Associated Sciences Consortium) (An Interactive Session)

Tuesday, Nov. 29 3:30PM - 5:00PM Room: S105AB

HP

AMA PRA Category 1 Credits™: 1.50
ARRT Category A+ Credits: 1.50

Participants

Patricia Kroken, Albuquerque, NM, (pkroken@comcast.net) (*Moderator*) Nothing to Disclose
Alexander Yule, DSc, Cardiff, United Kingdom (*Moderator*) Nothing to Disclose

LEARNING OBJECTIVES

Session attendees will 1) Gain practical industry knowledge that can be compared to their individual practice situations, 2) Understand the issues related to the implementation of ICD-10 and better prepare for the next stages and 3) Be able to compare examples of billing over-automation to their challenges maximizing revenue.

ABSTRACT

Radiology, as a business, increases in complexity each year as it responds to growing regulatory demands, downward revenue pressures and the need to do more with less. This session addresses the impact of ICD-10 after its first year of implementation and how reality matches to initial expectations. Did it live up to dire predictions or meet the promise of improved coding documentation? And what should we expect next? The session also reviews the trend of low-cost, highly automated billing options which have resulted in the commoditization of radiology billing; that is, the selection of billing options based primarily on price (rather than value). Examples of actual problems created by over-automation will be presented and the impact on revenue discussed. Together, the topics covered are timely and reflect common challenges for the business of radiology.

Sub-Events

MSAS34A Getting What You Pay For: The Commoditization of Radiology Billing

Participants

Patricia Kroken, Albuquerque, NM, (pkroken@comcast.net) (*Presenter*) Nothing to Disclose
Jennifer Kroken, MBA, Lewisville, TX (*Presenter*) Nothing to Disclose

LEARNING OBJECTIVES

The session is designed to provide physicians and administrative leadership with specific examples they can use to examine the effectiveness of their billing operations. Attendees can 1) Identify common industry problems with over-automation that may be occurring in their organizations. 2) Understand the revenue implications of "low bid" decisions related to billing. 3) Better understand the issues of price versus value.

ABSTRACT

The use of technology in radiology billing has been critical in lowering operational overhead, largely because increases in individual staff member productivity reduce the number of people needed to do the work. At the same time, competition has driven down billing company fees to the point where billing options have become commoditized; that is, dependent primarily on price. Have we gone too far? The presentation will review the impact of over-automation, evident as organizations struggle with providing the lowest cost options, and the financial consequences for physicians. Blinded examples from billing audits conducted over the past four years will be included to illustrate the types of problems encountered with low-cost billing options. The presenters make the case for seeking value in a billing relationship, rather than focusing strictly on price.

MSAS34B ICD-10 and Radiology: The Good, The Bad & The Ugly

Participants

Melody W. Mulaik, Powder Springs, GA, (melody.mulaik@codingstrategies.com) (*Presenter*) President, Coding Strategies, Inc;

LEARNING OBJECTIVES

1) The current overall status of ICD-10-CM after one year of implementation. 2) Specific areas of coding and documentation concerns for radiology practices. 3) How to identify specific areas of opportunity to minimize negative financial outcomes.

ABSTRACT

Effective October 1, 2015, healthcare organizations replaced the ICD-9 diagnosis and procedure coding system with ICD-10. Although ICD-10 codes are assigned by staff, or handled by an outsourced vendor, the implementation of ICD-10 has impacted radiologists in a variety of ways. For example, due to the structure and granularity of the ICD-10 code set, there is a need for new or additional information in the radiology report to allow proper coding and thus avoid payment denials and/or delays. This session is designed to give radiologists the information they need to ensure that they, and their organization, are doing everything possible to avoid payment delays and/or denials. The information flow process from the receipt of orders to the radiologists' dictation will be reviewed in detail to identify opportunities for process improvement and individual physician impact. Ample time will be provided for answer attendee questions.

Active Handout: Melody W. Mulaik

http://abstract.rsna.org/uploads/2016/16019617/ACTIVE_MSAS34B.pdf

MSCC34

Case-based Review of Nuclear Medicine: PET/CT Workshop-Lymphoma/Melanoma/Multiple Myeloma (In Conjunction with SNMMI) (An Interactive Session)

Tuesday, Nov. 29 3:30PM - 5:00PM Room: S406A



AMA PRA Category 1 Credits™: 1.50
ARRT Category A+ Credits: 1.50

Participants

Janis P. O'Malley, MD, Birmingham, AL (*Moderator*) Nothing to Disclose

Samuel E. Almodovar-Reteguis, MD, Homewood, AL (*Presenter*) Nothing to Disclose

LEARNING OBJECTIVES

1) Review where PET/CT fits into the assessment of lymphoma, melanoma and multiple myeloma. 2) Apply a systematic approach for evaluating PET/CT image quality and pathology. 3) Identify and discuss findings seen on PET/CT in lymphoma, melanoma and multiple myeloma.

ABSTRACT

MSES34

Essentials of Chest Imaging

Tuesday, Nov. 29 3:30PM - 5:00PM Room: S100AB

CH

AMA PRA Category 1 Credits™: 1.50
ARRT Category A+ Credits: 1.50

Participants

Sub-Events

MSES34A Sarcoidosis: Case-based Review

Participants

H. Page McAdams, MD, Durham, NC, (page.mcadams@duke.edu) (*Presenter*) Research Grant, General Electric Company; Consultant, MedQIA Imaging Core Laboratory ; Author, Reed Elsevier; Author, UpToDate, Inc; Research Consultant, F. Hoffmann-La Roche Ltd; Research Consultant, Boehringer-Ingelheim GmbH

LEARNING OBJECTIVES

1) Discuss classic clinical and radiologic features of thoracic sarcoidosis. 2) Discuss less common or less well known aspects of thoracic sarcoidosis including pulmonary hypertension, airway obstruction and drug-induced sarcoidosis. 3) Discuss the role of FDG-PET imaging in the diagnosis and management of thoracic sarcoidosis.

ABSTRACT

Sarcoidosis is a multisystem granulomatous disease of unknown etiology. This presentation will first briefly review the most common radiologic manifestations of thoracic sarcoidosis. Then, less common or less well known aspects of thoracic sarcoidosis will be discussed, including pulmonary hypertension, airway obstruction and drug-induced sarcoidosis. Finally, the role of FDG-PET imaging for diagnosis and management of thoracic sarcoidosis will be discussed.

Active Handout:H. Page McAdams

http://abstract.rsna.org/uploads/2016/16000882/MSES34A_Sarcoidosis_RSNA_2016_McAdams_Handout.pdf

Honored Educators

Presenters or authors on this event have been recognized as RSNA Honored Educators for participating in multiple qualifying educational activities. Honored Educators are invested in furthering the profession of radiology by delivering high-quality educational content in their field of study. Learn how you can become an honored educator by visiting the website at: <https://www.rsna.org/Honored-Educator-Award/>

H. Page McAdams, MD - 2012 Honored Educator

MSES34B Patterns of Lymphadenopathy in Common Thoracic Malignancies

Participants

Juliana M. Bueno, MD, Chicago, IL, (julianab@uchicago.edu julianab@uchicago.edu) (*Presenter*) Nothing to Disclose

LEARNING OBJECTIVES

1) Review clinically relevant pathways of lymphatic dissemination of common thoracic malignancies, including lung cancer, breast cancer and esophageal carcinoma. 2) Learn potential pitfalls in nodal staging of lung cancer and their impact in the patient's prognosis. 3) Learn key clinically relevant information to be included in staging reporting of these three common malignancies.

ABSTRACT

Medical imaging plays an essential role in the primary diagnosis and staging of neoplastic disease and in the selection of the most appropriate site for tissue biopsy. As such, it is one of the main components of the post treatment assessment in oncologic patients. In thoracic imaging, nodal staging is an important piece of information that directly impacts the prognosis of patients and therefore deserves careful assessment and an appreciation of the pathways of lymphatic dissemination in specific malignancies. Appropriate nodal staging will directly impact the prognosis and survival of oncologic patients. Knowledge of the most common pathways of lymphatic drainage and dissemination of disease in the chest, as well as the importance of specific nodal stations in the overall oncologic staging of the patient, will allow the radiologist to perform an accurate and detailed assessment. Including clinically relevant information in the report assists in deciding upon the most appropriate treatment option.

Active Handout:Juliana Marcela Bueno

http://abstract.rsna.org/uploads/2016/16000881/ACTIVE_MSES34B.pdf

MSES34C Imaging Techniques and Diagnostic Strategies in Pulmonary Embolism

Participants

Carole A. Ridge, MD, Dublin 7, Ireland (*Presenter*) Nothing to Disclose

LEARNING OBJECTIVES

This lecture will illustrate contemporary technical strategies to improve CT pulmonary angiography image quality and radiation dose and clinical strategies to facilitate the accurate diagnosis of pulmonary embolism and its complications.

ABSTRACT

200 CTPA's are performed every hour on emergency department patients in the US. This educational presentation aims to ensure that radiologists are familiar with key techniques to ensure accurate pulmonary embolism imaging, dose reduction, and diagnosis, with particular attention to underdiagnosis and overdiagnosis.

MSES34D Imaging of Patients with Hemoptysis

Participants

Diana Litmanovich, MD, Haifa, Israel, (dlitmano@bidmc.harvard.edu) (*Presenter*) Nothing to Disclose

LEARNING OBJECTIVES

1) The lecture will focus on airways related benign and malignant causes of hemoptysis. 2) Systemic approach to hemoptysis as a symptom will be discussed, including cause, source, and consequences. 3) Specific attention will be paid to ACR appropriateness criteria in assessment of hemoptysis. 4) Advantages and disadvantages of currently available imaging modalities will be discussed. 5) Optimal protocols for MDCT evaluation with emphasis on radiation dose reduction will be reviewed, including imaging of the airways, pulmonary vasculature and lung parenchyma.

ABSTRACT

RC401

RSNA Diagnosis Live™: High Resolution CT of Diffuse Lung Disease: Read Cases with the Experts (An Interactive Session)

Tuesday, Nov. 29 4:30PM - 6:00PM Room: E450A



AMA PRA Category 1 Credits™: 1.50
ARRT Category A+ Credits: 1.50

Participants

Georgeann McGuinness, MD, New York, NY (*Moderator*) Nothing to Disclose
Daria Manos, MD, FRCPC, Halifax, NS, (daria.manos@nshealth.ca) (*Presenter*) Speakers Bureau, F. Hoffmann-La Roche Ltd
Brett M. Elicker, MD, San Francisco, CA, (brett.elicker@ucsf.edu) (*Presenter*) Nothing to Disclose
Sharyn L. MacDonald, MBChB, Christchurch, New Zealand (*Presenter*) Nothing to Disclose

LEARNING OBJECTIVES

1) Understand the applications and limitations of HRCT in detecting and characterizing diffuse lung disease through the review and discussion of cases. 2) Apply correct usage of the HRCT lexicon to specific findings, to better elucidate pathophysiology and to refine differential considerations. 3) Develop diagnosis and management algorithms by working through problematic cases with the expert discussants.

ABSTRACT

This interactive session will use RSNA Diagnosis Live™. Please bring your charged mobile wireless device (phone, tablet or laptop) to participate.

Active Handout:Daria Manos

[http://abstract.rsna.org/uploads/2016/14000784/ACTIVE RC401manos handouts.pdf](http://abstract.rsna.org/uploads/2016/14000784/ACTIVE_RC401manos_handouts.pdf)

Active Handout:Sharyn Leigh Shirley MacDonald

[http://abstract.rsna.org/uploads/2016/14000784/RC401 MacDonald S handout F.pdf](http://abstract.rsna.org/uploads/2016/14000784/RC401_MacDonald_S_handout_F.pdf)

Active Handout:Brett M. Elicker

<http://abstract.rsna.org/uploads/2016/14000784/RSNA2016.pdf>

RC402

Managing your Career: How to Get Hired, Promoted Academically, and/or Advance to Partnership

Tuesday, Nov. 29 4:30PM - 6:00PM Room: N226

ED

AMA PRA Category 1 Credits™: 1.50
ARRT Category A+ Credit: 0

Participants

Jocelyn D. Chertoff, MD, Lebanon, NH, (jchertoff@gmail.com) (*Moderator*) Nothing to Disclose

LEARNING OBJECTIVES

1) The learner will be able to avoid significant pitfalls in the job hunt and hiring process. 2) The learner will be able to describe key steps to promotion. 3) The learner will be able to discuss the important factors in assessing a private practice job.

ABSTRACT

Sub-Events

RC402A How to Get Promoted

Participants

Jocelyn D. Chertoff, MD, Lebanon, NH (*Presenter*) Nothing to Disclose

LEARNING OBJECTIVES

View learning objectives under the main course title.

RC402B How to Look For a Job

Participants

C. Matthew Hawkins, MD, Decatur, GA (*Presenter*) Nothing to Disclose

LEARNING OBJECTIVES

View learning objectives under the main course title.

RC402C Private Practice Perspective

Participants

Scott M. Truhlar, MD, MBA, Coralville, IA (*Presenter*) Nothing to Disclose

LEARNING OBJECTIVES

View learning objectives under the main course title.

RC403

Imaging of the Cardiac Ventricles

Tuesday, Nov. 29 4:30PM - 6:00PM Room: N227B

CA CT MR

AMA PRA Category 1 Credits™: 1.50
ARRT Category A+ Credits: 1.50

FDA Discussions may include off-label uses.

Participants

Sachin S. Saboo, MD, FRCR, Dallas, TX, (sachin.saboo@utsouthwestern.edu) (*Moderator*) Nothing to Disclose

LEARNING OBJECTIVES

ABSTRACT

Sub-Events

RC403A Acquired Disease of the Right Ventricle (Including Secondary RV Disease Due to Pulmonary Disease)

Participants

Jens Bremerich, MD, Basel, Switzerland, (jens.bremerich@usb.ch) (*Presenter*) Nothing to Disclose

LEARNING OBJECTIVES

1) Better understand cardiopulmonary physiology. 2) Identify predictors of outcome in pulmonary diseases. 3) Know arguments for choosing the most useful imaging modality in specific situations.

ABSTRACT

Introduction: Right ventricular (RV) disease may be clinically inapparent or moderately symptomatic. It is even possible to survive without RV such as in patients after palliative cavo-pulmonary connection also referred to as Fontan procedure. Dysfunction may result in heart failure, thrombus formation or rhythm disturbances. Imaging is directed towards identification, characterisation and monitoring of RV disease, mass and function. Methods & Results: Echocardiography remains first line modality because of its ease of use and broad availability. It is particularly useful for assessment of the tricuspid and pulmonary valve. It is hampered, however, by the complexity of RV anatomy and its location behind the sternum, paracentral and peripheral pulmonary arteries can not be explored. Moreover, relevant interstudy and interobserver variability may be problematic in longitudinal monitoring of RV diseases. Computed Tomography provides an excellent overview of anatomy of RV and surrounding structures. Moreover, it can be completed within a single breath hold. Calcifications such as in constrictive pericarditis are readily identified, but more detailed tissue characterisation as well as functional analysis are limited. Magnetic Resonance Imaging (MRI) is the goldstandard for analysis of mass and function of the RV such as in Arrhythmogenic Right Ventricular Dysplasia. Moreover it provides excellent soft tissue characterisation in infarction, fatty infiltration, tumors and cardiac involvement in systemic diseases such as systemic sclerosis by means of quantitative mapping techniques. Conclusion: Echocardiography remains first line modality for imaging the RV because of its availability and ease of use. Advantages of CT are short examination time, excellent overview of cardiac and extracardiac anatomy as well as high sensitivity and specificity for calcifications. MRI is the goldstandard for function and mass and thus excellent for longitudinal monitoring. Detailed tissue characterisation enables characterisation of RV diseases.

RC403B Right Ventricular Failure in Congenital Heart Disease

Participants

Karen G. Ordovas, MD, San Francisco, CA (*Presenter*) Nothing to Disclose

LEARNING OBJECTIVES

1) To understand how sequela of surgical correction for congenital heart disease can impair right ventricular function. 2) To identify best method for measuring severity of right ventricular dysfunction by magnetic resonance. 3) To name surgical procedures that result on a systemic right ventricle.

ABSTRACT

RC403C Left Ventricular Cardiomyopathies

Participants

Seth J. Kligerman, MD, Denver, CO (*Presenter*) Nothing to Disclose

LEARNING OBJECTIVES

1) Recognize variable patterns of delayed enhancement of cardiac MRI. 2) Understand how the pathologic findings correlate with imaging findings. 3) Learn how these patterns in conjunction with left ventricular morphology allow for one to make an accurate diagnosis. 4) Discuss newer MRI sequences that allow for more accurate diagnosis.

RC403D MRI and CT of Cardiac Masses

Participants

Phillip M. Young, MD, Rochester, MN, (young.phillip@mayo.edu) (*Presenter*) Nothing to Disclose

LEARNING OBJECTIVES

1) We will review MRI and CT techniques for investigation of cardiac masses. 2) The role for tissue characterization in narrowing the differential diagnosis, and using imaging to help stage lesions, plan therapy, and anticipate complications will be reviewed. 3) The presentation will largely be case based.

ABSTRACT

.

RC404

Muscle-Tendon-Enteseal Unit: Form, Function, and Dysfunction with Emphasis on MR

Tuesday, Nov. 29 4:30PM - 6:00PM Room: E353C

MK **MR**

AMA PRA Category 1 Credits™: 1.50

ARRT Category A+ Credits: 1.50

Participants

Donald L. Resnick, MD, San Diego, CA (*Director*) Nothing to Disclose

Mini N. Pathria, MD, San Diego, CA (*Presenter*) Nothing to Disclose

Donald L. Resnick, MD, San Diego, CA (*Presenter*) Nothing to Disclose

Christine B. Chung, MD, San Diego, CA (*Presenter*) Nothing to Disclose

Brady K. Huang, MD, San Diego, CA (*Presenter*) Nothing to Disclose

LEARNING OBJECTIVES

1) Understand how variations in the macroscopic architecture of muscle relate to its physiological function, affect its risk of injury, and determine the pathoanatomy and imaging appearance following muscle strain. 2) Understand anatomy and histology of tendon, its normal and abnormal imaging appearances, and common patterns of tendon pathology based on anatomic location. 3) Review the anatomy of the tendon-enteseal unit with emphasis on the types of lesion that affect the region of the footprint, with emphasis on MR imaging.

RC405

Emergency Neuroradiology (An Interactive Session)

Tuesday, Nov. 29 4:30PM - 6:00PM Room: S406B



AMA PRA Category 1 Credits™: 1.50
ARRT Category A+ Credits: 1.50



Discussions may include off-label uses.

Participants

Michael H. Lev, MD, Boston, MA (*Moderator*) Consultant, General Electric Company; Institutional Research Support, General Electric Company; Stockholder, General Electric Company; Consultant, MedyMatch Technology, Ltd; Consultant, Takeda Pharmaceutical Company Limited; Consultant, D-Pharm Ltd

Sub-Events

RC405A Found Down

Participants

John L. Go, MD, Los Angeles, CA (*Presenter*) Nothing to Disclose

LEARNING OBJECTIVES

1) Choose the best imaging for each patient. 2) Discuss the Differential Dx for "found down". 3) Develop a "checklist" for imaging to identify significant findings. 4) Recognize imaging findings that will acutely change patient management.

ABSTRACT

The "found down" patient is unable to provide a history - and often unable to cooperate for a clinical exam. Up to 1/3 are mistriaged and require consultation to another service. Common "medical" conditions include: Hypoxia/Hypotension, Subarachnoid Hemorrhage Hypoglycemia/Hyperglycemia Drugs and Intoxicants Post-ictalCommon "surgical" conditions include: Extraaxial and Intraaxial Hemorrhage Hydrocephalus Herniation (e.g. from a neoplasm) Large Vessel Occlusion and InfarctionA systematic analysis using a "checklist" can help identify life-threatening lesions and may be life-saving.

RC405B Head & Neck Emergencies

Participants

Jenny K. Hoang, MBBS, Durham, NC (*Presenter*) Nothing to Disclose

LEARNING OBJECTIVES

1) Develop a systematic approach to evaluating patients with head and neck infections. 2) Recognize head and neck emergencies that result in morbidity and mortality presenting as fever, trauma, difficulty breathing, and bleeding.

RC405C Emergency Neuroradiology: Don't Miss these Lesions!

Participants

Michael H. Lev, MD, Boston, MA (*Presenter*) Consultant, General Electric Company; Institutional Research Support, General Electric Company; Stockholder, General Electric Company; Consultant, MedyMatch Technology, Ltd; Consultant, Takeda Pharmaceutical Company Limited; Consultant, D-Pharm Ltd

LEARNING OBJECTIVES

1) Summarize the role of imaging in the assessment of acute neurologic emergencies. 2) Apply an evidence based approach to devise effective and efficient neuroimaging algorithms. 3) Describe technological advances in CT and MRI as they relate to imaging acute neuro-vascular and traumatic injuries to the brain. 4) Determine imaging predictors in outcome assessment of cerebral hemorrhage and acute stroke.

ABSTRACT

RC406

Lumps and Bumps in the Head & Neck

Tuesday, Nov. 29 4:30PM - 6:00PM Room: E450B

HN NR

AMA PRA Category 1 Credits™: 1.50
ARRT Category A+ Credits: 1.50

Participants

Sub-Events

RC406A Cervical Lymphadenopathy

Participants

Peter M. Som, MD, New York, NY, (peter.som@mssm.edu) (Presenter) Nothing to Disclose

LEARNING OBJECTIVES

1) Understand the anatomy of the cervical lymph nodes and why these nodes are so important as predictors of survival. 2) Learn the criteria utilized to assess pathologic lymph nodes.

ABSTRACT

The cervical lymph nodes are the best predictors of the development of distant metastases from a head and neck cancer. As such, they are predictors of survival. Further, if metastatic tumor has spread outside of the node, the survival is reduced by half and the incidence of distant metastases is tripled. Because of these facts, a knowledge of how to evaluate these nodes is critical to someone interpreting head and neck imaging studies. This course will review how to classify and stage these cervical nodes and discuss criteria to assess when a metastatic node is present. It will also discuss how these metastatic nodes should be described in reports of these imaging studies.

RC406B Non-nodal Neck Masses

Participants

David R. De Lone, MD, Rochester, MN (Presenter) Nothing to Disclose

LEARNING OBJECTIVES

1) Have an organized approach to the imaging evaluation of a palpable neck mass. 2) Palpable pseudomasses will be discussed. 3) Construct a logical differential diagnosis based on the location, enhancement characteristics, and cystic/solid nature of the mass, considering neoplastic, inflammatory, and congenital etiologies.

RC406C Hemangiomas and Other Vascular Lesions

Participants

Deborah R. Shatzkes, MD, New York, NY, (shatzkes@hotmail.com) (Presenter) Nothing to Disclose

LEARNING OBJECTIVES

1) Understand what clinical and imaging features of a neck "lump" should suggest the possibility of a hemangioma or other vascular lesion. 2) Review current classification of vascular anomalies, and the biologic basis for this classification. 3) Describe the imaging features of common vascular tumors and malformations, specifically hemangiomas, venous and lymphatic malformations, and arteriovenous malformations.

ABSTRACT

Our understanding of vascular lesions has been hampered by loose and inconsistent terminology and by the lack of a coherent classification system. Following Mulliken's description of the biologic basis of disease in 1982 (PRS 69: 412-422), the International Society for the Study of Vascular Anomalies (ISSVA) was formed with the goal of classifying this diverse group of entities, and of defining nomenclature that would facilitate both clinical management and research in this area. The most important feature of this classification system is the division into vascular tumors and vascular malformations. The common hemangioma is by far the most important vascular tumor, while frequently encountered malformations include venous, lymphatic and arteriovenous lesions. Hemangiomas are proliferating endothelial neoplasms, while malformations are considered localized defects in angiogenesis and have quiescent epitheliums. It is important to reserve the term "hemangioma" for these vascular tumors only. This distinction drives the imaging appearance of these entities, with hemangiomas demonstrating signal characteristics compatible with cellular neoplasms, namely enhancement with only moderate T2 hyperintensity. Venous and lymphatic malformations, like all vascular malformations, are named by their vessels of origin. Lymphatic malformations image like sacs of lymph, with marked T2 hyperintensity but without enhancement. Venous malformations, however, enhance avidly, and demonstrate very high T2 signal given their relatively low cellularity. AVM's typically do not appear as discrete masses, but rather infiltrate tissues, causing hypervascularity and edema. The presence of vascular flow voids and mild T2 hyperintensity reflecting tissue edema are the hallmarks of AVM's.

GU Incidental Findings 2016 - What Is New and Helpful in Managing Them? (An Interactive Session)

Tuesday, Nov. 29 4:30PM - 6:00PM Room: E352

GUAMA PRA Category 1 Credits™: 1.50
ARRT Category A+ Credits: 1.50**Participants**

Lincoln L. Berland, MD, Birmingham, AL, (lberland@gmail.com) (*Coordinator*) Consultant, Nuance Communications, Inc;
Stuart G. Silverman, MD, Brookline, MA, (sgsilverman@partners.org) (*Presenter*) Author, Wolters Kluwer nv
Elaine M. Caoili, MD, MS, Ann Arbor, MI (*Presenter*) Nothing to Disclose
Susan M. Ascher, MD, Washington, DC, (aschers@gunet.georgetown.edu) (*Presenter*) Nothing to Disclose

LEARNING OBJECTIVES

1) Appreciate the need for and value of recommendations for managing incidental findings. The participants should also be able to choose from a variety of methods to bring these recommendations to the point of interpretation. 2) Identify incidental adnexal cystic lesions that require further evaluation to include the type and timing of follow up examinations. 3) Apply appropriate imaging criteria and thresholds to better distinguish benign adrenal adenomas from more clinically important lesions. 4) Manage incidental renal masses, even when they are incompletely characterized, such as when they are too small to characterize or detected on an examination that is not designed to evaluate them fully. Please bring your charged mobile wireless device (phone, tablet or laptop) to participate.

ABSTRACT

RC408

Trauma Imaging Pitfalls

Tuesday, Nov. 29 4:30PM - 6:00PM Room: N228



AMA PRA Category 1 Credits™: 1.50
ARRT Category A+ Credits: 1.50

Participants

Sub-Events

RC408A Abdomen (Solid Organs and Vessels)

Participants

Felipe Munera, MD, Miami, FL, (fmunera@med.miami.edu) (*Presenter*) Nothing to Disclose

LEARNING OBJECTIVES

1. Identify common pitfalls in interpretation of abdominal trauma CT studies - focus on solid organs and vascular structures. 2. Optimize CT acquisition techniques to reduce likelihood of missing potentially significant injuries. 3. Develop a search pattern that includes organs and structures where important lesions are commonly missed. 4. Describe strategies to improve detection of easily missed injuries

RC408B Diaphragm

Participants

Michael N. Patlas, MD, FRCPC, Hamilton, ON, (patlas@hhsc.ca) (*Presenter*) Nothing to Disclose

LEARNING OBJECTIVES

1) To describe direct and indirect signs of blunt and penetrating diaphragmatic injury. 2) To highlight factors affecting detection of diaphragmatic injury. 3) To discuss pitfalls in diagnosis of diaphragmatic injury.

ABSTRACT

The traumatic diaphragmatic injury is an uncommon entity. Blunt diaphragmatic injury is undiagnosed at initial presentation in 7-66%. Penetrating diaphragmatic injury can be occult in 7% of cases. Diaphragmatic injury does not resolve spontaneously and can cause disastrous complications. The misinterpretation in patients with diaphragmatic injury may be caused by suboptimal technique, failure to review portion of examination e.g. MPRs, or satisfaction of search error. Potential pitfalls in interpretation include congenital diaphragmatic hernias and atraumatic defects simulating diaphragmatic injury.

RC408C Bowel/Pelvis

Participants

Stephan W. Anderson, MD, Boston, MA (*Presenter*) Nothing to Disclose

RC408D Extremities

Participants

O. C. West, MD, Houston, TX (*Presenter*) Nothing to Disclose

LEARNING OBJECTIVES

1) Find upper extremity injuries that are difficult detect on screening radiographs. 2) Employ search patterns that may improve detection of easily missed injuries.

ABSTRACT

Summary of upper extremity pitfalls: Posterior shoulder dislocation; Supracondylar fracture (anterior humeral line); Monteggia fracture-dislocation (radio-capitellar line); Proximal radius including vertical head fracture (external oblique view), impacted neck fracture, flipped radial head fracture-dislocation, Galeazzi fracture-dislocation – beware the lateral radiograph. Imaging joints requires 3 radiographic projections. The 3rd view varies: Axillary view of shoulder and External oblique of elbow. The wrist needs 4 views: PA, lateral, external oblique and "Scaphoid" view (ulnar deviated PA view). Words to live by: watch for the least obvious of multiple injuries.

Active Handout: O. Clark West

[http://abstract.rsna.org/uploads/2016/16000641/ACTIVE RC408D.pdf](http://abstract.rsna.org/uploads/2016/16000641/ACTIVE_RC408D.pdf)

RC409

Pitfalls in Abdominal Imaging

Tuesday, Nov. 29 4:30PM - 6:00PM Room: E451B

GI

AMA PRA Category 1 Credits™: 1.50
ARRT Category A+ Credits: 1.50

FDA

Discussions may include off-label uses.

Participants

Sub-Events

RC409A Pitfalls in Hepatobiliary Imaging

Participants

Antonio Luna, MD, Jaen, Spain (*Presenter*) Nothing to Disclose

LEARNING OBJECTIVES

1) Identify the most common pitfalls in hepatobiliary imaging. 2) Differentiate them from pathological conditions using a multimodality approach with CT and MRI.

ABSTRACT

RC409B Pitfalls in Pancreas Imaging

Participants

Zhen J. Wang, MD, Hillsborough, CA (*Presenter*) Stockholder, Nextrast, Inc

LEARNING OBJECTIVES

1) Become familiar with the pitfalls in pancreas imaging techniques. 2) Learn the pitfalls in imaging evaluation of benign pancreatic diseases. 3) Review the pitfalls in imaging evaluation of pancreatic malignancies.

ABSTRACT

RC409C Pitfalls in Bowel Imaging

Participants

Benjamin M. Yeh, MD, San Francisco, CA, (ben.yeh@ucsf.edu) (*Presenter*) Research Grant, General Electric Company; Author with royalties, Oxford University Press; Shareholder, Nextrast, Inc;

LEARNING OBJECTIVES

1) Understand critical imaging features associated with the most common bowel emergencies. 2) Be able to tailor exams to suit specific clinical imaging scenarios, depending on patient history and clinical question. 3) Be familiar with common artifacts that can obscure or mimic clinical disease in and adjacent to bowel. 4) Understand how physiology, contrast material, and imaging technique affect cross-sectional imaging of bowel. 5) Provide cogent differential diagnoses based on CT and MR findings to direct patient care.

ABSTRACT

Imaging of the bowel and interpretation of radiological bowel images is arguably the most technically challenging aspect of abdominal imaging, with a high rate of missed diagnostic findings and misinterpretations. The bowel is highly changeable in appearance from scan to scan, and moment to moment. Bowel appearance depends not only on the disease state, but also lumen contents, timing of intravenous contrast material, and many technical image-related factors. Understanding of the mesenteric and bowel anatomy, normal and diseased bowel physiology and vascular flow, and the interaction of contrast agents, is critical to the accurate interpretation of bowel disease. In this talk we will discuss common pitfalls of technique and imaging. In addition, we will explore controversies regarding imaging technique which have become more pressing in recent years, including when to use positive versus neutral oral contrast agents versus no oral contrast in different clinical scenarios.

Active Handout: Benjamin M. Yeh

http://abstract.rsna.org/uploads/2016/16001267/RC409C_PitfallsInBowelImaging.v03syllabus.pdf

RC409D Pitfalls in Post-op Imaging

Participants

Kumaresan Sandrasegaran, MD, Carmel, IN, (ksandras@iupui.edu) (*Presenter*) Nothing to Disclose

LEARNING OBJECTIVES

1) To understand the postoperative anatomy after pancreatic and bowel surgery. 2) To differentiate between expected anatomy and postoperative complications. 3) To differentiate between expected post-op anatomy and tumor recurrence.

ABSTRACT

Honored Educators

Presenters or authors on this event have been recognized as RSNA Honored Educators for participating in multiple qualifying educational activities. Honored Educators are invested in furthering the profession of radiology by delivering high-quality educational content in their field of study. Learn how you can become an honored educator by visiting the website at: <https://www.rsna.org/Honored-Educator-Award/>

Kumaresan Sandrasegaran, MD - 2013 Honored Educator

Kumaresan Sandrasegaran, MD - 2014 Honored Educator

Kumaresan Sandrasegaran, MD - 2016 Honored Educator

RC410

Thyroid and Neck Ultrasound (An Interactive Session)

Tuesday, Nov. 29 4:30PM - 6:00PM Room: E451A



AMA PRA Category 1 Credits™: 1.50
ARRT Category A+ Credits: 1.50

Participants

Sub-Events

RC410A Thyroid Nodules: When and What to Biopsy

Participants

Mary C. Frates, MD, Sharon, MA (*Presenter*) Nothing to Disclose

LEARNING OBJECTIVES

1) Discuss the sonographic characteristics that are associated with a high probability that a thyroid nodule is likely malignant or likely benign. 2) Gain an understanding of the rationale of the current guidelines for recommending thyroid fine needle aspiration.

ABSTRACT

This presentation will review the epidemiology of thyroid nodules and thyroid cancer and correlate the sonographic findings of thyroid nodules with the risk of malignancy. Analysis of the sonographic features of thyroid nodules has become the preeminent non-invasive tool for analyzing the risk of malignancy of thyroid nodules and aids in selecting which nodules should undergo fine needle aspiration (FNA). A number of sonographic features have shown a high specificity for the diagnosis of thyroid cancer and include marked hypoechoogenicity, the presence of microcalcifications, infiltrating or micro-lobulated borders, and a taller-wide shape. Sonographic patterns can also identify those nodules with a very low risk of malignancy, making biopsy unnecessary in low risk adults. The current guidelines for recommending thyroid fine needle aspiration and the timing of sonographic follow-up imaging will also be discussed.

RC410B Thyroid Elastography

Participants

Richard G. Barr, MD, PhD, Youngstown, OH (*Presenter*) Consultant, Siemens AG; Consultant, Koninklijke Philips NV; Research Grant, Siemens AG; Research Grant, SuperSonic Imagine; Speakers Bureau, Koninklijke Philips NV; Research Grant, Bracco Group; Speakers Bureau, Siemens AG; Consultant, Toshiba Corporation; Research Grant, Esaote SpA; Research Grant, B and K Ultrasound; Research Grant, Hitachi Aloka Ultrasound

LEARNING OBJECTIVES

1) Explain the difference between strain and shear wave elastography. 2) Understand the techniques to be able to perform thyroid ultrasound elastography. 3) Apply ultrasound elastography into routine clinical practice of thyroid nodules.

ABSTRACT

RC410C Parathyroid and Other Neck Masses including Lymph Nodes Post-Thyroidectomy

Participants

Michael D. Beland, MD, Providence, RI, (mbeland@lifespan.org) (*Presenter*) Consultant, Hitachi, Ltd

LEARNING OBJECTIVES

1) Identify abnormal parathyroid glands based on sonographic characteristics. 2) Develop an accurate differential for cystic lesions in the neck based on sonographic characteristics, lesion location and clinical circumstances. 3) List the most common etiologies of other solid and cystic lesions located in the neck. 4) Recognize the sonographic characteristics that suggest metastatic disease in cervical lymph nodes.

ABSTRACT

RC411

Advances and Updates in SPECT/CT

Tuesday, Nov. 29 4:30PM - 6:00PM Room: S504CD



AMA PRA Category 1 Credits™: 1.50
ARRT Category A+ Credits: 1.50

Discussions may include off-label uses.

Participants

Sub-Events

RC411A SPECT/CT in Musculoskeletal Diseases

Participants

Christopher J. Palestro, MD, New Hyde Park, NY (*Presenter*) Nothing to Disclose

LEARNING OBJECTIVES

1) Describe the role of SPECT/CT in the workup of patients with malignancy. 2) Describe the role of SPECT/CT in musculoskeletal infection. 3) Use SPECT/CT to improve the accuracy of radionuclide studies for diagnosing musculoskeletal diseases.

ABSTRACT

RC411B SPECT/CT in Endocrine and Neuroendocrine Disorders

Participants

Esma A. Akin, MD, Washington, DC (*Presenter*) Nothing to Disclose

LEARNING OBJECTIVES

1) Through clinical case examples, this activity aims to refresh knowledge of SPECT-CT applications with emphasis on neuroendocrine disorders as well as parathyroid imaging.

ABSTRACT

RC411C Role of SPECT/CT in Lung Scintigraphy

Participants

Michael M. Graham, MD, PhD, Iowa City, IA (*Presenter*) Nothing to Disclose

LEARNING OBJECTIVES

The learner will understand that the interpretation of SPECT V/Q imaging is much simpler than the commonly used PIOPED criteria of the past.

ABSTRACT

RC412

Principles and Applications of 4D Flow MRA

Tuesday, Nov. 29 4:30PM - 6:00PM Room: E353A



AMA PRA Category 1 Credits™: 1.50
ARRT Category A+ Credits: 1.50

FDA Discussions may include off-label uses.

Participants

James C. Carr, MD, Chicago, IL (*Moderator*) Research Grant, Astellas Group Research support, Siemens AG Speaker, Siemens AG Advisory Board, Guerbet SA

Sub-Events

RC412A Technical Principles and Solutions

Participants

Michael Markl, PhD, Chicago, IL (*Presenter*) Institutional research support, Siemens AG; Consultant, Circle Cardiovascular Imaging Inc;

LEARNING OBJECTIVES

1) Understand basic principles of 4D flow MRI data acquisition. 2) Identify different variants of 4D flow sequences. 3) Explain methods for the 3D visualization and quantification of cardiovascular flow data acquired by 4D flow MRI.

ABSTRACT

The intrinsic motion sensitivity of magnetic resonance imaging (MRI) can be used acquire and quantify blood flow. 4D flow MRI can be employed to encode blood flow velocities along all dimensions and offers the possibility to acquire spatially registered information on three-directional blood flow simultaneously with the 3D anatomic data within a single examination. As a result, 4D flow MRI permits the assessment of three-directional blood flow with full volumetric coverage of cardiac chambers or cardio- or neurovascular regions of interest such as the thoracic aorta or the large cerebral arterial and venous system. A benefit compared to traditional imaging techniques is related to the possibility to visualize cardiac and vascular hemodynamics and retrospectively quantify blood flow at any location of interest. In addition to the 3D visualization of complex cardiac and vascular flow patterns, quantitative flow analysis can provide quantitative information on the impact of cardio- or neurovascular pathologies on altered hemodynamics associated with the presence of cardio- and neurovascular disease. The presentation will 1) Introduce methodological aspects related to the measurement of 3D blood in the human body based on 4D flow MRI; 2) Illustrate the potential of 4D flow MRI for the 3D visualization and quantification of cardiovascular hemodynamics; 3) Provide examples of clinically relevant questions and how 4D flow can be used to improve cardiovascular diagnostics.

RC412B Clinical Workflow and Implementation

Participants

Shreyas S. Vasanawala, MD, PhD, Stanford, CA (*Presenter*) Research collaboration, General Electric Company; Consultant, Arterys Inc; Research Grant, Bayer AG;

LEARNING OBJECTIVES

1) To know components required to implement clinically 4D flow. 2) To know types of clinically relevant data that can be extracted from 4D flow. 3) Become familiar with approaches to integrating 4D flow into clinical protocols.

ABSTRACT

4D flow is a time resolved volumetric phase contrast MRI technique. This presentation will cover essential components required to implement 4D flow in a clinical setting, review types of clinically relevant data that can be extracted from 4D flow, and present several approaches to integrating 4D flow into clinical MRI protocols. Essential components include a pulse sequence and post-processing software. Data that can be extracted includes blood flow, cardiovascular function, and anatomy. Protocols can be greatly simplified with 4D flow, enabling a decoupling of image acquisition and interpretation, thereby enhancing efficiency of patient, technologist, and radiologist time.

RC412C Aortic Applications

Participants

Michael D. Hope, MD, San Francisco, CA, (michael.hope@ucsf.edu) (*Presenter*) Nothing to Disclose

LEARNING OBJECTIVES

1) Review clinical scenarios where aortic flow data may help to identify patients at high risk for progressive disease. 2) Assess current data on emerging clinical applications of 4D Flow in the aorta. 3) Review 4D Flow-derived parameters that show promise for risk stratification of aortic disease.

ABSTRACT

We will focus on the emerging aortic applications of multidimensional MR flow imaging (4D Flow). The techniques and hemodynamic biomarkers that we will discuss can be applied broadly throughout the cardiovascular system. Two key issues must be addressed when considering these applications: 1) clear advantages over conventional imaging and 2) matching advanced imaging capabilities with clinical questions that change the management of patients with aortic disease. The goal is to provide a unique understanding

of how abnormal flow promotes or exacerbates disease. This understanding, in turn, could allow patients to be risk-stratified based on flow, guide medical therapy, and identify new pathways to target with drug therapy and patients that may benefit from early intervention.

RC412D Abdominal Applications

Participants

Scott B. Reeder, MD, PhD, Madison, WI (*Presenter*) Institutional research support, General Electric Company Institutional research support, Bracco Group

LEARNING OBJECTIVES

1) Understand the underlying principles of phase velocity MRA. 2) Be familiar with the currently available methods for phase velocity MRA. 3) Be familiar with important applications and examples of phase velocity MRA. 4) Understand current limitations and pitfalls associated with phase velocity MRA. 5) Be familiar with emerging applications of 4D flow MRI in the abdomen.

ABSTRACT

RC412E Cerebrovascular Applications

Participants

Patrick A. Turski, MD, Madison, WI (*Presenter*) Institutional Research support, General Electric Company

LEARNING OBJECTIVES

1) Develop a clinical protocol to generate 4DFlow images of the intracranial circulation. 2) Recognize the flow features of intracranial arterial stenosis and aneurysms. 3) Apply 4DFlow to precisely define AVM hemodynamics. 4) Develop an integrated approach to venous outflow assessment.

ABSTRACT

Accelerated 4DFlow MRI acquisition and reconstruction methods are now available to provide high resolution exams in clinically relevant imaging times. 4DFlow MRI not only provides images of vascular morphology but also acquires quantitative measurements of velocity throughout the imaging volume. Hemodynamic parameters such as flow volume, relative wall shear stress, streamlines, vorticity and pressure gradients can be derived from the velocity data. The combination of anatomical imaging, lumen visualization and physiological data derived from accelerated 4DFlow MRI augments the characterization of intracranial arterial stenosis, aneurysms, vascular malformations and dural sinus pathology. This presentation provides an update for radiologists interested in cerebrovascular applications of 4DFlow MRI.

RC414

Interventional Course (An Interactive Session)

Tuesday, Nov. 29 4:30PM - 6:00PM Room: S404CD



AMA PRA Category 1 Credits™: 1.50
ARRT Category A+ Credits: 1.50

Participants

Steven M. Zangan, MD, Chicago, IL (*Presenter*) Nothing to Disclose
Rakesh C. Navuluri, MD, Chicago, IL, (IR@uchicago.edu) (*Presenter*) Nothing to Disclose
Jafar Golzarian, MD, Minneapolis, MN (*Presenter*) Chief Medical Officer, EmboMedics Inc

LEARNING OBJECTIVES

1) Recognize vascular and non-vascular conditions and their image-guided treatment in the chest, abdomen and pelvis. Please bring your charged mobile wireless device (phone, tablet or laptop) to participate.

ABSTRACT

RC415

Digital Breast Tomosynthesis

Tuesday, Nov. 29 4:30PM - 6:00PM Room: E353B



AMA PRA Category 1 Credits™: 1.50
ARRT Category A+ Credits: 1.50

Participants

Cherie M. Kuzmiak, DO, Chapel Hill, NC, (Cherie_kuzmiak@med.unc.edu) (*Moderator*) Research Grant, FUJIFILM Holdings Corporation;

LEARNING OBJECTIVES

ABSTRACT

Sub-Events

RC415A The Nuts & Bolts of DBT Technology

Participants

Stamatia V. Destounis, MD, Scottsville, NY, (sdestounis@ewbc.com) (*Presenter*) Nothing to Disclose

LEARNING OBJECTIVES

1) Describe the DBT technology and history of design, testing and implementation. 2) Review important relevant literature- past and current. 3) Provide overview of implementation into a clinical practice. 4) Assess advantages and disadvantages of DBT.

ABSTRACT

RC415B Implementing DBT into Your Practice

Participants

Jocelyn A. Rapelyea, MD, Washington, DC (*Presenter*) Speakers Bureau, General Electric Healthcare Company; Research consultant, Q-view LLC.; Research consultant, QTUS

RC415C DBT-Directed Breast Biopsy

Participants

Liane E. Philpotts, MD, New Haven, CT, (liane.philpotts@yale.edu) (*Presenter*) Nothing to Disclose

LEARNING OBJECTIVES

1) Define the work-up and appropriate case selection for DBT stereotactic biopsy or needle localization. 2) Outline the basic steps in performing DBT-stereotactic biopsy and needle localization. 3) Discuss the challenges and limitations of DBT-stereo and provide trouble-shooting tips. 4) Review histological concordance and appropriate management options. 5) Discuss recent literature of performance outcomes.

ABSTRACT

Mitigation of Litigation (Sponsored by the RSNA Professionalism Committee)

Tuesday, Nov. 29 4:30PM - 6:00PM Room: N230B

PRAMA PRA Category 1 Credits™: 1.50
ARRT Category A+ Credits: 1.50**Participants**David M. Yousem, MD, Baltimore, MD, (dyousem1@jhu.edu) (*Moderator*) Royalties, Reed Elsevier; Royalties, Oakstone Publishing, LLC**LEARNING OBJECTIVES**

1) To understand the implications of the four components of a medical negligence case: a. duty to the patient, b. breach in the standard of care, c. causation between breach and harm, and d) damages (economic, pain and suffering, punitive). 2) To reflect on the patient and physician experience in going through a malpractice trial. 3) To apply practice habits that reduce the chance that you will be the subject of a medical malpractice suit, enhance patient safety, increase the likelihood of good outcomes, and prevent frivolous lawsuits. 4) To learn dos and don'ts once sued. 5) To comprehend the role of medical experts in establishing the standard of care and ensuring an equitable and fair judicial process. 6) To discuss ethics of testifying as expert.

ABSTRACT

A medical malpractice case requires establishing four components of the case: 1) the duty of the physician to the patient, 2) a breach in the standard of care (what a reasonably prudent person would do in a similar situation), 3) the establishment that the breach caused the subsequent harm to the patient, and 4) damages to the patient. Most malpractice cases are won or lost in determining whether a deviation in the standard of care occurred and whether that deviation truly caused the patient's damages. Expert witnesses are commonly employed to help establish the standard of care for the setting in question, although some experts also provide guidance as to the expected economic costs that will be incurred by the damaged plaintiff. Because of the high cost of medicolegal litigation, most cases that have minor damages never come to court but may be dropped or settled out of court. Because of the vagaries of a lay jury, many substantive cases are also settled out of court. One can reduce the chances that one will be sued by being cognizant of professional standards and guidelines that dictate certain behaviors such as timeliness of reporting, communication of important/relevant/critical/unexpected findings, and establishing good peer review systems that identify errors before they occur. Applying behaviors or work habits that enhance accuracy and efficiency and good practice patterns while also developing good physician-patient relationships are helpful for mitigation of litigation. Effective expert witnesses can help a lay jury understand the nuances of a case and establishing whether negligence has occurred. The credibility of expert witnesses is enhanced when they are impartial, do blinded unbiased reads, understand the specific practice patterns in which the defendant physicians are employed, and can explain complex issues to non-medical jury members.

Sub-Events**RC416A Elements of Legal Suits: Duty, Breach, Causation, Damages and the Links between Them****Participants**Kelly Yousem, JD, Owings Mills, MD (*Presenter*) Nothing to Disclose
Rosemary Schnall, Philadelphia, PA (*Presenter*) Stockholder, Johnson & Johnson**LEARNING OBJECTIVES**

View learning objectives under main course title.

ABSTRACT

The purpose of this presentation is to understand the main elements of a medical malpractice lawsuit. You will gain an understanding of the process as well as the legal reasoning behind litigation objectives. Additionally, we will discuss the standards of proof required and how expert witnesses are a necessary requirement in this process, for both Plaintiffs and Defendants.

RC416B Mitigation of Litigation: What the Radiologist Can Do To Reduce the Risk of Being Named in a Lawsuit**Participants**Michael M. Raskin, MD, JD, Tamarac, FL, (drraskin@bellsouth.net) (*Presenter*) Nothing to Disclose**LEARNING OBJECTIVES**

1) Recognize the two broad categories of radiologic errors: perception and interpretation.. 2) Analyze and compare specific actions to reduce errors. 3) Understanding why failure to communicate is one of the greatest problems facing radiologists today. 4) Apply survival strategies to mitigate the risk of being named in a law suit.

ABSTRACT

Failure to diagnose and failure to communicate are the two most frequent reasons why a radiologist is named in a lawsuit. Perception and interpretation errors will be analyzed and specific actions to reduce these errors will be compared. Communication errors of reporting critical results directly impacts on the ability of the radiologist to deliver quality patient care. The courts have consistently held that timely communication may be as important as the diagnosis itself. Radiology is so advanced in imaging technology but not in communicating imaging findings. Specific examples of communication errors will be discussed and analyzed. Potential solutions involving closed-loop communication will be addressed. Finally, a plan for implementation of specific strategies will be suggested.

Active Handout: Michael Mester Raskinhttp://abstract.rsna.org/uploads/2016/11/002102/ACTIVE_RC416B_Mitigation_of_Litigation_Handout.pdf

RC416C Expert Witness Testimony: Ethics and Qualifications for Being an Expert Witness

Participants

Ronald L. Eisenberg, MD, JD, Boston, MA, (rleisenb@bidmc.harvard.edu) (*Presenter*) Nothing to Disclose

LEARNING OBJECTIVES

1) Understand the role of an expert witness in malpractice lawsuits and ethical issues to consider to become a more effective and valuable expert witness.

ABSTRACT

Expert witnesses play essential roles in malpractice lawsuits. Radiologists considering becoming expert witnesses need to clearly understand that their duty is to provide honest opinions on technical issues to educate members of the jury so that they can render a more accurate verdict, rather than being advocates for the party that engaged them.

Honored Educators

Presenters or authors on this event have been recognized as RSNA Honored Educators for participating in multiple qualifying educational activities. Honored Educators are invested in furthering the profession of radiology by delivering high-quality educational content in their field of study. Learn how you can become an honored educator by visiting the website at: <https://www.rsna.org/Honored-Educator-Award/>

Ronald L. Eisenberg, MD, JD - 2012 Honored Educator

Ronald L. Eisenberg, MD, JD - 2014 Honored Educator

RC417

Emerging Technologies: Prostate Cancer Imaging & Management

Tuesday, Nov. 29 4:30PM - 6:00PM Room: S505AB



AMA PRA Category 1 Credits™: 1.50
ARRT Category A+ Credits: 1.50

Participants

Peter L. Choyke, MD, Rockville, MD, (pchoyke@nih.gov) (*Moderator*) Researcher, Koninklijke Philips NV; Researcher, General Electric Company; Researcher, Siemens AG; Researcher, iCAD, Inc; Researcher, Aspyrian Therapeutics, Inc; Researcher, ImaginAb, Inc; Researcher, Aura Biosciences, Inc

LEARNING OBJECTIVES

1) Understand current issues in prostate cancer relevant to imaging. 2) Understand the role of emerging technologies in the imaging and management of prostate cancer.

ABSTRACT

Prostate cancer is a major health issue. Imaging has made great strides in the last decade including the use of multiparametric MRI, MR-ultrasound fusion biopsies and most recently PET scanning. This refresher course explores emerging technologies in prostate cancer imaging and management.

Sub-Events

RC417A Introduction to Imaging in Prostate Cancer

Participants

Peter L. Choyke, MD, Rockville, MD, (pchoyke@nih.gov) (*Presenter*) Researcher, Koninklijke Philips NV; Researcher, General Electric Company; Researcher, Siemens AG; Researcher, iCAD, Inc; Researcher, Aspyrian Therapeutics, Inc; Researcher, ImaginAb, Inc; Researcher, Aura Biosciences, Inc

LEARNING OBJECTIVES

1) Understand the impact of new screening guidelines on imaging of prostate cancer. 2) Understand the issues facing clinicians treating prostate cancer.

ABSTRACT

This talk will review the current status of screening for prostate cancer and how stage migration is beginning to be seen. The problems of early detection, early recurrence and early metastases will be discussed. This talk will serve as a starting off point for the subsequent talks on new technologies.

RC417B Next Generation Prostate MRI

Participants

Baris Turkbey, MD, Bethesda, MD, (turkbeyi@mail.nih.gov) (*Presenter*) Nothing to Disclose

LEARNING OBJECTIVES

1) Understand current status and uses of multi-parametric MRI. 2) Understand role of MRI in assessment of prostate cancer aggressiveness and tumor heterogeneity. 3) Understand role of computer aided diagnosis systems in evaluation of prostate cancer aggressiveness and tumor heterogeneity.

ABSTRACT

RC417C Molecular Prostate Imaging: Chemistry to Clinic

Participants

Martin G. Pomper, MD, PhD, Baltimore, MD (*Presenter*) Shareholder, CTS, Inc; Board Member, CTS, Inc; Research Grant, CTS, Inc; Advisor, CTS, Inc; Institutional license agreement, Progenics Pharmaceuticals, Inc; Institutional license agreement, Advanced Accelerator Applications SA; Institutional license agreement, LI-COR, Inc; Institutional license agreement, BIND Therapeutics, Inc

LEARNING OBJECTIVES

View learning objectives under the main course title.

RC417D PET/MRI: Is Prostate Cancer a Perfect Fit?

Participants

Peter L. Choyke, MD, Rockville, MD, (pchoyke@nih.gov) (*Presenter*) Researcher, Koninklijke Philips NV; Researcher, General Electric Company; Researcher, Siemens AG; Researcher, iCAD, Inc; Researcher, Aspyrian Therapeutics, Inc; Researcher, ImaginAb, Inc; Researcher, Aura Biosciences, Inc

LEARNING OBJECTIVES

1) Understand the potential value of PET/MRI in prostate cancer.

ABSTRACT

PET/MRI offers the sensitivity and specificity of PET with the high contrast resolution of MRI. In the prostate this can be very useful in identifying prostate cancers and recurrent disease after treatment. This talk will review the various features of PET/MRI that make prostate cancer a "perfect fit" for it.

RC417E Hyperpolarized C-13 MR Molecular Imaging of Prostate Cancer

Participants

Daniel B. Vigneron, PhD, San Francisco, CA (*Presenter*) Research Grant, General Electric Company; Research Grant, GlaxoSmithKline

LEARNING OBJECTIVES

View learning objectives under the main course title.

RC418

Deconstructing Tumors with Imaging

Tuesday, Nov. 29 4:30PM - 6:00PM Room: S404AB



AMA PRA Category 1 Credits™: 1.50
ARRT Category A+ Credits: 1.50

FDA Discussions may include off-label uses.

Participants

Sub-Events

RC418A Imaging Proteomics Genomics Interaction - New Frontiers Ahead

Participants

Evis Sala, MD, PhD, New York, NY, (salae@mskcc.org) (*Presenter*) Nothing to Disclose

LEARNING OBJECTIVES

1) Learn the major differences between proteome and genome data. 2) Discuss how the proteome signal might be correlated with imaging features. 3) Provide insights into imaging of proteomics-genomics interaction.

ABSTRACT

Honored Educators

Presenters or authors on this event have been recognized as RSNA Honored Educators for participating in multiple qualifying educational activities. Honored Educators are invested in furthering the profession of radiology by delivering high-quality educational content in their field of study. Learn how you can become an honored educator by visiting the website at: <https://www.rsna.org/Honored-Educator-Award/>

Evis Sala, MD, PhD - 2013 Honored Educator

RC418B Imaging of Angiogenesis: What Do Vessels Tell Us about Tumors?

Participants

Roberto Garcia Figueiras, MD, PhD, Santiago de Compostela, Spain, (roberto.garcia.figueiras@sergas.es) (*Presenter*) Nothing to Disclose

LEARNING OBJECTIVES

1) Improve basic knowledge and skills relevant to the evaluation of angiogenesis in clinical practice. 2) Get an overview of the most relevant functional imaging modalities that are available. 3) Apply the most appropriate imaging technique for evaluating tumor angiogenic phenotype and tumor response. 4) Understand imaging limitations and technical requirements.

ABSTRACT

Tumor angiogenesis is the process whereby new blood vessels are formed in order to supply nutrients and oxygen to support the growth of tumors. Angiogenesis is a key cancer hallmark and an important target for cancer therapy. This lecture reviews the biological basis behind imaging features and the different imaging modalities used to assess the status of tumor neovasculature in vivo and tumor vascular changes secondary to different therapies.

Handout: Roberto Garcia Figueiras

http://abstract.rsna.org/uploads/2016/16000386/HANDOUT_RC418B.pdf

RC418C Multiparametric Imaging of Bone Marrow Metastatic Disease

Participants

Anwar R. Padhani, MD, FRCR, Northwood, United Kingdom, (anwar.padhani@stricklandscanner.org.uk) (*Presenter*) Advisory Board, Siemens AG; Speakers Bureau, Siemens AG; Researcher, Siemens AG; Speakers Bureau, Johnson & Johnson

LEARNING OBJECTIVES

1) To become familiar with the normal appearances of bone marrow on PET/MRI/CT scans and how these reflect underlying biologic properties. 2) To understand the biologic mechanisms responsible for osteoblastic and osteolytic lesions in malignancy settings. 3) To explain how imaging appearances of normal and pathologic bone marrow reflect therapy impacts. 4) To innumerate the professional challenges for implementing multiparametric imaging in bone therapy monitoring.

ABSTRACT

Honored Educators

Presenters or authors on this event have been recognized as RSNA Honored Educators for participating in multiple qualifying educational activities. Honored Educators are invested in furthering the profession of radiology by delivering high-quality educational content in their field of study. Learn how you can become an honored educator by visiting the website at: <https://www.rsna.org/Honored-Educator-Award/>

Anwar R. Padhani, MD, FRCR - 2012 Honored Educator

RC418D Imaging Tumor Metabolism with Hyperpolarized MRI

Participants

Kayvan Keshari, PhD, New York, NY (*Presenter*) Nothing to Disclose

LEARNING OBJECTIVES

1) Comprehend the basic principles of hyperpolarized MRS. 2) Assess the potential of using hyperpolarized probes to study cancer metabolism. 3) Assess the changes in cancer metabolism across multiple tumor types.

ABSTRACT

Oncogenic transformation has been shown to have a dramatic impact on the metabolic state of the cell. Recent work has shown that hyperpolarization of endogenous substrates can be used to trace metabolism in the setting of cancer, non-invasively in vivo. In this educational lecture, we will discuss the use of hyperpolarized ¹³C molecules in the setting of cancer imaging, spanning a number of molecules, which have been used preclinically as well as hyperpolarized pyruvate which has recently been used in the clinic.

RC420

Imaging Evaluation of Post-Radiation Therapy Normal Tissue Effects

Tuesday, Nov. 29 4:30PM - 6:00PM Room: S104A



AMA PRA Category 1 Credits™: 1.50
ARRT Category A+ Credits: 1.50

Participants

Christina I. Tsien, MD, Saint Louis, MO (*Moderator*) Speaker, Merck & Co, Inc

Sub-Events

RC420A Post-radiation Therapy CNS Imaging

Participants

Michael D. Chan, MD, Winston-Salem, NC (*Presenter*) Advisory Board, NovoCure Ltd
Tammie S. Benzinger, MD, PhD, Saint Louis, MO, (benzingert@wustl.edu) (*Presenter*) Research Grant, Eli Lilly and Company
Investigator, Eli Lilly and Company Investigator, F. Hoffmann-La Roche Ltd

RC420B Post-radiation Therapy Head and Neck Imaging

Participants

Allen M. Chen, MD, Los Angeles, CA (*Presenter*) Nothing to Disclose
Rajan Jain, MD, Hartsdale, NY (*Presenter*) Consultant, Cancer Panels; Royalties, Thieme Medical Publishers, Inc

LEARNING OBJECTIVES

1) Discuss the role of surveillance imaging in identification of radiation induced changes in normal tissue, so that these changes are not misinterpreted as evidence of persistent or recurrent tumor. 2) Describe imaging characteristics of radiation injury to various tissues including visceral mucosal space, salivary glands, bones and vascular structures in the neck as well as surrounding organs such as brain, skull base and lungs. 3) Discuss the advantage of early identification of these using case-based approach.

ABSTRACT

Radiation therapy for head and neck cancers can cause adverse effects and toxicity to the normal tissues in the irradiated regions. This does not only lead to a variety of comorbidities, but also present a challenging and complex appearance on surveillance imaging studies. Timely identification of some of these adverse effects can improve patient survival and quality of life.

RC420C Post-radiation Therapy Gynecologic Imaging

Participants

Akila N. Viswanathan, MD, Baltimore, MD (*Presenter*) Nothing to Disclose
Kathryn J. Fowler, MD, Chesterfield, MO (*Presenter*) Nothing to Disclose

LEARNING OBJECTIVES

1) Review and demonstrate the imaging findings of gynecologic malignancies following radiation therapy. 2) Review the imaging modalities used to assess response.

ABSTRACT

RC421

Advances in CT: Technologies, Applications, Operations-CT Operation

Tuesday, Nov. 29 4:30PM - 6:00PM Room: S103AB

CT **PH** **SQ**

AMA PRA Category 1 Credits™: 1.50
ARRT Category A+ Credits: 1.50

FDA Discussions may include off-label uses.

Participants

Ehsan Samei, PhD, Durham, NC (*Coordinator*) Research Grant, General Electric Company; Research Grant, Siemens AG
Norbert J. Pelc, ScD, Stanford, CA (*Coordinator*) Research support, General Electric Company; Research support, Koninklijke Philips NV; Consultant, Varian Medical Systems, Inc; Consultant, NanoX; Scientific Advisory Board, RefleXion Medical Inc; Scientific Advisory Board, Prismatic Sensors AB; Medical Advisory Board, OurCrowd, LP ;

Sub-Events

RC421A Statistical and Iterative Reconstruction and Image Domain Denoising

Participants

Norbert J. Pelc, ScD, Stanford, CA (*Presenter*) Research support, General Electric Company; Research support, Koninklijke Philips NV; Consultant, Varian Medical Systems, Inc; Consultant, NanoX; Scientific Advisory Board, RefleXion Medical Inc; Scientific Advisory Board, Prismatic Sensors AB; Medical Advisory Board, OurCrowd, LP ;

RC421B Protocol Optimization and Management

Participants

Mannudeep K. Kalra, MD, Boston, MA, (mkalra@mgh.harvard.edu) (*Presenter*) Technical support, Siemens AG; Technical support, Medical Vision

LEARNING OBJECTIVES

1.) CT protocol optimization begins with justification of clinical indication and proceeds to tailoring of scan parameters according to clinical region of interest, clinical indication, and patient size. Taking a nuanced and stratified approach to protocol stratification helps in the optimization process. 2) CT protocol management is a team effort involving attention to CT image quality and associated radiation doses. Medical physicists, radiologists, and CT technologists have a common responsibility in CT protocol optimization and management.

ABSTRACT

Optimization and management of CT protocols are joint responsibilities of medical physicists, radiologists and CT technologists. Attributes of optimized CT protocols include adaptation of image quality and radiation dose through suitable choice of scan parameters based on body area of interest, clinical indication, presence of prior imaging, patient size, and need for contrast enhancement. In an ideal practice, scan protocols must be divided according to the area of interest, and then clinical indication for which CT has been requested. Management of CT protocols must include frequent audits of image quality and radiation dose monitoring to ensure that good practices are maintained.

RC421C Dose Monitoring and Analytics

Participants

Joshua Wilson, PhD, Durham, NC, (joshua.wilson@duke.edu) (*Presenter*) Nothing to Disclose
Ehsan Samei, PhD, Durham, NC (*Presenter*) Research Grant, General Electric Company; Research Grant, Siemens AG

LEARNING OBJECTIVES

1) Describe conventional radiation dose monitoring workflows and analytics. 2) Critique the current shortcomings and future potential value of dose monitoring solutions. 3) Identify opportunities improving clinical operations and consistency with dose monitoring.

ABSTRACT

Recent legislative and accreditation requirements have driven rapid development and implementation of radiation dose monitoring platforms. Multiple solutions are available that require financial commitments and oversight. Once requirements are met, how can institutions derive added-value from their monitoring program by improving the quality of their clinical performance? Global alert thresholds, the standard in commercial products, naïve to system model and patient size have limited value. Setting a threshold presupposes a clinically-relevant level is known. For an arbitrary level, appropriately-dosed obese patients triggered false alerts, but over-dosed small patients were missed. Numerous study parameters must be retained because chronologic trends, the industry standard, are rarely useful without controlling for other moderators. Dashboards must be interactive enabling dynamic drill-down into cohorts. Dose databases require curation tools and maintenance, largely absent from all solutions, because wrong information will be inadvertently entered, and the utility of the analytics is entirely dependent on the data quality. Dose monitoring can satisfy requirements with global alert thresholds and patient dose records, but a program's real value is in optimizing patient-specific protocols, balancing image quality trade-offs that dose-reduction strategies promise, and improving the performance and consistency of a clinical operation.

Imaging for Personalized Medicine: Abdomen

Tuesday, Nov. 29 4:30PM - 6:00PM Room: S102C



AMA PRA Category 1 Credits™: 1.50
ARRT Category A+ Credits: 1.50

Participants

Kristy K. Brock, PhD, Houston, TX (*Moderator*) License agreement, RaySearch Laboratories AB; Development agreement, Varian Medical Systems, Inc;

ABSTRACT

The use of imaging and other biomarkers to increase the efficacy of treatment and decrease the risk of toxicity increased in the abdomen. Functional imaging and serum-based biomarkers can enable a more detailed understanding of the tumor, its characteristics, and early indications of its response to therapy. In addition, they can also be utilized to assess an individual patients risk for toxicity, enabling a personalize approach to radiotherapy. These advanced imaging techniques can be combined with anatomical information to generate high precision treatment plans which can be adapted over the course of treatment to account for identified uncertainties, changes, and deviations which may compromise the delivery of the intended treatment or identify the ability to re-optimize treatment to improve the therapeutic ration. In this session, technical and clinical concepts will be described to design and deliver personalized radiotherapy in the abdomen. Technical concepts will include incorporation of multi-modality imaging for treatment planning, image guidance at treatment, and functional and anatomical adaption. Clinical concepts will include functional targeting, clinical goals, and toxicity risks.

Sub-Events

RC422A IGRT and Anatomical Adaptation

Participants

Kristy K. Brock, PhD, Houston, TX (*Presenter*) License agreement, RaySearch Laboratories AB; Development agreement, Varian Medical Systems, Inc;

LEARNING OBJECTIVES

1) Describe the processes necessary for the safe and accurate integration of multi-modality imaging for treatment planning. 2) Understand the role of image guidance for abdominal radiotherapy. 3) Illustrate methods to perform functional and anatomical adaptation in the abdomen.

ABSTRACT

The use of imaging and other biomarkers to increase the efficacy of treatment and decrease the risk of toxicity increased in the abdomen. Functional imaging and serum-based biomarkers can enable a more detailed understanding of the tumor, its characteristics, and early indications of its response to therapy. In addition, they can also be utilized to assess an individual patients risk for toxicity, enabling a personalize approach to radiotherapy. These advanced imaging techniques can be combined with anatomical information to generate high precision treatment plans which can be adapted over the course of treatment to account for identified uncertainties, changes, and deviations which may compromise the delivery of the intended treatment or identify the ability to re-optimize treatment to improve the therapeutic ration. In this session, technical and clinical concepts will be described to design and deliver personalized radiotherapy in the abdomen. Technical concepts will include incorporation of multi-modality imaging for treatment planning, image guidance at treatment, and functional and anatomical adaption. Clinical concepts will include functional targeting, clinical goals, and toxicity risks.

RC422B Functional Targeting, Clinical Goals, and Toxicity Risks

Participants

Cullen M. Taniguchi, MD, PhD, Houston, TX (*Presenter*) Nothing to Disclose

LEARNING OBJECTIVES

1) Review methods to obtain, process and analyze tissue and serum based biomarkers for abdominal tumors. 2) Describe current dose/fractionation regimens as well as normal tissue constraints utilized in treating abdominal tumors. 3) Explain potential advantages of assessing treatment response with MRI and quantitative PET/SPECT (PERCIST) imaging over CT based response (RECIST) in abdominal tumors.

ABSTRACT

In order to deliver personalized radiation therapy in abdominal tumors, it is important to understand the methods used to obtain, analyze, and interpret serum and tissue based biomarkers. Most research to date has focused on identifying specific biomarkers used to personalize systemic or targeted therapies. Radiation-specific biomarkers are emerging and may eventually be used to determine whether radiation is indicated or identify specific radiation sensitizers for use in abdominal tumors. Radiation therapy planning has historically used computed tomography (CT)-based imaging. Molecular imaging using hybrid positron emission tomography (PET)/CT scanning or single-photon emission computed tomography (SPECT) imaging and functional magnetic resonance imaging (MRI) has provided new insights into the precise identification of gross tumor volume (GTV) and clinical tumor volume (CTV) and has provided response information during and after therapy. The effective use of PET/SPECT and MRI in clinical practice, however, requires an appreciation of the unique challenges inherent to these modalities. Fundamental physical issues of limited spatial resolution relative to the biological process, partial volume effects, image misregistration, motion management, and edge delineation must be carefully considered and can differ by agent or the method applied. Integration of PET/SPECT and MRI imaging into multicenter clinical trials and clinical practice can be particularly challenging due to differences in imaging protocols, machines, and anatomy. Imaging protocols that clearly outline scan and fusion parameters are crucial. Further,

interpretation of tumor response should be standardized, and scans should be obtained at consistent time intervals. In addition, it is important to consider novel tracers of tumor biology (e.g. hypoxia, proliferation, apoptosis) beyond the commonly used radiotracers. In this session, we will discuss these applications and challenges as well as provide guidance on how to integrate PET/SPECT/MRI into radiation treatment planning and assessing treatment response. Finally, we will evaluate common dose and fractionation regimens as well as established dose constraints used in treating abdominal tumors with conventional and stereotactic body radiation therapy.

RC423

MR Safety

Tuesday, Nov. 29 4:30PM - 6:00PM Room: S402AB

MR **PH** **SQ**

AMA PRA Category 1 Credits™: 1.50
ARRT Category A+ Credits: 1.50

FDA Discussions may include off-label uses.

Participants

Matthew A. Bernstein, PhD, Rochester, MN (*Director*) Research collaboration, General Electric Company;
Yunhong Shu, PhD, Rochester, MN (*Director*) Nothing to Disclose

LEARNING OBJECTIVES

1) List several MR Safety incidents and describe their root causes. 2) List a variety of commonly implanted Neurostimulators and MR Conditional Pacemakers. 3) Identify potential risks associated with scanning patients implanted with these devices using MRI in the clinical environment. 4) Describe special MR Safety hazards present in the MR interventional environment, and identify countermeasures to reduce the associated risks. 5) Describe MR Safety guidelines and recommendations to prevent accidents and injuries.

Handout: Yunhong Shu

[http://abstract.rsna.org/uploads/2016/16001093/MR safety - neurostimulator -handouts.docx](http://abstract.rsna.org/uploads/2016/16001093/MR%20safety%20-%20neurostimulator%20-%20handouts.docx)

Sub-Events

RC423A Case Review of Real MR Safety Incidents

Participants

Armen Kocharian, PhD, Houston, TX, (akocharian@houstonmethodist.org) (*Presenter*) Research collaboration, General Electric Company

LEARNING OBJECTIVES

1) Identify main safety risk factors from incident reviews at MR Imaging sites. 2) Assess and address the MRI safety potential risks. 3) Implement preventive measures in clinical practice for improved standard of care.

Active Handout: Armen Kocharian

[http://abstract.rsna.org/uploads/2016/16001094/RC423A Case Review of Real MR Safety Incidents.pdf](http://abstract.rsna.org/uploads/2016/16001094/RC423A%20Case%20Review%20of%20Real%20MR%20Safety%20Incidents.pdf)

RC423B MRI Safety of Deep Brain and Other Simulators

Participants

Yunhong Shu, PhD, Rochester, MN (*Presenter*) Nothing to Disclose

LEARNING OBJECTIVES

1) List a variety of commonly implanted neurostimulators. 2) Understand the importance of MRI as a diagnostic imaging tool for patient with implanted neurostimulator. 3) Identify the potential risks associated with scanning patient with implanted neurostimulator using MRI. 4) Describe MR safety guidelines and recommendations to prevent accidents and injuries.

ABSTRACT

A neurostimulator is a surgically placed programmable device. It delivers mild electrical signals to the targeted area through thin wires. The purpose is usually for pain relief or improving patient's ability to perform daily activities. There are a variety of commonly used neurostimulators include deep brain stimulator, spinal cord stimulator, vagus nerve stimulator and sacral nerve stimulator. MRI is clinically important for post-implantation evaluation. It is very likely that a patient will require an MRI scan after the neurostimulator is implanted. The risks of performing MRI on patients with neurostimulators are related to static magnetic field, gradient magnetic field and the RF field. The talk will provide an imaging physics overview on the potential risks and make recommendations for MR imaging safety procedure.

Handout: Yunhong Shu

[http://abstract.rsna.org/uploads/2016/16001095/MR safety - neurostimulator -handouts.docx](http://abstract.rsna.org/uploads/2016/16001095/MR%20safety%20-%20neurostimulator%20-%20handouts.docx)

RC423C MRI Conditional Pacemakers, What to Do?

Participants

Anshuman Panda, PhD, Scottsdale, AZ (*Presenter*) Nothing to Disclose

Active Handout: Anshuman Panda

[http://abstract.rsna.org/uploads/2016/16001096/RC423C Panda RSNA 2016 MR Conditional Pacemakers.pdf](http://abstract.rsna.org/uploads/2016/16001096/RC423C%20Panda%20RSNA%202016%20MR%20Conditional%20Pacemakers.pdf)

RC423D MRI Safety in the MR-Guided Interventional Environment

Participants

Krzysztof Gorny, PhD, Rochester, MN (*Presenter*) Nothing to Disclose

LEARNING OBJECTIVES

Presentation will include overview of interventional MRI practice within context of generally accepted principles of MRI safety. Description of the practice will be provided including example protocol for safety testing of previously unlabeled equipment considered for potential use inside Zone 4.

ABSTRACT

Handout:Krzysztof Gorny

[http://abstract.rsna.org/uploads/2016/16001097/Safety in the MRI hand out.pdf](http://abstract.rsna.org/uploads/2016/16001097/Safety%20in%20the%20MRI%20hand%20out.pdf)

RC424

How to Use the STARD (Standards for Reporting Diagnostic Accuracy Studies) and PRISMA (Preferred Reporting Items for Systematic Reviews and Meta-Analyses) Reporting Guidelines to Optimize Your Manuscript for Publication in Radiology

Tuesday, Nov. 29 4:30PM - 6:00PM Room: S502AB



AMA PRA Category 1 Credits™: 1.50
ARRT Category A+ Credits: 1.50

Participants

Herbert Y. Kressel, MD, Boston, MA (*Moderator*) Stockholder, Pfizer Inc; Stockholder, GlaxoSmithKline plc

LEARNING OBJECTIVES

1) To familiarize attendees with reasons why quality improvement initiatives are important for the dissemination of published research. 2) To discuss the components of the STARD criteria and why these are important for studies of diagnostic accuracy. 3) To describe the PRISMA statement and why these make up key components of high quality systematic reviews. 4) To enable authors to improve completeness of reporting in their submitted manuscripts, to demonstrate study quality and thus enhance the likelihood that their manuscripts will be favorably reviewed when submitted to journals such as Radiology for publication.

ABSTRACT

The purpose of this session is to describe STARD and PRISMA, two documents that aim to improve scientific study quality by improving reporting. The Editor-in-Chief of Radiology, Dr. Herbert Kressel, Professor Radiology at Harvard Medical School, will introduce the importance of quality metrics in scientific research. Dr. Patrick Bossuyt, Professor of Clinical Epidemiology at University of Amsterdam, and one of the original authors of the STARD manuscript, who recently worked to revise STARD, will discuss the components of the STARD criteria and why these are important for studies of diagnostic accuracy. Dr. Matthew McInnes, Associate Professor of Radiology at University of Ottawa, and our 2014 Eyer Editorial fellow will describe the PRISMA statement and the important key components of high quality systematic reviews. Dr. Deborah Levine, Professor of Radiology at Harvard Medical School and the Senior Deputy Editor of Radiology will describe how to put all of this information together into your final study plan and written manuscript. Our goal is to enable authors to improve completeness of reporting in their submitted manuscripts, to demonstrate study quality and thus enhance the likelihood that their manuscripts will be favorably reviewed when submitted for publication to Radiology as well as to other biomedical journals. Please see our publication information for authors at : <http://pubs.rsna.org/page/radiology/pia> as well as information about checklists at : <http://pubs.rsna.org/page/radiology/pia/checklists>

URL

<http://pubs.rsna.org/page/radiology/pia>

Sub-Events

RC424A Why Reporting Guidelines are Useful

Participants

Herbert Y. Kressel, MD, Boston, MA (*Presenter*) Stockholder, Pfizer Inc; Stockholder, GlaxoSmithKline plc

LEARNING OBJECTIVES

View learning objectives under the main course title.

RC424B STARD (Standards for Reporting Diagnostic Accuracy)

Participants

Patrick M. Bossuyt, PhD, Amsterdam, Netherlands, (p.m.bossuyt@amc.nl) (*Presenter*) Nothing to Disclose

LEARNING OBJECTIVES

View learning objectives under the main course title.

Active Handout: Patrick M. M. Bossuyt

http://abstract.rsna.org/uploads/2016/16001981/RC424B_RSNA_2016_-_Bossuyt_-_STARD_-_Handout.pdf

RC424C PRISMA (Preferred Reporting Items for Systematic Reviews and Meta-Analyses)

Participants

Matthew D. McInnes, MD, FRCPC, Ottawa, ON, (mmcinn@toh.on.ca) (*Presenter*) Nothing to Disclose

LEARNING OBJECTIVES

To be completed by Dr. Levine (we are co-presenting).

ABSTRACT

To be completed by Dr. Levine (we are co-presenting).

RC424D Putting It All Together

Participants

Herbert Y. Kressel, MD, Boston, MA (*Presenter*) Stockholder, Pfizer Inc; Stockholder, GlaxoSmithKline plc

LEARNING OBJECTIVES

View learning objectives under the main course title.

RC425

What's Up with the New Requirements for Diagnostic Imaging Services? The Joint Commission, Medicare and Beyond

Tuesday, Nov. 29 4:30PM - 6:00PM Room: N229



AMA PRA Category 1 Credits™: 1.50
ARRT Category A+ Credits: 1.50

Participants

Tyler S. Fisher, Gardena, CA, (tyler@therapyphysics.com) (*Presenter*) Nothing to Disclose
Andrea D. Browne, PhD, Oakbrook Terrace, IL (*Presenter*) Nothing to Disclose

LEARNING OBJECTIVES

1) Identify new requirements applying to medical imaging. 2) Assess the degree to which their current policies and procedures will meet the new requirements. 3) Develop and implement new policies and procedures that will satisfy the new requirements.

Active Handout: Tyler S. Fisher

http://abstract.rsna.org/uploads/2016/16001116/RC425_RSNA_2016_Presentation_Fisher.pdf

Active Handout: Andrea D. Browne

http://abstract.rsna.org/uploads/2016/16001116/rc425_11-2016_Handout.pdf

RC427

Incorporating Patient and Family Centered Care Principles into Your Practice

Tuesday, Nov. 29 4:30PM - 6:00PM Room: S102D

HP

AMA PRA Category 1 Credits™: 1.50
ARRT Category A+ Credits: 1.50

Participants

James V. Rawson, MD, Augusta, GA (*Moderator*) Nothing to Disclose

James V. Rawson, MD, Augusta, GA (*Coordinator*) Nothing to Disclose

LEARNING OBJECTIVES

1) Identify opportunities for Radiologist to Improve Patient Experiences. 2) Review tools for improving Patient Experiences.

Sub-Events

RC427A From Physician to Family Member Lessons Learned

Participants

Jennifer L. Kemp, MD, Denver, CO, (jkemp@divrad.com) (*Presenter*) Nothing to Disclose

LEARNING OBJECTIVES

View learning objectives under the main course title.

RC427B Technologist and Patient Interactions

Participants

Layne Mitchell, MBA, RT, Augusta, GA (*Presenter*) Nothing to Disclose

LEARNING OBJECTIVES

View learning objectives under the main course title.

RC427C Interacting with Parents: A Chance to Add Value

Participants

Lynn A. Fordham, MD, Chapel Hill, NC (*Presenter*) Nothing to Disclose

LEARNING OBJECTIVES

1) In this session we will review challenges and opportunities for talking with parents and their children.

ABSTRACT

RC427D Opportunities in Informatics to Increase Patient Value

Participants

Tessa S. Cook, MD, PhD, Philadelphia, PA (*Presenter*) Nothing to Disclose

LEARNING OBJECTIVES

View learning objectives under the main course title.

RC429

Body MRI: Technical Challenges (An Interactive Session)

Tuesday, Nov. 29 4:30PM - 6:00PM Room: E351

MR

AMA PRA Category 1 Credits™: 1.50
ARRT Category A+ Credits: 1.50

FDA

Discussions may include off-label uses.

Participants

Sub-Events

RC429A Motion Control Techniques in Body MRI

Participants

Hersh Chandarana, MD, New York, NY (*Presenter*) Equipment support, Siemens AG; Software support, Siemens AG; Advisory Board, Siemens AG;

LEARNING OBJECTIVES

1) Understand basic concepts of k-space and acquisition time. 2) Discuss various methods to accelerate acquisition by k-space undersampling. 3) Discuss motion robust acquisition schemes including non-Cartesian k-space sampling.

ABSTRACT

ABSTRACT: Assessment of multiple post-contrast phases after gadolinium contrast injection is essential for lesion detection and characterization, and thus is a routine component of abdominopelvic MRI. Contrast-enhanced multiphase MR examination is usually performed using a T1-weighted fat-saturated 3D volumetric interpolated sequence with Cartesian k-space sampling in a breath-hold. However, this method is sensitive to respiratory motion and can result in suboptimal images in patients who cannot adequately breath-hold. Techniques to overcome this major limitation include rapid imaging to decrease acquisition time and motion robust acquisition schemes. Concept of acquisition time and k-space will be discussed followed by discussion of techniques to perform rapid and motion robust imaging.

RC429B Which Contrast Should I Use?

Participants

Matthew S. Davenport, MD, Cincinnati, OH, (matdaven@med.umich.edu) (*Presenter*) Royalties, Wolters Kluwer nv; ;

LEARNING OBJECTIVES

1) Review common gadolinium-based contrast agents (GBCA). 2) Understand the strengths and weaknesses of various GBCA. 3) Learn the incidence and significance of various risks associated with GBCA administration.

ABSTRACT

This presentation will review the strengths and weaknesses of a variety of modern gadolinium-based contrast agents. Controversies, risks, and benefits will be presented. Practice optimization with respect to selection of a GBCA formulary will be discussed.

RC429C Optimizing Diffusion-Weighted Imaging

Participants

Dow-Mu Koh, MD, FRCR, Sutton, United Kingdom (*Presenter*) Nothing to Disclose

LEARNING OBJECTIVES

1) To understand how to get the best body diffusion-weighted MRI at 1.5T and 3.0T by optimizing image signal-to-noise and minimizing image artefacts. 2) To appreciate the additional challenges of body diffusion-weighted MRI at 3.0T. 3) To review newer imaging techniques that can be applied at 3.0T to improve body diffusion-weighted MRI including combinatorial fat suppression schemes, image-based shimming, reduced field-of-view acquisitions and readout-segmented echo-planar imaging techniques.

ABSTRACT

Body diffusion-weighted MRI (DWI) is now widely applied for disease evaluation, especially in oncology. DWI is relatively quick and easy to perform using single-shot echo-planar imaging (EPI) technique. However, imaging optimisation is important to ensure that high quality images are consistently attained. At both 1.5T and 3.0T, parameter optimization is necessary to maximize signal-to-noise (such as by reducing echo-times, using coarser matrix, thicker partition thickness, multiple signal averages) of the acquired images and to minimize potential artefacts (e.g. motion, chemical shift, eddy currents, Nyquist ghosting, susceptibility and G-noise) that will degrade image quality. Although body DWI is generally more robust at 1.5T, recent advances at 3.0T allow high quality DWI images to be obtained, including whole body studies. Imaging at 3.0T has the advantage of higher image signal-to-noise; but is more prone to artefacts arising from chemical shift (suboptimal fat suppression), susceptibility effects and image distortion. Hence, meticulous optimisation of fat suppression (e.g. using combinatorial fat suppression schemes) and avoidance of regions that may cause significant susceptibility artefacts are important. More recently, the introduction of advanced shimming (including image-based shimming option) has helped to improve DWI quality at 3.0T, particular for large field-of-view imaging. Image distortion and susceptibility artifacts can be further reduced using read-out segmented EPI techniques. The higher signal-to-noise at 3.0T also allows for high spatial resolution reduced field-of-view techniques to be applied. At 3.0T, there is also an opportunity to perform DWI studies on a hybrid PET-MRI system. To maximise information gained from such hybrid system, protocol design and clinical workflow

are important.

US for Thyroid Cancer: Diagnosis, Surveillance, and Treatment

Tuesday, Nov. 29 4:30PM - 6:00PM Room: E350



AMA PRA Category 1 Credits™: 1.50
ARRT Category A+ Credits: 1.50

Participants

Jill E. Langer, MD, Philadelphia, PA (*Presenter*) Nothing to Disclose
Kathryn A. Robinson, MD, Saint Louis, MO (*Presenter*) Nothing to Disclose
Sheila Sheth, MD, Cockeysville, MD (*Presenter*) Nothing to Disclose

LEARNING OBJECTIVES

1) Describe the sonographic characteristics of thyroid nodules that are suspicious for malignancy. 2) a. Discuss the Bethesda Cytology Classification of Thyroid FNA results and the risk of malignancy associated with each category. b. Describe the indications for new genetic tests that may be performed on FNAs obtained from thyroid nodules with indeterminate cytology. 3) a. Describe the technique of US-guided biopsy of thyroid nodules and cervical lymph nodes in patients who have undergone thyroidectomy for thyroid cancer. b. Discuss the rationale and method of performance of US-guided ethanol ablation of malignant cervical adenopathy in post thyroidectomy patients.

ABSTRACT

This presentation will consist of a three individual presentations. The first will review the sonographic characteristics of thyroid nodules that are suggestive of malignancy. Recommendations for selecting which thyroid nodules require ultrasound-guided biopsies which have been provided by both Radiology consensus conferences and published Endocrinology guidelines will be discussed. The second presentation will review with the Bethesda Cytology Classification of Thyroid FNA results and the risk of malignancy associated with each category. Additionally this presentation describes the indications for two new genetic tests that may be performed on FNAs obtained from thyroid nodules with indeterminate cytology. The last presentation will provide a detailed description of the technique for performing ultrasound guided biopsy of thyroid nodules and cervical lymph nodes. Various methods will be discussed and required equipment outlined. Possible complications, though rare, will be described. A comparison of the typical sonographic features of normal versus abnormal lymph nodes will be presented in an effort to identify those patients in whom sonographic follow up can be used instead of biopsy. A discussion of the possible advantages of adding thyroglobulin assay to cytologic evaluation will be provided. The rationale for and technique of performing ultrasound guided ethanol ablation of malignant cervical lymph nodes in patients with thyroid cancer will be undertaken.

RC432

Compensation

Tuesday, Nov. 29 4:30PM - 6:00PM Room: S103CD



AMA PRA Category 1 Credits™: 1.50
ARRT Category A+ Credit: 0

Participants

LEARNING OBJECTIVES

1) To learn about the implementation of fair market value compensation plans. 2) To understand the importance of utilizing appropriate benchmarks for clinical productivity metrics. 3) Provide a history of important legislation and policies that have had a significant impact on health care reform. 4) Review recent transformative health care legislation and policies that will impact radiology reimbursement. 5) Present concepts that can help radiology departments adapt to the changing reimbursement environment. 6) Define the need for, and importance and role of, the expert witness in the initiation and execution of a medical malpractice lawsuit. 7) Identify the factors that increase, and diminish, the value and effectiveness of the expert witness before a courtroom jury. 8) Appreciate the potential rewards, and the potential penalties, that can arise from testifying as an expert witness on behalf of the plaintiff, or the defendant.

Sub-Events

RC432A Radiology Compensation Issues.

Participants

Vincent P. Mathews, MD, Elm Grove, WI (*Presenter*) Nothing to Disclose

LEARNING OBJECTIVES

1) To learn about the implementation of fair market value compensation plans. 2) To understand the importance of utilizing appropriate benchmarks for clinical productivity metrics.

ABSTRACT

RC432B The Impact of Health Care Reform on Radiology Reimbursement and Revenue

Participants

Robert J. Witte, MD, Rochester, MN, (witte.robert@mayo.edu) (*Presenter*) Nothing to Disclose

LEARNING OBJECTIVES

1) Provide a history of important legislation and policies that have had a significant impact on health care reform. 2) Review recent transformative health care legislation and policies that will impact radiology reimbursement. 3) Present concepts that can help radiology departments adapt to the changing reimbursement environment.

RC432C Testifying as an Expert Witness: Rules, Compensation and Other Rewards, Prevarications and Penalties

Participants

Leonard Berlin, MD, Skokie, IL, (lberlin@live.com) (*Presenter*) Nothing to Disclose

LEARNING OBJECTIVES

1) Define the need for, and importance and role of, the expert witness in the initiation and execution of a medical malpractice lawsuit. 2) Identify the factors that increase, and diminish, the value and effectiveness of the expert witness before a courtroom jury. 3) Appreciate the potential rewards, and the potential penalties, that can arise from testifying as an expert witness on behalf of the plaintiff, or the defendant.

Targeted Treatment and Imaging of Liver Cancers: Basic to Advanced Techniques in Minimally-Invasive Therapies and Imaging

Tuesday, Nov. 29 4:30PM - 6:00PM Room: S403B



AMA PRA Category 1 Credits™: 1.50
ARRT Category A+ Credits: 1.50

FDA Discussions may include off-label uses.

Participants

Jinha Park, MD, PhD, Duarte, CA (*Presenter*) Speakers Bureau, Bayer AG;

Steven S. Raman, MD, Santa Monica, CA (*Presenter*) Nothing to Disclose

John J. Park, MD, PhD, Duarte, CA, (johnpark@coh.org) (*Presenter*) Proctor, Sirtex Medical Ltd; Advisory Board, Guerbet SA; Speakers Bureau, Medtronic plc

Marcelo S. Guimaraes, MD, Charleston, SC, (guimarae@musc.edu) (*Presenter*) Consultant, Cook Group Incorporated ; Consultant, Baylis Medical Company; Consultant, Terumo Corporation; Patent holder, Cook Group Incorporated

Andrew C. Price, MD, Gilbert, AZ, (Andrew.Price@bannerhealth.com) (*Presenter*) Nothing to Disclose

LEARNING OBJECTIVES

1) Discuss the role of the interventional radiologist in the treatment and management of patients with primary and metastatic liver cancer as part of the multidisciplinary team. 2) Learn best practice techniques in the treatment of liver cancers, with emphasis on both locoregional and focal therapeutic approaches, and indications for treatment. 3) Explore various tips and tricks for each treatment modality and learn how to avoid complications through good patient selection, choosing the appropriate techniques, and knowing what common mistakes to avoid. 4) Learn about newer and developing techniques and devices, their potential roles and indications, and potential pitfalls. 5) Explore advanced imaging modalities in the detection of tumors and for monitoring treatment response.

ABSTRACT

Primary and metastatic liver disease may benefit from combined techniques such as bland/chemoembolization and liver ablation. The presentation will provide the rationale for the association of techniques, patient selection, tips and tricks, equipment and supplies necessary, protective techniques and how to avoid complications. Also, it will be discussed the results and current literature to support the association of techniques.

Nerve Ultrasound Based on a Regional Approach: Elbow to Hand (Hands-on)

Tuesday, Nov. 29 4:30PM - 6:00PM Room: E264



AMA PRA Category 1 Credits™: 1.50
ARRT Category A+ Credits: 1.50

Participants

Carlo Martinoli, MD, Genova, Italy (*Presenter*) Nothing to Disclose
 Etienne Cardinal, MD, Montreal, QC (*Presenter*) Nothing to Disclose
 Mary M. Chiavaras, MD, PhD, Ancaster, ON (*Presenter*) Consultant, Toshiba Medical Systems Corporation; Research Grant, Arthrex, Inc; ;
 Joseph G. Craig, MD, Detroit, MI (*Presenter*) Nothing to Disclose
 Michael A. Dipietro, MD, Ann Arbor, MI (*Presenter*) Nothing to Disclose
 David P. Fessell, MD, Ann Arbor, MI (*Presenter*) Nothing to Disclose
 Ghiyath Habra, MD, Detroit, MI (*Presenter*) Nothing to Disclose
 Marnix T. van Holsbeeck, MD, Detroit, MI, (marnix@rad.hfh.eu) (*Presenter*) Consultant, General Electric Company; Stockholder, Koninklijke Philips NV; Stockholder, General Electric Company; Stockholder MedEd3D; Grant, Siemens AG; Grant, General Electric Company;
 Joseph H. Introcaso, MD, Neenah, WI (*Presenter*) Nothing to Disclose
 Jon A. Jacobson, MD, Ann Arbor, MI, (jjacobsn@umich.edu) (*Presenter*) Consultant, BioClinica, Inc; Royalties, Reed Elsevier; ; ;
 Viviane Khoury, MD, Philadelphia, PA, (Viviane.khoury@uphs.upenn.edu) (*Presenter*) Nothing to Disclose
 Marina Kislyakova, MD, Moscow, Russia, (mkisliakova@yandex.ru) (*Presenter*) Nothing to Disclose
 Andrea Klauser, MD, Reith bei Seefeld, Austria (*Presenter*) Nothing to Disclose
 Kenneth S. Lee, MD, Madison, WI, (klee2@uwhealth.org) (*Presenter*) Grant, General Electric Company; Research support, SuperSonic Imagine; Research support, Johnson & Johnson; Consultant, Echometrix, LLC; Royalties, Reed Elsevier
 Humberto G. Rosas, MD, Madison, WI (*Presenter*) Nothing to Disclose
 Matthieu Rutten, MD, Hertogenbosch, Netherlands (*Presenter*) Nothing to Disclose
 Courtney E. Scher, DO, Detroit, MI (*Presenter*) Nothing to Disclose
 Alberto S. Tagliafico, MD, Genova, Italy (*Presenter*) Nothing to Disclose
 Ximena L. Wortsman, MD, Santiago, Chile, (xworts@yahoo.com) (*Presenter*) Nothing to Disclose

LEARNING OBJECTIVES

1) Familiarize course participants with the ultrasound appearance of nerves and the scanning techniques used to image them in the distal upper extremity. 2) Emphasize the ultrasound anatomy of the median, ulnar, radial nerves and their divisional branches at the most common sites of entrapments, including the carpal tunnel and the cubital tunnel. 3) Learn the technique to image some minor nerves in their course throughout the distal upper extremity, such as the the lateral and the medial antebrachial cutaneous. 4) Outline the range of clinical conditions where ultrasound is appropriate as the primary imaging modality for nerve assessment.

ABSTRACT

In recent years, ultrasound of the musculoskeletal and peripheral nervous systems is becoming an increasingly imaging tool with an expanding evidence base to support its use. However, the operator dependent nature and level of technical expertise required to perform an adequate ultrasound assessment means that appropriate training is required. For this purpose, the present course will demonstrate the basic principles of musculoskeletal ultrasound with a special focus on nerves of the distal upper extremity (elbow to hand). The standardized techniques of performing an adequate ultrasound study of the median, ulnar, radial and their divisional branches, lateral cutaneous of the forearm and medial cutaneous of the arm and the forearm will be illustrated. The hands-on workshops will provide the opportunity to interactively discuss the role of ultrasound in this field with expert instructors. Participants will be encouraged to directly scan model patients. A careful ultrasound approach with thorough understanding of soft-tissue planes and extensive familiarity with anatomy are prerequisites for obtaining reliable information regarding the affected structure and the site and nature of the disease process affecting it.

Honored Educators

Presenters or authors on this event have been recognized as RSNA Honored Educators for participating in multiple qualifying educational activities. Honored Educators are invested in furthering the profession of radiology by delivering high-quality educational content in their field of study. Learn how you can become an honored educator by visiting the website at: <https://www.rsna.org/Honored-Educator-Award/>

Michael A. Dipietro, MD - 2016 Honored Educator
 Jon A. Jacobson, MD - 2012 Honored Educator

RC453

Clinical Decision Support: Impact and Lessons from Large Scale Implementations

Tuesday, Nov. 29 4:30PM - 6:00PM Room: S403A

IN

AMA PRA Category 1 Credits™: 1.50
ARRT Category A+ Credits: 1.50

Participants

Emanuele Neri, MD, Pisa, Italy, (emanuele.neri@med.unipi.it) (*Moderator*) Nothing to Disclose

LEARNING OBJECTIVES

1) To understand the strategy of implementation of a Clinical Decision Support System. 2) To learn from the evidences how the Clinical Decision Support System impact in the clinical practice.

Sub-Events

RC453A Results and Lesson from the Medicare Imaging Demonstration

Participants

Keith D. Hentel, MD, MS, New York, NY (*Presenter*) Nothing to Disclose

LEARNING OBJECTIVES

1) To understand the lessons learned in the Weill Cornell Implementation of CDS for the MID. 2) Apply lessons learned in the MID to guide future CDS implementations.

ABSTRACT

RC453B Massachusetts General Hospital

Participants

Jeffrey B. Weilburg, MD, Boston, MA (*Presenter*) Nothing to Disclose

LEARNING OBJECTIVES

View learning objectives under the main course title.

RC453C Virginia Mason

Participants

C. Craig Blackmore, MD, MPH, Seattle, WA, (craig.blackmore@virginiamason.org) (*Presenter*) Author with royalties, Springer Science+Business Media Deutschland GmbH

LEARNING OBJECTIVES

1) To understand the implementation of clinical decision support at Virginia Mason. 2) To apply lessons learned from successful implementation of clinical decision support. 3) To analyze factors contributing to the success or failure of clinical decision support in decreasing inappropriate imaging.

ABSTRACT

At Virginia Mason, we published one of the earliest clinical decision support programs for advanced imaging. That program differed in many important ways from other programs, including the Medical Imaging Demonstration project, by deploying a targeted intervention directed at a limited number of high cost/high utilization studies. Our clinical decision support system achieved 25% decreases in imaging across the included studies through use of a "hard stop" barrier whereby inappropriate imaging was not permitted to proceed.

RC453D Brigham and Women's Hospital

Participants

Ramin Khorasani, MD, Boston, MA (*Presenter*) Consultant, Medicalis Corp

LEARNING OBJECTIVES

1) Understand functional requirements and components for effective CDS for imaging. 2) Using a case example, review impact of large scale implementation of imaging CDS. 3) Summarize lessons learnt to inform impactful implementation of imaging CDS in the context of new federal regulations for imaging CDS (Protecting Access to Medicare Act, PAMA, of 2014).

ABSTRACT

Clinical Decision Support (CDS) has been recognized as an important tool in helping reduce inappropriate use of medical imaging to improve the quality of care and reduce waste by providing evidence-based recommendation to ordering providers at the time of order entry. Three federal regulations aimed to assess the impact of imaging CDS on use of high cost imaging, and promote and accelerate its use. 1. (Medicare Improvements for Patients and Providers Act or MIPPA) required CMS to perform a large scale demonstration project (Medicare Imaging Demonstration or MID; 2011-2014) to assess the impact of imaging CDS based on pre-determined professional society guidelines on utilization of ambulatory targeted high cost imaging procedures for medicare fee for service patients. 2. Stage two of Meaningful Use of health IT federal regulations provide modest financial incentives for adoption of

CDS, including for imaging, and 3. Promoting Evidence-Based care section of the Protecting Access to Medicare Act (PAMA) of 2014 mandates use of imaging CDS for specified ambulatory high cost imaging services as a requirement for payment for such services beginning January 2017. Despite these ongoing federal initiatives, adoption of imaging CDS has been limited in part because of ongoing debate on best practices for implementation and use of imaging CDS. In this session, speakers with experience in use of imaging CDS, including large scale implementation, will share their experience on impact of CDS, and lessons learnt from implementation of imaging CDS to help inform best practices for imaging CDS.

RC454

Health IT Policy Panel: The New Federal Requirement for Imaging Decision Support (H.R. 4302)

Tuesday, Nov. 29 4:30PM - 6:00PM Room: S504AB



AMA PRA Category 1 Credits™: 1.50
ARRT Category A+ Credits: 1.50

Participants

David B. Larson, MD, MBA, Los Altos, CA (*Moderator*) License agreement, Bayer AG; Potential royalties, Bayer AG

Sub-Events

RC454A Overview of the Imaging Decision Support Requirement

Participants

Curtis P. Langlotz, MD, PhD, Menlo Park, CA, (langlotz@stanford.edu) (*Presenter*) Shareholder, Montage Healthcare Solutions, Inc; Spouse, Consultant, Novartis AG;

LEARNING OBJECTIVES

1) Understand the requirements and scope of the U.S. Federal decision support requirement in the Protecting Access to Medicare Act of 2014. 2) Learn the legal definitions of appropriate use criteria and qualified provider-led entity. 3) Review the consequences of non-compliance. 4) Recognize the challenges CMS will face in implementing the law. 5) Recognize the challenges health care organizations will face in responding to the law. 6) Learn the latest information on implementation approach and timetable.

RC454B The Origins of the Imaging Decision Support Legislation

Participants

Keith J. Dreyer, DO, PhD, Boston, MA (*Presenter*) Medical Advisory Board, IBM Corporation

RC454C Experience and Recommendations of the High Value Health Care Collaborative

Participants

Keith S. White, MD, Murray, UT, (Keith.White@imail.org) (*Presenter*) Software support, Jidoka Systems

LEARNING OBJECTIVES

1) Understand the key differentiators of a Quality Improvement (QI) from a Quality Assurance (QA) program. 2) Understand how local teams should organize to establish QI programs focusing on Priority Clinical Areas (PCAs) to optimize local success in implementing PAMA regulations. 3) Identify pitfalls and strategies to mitigate risks of implementation of PAMA regulations. 4) Identify opportunities and strategies to optimize outcomes of local implementation of PAMA regulations.

ABSTRACT

Active Handout: Keith S. White

[http://abstract.rsna.org/uploads/2016/15003162/ACTIVE RC454C PAMA_Deliverable_Final.pdf](http://abstract.rsna.org/uploads/2016/15003162/ACTIVE_RC454C_PAMA_Deliverable_Final.pdf)

RC454D CMS Approach to Implementing the Legislation: Current Status

Participants

Joseph Hutter, Baltimore, MD (*Presenter*) Nothing to Disclose

LEARNING OBJECTIVES

1) Understand the key provisions of Section 218(b) of PAMA 2014. 2) Understand the CMS Final Rule setting up a new nationwide program for appropriate use criteria for imaging. 3) Understand the timetable for future components of the CMS program.

Data Collection, Organization and Analysis with Excel - A Hands-On Tutorial (Hands-on)

Tuesday, Nov. 29 4:30PM - 6:00PM Room: S401AB

AMA PRA Category 1 Credits™: 1.50
ARRT Category A+ Credits: 1.50**Participants**

Jaydev K. Dave, PhD, MS, Philadelphia, PA, (jaydev.dave@jefferson.edu) (*Presenter*) Nothing to Disclose
Raja Gali, MS, Philadelphia, PA, (raja.gali@jefferson.edu) (*Presenter*) Nothing to Disclose
Manish Dhyani, MBBS, Boston, MA (*Presenter*) Nothing to Disclose

LEARNING OBJECTIVES

1) Describe techniques for creating a spreadsheet to allow trouble-free data analysis. 2) Demonstrate key data management skills. 3) Describe tools for performing basic descriptive statistics. 4) Identify how to perform simple statistical tests and perform these tests with a sample dataset. 5) Understand how bad data (or bad data acquisition techniques) may corrupt subsequent data analyses. 6) Practice data plotting/representation techniques. 7) Identify differences between a spreadsheet and a database. 8) Identify statistical tasks that require more sophisticated software. Pre-requisites: Familiarity with Microsoft Windows and Microsoft Excel environment will be assumed

ABSTRACT

A spreadsheet program is commonly employed to collect and organize data for practicing quality improvement, for research, and for other purposes. In this refresher course, we will demonstrate to a user, familiar with Microsoft Excel environment, how this spreadsheet program may be used for such purposes. The course will begin with describing efficient approach for data acquisition and highlight key data management skills; and with reviewing common errors that may be avoided during data logging. Then we will provide a brief introduction on basic descriptive tests before proceeding with a hands-on tutorial using a sample dataset to calculate basic descriptive statistics, and to perform basic statistical tests like t-test, chi-square test, correlation analysis, etc. Effect of corrupted data on such analysis will also be demonstrated. The final hands-on component for this course will include data plotting and representation including the use of pivot tables. The course will conclude with a discussion on identifying differences between a spreadsheet and a database, limitations of a spreadsheet program and avenues where a dedicated statistical software program would be more beneficial. A list of some of these dedicated statistical software programs for analyses will also be provided. Pre-requisites: Familiarity with Microsoft Windows and Microsoft Excel environment will be assumed

RCB35

Making the Most of Google Docs: Docs, Slides, Forms, and Sheets (Hands-on)

Tuesday, Nov. 29 4:30PM - 6:00PM Room: S401CD

IN

AMA PRA Category 1 Credits™: 1.50
ARRT Category A+ Credits: 1.50

Participants

Ross W. Filice, MD, Washington, DC (*Presenter*) Nothing to Disclose
Aaron P. Kamer, MD, Indianapolis, IN (*Presenter*) Nothing to Disclose
Andrew B. Lemmon, MD, Atlanta, GA, (alemmon@emory.edu) (*Presenter*) Nothing to Disclose
Thomas W. Loehfelm, MD, PhD, Palo Alto, CA (*Presenter*) Nothing to Disclose
Marc D. Kohli, MD, San Francisco, CA (*Presenter*) Nothing to Disclose

LEARNING OBJECTIVES

1) Describe the benefits and drawbacks of using Google tools for collaborative editing. 2) Explain issues related to storing protected health information in Google Drive. 3) Demonstrate the ability to use the Google productivity applications for collaboration on document, spreadsheet, online form and presentation creation.

ABSTRACT

Note: Attendees should have or create a Google account prior to coming to the session. In today's busy environment, we need tools to work smarter, not harder. Google's suite of productivity applications provides a platform for collaboration that can be used across and within institutions to produce documents and presentations and to obtain and work-up data with ease. However, with increased sharing, security concerns need to be addressed. At the end of the session, learners should be able to demonstrate creating, sharing, and editing a document as a group.

RCC35

Ergonomics

Tuesday, Nov. 29 4:30PM - 6:00PM Room: S501ABC



AMA PRA Category 1 Credits™: 1.50
ARRT Category A+ Credits: 1.50

Participants

William J. Weadock, MD, Ann Arbor, MI (*Moderator*) Owner, Weadock Software, LLC

LEARNING OBJECTIVES

1) The attendee will learn how the radiology reading room environment can physically affect the radiologist. 2) Learn about repetitive stress injuries and how they may affect radiologists and technologists. 3) Learn about how PACS workstations (including mice, keyboards, screens, etc.); room lighting, sounds and temperature; and room furniture may be optimized to help prevent repetitive stress injuries. 4) Learn how radiologic technologists can also be affected by repetitive stress injuries.

ABSTRACT

This presentation will review the features of a reading a study at a PACS, and the interactions of the radiologist with the various devices. This includes desktops/tables height, chairs, keyboard location, monitor position, mouse position (and cleanliness), microphone positioning, room temperature, sound volume, ambient light, and body positioning. Each of these components will be discussed, showing how to prevent future problems with repetitive stress disorders. The goal is to raise awareness of ergonomics for the radiologist.

Sub-Events

RCC35A Introduction to Ergonomics

Participants

William J. Weadock, MD, Ann Arbor, MI (*Presenter*) Owner, Weadock Software, LLC

LEARNING OBJECTIVES

View learning objectives under main course title.

RCC35B Lessons Learned From Our Reading Room of the Future Lab

Participants

Eliot L. Siegel, MD, Baltimore, MD (*Presenter*) Board of Directors, Brightfield Technologies; Board of Directors, McCoy; Board of Directors, Carestream Health, Inc; Founder, MedPerception, LLC; Founder, Topoderm; Founder, YYESIT, LLC; Medical Advisory Board, Bayer AG; Medical Advisory Board, Bracco Group; Medical Advisory Board, Carestream Health, Inc; Medical Advisory Board, Fovia, Inc; Medical Advisory Board, McKesson Corporation; Medical Advisory Board, Merge Healthcare Incorporated; Medical Advisory Board, Microsoft Corporation; Medical Advisory Board, Koninklijke Philips NV; Medical Advisory Board, Toshiba Corporation; Research Grant, Anatomical Travelogue, Inc; Research Grant, Anthro Corp; Research Grant, Barco nv; Research Grant, Dell Inc; Research Grant, Evolved Technologies Corporation; Research Grant, General Electric Company; Research Grant, Herman Miller, Inc; Research Grant, Intel Corporation; Research Grant, MModal IP LLC; Research Grant, McKesson Corporation; Research Grant, RedRICK Technologies Inc; Research Grant, Steelcase, Inc; Research Grant, Virtual Radiology; Research Grant, XYBIX Systems, Inc; Research, TeraRecon, Inc ; Researcher, Bracco Group; Researcher, Microsoft Corporation; Speakers Bureau, Bayer AG; Speakers Bureau, Siemens AG;

RCC35C No Strain, No Pain: A Guide to Reducing Musculoskeletal Strain and Eye Fatigue Among Radiologists

Participants

Rebecca L. Seidel, MD, Atlanta, GA (*Presenter*) Nothing to Disclose

MSRO39

BOOST: Breast-eContouring

Tuesday, Nov. 29 4:45PM - 6:00PM Room: S104B



AMA PRA Category 1 Credits™: 1.25
ARRT Category A+ Credits: 1.50

Participants

Jean L. Wright, MD, New York, NY (*Presenter*) Nothing to Disclose

Atif J. Khan, MD, New Brunswick, NJ (*Presenter*) Consultant, Elekta AB; Consultant, Vertex Pharmaceuticals Incorporated; Speaker, Elekta AB; Speaker, Vertex Pharmaceuticals Incorporated; Research funded, Elekta AB; Research funded, Cianna Medical, Inc

LEARNING OBJECTIVES

1) Know where to locate the available resources for optimal contouring of breast cancer radiation targets. 2) Understand the contouring guidelines in contemporary breast radiation protocols and know standard contouring nomenclature currently used in these studies. 3) Understand how contouring represents a critical component for optimal planning in breast cancer. 4) Carry out contouring on representative CT images for two scenarios: intact breast, and chest wall and regional nodes.